DEPARTMENT OF BIOLOGICAL SCIENCES

DIVERSE ROLES OF FOCAL ADHESION KINASE IN VERTEBRATE DEVELOPMENT

NICOLETTA I. PETRIDOU

A Dissertation Submitted to the University of Cyprus in Partial Fulfillment of the Requirements for the Degree of Doctor of Philosophy

OCTOBER 2015

VALIDATION PAGE

Doctoral Candidate: Nicoletta I. Petridou

Doctoral Thesis Title: DIVERSE ROLES OF FOCAL ADHESION KINASE IN VERTEBRATE DEVELOPMENT

The present Doctoral Dissertation was submitted in partial fulfillment of the requirements for the Degree of Doctor of Philosophy at the ***Department of Biological Sciences*** *and was approved on 22nd of October 2015 by the members of the* ***Examination Committee***.

Examination Committee:

Research Supervisor: Paris Skourides, Assistant Professor, Department of Biological Sciences, UCY

Committee Member: Niovi Santama, Associate Professor, Department of Biological Sciences, UCY

Committee Member: Pantelis Georgiades, Associate Professor, Department of Biological Sciences, UCY

Committee Member: Maddy Parsons, Professor of Cell Biology, King's College London

Committee Member: George Zachos, Assistant Professor, Biology Department, University of Crete

DECLARATION OF DOCTORAL CANDIDATE

The present doctoral dissertation was submitted in partial fulfillment of the requirements for the degree of Doctor of Philosophy of the University of Cyprus. It is a product of original work of my own, unless otherwise mentioned through references, notes, or any other statements.

Nicoletta I. Petridou

.....

Περίληψη

Η κινάση των εστιακών προσκολλήσεων (Focal Adhesion Kinase, FAK) είναι μία μη-υποδοχέας κινάση τυροσίνης σημαντική για σηματοδότηση προερχόμενη από αλληλεπιδράσεις ιντεγκρινών-εξωκυττάριου υποστρώματος και εμπλέκεται σε διαδικασίες κυτταρικής προσκόλλησης και μετανάστευσης. Η FAK είναι απαραίτητη στην εμβρυική ανάπτυξη, καθώς ποντίκια με διαγραφή του γονιδίου της FAK παρουσιάζουν εμβρυικό θάνατο λόγω ελαττωματικής μορφογένεσης του μεσοδέρματος. Παρόλα αυτά, οι συγκεκριμένοι ρόλοι της πρωτεΐνης FAK στην εμβρυογένεση παραμένουν ως επί το πλείστον άγνωστοι. Σε αυτή τη μελέτη, διερευνήσαμε τη λειτουργία της FAK κατά την εμβρυική ανάπτυξη των σπονδυλωτών χρησιμοποιώντας ως πειραματικό μοντέλο το βάτραχο *Xenopus laevis*. Δημιουργώντας ένα ισχυρό πρωτεϊνικό αναστολέα της FAK καταφέραμε να χαρακτηρίσουμε το ρόλο της στο πρώιμο έμβρυο. Αναστολή της FAK στο ραχιαίο μεσόδερμα οδήγησε σε φαινότυπο παρόμοιο με αυτόν των ποντικών που δεν εκφράζουν FAK και επιπλέον, αποκάλυψε ότι η λειτουργία της FAK στα κεντροσωμάτια κατά τη μίτωση είναι σημαντική στην επιβίωση του μεσοδέρματος. Αναστολή της FAK στο νευροεκτόδερμα οδήγησε στην ανακάλυψη ενός νέου ρόλου κατά τη γαστριδίωση. Συγκεκριμένα, δείχνουμε ότι η FAK είναι απαραίτητη κατά την επιβολή, τη μορφογενετική κίνηση που επιτρέπει στο εκτόδερμα να περικλείσει το έμβρυο. Δείχνουμε ότι η σηματοδότηση προερχόμενη από φιμπρονεκτίνη κατά την επιβολή μεταδίδεται μέσω της FAK με ως αποτέλεσμα να ρυθμίζεται η πολικότητα και παρεμβολή των εκτοδερμικών κυττάρων. Επιπλέον, αποτυχία της επιβολής οδηγεί στο σταμάτημα της γαστριδίωσης, ένας φαινότυπος που διασώζεται με μηχανική ή φαρμακολογική ελευθέρωση της τάσης στον ιστό, αποδεικνύοντας ότι η επιβολή παίζει ένα επιτρεπτικό ρόλο στη γαστριδίωση και επεκτείνοντας την μηχανοβιολογική κατανόηση της γαστριδίωσης.

Περαιτέρω πειραματικές διεργασίες ανακάλυψαν ένα συντηρημένο ρόλο της FAK στη ρύθμιση του προσανατολισμού της μιτωτικής ατράκτου σε διάφορους ιστούς, συμπεριλαμβανομένων θηλαστικών κυττάρων σε καλλιέργεια και επιθηλιακά όργανα στο έμβρυο. Ένας από τους μηχανισμούς με τους οποίους η μιτωτική άτρακτος προσανατολίζεται είναι μέσω αναγνώρισης εξωτερικών δυνάμεων. Όμως, είναι ελάχιστα κατανοητό το πώς αυτές οι δυνάμεις αναγνωρίζονται και μεταφράζονται ενδοκυτταρικά σε βιοχημικά σήματα. Σε αυτή τη μελέτη παρέχουμε τα πρώτα στοιχεία της μοριακής σύνδεσης μεταξύ των εξωκυτταρικών μηχανικών ερεθισμάτων και του προσανατολισμού της ατράκτου. Δείχνουμε ότι η αναγνώριση των δυνάμεων επιτυγχάνεται μέσω ενεργοποίησης της ιντεγκρίνης β1 ανεξάρτητης της πρόσδεσης με συνδέτη, στον πλευρικό φλοιό των μιτωτικών κυττάρων. Αυτό οδηγεί στην προσέλκυση

πρωτεϊνών των εστιακών προσκολλήσεων συμπεριλαμβανομένων της FAK, p130Cas και Src στον πλευρικό φλοιό για να σχηματίσουν ένα φλοιώδες μηχανοαισθητήριο σύμπλοκο (Cortical Mechanosensory Complex, CMC) το οποίο είναι υπεύθυνο για τη μεταγωγή του σήματος στην άτρακτο. Επιπλέον, δείχνουμε ότι τα μέλη του CMC και οι μεταξύ τους αλληλεπιδράσεις είναι απαραίτητες για τον προσανατολισμό της ατράκτου, παρέχοντας λεπτομέρειες ως προς το μηχανισμό λειτουργίας του CMC. Προτείνουμε ότι η πολωμένη ενεργοποίηση της ιντεγκρίνης β1 οδηγεί στην ασύμμετρη προσέλκυση των πρωτεϊνών του CMC στο μιτωτικό φλοιό. Αυτό έχει ως αποτέλεσμα τη φωσφορυλίωση της p130Cas μέσω ενός FAK/Src συμπλόκου το οποίο μέσω ενός απροσδιόριστου ακόμα μηχανισμού ευθυγραμμίζει την άτρακτο με το διάνυσμα της μεγαλύτερης εξωτερικής δύναμης. Αυτά τα ευρήματα δείχνουν ότι οι πρωτεΐνες των εστιακών προσκολλήσεων μπορούν να μεταδώσουν μηχανικά ερεθίσματα στο κύτταρο στην απουσία εξωκυτταρικών συνδετών και εισηγούνται ότι έχουν προσαρμοστεί για λειτουργίες εξαρτώμενες και ανεξάρτητες της κυτταρικής προσκόλλησης.

Abstract

The Focal Adhesion Kinase (FAK) is a non-receptor tyrosine kinase crucial for integrin-extracellular matrix (ECM) signal transduction and involved in a wide variety of biological processes including cell adhesion and migration. FAK is necessary for embryonic development since targeted disruption of the FAK gene in mice results in embryonic lethality due to general mesodermal deficiency. However, its specific roles in embryogenesis remain largely unknown. In this study, we explored FAK function during vertebrate embryonic development using *Xenopus laevis* as a model system. By generating a powerful dominant negative of FAK we managed to address FAK function in the early embryo. FAK inhibition in the dorsal mesoderm elicited defects similar to those reported in FAK null mice but in addition, revealed that FAK's centrosomal function during mitosis is essential for mesodermal survival. FAK inhibition in the prospective neuroectoderm however, uncovered a previously unidentified role of FAK during *Xenopus* gastrulation. Specifically, we show that FAK is necessary during epiboly, the morphogenetic movement that allows the ectoderm to encompass the entire embryo. We show that a fibronectin-derived signal transduced by FAK governs cell polarity and cell intercalation of ectodermal cells during epiboly. Moreover, failure of epiboly results in gastrulation arrest that can be rescued by both mechanical and pharmacological release of tension within the tissue, demonstrating that epiboly is permissive for gastrulation and furthering our mechanobiological understanding of gastrulation.

Additional work revealed a conserved role of FAK in the control of spindle orientation in several tissues including mammalian cells in culture and epithelial organs in the vertebrate embryo. One of the mechanisms by which the spindle is oriented is through sensing of external forces. However, how are these forces sensed and translated into biochemical signals intracellularly to orient the spindle is poorly understood. In this study we provide the first evidence of the molecular link between external mechanical stimuli and spindle orientation. We show that force sensing is achieved through ligand independent integrin β1 activation at the lateral cortex of mitotic cells. We go on to show that this activation elicits the recruitment of several focal adhesion proteins including FAK, p130Cas and Src to the lateral cortex to form a Cortical Mechanosensory Complex (CMC) which is responsible for the transduction of the signal to the spindle. Further analysis revealed that all three members of the CMC and interactions between them are essential for spindle orientation, providing mechanistic details with respect to the manner in which the CMC operates. Specifically, we propose that polarized activation of integrin β1 leads to the asymmetric recruitment of CMC proteins at the mitotic

cortex. This results in the phosphorylation of p130Cas through a FAK/Src complex which, through a yet undefined mechanism, aligns the spindle with the major external force vector. These findings show that focal adhesion proteins can transduce external mechanical stimuli to the cell in the absence of extracellular ligands and suggest that evolutionary they were adapted for both adhesion dependent and independent functions.

Acknowledgments

"When you set sail for Ithaka, wish for the road to be long, full of adventures, full of knowledge".

C.P. Cavafy

I have always considered the completion of my PhD studies, my personal "Ithaka". My journey to "Ithaka" has been long, difficult but also an enjoyable experience filled with knowledge and precious memories. A journey that would not have been possible without the invaluable support of several people.

To this select group, I would like to give special thanks beginning with my supervisor, Dr. Paris A. Skourides, for giving me the opportunity to join his lab, work on this exciting project and encouraging me to explore any question that came into my mind. Besides the excellent scientific guidance, his crazy ideas, the funny nicknames and the sometimes unreasonable for me ways to comprehend things made me open my eyes and look the bigger picture and finally be able to think outside the box. This is a priceless gift that I will carry for life. I am grateful to all the members of my committee; the external members Dr Maddy Parsons and Dr George Zachos and the internal members Dr Niovi Santama and Dr Pantelis Georgiades for reading my thesis, attending my defense and providing excellent comments and suggestions.

I would also like to thank all the former and current members of the *Xenopus* lab especially Dr Panayiota Stylianou, Evanthia Papazachariou and Stephanie Razi for their collaboration on this work. Some of the members of the lab I do not consider them only as excellent colleagues but as my second family. Dr Panayiota Stylianou was and will always be my "lab mum". I am grateful not only for the scientific knowledge that she provided me with, but also for her support, patience and her unique way to solve all of my problems in no time! I would also like to thank my "aunts" Dr Maria Andreou and Dr Andriani Ioannou, my "brother" Dr Neofytos Christodoulou and my "sister" Dr Ioanna Antoniades for all the amazing memories that we created together throughout the years.

Many special thanks to all of my friends for reminding me that there is life outside the lab and for being next to me during the most important moments of my life, to all the ups and downs. I feel extremely lucky that I met these amazing people and that they are a part of my life, especially George Karaolis, Vasiliki Vasiliou and Isabella Prokopiou.

Last but most importantly, I would like to thank my family especially my parents Yiannakis and Thelma, my brother Socrates and my grandmother Niki. My parents have always been the driving force to everything I have accomplished so far, supported me in success and failure and taught me to have patience in every obstacle. They both showed me that each problem has its own solution and a problem might not be that of an issue upon some shopping with mum or a nice glass of wine with dad.

With the help of these people this goal of my life is finally achieved, and I have finally reached my “Ithaka”. However according to C.P. Cavafy…

“Ithaka gave you the marvelous journey. Without her you would not have set out. She has nothing left to give you now. And if you find her poor, Ithaka won’t have fooled you. Wise as you will have become, so full of experience, you will have understood by then what these Ithakas mean”.

Dedication

To my parents,

Yiannakis and Thelma

Table of Contents

I. List of Figures

II. List of Tables

III. List of Movies

Movie 1: FA turnover in FF expressing cells in culture.
XL177 cell transfected with FF-GFP and imaged for FA assembly and disassembly. Images were acquired every 5 minutes for 1 hour.

Movie 2: FA turnover in FRNK expressing cells in culture.
XL177 cell transfected with GFP-FRNK and imaged for FA assembly and disassembly. Images were acquired every 5 minutes for 1 hour.

Movie 3: FA disassembly in FF expressing cells in culture.
XL177 cell transfected with FF-GFP and imaged at high magnification for FA disassembly. Images were acquired every 5 minutes for 1 hour.

Movie 4: FA disassembly in FRNK expressing cells in culture.
XL177 cell transfected with GFP-FRNK and imaged at high magnification for FA disassembly. Images were acquired every 5 minutes for 1 hour.

Movie 5: FA formation and migration of FF expressing mesodermal cells.
High magnification imaging of a mesodermal explant on FN coated glass coverslips for a 2 hour period. Cells are labelled with memCherry (red) and FF-GFP expressing cells are shown in green. FF-GFP expressors form very strong and numerous FAs which fail to disassemble and despite the undiminished protrusive activity, fail to migrate and are overtaken by surrounding cells.

Movie 6: Mesodermal tissue migration in explants.

Time lapse recording of a control AC induced with activin on FN coated glass coverslips. The AC was held in place by a glass bridge. The explant was imaged for approximately 4 hours. The explant spreads as cells are migrating out in all directions.

Movie 7: Mesodermal tissue migration in FF expressing explants.

Time lapse recording of an AC induced with activin on FN coated glass coverslips expressing FF-GFP on one side. The AC was held in place by a glass bridge. The explant was imaged for approximately 4 hours. Mesoderm migration is reduced at the FF-GFP expressing area of the explant whereas in non-expressing areas the explant extends as cells are migrating out.

Movie 8: Elongation of the A-P axis in *Xenopus* embryos.

Time lapse movie of a control embryo undergoing A-P axis elongation from neurula until tadpole stage. Images were acquired every 10 minutes.

Movie 9: Elongation of the A-P axis in FF expressing *Xenopus* embryos.

Time lapse movie of an FF injected embryo in the mesoderm undergoing A-P axis elongation from neurula until tadpole stage. Images were acquired every 10 minutes.

Movie 10: Blastopore closure during *Xenopus* gastrulation.

Time lapse movie of an FF injected embryo (left), rescued embryo (FF + FAK K38A injected, middle) and control embryo (right) undergoing gastrulation. Images were acquired every 10 minutes from stage 10.5 until 12.5.

Movie 11: Laser ablations and spindle re-orientation in *Xenopus* embryos.

Time lapse recording of spindle rotation in the epidermal cells of *Xenopus* stage 11 embryos injected with GFP-EMTB. A cell near the mitotic cell was ablated to generate tension perpendicular to the initial axis of the spindle leading to spindle rotation of the spindle towards the tension axis. Images were acquired every 2 minutes for a period of 10 minutes.

Movie 12: Laser ablations and spindle re-orientation in *Xenopus* FAK morphant embryos.

Time lapse recording of spindle rotation in the epidermal cells of *Xenopus* stage 11 embryos injected with GFP-EMTB and FAK MO. A cell near the mitotic cell was ablated to generate tension perpendicular to the initial axis of the spindle resulting to an almost null response by the spindle of morphant cells. Images were acquired every 2 minutes for a period of 10 minutes.

1. General Introduction

1.1. Cell adhesive interactions

Cells display adhesive interactions either between them which link cells into functional tissues and organs, or with the extracellular matrix (ECM) which provides mechanical anchoring of the cells and regulate precisely cell positioning within a multicellular organism (Heisenberg and Fassler 2012). Defective cell adhesion has been associated with abnormal embryonic development and wound repair and was linked with several diseases including immune, hematological and dermatological disorders, fibrotic, neurodegenerative and cardiovascular diseases, muscular dystrophies, tumor malignancies and metastasis (Morgan, Humphries et al. 2007, Geiger and Yamada 2011, Winograd-Katz, Fassler et al. 2014).

Cell-ECM interactions permit bidirectional biochemical and mechanical signal transduction that is crucial for many cellular functions including cell migration, proliferation and differentiation at the cell level and tissue remodeling, morphogenesis and wound healing at the organism level (Petit and Thiery 2000). Cell adhesion at the ECM is achieved through the engagement of cell surface receptors with ECM components, and the cell response to cell adhesion is mediated through the formation of cell-matrix adhesion complexes that eventually link the ECM with the microfilament system (Lock, Wehrle-Haller et al. 2008) (**Figure 1**). ECM components vary according to the type of matrix, such as tissue culture surfaces, basement membranes, connective tissue or tendons. Some of the major ECM components include the proteins collagen, laminin, fibronectin (FN), vitronectin (VN), perlecan and glycosaminoglycans (**Figure 1**). The ECM does not only provide physical support to the cells but according to its chemical composition, its dimensionality (if it exists in 2D surfaces or in a 3D environment such as in organs) and its mechanical properties, it enables micro-environmental sensing that precisely controls the activation of intracellular signaling, cell morphology, migration, proliferation, pattern of gene expression, stem cell fate choice and tumor progression (Geiger and Yamada 2011).

Besides the molecular diversity of the ECM components, there is also variety in their cell surface receptors. There are two types of cell surface receptors that recognize ECM components; integrin and non-integrin receptors. Non-integrin receptors mediate multiple adhesive interactions and include the proteoglycans syndecans, the tyrosine kinase receptors discoidin domain receptor 1 and 2, selectins, CD44, RHAMM and uPAR (urokinase-type plasminogen activator receptor) (Beauvais and Rapraeger 2004, Vogel, Abdulhussein et al. 2006, Smith and Marshall 2010, Geiger and Yamada 2011). However, the major cellular

receptors for ECM proteins are the well characterized transmembrane proteins, called integrins (**Figure 1**). Integrins have the ability to form morphologically, structurally and dynamically distinct adhesion types even within the same cell simultaneously, which are all referred with the name "adhesome". The integrin adhesome exhibits high molecular complexity in respect to its morphology, composition and regulation, characteristics that provide both physical-structural capacities and sensing-signaling activities to the cell (Geiger and Yamada 2011).

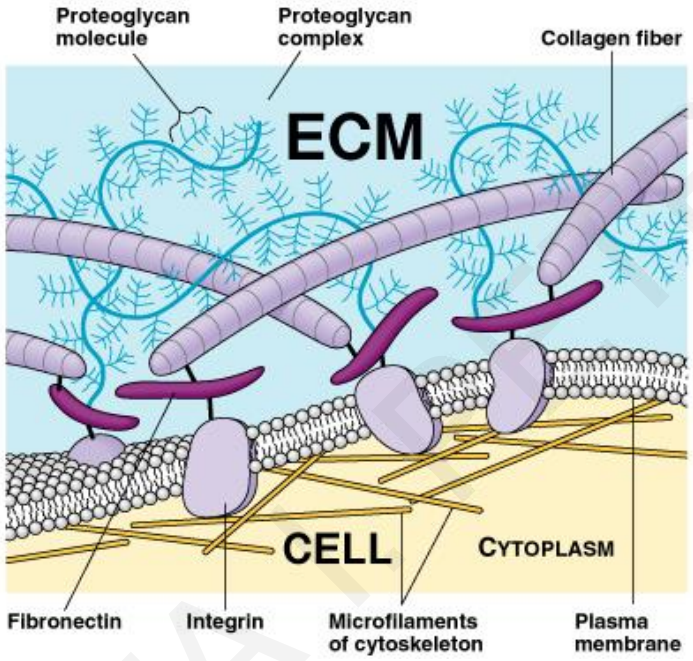

Figure 1: Schematic representation of cell-ECM adhesion.

The transmembrane receptors integrins interact with several ECM components through their extracellular domains and are linked with the microfilament system intracellularly. Adapted from 1999 Addison Wesley Longman, Inc.

1.2. The integrin adhesome; structure, composition and dynamic plasticity.

Within the integrin adhesome, several scaffolding and regulatory interactions take place in order to permit the bidirectional signal transduction between the cell exterior and the cytoskeleton. Scaffolding interactions mainly control the mechanical anchoring of integrins to the actin cytoskeleton, including actin-associated and adaptor proteins, whereas the regulatory interactions provide the dynamic plasticity at the adhesion site and include mainly signaling molecules, such as kinases, phosphatases, Rho-family GTPases and their regulators. To date, the adhesome network consists of over 232 components, of which 148 are intrinsic molecules of the adhesion complex and 84 transiently associate with the adhesion site (Winograd-Katz, Fassler et al. 2014).

The molecular architecture of the integrin adhesome has been studied for many years and it is still under intense investigation, since as mentioned above according to the ECM environment, the adhesome can dynamically change its morphology and structure, and as a result leading to discrepancies in its exact composition (Cukierman, Pankov et al. 2001). However, extensive work in 2D cultures has revealed core protein members of the adhesome that are described in more detail below. Briefly, the key molecules of the adhesome, integrins, are large class I transmembrane, heterodimeric proteins consisting of non-covalently linked α and β subunits. They contain extracellular domains with ECM binding sites, traverse the plasma membrane and form the cytoplasmic units which link the ECM with the actin cytoskeleton through the formation of the multiprotein signaling and scaffolding complex (Campbell and Humphries 2011) (**Figure 2**). Some examples of the scaffolding proteins that associate directly with the cytoplasmic domains of integrins are the cytoskeletal proteins talin, α-actinin and filamin (Horwitz, Duggan et al. 1986, Otey, Pavalko et al. 1990, Sharma, Ezzell et al. 1995) (**Figure 2**). Proteins of the adhesome that do not associate directly with integrins are vinculin, VASP (vasodilator-stimulated phosphoprotein), zyxin, p130Cas and tensin (Geiger 1979, Lo, An et al. 1994, Sakai, Iwamatsu et al. 1994, Beckerle 1997, Rottner, Behrendt et al. 1999) (**Figure 2**). Examples of regulatory proteins of the adhesome are FAK (Focal Adhesion Kinase), paxillin and ILK (Integrin-Linked Kinase) (Schaller, Otey et al. 1995, Hannigan, Leung-Hagesteijn et al. 1996) (**Figure 2**). Other regulatory proteins that are not necessarily part of the adhesion complex but they regulate its dynamic nature are the calcium-dependent protease calpain (Beckerle, Burridge et al. 1987), the kinases PI3K (phosphoinositide 3-kinase) and PKC (Protein Kinase C) (Carpenter and Cantley 1996, Ng, Squire et al. 1999), the phosphatases SHP-2 (Yu, Qu et al. 1998) and PTP-PEST (Garton and Tonks 1999), the motor protein kinesin-1(Krylyshkina, Kaverina et al. 2002), endocytosis regulatory molecules such as caveolin-1 (Nethe and Hordijk 2011) and dynamin-2 (Ezratty, Partridge et al. 2005) and regulators of actin dynamics such as the Arp2/3 complex (Pollard 2007) (**Figure 2**).

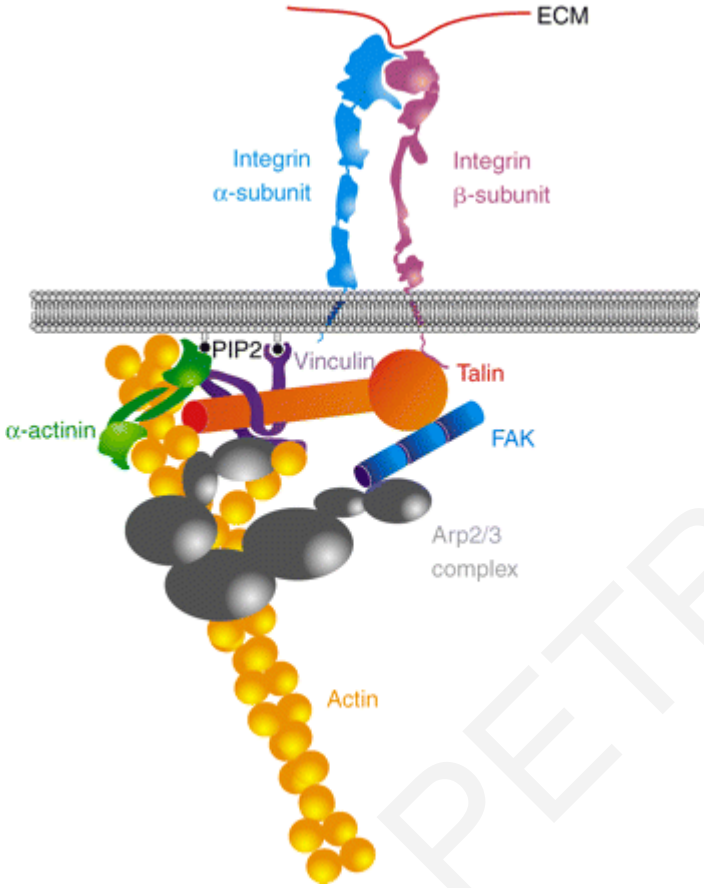

Figure 2: Adhesome structure and composition.

Schematic representation of the actin-integrin linkage mediated by the multiprotein complex formed on the cytoplasmic tails of the integrin heterodimer. The members of the adhesome shown are integrins (α and β transmembrane subunits), talin and α-actinin (scaffolding proteins that interact directly with integrin and actin), vinculin (scaffolding protein that does not interact directly with integrin), FAK (intrinsic regulatory protein of the adhesome) and Arp2/3 complex (regulatory protein that associates transiently with the adhesome). Adapted from (Vicente-Manzanares, Choi et al. 2009).

In a migratory cell, the adhesome can be classified at least into four different types of cell adhesion structures depending on the cell type, cell environment, size, morphology and location of the adhesion structure, and all types can all be present simultaneously (Dubash, Menold et al. 2009, Geiger and Yamada 2011). During cell migration, regulated actin polymerization drives the formation and extension of polarized protrusions at the cell membrane, which consist of lamellipodia or filopodia that become stabilized, mature and form the different types of adhesions at the cell front. Actin has a branched arrangement at the lamellipodium and its polymerization is driven by the Arp2/3 complex and is regulated by the effects of Rho GTPases, Rac and Cdc42, on the proteins of the WASP (Wiskott-Aldrich Syndrome Protein) and WAVE (WASP-family verprolin-homologous protein) family (Parsons, Horwitz et al. 2010). This protrusive activity brings the integrin expressing membranes in contact with the ECM ligand

and leads to integrin activation which is followed by a hierarchical recruitment of several proteins to the adhesome. The first type of adhesions in migrating cells is the nascent adhesions which are small short-lived adhesions formed at the lamellipodium immediately behind the leading edge (**Figure 3**). They have a dot-like shape, they consist of only a few hundred protein molecules positive for actin, VASP, α-actinin, talin and paxillin, and they transduce signal that promotes actin polymerization (Alexandrova, Arnold et al. 2008). Nascent adhesions can either turn over within 60 seconds or can mature to larger, same-shaped adhesions referred as focal complexes (FCs) (**Figure 3**). FCs have a longer lifetime (several minutes) and reside slightly back form the leading edge at the lamellum-lamellipodium interface (Parsons, Horwitz et al. 2010). Specifically, vinculin binding on talin leads to clustering of active integrins and the integrin-actin link is strengthened through the binding of the vinculin tail on actin (Galbraith, Yamada et al. 2002, Humphries, Wang et al. 2007). FCs mature further and transform into focal adhesions (FAs) which are longer and elongated structures that reside at the termini of the stress fibers (**Figure 3**). FAs are not formed only at the leading edge but also at the center and the periphery of the cell. FAs mature further by increasing their length and surface and their structural role is the linkage of the ECM with the actin cytoskeleton (Parsons, Horwitz et al. 2010, Geiger and Yamada 2011, Huttenlocher and Horwitz 2011). At this point, dendritic actin at the lamellum-lamellipodium interface depolymerizes and reorganizes into parallel bundles and actomyosin contraction regulated by the activity of Rho and its effectors ROCK (Rho-associated protein Kinase) and mDia1, creates traction forces that promote the forward movement of the cell (Parsons, Horwitz et al. 2010). Maturation of the FAs involves changes in their protein composition, for example zyxin is recruited, paxillin becomes phosphorylated and this transition happens when the leading edge stops advancing (Zaidel-Bar, Ballestrem et al. 2003, Ballestrem, Erez et al. 2006). For the polarized forward movement of the cell, FA disassembly at the cell rear is required. Cell polarization requires polarized myosin activation inside the cell that determines the cell rear (Vicente-Manzanares, Newell-Litwa et al. 2011). FA disassembly happens in two populations of adhesions, at the rear and at the front of the cell and are regulated by different mechanisms. At the cell front, FA turnover is due to actin de-polymerization and reorganization. At the trailing edge of the cell, FA disassembly is accompanied with retraction and "sliding" of the FAs as the cell moves inwards. This process mainly depends on Rho kinase and myosin II activity (Parsons, Horwitz et al. 2010). Other mechanisms controlling FA turnover is through FAK signaling and proteolytic cleavage of several FA proteins, such as FAK, paxillin and talin by the protease calpain (Ilic, Furuta et al. 1995, Franco, Rodgers et al. 2004, Chan, Bennin et al. 2010, Cortesio, Boateng et al. 2011, Bate, Gingras et al. 2012). Moreover, FA disassembly is also regulated by dynamin 2-dependent

integrin endocytosis through microtubule targeting of the FAs, a process independent of RhoA activity (Ezratty, Partridge et al. 2005) and through caveolin-1 dependent lipid raft endocytosis of the rear FAs, a process based on Rac1 activity (Nethe and Hordijk 2011). The last type of adhesion complex is fibrillar adhesions (FBs), which are elongated, have long residence time, are located in the center of the cell and they are formed along the matrix fibrils (**Figure 3**). These adhesions are involved in the assembly and reorganization of the FN matrix, a component of the ECM (Parsons, Horwitz et al. 2010, Geiger and Yamada 2011). FBs are enriched in tensin, parvins and FN but are devoid of any enzymatic activity and as a result there is no tyrosine phosphorylation detected on them (Dubash, Menold et al. 2009). During their formation the α5β1 integrin receptor is translocated form the FAs towards the cell center by transforming the sustained actomyosin-generated tension of the FAs into directed movement along the actin filaments (Pankov, Cukierman et al. 2000).

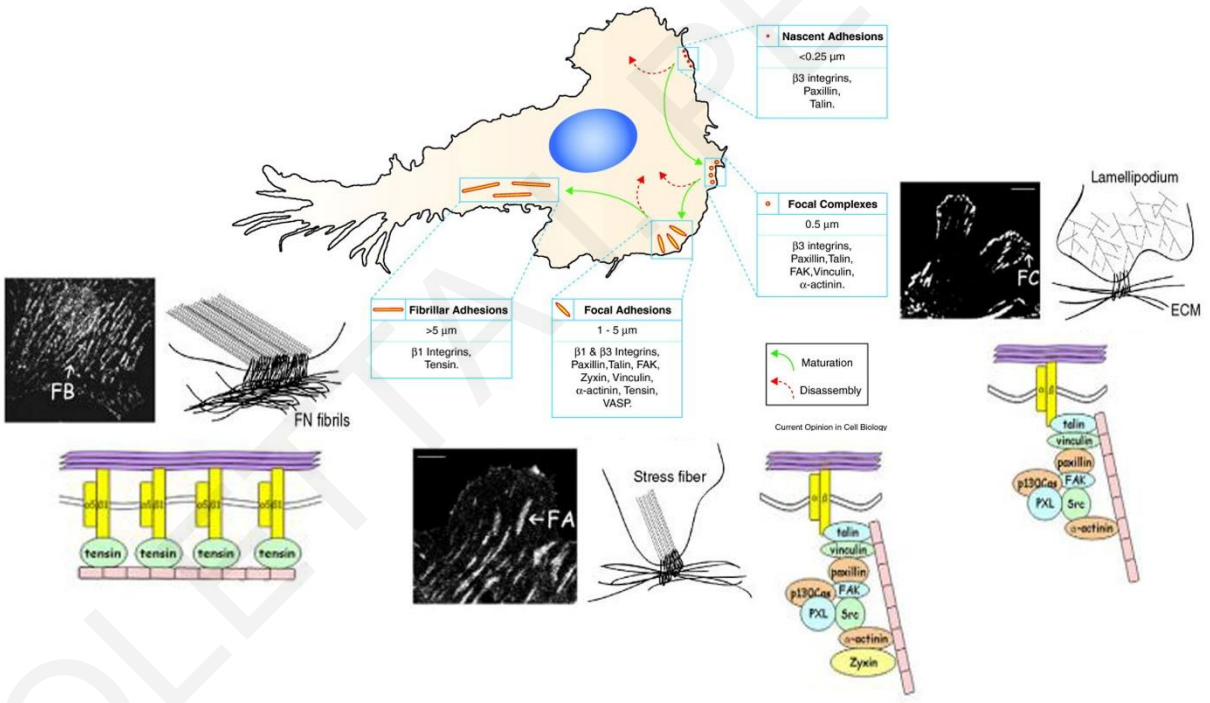

Figure 3: Types of cell adhesions.

The nascent adhesions are the first type of cell adhesion formed at the leading edge and they are enriched in paxillin and talin. They can turnover or mature into FCs. FCs are larger with a dot-like shape and are composed of almost all the main FA proteins. The transition from the nascent adhesions to the FCs is promoted by the recruitment of vinculin at the adhesion complex through its binding on talin. FCs mature further into elongated and larger structures called FAs. FA formation is accompanied with the reorganization of the actin cytoskeleton into stress fibers, where actomyosin contraction takes place that promotes the forward movement of the cell. FAs mature further into FBs that are located at the cell center and are responsible for the formation and remodeling of the FN matrix. Adapted from (Parsons, Horwitz et al. 2010).

1.3. Proteins of the integrin adhesome; structure, activation mechanisms and roles in embryonic development

Defects in the structure, composition or dynamic nature of the adhesome are associated with aberrant cell migration, proliferation, survival and differentiation, processes that are fundamental during embryonic development. Disruption of the genes of most of the core proteins of the adhesome in mice, result in embryonic lethal phenotypes highlighting the importance of cell-ECM adhesion during embryogenesis (Wiesner, Legate et al. 2005). Below there is an overview of the major adhesome proteins that their role in cell-ECM adhesion is crucial in tissue morphogenesis.

1.3.1. Integrins

Integrins are large class I transmembrane, heterodimeric proteins consisting of non-covalently linked α and β subunits. They belong in the glycoprotein receptor family, where most of the receptor dimer is extracellular (globular head) and it contains binding sites for ECM ligands. Both units traverse the plasma membrane and form the cytoplasmic units (tails). The cytoplasmic tails are usually unstructured but all subunits have a single membrane-spanning helix. There are 18 α and 8 β integrin subunits that can associate to each other and form 24 distinct integrin α-β heterodimers. Although integrins were initially believed to be restricted to metazoans, there is evidence that homologous sequences of the domains of the α-β subunits are found in prokaryotes (Johnson, Lu et al. 2009). Each integrin displays a unique expression pattern and ECM binding specificity resulting in differential bidirectional signal transduction (Hynes 2002). Thus, the 24 different receptors can be separated into several groups according to their extracellular ligands (**Figure 4**). For example, integrins α5β1, αvβ3, α4β1 bind to FN, integrins α1β1, α6β1 recognize collagen and integrins α2β1, α3β1, α6β1 bind to laminin (Huttenlocher and Horwitz 2011).

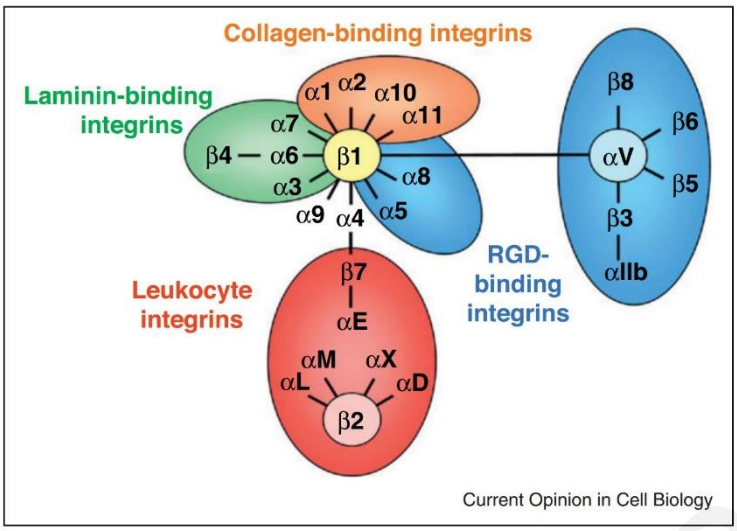

Figure 4: Schematic representation of the mammalian integrins and their ligands.
Classification of integrin according to their ligand binding specificity. Each line represents an integrin heterodimer. Adapted from (Margadant, Monsuur et al. 2011).

There are three regions in the integrin heterodimer that recognize acidic motifs of the proteins of the ECM, the EGF-hand-like motifs in the amino-terminal domain of the α subunit, a region near the amino-terminus of the β subunit and the A-domain (Humphries 1996). Moreover, all integrin-ligand interactions depend on the presence of the bivalent cations Mg^{++}, Ca^{++} and Mn^{++} (Campbell and Humphries 2011). The main classification groups of integrins based on their specificity for the ECM ligands are the following:

- RGD-binding integrins:

This group consists of all five αV integrins, β1 integrins (α3, α5) and αIIbβ3 that bind to ligands containing the RGD domain (Arg-Gly-Asp) (Campbell and Humphries 2011). The RGD binding is identical between the different integrins, in the interface between the two subunits. The basic residue (Arg) fits in a β-propeller in the α subunit and the acidic residue (Asp) interacts with the cation bound in the β-I-domain (Takagi 2004, Xiao, Takagi et al. 2004). This family includes many ECM and soluble vascular ligands. The most known ligand of this group is FN but there are also other members such as VN, fibrinogen, prothrombin, and thrombospondin (Plow, Haas et al. 2000).

- LDV-binding integrins:

The members of this group recognize the acidic motif LDV and include the integrins α4β1, α9β1, α4β7, αEβ7 and all members of β2 subfamily. The consensus sequence of the LDV motif is L/I-D/E-V/S/T-P/S. Such ligands are FN, VCAM-1 (Vascular Cell Adhesion Molecule 1)

and MAdCAM-1 (Mucosal Addressin Cell Adhesion Molecule-1). The binding of the LDV-containing ligands is believed to be very similar with that in the RGD-containing ligands (Humphries, Byron et al. 2006).

- A-domain β1 integrins:

Integrins containing the α-I-domain (α1, α2, α10, α11) and β1, bind to a collagenous CFOGER motif to interact with laminin and collagen (Campbell and Humphries 2011{Emsley, 2000 #355)}. This specific binding is crucial for proper embryonic development, tissue maintenance and repair, hemostasis and host defense (Harburger and Calderwood 2009).

- Non-αA-domain-containing laminin-binding integrins:

This family contains only highly selective laminin receptors (three β1-integrins – α3, α6, α7, and α6β4 integrin) (Plow, Haas et al. 2000, Humphries, Byron et al. 2006).

Some other known ligands that are not classified to the above groups are E-cadherin, fibrillin, VEGF-C (Vascular Endothelial Growth Factor), VEGF-D, heparin, ADAM family (A Disintegrin And Metalloproteinase) and ICAM-4 (InterCellular Adhesion Molecule) (Plow, Haas et al. 2000, Humphries, Byron et al. 2006).

The formation of the adhesome is based on integrin activation, which can be induced either by "inside-out" signaling (cytoplasmic events), or by "outside-in" signaling (extracellular ligand binding) that cause structural changes to the integrin heterodimer from an inactive bent state to an active open state (Margadant, Monsuur et al. 2011). Conformational changes involve interactions between the head and the legs. The head is comprised by the extracellular part of the α subunit, a seven bladed-propeller, and of the β subunit (βI domain). The α subunit leg consists of the Ig-like thigh domain and two calf domains, and the β subunit leg includes the hybrid domain (immunoglobin fold), the pleckstrin/semaphoring/integrin domain, four EGF-like repeats and the proximal β tail domain (cystatin-like fold) (Xiong, Stehle et al. 2001, Liddington 2014) (**Figure 5**). Integrin conformations exist in a dynamic equilibrium depending on the level of affinity for ECM ligands (low, intermediate, high). Studies using monoclonal antibodies showed that in the inactive conformation, there are bonds between the tails, legs and head that keep the heterodimer in a bent conformation, facing the plasma membrane, displaying low affinity for ligand and preventing the cytoplasmic tails from interacting with cytoplasmic proteins. Structural data revealed an intermediate "primed" state, in which the heterodimer acquires an extended head conformation but the ligand affinity is low. In the active open state, the cytoplasmic tails separate, the hybrid domain separates from the βI domain and the propeller leading to conformational changes so as the integrin heterodimer acquires high affinity binding

sites for the head and the tails and becomes fully activated (Luo and Springer 2006, Liddington 2014) (**Figure 5**).

Moreover, FRET studies in adherent cells confirmed the above model. By using integrin mutants and monoclonal antibody reporters, Askari and coworkers imaged integrin α5β1 conformation. When preventing the dissociation of the two cytoplasmic units, the integrin heterodimer adopted a bent inactive conformation at the FAs and was unable to mediate cell spreading (Askari, Tynan et al. 2010).

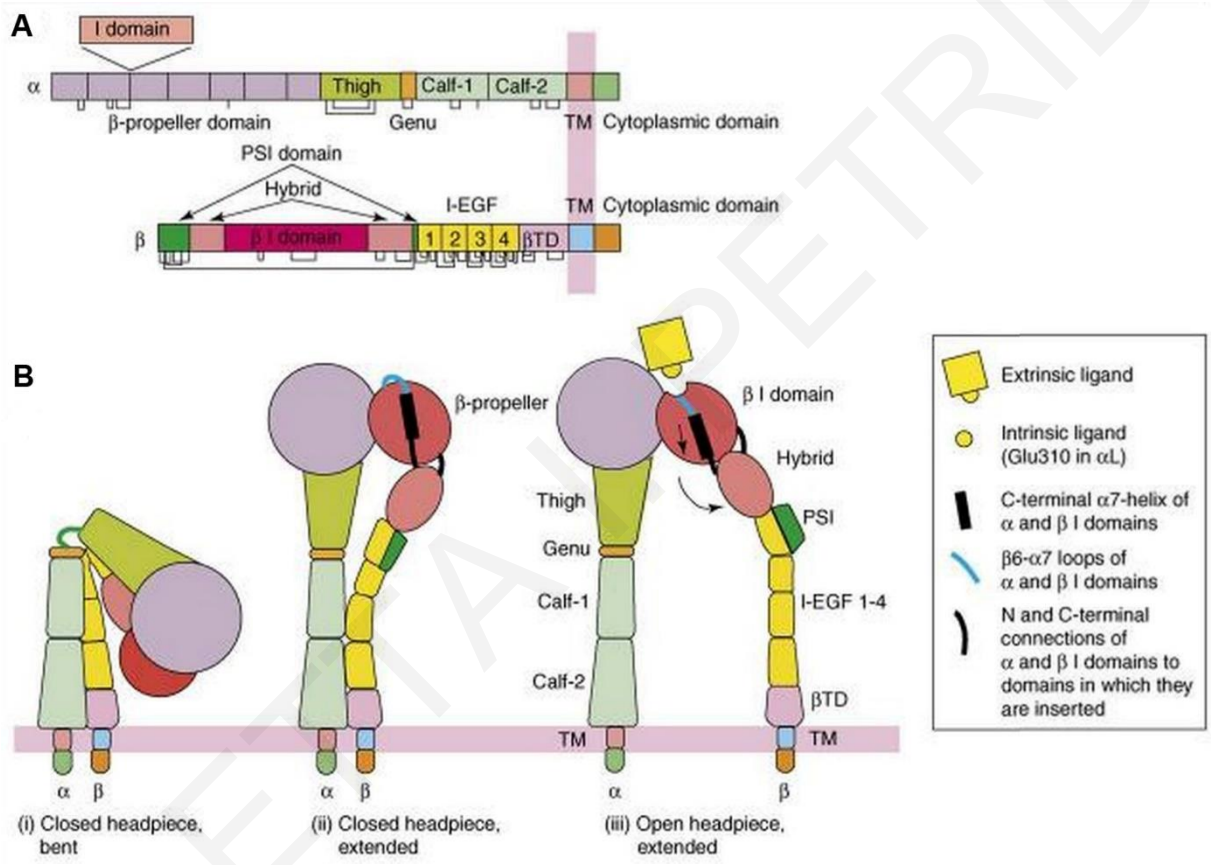

Figure 5: Integrin activation and conformational changes.
Schematic representation of the integrin architecture in the primary structure (A) and conformational changes between the three states of the heterodimer (B). Adapted from (Luo and Springer 2006).

In the high affinity state, two NPxY motifs on the cytoplasmic tail of the β subunit are exposed, which are the binding sites of talin and kindlin (Valdembri and Serini 2012). The binding of talin to the first membrane proximal NPxY motif has a key role in integrin activation, since it disrupts the inhibitory interactions between the membrane proximal regions of α and β tails (Tadokoro, Shattil et al. 2003, Wegener, Partridge et al. 2007). Kindlin binding to the second membrane distal NPxY motif of the β subunit is necessary for integrin activation since

inhibition of kindlin binding blocks this process and it seems that kindlins have a synergistic role with talin for integrin activation (Kloeker, Major et al. 2004, Montanez, Ussar et al. 2008, Goult, Bouaouina et al. 2009). The recruitment of these proteins is concomitant with integrin clustering which occurs in several phases of the maturation of the adhesome, mainly through homo-oligomerization and lateral diffusion (Wiseman, Brown et al. 2004, Li, Metcalf et al. 2005). Integrin clustering is associated with the formation of the multiprotein signaling complex which is responsible for downstream signal transduction since integrins lack enzymatic activity (Campbell and Humphries 2011).

The importance of integrins during embryonic development is highlighted by the integrin gene knockout phenotypes of transgenic mice. There are knockout mice for almost every subunit and most of them have severe developmental defects with some leading to embryonic lethality (Hynes 2002). Integrin β1 homozygous null mice display peri-implantation lethality by E6.5. Generation of chimeric mice using β1 integrin deficient embryonic stem cells, showed that E8.5 embryos exhibit abnormal morphogenesis with gastrulation and neurulation failure (Fassler and Meyer 1995). Another study supports the above findings and also suggests that β1 integrins are required for normal morphogenesis of the inner cell mass of the blastocysts. Inner cell mass outgrowths from integrin β1 null blastocysts showed abnormal morphogenesis and migration of the extraembryonic mesoderm (Stephens, Sutherland et al. 1995). Conditional knockout of integrin β1 in mouse neural crest precursor cells resulted in severe neuronal defects that led to lethality one month after birth. Disruption of integrin β1 caused defective migration of the neural crest derivatives, such as Schwann cells, along the axons, abnormal maturation of the Schwann cells in neuromascular synaptogenesis and defective axon segregation (Pietri, Eder et al. 2004). Embryonic lethality is also caused by the deletion of the integrin β8 gene. Integrin β8 null embryos die by E11.5 due to defective vascular development at the placenta, the yolk sac and at the nervous system and display extensive intracerebral hemorrhage (Zhu, Motejlek et al. 2002). Finally, integrin α5 null mice show embryonic lethality by day E10-11 accompanied by severe mesodermal defects such as shortening of the posterior trunk and vascular and extraembryonic defects (Yang, Rayburn et al. 1993).

1.3.2. Talin

Talin is one of the most important players in regulating adhesion dynamics because it controls integrin activation and it can link integrins with the actin cytoskeleton directly. Talin is a 270KDa F-actin binding homodimeric protein that was identified as a cytoplasmic integrin ligand (Horwitz, Duggan et al. 1986) and is one of the first proteins recruited at the adhesome.

Talin interacts through its N-terminal globular head with the conserved membrane proximal NPxY motif in β integrin tails (Garcia-Alvarez, de Pereda et al. 2003) (**Figure 6**). Talin head contains a characteristic FERM domain (Four-point-one, Ezrin, Radixin, Moesin) with basic amino acids that also interacts with the negatively charged PIP_2 (phosphatidylinositol-4,5-biphosphate), PIPKIγ (phosphatidylinositol-4-phosphate 5-kinase type 1γ), and with FAK (Martel, Racaud-Sultan et al. 2001, Di Paolo, Pellegrini et al. 2002, Chen and Chen 2006) (**Figure 6**). Through its elongated rod-shaped C-terminal domain, talin interacts with vinculin and actin (Hemmings, Rees et al. 1996, Bass, Patel et al. 2002) (**Figure 6**). Its autoinhibited head-tail conformation can be released by regulated proteolysis or by binding to PIP_2, or through Src signaling (Goksoy, Ma et al. 2008). Talin can induce conformational changes in integrin cytosolic tails, which are transmitted through the plasma membrane in order to increase the affinity of the head domain of integrins for ECM ligand binding (Critchley 2009). Cells deficient for talin 1 and 2 display defective FA assembly, FAK mediated signaling and traction force generation (Zhang, Jiang et al. 2008).

Talin deficient mice exhibit embryonic lethality by E8.5-9.5 due to failure of cell migration during gastrulation. Although these embryos develop normally until implantation, at gastrulation stage the mesoderm fails to migrate from the posterior side of the embryo to the extraembryonic regions and as a result the extraembryonic tissues are disorganized leading to lethality (Monkley, Zhou et al. 2000).

1.3.3. Vinculin

Vinculin is a 116KDa, actin-binding protein. It is composed of a globular head domain, short proline-rich sequences and a tail domain. In its autoinhibited conformation, the tail binds the head masking the binding sites for its partners. Vinculin head domain binds to talin, whereas the tail binds to F-actin, paxillin, PIP_2 and the Arp2/3 complex (Peng, Nelson et al. 2011) (**Figure 6**). Although vinculin does not bind directly to β integrin tails, is important for integrin mediated cell adhesion by stabilizing the FAs during cell migration (Ziegler, Liddington et al. 2006). Vinculin is recruited at nascent adhesions through its binding on the talin molecule and this interaction is accompanied by the maturation of the nascent adhesions into FCs (Zaidel-Bar, Ballestrem et al. 2003). Vinculin regulates integrin function by recruiting PIPKIγ leading to increased local PIP_2 production that bind talin, resulting in high affinity of talin for integrins. Moreover, these events activate vinculin leading to the stabilization of the initial integrin clustering, since it crosslinks actin with the nascent FC (Wiesner, Legate et al. 2005). Vinculin null cells display reduced adhesion to several substrates such as FN, VN, collagen and laminin,

smaller and decreased number of FAs which turnover rapidly, leading to increased locomotion and increased integrin-stimulated migration (Coll, Ben-Ze'ev et al. 1995, Xu, Baribault et al. 1998, Saunders, Holt et al. 2006). Thus, vinculin is believed to regulate cell-ECM adhesions by stabilizing the adhesion complexes and enhancing integrin clustering (Carisey and Ballestrem 2011).

Vinculin null embryos die between E8 to E10 days of gestation. They are small, exhibit cranial neural tube defects, diminished ventricles and somites and abnormal heart development (Xu, Baribault et al. 1998).

1.3.4. Paxillin

Paxillin is a 68KDa modular adaptor protein (Deakin and Turner 2008). Paxillin contains in its N-terminus five LD (Leucine and Aspartate rich – consensus sequence LDXLLXXL) repeats of 13 amino acids each and in its C-terminus 4 LIM (Lin11, Isl-1, Mec-3) domains, both mediating several protein-protein interactions (Wiesner, Legate et al. 2005). Paxillin interacts through its N-terminal with the actin-associated protein vinculin and FAK and through its C-terminal with tubulin and PTP-PEST (Deakin and Turner 2008) (**Figure 6**). Moreover, paxillin can bind directly the α4 integrin cytoplasmic tail and β1 integrin peptides (Schaller, Otey et al. 1995, Liu, Thomas et al. 1999). Paxillin contains multiple sites that are subjected to phosphorylation by tyrosine kinases (FAK/Src complex) and serine/threonine kinases (p-21 activated kinase -PAK- , Cyclin-dependent-like kinase 5 -Cdk5-), that act as scaffolds to generate binding sites for other proteins of the adhesome (Wiesner, Legate et al. 2005). Paxillin regulates the dynamic plasticity of the integrin adhesome by controlling the spatiotemporal activation of the Rho GTPases that regulate actin dynamics during cell migration (Deakin and Turner 2008). Paxillin null cells display defective cell spreading on FN and laminin, reduced tyrosine phosphorylation of FAK, reduced locomotion and aberrant cortical cytoskeleton (Hagel, George et al. 2002, Wade, Bohl et al. 2002). Loss of paxillin is also associated with reduced FA disassembly rates (Webb, Donais et al. 2004).

Paxillin knockout mice show embryonic lethality at E9.5 with severe developmental abnormalities in mesodermal derived tissues such as the somites and the heart concomitant with shortening of the anterior-posterior (A-P) axis (Hagel, George et al. 2002).

1.3.5. p130Cas

Cas (Crk-associated substrate, p130Cas) is a scaffolding protein member of the adhesome, originally discovered as a tyrosine phosphorylated protein in cells transformed with the v-Crk and v-Src oncogenes (Reynolds, Kanner et al. 1989, Matsuda, Mayer et al. 1990). Cas consists of an N-terminal SH3 domain (Src homology domain 3) that interacts with FAK (**Figure 6**), PTP-PEST and Pyk2 (Protein Tyrosine Kinase 2), a substrate domain (SD) which contains 15 tyrosine residues that become phosphorylated by Src (**Figure 6**) and serve as binding sites for Crk and Nck, a Src Binding Domain (SBD) near the C-terminus and a conserved C-terminal Cas-family homology domain that contains binding sites for Cas and PI3K (Defilippi, Di Stefano et al. 2006). Cas null cells display defective cell spreading, disorganized actin stress fibers and abnormal actin bundling (Honda, Nakamoto et al. 1999). Cas when phosphorylated, recruits Crk and Nck and regulates cell migration through protrusion of the leading edge plasma membrane, and also enhances the rates of FA assembly and disassembly (Klemke, Leng et al. 1998, Rivera, Antoku et al. 2006, Meenderink, Ryzhova et al. 2010). In addition, Cas null cells display reduced FA disassembly rates, when compared to control cells (Webb, Donais et al. 2004).

The Cas mouse knockout is embryonic lethal at E12.5 with defects mainly in the heart and blood vessels (Honda, Nakamoto et al. 1999).

1.3.6. FAK

FAK is a 125KDa non-receptor tyrosine kinase that is recruited to FAs, shown to be activated by integrin signaling and to act as a phosphorylation regulated signaling scaffold to control adhesion turnover, cell migration, activation of Rho family GTPase and crosstalk between integrins and growth factor signaling (Mitra, Hanson et al. 2005). Upon integrin mediated adhesion, FAK becomes tyrosine phosphorylated and subsequently activated (Zachary 1997). Signaling molecules, like c-Src and PI3K, are recruited into complexes with FAK (**Figure 6**), leading to the transduction of integrin signaling (Parsons and Parsons 1997, Reiske, Kao et al. 1999). The protein is composed of three main domains, the N-terminal FERM domain, the central catalytic kinase domain and the C-terminal focal adhesion targeting (FAT) domain. The FERM domain of FAK was found to bind peptides of the β1 integrin cytoplasmic tail, PIP_2 and GFRs (Growth Factor Receptors) (Schaller, Otey et al. 1995, Sieg, Hauck et al. 2000, Chen and Chen 2006, Cai, Lietha et al. 2008). The C-terminus contains the FAT domain, a four-helix bundle shown to be both necessary and sufficient for FA targeting (Hildebrand, Schaller et al.

1993, Hayashi, Vuori et al. 2002). In addition, the C-terminus contains binding sites for the integrin ligands talin and paxillin (Chen, Appeddu et al. 1995, Hildebrand, Schaller et al. 1995) (**Figure 6**). Upon integrin activation, FAK becomes autophosphorylated on Tyr397 (Eide, Turck et al. 1995), creating a high affinity binding site for Src family kinases which further phosphorylate FAK on several residues creating more binding sites for other scaffolding and signaling proteins such as Cas and RhoGAP GRAF (GTPase regulator associated with FAK). The FAK/Src complex binds to and activates several proteins that regulate the dynamics of the actin cytoskeleton (Hall, Fu et al. 2011). FAK deficient fibroblasts display impaired integrin dependent cell migration, defects in cell spreading, increased number and size of FAs suggesting a role of FAK in FA turnover (Ilic, Furuta et al. 1995).

FAK null mice display early embryonic lethality by E8.5 due to generalized mesodermal defects especially in the axial mesodermal tissues and the cardiovascular system (Furuta, Ilic et al. 1995).

1.3.7. c-Src

c-Src is a non-receptor tyrosine kinase and is a member of the Src family kinases (SYFs). It is composed of a myristoylated N-terminus, SH3, SH2, a linker segment, and tyrosine kinase domain which contains its autophosphorylation site and a short tail at the C-terminus (Parsons and Parsons 2004). Src binds phosphorylated FAK on Tyr397 through its SH2 domain leading to phosphorylation of FAK/Src downstream targets such as Cas and paxillin (**Figure 6**). Src null fibroblasts exhibit reduced adhesion and spreading on FN (Kaplan, Swedlow et al. 1995). Moreover, the adhesomes appear abnormal in Src null cells including reduced phosphotyrosine levels and increased size and density of the FBs (Volberg, Romer et al. 2001). In addition, SYF-/- cells show a 19-fold reduction of FA disassembly rates compared to WT cells. In agreement, disruption of the kinase activity of Src also resulted in similar results highlighting the importance of Src signaling in cell migration (Webb, Donais et al. 2004).

However, the phenotype of c-Src null mice is quite different from those caused by deletion of the genes of the adhesome proteins, where the main defect is osteoporosis (Soriano, Montgomery et al. 1991) probably attributed however, to compensatory roles of the other protein members of the SYF family.

1.3.8. Fibronectin

Fibronectin (FN) is a major component of the ECM but it can be considered as a member of the adhesome since it is the major ligand of cells in culture. FN is a high molecular weight glycoprotein and exists either in a soluble form in the blood or in an insoluble form in the ECM, secreted usually by fibroblasts (Pankov and Yamada 2002). FN is composed of two nearly identical subunits (250KDa each), covalently linked with disulfide bonds at the C-terminal and each subunit consists of three types of repeats: 12 type I, 2 type II and 15-17 type III. FN interacts with many integrin heterodimers (α3β1, α5β1, αvβ1, αvβ3) mainly through its RGD sequence located in the central cell binding domain (type III 9-10). Moreover, the FN molecule contains binding domains for other proteins of the ECM, such as collagen, fibrin and heparin (Singh, Carraher et al. 2010).

FN null mice phenotype is embryonic lethal by day E8.5 due to failure in development of embryonic and extraembryonic vasculatures. FN null embryos exhibit short A-P axis, lack of somites, deficient head and trunk mesoderm, phenotypes attributed to defective mesodermal migration and adhesion (George, Georges-Labouesse et al. 1993).

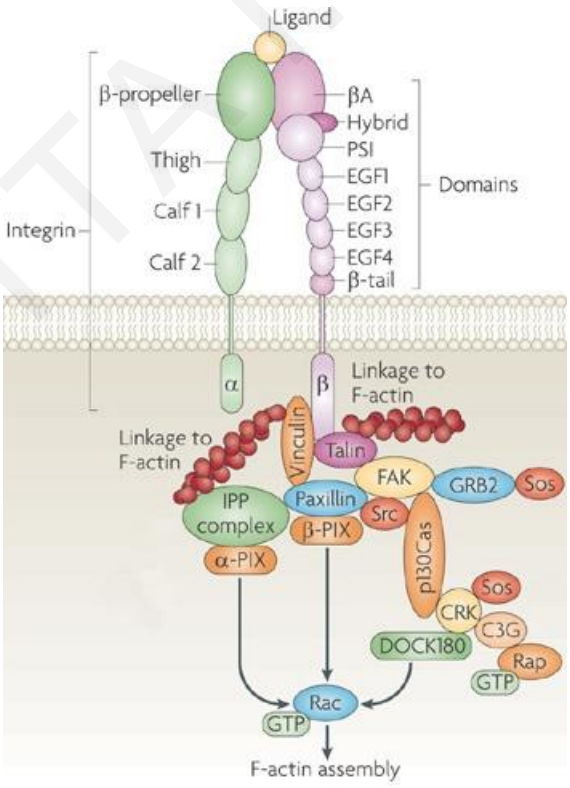

Figure 6: Interactions of the FA proteins within the adhesome.

Schematic representation of the multiple interactions taking place within the adhesome in order to link the ECM with the actin cytoskeleton. Adapted from (Smith and Marshall 2010).

1.4. Mechanotransduction through the adhesome

Cells can sense and respond to both chemical and mechanical signals. The ability of the cells to detect, react and translate mechanical forces into biochemical signals is called mechanotransduction. Cells have developed several sensory elements that convert the mechanochemical signal including ion channels, sensory cilia, cell-cell contacts and the adhesome. Forces can be either generated internally (from the cytoskeleton) or applied externally (from the physical environment) (Vogel 2006, Tilghman and Parsons 2008). Thus, each component of the mechanical link between the ECM, integrins and the contractile actin cytoskeleton are prime candidates of mechanotransduction in adherent cells (Schwartz 2010).

Tension is generated on a physical object when a pulling force is applied at the one side and an opposite pulling or a resisting force is applied on the other side. Similarly, at the adhesion site, contraction of the actin cytoskeleton generates force and the adhesome resists the contraction, and vice versa, i.e. ECM rigidity generates forces that are anticipated by the cytoskeleton network (Tilghman and Parsons 2008) (**Figure 7**). Internal forces are generated through signaling pathways that lead to activation and phosphorylation of the myosin light chain (MLC), which subsequently increases the affinity of myosin for actin resulting in increased contractility of the actomyosin complex (**Figure 7**). This pathway usually acts in parallel to the Rho-GTPase activation pathway, in which ROCK becomes activated and inhibits (through phosphorylation) the myosin phosphatase, thus enhancing MLC phosphorylation and actin contractility (Jaalouk and Lammerding 2009).

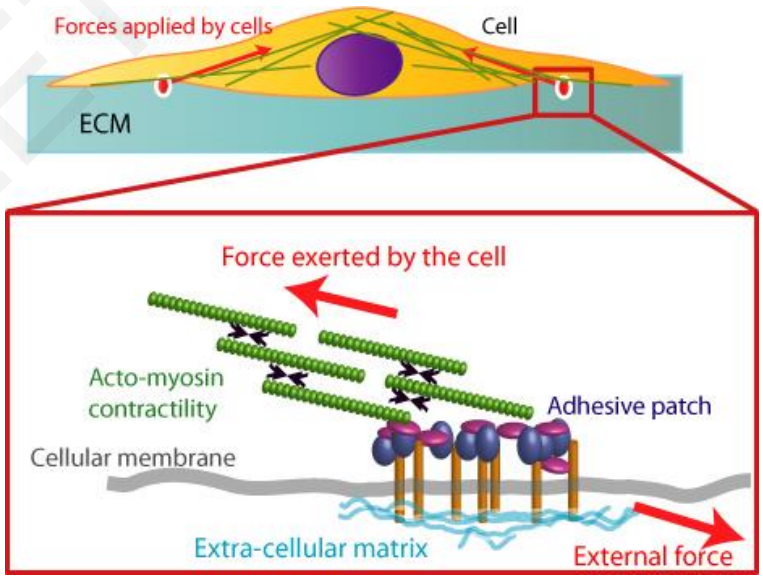

Figure 7: Equilibrium of internal and external forces sensed at the adhesion site.

Schematic illustration of how tension is generated at FAs. Adapted from (Ladoux and Nicolas 2012).

It is now well established that adhesions strengthen in response to force (Schwartz and DeSimone 2008) (**Figure 8**). The first evidence that the members of the adhesome are mechanosensory molecules, came from studies showing that cells seeded on rigid substrates form stronger adhesions when compared to cells seeded on soft substrates (Choquet, Felsenfeld et al. 1997, Pelham and Wang 1997). Moreover, cell stretching was shown to cause growing and maturation of the FAs. Specifically, application of mechanical force on small dot-like, vinculin-containing adhesions using a micropipette resulted in local assembly and elongation of the adhesion (Riveline, Zamir et al. 2001). In agreement, treatment of cells with contractility inhibitors decreased force on adhesions resulting in FA disassembly (Balaban, Schwarz et al. 2001, Chen, Alonso et al. 2003).

Specific roles in mechanotransduction have been identified for almost all the core protein members of the adhesome. Concerning integrins, initial studies showed that force application on integrins either internally (beads coated with a FN variant that does not support FA formation) or externally (laser tweezers), can strengthen the adhesion site leading to its maturation (Galbraith, Yamada et al. 2002). Molecular dynamics simulations suggested that the β subunit is able to change conformation from inactive to active state through mechanical force (Puklin-Faucher, Gao et al. 2006). Application of biaxial stretch in NIH3T3 cells seeded on an elastic membrane coated with FN, led to conformational activation of the αvβ3 heterodimer. This activation depends on PI3K and leads to increased affinity for ligand binding (Katsumi, Naoe et al. 2005). Moreover, it was shown that force application on the α5β1 heterodimer strengthens the bond between α5β1 and FN by triggering the integrin switch from the relaxed to the tensioned state (Friedland, Lee et al. 2009). The strengthening of ligand binding upon force application results in the formation of catch bonds which stabilize the heterodimer in the high affinity state. Atomic force microscopy revealed that force affects the lifetime of the catch bond (Kong, Garcia et al. 2009) and in agreement with this observation, cyclic forces applied on the α5β1-FN bond were shown to reinforce the bond by increasing its lifetime (Kong, Li et al. 2013). In a recent paper, Ferraris and coworkers have shown that integrin β1 can become activated independently of ligand binding in response to membrane tension. In this study, the authors generated an artificial system in which cells adhered on VN independently of integrins, relying instead on uPAR-mediated adhesion. Under these conditions there was integrin β1 signaling downstream of conformational changes of the receptor but in the absence of ligand engagement. This signaling requires force generation at the cell-ECM interface and atomic force microscopy revealed that it is derived by membrane tension (Ferraris, Schulte et al. 2014).

Most of the members of the cytosolic complex of the adhesome also respond to mechanical forces. Force has been shown to expose cryptic sites in several proteins including paxillin, FAK and Cas by stretching Triton-X cytoskeletons. In this system cells lack a surrounding membrane, thus the remaining cytoskeleton can react with cytoplasmic cell extracts without being affected by changes in the ionic environment. Biaxial stretch of the cytoskeleton revealed that the above proteins bind preferentially to stretched triton cytoskeletons, suggesting that matrix forces are transduced through force dependent conformational changes of the members of the adhesome and the cytoskeleton (Sawada and Sheetz 2002). Another well characterized response to mechanical forces that involves exposure of cryptic binding sites is the binding of vinculin on talin. As mentioned above, it was initially observed that the binding of vinculin on talin occurs during the maturation of the nascent FAs into FCs. The Vinculin Binding Sites (VBS) on the talin rod are masked in the talin helical bundle (Gingras, Vogel et al. 2006), suggesting that the bundle must rearrange its structure so as the talin molecule unfolds (Papagrigoriou, Gingras et al. 2004). Support comes from molecular dynamics simulations at FAs where it was shown that vinculin recruitment is enhanced by locally applied tensile forces (Lee, Kamm et al. 2007, Hytonen and Vogel 2008). This was later confirmed in a study by the Sheetz group, in which by using molecular tweezers showed that force can stretch single talin rods and expose the cryptic VBS (del Rio, Perez-Jimenez et al. 2009) (**Figure 8**). Moreover, a role of vinculin in mechanotransduction is highlighted by the fact that vinculin null cells do not respond by reducing their adhesive forces after inhibition of contractility (Dumbauld, Shin et al. 2010). The same holds true for FAK null cells which in addition with the above phenotype, they also do not respond to changes in contractility by affecting FA assembly (Dumbauld, Shin et al. 2010). Moreover, FAK shows increased tyrosine phosphorylation upon LPA (lysophosphatidic acid) induced increased contractility and upon cell stretching (Seufferlein and Rozengurt 1994, Hamasaki, Mimura et al. 1995) (**Figure 8**). A more prominent role of FAK in mechanotransduction was suggested when studying cell migration of flexible polyacrylamide substrates. Normal cells tend to re-orient their movement upon local application of force and also sensing the rigidity of the substrate and migrate from soft to rigid substrates (durotaxis). However, FAK null cells fail to respond to changes in substrate stiffness consistently exhibiting lower traction forces (Wang, Dembo et al. 2001). Another member of the adhesome shown to respond to increased contractility by increased phosphorylation is Cas (Seufferlein and Rozengurt 1994) (**Figure 8**). Direct evidence for its implication in mechanotransduction came from a study in which the SD of Cas was mechanically stretched in an *in vitro* protein stretch assay. The authors showed that stretching exposed the 15 tyrosine residues of the SD enhancing their phosphorylation by Src and resulting in Rap1 activation.

Moreover, *in vivo* mechanical extension of Cas was correlated with regions under higher tensile force (Sawada, Tamada et al. 2006). Zyxin, a mature FA protein was also implicated in mechanotransduction. Although in normal cells, uniaxial stretching of cells leads to actin polymerization, loss of zyxin function decreased the force induced actin polymerization (Hirata, Tatsumi et al. 2008). Moreover, uniaxial stretch of fibroblasts increased Src kinase activity leading to increased phosphorylation of Cas, FAK and paxillin (Sai, Naruse et al. 1999) (**Figure 8**). In agreement, Src was shown to change its conformation upon tension (Na, Collin et al. 2008). Lastly, force was shown to influence FN fibrillogenesis. *In vitro* single molecule force spectroscopy showed that the type III repeats domains can be unfolded in an hierarchic fashion according to the force magnitude applied on the molecule (Oberhauser, Badilla-Fernandez et al. 2002). Moreover, molecular dynamics simulations revealed conformational changes at the cell binding site of the FN molecule above a force threshold and that a stepwise unfolding process exposes the RGD sequence (Krammer, Lu et al. 1999, Gee, Ingber et al. 2008).

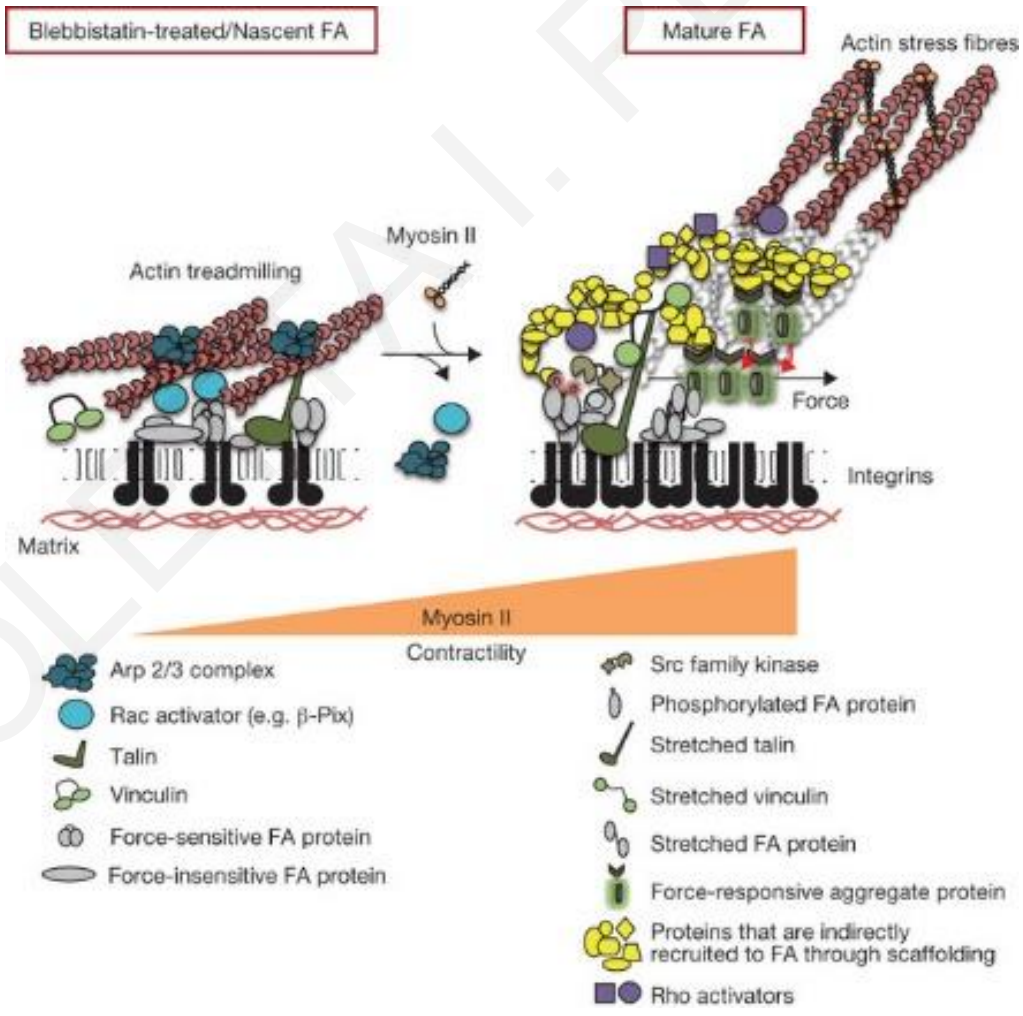

Figure 8: Changes in the composition of the adhesion complexes in response to force.

Schematic representation of the maturation of the adhesion site in response to mechanical forces (either internal from actomyosin contractility or external from the substrate). Tension leads to maturation of the adhesion site from nascent FAs to FCs. This process is accompanied with changes in the conformation of the protein members of the adhesome leading to changes in its composition. Some examples illustrated include integrin clustering, the extension of the talin molecule and the binding of vinculin, the increased kinase activity of Src, the increased phosphorylation of several proteins (such as FAK, paxillin, Cas) and the increased contractility caused by the assembly of the actomyosin complex. Adapted from (Gallegos, Ng et al. 2011).

1.5. Focal adhesion kinase: Structure, interactions and function

FAK was originally discovered as a FA associated protein which is highly tyrosine phosphorylated upon expression of the Rous sarcoma virus encoded oncoprotein, pp60v-src (Hanks, Calalb et al. 1992, Schaller, Borgman et al. 1992). FAK is generally expressed in most tissues (Schaller 2010) and specifically is highly expressed during embryonic development and then its expression drops but remains in adult non-neuronal tissues (Burgaya, Menegon et al. 1995). Moreover, FAK displays increased expression and altered phosphorylation in many tumors, correlated with poor prognosis (McLean, Carragher et al. 2005), and as a result is considered a therapeutic target. FAK together with Pyk2 are the sole members of the FAK family of non-receptor protein tyrosine kinases and they display 46% identity and 65% similarity at the protein level. Although loss of FAK is accompanied by embryonic lethality, Pyk2 is not an essential gene and displays more restricted expression pattern compared to FAK (Schaller 2010). However, in some functional aspects these two proteins display compensatory roles (Hall, Fu et al. 2011). FAK is evolutionary conserved in mammalian species and in lower eukaryotic organisms (Parsons 2003). Its sequence is highly conserved across species (human compared to mouse: 97% identity, frog: 90% identity, *Zebrafish*: 79% identity) (Schaller 2010). Although FAK is a well established kinase, it displays both scaffolding and signaling roles and thus it exhibits a variety of kinase dependent and independent functions, highlighting the complexity and diversity of the processes that it is involved.

1.5.1. Domain Structure

As mentioned above, FAK is composed of three structurally distinct domains, an N-terminal FERM domain, a central catalytic kinase domain and a C-terminal FAT domain. Although none of the main three domains is unique to FAK, all of them display FAK specific modifications that result in its tight regulation of function. The three domains are linked through two flexible

linker regions that contain conserved sequences that promote interactions with other proteins (Arold 2011) (**Figure 9**).

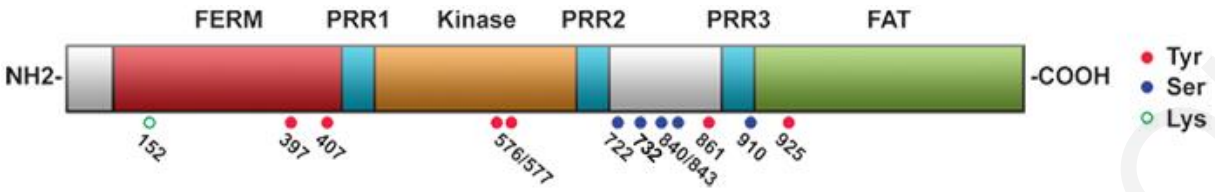

Figure 9: Schematic diagram of the domains and major phosphorylation sites of FAK.
Adapted from http://atlasgeneticsoncology.org/Genes/PTK2ID41898ch8q24.html

- **FERM domain:**

The N-terminus of FAK consists of approximately 300 amino acids (33-362 amino acids, the first 30 amino acids are part of the N-terminus but not part of the FERM domain). The FERM domain is named after its homology with the proteins protein 4.1, ezrin, radixin and moesin. It is trilobed, arranged in a "clover-leaf"-like structure and contains the F1, F2 and F3 subdomains (Ceccarelli, Song et al. 2006). The F1 lobe (33-127 amino acids) has an ubiquitin-like fold and it consists of five stranded β-sheet caped by an α-helix. The F2 lobe (128-253 amino acids) folds like acyl-CoA binding protein (all α-helical) and the F3 lobe (254-352 amino acids) exhibits the pleckstrin homology phosphotyrosine binding domain fold that is a β-sandwich capped by a COOH-terminal α-helix (Pearson, Reczek et al. 2000, Ceccarelli, Song et al. 2006) (**Figure 10**). The F1 lobe contains the first Nuclear Export Signal (NES) and the F2 lobe contains a "basic patch" which acts as a Nuclear Localization Signal (NLS) (Lim, Chen et al. 2008, Ossovskaya, Lim et al. 2008).

The FERM domain of FAK promotes several protein-protein interactions, including its direct binding on the kinase domain of FAK, which inhibits FAK activation. This autoinhibitory interaction plays a key role in regulating FAK's enzymatic activity, a subject that will be described in detail below. Other known binding partners of the FERM domain include GFRs, such as Epidermal GFR (EGFR), Hepatocyte GFR (HGFR), Platelet-Derived GFR (PDGFR), Insulin-like GFR (IGF-IR) and Vascular Endothelial GFR (VEGFR) (Sieg, Hauck et al. 2000, Chen and Chen 2006, Garces, Kurenova et al. 2006, Zheng, Kurenova et al. 2009) (**Figure 13**). The interaction of the FERM domain with HGFR involves residues in the "basic patch" of the F2 lobe, the same sequence that is also involved in the interaction with PIP_2 (Cai, Lietha et al. 2008). These interactions are crucial for the role of FERM in FAK activation and they will be dicussed further below. It was aslo shown that the FERM domain associates with the

cytoplasmic tails of integrin β1 *in vitro* (Schaller, Otey et al. 1995), however, no direct *in vivo* binding has been demonstrated between FAK and integrins and exogenously expressed FERM does not localize to FAs (Lawson, Lim et al. 2012). Althought the FAK FERM domain is not sufficient for FA localization, recent studies have shown that it is important for stabilizing the molecule at FAs (Brami-Cherrier, Gervasi et al. 2014).

The FERM domain is also responsible for regulating FAK function in the nucleus. Besides the fact that the FERM F2 lobe promotes nuclear localization of FAK (Lim, Chen et al. 2008), it was identified that the FERM F1 lobe can bind the N-term transactivation domain of p53 and inhibit p53-induced apoptosis (Golubovskaya, Finch et al. 2005). Moreover, the FERM F3 lobe associates with MDM2 (mouse double minute 2 homolog) so as a FAK/MDM2/p53 complex is formed which promotes the ubiquitination and proteasomal degradation of nuclear p53 (Lim, Chen et al. 2008). Moreover, the FERM domain undergoes sumoylation at the ε-amino position of Lys152 (**Figure 9, Figure 13**) upon interaction with the protein inhibitor of activated STAT1 (Signal Transducer and Activator of Transcription). This modification leads to increased phosphorylation levels of FAK on Tyr397 and it was proposed that its physiological role is to facilitate direct signaling between FAs and the nucleus (Kadare, Toutant et al. 2003).

Finally, the FERM domain interacts with actin associated proteins, influencing in this way the interplay with the actin cytoskeleton. Such examples are N-WASP, Arp2/3 complex and Ezrin, where binding of Ezrin on the FERM domain of FAK increases FAK activation in an integrin independent manner (Poullet, Gautreau et al. 2001). It is believed that the FERM domain acts as a scaffold for the two to create a complex that is present in nascent lamellipodia. Interestingly, this complex seems to form when FAK is in the unphosphorylated form and it dissociates upon activation (Serrels, Serrels et al. 2007).

The above observations suggest that the FERM domain controls the transmission of information between the nucleus and the cell cortex, so that the processes that take place at the cell boundaries (such as directional migration) can communicate with the processes that happen in the nucleus (such as proliferation) (Frame, Patel et al. 2010).

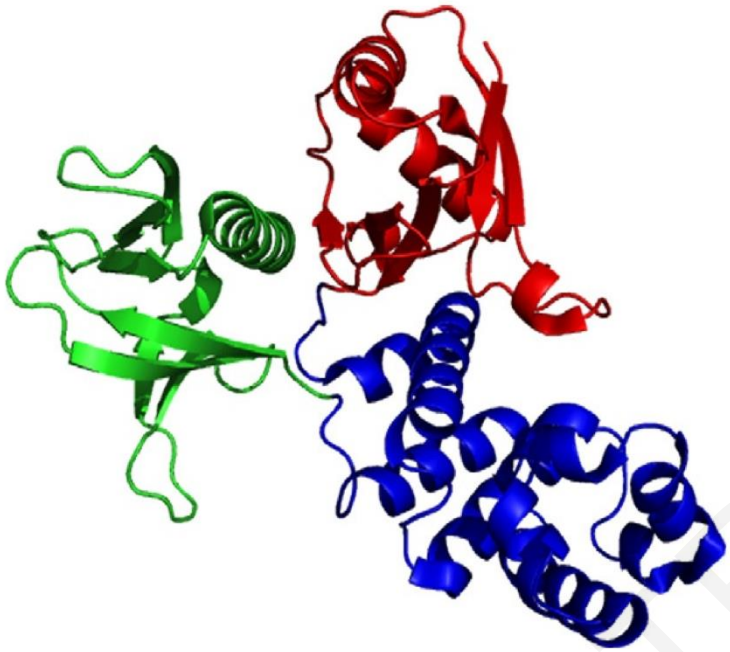

Figure 10: Structure of the FERM domain of FAK.
F1 lobe is shown in red, F2 in blue and F3 in green. Adapted from (Hall, Fu et al. 2011).

- **FERM-Kinase domain linker segment:**

This region of FAK contains the major site of autophosphorylation Tyr397 (Eide, Turck et al. 1995) and the proline-rich region 1 (PR1) (**Figure 9**). Although, it is believed that autophosphorylation is happening mainly *in trans* since kinase inactive FAK can become transphosphorylated on Tyr397 (Sieg, Hauck et al. 2000), there is also evidence for *cis* autophosphorylation. Studies using alternative splicing isoforms of FAK in the brain in which the amino acids surrounding the Tyr397 site differ, have identified that FAK can be either autophosphorylated intramolecularly or intermolecularly. Interestingly, insertion of 7 residues between Tyr397 and the kinase domain in neuronal FAK splice forms promotes *cis* phosphorylation rather than *trans*, probably due to different conformation of the molecule in the autoinhibited state that would preferentially allow *cis* phosphorylation (Toutant, Costa et al. 2002). The phosphorylated Tyr397 serves as a binding site for SH2 domain containing proteins, including Src family kinases and PI3K (Schaller, Hildebrand et al. 1994, Chen, Appeddu et al. 1996) (**Figure 13**). PI3K binds on this site through its p85 subdomain (Chen, Appeddu et al. 1996) and this binding results in the activation of the PI3K/Akt pathway which has a role in preventing cell apoptosis (Franke, Kaplan et al. 1997). The binding of Src to this site is enhanced by the interaction of the SH3 domain of Src with the PR1 domain of FAK (RXXPXXP motif – RALPSIP sequence) upstream of Tyr397 (amino acids 371-374) (Thomas, Ellis et al. 1998). Binding of Src leads to phosphorylation of FAK in the activation loop and the

C-terminus. Other SH2 containing proteins shown to bind this site are phospholipase Cγ (PLCγ) (Zhang, Chattopadhyay et al. 1999), suppressor of cytokine signaling which promotes polyubiquitination and degradation of FAK (Liu, Cote et al. 2003), Grb7 (Growth factor receptor bound protein 7) which becomes phosphorylated by FAK on Tyr188 and Tyr338 (Han and Guan 1999, Chu, Huang et al. 2009), Shc adaptor protein and p120 RasGAP (Mitra, Hanson et al. 2005) (**Figure 13**). The linker segment also contains tyrosine 407 (**Figure 9**), which when phosphorylated has been shown to be negatively associated with the processes of cell spreading, adhesion and migration. Moreover, phosphorylation of FAK on Tyr407 correlates with decreased Tyr397 phosphorylation (Lim, Park et al. 2007).

- **Central Catalytic Kinase domain:**

The kinase domain includes Lys454, which is in the ATP binding site and is essential for catalytic activity. It is highly conserved in the eukaryotic protein kinase superfamily. When it is substituted by Arg (K454R, kinase dead mutant –KD-) the kinase loses its ability to phosphorylate (Calalb, Polte et al. 1995). The kinase domain also contains the residues Tyr576, Tyr577 (**Figure 9**) that become phosphorylated from Src upon binding on P-Tyr397, and they regulate the catalytic activity of the kinase in an adhesion dependent manner. These residues are located in the activation loop of the kinase domain (576-600 amino acids), they are ATP binding sites and their phosphorylation confers full enzymatic activity to FAK (Calalb, Polte et al. 1995) (**Figure 11**). Activated FAK together with Src phosphorylate substrates that are related with cell migration processes, such as phosphorylation of Cas protein at the sequence YDYVHL (Tachibana, Urano et al. 1997) and of paxillin at Tyr118 and Tyr31 (Bellis, Miller et al. 1995, Schaller, Otey et al. 1995), residues that are required for FA turnover (Webb, Donais et al. 2004).

The crystal structure of the kinase domain revealed a disordered activation loop when compared to structures of other protein kinases such as Aurora-A and ephrin receptor A2. Specifically, the activation loop has an open conformation, suggesting that post-translational and mutational changes can modulate the catalytic activity (Nowakowski, Cronin et al. 2002). Such example is the mutation of the residues Lys578 and Lys581 into glutamic acid (known as "SuperFAK") that leads to increased catalytic activity and hyperphosphorylation of FAK downstream substrates such as tensin and paxillin in an adhesion dependent manner (Gabarra-Niecko, Keely et al. 2002). Moreover, an unusual short range disulphide bond at the N-terminal lobe of the kinase between the conserved residues C456 and C459 was identified, but its physiological significance is not clear (Nowakowski, Cronin et al. 2002).

Other important features of the kinase domain are the residues residing at the C-term of the kinase which seem to restrict access of the kinase to Tyr397 in the autoinhibitory conformation, supporting the FERM-Kinase interaction (Lietha, Cai et al. 2007). In addition, the FAK kinase domain contains the second NES signal (Ossovskaya, Lim et al. 2008). Finally, one of the known binding partners of the kinase domain of FAK is FIP200 (FAK family Interacting Protein 200), which when bound it inhibits FAK kinase to prevent "leaking" of FAK enzymatic activity (Abbi, Ueda et al. 2002) (**Figure 13**).

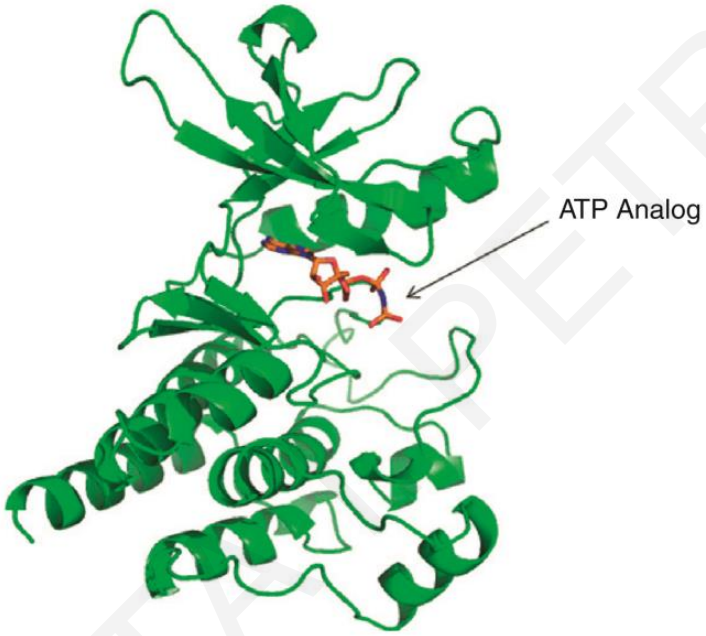

Figure 11: Structure of the FAK kinase domain.
Indication of the ATP binding site in the activation loop of the kinase domain. Adapted from (Hall, Fu et al. 2011).

- **Kinase-FAT domain linker segment:**

This unstructured region contains PR2, PR3 and several serine and tyrosine residues, which when phosphorylated mediate several protein interactions (**Figure 9**). PR2 is recognized by the N-terminal SH3 domain of the adaptor protein Cas (Harte, Hildebrand et al. 1996) (**Figure 13**). Several models have implicated the requirement of the FAK/Src complex for full activation of Cas. FAK is believed to phosphorylate Cas on Tyr762 (YDYVHL), which is recognized by the SH2 domain of Src leading to phosphorylation of the tyrosine residues of the Cas SD (Tachibana, Urano et al. 1997). However, it was afterwards shown that the kinase activity of FAK is dispensable for Cas phosphorylation and that FAK acts as a scaffold to recruit both Src and Cas so as Src can phosphorylate Cas SD (Fonseca, Shin et al. 2004). Cas SD

phosphorylation sites bind the SH2 containing protein Crk, resulting in increased Rac activation, enhanced membrane ruffling and lamellipodia formation promoting cell migration (Sharma and Mayer 2008).

With respect to the serine residues residing in the linker segment shown to be phosphorylated (Serine 722, 843 and 910) (**Figure 9**), it is generally believed that serine phosphorylation of FAK is accompanied by tyrosine dephosphorylation and inactivation (Ma, Richardson et al. 2001). Such process takes place during mitosis, when cells disassemble their FAs (Yamaguchi, Mazaki et al. 1997). Phosphorylation of Ser722 which is located five amino acids C-terminally to the Cas binding region, alters the binding properties of Cas on FAK (Ma, Richardson et al. 2001). The modification of this residue is regulated by the Glycogen synthase 3 and the PP1 phosphatase and Ser722 phosphorylation is associated negatively with FAK catalytic activity (Bianchi, De Lucchini et al. 2005). The Ser732 residue is a substrate of Cdk5 and becomes phosphorylated during mitosis. Ser732 phosphorylated FAK co-localizes with γ-tubulin in the perinuclear region of the cell, at the MTOC (Microtubule Organizing Center) in neurons (Xie, Sanada et al. 2003) and at the centrosome during endothelial cell mitosis (Park, Shen et al. 2009). P-Ser732 FAK at the centrosome associates with dynein and is required for proper spindle integrity and mitosis progression (Park, Shen et al. 2009). Serine 910 is phosphorylated by ERK (Extracellular signal Related Kinase) and acts as a binding site for PIN1 and PTP-PEST during the formation of the lamellipodia. Specifically, PIN1 interaction results is propyl isomerization of FAK and dephosphorylation of Tyr397 by PTP-PEST, a process associated with Ras mediated cell migration, invasion and metastasis (Zheng, Xia et al. 2009).

Another important residue of the linker segment is Tyr861 which is a substrate of Src (Calalb, Zhang et al. 1996) (**Figure 9**). Phosphorylation of Tyr861 was shown to increase the binding of Cas on FAK (Lim, Han et al. 2004). Interestingly, this phosphorylation is uncoupled from integrin adhesion signaling (Slack, Adams et al. 2001) and it regulates FAK enzymatic activity since it enhances autophosphorylation on Tyr397 (Leu and Maa 2002).

Last, this region also contains the PR3 which is a binding site for the SH3 domains of ASAP1 (ARF [ADP Ribosylation Factor] GTPase-activating protein GAP) (Liu, Loijens et al. 2002) and GRAF (Hildebrand, Taylor et al. 1996), both interactions implicated in the formation and organization of the FAs (**Figure 13**).

- **FAT domain:**

The C-terminus of FAK contains the FAT domain, a four-helix bundle which has been shown to be both necessary and sufficient for FA targeting (Hildebrand, Schaller et al. 1993, Chen, Appeddu et al. 1995, Hildebrand, Schaller et al. 1995, Hayashi, Vuori et al. 2002). The crystal structure of the FAT domain displays similarity with those found in other FA proteins such as the C-terminal vinculin tail, Cas, apolipoprotein 3 and a-catenin (Hayashi, Vuori et al. 2002).

NMR and X-ray crystallography show that it is composed by four amphipathic α-helices that assemble into an antiparallel four-helix elongated bundle with an up-down-up-down right-handed turn (Hayashi, Vuori et al. 2002, Hoellerer, Noble et al. 2003, Prutzman, Gao et al. 2004) (**Figure 12**). The FAT domain contains two hydrophobic patches on opposite faces flanked by basic residues which maintain its globular form and mediate several interactions. The first one lies at the interface of α-helices 1 and 4 and the second one at the interface of α-helices 2 and 3 (Hayashi, Vuori et al. 2002, Liu, Guibao et al. 2002). These sites interact with the LD2 and LD4 motifs of paxillin which when bound, the FAT-paxillin complex forms a six-helix bundle. Specifically, the hydrophobic surface of the LD motifs interacts with the hydrophobic patches of the FAT domain and the acidic residues of the LDs with the basic residues flanking the two patches of FAT (Hayashi, Vuori et al. 2002). Analysis of the structure of the FAT domain bound to LD2-LD4 mimicking peptides revealed that the two interactions display different thermodynamic properties and that the conformation of the FAT domain changes upon LD2 binding on helix 4 (Gao, Prutzman et al. 2004). Although the binding of these two motifs on the two patches was believed to be interchangeable, it was later identified that LD4 binds specifically to only a single site between the helices 2 and 3 (Bertolucci, Guibao et al. 2005). Interestingly, paxillin binding on the FAT domain is believed to stabilize the FAT domain structure, suggesting a critical role of paxillin in determining the localization and affinity of FAK for FAs. It is believed that a "hinge" region between the C-term of helix 1 and the N-term of helix 2 (941-951 amino acids) together with a PR region can induce strain and promote conformational change between an "open" and a "close" state of the FAT domain. Importantly, a FAK mutant that abolishes paxillin binding (V955A/L962A) displays an open conformation of FAT supporting the above hypothesis (Prutzman, Gao et al. 2004). The physiological significance of paxillin binding on FAK is that the paxillin phosphorylation by FAK activates downstream signalling to regulate processes of cell migration. Specifically, paxillin binds to PKL/Git2 (Paxillin Kinase Linker) and β-pix (Cdc42 guanine nucleotide exchange factor) which then recruit Rac and PAK to the complex. FAK/paxillin mediated

phosphorylation of β-pix affects Rac activity and controls cell polarization, lamellipodia formation and directional migration (Chang, Lemmon et al. 2007, Yu, Deakin et al. 2009).

An important tyrosine residue residing in the FAT domain is Tyr925, which becomes phosphorylated by Src (Schlaepfer and Hunter 1996) (**Figure 9**). Adhesion dependent Tyr925 phosphorylation creates a binding site for the SH2 domain of the GFR-Bound protein 2 (Grb2) (Schlaepfer, Hanks et al. 1994) (**Figure 13**). Due to the fact that this tyrosine residue resides within the α-helix 1 of the FAT domain, phosphorylation of this site and recognition by Grb2 is poor within this structure suggesting that a conformational change of the FAT domain is needed. Support for this hypothesis comes from studies showing that the α-helix 1 can be displaced to enable conformational change from an α helical to an extended form so the peptide sequence containing Tyr925 will be exposed (Dixon, Chen et al. 2004, Zhou, Feng et al. 2006). The FAK/Grb2 interaction leads to ERK1/2 mediated activation of the Ras pathway which eventually activates the mitogen activated protein kinase (MAPK) (Schlaepfer, Hanks et al. 1994). The Grb2 binding site partially overlaps with one of the two paxillin LD-motif binding sites (Liu, Guibao et al. 2002, Gao, Prutzman et al. 2004) suggesting that the processes of paxillin binding and Tyr925 phosphorylation are inter-dependent. Interestingly, the paxillin defective binding mutant of FAK (V955A/L962A) used in the study by Prutzman et al. that displays an open FAT conformation, exhibits increased phosphorylation on Tyr925 supporting the above notion (Prutzman, Gao et al. 2004). Moreover, expression of FAK Y925F in FAK nulls leads to increased interaction of FAK with unphosphorylated paxillin and blocks FA turnover suggesting that this residue becomes phosphorylated mainly during FA disassembly. In contrast, expression of the phosphomimetic mutant FAK Y925E leads to increased phosphorylation of paxillin at FAs and in increased formation of nascent FAs (Deramaudt, Dujardin et al. 2011). Thus, paxillin binding on FAK is a key step in the regulation of the structure of the FAT domain and in downstream signaling.

Another important binding partner of the FAT domain of FAK which is important for FAK function, is the FA protein talin (Lawson, Lim et al. 2012) (**Figure 13**). Interestingly, the bundle structure of the FAT domain is not necessary for talin binding, since a deletion mutant that lacks most of α-helices 1 and 2 binds talin normally (Hayashi, Vuori et al. 2002). Talin-FAK interaction is mediated through the FERM F3 lobe of talin and the C-terminal region of FAK (Chen, Appeddu et al. 1995). The exact talin binding site on the FAT domain of FAK is on E1015 residue, which is exposed on the surface and does not participate in paxillin binding (Lawson, Lim et al. 2012). FAK-talin binding is required for FA turnover but interestingly, at nascent FAs (early spreading adhesions formed within the first 15 minutes after plated on FN)

FAK recruitment was found to be upstream of that of talin, since in FAK null MEFs talin did not localize at nascent FAs. This was a surprising finding since talin is an activator of integrins and is believed to be the first molecule recruited at integrin sites (Zhang, Jiang et al. 2008, Wang, Ballestrem et al. 2011). However, this was not the case in mature FAs suggesting that different mechanisms regulate the hierarchy of FA protein recruitment at FAs (Lawson, Lim et al. 2012, Lawson and Schlaepfer 2012).

In addition, the FAT domain binds the C-terminal coiled coil domain of p190RhoGEF, leading to its phosphorylation and activation of RhoA (**Figure 13**). Interestingly, this interaction also requires the integrity of the FAT domain structure since an L1034S mutant which disrupts the conformation of FAT, impairs this interaction (Zhai, Lin et al. 2003). This signaling pathway has been linked with the role of FAK in neural development since it regulates axonal branching and synapse formation in Purkinje and hippocampal neurons (Rico, Beggs et al. 2004). Moreover, the FAT domain binds to STAT1 relating FAK with the transcription signaling pathway (Xie, Zhao et al. 2001) and to MBD2 (Methyl-CpG-binding protein 2) leading to reduced histone binding of HDAC1 (histone deacetylase 1) altering chromatin structure and gene expression (Luo, Zhang et al. 2009).

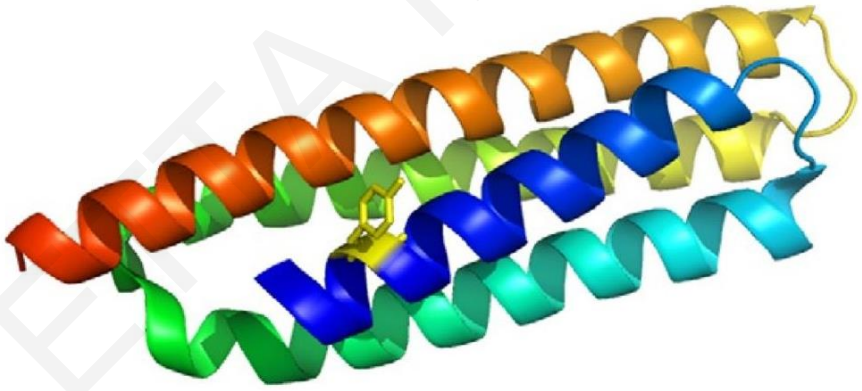

Figure 12: Structure of the FAT domain of FAK.
Schematic representation of the four-helix bundle (N-term with blue, C-term with red). Tyrosine 925 is shown as a yellow feature. Adapted from (Hall, Fu et al. 2011).

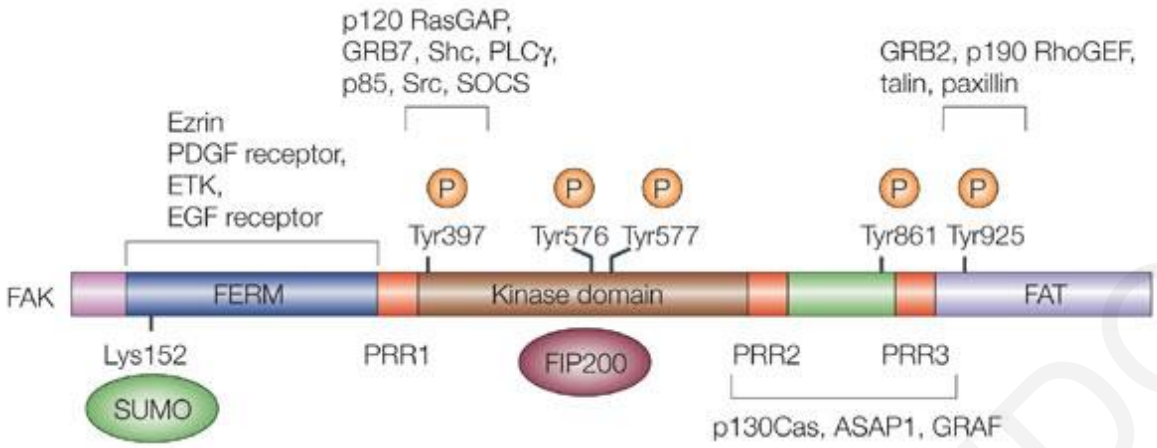

Figure 13: FAK domains and binding partners.

Schematic illustration of the FAK domains, the major phosphorylation sites and their binding partners. Adapted from (Mitra, Hanson et al. 2005).

1.5.2. Mechanisms of FAK activation

FAK as a multifunctional protein its regulated by crosstalk signaling between ECM and growth factors (Parsons 2003). The FERM domain of FAK was originally discovered as a key feature in the regulation of FAK activity. One of the early studies supporting this notion came by Cooper and coworkers, where FERM overexpression was shown to suppress the enzymatic activity of FAK both *in vitro* and *in vivo*, by interacting with the kinase domain *in trans* (Cooper, Shen et al. 2003). Furthermore, expression of the F1 and F2 lobes was found to inhibit FAK phosphorylation, providing evidence that these two lobes of the FERM domain regulate FAK's enzymatic activity (Cohen and Guan 2005). However, deletion of the FERM domain of FAK resulted in enhanced enzymatic activity providing evidence that intramolecular interactions between the FERM and kinase domains might take place in order to inhibit FAK activation (Jacamo and Rozengurt 2005). In agreement with this hypothesis, a point mutation of Lys38 to Ala in the FERM domain which weakens the interaction between the N-terminus and the kinase domain has been shown to result in increased FAK phosphorylation and its downstream target paxillin (Cohen and Guan 2005). Resolution of the crystal structure of the autoinhibited FAK (fragment containing the FERM and Kinase domains) revealed the molecular and structural basis of the mechanism of autoinhibition (**Figure 14**). Specifically, an interaction between the residue Phe596 in the C-lobe of the kinase domain and the hydrophobic pocket of the F2 lobe of the FERM domain (consisting of the residues Tyr180, Met183, Leu197 and Val196) was identified. Moreover, F1 lobe (containing the residue Lys38) interacts with the FERM-Kinase linker segment and with the N-lobe of the kinase domain preventing the stereochemical access

of the kinase domain to its substrates, sequestering Tyr397 from the catalytic cleft, preventing its autophosphorylation and masking tyrosines 576 and 577 in the activation loop from Src (Lietha, Cai et al. 2007) (**Figure 14**). Thus the FERM domain blocks FAK activation by blocking the activation loop, masking Tyr397 and hindering Src recruitment.

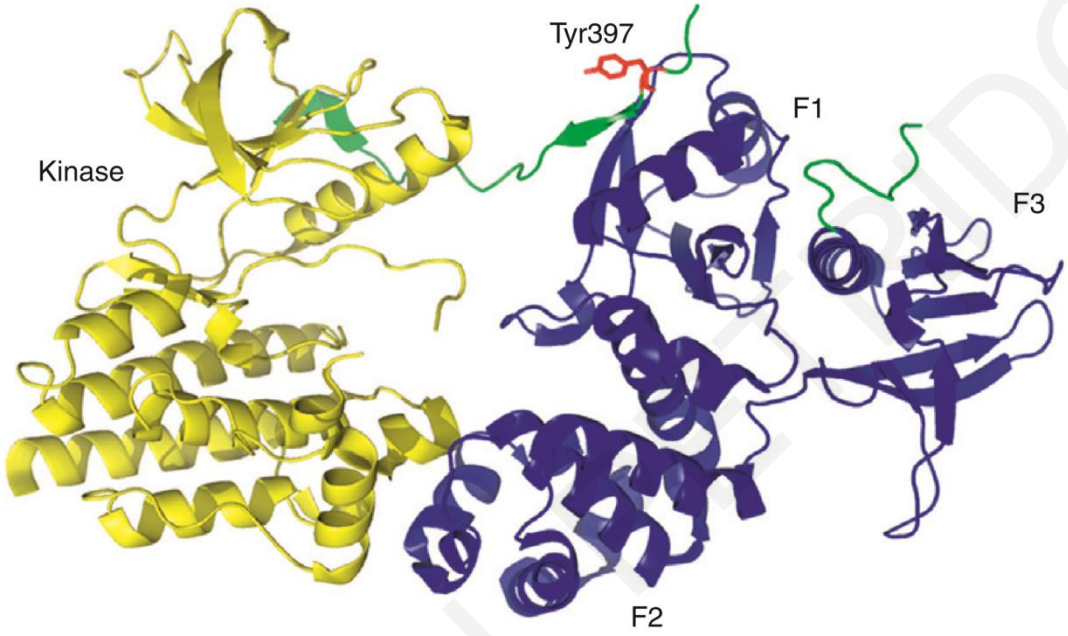

Figure 14: The structure of the FERM and Kinase domains of FAK in the autoinhibited conformation. FERM domain is shown in blue and the Kinase domain in yellow. F1 lobe interacts with the N-term of the kinase, F2 lobe interacts with the C-term of the kinase and Tyr397 (red feature) is away from the catalytic cleft. Adopted from (Hall, Fu et al. 2011).

FAK activation is achieved by the release of the FERM-Kinase autoinhibitory interactions. Although the mechanism is not precisely characterized it is believed that a basic patch in the F2 lobe composed of the residues 216-KAKTLR-221 is essential. This basic patch was found to interact with PIP_2 and HGFR (Cai, Lietha et al. 2008, Chen, Chan et al. 2011) (**Figure 15**). Specifically, using a FRET-based FAK biosensor it was shown that FAK can acquire an open conformation when bound to PIP_2 containing vesicles providing direct evidence that these lipids are capable of changing FAK´s structure. In the case of the binding of the FERM domain on the c-Met receptor (HGFR), it was observed that this interaction leads to the phosphorylation of FAK on Tyr194 by c-Met which probably interacts with the basic patch resulting in increased FAK activation (Chen, Chan et al. 2011).

However, the fact that FAK activation takes place primarirly at FAs suggests mechanisms that combine signals from integrins through the FAT domain and from FERM domain interactions. It is possible that FERM mediated interactions induce clustering of FAK molecules to promote *trans* autophosphorylation, especially in areas that promote clustering such as the FAs. This hypothesis was recently supported from work by the Arold group, who showed that FERM:FERM domain interactions take place leading to FAK dimerization at FAs which is stabilized further by FERM:FAT interactions. Specifically, the residue W266 within the FERM domain was found to be essential for the FERM:FERM interactions. Mutation of this amino acid into Ala affected FAK dimerization and resulted in decreased recruitment and stability of FAK at FAs and abolishment of FAK autophosphorylation (Brami-Cherrier, Gervasi et al. 2014), supporting earlier studies that Tyr397 autophosphorylation takes place intermolecularly and it requires dimerization (Toutant, Costa et al. 2002). In addition, an *in trans* interaction between the basic patch of the FERM F2 lobe and the FAT domain was found to stabilize the dimerization. Paxillin binding re-inforces the FERM:FAT interaction suggesting that paxillin binding controls FAK dimerization (Brami-Cherrier, Gervasi et al. 2014).

The eventual opening of the FAK molecule leads to exposure of Tyr397 for autophosphorylation. This phosphorylation site together with the unmasking of the nearby PR1 act as a binding site for Src´s SH2 and SH3 domains which blocks the inhibitory interaction between the FERM-kinase linker and the FERM domain (Ceccarelli, Song et al. 2006). Src binding and the exposure of the FAK activation loop leads to full catalytic activation of FAK, through phosphorylation on Y576 and Y577 (Calalb, Polte et al. 1995) (**Figure 15**). Upon phosphorylation, the activation loop acquires a β-hairpin conformation which is stabilized by hydrogen bonds formed between the phosphate group on Tyr577 and the residues Ser580, Ala579 and Arg569. It is believed that phosphorylation of the kinase activation loop blocks the interaction of the kinase domain with the FERM domain maintaining FAK in its open, active conformation (Lietha, Cai et al. 2007). Restoration to the autoinhibited conformation depends on phosphatase activity, a process which has not been well characterized (Hall, Fu et al. 2011).

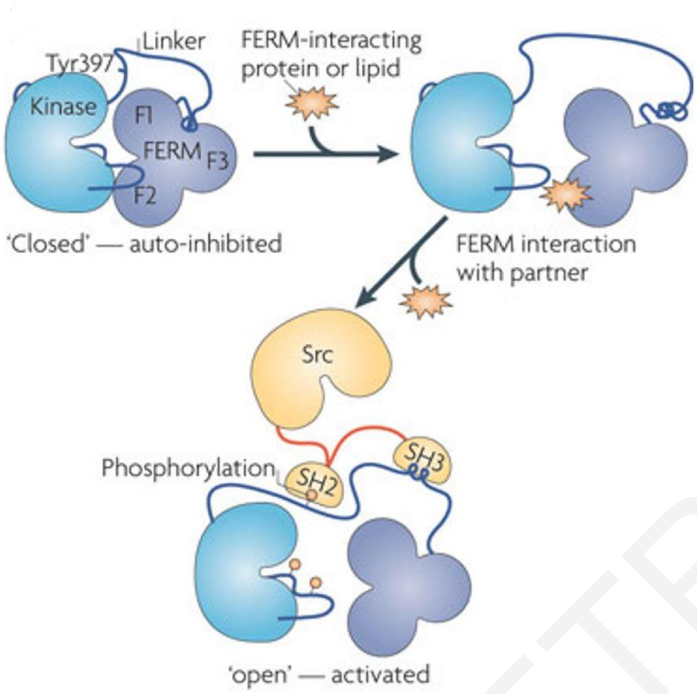

Figure 15: Conformational change of FAK from the autoinhibited state to the active form.
FAK autoinhibitory state is released when the FERM domain is bound to a protein or lipid partner (GFR or PIP_2). Now the Tyr397 site is available for autophosphorylation leading to Src recruitment, phosphorylation of the tyrosines of the activation loop and full activation of FAK. Adapted from (Frame, Patel et al. 2010).

Another regulator of FAK activation, is its physiologically expressed dominant negative (DN) FRNK (FAK-related non kinase) which encompasses the FAK C-terminus of FAK. FRNK is transcribed from a second promoter and is expressed through the transcription elements between the 3'-most exon of the kinase domain and the first exon of the C-terminus (Nolan, Lacoste et al. 1999). FRNK overexpression inhibits cell spreading and cell migration (Richardson, Malik et al. 1997, Taylor, Mack et al. 2001). Since FA targeting has been shown to be necessary for FRNK's DN activity (Cooley, Broome et al. 2000), it is believed that it inhibits FAK through competition with endogenous FAK at the FAs (Richardson, Malik et al. 1997, Sieg, Hauck et al. 1999). Moreover, it was shown that cleavage of FAK from the protease caplain creates FRNK-like elements suggesting an alternative mechanism of control of FAK activity (Chan, Bennin et al. 2010).

1.5.3. FAK in cell migration, development and disease

FAK has long been considered a key regulator of embryonic development, since it regulates not only cell migration which is fundamental for the morphogenetic movements during development but as mentioned above, it also controls cell proliferation, apoptosis, survival and gene expression. However, most of the known knowledge of FAK is concentrated in the area of cell migration since it is associated with severe diseases such as tumorigenesis.

As mentioned above, FAK null cells display increased number and size of FAs, however since FAs are formed, it is clear that FAK is not required for FA formation. These FAs are formed primarily at the cell periphery and are enmeshed in a cortical actin ring, not connected to longitudinal stress fibers, suggesting that these cells don't respond to contractility and polarization (Ilic, Furuta et al. 1995). Interestingly, this phenotype is rescued by expression of constitutively active Src, indicating that the overall phenotype stems from impaired activation of Src (Hsia, Mitra et al. 2003). The specific roles of FAK in cell migration mainly concern the process of polarization, direction of cell migration, regulation of the protrusive activity at the leading edge and of the retraction at the trailing edge (Schaller 2010) (**Figure 16**).

FAK is believed to regulate cell protrusive activity through the promotion of actin branching and nucleation of F-actin assembly, a process involving the association of FAK dependent phosphorylation of N-WASP and activation of the Arp2/3 complex at the leading edge of the cells (Serrels, Serrels et al. 2007). FAK's role in cell polarization is evident from Golgi re-orientation experiments upon wound healing, where FAK downregulated cells exhibit broad random lamellipodia instead of forming a leading edge (Tilghman, Slack-Davis et al. 2005). This process is regulated by a complex consisting of FAK, p120RasGAP and p190RhoGAP which phosphorylates p120RasGAP, leading to its FA recruitment to drive cytoskeletal changes and guides polarization (Tomar, Lim et al. 2009). Concerning FAK's role in FA turnover, besides the phenotype of FAK null mouse embryonic fibroblasts (MEFs) (Ilic, Furuta et al. 1995), FAK null macrophages also show defective disassembly at the leading edge (Owen, Pixley et al. 2007). Moreover, LPA treatment to promote retraction of the trailing edge in FAK downregulated cells led to impaired FA disassembly at the rear of the cell (Iwanicki, Vomastek et al. 2008) (**Figure 16**). The mechanism behind FAK's role in FA turnover involves RhoA activation. The FAK null MEF phenotype is similar to that induced by overactivation of Rho and indeed FAK null fibroblasts exhibit elevated levels of active Rho (Ren, Kiosses et al. 2000). The mechanism behind FAK mediated control of Rho activity depends on interactions between FAK and several modulators of Rho activity. GRAF (which binds FAK on PR3) blocks Rho activation and formation of stress fibers, suggesting that FAK-GRAF interaction influences this

process (Taylor, Macklem et al. 1999). Moreover, FAK binds the Rho-activating GEF, PDZRhoGEF which is required for FA disassembly at the rear of the cell (Iwanicki, Vomastek et al. 2008). In addition, FAK binds p190RhoGEF, which when overexpressed enhances RhoA activation (Lim, Lim et al. 2008). FAK mediated FA turnover was also shown to be regulated by Tyr925 phosphorylation and Grb2 binding on FAK, an interaction that recruits dynamin in complex to promote microtubule dependent FA disassembly (Ezratty, Partridge et al. 2005) (**Figure 16**).

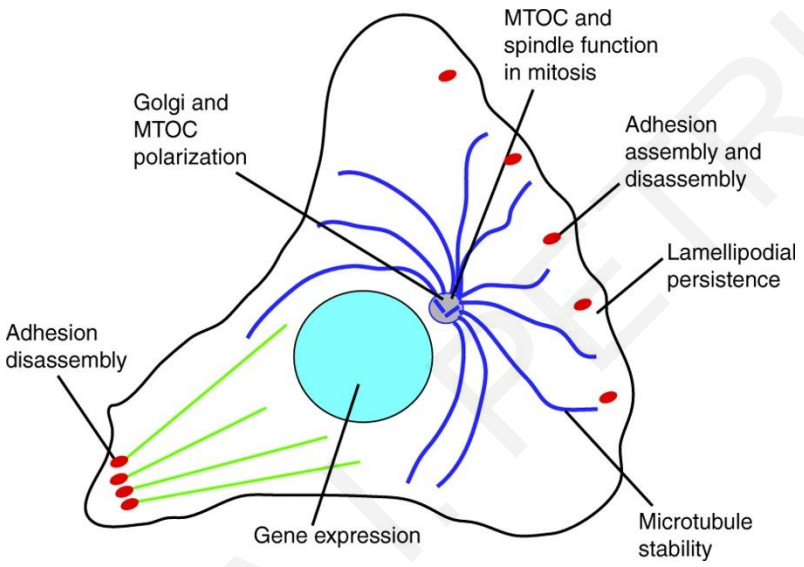

Figure 16: Schematic representation of the roles of FAK in a migrating cell.
FAK controls cell protrusive activity at the leading edge, cell polarization and FA disassembly at the front and the rear of the cell. Adapted from (Schaller 2010).

The early embryonic lethal phenotype of the FAK null mice (Furuta, Ilic et al. 1995) was initially attributed to defects in cell migration, since this phenotype was similar to those observed in FN and integrin α5 knockouts (George, Georges-Labouesse et al. 1993, Yang, Rayburn et al. 1993), suggesting that FAK mediates FN-integrin signaling required for early embryonic development. The most prominent phenotype of the FAK knockout embryos was the defective cardiovascular system (Furuta, Ilic et al. 1995). Interestingly, mice expressing a FAK deletion mutant that lacks exon 15 which encoded the Tyr397 site, show embryonic lethality at E14.5 instead at E8.5, indicating autophosphorylation dependent and independent functions of FAK. However, these mice displayed similar defects to the FAK nulls, including hemorrhages, edema, delayed artery formation and defective vascular remodeling (Corsi, Houbron et al. 2009). In addition, endothelial cell specific FAK knockouts displayed embryonic lethality between E10.5 to E11.5, with irregular vasculature, dilated capillaries and

hemorrhages. Those defects were attributed to endothelial cell apoptosis leading to reduced vessel growth and increased vessel regression (Braren, Hu et al. 2006). However, vasculogenesis which takes place early on in development, appeared normal (Shen, Park et al. 2005). An endothelial cell specific FAK kinase defective mutant knock-in extended lifespan to E13.5, however these embryos also displayed vessel dilation, increased permeability of the endothelial cells, suggesting that the kinase activity of FAK is necessary for vascular development (Zhao, Peng et al. 2010). The role of FAK in vascular integrity was later characterized further using inducible endothelial cell specific knockout and FAK KD (K454R mutation) knock-ins, where it was shown that FAK prevents VEGF stimulated permeability. It is believed that VEGF activates FAK leading to its localization at the cell-cell junctions, interacting with VE cadherin, leading to β-catenin phosphorylation and dissociation from the junctions to promote vasculogenesis (Chen, Nam et al. 2012).

The well characterized role of FAK in angiogenesis and cell migration has established FAK as a therapeutic target for tumorigenesis. FAK displays elevated mRNA levels in several human malignancies including invasive breast cancers and tumors in ovaries, colon, thyroid, prostate, liver, stomach, skin and bone and its increased expression is associated with poor prognosis (Parsons, Slack-Davis et al. 2008). Interestingly, increased FAK activation is associated with tumor progression (Zhao and Guan 2009). Moreover, maintenance of a balance between kinase dependent and independent functions of FAK is crucial for tumor associated processes such as invasion, altering tumor microenvironment (pH, stiffness), survival, growth, transcription and EMT (epithelial to mesenchymal transition). Up to date, small molecule inhibitors have been synthesized and are currently candidates as chemotherapeutic agents in preclinical and clinical trials (Sulzmaier, Jean et al. 2014).

2. Methodology

2.1. *Xenopus* frogs, embryos and embryo manipulation

2.1.1. Frogs

Adult frogs were obtained from the international suppliers NASCO (United States) and *Xenopus* express (France/UK). New frogs were kept separately from the older ones and a recovery period of minimum two weeks was allowed prior experimentation (Hazel L. Sive 2000).

2.1.2. Egg collection and *in vitro* fertilization

Egg collection starts with the induction of ovulation which is achieved by injection of 600-750 units of human Chorionic Gonadotropin (hCG; Chorulon/Sigma) into the dorsal lymph sac of the female frog. Using a fine needle (26 gauge, Fisher) attached to a 1 ml syringe, the injection was performed posteriorly, at the level of the hind limb near the lateral line "stitch". Primed frogs are kept at 18-20°C and ovulation starts approximately 12 hours after injection. When the female frog is ready for ovulation the cloaca becomes red and swollen (Hazel L. Sive 2000).

Egg collection from the primed female frog was achieved by holding the frog properly and applying lateral and vertical pressure by massaging the belly. Eggs were collected in a clean glass petri dish containing 0.33x MMR (Marc's Modified Ringers, Annex 7.2). The egg collection process lasts 2-3 minutes and it can be repeated 6-8 times during the day. Each batch of oocytes obtained from the female frog was kept in a separate glass petri dish (Hazel L. Sive 2000).

Fertilization was performed *in vitro* immediately after laying and time of fertilization was noted. In order to isolate the testes for the fertilization, a male frog is sacrificed by submerging it in 0.05% benzocaine for 30 minutes at RT (Room Temperature). The testes lie at the base of the fat bodies, they are 1 cm long, and they are removed from the body by the use of scissors and forceps (Hazel L. Sive 2000). The isolated testes are stored at 4^{o}C, in 10% newborn calf serum, 90% Leibovitz (L-15 Medium Leibovitz) with antibiotic (0.05 mg/ml gentamycin) for 5-7 days. Before *in vitro* fertilization, excess 0.3x MMR buffer was removed from the petri dish containing eggs using a plastic pipette. A small piece of testis was cut and macerated using forceps and mixed with the eggs in order to evenly distribute the sperm throughout the eggs.

The eggs were left for 20 minutes in order for fertilization to occur. The first sign of a successful fertilization is the rotation of the embryos so that the animal hemisphere faces upwards (pigmented half). Then the embryos are kept in 0.33x MMR.

2.1.3. Microinjections and embryo maintenance

The embryos are protected by thick, jelly membranes that make the micromanipulation procedures impossible. The jelly is removed after the bathing and swirling of the embryos in 1.8% Cysteine buffer (Annex 7.2) for 2-4 minutes (Hazel L. Sive 2000). When the embryos begin packing closely together and the jelly coats can be seen floating in the buffer, the cysteine was promptly removed and the fertilized eggs were rinsed at least 10 times in an excess of 0.33x MMR. If these embryos are going to be used for microinjections, the healthy ones are selected and placed in 4% Ficoll (Annex 7.2) or else they are maintained in 0.1x MMR.

Ficoll collapses the vitelline space, reduces the pressure on the embryo and therefore prevents leakage upon microinjection procedure. The embryos were injected using glass capillary pulled needles, forceps, a Singer Instruments MK1 micromanipulator and Harvard Apparatus pressure injector. Embryos were staged according to Nieuwkoop and Faber (Nieuwkoop 1994) and were injected mainly with mRNAs (or plasmid DNAs) encoding a protein or a mutant protein of interest and morpholino oligonucleotides (MOs). In each case careful calibration of the needle was performed in order to tune the injection volume and control the concentration of the injected reagent into the embryo. The targeting according to the *Xenopus* fate map (Dale and Slack 1987) and the amount of the injections depended on the individual experiments and this information is stated in the description of the experiments in the Results sections. After injections, embryos were kept in Ficoll for 2 hours and then washed and maintained in 0.1x MMR. Embryos were allowed to develop to the desired stage and then imaged live, dissected, or fixed.

2.1.4. Explants and microdissections

All explants were performed with the use of forceps and hair-knives.

2.1.4.1. AC explants for mesodermal migration assay

These explants were performed as previously described (Alfandari, Cousin et al. 2001). Briefly, ACs were dissected from stage 8 embryos, placed on 50 μg/ml FN coated glass coverslips in

DFA (Danilchik's for Amy) explant culture media (Annex 7.2) containing gentamycin and the mesodermal inducing agent activin (10ng/ml). The ACs were held in place by glass bridges and imaged live.

2.1.4.2. AC explants for spindle orientation assay

ACs from stage 9 embryos were dissected and cultured on agarose coated dishes in DFA containing gentamycin until sibling embryos reached stage 15. Then ACs were fixed and processed for immunofluorescence experiments.

2.1.4.3. Convergent Extension assay

ACs were dissected from stage 8 embryos, cultured on agarose coated dishes in 0.5x MMR containing gentamycin and activin until sibling embryos completed neurulation. The explants were then fixed and imaged under a Zeiss LumarV12 fluorescent stereomicroscope.

2.1.4.4. Radial Intercalation explants

Radial intercalation explants were performed as previously described (Marsden and DeSimone 2001). Briefly, the NIMZ was dissected from a control stage 10 embryo, the outermost epithelium was removed, the deep involuting cells were shaved and the explant was placed on a FN coated charged coverslip. A similar explant was dissected from injected embryos, the deep cells were shaved but the epithelium was retained and it was positioned above the control explant. The explants were held in place by the use of glass bridges. The reverse explant system was also performed. The explants were kept in place until the sibling embryos completed gastrulation and then were fixed, immunostained, cleared and imaged under a confocal LSM710 microscope.

2.1.4.5. AC excision in whole embryos

This manipulation was previously described (Keller and Jansa 1992). The vitelline membrane was carefully removed from both experimental and control stage 11 embryos. The release of tension from the AC tissue of embryos undergoing gastrulation was carried out by generating an incision at the AC using a hair-knife and removing a very small piece of the ectodermal

tissue. Embryos were then monitored for blastopore closure for 20 minutes and compared with non-manipulated sibling embryos.

2.1.5. Drug treatments in embryos

For the examination of the specificity of the phospho-antibodies P-Y397 FAK and P-Y576 FAK, two-cell stage embryos were treated with 10 μM of the Src inhibitor PP2 (Sigma) until gastrula stages. ROCK inhibitor (Sigma) (7 mM) was injected in the blastocoel at stage 10 as described previously (Woolner and Papalopulu 2012). Nocodazole treatment of tadpoles was performed at 50 nM, 20 minutes upon wounding with the gastromaster microsurgery instrument and left for 40 minutes until fixation. For the effects of Src kinase activity inhibition on spindle orientation in the *Xenopus* epidermis, embryos were treated with 8 μM of Src inhibitor PP2 from stage 9 until stage 15 and then they were fixed and processed for immunofluorescence. For the activation of the inducible FF-GR DN for the radial intercalation experiments, stage 10.5 embryos were incubated in 10 mM dexamethasone (Santa Cruz) at 14^{o}C. Activation of the FF-GR for the evaluation of the effects on pronephros morphogenesis was performed by incubating the embryos with 10 mM dexamethasone in 0.1x MMR from stage 33/34 until either stage 35/36 for imaging cell divisions or stage 40 for evaluation of the pronephros morphology.

2.1.6. Heart injections

Tadpoles were anesthetized by placing them in 0.01% Benzocaine in 0.1x MMR. Embryos were placed in slides containing silicone gaskets so that the tadpoles would be placed on their sides and held there by the use of forceps. A total of 5 nl of Quantum Dots (QDs) Qtracker 800nm (Q21071MH, Invitrogen) was injected into the heart of each embryo. Embryos were then kept in 0.1x MMR until they woke up and were re-anesthetized for imaging.

2.2. DNA constructs and morpholino oligonucleotides

All constructs were generated using standard molecular biology techniques and were verified for correct coding by DNA sequencing.

2.2.1. Cloning

All FAK constructs were generated from the FAK chicken variant (GenBank AAA48765.1). All plasmids generated in this project by PCR are listed in **Table 1**. The DNA amplification reactions were performed using AccuPrime™ Pfx SuperMix (1234-040, Invitrogen) which contains 22 U/ml Thermococcus species KOD thermostable polymerase complexed with anti-KOD antibodies, 66 mM Tris-SO_4 (pH 8.4), 30.8 mM $(NH_4)_2SO_4$, 11 mM KCl, 1.1 mM $MgSO_4$, 330 µM dNTPs, AccuPrime proteins and stabilizers.

Generated Construct	**Primers**	**Template DNA**
pCS108 HA-FERM	F/HA: ATGCGGCCGCATGTACCCATACGATGTTCCAGATTACGCT R/FERM: TTTCTCGAGTTAATCTATTATCTCTGCATAGTCATCTGT	pKH3 HA-FAK
pCS108 HA-FERM Y397F	F/HA R/FERM Y397F: TTTCTCGAGTTAATCTATTATCTCTGCAAAGTCATCTGT	pKH3 HA-FAK Y397F
pCS108 HA-FAK Δ375	F/HA R/FAK: TTTCTCGAGTTAGTGGGGCCTGGACTGGCTGATCATTTT	pKH3 HA-FAK Δ375
pCS108 HA-FF	F/HA R/FERM F/FRNK: AAATCTAGAGGTAGCGGCAGCGGTAGCAGGTTTACTGAACTTAAAGCAC R/FAK	pKH3 HA-FAK
pCS108 HA-FRNK	F/HA R/FAK	pKH3 HA-FRNK
pCS2++ HA-FAK K38A	F/HA R/FAK	pKH3 HA-FAK K38A
pCS2++ HA-FAK K454R	F/HA R/FAK	pKH3 HA-FAK K454R
pCS108 HA-FF S732A	F/FF S732A: AGTGAAGGGTTTTATCCGGCTCCTCACGATATGGTACAG R/FF S732A: CTGTACCATATCGTGAGGAGCCGGATAAAACCCTTCACT	pCS108 HA-FF
pCS108	F/HA R/ΔFAT:	pCS2++ HA-FAK

HA FAK ΔFAT	AACTCGAGTCTTCACGCCTTCGTTGTAGCTGTCCACGGGG	
pCS108 GFP FAK ΔFAT	F/GFP: AAAGCGGCCGCATGGTGAGCAAGGGCGAGGAGCTG R/ΔFAT	pCS2++ GFP FAK
pCS2++ HA-FAK L1034S	F/FAK-L1034S: GCTGTGGATGCCAAGAACTCGCTGGATGTCATCGATCAAGC R/FAK-L1034S: GCTTGATCGATCACATCCAGCGAGTTCTTGGCATCCACAGC	pCS2++ HA-FAK
pCS2++ GFP-FAK L1034S	F/FAK-L1034S R/FAK-L1034S	pCS2++ GFP-FAK
pCS2++ GFP-FAK E1015A	F/FAK-E1015A: CCAGCCTGCAGCAGGCGTACAAGAAGCAAAT GCT R/FAK-E1015A: AGCATTTGCTTCTTGTACGCCTGCTGCAGGCTGG	pCS2++ GFP-FAK
pCS2++ GFP-Paxillin Rescue	F/Pxn Rescue 1: ATGGAAGAATTCGACGCCCTGCTGGCGGACTTGGAGTCTACC R/Pxn Rescue 1: GGTAGACTCCAAGTCCGCCAGCAGGGCGTCGAATTCTTCCAT F/Pxn Rescue 2: ATGGAAGAATTCGATGCGCTCTTGGCGGACTTGGAGTCTACC R/Pxn Rescue 2: GGTAGACTCCAAGTCCGCCAAGAGCGCATCGAATTCTTCCAT	pCS2++ GFP-Paxillin
pCS108 GFP F-GR-F	F/GFP2: AAAGGATCCATGGTGAGCAAGGGCGAGGAGCTG R/FERM: TTTGCGGCCGCATCTATTATCTCTGCATAGTCATCTGT F/GR: AAAGCGGCCGCATCTGAAAATCCTGGTAACAAAACA R/GR: TTTGATATCCTTTTGATGAAACAGAAGTTT F/FRNK R/FAK	pCS2++ GFP-FAK pSP64T Xbra-GR
pCS2++ GFP FAK P712/715A	F/FAK P712/715A: GGATCAGATGAAGCTGCTCCCAAGGCCAGCAGGCCTGGTTAC R/FAK P712/715A: GTAACCAGGCCTGCTGGCCTTGGGAGCAGCTTCATCTGATCC	pCS2++ GFP FAK
pCS2++	F/FAK P712/715A R/FAK P712/715A	pKH3 HA FAK

HA FAK P712/715A		
pCS2++ GFP FAK I936E/I998E	F/FAK I936E: CCGGGCTGGTGAAAGCTGTCGAAGAGATGTCCAG TAAAATACAG R/FAK I936E: CTGTATTTTACTGGACATCTCTTCGACAGCTTTCA CCAGCCCGG F/FAK I998E: AACTCTGACCTGGCTGAGCTCGAAAACAAGATGA AGCTGGCCCAG R/FAK I998E: CTGGGCCAGCTTCATCTTGTTTTCGAGCTCAGCCA GGTCAGAGTT	pCS2++ GFP FAK
pCS2++ GFP FAK Y925F	F/FAK Y925F: GACCGCTCCAATGACAAAGTCTTTGAGAATGTAA CCGGGCTG R/FAK Y925F: CAGCCCGGTTACATTCTCAAAGACTTTGTCATTGG AGCGGTC	pCS2++ GFP FAK

Table 1: **List of constructs generated by PCR and the primers used for each cloning.**
Abbreviations: F, forward primer; R, reverse primer; HA, hemagglutinin.

The GFP FRNK and GFP FAK sequences were subcloned from the adenoviral shuttle vector pShuttle to the pCS2++ vector using the restriction enzymes BglII/NotI. The HA ΔFERM/K454R pCS2++ construct was generated by subcloning a fragment of FAK containing the K454R mutation form the HA FAK K454R pCS2++ plasmid followed by ligation to the plasmid of HA ΔFERM pCS2++. The constructs F-GFP-F and F-mCherry-F were generated by inserting the GFP sequence from pEGFP-N1 or mCherry sequence from pShuttle mCherry-tubulin (Addgene) at the XbaI site of the HA FF construct.

2.2.2. Mutagenesis

The constructs pCS108 HA FF S732A, pCS108 HA FF L1034S, pCS108 HA FF E1015A, pCS2++ HA FAK L1034S, pCS2++ GFP FAK L1034S, pCS2++ HA FAK E1015A, pCS2++ GFP FAK E1015A, pCS2++ HA FAK P712/715A, pCS2++ GFP FAK P712/715A, pCS2++ GFP FAK I936E/I998E and pCS2++ GFP paxillin Rescue were generated by site-directed mutagenesis with the primers listed in **Table 1**. The primers for the mutagenesis PCR reaction were designed such that both primers contain the desired mutation and annealed to the same sequence on opposite strands of the plasmid. The primers were between 25-45 bases, the

melting temperatures (T_m) were ≥ 78°C, the GC content over 40% and the mutated sequence was located in the middle of the primers. The reaction was performed as followed: In a PCR tube we added 125ng of each primer 22.5μl Accuprime (Invitrogen) polymerase mix and 100ng of the template DNA. The cycling conditions were: 95°C for 1 minute, 18 cycles of 95°C for 50 seconds, 60°C for 50 seconds and 68°C for time depending on the size of the vector (1.5 minute per Kb of plasmid) and last 1 cycle at 68°C for 10 minutes. The PCR was immediately cooled to 37°C, 1μl of Dpn1 (10U/μl) restriction enzyme was added and the reaction incubated for 1 hour at 37°C. 2 μl of the PCR reaction was then used for transformation in TOP10 cells (Invitrogen).

2.2.3. Provided plasmids

The plasmids pKH3 HA FAK, pKH3 Δ375, pKH3 HA FRNK, pKH3 HA FAK K38A, pKH3 K454R, pKH3 HA FAK Y397F were kindly provided by Dr. Guan lab. The pRK GFP Paxillin construct was provided by Dr Kenneth Yamada lab. The plasmids membraneCherry (memCherry) pCS2+ and histoneGFP (hGFP) pCS2+ were kindly provided by Chenbei Chang lab. The HA Par6 pCS2+ plasmid was provided from Ira O. Daar lab. The H2B-mRFP1 (hRFP) pCS2 plasmid was provided by Reinhard Koster lab. The EMTB-3xGFP pCS2 was provided by Brian J. Mitchell lab. The pEGFP C1-LGN construct was kindly provided by Fumiko Toyoshima Lab. The HAβ1 pSP64T construct was provided by Douglas DeSimone lab. The pCS2 GFP Utrophin plasmid was provided by Dr. John Wallingford. All p130Cas constructs (pLZRS-MS-GFP Cas WT, pLZRS-MS-GFP Cas 15F, pLZRS-MS-GFP Cas mPR, pLZRS-MS-Zeo-Cas WT venus, pLZRS-MS-Zeo-Cas ΔSH3 venus) were provided by Dr. Steven Hanks. The pEGFP FAK S732A plasmid was provided by Dr Li-Huei Tsai lab.

2.2.4. Morpholinos

The sequence of FAK MO is 5'-TTGGGTCCAGGTAAGCCGCAGCCAT-3' (Fonar, Gutkovich et al. 2011), of Vinculin MO is 5'-TATGGAAGACCGGCATCTTGGCAAT-3' and of paxillin MO is 5'-CAGCAATGCATCCAGGTCATCCATG-3'. The Paxillin MO sequence is based on a previously published paxillin MO with slight differences (Iioka, Iemura et al. 2007).

2.3. cDNA, mRNA synthesis and RT-PCR

2.3.1. RNA isolation and cDNA synthesis

Embryos were placed in an autoclaved 1.5 ml capped centrifuge tube (~5 per tube). 500 µl TRIzol reagent (Invitrogen) was added, and embryos were homogenized by pipetting until the sample was uniform. The sample was allowed to incubate for 10 minutes at RT. Tubes were then centrifuged at 14000 rpm for 10 minutes at 4°C. The supernatant was removed and placed into a new autoclaved 1.5 ml tube. An equal volume of chloroform was added, the tubes were vortexed for 15 seconds and allowed to incubate at RT for 3 minutes. Tubes were then spun in a 4°C microfuge at 12000 rpm for 15 minutes. The top phase was placed into a new autoclaved tube. 500 µl of isopropanol was added and the tubes were allowed to stand for 10 minutes at RT, spun at 12000 for 10 minutes at 4°C, the supernatant was decanted and the pellet was washed with 500 µl RNAase-free 70% ethanol and RNA was recovered by centrifugation at 9000 rpm for 5 minutes at 4°C. The supernatant was removed and the pellet was allowed to dry before resuspending it in 30 µl of sterile water. cDNA was then synthesized from RNA using the SuperScriptIII First strand synthesis kit from Invitrogen.

2.3.2. mRNA synthesis

All constructs were *in vitro* transcribed into mRNA using mMessage mMachine SP6 or T7 kit (Ambion).

2.3.3. RT-PCR

For RT-PCR, cDNA was synthesized as described above for different developmental stages. PCR was carried out using specific primer pairs for Actin, MyoD, Xbra, Chrd and Sox2.

2.4. Whole-mount *in situ* hybridization

Whole-mount *in situ* hybridization (ISH) of *Xenopus* embryos was performed according to Harland (1991) (Smith and Harland 1991). The basic ISH steps are as follows:

Digoxigenin labelled probe preparation: Antisense digoxigenin labeled RNA probes were synthesized by *in vitro* transcription from linearized plasmid templates using bacteriophage

RNA polymerases (T3, T7 or SP6) and a ribonucleotide mixture in which the UTPs are labeled with digoxigenin (DIG-11-UTP). The probe was stored at -80° until use.

Day1 of ISH: The embryos were first transferred to 4 ml glass vials and rehydrated through a methanol series. Next the embryos were permeabilized by incubation at RT for 5 minutes in 10 µg/ml Proteinase K, washed 2x5 minutes in 0.1 M Triethanolamine pH7-8 (TEO), 2x5 minutes in TEO with acetic anhydride and then post fixed in 4% PFA (paraformaldehyde) for 20 minutes at RT. Embryos were then incubated for 5-6 hours in hybridization solution (Annex 7.2) at 60-65°C and then incubated overnight at 60-65°C in hybridization solution containing the probe. Probes used: Xbra, MyoD, Sox2, Gsc and Chrd.

Day2 of ISH: Post-hybridization washes in SSC, RNase treatment at 37°C, block, and antibody incubation (Anti-DIG-AP fab fragments. 1:2000) at 4°C overnight or 4 hours at RT followed by a brief wash in 1x MAB (Maleic Acid Buffer, Annex 7.2) and then overnight wash in 1x MAB at 4°C .

Day3-4 of ISH: Post-antibody washes with MAB solution (5x1 hour washes for overnight antibody incubation and 4x10 minutes washes for 4 hours RT antibody incubation) and washed in Alkaline Phosphatase buffer (Annex 7.2) which contained levamisole to inhibit endogenous phosphatases (2x10 minutes washes). Visualization of the probe was performed with BM purple. Color development time varied depending on the probe used. To stop the color reaction, the embryos were washed in 1x MAB and fixed overnight in 1x MEMFA (Annex 7.2) at RT. Embryos were then bleached in bleaching solution (Annex 7.2). Bright field images were captured on a Zeiss LumarV12 fluorescent stereomicroscope.

2.5. Tunel Assay

Tunel assay of *Xenopus* embryos was performed according to the Harland protocol (Conlon laboratory, North Carolina). Briefly, embryos were fixed in 1x MEMFA (Annex 7.2) at RT, dehydrated in methanol and rehydrated in 1x SSC. Embryos were bleached under direct light in bleaching solution containing formamide and hydrogen peroxide. Then embryos were incubated for 1 hour at RT in TdT buffer (Invitrogen). 1 µl of 15 U/ml TdT enzyme (Invitrogen) and 0.1 µl of DdUTP (Roche) per 100 µl buffer were added to the buffer solution and the embryos were incubated overnight at RT. Then embryos were first washed 2x1 hour at 65°C in 1 mM EDTA/PBS and washed in 1xPBS 4x1 hour at RT followed by 2x5 minutes washes in 1x MAB. Embryos are then blocked in 2% BMB blocking solution (Annex 7.2) for 1 hour at RT and incubated in a 1:3000 dilution of anti-digoxigenin AP antibody in BMB block for 4 hours RT or overnight at 4°C. Antibody was washed away by 5x1 hour washes in MAB.

Endogenous phosphatases are blocked by 2x10 minutes washes in alkaline phosphatase buffer and then NBT/BCIP was added to the embryos. Chromogenic reaction was stopped by a quick wash in MAB and then the embryos were fixed overnight in 1x MEMFA and stored in 1x SSC.

2.6. Cell culture

2.6.1. Cell lines

HeLa (ATCC), NIH3T3 (ATCC) and MDCK (ATCC) cells were cultured in DMEM with 10% Fetal Bovine Serum (FBS) at 37ºC. The FAK-/- cell line (ATCC) was cultured in DMEM with 10% FBS and 1mM sodium pyruvate at 37ºC. The Cas -/- and Cas reconstituted cells (provided by Dr Sara Cabodi) were cultured in DMEM with 10% FBS and 1mM L-Glutamine at 37ºC. *Xenopus* XL177 and A6 cells were cultured in 70% L-15 medium Leibovitz, 15% FBS and 2mM L-glutamine at RT.

2.6.2. Drug treatments in cells in culture

For the examination of the role of FAK's kinase activity in spindle orientation the FAK inhibitor PF-228 (Sigma) was added in HeLa and NIH3T3 cells at 10 and 5 mM for 24 hours, respectively. For the activation of the inducible FF construct in HeLa cells dexamethasone was added at a concentration of 100 nM for 3 hours. For the disruption of the astral microtubules HeLa cells were treated with 10 nM of nocodazole for 30 minutes at 37 ºC. For the disruption of the RFs, HeLa cells were treated with 0.5 μg/ml of Cytochalasin D for 1 hour at 37 ºC. For integrin blocking experiments, the P4C10 antibody (0.45 μg/ml) was added to the cells for 40 minutes at 37 ºC before fixation. For integrin overactivation experiments, cells were treated with 10 μg/ml or 50 μg/ml of RGD peptide for 1 hour, or with 0.625 μg/ml 9EG7 for 1 hour or with 10 μg/ml of RGD for 30 minutes followed by treatment with 10 μg/ml of RGD and 0.625 μg/ml 9EG7 for another 30 minutes at 37 ºC.

2.6.3. Cell transfections

HeLa, NIH3T3, FAK-/-, Cas-/- and Cas reconstituted cells were transfected using Lipofectamin 2000 (Invitrogen) whereas XL177 and A6 cells were transfected by electroporation (Invitrogen) according to the manufacturer's protocol.

2.6.4. Cell adhesion assays

2.6.4.1. Cell adhesion on substrates

Coating of charged coverslips with FN (Invitrogen) and VN (Sigma) was performed for 2 hours at 37 ^{o}C prior cell seeding. Poly-L-Lysine (PLL, Santa Cruz) coating was performed for 30 minutes at RT. In all experiments except those where parallel cell adhesion on FN, VN or PLL was performed, cells were adhered overnight on 10 μg/ml FN coated coverslips. For experiments comparing cells seeded on FN vs VN, cells were seeded on 10 μg/ml FN or 20 μg/ml VN for 4 hours before fixation. Cells on PLL were adhered for 1 hour before fixation.

Plating of the FAK-/- and HeLa cells on FN micropatterned coverslips (CYTOO) was performed according to the manufacturer's protocol.

2.6.4.2. Three-dimensional adhesion assay

The adhesion of HeLa cells between two coverslips was performed as follows: Bottom coverslips were charged, spotted with silicone grease at the edges and then coated with 50 μg/ml FN for 1 hour at 37^{o}C. Top coverslips were also charged and coated either with PLL or FN. Cells were seeded on the bottom FN coated coverslips and allowed to adhere for 15 minutes. After initial attachment and while cells were still round, the second coverslip was secured in place on top using the silicone grease spots and carefully lowered under an inverted microscope until it contacted the cells. Cells were grown for 6 hours at 37^{o}C and then were either imaged live or fixed and processed for immunofluorescence.

2.7. Immunofluorescence

2.7.1. Specificity of phospho-antibodies

The phosphospecific FAK antibodies although previously characterized were tested further for specificity. The P-Y576 FAK antibody which was used extensively was tested in FAK knockout cells where it fails to detect FAs in immunofluorescence experiments (**Figure 17A**). Additionally, 30 ng of FAK MO was injected on both blastomeres of two cell-stage embryos to knockdown endogenous FAK expression. In morphant tadpoles staining of the intersomitic

boundaries with the anti P-Y576 antibody (**Figure 17B**) is significantly reduced suggesting that the antibody is specific.

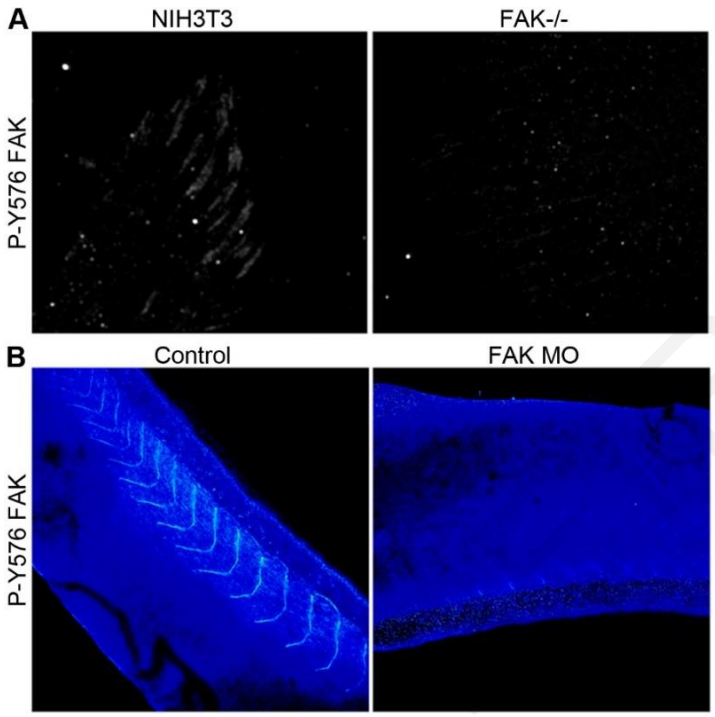

Figure 17: Specificity of the phospho-FAK antibodies.
(A) P-Y576 FAK antibody staining on NIH3T3 and FAK null cells showing no FA signal of phospho-FAK in the FAK nulls. (B) P-Y576 FAK antibody on control and FAK MO injected tadpoles showing loss of intersomitic phospho-FAK staining in the morphants.

2.7.2. Immunofluorescence in cultured cells

Immunofluorescence on HeLa, NIH3T3, XL177, A6, MDCKs, FAK-/-, Cas-/- and Cas reconstituted cells was carried out as follows: cells were washed 3 times in PBS and then fixed for 15 minutes in 4% PFA. Fixation was followed by incubation of cells in 50 mM glycine, pH 8. Then the cells were permeabilized in Triton-X solution. The concentration and time of Triton treatment was varied from 0.03% - 0.2% and 6 - 10 minutes depending on the primary antibodies and the cell lines used. Then, cells were washed 3 times in PBS and blocked in 10% Normal Donkey or Goat Serum for 30 minutes. Cells were incubated with the primary antibodies either 90 minutes RT or overnight at 4^{o}C. All primary antibodies used are listed in **Table 2**. Cells were then washed several times in PBS and incubated with secondary antibodies (**Table 3**). Staining of the F-actin was performed using phalloidin (Phalloidin 488 A12379 Invitrogen, Phalloidin 633 A22284 Invitrogen), whereas DNA staining was performed by the

use of TO-PRO 3 or Hoechst (Invitrogen). Mounting was performed in prolong gold antifade media.

When staining phosphorylated proteins, fixation was performed in the presence of 1 mM Sodium Orthovanadate. When active or total integrin β1 staining was performed, cells were blocked in 10% Normal Donkey Serum (Jackson Immunoresearch) right after glycine incubation and then incubated with the integrin antibodies before triton treatment in order to preserve the specificity of the antibodies against their epitopes for 90 minutes at RT. Cells were then washed, permeabilized using 0.03% Triton-X for 6 minutes, blocked again for 15 minutes and incubated with the primary antibodies for 90 minutes RT or overnight at 4ºC.

Primary Antibodies (IF)	**Dilution (cultured cells)**	**Dilution (*Xenopus* embryos)**
Active integrin β1 9EG7 rat (550531 BD Pharmigen)	1:250	-
Active integrin β1 HUTS-21 m (556048 BD Pharmigen)	1:250	-
atypical PKC r (sc-216, Santa Cruz)	-	1:250
β-catenin r (sc-7199, Santa Cruz)	-	1:500
β-tubulin m (E7, Hybridoma Bank)	1:250	1:250
E-cadherin m (5D3, Hybridoma Bank)	-	1:50
FAK m (05-537, Millipore)	1:500	1:200
GFP r (A11122, Invitrogen)	-	1:500
Fibronectin (4H2, provided by DeSimone Lab)	-	1:400
HA m (sc-7392, Santa Cruz)	1:500	1:100
HA r	1:500	1:250

sc-805		
Histone H3 Trimethyl Lysine 9 m (NBP1-30141, Novus)	-	1:500
integrin β1 m (8C8, Hybridoma Bank)	-	1:100
integrin β1 AIIB2 rat (Hybridoma Bank)	1:500	-
Integrin β1 K20 m (sc-18887, Santa Cruz)	1:50	-
integrin β1 TS2/16 m (sc-53711, Santa Cruz)	1:500	-
NuMA r (ab36999, Abcam)	1:500	-
Paxillin m (610569, BD Biosciences)	1:1000	1:500
Phospho-Ser10 H3 r (06-570, Millipore)	1:1000	1:500
Phospho-Ser20 Myosin light chain r (ab2480, Abcam)	-	1:500
Phospho-Ser473 Akt r (sc-7985, Santa Cruz)	-	1:300
Phospho-Tyr165 p130Cas r (4015, Cell Signaling)	1:50	1:50
Phospho-Tyr762 p130Cas r (PP1451, ECM Biosciences)	-	1:100
Phospho-Tyr416 Src r (2101, Cell Signaling)	1:100	1:100
Phospho-Tyr397 FAK r (44624G, Invitrogen)	-	1:500
Phospho-Tyr397 FAK r (ab4803, Abcam)	-	1:2000

Phospho-Tyr576 FAK r monoclonal (700013, Invitrogen)	1:200	-
Phospho-Tyr576 FAK r (44652G, Invitrogen)	1:500	1:500
Phospho-Tyr576 FAK r (sc-16563-R, Santa Cruz)	-	1:500
Phospho-Tyr861 FAK r (44626G, Invitrogen)	-	1:500
Phospho-Tyr31 Paxillin r (sc-14035, Santa Cruz)	-	1:150
Vinculin m (VN 3-24, Hybridoma Bank)	1:500	-
ZO-1 r (617300, Invitrogen)	-	1:500

Table 2: List of primary antibodies used for immunofluorescence in cells in culture and in the *Xenopus* embryos.

Abbreviations: IF, Immunofluorescence; m, mouse; r, rabbit.

Secondary Antibodies (IF)	**Dilution**
Alexa Fluor 488 anti-mouse (A11029, Invitrogen)	1:500
Alexa Fluor 488 anti-rabbit (A11034, Invitrogen)	1:500
Alexa Fluor 633 anti-mouse (A21052, Invitrogen)	1:250
Alexa Fluor 633 anti-rabbit (A21070, Invitrogen)	1:250
Cy3 anti-mouse (715-165-150, Jackson Immunoresearch)	1:500
Cy3 anti-rabbit (711-165-152, Jackson Immunoresearch)	1:500
Cy3 anti-rat	1:500

(712-165-153, Jackson Immunoresearch)	

Table 3: List of secondary antibodies used for immunofluorescence of cells in culture and in the *Xenopus* embryos.

Abbreviations: IF, Immunofluorescence.

2.7.3. Live immunofluorescence

Live imaging of active integrin β1 was performed by treating seeded cells for 30 minutes with the 9EG7 antibody (0.15 μg/ml) in media, followed by three media washes and incubation with Cy-3 anti-rat secondary antibody for 30 minutes. Cells were then washed with media and imaged.

2.7.4. Immunofluorescence in *Xenopus* embryos

Embryos were fixed in 1x MEMFA (Annex 7.2) for 2 hours at RT, permeabilized in PBST (Annex 7.2) either overnight or 5-6 hours. Embryos were dissected (AC excision or sagittal sections) at this step if necessary. Then embryos were blocked for 30 minutes in 10% Normal Donkey Serum. Primary antibodies (**Table 2**) were incubated overnight at 4 ^{o}C or 5-6 hours RT. Embryos were washed in PBST and incubated for 2 hours with secondary antibodies (**Table 3**) at RT, washed several times and post-fixed in 1x MEMFA. Clearing of the embryos was performed after methanol dehydration followed by immersing them in Murray's Clearing Medium. Immunofluorescence of *Xenopus* ACs was performed as whole mount immunostaining but the permeabilization step was for 2 hours. Immunofluorescence for the *Xenopus* pronephros was performed as whole-mount immunostaining with the difference that the tadpoles were treated with 0.01% Triton in 0.1x MMR for 3 minutes prior fixation to avoid staining of the epidermis in order to facilitate imaging of the deep tissue. FITC-labelled *Lycopersicon Esculentum* (Tomato) Lectin (1:500, Vector Labs) was used for pronephros staining together with the secondary antibodies.

2.8. Immunoprecipitation and immunoblotting

2.8.1. Protein lysates preparation

Protein lysates were prepared by homogenizing cells or embryos in ice cold RIPA lysis buffer (Annex 7.2) supplemented with phosphatase inhibitors (5 mM Sodium Orthovanatate, Na_3VO_4) and protease inhibitors (1 mM phenylmethanesulfonyl fluoride, Protease cocktail, Sigma). Homogenates were cleared by centrifugation at 15000 g for 30 minutes at 4°C for embryos or 10000 g for 5 minutes at 4°C for cells. Protein levels were determined by bicinchoninic acid assay using the Magellan™ Data Analysis software (Tecan).

2.8.2. Immunoprecipitation

Immunoprecipitation from *Xenopus* protein lysates was performed as previously described (Klymkowsky Lab Methods). For immunoprecipitation the protein lysates from embryos were prepared in MK's buffer (Annex 7.2, protease inhibitors and sodium orthovanatate). 500 µl of protein lysate was incubated with 1 µl of GFP mouse monoclonal antibody (A1120, Invitrogen) in end-over-end rotation for 2 hours at 4ºC. 30 µl of protein-G-agarose beads (Santa Cruz) were added in the lysate-antibody mix and incubated with end-over-end rotation for 2 hours at 4ºC. Beads were recovered by centrifugation for 2 minutes at 2000 rpm at 4ºC (the supernatant is the soup). The pellet was resuspended in MK's buffer and washed for 1 minute at 4ºC with end-over-end rotation. Beads were recovered by centrifugation for 2 minutes at 2000 rpm at 4ºC and washed twice with MK's buffer with 1 minute at 4ºC end-over-end rotation between the centrifugation steps. At the last centrifugation the supernatant was removed as completely as possible without disturbing the beads. Beads were spun down, resuspended in 1x SDS buffer containing β-mercaptoethanol, heated at 80ºC for 5 minutes and spun down to the bottom of the tube. The supernatant was then stored at -80ºC until use.

2.8.3. Western Blot

The lysates were loaded on 7.5% SDS-polyacrylamide gels with the WesternC ladder (Bio-Rad). The proteins were transferred onto nitrocellulose membrane, blocked in 5% BSA (Bovine Serum Albumin) (for phospho-antibodies) or 5% milk (in TBST: 1X TBS & 0.1% Tween). The blotting was performed by incubation of the primary antibodies in 3% BSA (for phospho-antibodies) or 3% milk, overnight at 4°C. The primary antibodies used are listed in **Table 4**.

Visualization was performed using HRP-conjugated antibodies (1 hour incubation RT) (1:15000, sc-2301 or sc-2302 Santa Cruz) and detected with LumiSensor (GeneScript) on UVP iBox. Densitometry analysis was carried out using the Vision Works LS Software. The analysis of the phospho-FAK signal was carried out by normalization of the phospho-FAK signal against total FAK averaging values from three independent experiments.

Primary antibodies (WB)	**Dilution**
Actin r (sc-1616, Santa Cruz)	1:1000
FAK m (2A7, Upstate Biotechnology)	1:200
FAK m (05-537, Millipore)	1:500
Fibronectin m (4H2, DeSimone Lab)	1:500
HA r (NB600363, Novus)	1:500
Paxillin m (610569, BD Biosciences)	1:5000
Phospho-Ser732 FAK r (44590G, Invitrogen)	1:500
Phospho-Tyr397 FAK m (MAB1144, Chemicon Millipore)	1:200
Phospho-Tyr397 FAK r (ab4803, Abcam)	1:3000
Phospho-Tyr576 FAK r (44652G, Invitrogen)	1:200
Phospho-Tyr576 FAK r monoclonal (700013, Invitrogen)	1:500
Phospho-Tyr861 FAK r (44626G, Invitrogen)	1:200
Phospho-Tyrosine PY20 m (sc-508, Santa Cruz)	1:250

Table 4: List of primary antibodies used for western blot.
Abbreviations: WB, Western Blot; m, mouse; r, rabbit.

2.9. Imaging

Embryos, explants and cultured cells were imaged either under a Zeiss Axio Imager Z1 microscope, using a Zeiss Axiocam MR3 and the Axiovision software 4.8, or a Zeiss LumarV12 stereomicroscope or under a laser scanning confocal LSM710 microscope (Zeiss).

2.9.1. Fluorescent Recovery After Photobleaching - FRAP

FRAP experiments were conducted using a Plan-Apochromat 63×/1.40 oil DIC M27 objective lens at the LSM 710 confocal microscope. The 488 nm and 543 nm laser lines were used for GFP and mCherry excitation respectively. Emissions of GFP and mCherry were detected between 493-538 and 600-685 nm respectively. Photobleached regions consisted of a rectangle enclosing selected FA region. Fluorescence within the rectangle was measured at lower power before bleaching and the photobleaching was carried out with full laser power, which effectively reduced the fluorescence to background levels. Recovery was followed using low laser power at various time intervals until the intensity reached a steady plateau. Negligible bleaching occurred while imaging the recovery process at low power, as verified in control experiments. Fluorescence during recovery was normalized to the prebleach intensity. Relative recovery rates were compared using half time for recovery of fluorescence towards the asymptote. The fluorescence recovery curve was fitted by single exponential function, given by $F(t)=A(1-e^{-R})+B$; where F(t) is the intensity at time t, A and B are the amplitudes of the time-dependent and time-independent terms, respectively; τ is the lifetime of the exponential term (time constant); and the recovery rate is given by $R=1/\tau$. Immobile fractions were calculated by comparing the intensity ratio in the bleached area just before bleaching and after recovery. Analysis of the results was performed using the ZEN2010 software.

2.9.2. Fluorescence Loss In Photobleaching - FLIP

For the FLIP experiments photobleached regions consisted of a rectangle enclosing the selected region of the cell which was repetitively photobleached during the experiment. Analysis of the results was performed using the ZEN2010 software.

2.9.3. Time lapse imaging of cell divisions in the presence or absence of mechanical tension.

Live imaging of cell divisions described in **Figure 76** was performed as mentioned below. Imaging of gastrula embryos under conditions of reduced tension was performed by placing the embryos on a drop of vaseline in a slide with a 2 mm silicone gasket and held in place by a glass coverslip, which was not in contact with the embryo. Optical sections were acquired every 2 minutes for a 40 minute period. Imaging of embryos under conditions of increased tension was performed by placing the embryos in a slide with a 1 mm silicone gasket, applying in this way external mechanical force directly on the embryo and imaged as described above.

2.9.4. Laser ablations

Laser ablation experiments were conducted using the LSM 710 confocal microscope and a Plan-Apochromat 63×/1.40 oil DIC M27 objective lens (Zeiss). An early mitotic cell was selected and an image was acquired to determine the orientation of the division axis. For the data presented in **Figure 78**, wounds were performed in the two neighboring cells in the axis perpendicular to the long axis of the spindle by using the 488 and 543 nm laser lines simultaneously, 50 iterations at 100% power and the mitotic cell was imaged every 15 seconds until the beginning of cytokinesis. For the data presented in **Figure 79** laser ablations were contacted as described above with the differences that the embryos were placed in high salt solution (0.33x MMR) and only one cell near the mitotic cell was ablated in order to create a smaller wound that will not cause severe cell deformation.

2.10. Image and statistical analysis

All intensity profiles and color coded images were generated by using the ZEN2010 software. All graphs constructed and the statistical analysis of the data was performed by using Image J, Adobe Photoshop, GraphPad, office Microsoft excel 2013 and MATLAB.

2.10.1.Spindle angle in Z-axis and XY plane

Quantification of the orientation of the division axis of metaphase cultured and epithelial cells was carried out with ImageJ using the Z-projections of the images. The angle between the line connecting the two spindle poles and the line extending from the one spindle pole parallel to

the substrate was measured. Quantification of spindle orientation in the cells of the outermost cell layer of the *Xenopus* epithelium was carried out as described above, by measuring the angle between the line connecting the two spindle poles and the line extending from the one spindle pole parallel to the apical surface of the cell.

Quantification of spindle orientation at the XY plane was performed by measuring the angle formed between the line connecting the two spindle poles and the long axis of the micropattern in cultured cells or the long axis of the cell in epithelia. Statistical analysis including analysis of variance and two-tailed unpaired t-test for parametric distributions and Kruskal–Wallis and Mann–Whitney tests for non-parametric distributions and graph construction was performed by the GraphPad software.

2.10.2.Spindle size

The spindle size was determined by measuring the length and width of the mitotic spindle of metaphase cells. Maximum intensity projections were used for the measurements. The width was measured at the widest point of the mitotic spindle, usually at the center of the spindle. As in the 3D, the spindle angle must also be considered and the actual length corresponds to the hypotenuse of the right triangle that connects the two poles, we calculated the length of the mitotic spindle as cosα/A, where α is the average spindle angle and A the length of the spindle in the maximum intensity projections. This process was performed both in control and experimental samples.

2.10.3.Spindle centering

Spindle centering was calculated by measuring the distance from each spindle pole of a metaphase cell to the nearest point at the cell cortex and then the distance with the greatest value was divided by the distance with the smallest value. Off-center spindles were defined when the above ratio was greater than 1.5.

2.10.4.LGN and active integrin β1 cortical crescent

The correlation of the spindle poles to the LGN cortical crescent was performed by measuring the angle formed between the line connecting the center of the metaphase plate perpendicularly to the cell cortex and the line extending from the center of the LGN cortical crescent towards

the center of the metaphase plate. The spindles that displayed an angle between 30^{o} and 90^{o} were considered as uncoupled with the LGN cortical localization.

The correlation of spindle orientation to the active integrin β1 cortical polarity crescent was performed by measuring the angle formed between the line connecting the center of the metaphase plate perpendicularly to the cell cortex and the line extending from the center of the active integrin β1 cortical crescent towards the center of the metaphase plate. The angular distribution plot was constructed by using MATLAB.

2.10.5. Spindle rotation

For the average degree of spindle rotation in *Xenopus* embryos, the angle between the long axis of the spindle at the first time point and the next time point was measured. In order to calculate the average number of spindle rotations per frame, for each metaphase cell, the number of rotations above 20^{o} was counted and divided by the number of total rotations. The frequency was calculated by dividing this result with the time interval between the frames.

The quantification of the spindle rotation after laser ablation was performed by measuring the angle between the final division axis before cytokinesis and the axis of the induced tension which corresponds to the long axis of the cell after it changes its shape. The frequency of the above spindle angle was calculated as the number of divisions that had a spindle angle in the indicated categories divided by the total number of divisions.

2.10.6.Cell shape – spindle angle correlation

The correlation between cell shape and spindle angles was evaluated by measuring the length and width for each cell as well as the angle of deviation of each spindle from the cells long axis. For the statistical analysis both Kruskal–Wallis and Mann–Whitney tests were performed between controls, FAK MO and nocodazole treated cells comparing all values or after setting a length to width ratio (L/W) threshold of three.

2.10.7. *Xenopus* pronephros thickness

The average thickness of the *Xenopus* distal pronephros was quantified by measuring the thickness of the pronephros in 20 different areas of the distal part in each embryo by using the

Zen2009 Light Edition Software. The average thickness in each embryo was used for the two-way analysis of variance test to compare the thickness in control and experimental samples.

2.10.8. Spindle angle – active integrin β1 correlation

The correlation of spindle misorientation with the levels of integrin β1 cortical activation was performed by measuring the spindle angle and the ratio of basal to mid-lateral cortex intensity of active integrin β1 for each metaphase cell. Pearson correlation coefficient (r) was calculated for the two variances, where $-1 < r < 1$ and graphs were constructed in Microsoft Excel 2013.

3. Chapter I

3.1. Introduction Chapter I

3.1.1. *Xenopus* embryonic development

3.1.1.1. *Xenopus laevis* as an experimental model

Xenopus, the African clawed frog, has been widely used for many years as an experimental model not only for early vertebrate development but also for basic cell and molecular biology, neurobiology, toxicology and as a model for human diseases. There are two species of *Xenopus*, *Xenopus laevis* and *Xenopus tropicalis*. *Xenopus laevis* exhibits several advantages in comparison to other vertebrate model systems, making it ideal for studies in the above research areas. *Xenopus* females can be easily induced with simple hormone injection (hCG) to lay eggs repeatedly in a controlled manner. Large amount of eggs can be collected from the same frog several times per day allowing high throughput biochemical studies. Fertilization takes place *in vitro*, with a slight mixing of the sperm with the oocytes. The ability to manipulate the time of fertilization is crucial for further experimental procedures, since *Xenopus* embryonic development is synchronized providing the ability to acquire a large number of embryos of the same stage. Moreover, oocytes are large (diameter approximately 1.4 mm) allowing extensive micromanipulation, microinjections and microdissections. The eggs are maintained in simple media since they develop externally and they contain high percentage of yolk at their vegetal side which is sufficient for their growth. Embryos grow fast and develop into a tadpole (whole organism with fully functional organs and systems) only in a couple of days upon fertilization (Hazel L. Sive 2000) (**Figure 18**). One of the greatest advantages of *Xenopus* as an experimental model of embryogenesis is its well characterized fate map, which means that from early on, the cell fate of each embryonic cell is known allowing targeted loss and gain of function experiments in specific tissues. Gain of function approaches include overexpression of either proteins that can be found endogenously or constructs that encode constitutively active forms of the protein of interest by injecting the mRNA encoding the protein in question. Loss of function approaches include either injection of mRNA encoding DN constructs, or morpholino oligonucleotides (MOs), which are DNA analogues that block either translation or splicing, or the more recently developed approaches Transcription Activator-Like Effector Nuclease (TALEN) and Clustered Regularly Interspaced Short Palindromic Repeats (CRISPR) that target directly the genomic DNA of the protein of interest (Wang, Shi et al. 2015). The main drawback

of *Xenopus laevis* is its pseudotetraploid genome which in combination with long generation time make genetic manipulation quite challenging (Hazel L. Sive 2000).

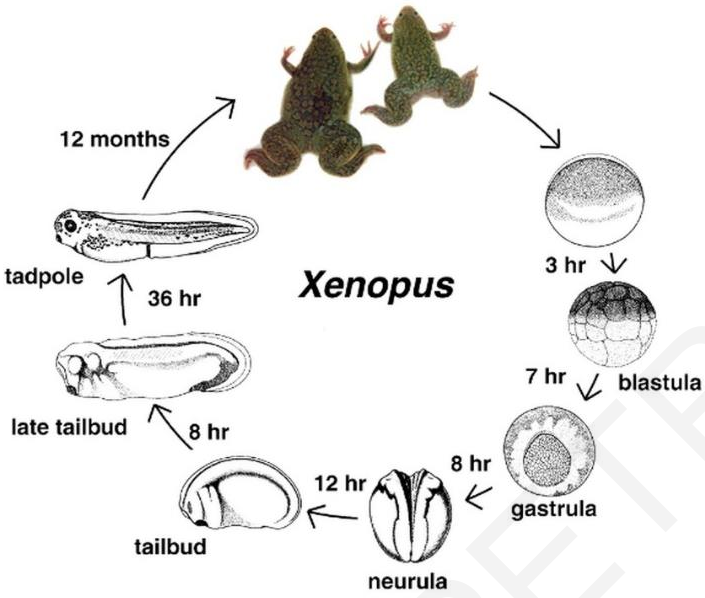

Figure 18: Main developmental stages of *Xenopus* embryonic development and metamorphosis.
Adapted from Xenbase, http://www.xenbase.org/anatomy/intro.

3.1.1.2. Developmental stages of *Xenopus* embryogenic development

From oocyte to zygote:

Xenopus oocytes are surrounded by two types of ECM. The vitelline membrane which is in direct contact with the egg and the outer jelly coat layers (Olson and Chandler 1999). Moreover, they display animal – vegetal polarity with the animal pole (AP) showing pigmentation and the white vegetal pole (VP) containing the yolk (Hazel L. Sive 2000). During fertilization only one sperm enters the animal region leading to a sudden increase of calcium. This leads to the exocytosis of cortical granules at the surface of the egg and to the lifting of the vitelline membrane. As a consequence, the zygote can now rotate freely under the effect of gravity, which leads to the upward rotation of the AP. As a result, cortical rotation takes place by 30º, the peripheral cytoplasm is rearranged and the future dorsal side of the embryo is determined (opposite from the sperm entry site) (Whitaker 2006). The development of the embryos until the basic body plan is determined, involves three main stages. The first is called cleavage-blastula, gastrulation and neurulation.

Cleavage and blastula formation:

Approximately 2 hours after fertilization the first cleavage takes place. In the amphibian embryo, the first cleavage starts at the AP and extends slowly to the VP due to the high amounts of yolk that it contains. The first cleavage divides the embryo into left and right (determines the left-right axis, L-R), whereas the second one is again vertical but perpendicular to the first and determines the dorsal-ventral (D-V) axis. The third division separates the AP from the VP (Elinson 2011). The cleavages continue until the blastula stage creating inner and outer cells with different fates due to controlled orientation of the mitotic spindle, where the spindle either becomes oriented parallel or perpendicularly to the apical surface. Spindle orientation of the *Xenopus* blastomeres is determined by the shape of the cells, where they divide along their long axis (Strauss, Adams et al. 2006). During the cleavages a cavity filled with fluid, called the blastocoel, is formed from the first division, expands until blastula stage and it is sealed from the outside with tight intracellular junctions (Fesenko, Kurth et al. 2000). The *Xenopus* blastula wall is multilayered in all regions but it varies in thickness. The blastocoel wall at the top animal part (blastocoel roof - BCR) is a multilayered epithelium which has one outer and two inner cell layers, where the outer blastomeres show apicobasal polarity (they contain tight junctions) and the inner blastomeres are intimately attached to the outer layer without an intervening basal lamina (Shook and Keller 2003). The BCR is covered by a rich FN matrix that is essential for gastrulation (Winklbauer and Keller 1996). This wall thickens towards the marginal zone (MZ) and is distinct from the vegetal mass (Winklbauer 2009). At mid-blastula stage, mid-blastula transition occurs, which is the beginning of the zygotic genome transcription. At late blastula stages the animal cap (AC- the animal top part of the AP) is fated to become epidermis, the MZ will give rise to mesodermal tissues and the VP will give rise to endodermal tissues (**Figure 19**) (Hazel L. Sive 2000).

Gastrulation:

During gastrulation several morphogenetic movements take place simultaneously leading to massive cell rearrangements so as the three germ layers (ectoderm, mesoderm, endoderm) acquire the proper positions in the developing embryo (**Figure 19**). Ectoderm, the exterior germ layer, forms the skin, nervous system, lens, ears, and cement gland. Mesoderm, the middle germ layer, forms the gastrointestinal tract, notochord, somites, kidneys, blood, blood vessels, heard, gonads and limbs. Endoderm, the most internal germ layer, forms the epithelial layer of the gastrointestinal tract, lungs, liver, and bladder. The first sign of gastrulation is the appearance of the elongated endodermally derived bottle cells (a condensed area of pigmentation on the

dorsal side of the embryo) responsible for the morphogenetic movement of invagination through which they form the blastopore lip (**Figure 19**). Involution of the dorsal marginal zone (DMZ) begins at the blastopore lip, while the prospective mesoderm (deep involuting layer) and endodermal cells (superficial involuting area) become internalized. The outcome of the involution is the positioning of the mesodermal and endodermal precursors along the future D-V and A-P axis (Winklbauer 2009). Invagination and involution progress to the lateral tissues and to the ventral side where now the blastopore forms a full circle at the vegetal side of the embryo. While blastopore closes, the mesoderm and endoderm are completely internalized and the blastocoel is replaced by the archenteron, a cavity that begins to form dorsally during involution and expands throughout gastrulation (Hazel L. Sive 2000) (**Figure 19**). The vegetal mass contributes to internalization by undergoing vegetal rotation, a movement by which the vegetal cells surge animally and outwards (Winklbauer and Schurfeld 1999). Concomitant with the involution steps, morphogenetic movements of the involuting mesoderm take place so as mesodermal progenitors will become properly positioned along the A-P axis that will lead to elongation of the embryo along this axis. Mesoderm cells undergo mesodermal migration where they extend lamellipodia and migrate as a multilayered coherent cell mass on the FN matrix of the BCR that provides directional information (Winklbauer, Nagel et al. 1996). In *Xenopus*, A-P axis elongation is an integral part of gastrulation, where the presumptive notochord (dorsal section of the IMZ – involuting marginal zone) and somitic mesoderm (lateral section of the IMZ) rearrange by mediolateral and radial intercalation in order to lengthen and narrow the involuting tissue. This movement is called convergent extension (CE), and starts during involution contributing to blastopore closure and continues to tailbud stages (Winklbauer 2009) (**Figure 19**). During CE, IMZ cells display mediolaterally polarized protrusive activity that allows convergence along the mediolateral axis and extension along the future A-P axis (Keller, Shook et al. 2008). Similarly, CE occurs at the BCR in the future central nervous system so as the neuroectodermal tissue will elongate in the same manner (Keller, Shih et al. 1992). Finally, while mesoderm and the endoderm become internalized, the morphogenetic movement of epiboly takes place concurrently, where the prospective ectoderm thins, spreads and moves towards the vegetal pole so as it will encompass the entire embryo by the end of gastrulation (**Figure 19**) (Keller 1980).

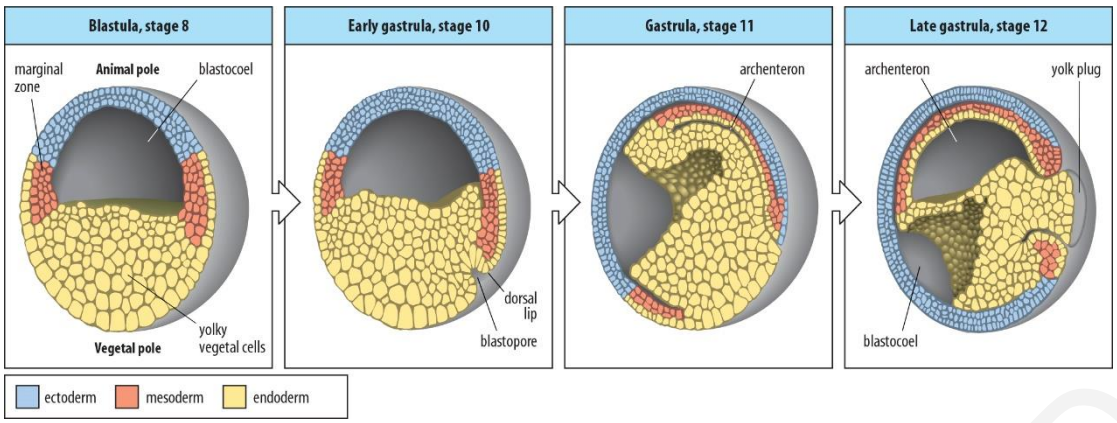

Figure 19: *Xenopus* gastrulation.

At blastula stage the AC at the AP consists of three cell layers, the MZ (prospective mesoderm) is in the middle and the vegetal mass (prospective endoderm) resides at the VP. The AP is separated from the vegetal mass by a fluid containing cavity, the blastocoel. Gastrulation begins with the formation of the blastopore lip at the dorsal side of the embryo, where mesoderm involutes, migrates towards the AC through integrin-FN interactions and at the same time it undergoes CE leading to thinning and lengthening along the future A-P axis. Mesoderm involution leads to the formation of a cavity, called the archenteron which expands during gastrulation and replaces the blastocoel. As gastrulation proceeds, the blastopore is formed laterally and eventually ventrally and together with the morphogenetic movement of epiboly (spreading of the ectoderm towards the blastopore) is closes to engulf the mesoderm and endoderm.

Adapted from http://www.mun.ca/biology/desmid/brian/BIOL3530/DEVO_03/devo_03.html.

As mentioned above, the *Xenopus* BCR at blastula stage consists of three epithelial cell layers, a superficial cell layer and two deep cell layers. During *Xenopus* epiboly, the superficial cells flatten and spread towards the blastopore, while the deep cells extend protrusions towards each other and intercalate by local migration so that by early gastrula they consist of a single cell layer. Epiboly starts at the BCR and is expanded towards the MZ (**Figure 20**) (Keller 1980). It is believed that the guiding cue for epiboly is the FN fibrillar matrix that resides beneath the innermost cell layer (Marsden and DeSimone 2001).

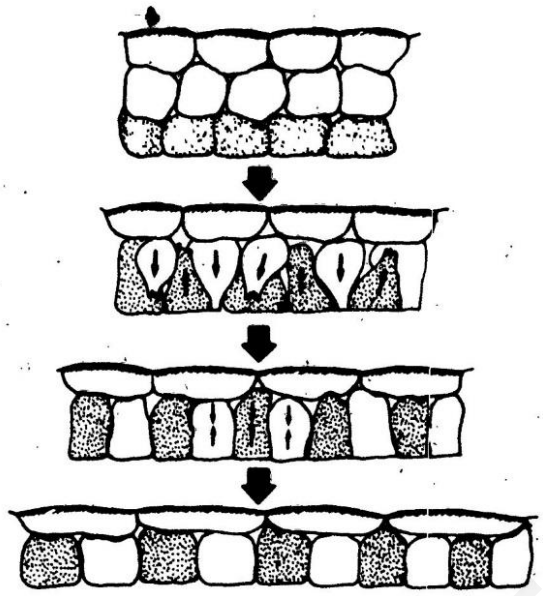

Figure 20: Epiboly of the *Xenopus* BCR.

The three-cell layered BCR at the AC becomes two cell-layered due to radial intercalation of the inner epithelial layers. At the same time, cells acquire a flattened and spread morphology. Adapted from (Keller 1980).

FN matrix assembly is an essential process for vertebrate development and FN fibrillogenesis at the BCR is quite similar to the *in vitro* mechanisms that were shown to regulate this process. As described above, FN matrix assembly in cells in culture is mediated by the FBs, while during their formation the α5β1 integrin receptor is translocated form the FAs towards the cell center by transforming the sustained actomyosin-generated tension of the FAs into directed movement along the actin filaments (Pankov, Cukierman et al. 2000). Their formation is linked to changes in cell shape leading to conformational changes in the FN molecule promoting the elongation of the FN fibrils and FN matrix assembly. Their translocation stretches the FN molecules and promotes FN-FN interactions necessary for the fibrillogenesis. Also, FN fibrillogenesis is promoted by cytoskeletal tension, where Rho-mediated contractility exposes cryptic sites of FN to promote the intermolecular interactions (Zhong, Chrzanowska-Wodnicka et al. 1998) and requires integrin activation (LaFlamme, Thomas et al. 1994) (**Figure 21**).

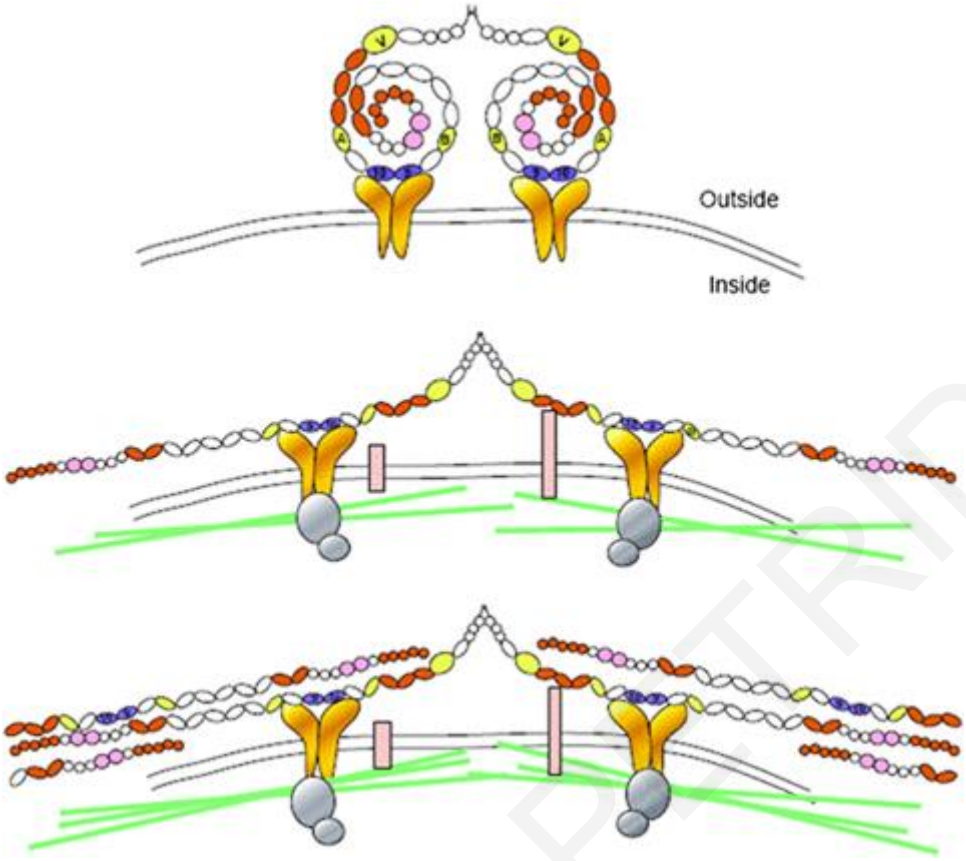

Figure 21: FN fibrillogenesis in cells in culture.

Compact soluble FN binds integrin α5β1 leading to reorganization of the actin cytoskeleton. Cell contractility induced by actin rearrangements exposes cryptic sites on the FN molecule in order to acquire an extended conformation and to promote matrix assembly through FN-FN interactions. Adapted from (Henderson, Nair et al. 2011).

FN fibrillogenesis in the *Xenopus* BCR shares common mechanisms with the *in vitro* situation such as the necessity of integrin binding, since it is inhibited by RGD peptides, and proper actin cytoskeleton. Moreover, FN fibrillogenesis in *Xenopus* is blocked by expression of its N-terminal domain which is required for the FN-FN interactions that take place during matrix assembly (Winklbauer and Stoltz 1995). Matrix assembly on the BCR starts at the onset of gastrulation as a cell autonomous process, which is prevented by cell-cell contact. Although the cells require free cell surface, at the same time they must be a part of a larger cohesive tissue so as they can provide the required mechanical forces in order to properly generate the matrix (Winklbauer 1998). Proteins of the FA complex were shown to regulate FN matrix assembly in *Xenopus*. Loss of FAK function using its DN FRNK led to reduced FN matrix assembly on the BCR in *Xenopus* embryos (Kragtorp and Miller 2006) and overexpression of the tyrosine phosphatase PTP-PESTr also prevented fibrillogenesis on the BCR (Cousin and Alfandari 2004). In addition, FN matrix assembly in *Xenopus* was shown to be regulated by cytoskeletal

tension through filamentous actin (Winklbauer and Stoltz 1995, Davidson, Dzamba et al. 2008) and by mechanical tension through morphogenetic events (Dzamba, Jakab et al. 2009).

At the organismal level, the tension experienced by the cells is not derived only by endogenous or exogenous cytoskeletal forces but also by mechanical forces created during morphogenesis (Davidson 2011). During vertebrate embryogenesis, especially during gastrulation, morphogenetic movements alter mechanical tension. For example, radial intercalation likely releases tension from the embryo, whereas bottle cell formation increases tension. All morphogenetic movements require tight regulation of force production and mechanical resistance to these forces in order to be coordinated and drive morphogenesis. Mechanical failures during morphogenesis, such as insufficient force or elevated mechanical resistance, lead to developmental defects (Davidson 2011). As a result, in a multilayered sheet the tension that promotes FN fibril assembly is likely generated by different mechanisms from that in cultured cells. For example, increased or decreased mechanical force were shown to promote or inhibit FN fibril assembly in the BCR, respectively (Dzamba, Jakab et al. 2009).

The DeSimone group initially showed by injecting FN function-blocking antibodies in the blastocoel that the matrix is required for the morphogenetic movement of epiboly. Specifically, loss of FN fibrils resulted in a thick multilayered AC with misoriented cell divisions, suggesting that the FN matrix provides a polarizing signal that orients these cells to intercalate radially and divide in a certain orientation (Marsden and DeSimone 2001) (**Figure 22**).

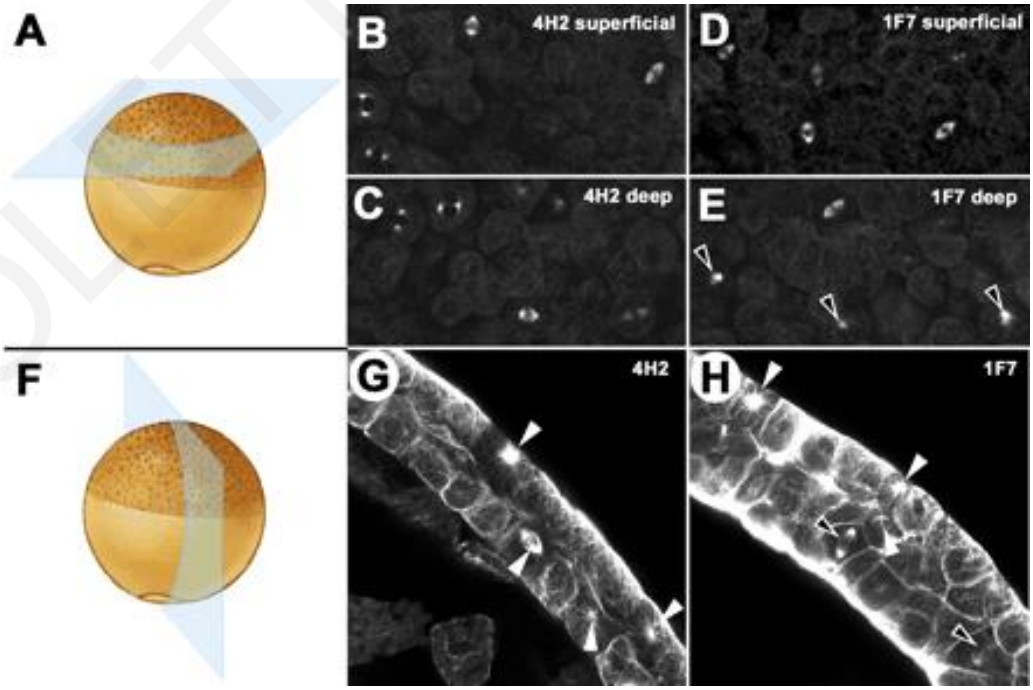

Figure 22: Disruption of FN fibrillogenesis in *Xenopus* results in AC thickening and spindle misorientation. AC views either from the BCR (upper panel) or from the side (lower panel) from embryos treated either with a FN non-functional antibody (4H2) or a FN blocking antibody (IF7). Inhibition of FN fibrillogenesis leads to spindle misorientation of the cells of the inner epithelial layer of the AC and to the thickness of the AC more than two cell layers. Adapted from (Marsden and DeSimone 2001).

The existence of a polarity signal became evident in radial intercalation explants, where the dorsal non-involuting MZ (NIMZ) from two different embryos were dissected and placed the one on top of the other either adhering either on FN or BSA. When the explant was in contact with the FN matrix, intercalation of the top cells towards the substrate took place, whereas this was absent when the explant was in contact with BSA. These results suggested that a FN-derived polarity signal can instruct cells at a distance to intercalate radially. Importantly, loss of integrin β1 function by the use of an integrin DN resulted in a similar phenotype suggesting that FN-integrin interactions are necessary for the transduction of this polarity signal (Marsden and DeSimone 2001). Further studies confirmed these results either using FN MOs or more interestingly, the DN construct FN 70KD (Davidson, Marsden et al. 2006, Rozario, Dzamba et al. 2009). Although the use of this DN disrupted FN fibrillogenesis but at the same time maintained the FN-integrin interactions necessary to promote cell polarization, it led to radial intercalation failure indicating that the FN-integrin interactions are not sufficient to promote cell polarity, but rather the physical state of the matrix is. This raised the possibility that the FN matrix also has a structural role in the embryo by which it generates and maintains tension to regulate radial intercalation (Rozario, Dzamba et al. 2009). Thus, defective radial intercalation may be attributed not only to abnormal FN-integrin interactions that promote cell polarization but also to defective transduction of mechanical tension during embryogenesis that may lead to loss of polarization.

Besides epiboly, FN was also shown to regulate cell polarity during CE by orienting the cellular protrusions of the DMZ cells (Davidson, Marsden et al. 2006). Also, fibrillar FN remodeling along the somitic mesoderm/endoderm boundary and at the notochord/somitic mesoderm boundary is important during gastrulation and neurulation (Davidson, Keller et al. 2004).

Neurulation and organogenesis:

Neurulation begins at the end of gastrulation, and is the process by which the neural tube and neural crest cells are formed. The ectoderm at the dorsal side of the embryo, thickens and undergoes cell shape and cell adhesion changes so as the neural folds form, elevate, converge towards the midline and eventually fuse to form the neural tube. The cells at the tips of the

neural folds lie between the neural tube and the underlying epidermis and become neural crest cells (Hazel L. Sive 2000). During neurulation, both the neural ectoderm and the underlying mesoderm undergo CE and A-P axis elongation is now more prominent (Keller, Shih et al. 1992).

At the end of neurulation, the early tailbud keeps elongating along the A-P axis through CE and at the same time organogenesis takes place including the somites, the pronephros, the heart, neural development (spinal cord, hindbrain, midbrain, forebrain) and vascular development. *Xenopus* somitogenesis is the process by which the paraxial mesodermal cells are subdivided in repeating units called the somites (Pourquie 2001). Somitogenesis is a wave-like process while the embryo extends posteriorly producing the somites one by one from the anterior towards the posterior side. The paraxial mesodermal cells elongate perpendicularly to the notochord and narrow along their A-P axis (Wilson, Oster et al. 1989). Each somite rotates 90^{o} relative to the A-P axis and individual somites become single blocks of spindle-shaped cells that lie parallel to the notochord (Keller 2000). FA proteins were found to have a role in *Xenopus* somitogenesis including FAK, Ena/Vasp, FN and integrins (Kragtorp and Miller 2006, Kragtorp and Miller 2007). Another mechanism shown to contribute to A-P axis elongation is apoptosis in the notochord which correlates with notochord extension through vacuolization (Malikova, Van Stry et al. 2007). The development of the vasculature system in *Xenopus* in achieved through two processes; vasculogenesis and angiogenesis. During vasculogenesis the endothelial tube and the primary vessels are generated through migration of the angioblasts from the lateral plate mesoderm and differentiation into endothelial cells. Angiogenesis promotes the sprouting of new vessels from the primary vessels and their remodeling (Hanahan 1997).

3.1.2. The role of FAK during *Xenopus* embryonic development

The temporal and spatial expression patterns of FAK are well studied. Northern blot analysis showed that there is maternal mRNA and that its levels decrease during cleavages until the mid-blastula stage (stage 7-9), whereas at the onset of gastrulation they increase (stage 9-10.5). At late gastrula (stage 12.5), the levels of FAK mRNA decrease again. This reduction continues until neurulation (stage 20), while at tailbud (stage 26) and tadpole stages (stage 33-34) FAK mRNA levels are steadily increasing (Zhang, Wright et al. 1995). The same pattern is valid for the levels of protein expression of FAK with an exception at neurula stage, where protein levels are stable, instead of decreasing, until stage 35 (Hens and DeSimone 1995). FAK is ubiquitously expressed and immunohistochemical techniques showed that during gastrulation,

FAK is enriched at mesoderm, ectodermal MZ and in the cells of the BCR, whereas during stages 21-22 and onwards, it is mainly expressed in the somites. FAK activation (phosphorylated on Tyr397) is initially detected at the onset of gastrulation and it remains until stage 35 (Hens and DeSimone 1995). Whole-mount ISH showed that FAK is enriched in the central nervous system (head, retina, lens, rhombomeres, forebrain, midbrain, hindbrain). The above expression patterns indicate that FAK functions through integrin dependent signaling since these areas are subjected to cell migration events through cell-ECM interactions (Hens and DeSimone 1995). It has been shown in *Zebrafish* that FAK is expressed throughout the duration of early development but it displays three different phases according to its phosphorylation status: Primarily, during the first cleavages and during gastrulation, FAK is unphosphorylated and inactive. Then, during the segmentation stage (division of mesoderm into somites) FAK is moderately phosphorylated. Finally, FAK has its maximal phosphorylation after the segmentation. Activated FAK (P-Tyr397) in *Zebrafish* is first seen at the end of gastrulation (Henry, Crawford et al. 2001), whereas in *Xenopus* it is detectable from the onset of gastrulation (Hens and DeSimone 1995) and in mice, after the late mid-gestation stage (Corsi, Houbron et al. 2009). Whole-mount ISH in *Zebrafish* has showed that activated FAK is clearly present at the notochord periphery, where the cells of the notochord make adhesive contacts with the ECM surrounding the notochord, at the recently formed somite boundaries and at the intersomitic furrows (Henry, Crawford et al. 2001).

Functional studies showed that FAK regulates a variety of developmental processes during *Xenopus* embryogenesis. In *Xenopus*, FRNK expression is not detectable, neither at the mRNA, nor at the protein level (Hens and DeSimone 1995) however, FRNK was used as a DN in *Xenopus* embryos during somitogenesis. It has been reported that injection of 500pg of FRNK can act as a DN, and cause a significant decrease in autophosphorylation of FAK at the stage of somitogenesis. Moreover, overexpression of FRNK leads to defects in somite formation such as disruption of intersomitic boundaries *in vivo* probably due to impaired FN matrix assembly, cell adhesion and migration (Kragtorp and Miller 2006). This is in agreement with a study by Stylianou et al., in which injection of 500pg of FRNK in the DMZ of four-cell stage embryos followed by dissection and dissociation of the DMZ at late blastula stage and then plating on FN coated wells, led to failure of spreading and migration of FRNK overexpressing cells (Stylianou and Skourides 2009).

In the first study attempting FAK downregulation in *Xenopus* using antisense MOs, it was shown that the major phenotype of FAK morphant tadpoles was pronounced pericardial edema, cardiac dysmorphogenesis and lethality by stage 42. Embryonic hearts from morphant embryos

exhibited bent heart tubes that failed to undergo the process of looping morphogenesis. Detailed characterization of the phenotype revealed that defective cardiogenesis is not a result of cell differentiation, migration and fusion of the cardiac precursors but rather due to reduced myocyte proliferation in the heart tubes in response to fibroblast growth factors and other cardiotrophic factors. Moreover, these embryos also exhibited anterior defects (diminished head size) and shortening of the A-P axis (Doherty, Conlon et al. 2010). The fact that FAK downregulation in *Xenopus* resulted in defects in heart morphogenesis is in agreement with the phenotype of the FAK knockout mice which display extensive defects in the formation of the heart and the vasculature. However, it is quite surprising that no earlier phenotypes were observed which were expected from the early embryonic lethal phenotype of the FAK null mice (Furuta, Ilic et al. 1995), probably explained by the insufficient downregulation of FAK in earlier stages (Doherty, Conlon et al. 2010).

An independent study using a different FAK MO and a combination of splice-blocking FAK MOs lead to more effective FAK downregulation at neurula stages and revealed that FAK downregulation leads to increased expression of anterior neural markers and reduced posterior neural markers resulting in embryo anteriorization. This anteriorized phenotype is accompanied by short A-P axis and inhibition of neural plate folding and CE. This study also showed that Wnt3a acts downstream of FAK signaling to regulate A-P cell fate specification in the developing neural plate (Fonar, Gutkovich et al. 2011). A more recent study used another FAK MO that effectively downregulated FAK at gastrula stages. FAK morphant embryos displayed several defects during gastrulation, neurulation, A-P axis elongation and somitogenesis. However, the most prominent defect was in the speed and persistence of mesendoderm single and collective cell migration, attributed to defective cell spreading and reduced traction forces in FAK morphant cells. FAK morphant cells displayed disorganized keratin filaments and impaired interaction between pakoglobin and cadherin possibly contributing to defective coordination of collective mesendoderm migration (Bjerke, Dzamba et al. 2014).

3.2. Results Chapter I: FAK regulates embryonic development in *Xenopus* during gastrulation and organogenesis through different mechanisms

3.2.1. Expression and phosphorylation pattern of FAK during *Xenopus* early development

As a first approach to gain insight into the function of FAK during *Xenopus* embryonic development, we initially examined the expression, localization and activation pattern of endogenous FAK during different developmental stages of *Xenopus* embryogenesis. *Xenopus* FAK was originally cloned by Zhang et al. and its expression was analyzed in detail by the DeSimone group (Hens and DeSimone 1995, Zhang, Wright et al. 1995). It was determined that FAK is expressed maternally and that elevated levels are found in the highly mophogenetically active mesodermal tissues. In addition, FAK was enriched at the intersomitic boundaries which also display enriched integrin expression and deposition of ECM proteins such as FN (Kragtorp and Miller 2006, Kragtorp and Miller 2007). Additionally, increased levels of expression and phosphorylation of FAK were observed during gastrulation indicating that FAK may be involved in regulating embryonic cell adhesive behavior and morphogenesis (Hens and DeSimone 1995, Zhang, Wright et al. 1995). We initially performed detailed characterization of the spatiotemporal expression and phosphorylation of FAK. We examined the endogenous levels of the main phosphorylation sites of FAK, tyrosines 397, 576 and 861 by western blotting (**Figure 23**) using previously characterized antibodies against the phosphorylated forms of the above sites. As shown in **Figure 23**, all three sites are phosphorylated in all developmental stages we examined including pre-gastrula stages. Phosphorylation of Tyr397 follows a similar pattern to what was reported by Hens and DeSimone for total phospho-FAK, i.e. phosphorylation increases during development with an increase observed during gastrulation (Hens and DeSimone 1995). A similar increase is observed for phosphorylation of tyrosines 576 and 861 however, for these two sites a drop is observed during neurulation (**Figure 23**).

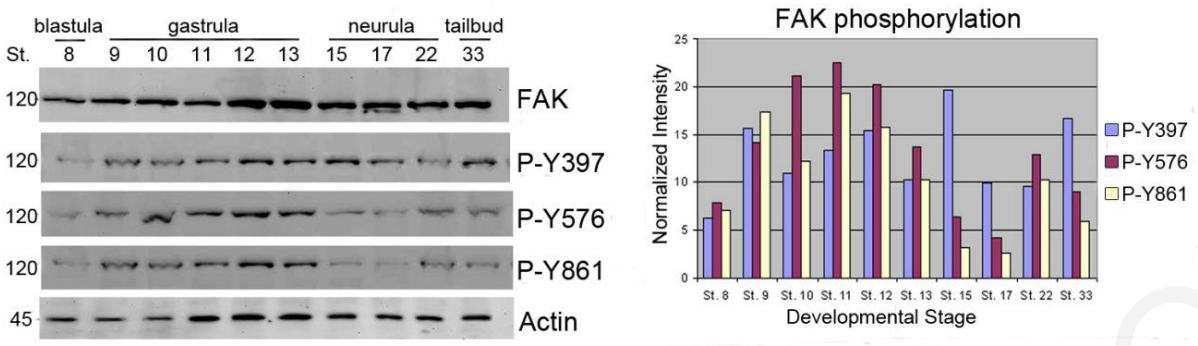

Figure 23: FAK expression and phosphorylation pattern during *Xenopus* development.
Western Blots from extracts of equal numbers of embryos probed with antibodies against the C-terminus of FAK or against the phosphorylated tyrosine residues indicated. FAK is phosphorylated on all three residues before and after gastrulation. The intensity values from the densitometry analysis of the western blots were normalized against total FAK amount.

Moreover, whole mount indirect immunofluorescence against the above phospho-tyrosine sites of FAK shows that phosphorylated active FAK is localized at the plasma membrane of the cells (**Figure 24**) suggesting that FAK activation takes place at the plasma membrane as expected from the distribution of integrins in these cells (Joos, Whittaker et al. 1995) and its FA localization in adherent cells (Mitra, Hanson et al. 2005). Elevated levels of phosphorylated FAK were seen in the highly morphogenetic mesodermal tissues suggesting a possible involvement of FAK in these movements (**Figure 24**, white arrowheads), again as expected from the well known role of FAK in cell migration. Moreover, this is supported by the fact that FAK has crucial roles in mesodermally derived tissues as is evident from the early lethality of the FAK null mice due to generalized mesodermal defects (Furuta, Ilic et al. 1995). The fact that FAK null mice in which a KD mutant of FAK (K454R) was introduced display similar defects in the mesodermally derived tissues (Lim, Chen et al. 2010) is in agreement with the enriched phosphorylation of FAK in the mesoderm of *Xenopus* embryos, highlighting kinase activity dependent roles of FAK. Examination of the localization pattern of a downstream target of active phosphorylated FAK, the tyrosine phosphorylated FA protein paxillin (Tyr31) at these stages, reveals a similar pattern to that of phosphorylated FAK (**Figure 24**) supporting integrin dependent activation of FAK in the mesoderm of *Xenopus* early embryos.

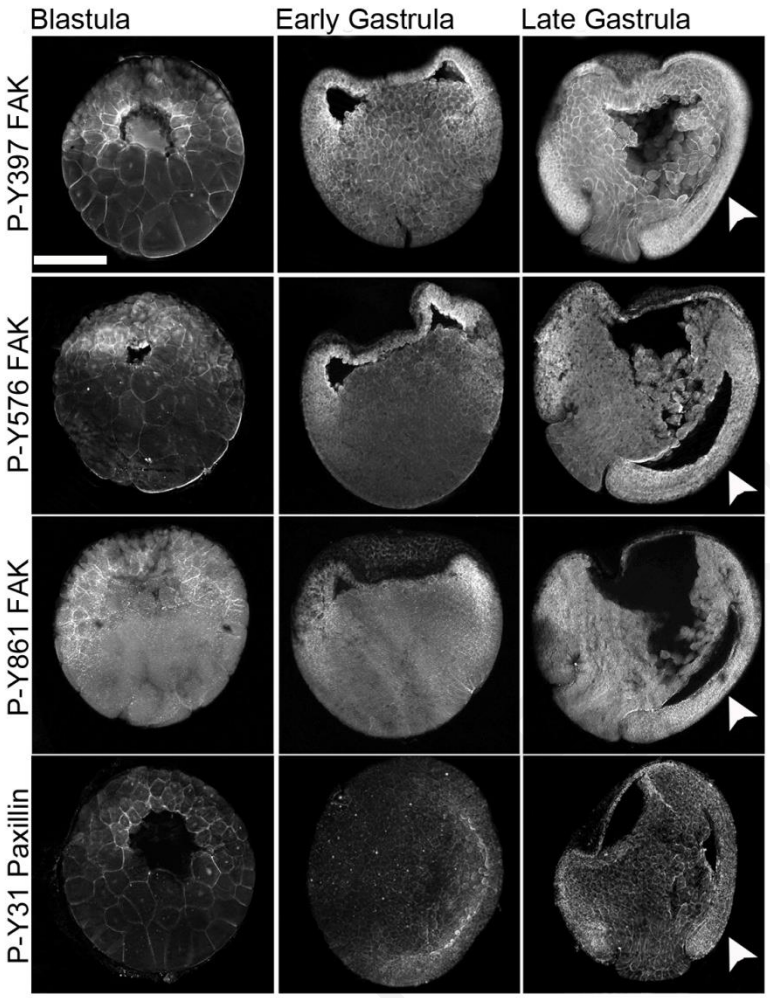

Figure 24: FAK displays enriched activation at the mesoderm of the early *Xenopus* embryo.
Blastula, early gastrula and late gastrula embryos stained with P-Tyr397, P-Tyr576, P-Tyr861 and P-Tyr31paxillin antibodies as indicated. Phosphorylated FAK and paxillin can be detected on the plasma membrane from early blastula stages including the apical region of superficial blastomeres. During gastrulation elevated levels of phosphorylation are detected in the highly morphogenetic mesodermal tissues (white arrowheads). Scale bar: 400 μm.

3.2.2. FAK activation in the early *Xenopus* embryo is not always associated with integrin expression

Detailed characterization of FAK activation pattern in the mesodermal tissues of gastrula stage *Xenopus* embryos was performed through optical sectioning. High magnification optical sections of the blastopore lip reveal that the mesoderm contains much higher levels of phosphorylated FAK (**Figure 25A**, white arrow) compared to the adjacent endoderm of the blastopore (**Figure 25A**, red arrow) as well as the single layer of endodermal cells that will line the archenteron and surround the mesoderm (**Figure 25A**, white arrowheads). In addition, the superficial cells of the ectoderm on the AC display lower levels of FAK phosphorylation

compared to the deep cells (**Figure 25B**), indicating roles of FAK in these cells that might not be exclusively based on its kinase activity, or that a baseline of FAK phosphorylation is required in these cells. The detection of phosphorylated FAK prior to gastrulation including early blastula stages and the presence of phosphorylated FAK on the apical surface of superficial cells is surprising (**Figure 24** and **Figure 25C**). Prior to gastrulation there is no FN secretion (Danker, Hacke et al. 1993), and no laminin expression (Fey and Hausen 1990). In addition, cells from *Xenopus* embryos are unable to spread or migrate on FN prior to gastrulation (Ramos and DeSimone 1996). These taken together, suggest that there is little, if any cell-ECM signaling at these early stages of development and thus FAK phosphorylation is most likely integrin independent or at least integrin dependent but in an ECM ligand independent manner. This notion is also supported by the presence of phosphorylated FAK at the apical surface of superficial blastomeres which are clearly not exposed to the ECM (**Figure 25C**). The apical surface of each superficial cell is isolated from the basolateral region with tight junctions which prevent diffusion of membrane bound molecules between the two areas (Fesenko, Kurth et al. 2000). Thus, it is likely that FAK at the apical surface of these cells is exclusively activated through mechanisms independent of integrin signaling. Importantly, high magnification optical sections from superficial ectodermal cells of the AC reveal that the level of FAK phosphorylation is identical between the apical and basolateral regions (**Figure 25C**), whereas in the cells facing the blastocoel there is an elevation of FAK phosphorylation at the basal compared to the basolateral region in these cells (**Figure 25D**). It should also be noted that in these high magnification images of deep ectodermal cells the phospho-FAK signal in the basolateral region appears relatively uniform and no FA like structures can be detected. However, on the basal surface of these cells which is facing the FN network of the BCR, the phospho-FAK staining is of higher intensity with clearly visible high intensity foci which may represent FA like structures (**Figure 25D**).

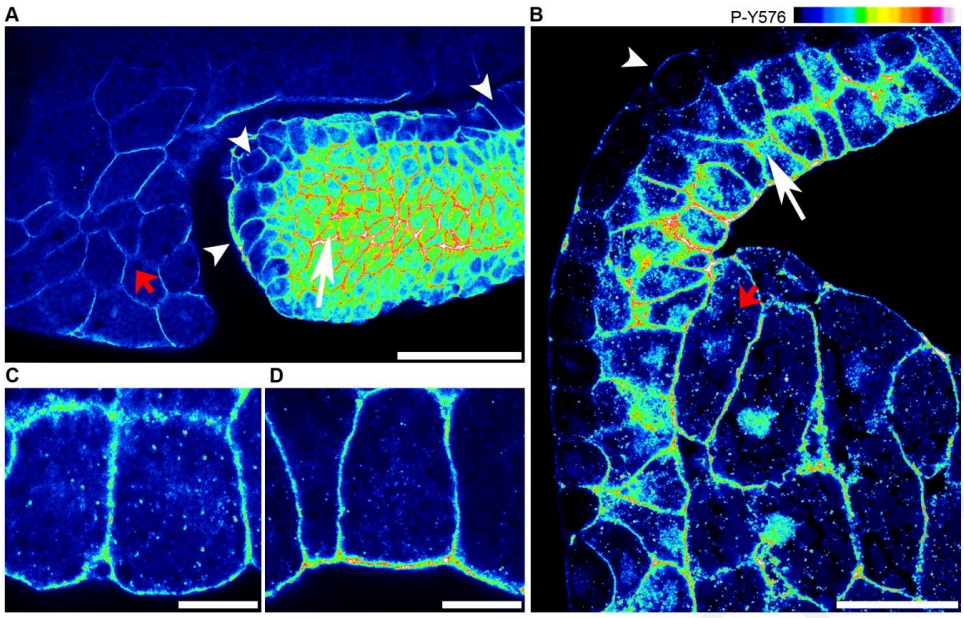

Figure 25: FAK is heavily phosphorylated in mesodermal tissues.
(A) Intensity color coded confocal section of the dorsal lip region from a whole mount immunostained gastrula stage embryo using a P-Tyr576 FAK antibody. Mesodermal cells (white arrow) display much higher levels of phospho-FAK than endodermal cells lining the forming archenteron (white arrowheads) and the endodermal cells of the blastopore (red arrow). (B) Same as (A) but showing the anterior mesendoderm and the AC. The superficial cells of the AC (white arrowhead) show lower levels of phospho-FAK signal compared to deep cells (white arrow) and mesendodermal cells (red arrow). (C) High magnification color coded narrow optical section of superficial cells of the AC reveals that the apical surface of these cells display similar levels of phospho-FAK compared to the basolateral region while (D) the basal region of the deep cells of the AC facing the FN ECM display significantly elevated levels of phospho-FAK compared to the basolateral region. Scale bars: (A) 100 μm, (B) 50 μm, (C, D) 10 μm.

This differential pattern of FAK phosphorylation may be attributed to differences in the cell context, such as the presence of integrins. Thus, we examined the possibility that FAK activation at the apical surface of the outermost epithelium in the early embryo is integrin independent by comparing the localization of phosphorylated FAK in relation to that of integrins. Double whole mount *in situ* immunofluorescence using P-Tyr397 and integrin β1 antibodies were carried out and embryos were imaged on a confocal microscope (**Figure 26**). α5β1 integrin is ubiquitously expressed and is the primary integrin heterodimer responsible for both mesoderm migration on FN as well as control of FN deposition by AC cells on the BCR (Joos, Whittaker et al. 1995). As seen in **Figure 26**, phosphorylated FAK is localized tightly on the membrane in a similar fashion to integrin β1 at sites of cell–cell contact (white arrowhead). However, despite strong phospho-FAK signal on the apical surface of superficial cells, no integrin β1 staining can be detected in this region of the cell (**Figure 26A,** red arrow),

but interestingly integrin β1 is localized in the basolateral areas of the cells of the outermost epithelium where there is no ECM surrounding them. This is in agreement with previous reports indicating that integrin α5 is also not detectable on the apical surface of these cells (Joos, Whittaker et al. 1995). On the other hand, in cells facing the blastocoel where FN fibrils are assembled (Winklbauer and Stoltz 1995), both activated FAK and integrins are found on the basal surface (**Figure 26B**). This could be interpreted as integrin based elevation since FN is lining the blastocoel and both α5 and β1 integrins are present in this region (Joos, Whittaker et al. 1995, Marsden and DeSimone 2001).

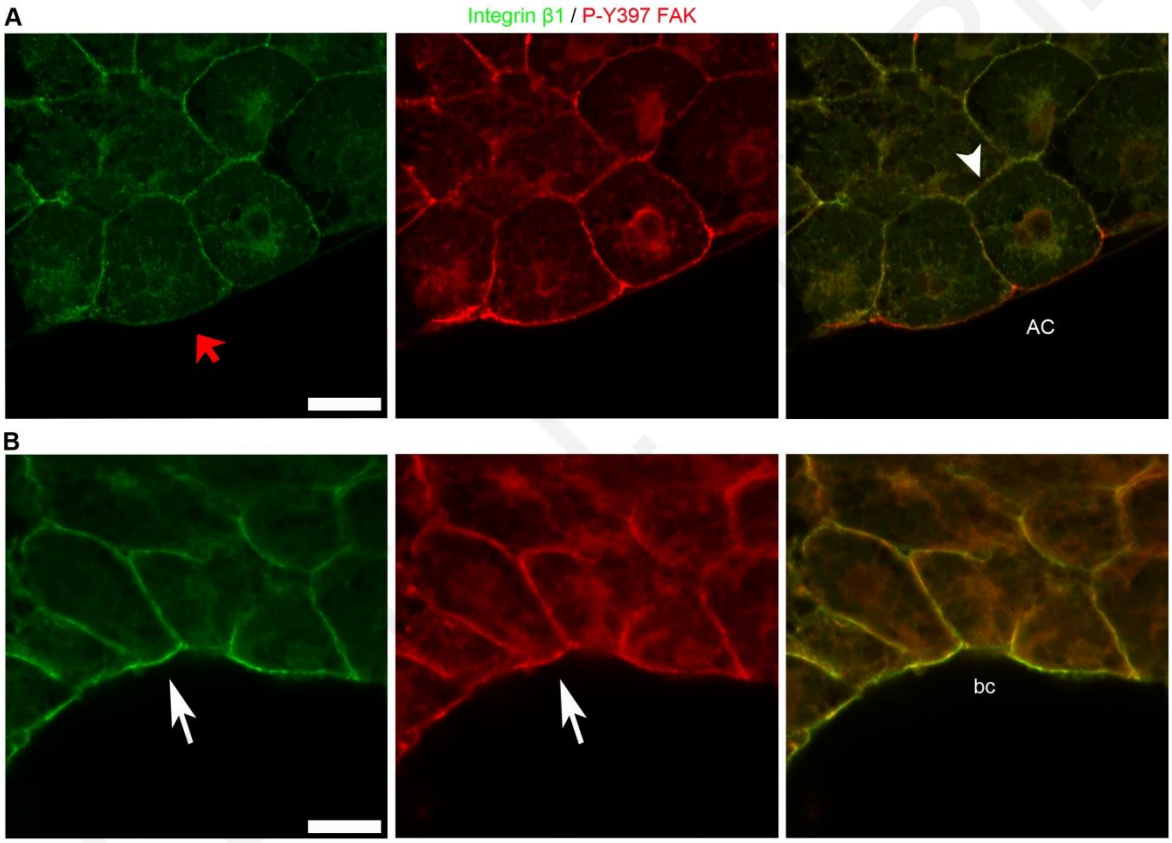

Figure 26: FAK is activated in integrin-free regions of the cells of the *Xenopus* AC.
(A) Confocal optical sections from whole mount immunostained embryos using integrin β1 and P-Tyr397 FAK antibodies. Integrin β1 and P-Tyr397 FAK co-localize on the plasma membrane at cell-cell boundaries (white arrowhead). However, phosphorylated FAK is also present on the apical region of the outermost cells of the embryo where integrin β1 is absent (red arrow). (B) Same embryo as above but the cells facing the blastocoel cavity are imaged. Integrin β1 and P-Tyr397 FAK co-localize on the basal surface of the cells facing the blastocoel (white arrows). Abbreviations: AC, Animal Cap; bc, blastocoel. Scale bars: (A, B) 30 μm.

3.2.3. The FERM domain is both necessary and sufficient for plasma membrane localization of FAK in the apical surface of the outermost epithelial cells

The above data raised the possibility that FAK is primarily activated through an integrin independent mechanism at the apical surface of the cells of the outermost epithelium of the early *Xenopus* embryo. Thus, the apical surface of the *Xenopus* outermost epithelium is an excellent tool to study integrin independent activation of FAK *in vivo*.

Since this mechanism seems to be integrin independent we postulated that the C-terminal domain of FAK that is necessary and sufficient for FAK's localization at the FAs would be dispensable. Thus, we examined the localization of FRNK, which is a DN of FAK that acts through its ability to localize at FAs (Sieg, Hauck et al. 1999). Expression of FRNK in these cells resulted in a diffused cytosolic localization which fails to mimic the tight membrane localization of active FAK in this context (**Figure 27**), supporting the integrin independent FAK activation at the apical surface of these cells.

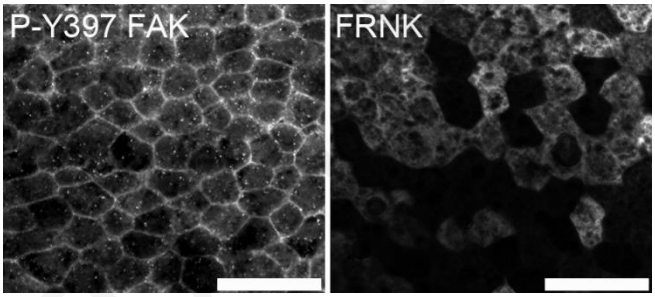

Figure 27: FRNK localization is not similar to the localization of active FAK in cells of the AP.
Localization of P-Tyr397 FAK and FRNK in AP cells of stage 10 *Xenopus* embryos. P-Tyr397 FAK shows strong membrane localization while FRNK is primarily cytoplasmic in these cells. Scale bars: 40 μm.

In an effort to address which domain of FAK is responsible for the integrin independent activation of the molecule we generated several FAK deletion mutants and examined their localization in the apical surface of the cells of the AP. Each construct was expressed as an HA (hemagglutinin) tagged protein through mRNA injection at the two AP-dorsal blastomeres of four-cell stage embryos, and embryos were subsequently processed for whole mount immunofluorescence using a monoclonal anti-HA antibody. Specifically, expression of the N-terminal FERM domain of FAK, which has been shown to bind PIP_2 and GFRs (Chen and Chen 2006, Cai, Lietha et al. 2008), exhibits a strong plasma membrane localization in the integrin-free apical surface of these cells and is also found on plasma membrane associated vesicles (**Figure 28A**). This pattern closely matches that of phosphorylated FAK (**Figure 28B**)

suggesting that the FERM domain rather than the FAT domain is responsible for membrane localization of active FAK in the embryo. To further investigate the role of the FERM domain in the localization of activated FAK we examined the localization of the full length FAK K38A point mutant, in which the FERM kinase domain interaction is compromised, and compared it to that of the Δ375 mutant, which lacks the FERM domain (Cohen and Guan 2005). Both constructs are constitutively active: in the case of the K38A mutant, due to the loss of the FERM-kinase inhibitory interaction and in the case of the Δ375 due to the absence of the FERM domain. The two constructs exhibit significant differences in terms of their ability to localize to the plasma membrane with the K38A exhibiting strong membrane localization while the Δ375 is very diffuse and appears completely absent from the plasma membrane in the cells of the AC (**Figure 28C,D**). These results suggest that the FERM domain is both necessary and sufficient for the localization of FAK on the apical surface of the epithelial cells.

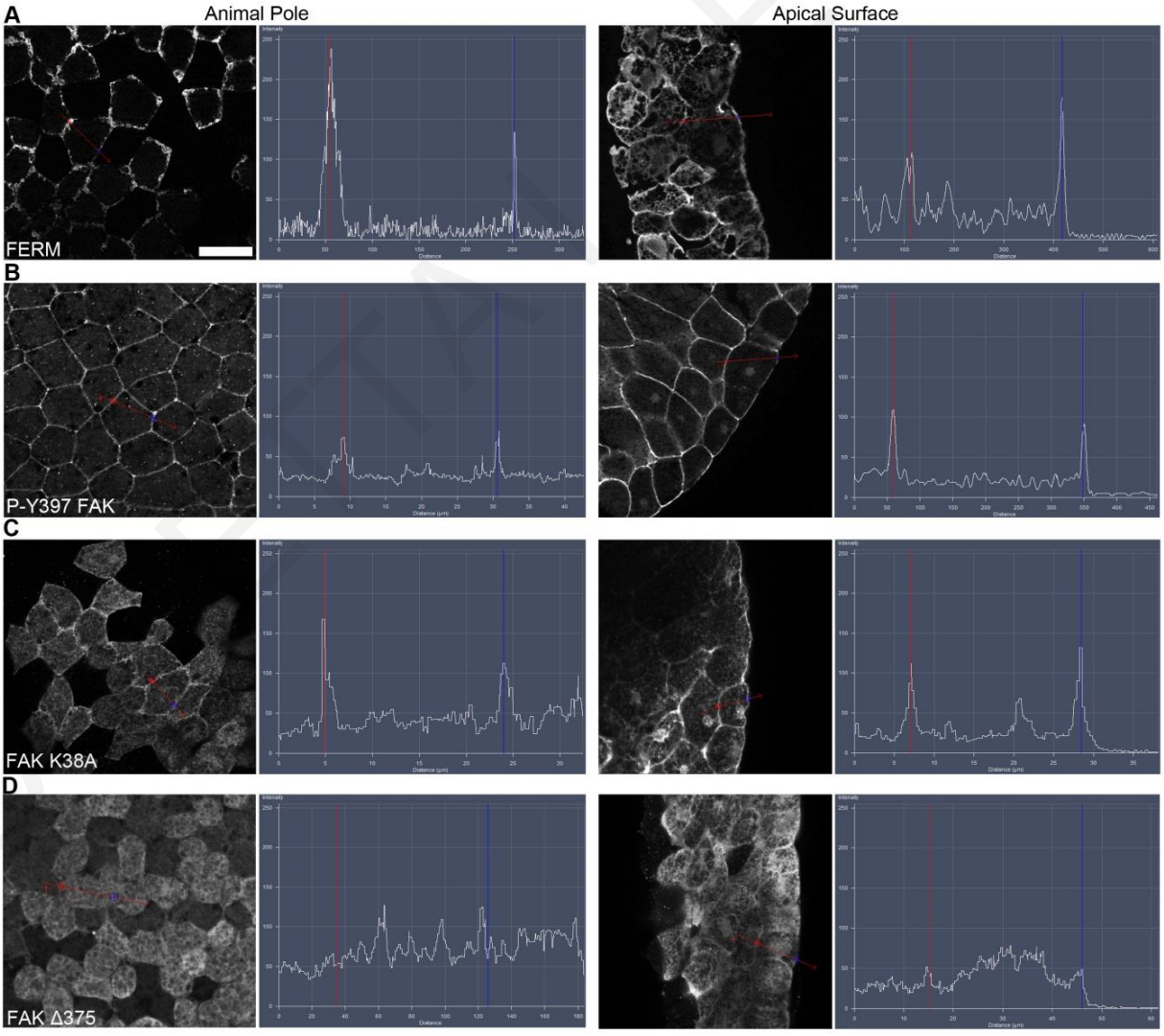

Figure 28: The FERM domain is necessary and sufficient for plasma membrane localization of FAK at integrin-free regions.

Confocal images and intensity profiles of the indicated constructs after whole mount immunostaining. The first column are top views of superficial cells of the AC in intact embryos and the second column are views from sagittally sectioned embryos that reveal the localization of each construct on the apical surface of superficial cells. Apical region of superficial blastomeres is to the right. (A) The FERM domain shows strong plasma membrane localization in the top view and is strongly localized to the apical surface. (B) Endogenous phosphorylated FAK shows strong plasma membrane localization in the top view and is localized on the basolateral and apical surface of the cell. (C) Full length FAK with the point mutation K38A exhibits strong membrane localization. (D) Deletion of the FERM domain (Δ375 FAK) abolishes the plasma membrane localization of FAK. Scale bars: 25 μm.

3.2.4. Expression of the N-terminal domain of FAK leads to elevated phosphorylation of endogenous FAK and downstream targets in a Src dependent manner

Since the presence of the FERM domain of FAK is crucial for FAK's localization in integrin-free regions of the cells we went on to further explore the role of the FERM domain in the activation of FAK in *Xenopus*. Initially, we examined the effects of FERM domain overexpression in the developing embryo. Embryos were injected with the FERM domain at the AP at the one blastomere of two-cell stage embryos and were allowed to develop to tadpole stages. FERM expressing embryos developed normally and were identical to controls suggesting that FAK function was not inhibited (data not shown). To examine the effects of FERM expression on endogenous FAK the experiment was repeated and embryos were either fixed or lysed at gastrula stage. As shown in **Figure 29**, cells expressing FERM, show elevated levels of endogenous phosphorylated FAK on tyrosines 576 and 861 compared to un-injected neighboring cells suggesting that FERM expression leads to activation of endogenous FAK (**Figure 29A, B**). This is a surprising finding and several experiments described in the materials and methods section were carried out to ensure that the phospho-FAK antibodies used were in fact specific in this context (**Figure 17**).

To confirm the activation of FAK in FERM overexpressing embryos western blotting experiments and densitometry analysis were carried out. Lysates from FERM injected embryos contain comparable levels of total FAK as controls but elevated phosphorylation on tyrosines 397, 576 and 861 (**Figure 29C**). In addition, blotting of the HA FERM with an anti P-Tyr397 antibody shows that the exogenously expressed protein is phosphorylated on Tyr397 in agreement with previously published work (**Figure 29C**, 2nd row) (Sieg, Hauck et al. 2000, Toutant, Costa et al. 2002).

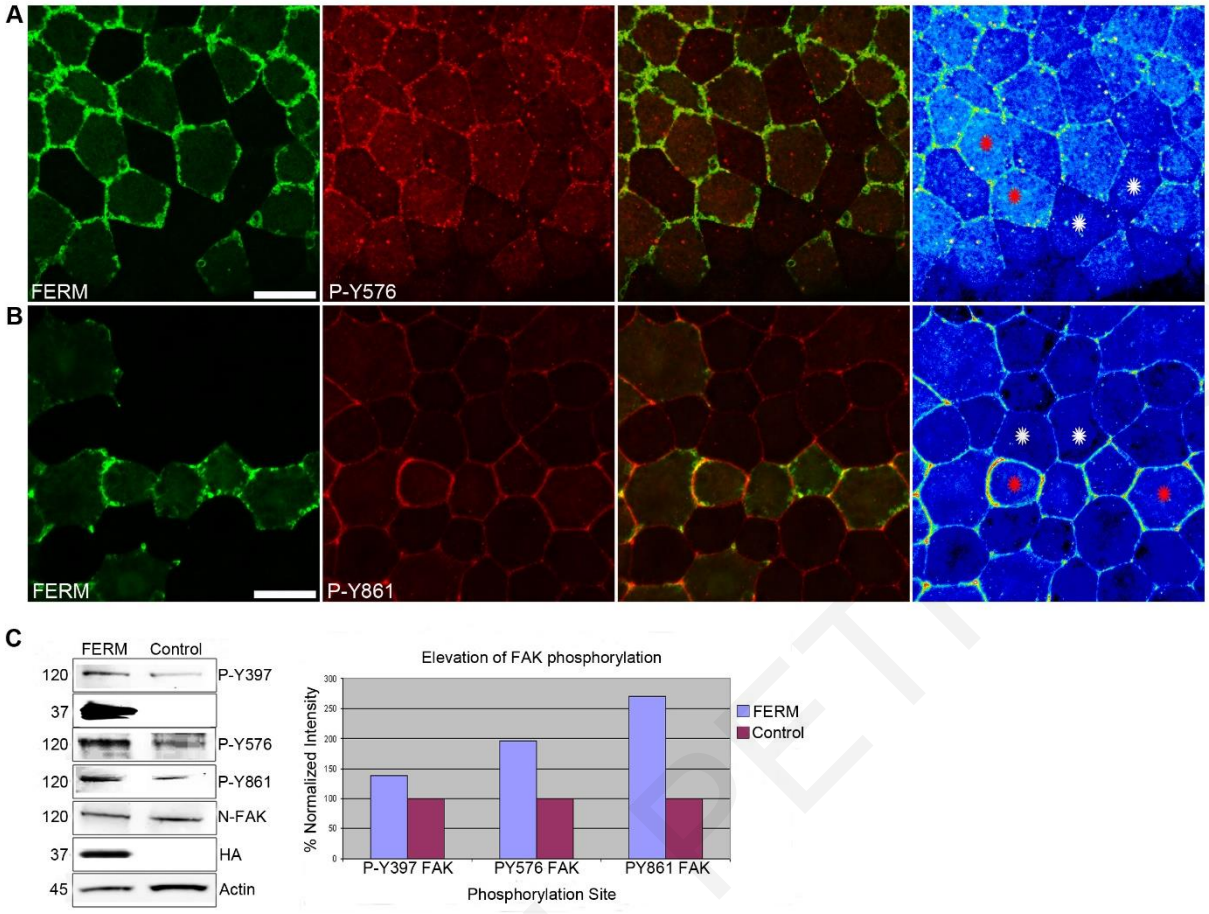

Figure 29: FERM expression leads to activation of endogenous FAK.

HA FERM injected embryos in one blastomere at the AP of two-cell stage embryos were processed for whole mount immunostaining using an HA antibody (green) to reveal expressing cells and a phospho-specific Tyr576 antibody (red). In each case individual signals for each antibody are shown in addition to a merged image and finally an intensity color coded image of the phospho-specific antibody signal. Injected cells are indicated with red stars and un-injected cells with white stars. Levels of P-Tyr576 (A) and P-Tyr861 (B) are elevated in FERM overexpressing cells compared to controls. (C) Total lysates from HA FERM injected gastrula stage embryos contain comparable levels of endogenous FAK as un-injected controls but elevated levels of phosphorylated FAK on tyrosines 397, 576 and 861. Blotting using the anti-P-Tyr397 antibody shows that the exogenously expressed FERM is heavily *in trans* phosphorylated on tyrosine 397 (2nd row). The intensity values from the densitometry analysis were normalized against total FAK and present the average increase in phosphorylation from three independent experiments. Scale bars: (A, B) 40 µm.

Expression of the N-terminus of FAK has been previously shown to block integrin dependent FAK activation (Cooper, Shen et al. 2003, Cohen and Guan 2005). To preclude the possibility that the observed effect is *Xenopus* specific we expressed the FERM domain in *Xenopus* A6 cells and examined the effects on endogenous levels of P-Tyr576 via indirect immunofluorescence. As shown in **Figure 30** FERM expression in *Xenopus* adherent cells results in a moderate reduction of phospho-576 levels indicating that FERM expression does in

fact block FAK activation in cultured *Xenopus* cells. The opposite results obtained *in vivo* and *in vitro* with regard to the effects of FERM expression may be explained by a differential effect of FERM expression in integrin vs non integrin based activation of FAK. Expression of the N-terminus of FAK in FAK null cells has been shown to actually partially rescue the EGF induced cell migration defect suggesting that the FERM domain can partially transduce growth factor based signals autonomously supporting this possibility (Sieg, Hauck et al. 2000).

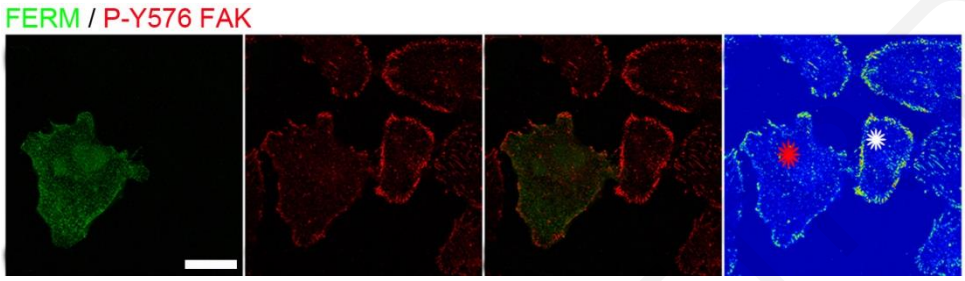

Figure 30: FERM overexpression in adherent *Xenopus* cells leads to reduction of FAK phosphorylation. Confocal images of A6 *Xenopus* cells transfected with HA FERM. Cells were stained with anti-HA and anti-P-Tyr576 antibodies. Transfected cells are shown with red stars and controls with white stars. FERM transfected cells show reduced levels of Tyr576 phosphorylation suggesting that FERM expression blocks FAK activation in these cells. Scale bars: 20 μm.

Since tyrosine 397 is a known Src binding site (Schaller, Hildebrand et al. 1994) and tyrosines 576 and 861 are targets of Src (Calalb, Polte et al. 1995, Calalb, Zhang et al. 1996) we went on to examine the possibility that an intact tyrosine 397 was required for the FERM induced activation of FAK. We generated a FERM Y397F construct and the construct was overexpressed in *Xenopus* embryos. As shown in **Figure 31**, cells expressing FERM Y397F do not display elevated levels of phosphorylation on tyrosines 576 and 861 (**Figure 31A, B**) suggesting that the observed activation of endogenous FAK is dependent on Src.

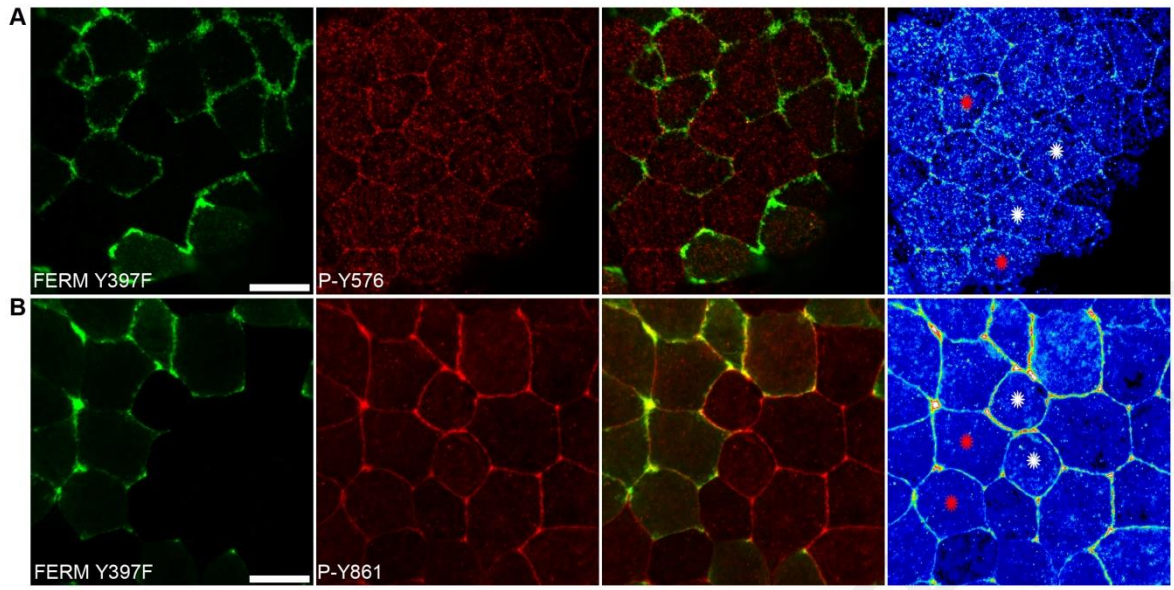

Figure 31: Expression of FERM Y397F construct does not lead to endogenous FAK activation.
Top views of embryos expressing the HA FERM Y397F construct and stained for HA (green) and phospho-specific antibodies against Tyr576 (A), or Tyr861 (B), showing no effect on the phosphorylation levels of endogenous FAK by the expression of the construct. Scale bars: (A, B) 40 μm.

This is also supported by the fact that in embryos treated with the Src inhibitor PP2, tyrosine phosphorylation on both 576 and 861 is severely reduced indicating that, in the developing embryo, FAK phosphorylation of the above residues is dependent on Src (**Figure 32**).

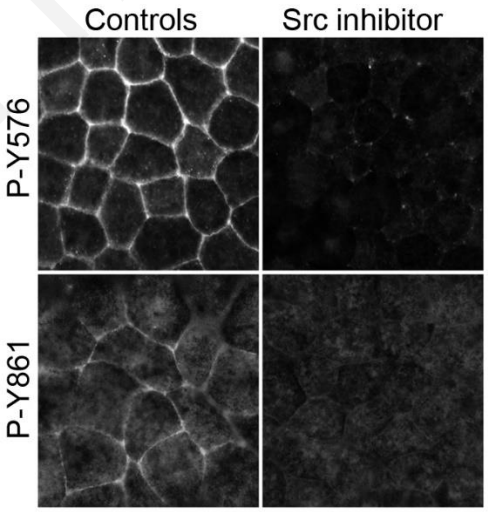

Figure 32: Src-dependent phosphorylation of FAK in the *Xenopus* embryos.
Control and Src inhibitor treated *Xenopus* gastrula embryos stained for phosphorylated FAK on Tyr576 and Tyr861.

Finally, to confirm the FERM induced activation of endogenous FAK we examined the phosphorylation status of p130Cas and paxillin, two FAK/Src downstream targets (Richardson, Malik et al. 1997, Tachibana, Urano et al. 1997). Expression of FERM, but not FERM Y397F, leads to elevated phosphorylation of both paxillin and p130Cas, but not of Akt which is a substrate of PI3K (Franke, Kaplan et al. 1997) (**Figure 33**) (Franke, Kaplan et al. 1997). These results show that FERM expression in integrin-free regions of the *Xenopus* outermost epithelial cells leads to activation of endogenous FAK and subsequent phosphorylation of FAK-Src targets in a tyrosine 397 dependent manner.

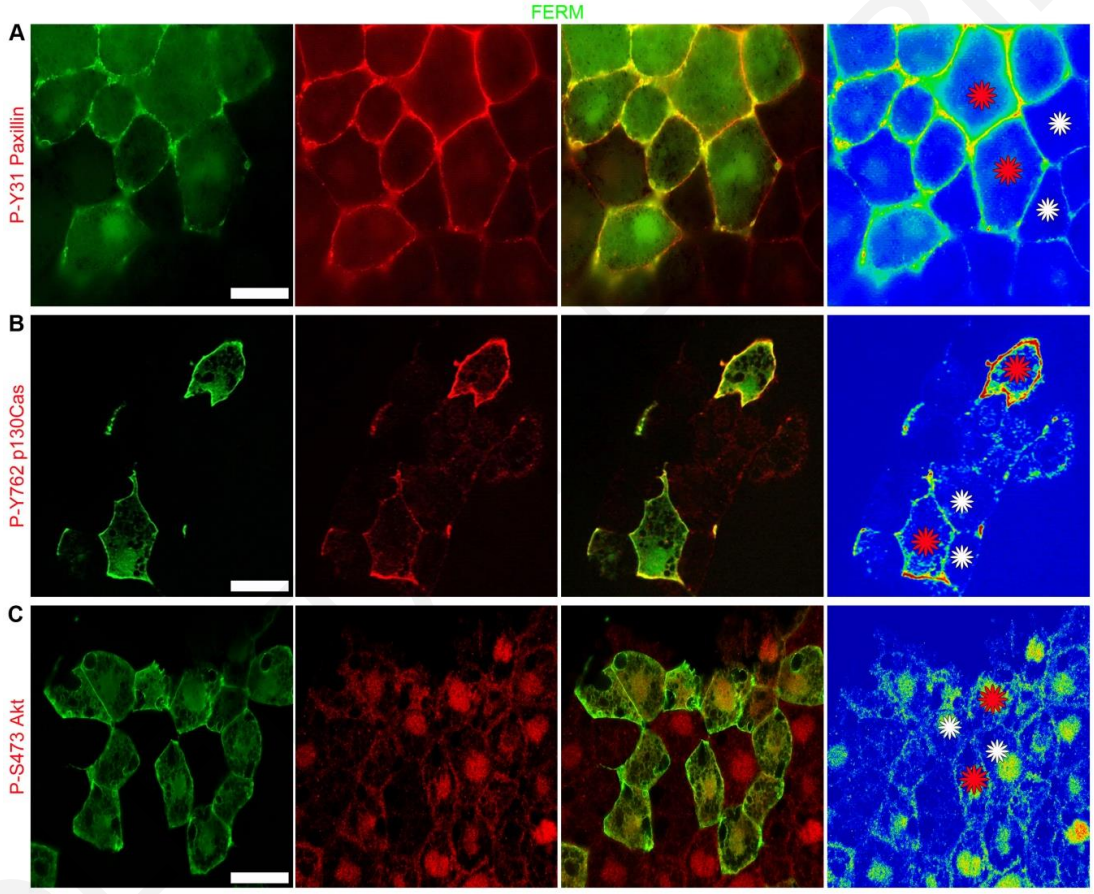

Figure 33: The FERM domain activates endogenous FAK leading to increased phosphorylation of FAK/Src targets.

(A) Embryos injected with HA FERM mRNA in two blastomeres, at the AP, at the four cell stage were processed for immunofluorescence using anti-HA (green) and anti-P-Tyr31 paxillin (red) antibodies. FERM expressing cells display elevated levels of phosphorylated paxillin. (B) Same as (A) but comparing phosphorylation levels of p130Cas on tyrosine 762 between FERM expressing and control cells. FERM expressing cells show elevated levels of P-p130Cas. (C) Same as (A-D) but comparing levels of phosphorylated Akt on serine 473 between FERM expressing and control cells. Levels of P-Akt are comparable in FERM expressing cells to those of control neighboring cells. Red stars indicate FERM injected cells and white stars indicate control un-injected cells. Scale bars: 20 μm.

3.2.5. FRNK does not act as a DN of FAK during early *Xenopus* development

Although in the integrin-free regions of the embryo FAK seems to be regulated exclusively through its N-terminal domain and that the C-terminal domain is dispensable, these areas constitute only a small minority of the embryo, corresponding to the apical surface of the outermost epithelial cells of the embryonic skin. In order to further examine the embryonic role of FAK we focused on the integrin aspect of FAK activation. Thus, as an initial approach we utilized FRNK, the bona fide DN of FAK which has been previously shown to block cell spreading and integrin based tyrosine phosphorylation of endogenous FAK, paxillin, and tensin *in vitro* (Richardson and Parsons 1996, Richardson, Malik et al. 1997). We injected FRNK at the DMZ of gastrula stage embryos, where mesoderm morphogenesis takes place in an integrin dependent fashion. Expression of FRNK in DMZ cells, where FAK is also most highly phosphorylated, had no effect on the levels of phosphorylation of FAK on tyrosines 397 and 576 during gastrulation *in vivo* as determined by immunofluorescence and western blotting (**Figure 34**).

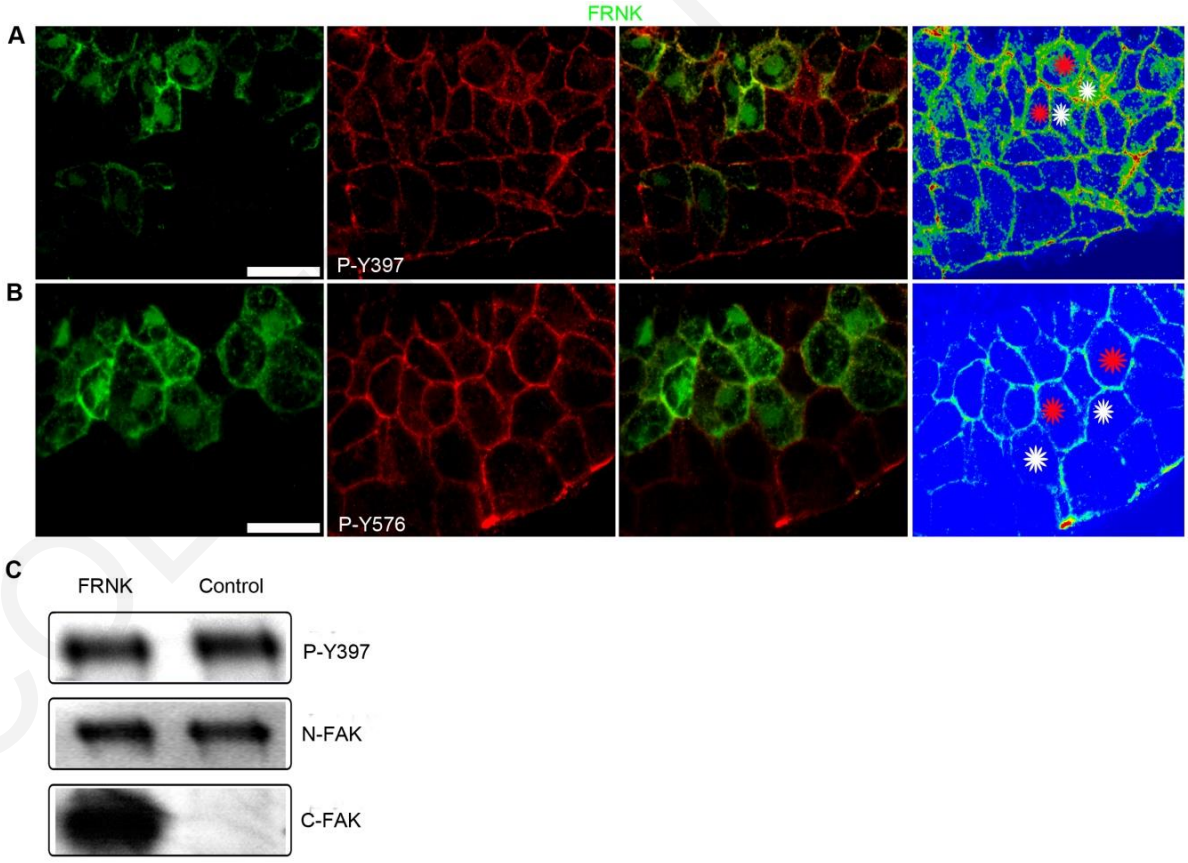

Figure 34: FRNK does not act as a DN in early *Xenopus* embryos.

Optical sections of whole mount immunostained embryos injected with 1ng GFP FRNK at the two dorsal blastomeres at the four-cell stage. Embryos were stained with anti-GFP and anti-P-Tyr397 (A), or anti-P-Tyr576

(B). FRNK injected cells are indicated with red stars and control cells with white stars. FRNK expression fails to reduce the phosphorylation levels of endogenous FAK on Tyr397. (C) Western blot analysis of control and injected gastrula stage embryos with 1 ng FRNK at the AP of both blastomeres of two-cell stage embryos. FRNK expression fails to reduce endogenous FAK phosphorylation on tyrosine 397. FRNK expression was verified using a FAK antibody raised against the C-terminus of the protein. Scale bars: (A, B) 40 μm.

This is in contrast to the clear downregulation of phosphorylation on both tyrosine 397 and 576 seen when we expressed FRNK via transfection in the *Xenopus* A6 cell line (**Figure 35**), showing that the lack of DN activity of FRNK is specific to the early vertebrate embryo.

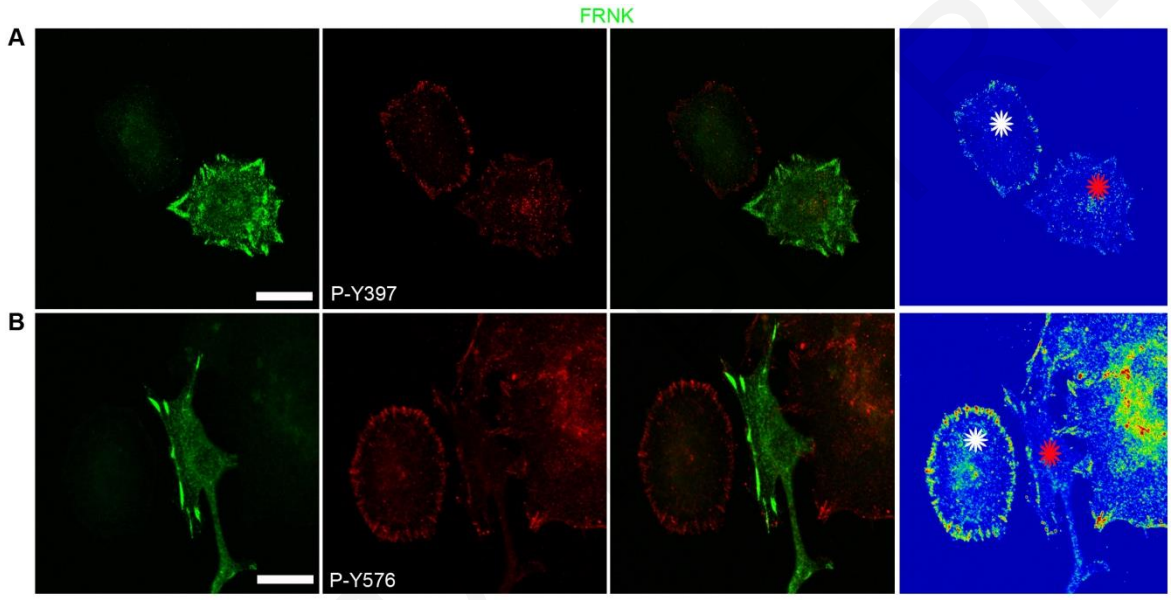

Figure 35: Verification of the DN activity of FRNK in *Xenopus* adherent cells.
Confocal images of A6 *Xenopus* cells transfected with GFP FRNK. Cells were stained with anti-GFP and anti-P-Tyr397 (A) or anti-P-Tyr576 (B) antibodies. FRNK expression leads to reduction of the phosphorylation levels of FAK at the FAs. Transfected cells are indicated by red stars, control cells with white stars. Scale bars: 20 μm.

The lack of DN activity of FRNK is in agreement with the fact that FRNK fails to localize at the plasma membrane in AC cells unlike phosphorylated endogenous FAK which is found exclusively on the plasma membrane in these cells, as shown above (**Figure 27**).

However, the lack of DN of FRNK in the DMZ, where mesodermal morphogenesis is primarily based on integrin signaling, suggests that FRNK is not able to sufficiently inhibit FAK function in this context. Previous work from our group has shown that FRNK does in fact reduce endogenous FAK phosphorylation of mesodermal explants plated on FN and we show now that it can do the same in *Xenopus* cell lines (Stylianou and Skourides 2009). In all these cases however, FAK phosphorylation primarily derives from cell-ECM adhesion. Support comes

from the fact that FRNK's DN function is based on its FAT domain (Richardson and Parsons 1996) suggesting that targeting to integrin-based complexes is the mechanism through which FRNK acts. This suggests that in the absence of the ability to target non-integrin based FAK complexes, FRNK would not be able to act in a DN fashion. Our data suggest strong context dependence with regards to the DN activity of FRNK. Thus, the lack of DN activity of FRNK in the early embryo can be explained by two hypotheses. Either that in the context of the embryo FAK activation might not be exclusively integrin dependent, or that FRNK in this context does not have sufficiently high affinity for integrin complexes. In either case the above suggest that the C-terminus of FAK is not sufficient to target FAK in its complexes *in vivo* and that both integrin dependent and integrin independent mechanisms might regulate FAK activation in the embryo.

3.2.6. The FERM and FAT domains cooperate to target FAK at the plasma membrane in the embryo, and at FAs in cultured cells

Since the FERM domain of FAK seems to be the major determinant of FAK's localization in the embryo, we examined and compared the localization of FERM and FRNK in the DMZ cells where we hypothesize that both integrin dependent and independent mechanisms regulate FAK function. We noticed that neither the FAT nor the FERM domain of FAK, are sufficient to strongly target FAK to the plasma membrane of these cells (**Figure 36A**). Thus, we wanted to explore the possibility that the FERM and FAT domains cooperate to target active FAK at the plasma membrane and generated FERM-FRNK (FF), a construct which contains the N and C terminus sequences of FAK (**Figure 36B**). By removing the kinase domain, we wanted to mimic the active conformation of FAK in which the FERM domain is free to bind PIP_2 and GFRs (Sieg, Hauck et al. 2000, Chen and Chen 2006, Cai, Lietha et al. 2008) (integrin independent interactions) and at the same time the FAT domain is able to interact with its binding partners, such as paxillin and talin (Sieg, Hauck et al. 1999, Hayashi, Vuori et al. 2002, Lawson, Lim et al. 2012) (integrin dependent interactions). Combining the two regions resulted in a dramatic change in localization, as shown in **Figure 36A**. FF is almost exclusively localized at the plasma membrane, unlike FRNK and FERM, mimicking the localization of endogenous phosphorylated FAK. To explore the role of the FERM domain in the localization of FAK further, we compared the localization of FF and FRNK in cultured cells after generating GFP fusions of the two constructs. As shown in **Figure 36C** FRNK localizes in the cytosol and FAs, while FF is predominantly localized on FAs with little signal in the cytosol. In addition, FF expressors have FAs throughout the cell while in FRNK expressors FAs are primarily found in

the cell periphery. FF expressing cells contained visibly more and stronger FAs than FRNK and control cells (**Figure 36D**). To preclude the possibility that FF appeared to have stronger localization on FAs compared to FRNK was due to the fact that FF expression induces stronger and more abundant FAs than FRNK, we co-transfected GFP-FRNK with FF-mCherry. As shown in (**Figure 36E**) FRNK and FF co expressing cells show a similar increase in abundance of FAs as seen in FF alone and all these FAs contain both FF and FRNK. However, FF displays much lower cytoplasmic signal than FRNK, again confirming that FF has a higher affinity for these complexes than FRNK and suggesting a role for the FERM domain in the localization of FAK at FA complexes.

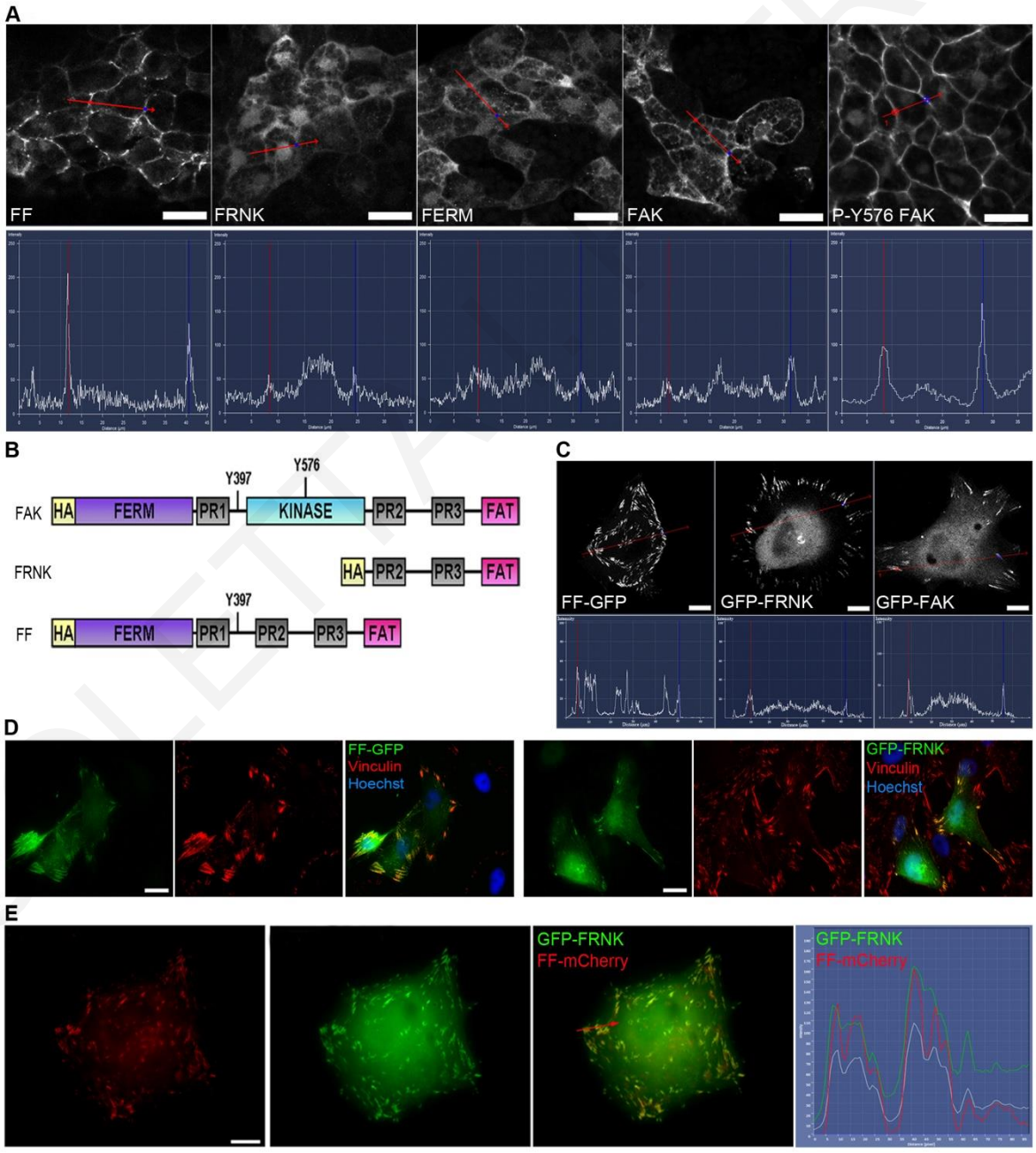

Figure 36: The FERM and FAT domains cooperate to target FAK at the plasma membrane in the embryo and at FAs in cultured cells.

(A) Confocal images and intensity profiles of gastrula stage embryos injected with 300pg of WT FAK or HA-tagged FAK mutants FF, FRNK and FERM at the DMZ and stained with anti-HA antibody or control embryos stained with anti-P-Tyr576 FAK. (B) Schematic representation of the FF construct, consisting of the N-terminal FERM domain together with PR1 domain and the Tyr397 autophosphorylation site, and the C-terminal FAT domain together with the PR2 and PR3 domains. (C) Confocal images and intensity profiles of live XL177 cells transfected with FF-GFP, GFP-FRNK or GFP-FAK. (D) Wide field images of XL cells transfected with either FF-GFP or GFP-FRNK (green) and stained with anti-vinculin (red) and hoechst (blue). (E) Confocal image and intensity profile of the FAs of XL cells co-transfected with GFP FRNK and FF-mCherry showing FF and FRNK co-localization at the same FAs. Scale bars: (A, D) 20 μm, (C) 10 μm, (E) 2 μm.

3.2.7. *In vitro* characterization of the FF construct as a DN of FAK

This higher affinity of FF for FA localization in adherent cells and tight plasma membrane localization in the context of the embryo, in both cases mimicking the localization of endogenous phosphorylated FAK, suggests that it can effectively displace activated FAK from its complexes and act as a strong DN of FAK. In order to address this question, we expressed either WT FAK alone or in combination with FF in adherent cells and compared the localization of FAK in the two cases. As shown FF expression displaces full length FAK from FAs (**Figure 37A**) and nearly eliminates FAK phosphorylation on these complexes (**Figure 37B**), demonstrating a strong DN activity.

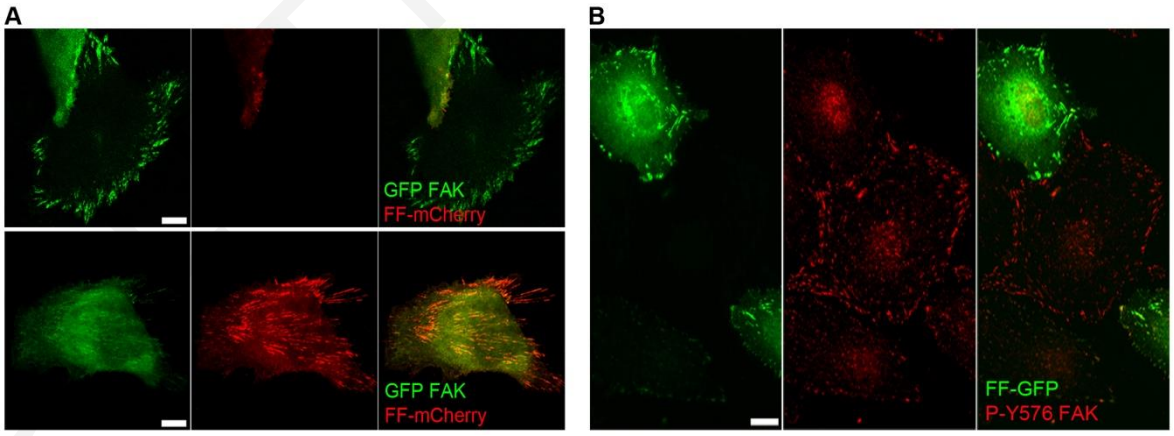

Figure 37: FF displaces endogenous FAK from FAs and eliminates its phosphorylation.

(A) Confocal images of XL177 cells co-transfected with FF-mCherry and GFP FAK showing FAK displacement from FF positive FAs. (B) Wide field images of XL177 cells transfected with FF-GFP and stained with P-Tyr576 FAK. Scale bars: (A) 10 μm (B) 20 μm.

To better understand the mechanism underlying the higher affinity of FF for FAs we carried out FRAP and FLIP experiments on cells expressing GFP-FRNK and FF-GFP (**Figure 38A, B**). As shown, FF displays a much slower recovery and has a larger immobile fraction compared to FRNK suggesting slower turnover of FF on FAs (FF $t^{1/2}$: 11.01 ± 1.74 seconds, FRNK $t^{1/2}$: 2.6 ± 0.4 seconds, **Figure 38A'**, Immobile fraction FF: 30.3 ± 4.5%, FRNK: 9.78 ± 1.4%, **Figure 38A''**). Moreover, FLIP experiments revealed that FF is retained more at the FAs than FRNK (**Figure 38B**).

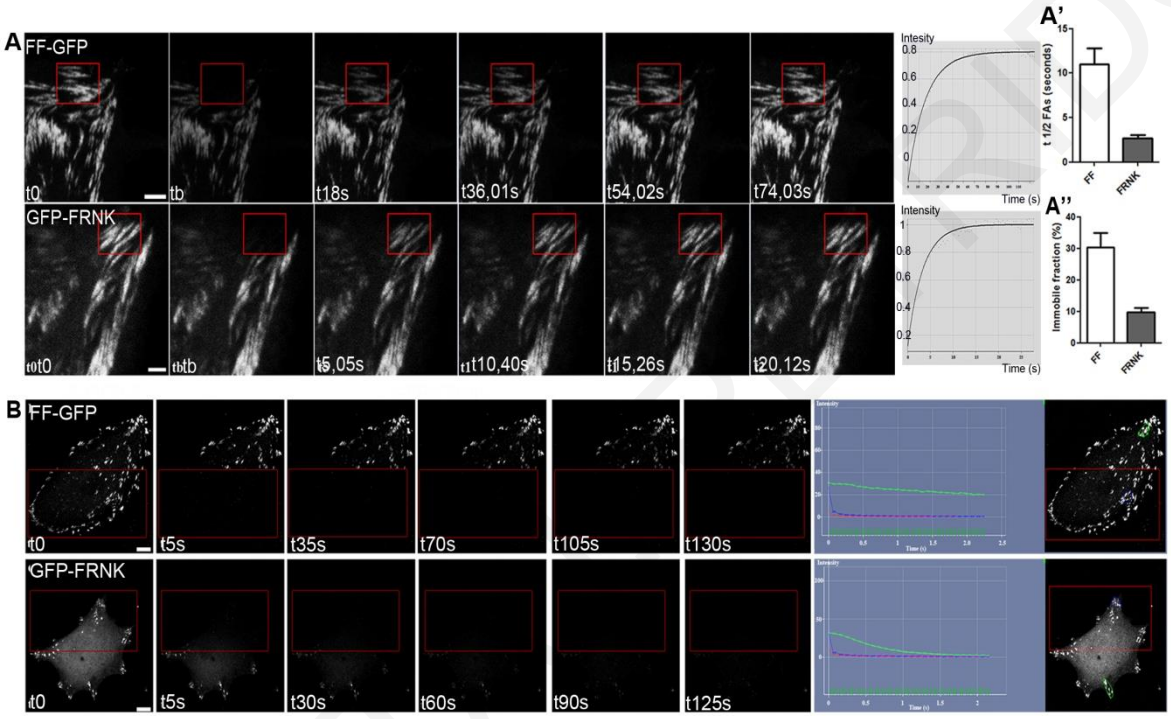

Figure 38: FF exhibits longer residence times on FAs compared to FRNK.

(A) FRAP experiments comparing FF-GFP and GFP-FRNK. FF displays slower recovery and larger immobile fraction than FRNK (B) FLIP experiments comparing loss of FF-GFP and GFP-FRNK. Rate of loss of FF is slower than FRNK. Abbreviations: tb, time of bleaching. Scale bars: (A) 2 μm, (B) 10 μm.

To preclude the possibility that these differences arise due to changes induced by FF on the FA complexes we carried out FRAP experiments in cells co-transfected with FF-mCherry and GFP-FRNK (**Figure 39A**). These experiments gave similar results with the recovery rate of FF being significantly slower than that of FRNK. We went on to carry FLIP experiments on FF-mCherry and GFP-FRNK co-transfected cells. As shown in **Figure 39B**, loss of FF from FAs is slower than loss of FRNK, confirming that FF has longer residence times on FAs. These data show that the FERM domain is required for the localization of FAK on the plasma membrane in the embryo and has an important role for FAK's affinity and dynamics on FA complexes in cultured cells.

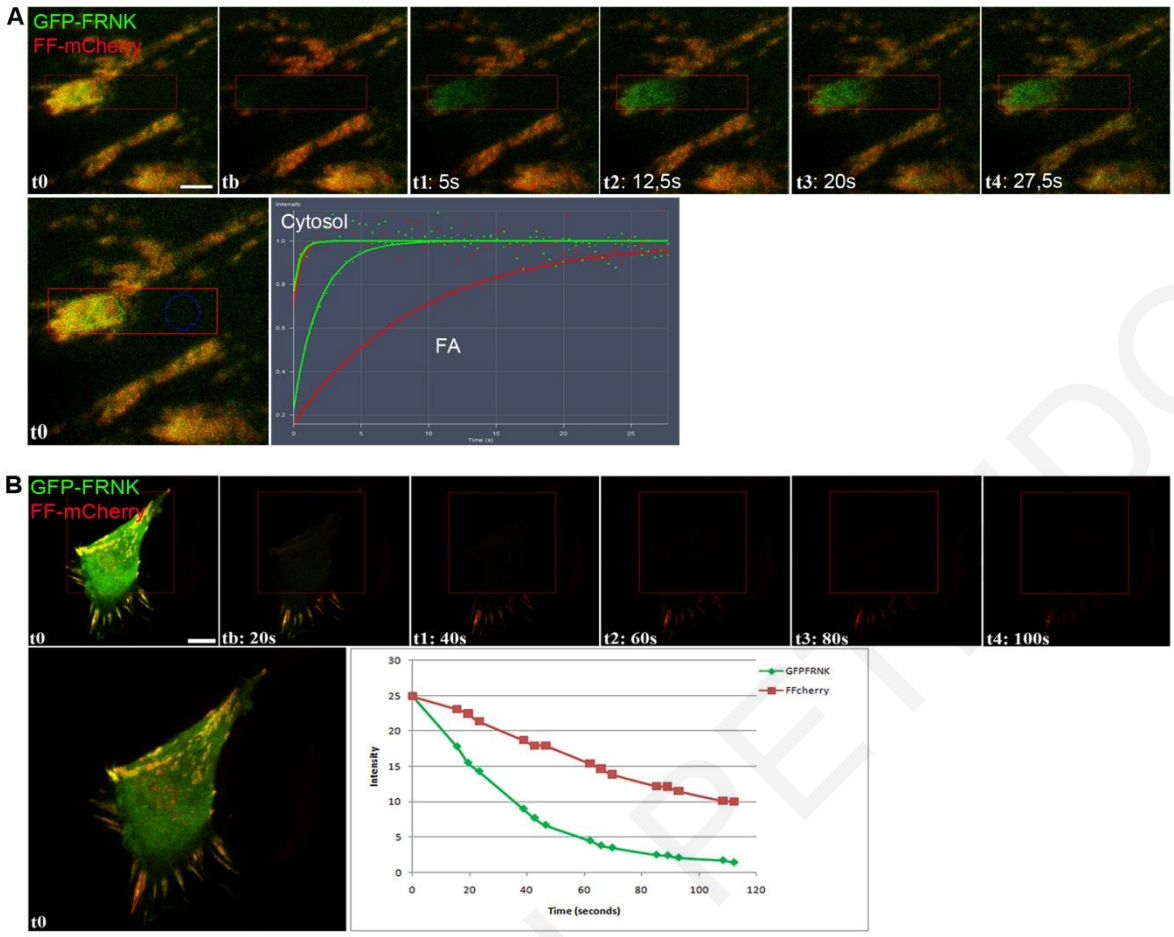

Figure 39: The higher affinity of FF for FAs than FRNK is not due to differences of the FA complex induced by FF expression.

(A) FRAP experiments on a FF-mCherry and GFP-FRNK co-expressing cell. A total of 60 frames were acquired. FF recovery at the FA is much slower while diffusion rates of the two constructs as evidenced by their recovery in the cytosol is comparable and much faster. (B) FLIP experiments of a cell expressing FF-mCherry and GFP-FRNK. A total of 50 frames were acquired. Rate of loss of FF is slower than that of FRNK. Abbreviations: tb, time of bleaching. Scale bars: (A) 2 µm, (B) 10 µm.

3.2.8. FF expression blocks cell migration by blocking FA turnover in adherent cells

Fibroblasts from FAK null mice show a significant increase of FA number and size and decreased migration rates (Ilic, Furuta et al. 1995), which can be restored by re-expression of WT FAK (Sieg, Hauck et al. 1999). Restoration requires the kinase activity of FAK as well as an intact Tyr397 (Cary, Chang et al. 1996). These data led to the conclusion that FAK is required for FA turnover and that the FAK kinase activity is required for FAK to perform this function. Overexpression of FRNK has been shown to decrease the rates of cell spreading and migration and induce the formation of enlarged FA complexes (Richardson, Malik et al. 1997,

Sieg, Hauck et al. 1999, Taylor, Mack et al. 2001), presumably by displacing FAK from the FAs and sequestering key regulatory proteins required for efficient FAK signaling.

As shown above, FF expressing cells display a marked increase in the numbers and size of FAs compared to FRNK and control cells, suggesting that FF leads to a more dramatic reduction of FA turnover compared to FRNK. To explore this possibility further, FF and FRNK expressing cells were imaged using time lapse fluorescence microscopy. As shown in **Figure 40A** and **Movie 1**, a typical FF expressing cell completely fails to disassemble its FAs while a FRNK expressing cell has completely disassembled all its FAs (**Movie 2**) and generated new ones within the same time frame (1 hour). FF cells also have ventral adhesions and time lapse sequences reveal how these materialize (**Figure 40B**). As the cell moves forward, anterior FAs fail to disassemble becoming ventral adhesions (yellow box). At the same time, posterior FAs also fail to disassemble and as the cell retracts the cell membrane is torn leaving the FF-GFP containing FAs behind (**Figure 40B**, white arrowheads). Time lapse movies of FF-GFP and GFP-FRNK reveal that the enlargement of FAs in FF expressors occurs primarily during the retraction of filopodia (**Movies 3** and **4** respectively).

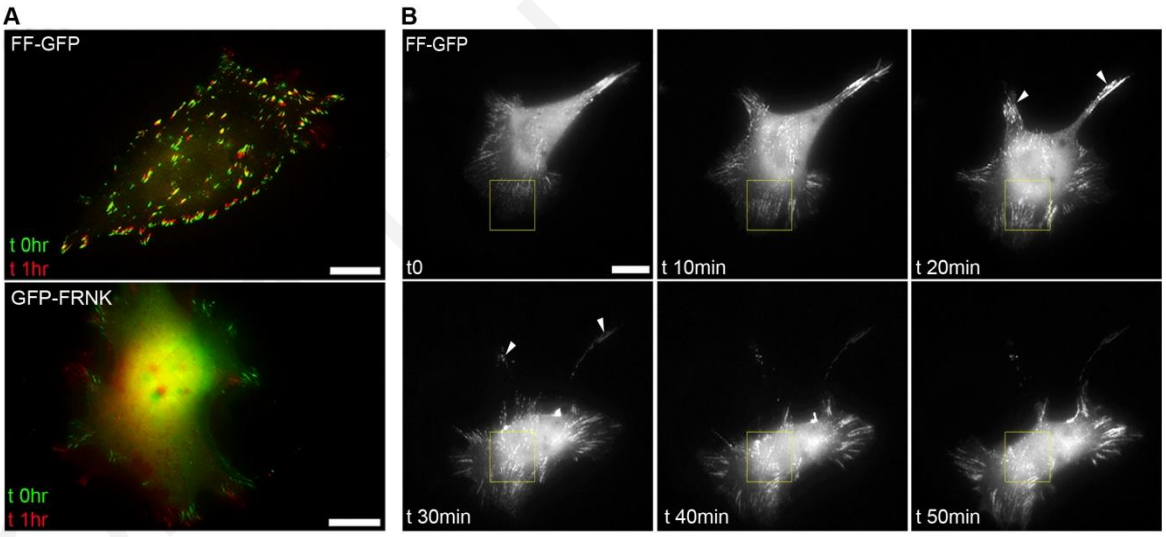

Figure 40: FF expression blocks FA turnover in adherent cells and cell migration.
(A) High magnification wide field live imaging of FA turnover in FF-GFP or GFP-FRNK transfected XL177 cells. Cells were imaged for a period of 1 hour. The merged image is composed from the first (green) and last time point (red). (B) Stills from a time lapse movie of an FF-GFP transfected XL migrating cell imaged for 50 minutes showing FA disassembly failure at the cell rear (white arrowheads) and at the cell front (yellow box) leading to the formation of ventral adhesions. Scale bars: (A) 20 μm, (B) 10 μm.

FF showed different dynamics on FAs and higher affinity compared to FRNK and it has been suggested in previous studies that the FERM domain has a role in the recruitment of FAK at the sites of FA formation possibly via binding of locally generated PIP_2 (Cai, Lietha et al. 2008). If this hypothesis is correct, one would expect FF to be recruited to nascent FAs prior to FRNK. To test this hypothesis, we co-transfected and imaged FF-mCherry and GFP-FRNK expressing cells. As shown in the stills from **Figure 41A**, FF (red) enrichment appears first on two nascent adhesions and FRNK enrichment follows (green). In addition, we also noted that FF would also form very transient adhesions on which FRNK fails to localize (**Figure 41B**). These results suggest that the FERM domain plays a role in the recruitment of FAK to nascent adhesions. Overall, the data presented show that FF expression leads to a more severe reduction of FA turnover compared to FRNK and as a result leads to a dramatic block of cell migration.

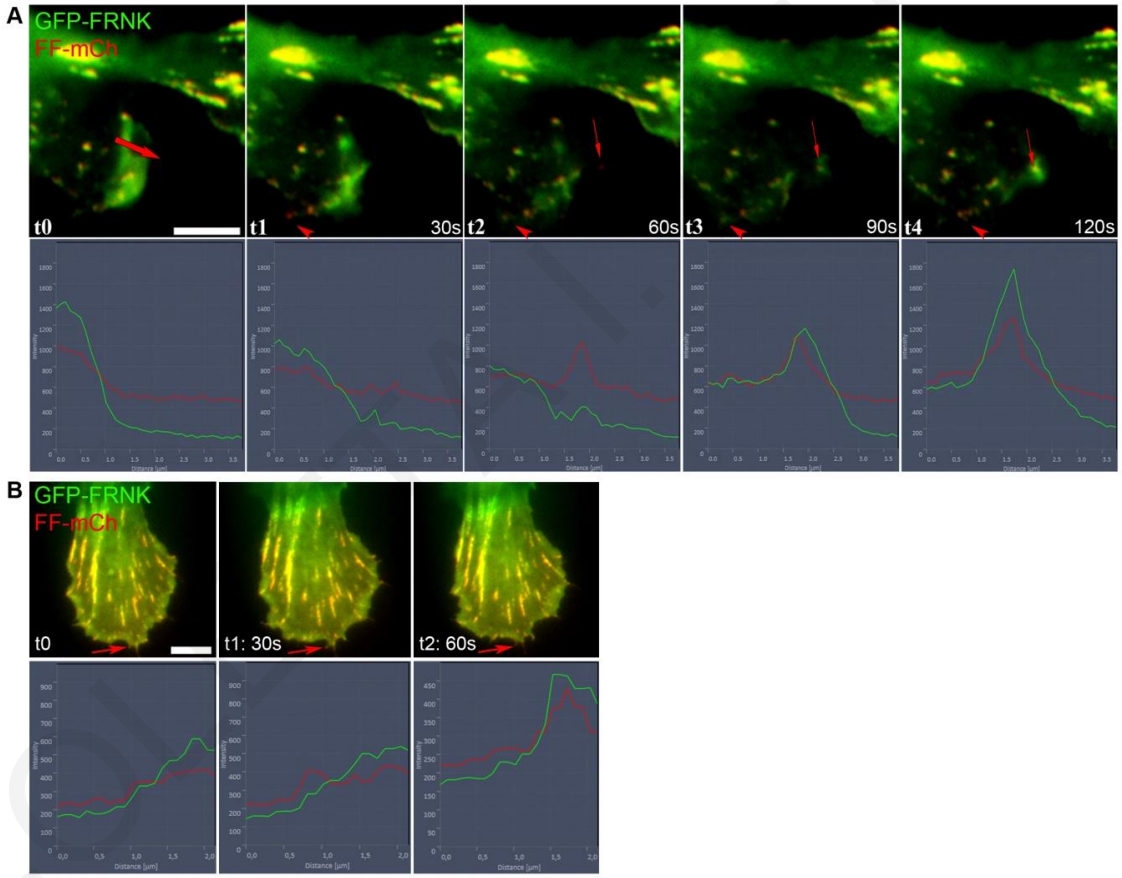

Figure 41: FF displays earlier enrichment on nascent FAs compared to FRNK.

(A) High magnification stills from a time lapse movie of an XL cell transfected with FF-mCherry and GFP-FRNK and intensity profile from the region indicated with an arrow on t0. The red arrow at t2, t3 and t4 shows early enrichment of FF at the newly formed adhesion followed by the subsequent enrichment of FRNK. A second nascent adhesion is shown with an arrowhead. (B) Transient adhesion shows FF enrichment but no FRNK enrichment (red arrow). Scale bars: (A, B) 5µm.

3.2.9. Characterization of the DN effect of FF on FA turnover

In order to characterize the higher affinity of FF for FAs, to explore how it blocks cell migration and to gain insight into FAK function in these complexes we generated point mutants of FF that abolish the interactions of the FAT domain with other FA proteins. Specifically, we generated FF L1034S and FF E1015A point mutants that disrupt the interaction of FAK with paxillin and talin respectively (Sieg, Hauck et al. 1999, Lawson, Lim et al. 2012), and transfected them in adherent cells and compared the phenotype to that of WT FF. Time lapse movies of the three constructs were acquired as described in **Figure 40**. Cells expressing FF L1034S disassembled their FAs in a greater extent than WT FF (**Figure 42A**), indicating that the interaction of FAK with paxillin enhances the localization of FAK at the FAs. Concerning the interaction of FAK with talin, the E1015A mutation on FF resulted in block of FA turnover in a subset of FAs, mainly the ventral FAs (**Figure 42**, white arrows), whereas peripheral FAs appeared to be able to disassemble more effectively than those in WT FF expressing cells (**Figure 42A**). These results indicate that the FAK-talin interaction is more important for the turnover of peripheral FAs, which are usually localized at the leading edge of the cell. Support comes from the fact that introduction of a FAK mutant that abolishes talin binding in FAK null cells does not rescue FA turnover at the leading edge of the cell (Lawson, Lim et al. 2012). This suggests that the FF E1015A mutant does not disrupt the role of talin in this pool of FAs by recruiting it in a FAK deficient complex, highlighting the role of talin in these complexes. These results were also confirmed by FRAP experiments, where the FF L1034S construct displayed faster recovery rates than WT FF, whereas the FF E1015A construct had faster kinetics only at peripheral FAs (**Figure 42B**).

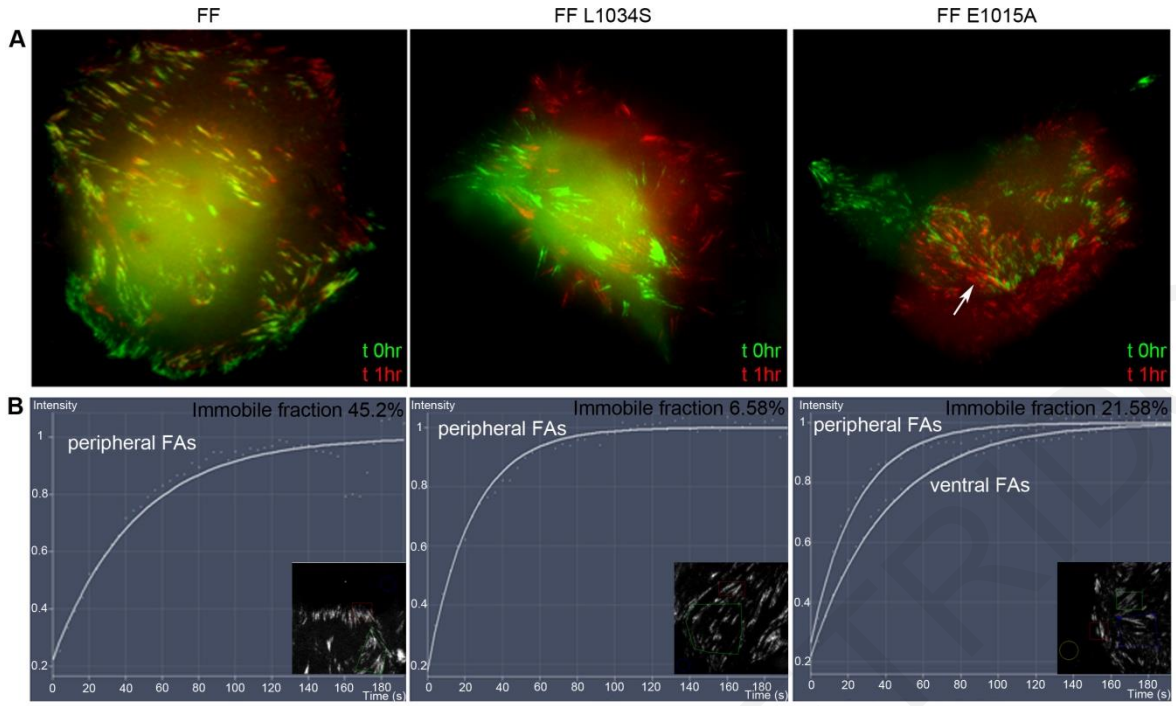

Figure 42: Disruption of the binding partners of the FAT domain leads to impaired DN activity of FF on FA turnover.

(A) High magnification wide field live imaging of FA turnover in FF-GFP, FF-GFP L1034S and FF-GFP E1015A expressing XL177 cells. Cells were imaged for a period of 1 hour. The merged image is composed from the first (green) and last time point (red). (B) Representative FRAP experiments of the above cells (50 frames were acquired for a 200 second period).

3.2.10. FF expression blocks FA turnover and cell migration in mesodermal tissues of the *Xenopus* embryos

To further explore the effects of FF expression on cell migration we expressed FF in mesodermal explants. As shown in **Figure 43A**, FF-GFP expressing cells (green) spread and form very strong FAs. Such strong adhesions are normally absent from migrating mesodermal cells (Wacker, Brodbeck et al. 1998, Stylianou and Skourides 2009). FF expression in this case also blocks FA turnover, preventing these cells from migrating despite the fact that protrusive activity is not affected. Within a short time period, FF expressing cells at the leading edge of the explant are left behind as control cells overtake them (**Figure 43A, Movie 5**). Support comes from experiments where GFP paxillin was used as an FA marker, instead of examining the dynamics of FF on FAs. Specifically, embryos were injected at the one-cell stage with GFP paxillin and at the one blastomere at the two-cell stage with FF + histone RFP and mesodermal explants were dissected as described. As can be seen, cells not expressing FF show a smooth and diffused paxillin signal, whereas paxillin localization in FF expressing cells is punctate and

concentrated at the ECM interface reassembling FA-like structures (**Figure 43B**). Moreover, FRAP experiments were conducted in order to identify how the dynamics of paxillin change in the presence of FF. FF expression resulted in slower recover rates of paxillin at FAs when compared to control cells (**Figure 43C**) confirming that expression of FF affects FA turnover also at the tissue level.

In addition, expression of FF in activin-induced ACs, which normally spread and migrate as a cohesive sheet in all directions when plated on FN (**Movie 6**), blocks spreading, and migration is reduced in the GFP-positive areas (**Movie 7**).

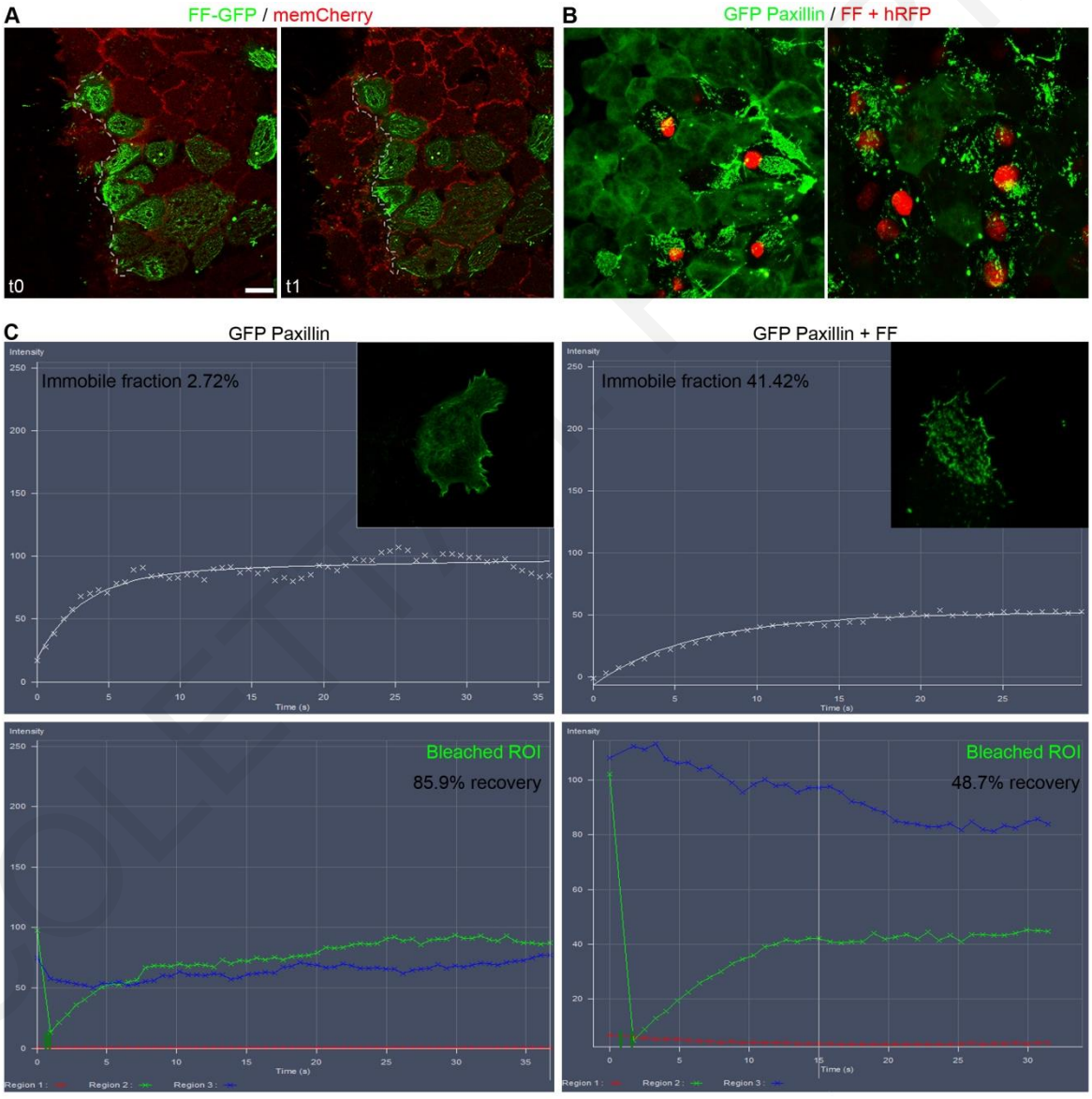

Figure 43: FF expression blocks FA turnover and cell migration in mesodermal tissues.

(A) The first (t0) and last (t1) time point of a 2 hour time lapse movie of a mesodermal explant placed on FN coated coverslips injected with memCherry (red) and FF-GFP (green), showing blockage of cell migration in FF

expressing cells. (B) Representative images of a mesodermal explants expressing GFP Paxillin (green) either alone or together with FF (co-injected with histone RFP), showing exclusive localization of paxillin at the FAs in the FF expressing cells and induction of large ventral FAs. (C) Representative examples of FRAP experiments of single mesodermal cells of *Xenopus* expressing what has been described in (B). Abbreviations: ROI, Region of interest. Scale bars: (A) 20 μm.

3.2.11.FF expression in *Xenopus* leads to loss of mesodermal tissues and severe shortening of the A-P axis

Since we have established that FF acts as a strong DN of FAK both in adherent cells and in mesodermal tissues, we went on to test if this construct can block FAK function in the embryo in order to address the precise roles of FAK in morphogenesis. FAK has a crucial role in mesoderm morphogenesis, since the major defect reported in FAK knockout mice is loss of mesodermally derived tissues such as the notochord and the somites leading to truncated A-P axis (Furuta, Ilic et al. 1995). Moreover, the phenotype of FAK nulls is extremely similar to the FN null mice, which also exhibit early embryonic lethality by E10.5 due to defects in mesodermally derived tissues. Specifically, FN deficient mice have short A-P axis, defects in heart and vessel development, abnormal head and trunk mesoderm and they lack somites (George, Georges-Labouesse et al. 1993). We thus decided to target FF to the dorsal mesoderm via DMZ injection at the four-cell stage. Injection of 500pg FF in the dorsal mesoderm lead to smaller curved and severely shortened embryos, the majority of which died by early tadpole stages (**Figure 44A**). The phenotype could be rescued via co-injection of 150pg of the constitutively active FAK K38A point mutant, indicating that the phenotype is specific (**Figure 44A**). Interestingly, injection of 500pg of FRNK has a mild impact on development (**Figure 44A**) and examination of the phosphorylation status of FAK shows that FF is more effective in blocking FAK phosphorylation *in vivo* (**Figure 44B**). To further address the specificity of the FF phenotype in the shortening of the A-P axis, we combined FAK MO injections with FF expression and as shown in **Figure 44C**, FF and FAK MO act synergistically, suggesting that FF elicits the phenotype via inhibition of FAK activity.

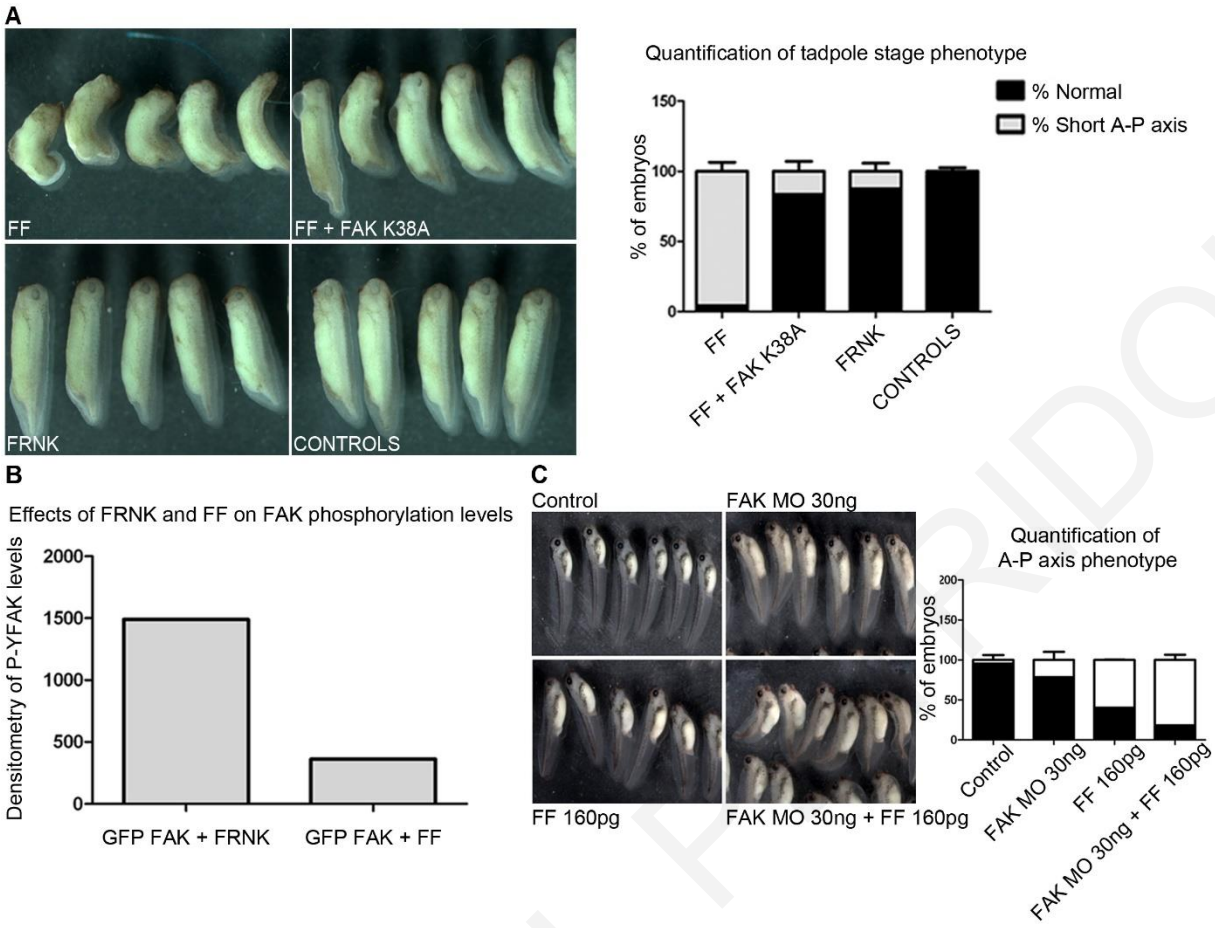

Figure 44: FF expression in the mesoderm leads to severe shortening of the A-P axis of the embryos.
(A) Injection of 500pg of FF at the DMZ of 4-cell stage embryos leads to severe shortening of the A-P axis (95.83 ± 6.45%, n=149) when compared with control and FRNK (12.45 ± 5.87%, n=136) injected embryos. This phenotype is rescued by co-injection of 150pg of FAK K38A (16.41 ± 7.1%, n=136). (B) Densitometry analysis of the phosphorylated levels (blotted with PY20) of immunoprecipitated exogenously expressed GFP FAK from lysates from gastrula stage embryos co-injected with GFP FAK + FRNK or GFP FAK + FF at 2 dorsal-AP blastomeres at the four-cell stage. Phosphorylated FAK has been normalized with total FAK. (C) Injection of 160pg of HA FF or 30ng of FAK MO at the DMZ of 4-cell stage embryos leads to mild A-P shortening whereas the combination of the above same amounts leads to severe A-P shortening.

Time lapse imaging of A-P axis elongation in control and FF injected embryos revealed that the shortening of the A-P axis happens later on in development, i.e. after tailbud stages (**Movies 8** and **9**). Interestingly, FF injected tadpoles in the mesoderm displayed extensive loss of dead cells during A-P axis elongation (**Movie 9**), raising the hypothesis that inhibition of FAK in the mesoderm leads to shortening of the A-P axis through the loss of the mesodermal tissues. In order to address if FAK inhibition affects mesodermal development, we performed whole-mount ISH and RT-PCR experiments to examine mesodermal induction and patterning in the presence of FF. FF expressing embryos display normal mesoderm induction and marker

expression at gastrula and neurula stages (Xbra - *Xenopus* Brachyury - and MyoD) similarly to control, FRNK injected and rescued embryos (**Figure 45A-C, E**). However, FF expressing embryos display extensive loss of somitic mesoderm (MyoD) (**Figure 45B, C, E**, red arrowheads) at tadpole stages while no effect is seen in the expression of Sox2 (**Figure 45D, F**). This phenotype was absent in FRNK expressing embryos and importantly it was rescued by expression of FAK K38A (**Figure 45E**). It has been previously shown that FRNK expression in the somitic mesoderm in *Xenopus* led to disrupted somite formation (Kragtorp and Miller 2006). However, when we compared the effects of FF and FRNK on somite formation, we observed that whereas FRNK injected embryos display mild defects in the intersomitic boundaries compared to controls, FF injected embryos display severe disruptions of the intersomitic boundaries, lack of boundaries in certain areas, misorientation of the somitic cells, reduced phospho-tyrosine staining at the boundaries and overall disruption of structure and loss of tissue in agreement with the reduced marker expression in ISH experiments. This phenotype was rescued by co-injection of 150 pg of FAK K38A, indicating that is specific to loss of FAK function (**Figure 45G**). Moreover, despite normal patterning at gastrula stages, Xbra staining of the notochord appeared wider (**Figure 45A,** yellow arrowhead) while the MyoD expression domain at neurula stages was wider and positioned at the posterior (**Figure 45C, D,** white arrowheads). This coupled with the dorsally bend tadpole stage embryos suggested that CE movements may be affected. However, AC elongation assays showed that FF expressing ACs elongate to the same extent as controls (**Figure 45H**), suggesting that the mild early mesodermal morphogenesis problems may be due to defective mesoderm migration and possibly radial intercalation of the mesoderm. This result is in agreement with the results for the time lapse movies of A-P axis elongation of FF injected embryos which appear to develop normally at gastrula and neurula stages supporting the notion that the morphogenetic movements of the mesoderm during gastrulation and neurulation are unaffected.

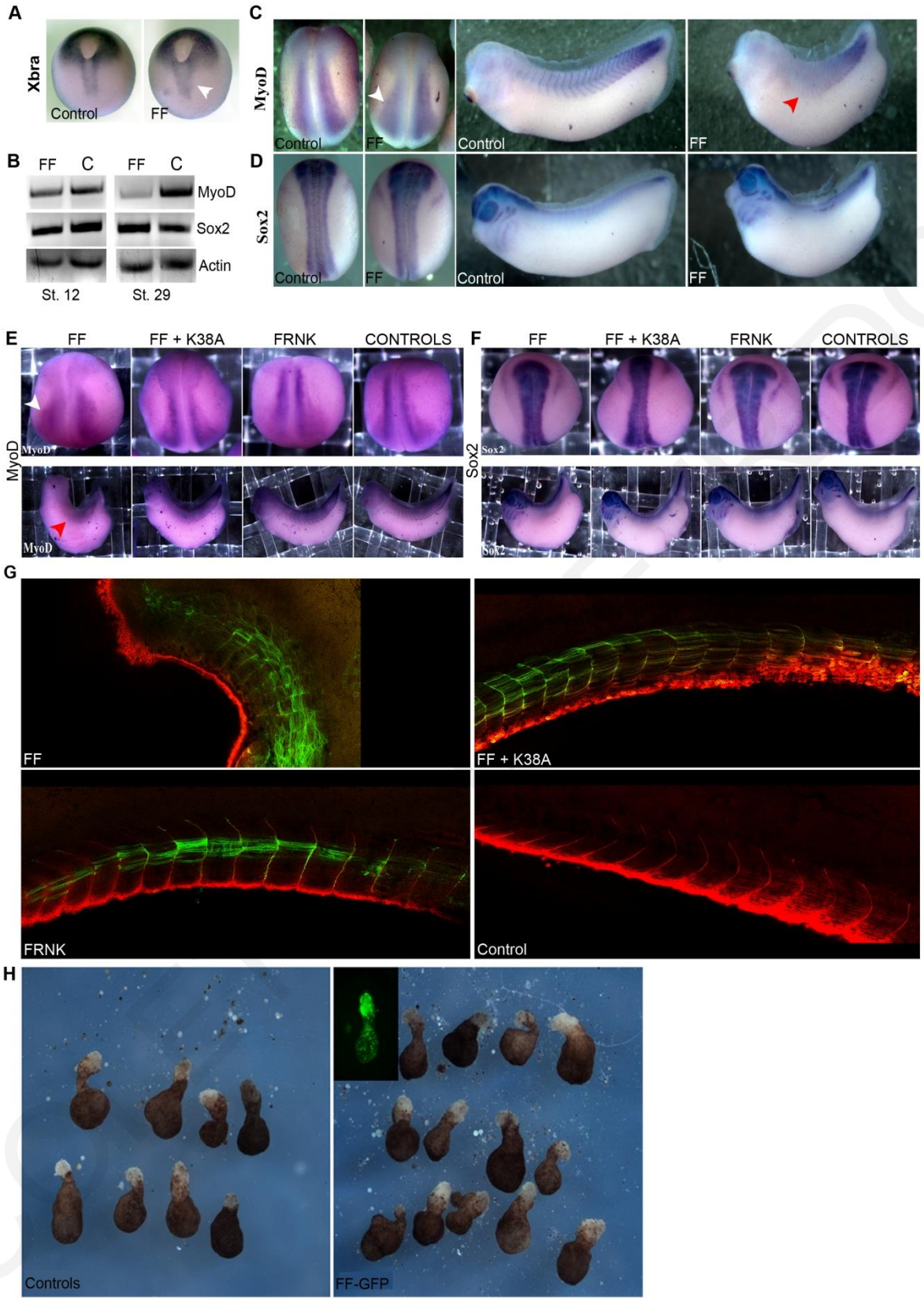

Figure 45: FF expression in the mesoderm leads to loss of somitic mesoderm and to short A-P axis.

(A) Whole mount ISH for Xbra of gastrula stage control embryos or embryos injected with 500pg FF at the 2 dorsal blastomeres at the four-cell stage. (B) RT-PCR of gastrula and tadpole stages of control embryos or embryos injected with 500pg FF 2 out of 4 DMZ for MyoD, Sox2 and Actin showing loss of MyoD in FF injected embryos. (C, D) Whole mount ISH for MyoD and Sox2 of neurula and tadpole stage control embryos and embryos injected

with FF as described above. (E, F) Whole mount ISH for MyoD and Sox2 of neurula and tadpole stage control, rescued embryos or embryos injected with FF and FRNK. (G) Maximum Intensity Projections of *Xenopus* tadpoles injected with the indicated constructs together with memGFP, showing severe defective somitic morphogenesis in FF injected embryos. (H) AC elongation assays on control and FF-GFP expressing ACs showed no effect of FF on CE movements.

3.2.12. The loss of mesodermal tissues induced by FAK loss of function is due to apoptosis stemming from cell division defects

The overall severity of the A-P axis elongation defects together with the specific loss of somitic mesoderm in FF expressing embryos suggests defects in the survival of the mesodermal cells. To explore this possibility we performed tunel staining of FF expressing embryos neurula and tadpole embryos and observed increased apoptosis beginning at neurula stages (**Figure 46A**). In order to probe the cause of apoptosis we performed immunofluorescence experiments of FF expressing embryos co-injected with histone GFP which revealed a large number of anaphase bridges from late gastrula stages onwards suggesting that FF expression induces mitotic defects and apoptosis (**Figure 46B**).

Since Ser732 phosphorylation of FAK has been shown to play a role in centrosome function during mitosis (Park, Shen et al. 2009), we examined the effects of FF expression on the levels of endogenous P-Ser732. FF expression leads to a reduction of P-Ser732 levels and FF itself is heavily phosphorylated on Ser732 (**Figure 46C**). Since phosphorylation of Ser732 has been shown to be essential for the association of endogenous FAK with dynein, we postulated that FF's DN activity with respect to the centrosomal function would require this residue. We thus generated a Ser732 point mutant that substituted Serine to Alanine (FF-S732A), and compared the effects of its expression to that of FF. As shown in **Figure 46B**, FF-S732A expression fails to induce mitotic defects resulting in a much milder phenotype compared to FF (**Figure 46D**), suggesting that at least part of the FF phenotype is due to effects of FF on centrosome function through Ser732. These results suggest that the role of FAK in mesodermal survival is primarily associated with FAK's role in cell division and survival through the phosphorylation of the Ser732 residue.

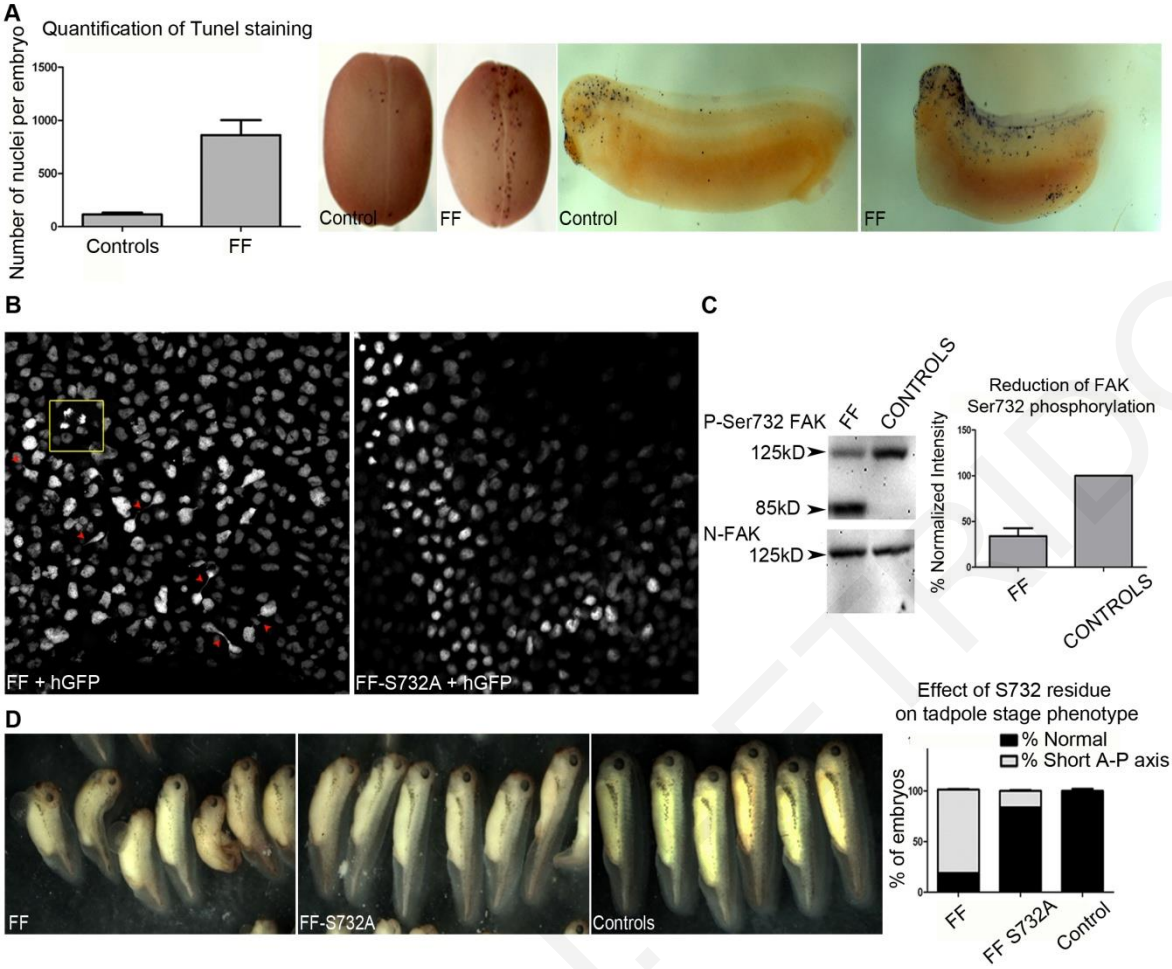

Figure 46: Phosphorylation of FAK on Ser732 regulates cell division and apoptosis in mesodermal tissues. (A) Tunel assay on control and FF injected embryos at the DMZ at the four-cell stage. Quantification of the apoptotic nuclei at the tadpole stages shows a 7-fold increased apoptosis in FF expressors (861.67 ± 140.96 apoptotic nuclei compared to 114.67 ± 17.79 apoptotic nuclei in controls, n=6, two independent experiments). (B) Confocal images of embryos co-injected with histone GFP and HA FF or HA FF-S732A to visualize mitotic cells showing the formation of anaphase bridges (red arrowheads) and multipolar spindles (yellow box) in FF expressors. (C) Western blot and densitometry analysis of the effect of HA FF expression on the reduction of the phosphorylation levels of P-Ser732 endogenous FAK and Ser732 phosphorylation of FF (lower band in FF lane). (D) Control and injected tadpole embryos with FF or FF-S732A at the DMZ at the 4-cell stage and statistical analysis of the shortened A-P axis phenotype.

3.2.13. Generation of an inducible form of the FF DN construct

Although the use of MOs to study later functions of a protein during development is quite common, this approach is not ideal when the protein of interest is involved in processes concerning cell survival and apoptosis. The reason behind this, is that in order to address the function of a protein in developmental processes that occur later on in embryogenesis, such as vasculogenesis and organ development, the precursors needed for these processes have to be

unaffected until the developmental stage where these processes begin. So if the protein of interest is involved in cell survival, then the potential defects of the latter developmental processes can be attributed to the loss of the precursors or even loss of inductive interactions required for the formation of an organ from tissues not involved directly in its formation. Given the fact that FAK is involved in cell survival and apoptosis of mesodermally derived tissues, the use of the available MOs or the FF DN to study late developmental roles of FAK is problematic. Thus, in order to explore FAK's involvement in late embryonic development we generated an inducible FF DN based on the hormone binding domain of the glucocorticoid receptor (GR). This type of inducible systems have been widely used in *Xenopus* and they are based on the insertion of the hormone binding domain of the GR in the construct of interest (Kolm and Sive 1995, Tada, O'Reilly et al. 1997). When the construct is expressed in the cell it is not functional because it is sequestered by the heat-shock apparatus of the cell HSP90, which binds the hormone binding domain, creating a complex that covers the entire molecule and masks its binding sites. Addition of dexamethasone (DEX) that binds the GR, leads to the release of the construct and its activation. We generated the inducible FF-GR by inserting the ligand binding domain of the GR between the FERM and the FAT domains of the molecule. In order to test it, we transfected FF-GR in HeLa cells and examined its localization. As shown, in the absence of induction, FF-GR is localized primarily in the cytosol, while after induction it is localized exclusively at FAs (**Figure 47A**). In addition, after induction FF-GR transfected cells display ventral FAs indicating defective cell migration similarly to the FF DN, showing that this construct is functional (**Figure 47A**). Importantly, activation of the FF DN is reversible, since removal of the inducing agent leads to the loss of the localization of FF on FAs and to disassembly of the ventral FAs (**Figure 47A**). In addition, to ensure its functionality *in vivo*, we injected FF-GR at the DMZ of *Xenopus* embryos, where we have shown before that loss of FAK function in mesodermal tissues leads to shortened A-P axis of the embryos. Induction of the construct after gastrulation leads to severe shortening of the A-P axis (**Figure 47B**), establishing this construct as a powerful tool to study FAK function during later stages in development.

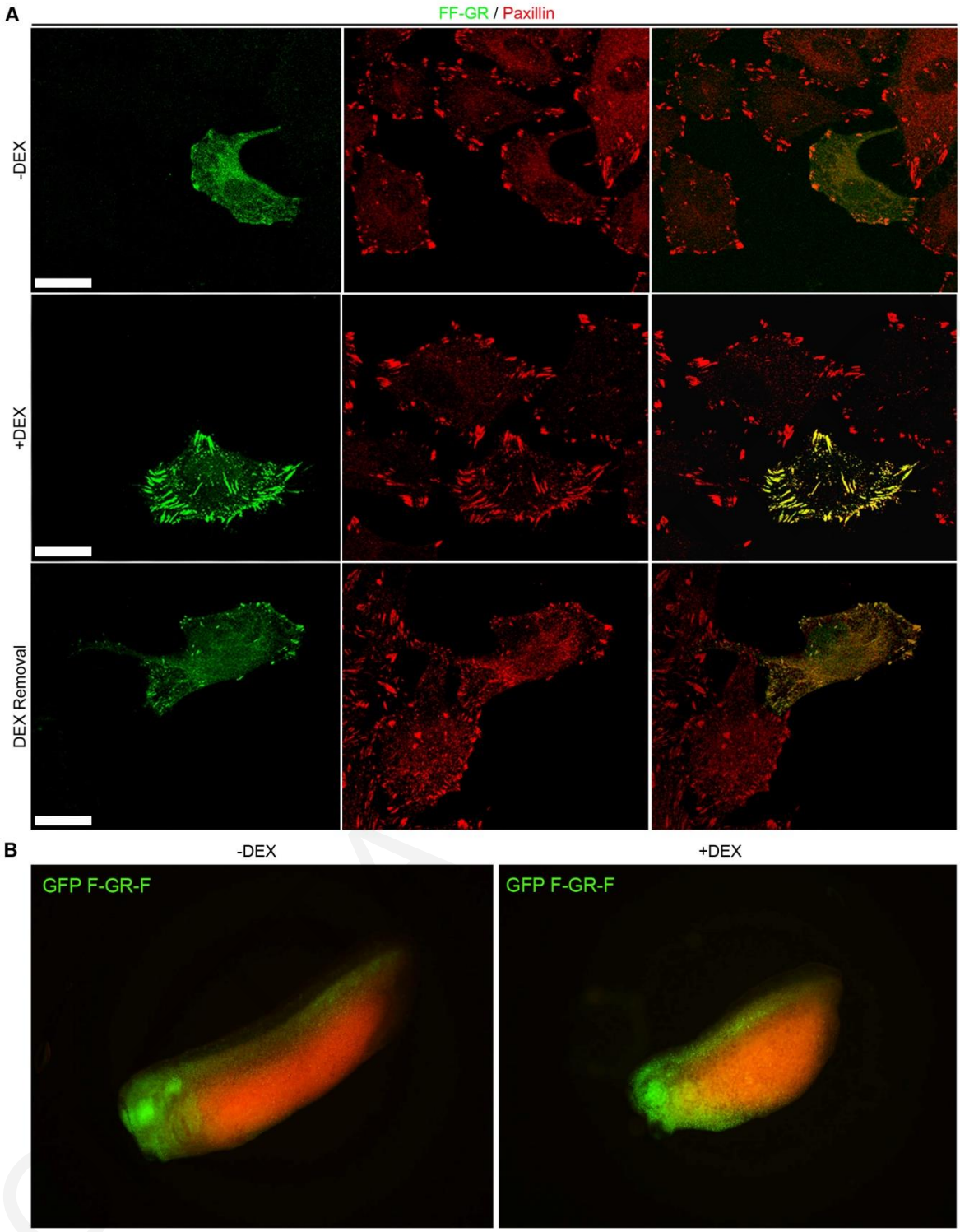

Figure 47: Characterization of the inducible FF DN *in vitro* and *in vivo*.

(A) HeLa cells expressing FF-GR in the absence of the inducing agent show no FA localization and no effect on the FA formation. When cells are treated with 100 nM of DEX, FF localizes almost exclusively at FAs and leads to formation of ventral FAs. 3 hours after the removal of DEX, FF expressing cells disassemble their ventral FAs and FF is localized primarily back to the cytosol. (B) Expression of the FF-GR construct in the mesodermal tissues of *Xenopus* leads to shortening of the A-P axis only upon induction. Scale bars: (A) 20 μm.

3.2.14. Inhibition of FAK function results in defective vascular development

As mentioned above, FAK knockout mice display general deficiency in mesoderm including abnormal vasculature development (Furuta, Ilic et al. 1995). FAK's role in the cardiovascular system was later confirmed using a conditional knockout of FAK in endothelial cells which resulted in defective development of the embryonic vasculature (Shen, Park et al. 2005). Support also comes from conditional mice where either the Tyr397 autophosphorylation site or the R454 site was mutated, which again display defective vascular development including hemorrhages, deficient vascular remodeling and delayed artery formation (Corsi, Houbron et al. 2009, Lim, Chen et al. 2010). Blood vessel formation in *Xenopus* is accomplished in two phases, vasculogenesis, where the endothelial cells precursors, angioblasts, migrate from the lateral plate mesoderm and differentiate into endothelial cells to form endothelial tubes and primary vessels and angiogenesis, where the existing primary vessels remodel and extent new vessels (Bussolino, Mantovani et al. 1997, Hanahan 1997, Risau 1997).

In order to explore the role of FAK in the development of the *Xenopus* vascular system, we initially injected low amount of FF (100pg) that it will not cause embryonic lethality, at the mesoderm and embryos were allowed to develop until tadpole stages. Examination of these tadpoles revealed scattered variably sized hemorrhages consistent with a role of FAK in angiogenesis and vascular development (**Figure 48A**). To gain further insight into how FAK regulates vascular development we utilized the inducible FF-GR DN, described above. Embryos were injected with 150 pg of FF-GR targeting the vascular system at the blastomeres C2, C3 or C4 at the 16-cell stage which give rise to the main vessels including dorsal aorta (da), cardinal veins, intersomitic vessels (isv) and dorsal lateral anastomosing vessel (dlav) and were induced with DEX in different stages of development. Specifically, FF was activated at stage 22 at the onset of angiogenesis, where the formation of the main vessels of the trunk and tail starts. At this developmental stage vasculogenesis is completed so activation of FF in this stage will not be able to affect the integrity or the migration process of the endothelial precursors. Phenotypic analysis of these embryos revealed hemorrhages, similarly to FF injected embryos (**Figure 48B**).

Detailed examination of the vascular system of these embryos at stage 45 by injecting QDs in the heart revealed structural defects in the main vessels. Specifically, the connection of the dlav to the posterior cardinal vein (pcv) was defective at the trunk (**Figure 48C**, red star) and the isv were abnormal and incoherent (**Figure 48C,** white arrows). Moreover, in the area of the tail the pcv and dlav displayed discontinuities. These phenotypes were absent in embryos injected with FF-GR but were not treated with DEX (**Figure 48C**). The above experiments were repeated but

the FF-GR was induced at st.38, by which time the da, pcv and dlav have fully formed. No obvious abnormalities were observed in the structure of these vessels at st.45 (**Figure 48C**). However, extensive abnormalities were observed in the isv, especially at the tail region probably due to the fact that during development, the trunk isv form first and then those of the tail, so at the time of induction the trunk isv were already formed (**Figure 48C**, yellow arrowheads). These results suggest that FAK is essential in the process of angiogenesis.

Since FF-injected *Xenopus* embryos, like FAK null mice display hemorrhages, we examined the possibility that FAK is important for the integrity of the blood vessels. In order to do this, FF-GR injected embryos which were induced at stage 22 were removed from DEX at stage 45, where the main vasculature was completely formed, and examined for hemorrhages at stage 52. Embryos were injected in the heart with QDs and imaged to identify leakage of the QDs from the vessels. Removal of DEX partially rescued the hemorrhages observed in the embryos remained in the inducing agent, as can been seen from the absence of QD signal all over the tadpole, suggesting that FAK has a role in maintaining vessel integrity (**Figure 48D**).

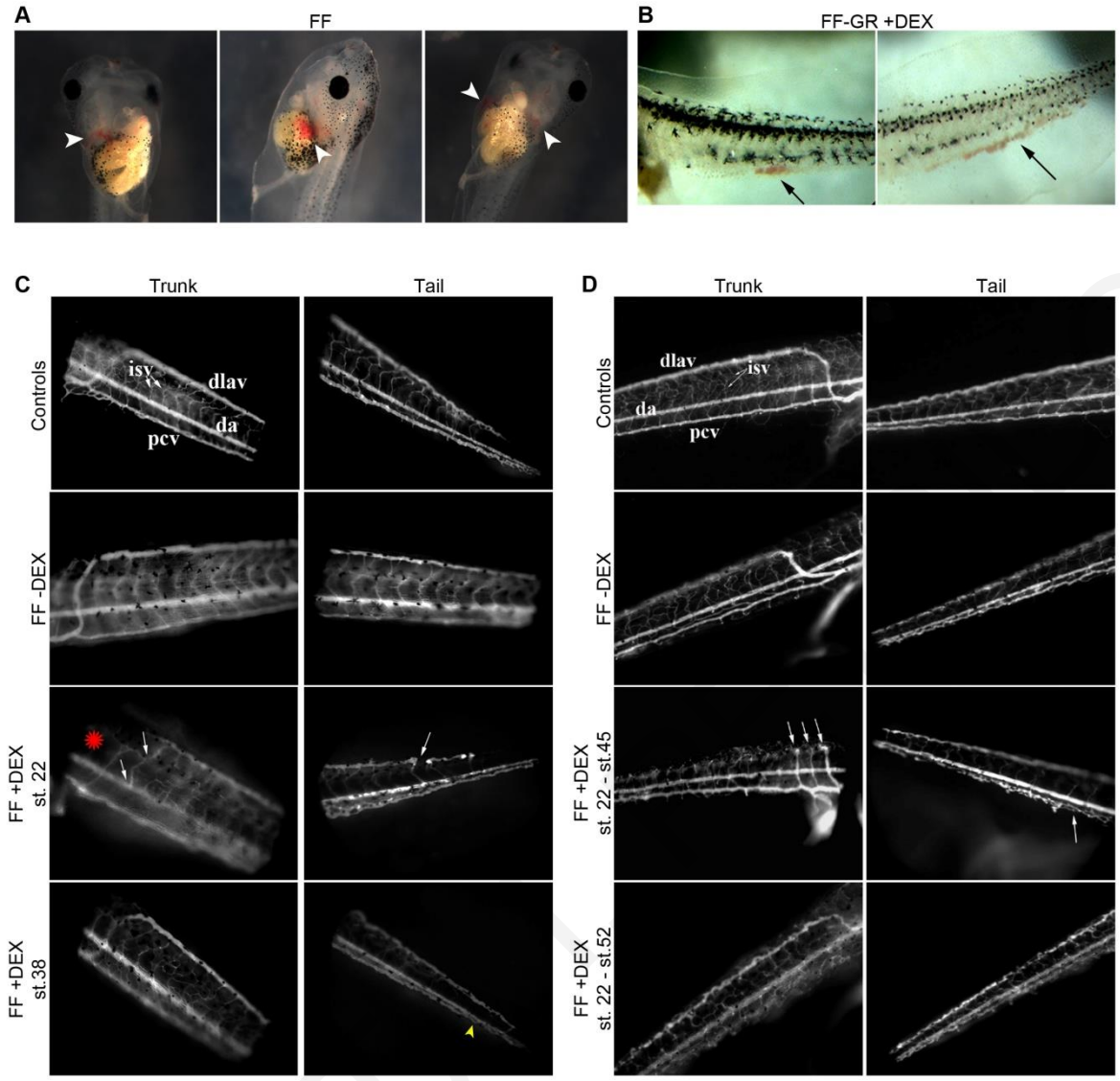

Figure 48: FAK is required for proper angiogenesis during *Xenopus* development.

(A) Representative images of tadpoles injected with 100pg of FF at the mesoderm. Hemorrhages are indicated by the white arrowheads. (B) Hemorrhages at the tails of tadpoles injected with the inducible FF (DEX was added at stage 22). (C) Fluorescent images from control tadpoles, or tadpoles injected with FF-GR, either non-induced, or induced at two different stages of development. Embryos were injected in the heart with QDs at stage 45 and imaged immediately. (D) Same as (C) but FF-GR injected embryos were either maintained in DEX until stage 52, or removed from DEX at stage 45.

3.2.15.FAK signals cell polarity during *Xenopus* epiboly

Since FF acts as a strong DN both in adherent cells and in the embryo, combined with the inability of FRNK to block FAK function during early embryogenesis, we used FF to address the diverse roles of FAK in tissue morphogenesis of the *Xenopus* embryos. FAK is a major transducer of integrin signaling and the earliest integrin dependent process described in *Xenopus* is the FN fibrillogenesis taking place on the BCR. In addition, FAK is expressed in the AC of *Xenopus* embryos and is specifically expressed and activated in the deep cells of the AC co-localizing with FN suggesting a possible role in this process (**Figure 26B**) (Hens and DeSimone 1995).

In an effort to address the role of FAK in *Xenopus* early morphogenesis we decided to test if FF expression could block endogenous FAK function in the embryo. As shown in **Figure 49A**, injection of 500pg of FF in the AC leads to severe gastrulation defects including failure of blastopore closure. These defects are partially rescued by co-expression of K38A FAK, which speeds up blastopore closure (**Figure 49A** and **Movie 10**). This phenotype was not rescued by expression of a FAK construct lacking the N-terminal domain (FAK Δ375) (**Figure 49B**), stressing the requirement of the FERM domain for FAK's function in this context. Interestingly, FF-S732A expression induced identical phenotypes as FF concerning block of blastopore closure (**Figure 49C**) suggesting that FAK's role in the epithelial tissues during gastrulation is independent from the centrosomal function of FAK.

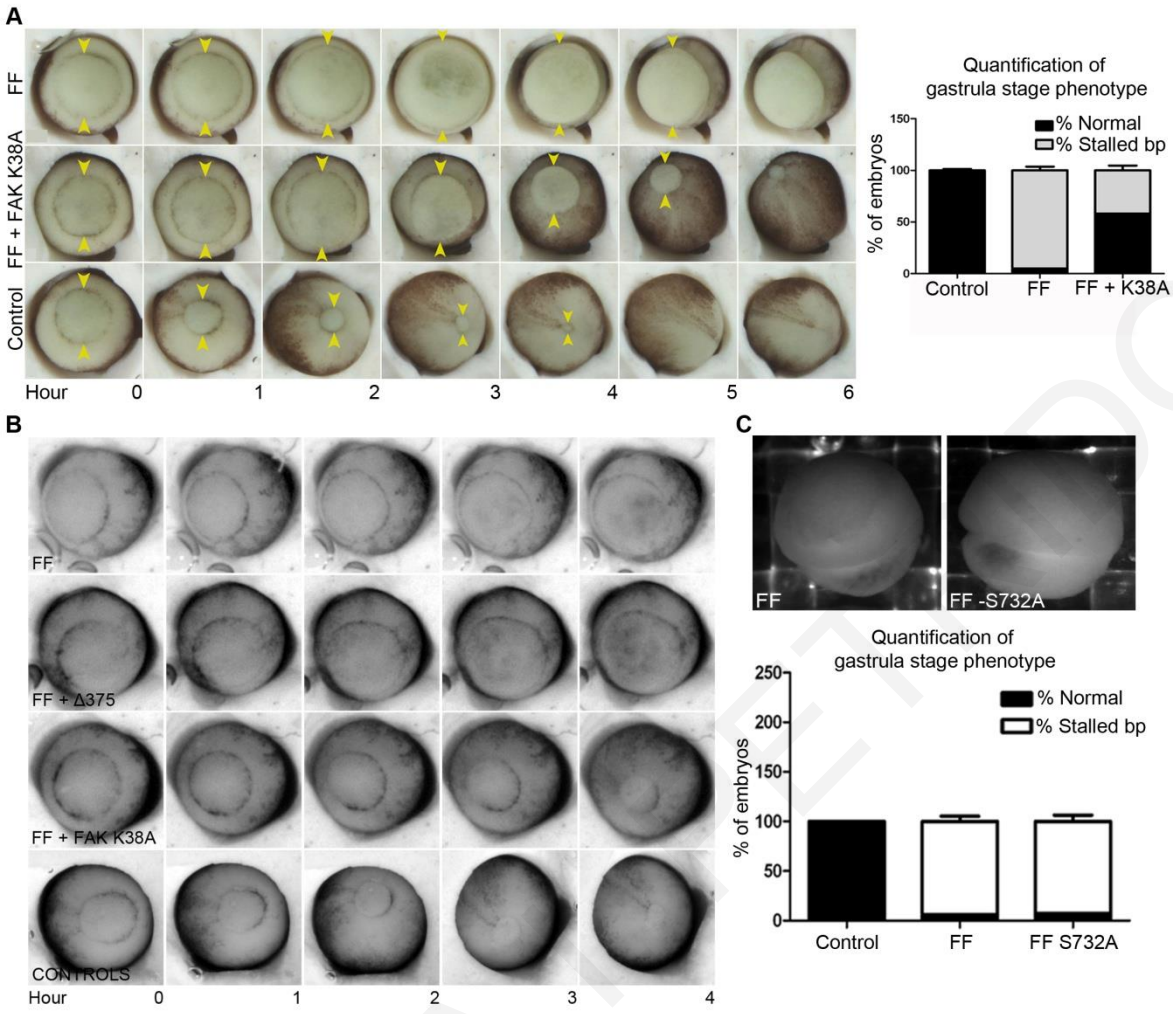

Figure 49: FF expression at the AC leads to stalled blastopore and gastrulation failure.

(A) Stills from a movie showing blastopore closure in controls and embryos injected with 500 pg HA FF (95.05 ± 3.7% stalled blastopore, n=211) or 500 pg HA FF + 150 pg FAK K38A (41.97 ± 4.7% stalled blastopore, n=128,) from three independent experiments. Yellow arrowheads show the progress of blastopore closure. (B) Time lapse images of blastopore closure in control embryos or injected with 500 pg FF, 500 pg FF + 150 pg FAK Δ375 and 500 pg FF + 150 pg FAK K38A in both blastomeres at the two-cell stage. FAK Δ375 fails to rescue the FF-induced blastopore closure defect (32 out of 35 embryos with stalled blastopore) whereas FAK K38A expression partially rescued this phenotype (13 out of 35 embryos with stalled blastopore). (C) Gastrula stage embryos injected with HA FF or HA FF-S732A and statistical analysis of the stalled blastopore phenotype from three independent experiments.

In order to gain insight into the role of FAK during gastrulation, we performed whole mount ISH experiments for mesodermal and neural markers in FF injected and control embryos. Embryos were sectioned sagittally and imaged. We noticed that, in FF expressing embryos the prospective mesodermal and neural tissues display proper induction and patterning as can be seen from the expression of the pan-mesodermal marker Xbra, the head mesoderm marker goosecoid (Gsc), the dorsal mesoderm marker Chordin (Chrd) and the pan-neural marker Sox2

(**Figure 50A-E**). However, the blastocoel is displaced vegetally, the archenteron fails to form and the mesoderm only involutes partially leaving un-internalized chordin and Gsc expressing cells in the dorsal vegetal region of the embryo (**Figure 50B, C**). In agreement with the failure of the Δ375 construct to rescue the FF phenotype, expression of FRNK which lacks the FERM domain does not induce any appreciable gastrulation defects confirming the requirement of the FERM domain for the DN function in this context (**Figure 50A-D**).

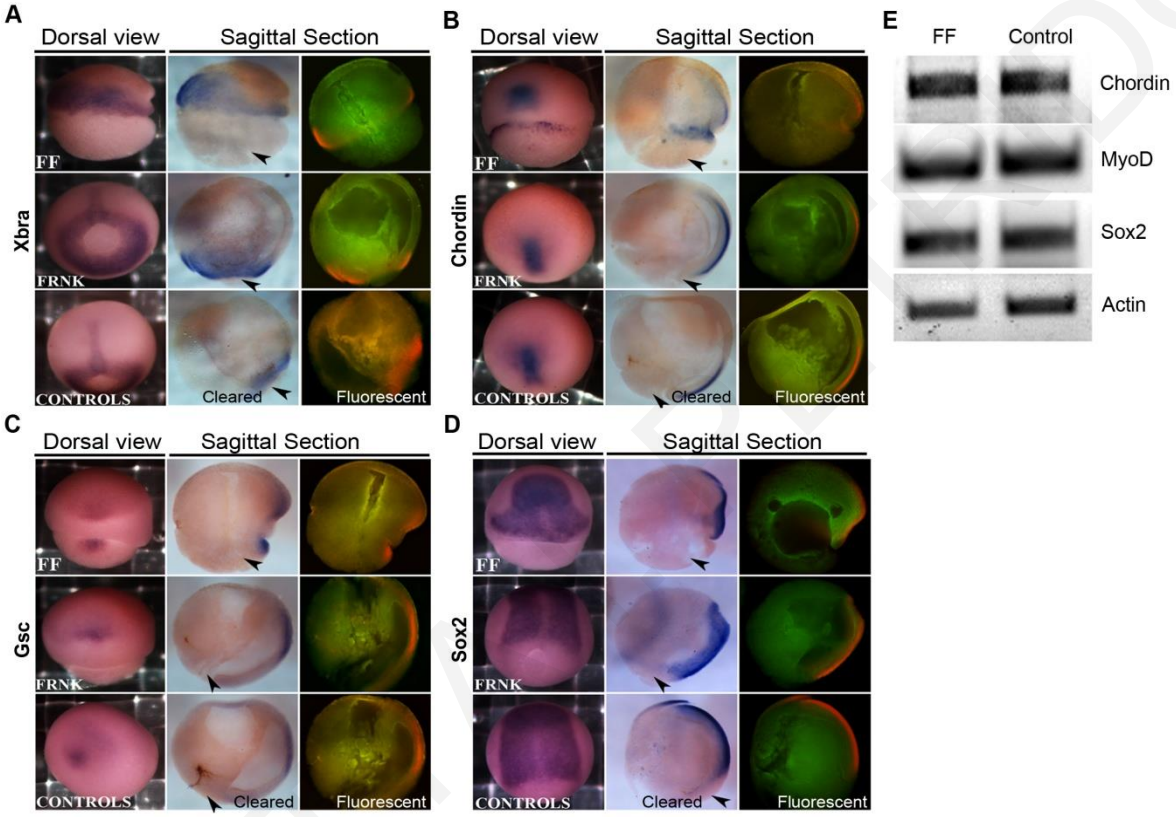

Figure 50: FF expression at the AC leads to blastopore closure arrest without affecting mesoderm and neural induction and patterning.

Whole mount ISH of control and embryos injected with HA FF and HA FRNK for the mesodermal markers Xbra (A), Chrd (B) and Gsc (C) and the neural marker Sox2 (D). Black arrowheads show the blastopore. (E) RT-PCR for the markers Chrd, MyoD and Sox2 and for Actin as a loading control from control and FF injected mid-gastrula stage embryos.

More detailed characterization of sagittally sectioned FF expressing embryos during early and late gastrulation, revealed a visible thickening of the BCR suggesting that epiboly and radial intercalation are blocked (**Figure 51A, B**, red arrowhead). In addition, while normally, cell divisions in the BCR are parallel to the plane of the epithelium, spindle orientation in FF expressors is randomized showing loss of polarity (**Figure 51C**, white arrowheads). Dose response of a previously characterized FAK MO showed no early gastrulation defects (Fonar,

Gutkovich et al. 2011). However, sectioning of morphant embryos at gastrula stages revealed epiboly defects albeit milder than those induced by FF expression (**Figure 51D**). Epiboly occurs in two distinct phases beginning at the AC and spreading to the MZ as gastrulation proceeds (Keller 1980) and morphants display more prominent thickening in the MZ suggesting that the MO is more effective in preventing later intercalative activities as the maternal pool of FAK is slowly depleted. This is in agreement with the fact that FAK MO only reduces FAK protein levels by 50% at early gastrula stages (**Figure 51E**).

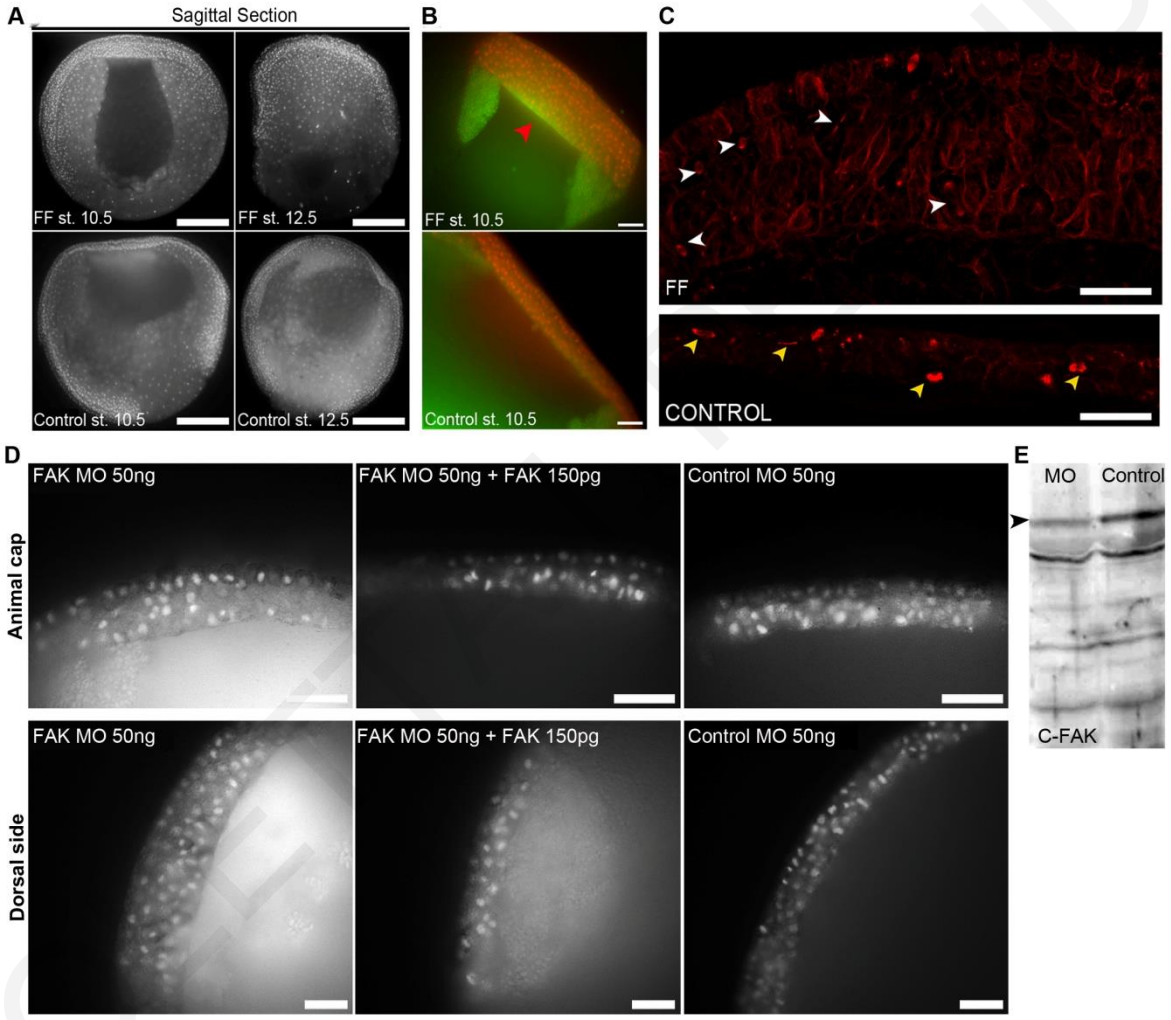

Figure 51: FF expression in the AC leads to epiboly failure and loss of polarity in the epithelial cells at the AP.

(A) Wide field images of sagittal sections of early and late gastrula stage control and HA FF injected embryos stained with Hoechst, showing thick AC in FF expressing embryos. (B) Wide field images of the AC of the same embryos showing epiboly failure in HA FF injected (red arrowhead). (C) HA FF injected and control stage 11 embryos stained with β-tubulin antibody to image spindle orientation (78.7% misoriented spindles, n= 61, three independent experiments). (D) Injection of 50 ng of FAK MO and 50 pg of histone RFP as a lineage tracer either at the AC (upper panel) or at the dorsal side of the embryo (lower panel) leads to defective epiboly and the

phenotype is rescued with expression of 150 pg of WT FAK. The epiboly defect is more pronounced in the MZ (lower panel). (E) Western blot analysis of lysates from FAK MO injected and control embryos with the C-903 FAK antibody showing an approximately 50% reduction of endogenous FAK at early gastrula stage. Scale bars: (A) 500 µm, (B) 100 µm, (C, D) 50 µm.

The gastrulation defects observed in FF expressors are quite similar to what was observed when FN fibrillogenesis is inhibited (Marsden and DeSimone 2001, Davidson, Marsden et al. 2006) suggesting that FF may be eliciting these by blocking FN fibrillogenesis. FN staining of stage 11 FF expressors however, shows that a dense fibrillar matrix is present (**Figure 52A**) and FN protein levels are unaffected suggesting that FF does not elicit its effect through the loss of the FN matrix (**Figure 52B**). However, in FF expressors the fibrils appear thicker than controls (**Figure 52A**) and sagittal sections of FF expressing embryos reveal a dense network of FN on the BCR and ectopic fibrils between the cells of the AC (**Figure 52A,** red arrowhead), in agreement with the slow FA turnover and loss of polarity elicited by FF expression. Importantly, conditioned substrates from FF ACs support cell adhesion and migration, providing evidence that the FN fibrillar matrix deposited should be able to signal polarity (data not shown).

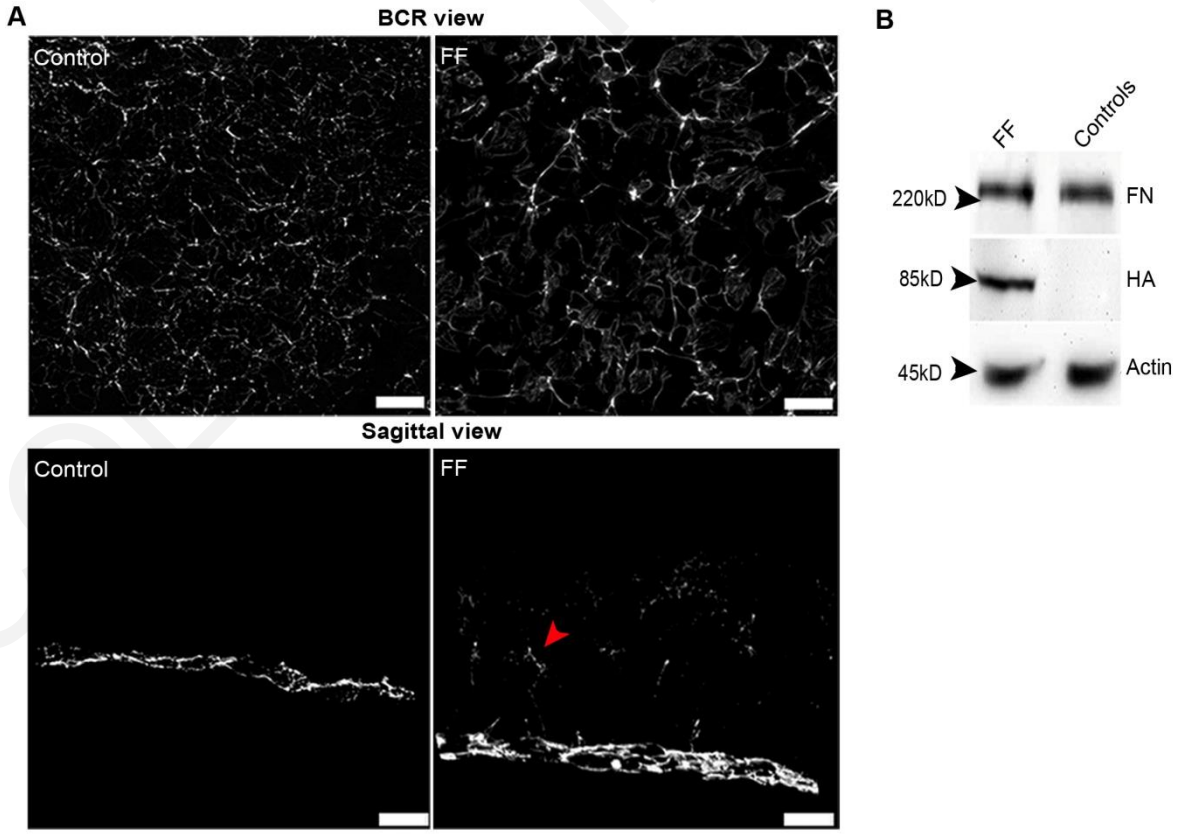

Figure 52: FF expressing ACs retain the FN matrix that provides signal polarity.

(A) Confocal images of the FN matrix on the BCR of control and FF-GFP injected embryos at stage 11 and sagittal sections from embryos of the same experiment showing ectopic FN fibril formation between the inner cells of the AC in FF injected embryos (red arrowhead). (B) Western blot analysis shows similar expression levels of FN between HA FF injected and control embryos. Scale bars: (A) 20 μm.

Another possible mechanism through which FF may be blocking epiboly is through the inhibition of adhesive complex turnover. To explore this possibility we used MOs against *Xenopus* Vinculin. Vinculin null cells adhere poorly and have been shown to display increased migration rates and faster turnover of FA complexes (Coll, Ben-Ze'ev et al. 1995). FRAP experiments comparing FF-GFP recovery in FF alone and FF + vinculin MO injected explants show that vinculin knockdown leads to fewer and smaller adhesions in these cells in addition to increased turnover of FF in a similar fashion to FAK K38A (**Figure 53A**). However, unlike FAK K38A which rescues epiboly, vinculin knockdown fails to do so (**Figure 53B**) suggesting that the effects of FF on FA turnover are not responsible for the phenotype. As an alternative approach, we utilized the FF L1034S mutant, where as shown above displays significantly faster turnover on FAs and fails to block FA disassembly. However, this mutant also blocks epiboly effectively uncoupling FA turnover from the epiboly defects (**Figure 53C**).

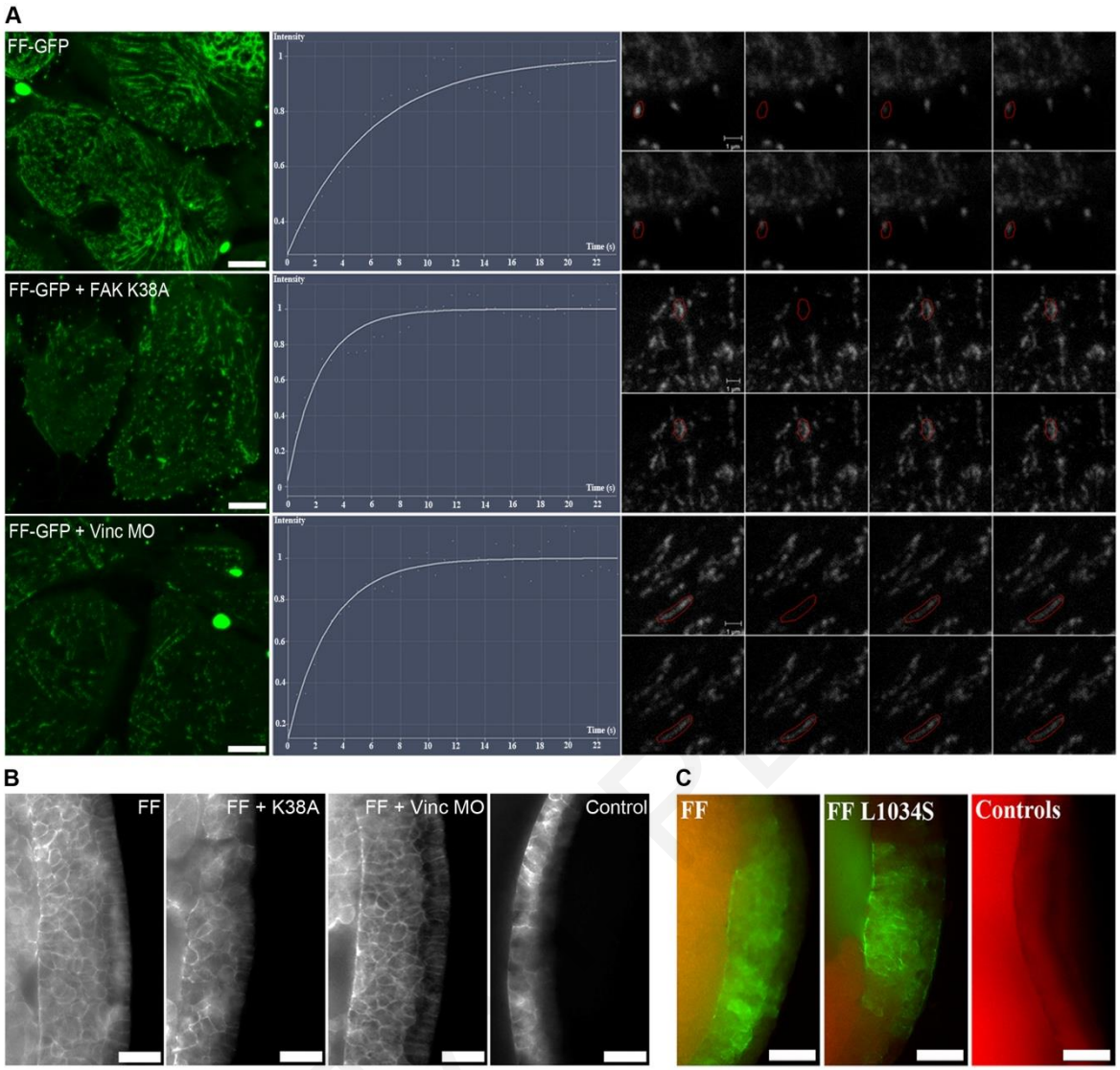

Figure 53: Epiboly failure through FAK loss of function is not associated with FA turnover defects.
(A) FRAP experiments on FF-GFP expressing inner ectodermal cells alone, co-injected with HA FAK K38A, or Vinculin MO. A total of 40 frames were acquired in a 24.4 second period. Vinculin MO injection, as well as FAK K38A expression, increases the turnover rates of FF on FAs formed by the cells of the AC. (B) Wide field images of gastrula stage control and embryos injected with FF, FF + FAK K38A, FF + vinculin MO stained with β-catenin antibody to visualize the cell boundaries. (C) Wide-field images of the AC of gastrula stage embryos injected with 500 pg of FF-GFP or FF-GFP L1034S in both AP blastomeres at the two-cell stage showing similar epiboly defects. Abbreviations: Vinc, vinculin. Scale bars: (A) 5 μm, (B) 50 μm, (C) 20 μm.

Previous studies in *Xenopus* have demonstrated that FN can provide signals that instruct cells to intercalate in the plane perpendicular to the matrix, and that these signals can act at a distance (Marsden and DeSimone 2001). Our results suggest that FF expression leads to loss of polarity in the cells of the BCR by blocking these signals. If in fact FF blocks integrin signals required for polarization, one would expect that restricted FF expression in the cells in contact with the FN matrix would be sufficient to block directional intercalative behavior. To test this

hypothesis, we took advantage of the deep layer explant developed by Marsden and DeSimone (2001). In this explant, a DMZ tissue is cut from one embryo and layers of deep cells lining the blastocoel are shaved and placed on a FN coated coverslip. Another DMZ fragment is cut, the majority of deep cells removed and then positioned over the deep explant. As shown in **Figure 54A**, when the deep explant in contact with the FN is expressing FF-GFP, little or no intercalation takes place from the overlying tissue and the GFP positive FF explant remains coherent (dashed line). However, when a control deep explant is overlaid with an FF-GFP expressing superficial explant, FF cells intercalate into the control and GFP positive cells can be seen interspersed between the controls (**Figure 54B**). This shows that FF expression specifically blocks the FN-dependent signal originating from the cells in direct contact with the substrate and that FF expressing cells can in fact polarize and intercalate if the signal is provided by control cells.

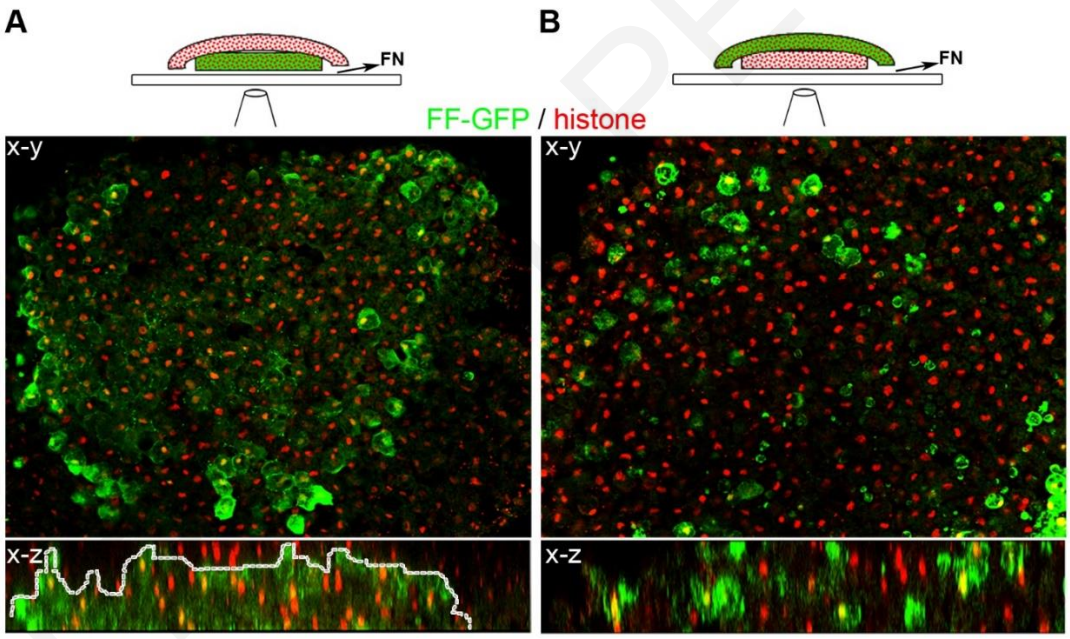

Figure 54: FAK signals the FN-derived polarity signal to guide radial intercalation during *Xenopus* epiboly. Radial intercalation explants from control and FF-GFP injected embryos. (A) The deep cell layer explant dissected from an FF-GFP injected embryo (green and red signal) was placed on a FN coated coverslip and another explant from a control embryo (red signal only) was placed on top. Explants were cultured for 3 hours, fixed and stained with anti-histone H3 (nuclei, red signal) and anti-GFP (green signal) antibodies. They were subsequently cleared and Z-stacks were acquired on a confocal microscope. A single optical section at the level of the FN (x-y) and a vertical reconstruction of the Z-stack (x-z) are shown. The FF-GFP expressing explant (green with red dots) remains coherent and no GFP-negative cells have intercalated into it. A clear boundary is visible between the two explants (dashed line). (B) In the reverse explant with control tissue (red dots) placed on FN and FF-GFP injected explant on top (green with red dots), radial intercalation takes place normally and there is extensive cell mixing without any visible boundaries between the two explants.

3.2.16. Epiboly plays an essential but permissive role during *Xenopus* gastrulation

The block of epiboly in FF expressors leads to the delay or failure of blastopore closure as well as partial block of involution. We postulated that this is due to the fact that in the absence of radial intercalation and BCR thinning, the mesodermal belt and the blastopore are held back and are unable to move vegetally. This coupled with the fact that mediolateral intercalation proceeds normally, leads to constriction of the embryo at the equatorial region and produces the characteristic mushroom shaped embryos also seen in the 70KD FN experiments (Rozario, Dzamba et al. 2009). If this explanation is correct, one would expect increased tension in FF expressing ACs. Phalloidin staining in combination with β-catenin staining, shows that cells in FF expressing ACs display stronger actin staining and have many protrusions compared to controls suggesting they are under increased mechanical tension (**Figure 55A**). The levels of β-catenin and C-cadherin are similar between FF and controls, suggesting that FF does not elicit its effect via strengthening of cell-cell adhesions (**Figure 55A, B**). Staining of FF and control ACs with a phospho-MLC antibody revealed that FF expressing ACs have higher levels of phosphorylated MLC especially in the apical surface of the deep cells (**Figure 55C**), suggesting that FF BCRs are under increased mechanical tension and respond with increased contractility. In addition, levels of phosphorylated MLC are elevated both in expressing as well as in control cells suggesting that FF expression does not cell autonomously lead to Rho activation, but rather the increased tension in the AC leads to elevated phosphorylation of MLC (**Figure 55C'**). This result is consistent with the above postulated explanation that the failure of blastopore closure is a result of the block of epiboly and the mechanical linkage of the mesodermal belt to the AC.

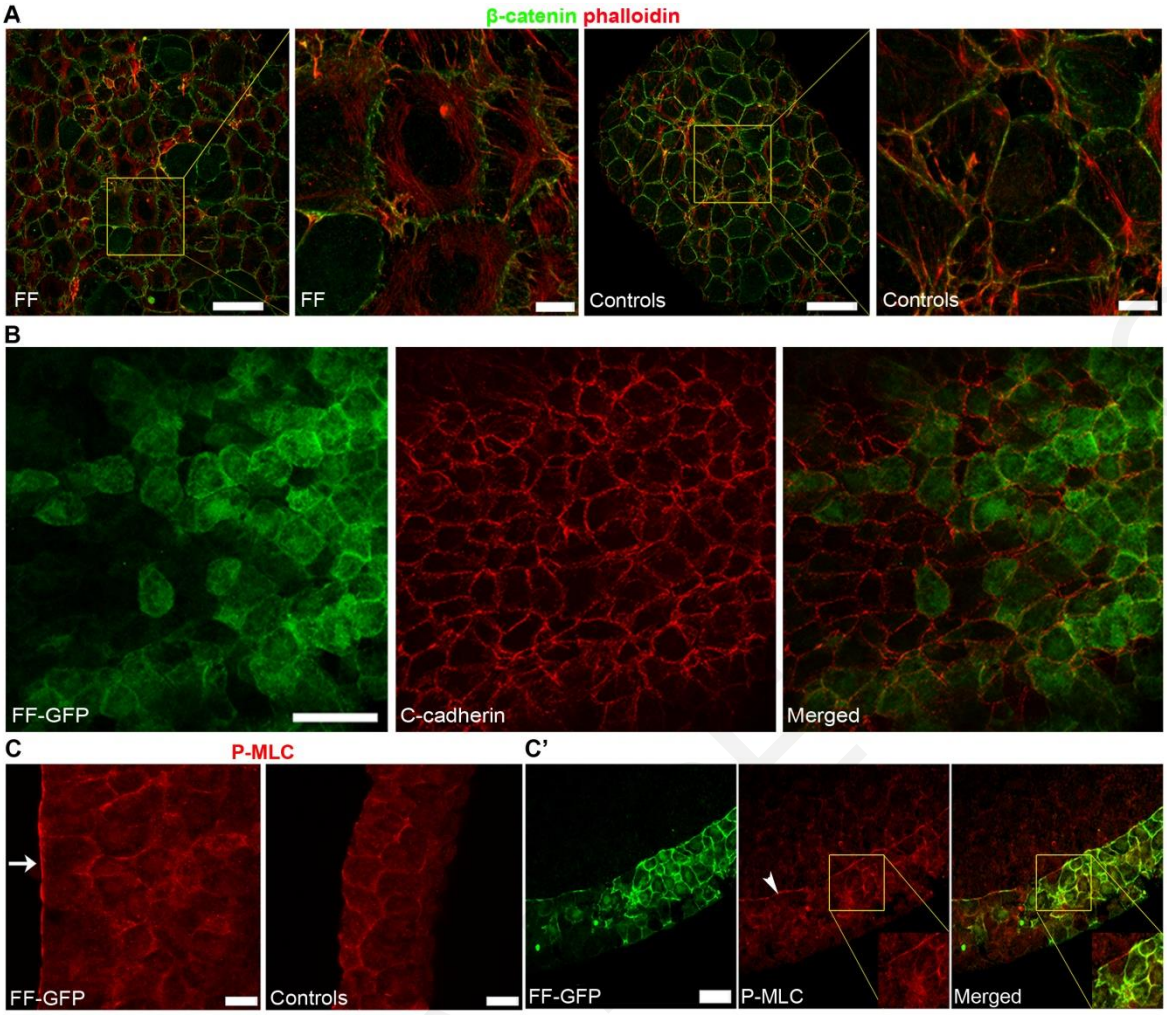

Figure 55: FF expression in the AC leads to increased tension and elevated phosphorylation of MLC.
(A) Low and high magnification confocal images and maximum intensity projections of the inner cell layer of the AC in FF injected and control gastrula embryos stained with β-catenin (green) and phalloidin (red). (B) Confocal image of the inner side of the AC from FF-GFP injected gastrula stage embryo stained with anti-GFP (green) and anti-C-cadherin (red) showing that FF expressors do not display stronger adherens junctions or elevated levels of C-cadherin. (C) Confocal images of FF-GFP injected and control embryos stained for P-MLC showing elevated P-MLC at the inner apical surface facing the blastocoel in FF injected (white arrow). (C') Elevation of P-MLC is not cell-autonomous since elevation is seen in both FF expressing (green) and non-expressing cells of the BCR (yellow box, white arrowhead). Scale bars: (A) 10 μm, (B, C') 50 μm, (C) 20 μm.

To confirm that FF expression in the AC leads to increased tension that subsequently blocks epiboly, we decided to relieve the tension within the FF expressing ACs. To do so, we generated an incision on the BCR of FF expressing embryos and monitored the progress of blastopore closure. In **Figure 56A**, two representative sibling embryos are shown. Generating an incision on the BCR of an FF embryo (**Figure 56A'**) led to the abrupt speeding up of blastopore closure compared to the FF control which remained stalled. In agreement with previous reports, such small incisions only affect blastopore closure rates of control embryos marginally (data not

shown) (Keller and Jansa 1992). The incision on the BCR relieves tension within the AC and allows the mesodermal belt to move vegetally suggesting that epiboly plays an essential but *permissive* role during *Xenopus* gastrulation. Interestingly, injection of an inhibitor of ROCK at stage 10 to chemically relive tension within the AC of FF expressing embryos has the same effect, rescuing blastopore closure and dissection of ROCK inhibitor treated FF expressing embryos revealed a thinned AC (**Figure 56B, C**). This result in combination with the non-cell autonomy of MLC phosphorylation elevation suggests that loss of polarity by FF expression leads to defective epiboly which in turn leads to increased tension and stiffness in the AC. Inhibition of ROCK leads to a reduction of tissue stiffness and improved tissue rheology allowing the AC tissue to deform in response to the pulling forces of the mesodermal belt leading to thinning of the AC and rescuing blastopore closure.

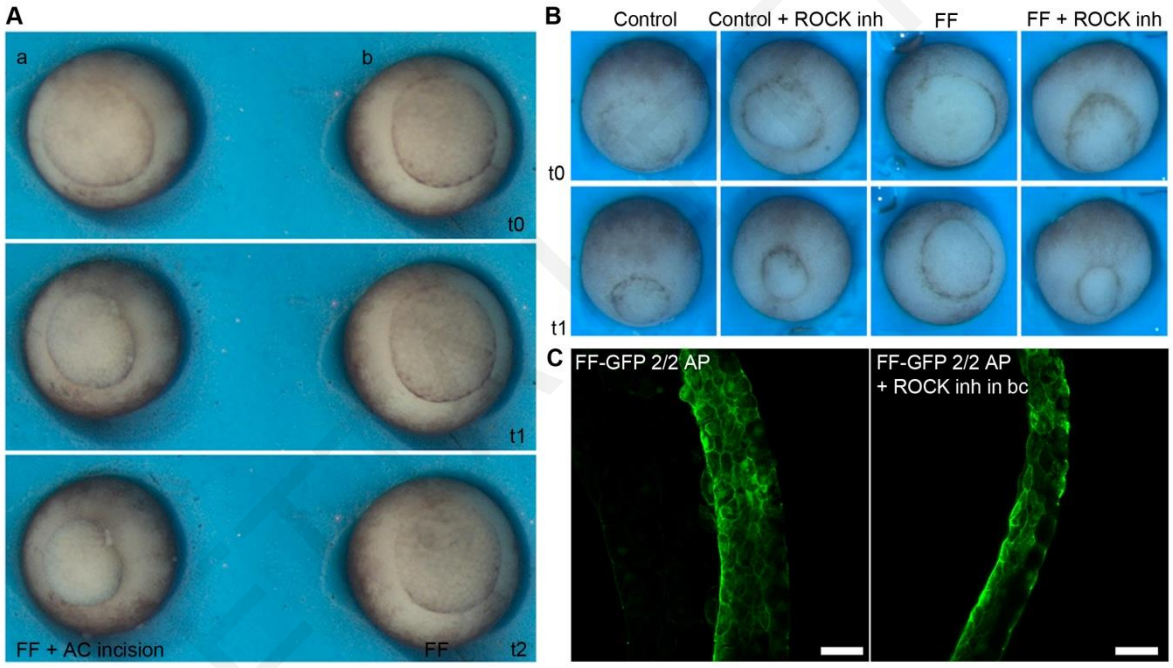

Figure 56: Epiboly has a permissive role during *Xenopus* gastrulation.

(A) FF blastopore closure failure is rescued by a small incision on the BCR (panel a), t0: FF injected embryos before AC incision, t1: first time point immediately after incision, t2: second time point after incision. (B) FF blastopore closure failure is also rescued by pharmacological release of tension by injecting the ROCK inhibitor in the blastocoel at stage 10. (C) Sagittal sections of FF-GFP injected embryos, non-treated or treated with the ROCK inhibitor showing thinning of the AC and epiboly rescue. Abbreviations: AP, Animal Pole; bc, blastocoel. Scale bars: (C) 50 μm.

3.3. Discussion Chapter I

3.3.1. Differential regulation of FAK depending on the cell and tissue context

FAK is a cytoplasmic kinase shown to be involved in a number of diverse processes including cell adhesion, migration, proliferation and survival. It has also been shown to be necessary for embryonic development since FAK knockout mice die early during development due to defects of the axial mesoderm (Furuta, Ilic et al. 1995). FAK as a FA protein has been primarily studied with respect to integrin-based activation on 2D matrices. On such matrices it has been shown to be activated downstream of integrin clustering and to have an important role in the assembly and disassembly of FAs (Guan 1997, Guan 1997, Cary and Guan 1999, Ren, Kiosses et al. 2000, Webb, Donais et al. 2004, Hamadi, Bouali et al. 2005). However, FAs are much smaller on soft matrices and different in structure, localization, and function in cells embedded in 3D matrices which resemble the *in vivo* setting better (Fraley, Feng et al. 2010, Harunaga and Yamada 2011, Prager-Khoutorsky, Lichtenstein et al. 2011). In addition, cell polarization also depends on matrix rigidity and is controlled by mechanosensing at the FAs (Prager-Khoutorsky, Lichtenstein et al. 2011). FAK's phosphorylation is much lower in cells grown on soft matrices and surprisingly no tyrosine 397 phosphorylation can be detected on 3D matrix adhesions (Pelham and Wang 1997, Cukierman, Pankov et al. 2001, Gonzales, Weksler et al. 2001). In fact downregulation of some proteins has the opposite effect in terms of their role in cell migration when tested on 2D vs 3D matrices. Overall, it appears that regulation of 2D cell motility by FA proteins is not necessarily predictive of regulation of cell motility in a 3D environment (Fraley, Feng et al. 2010). Things get even more complicated when examining FA proteins in the context of a living organism in which case not only the cell is faced with a 3D matrix but it also faces a 3D cell–cell adhesion network. These differences raise the need for the study of adhesion molecules, like FAK, in an *in vivo* setting in order to allow the integration of the valuable knowledge generated with respect to FAK signaling *in vitro* back to a more physiologically relevant context.

Here we explore the activation of FAK in the context of the *Xenopus* embryo. We initially examined FAK phosphorylation on three major tyrosine residues 397, 576 and 861 during development. In agreement with previously published work, we observed elevated FAK phosphorylation on all three residues during gastrulation suggesting a possible role of FAK in embryonic morphogenesis (Hens and DeSimone 1995, Zhang, Wright et al. 1995). Specifically, phospho-FAK levels were elevated in the mesoderm compared to the endoderm in gastrula

stage embryos and deep cells of the AC facing the BCR displayed elevated levels of phospho-FAK compared to the cells of the outermost epithelium. Surprisingly, phosphorylation was detected on all three residues from early blastula stages before the mid-blastula transition and well before the initiation of gastrulation and cell movements. What the role of FAK during these early developmental stages might be is not known, but the mechanism of activation is not likely to rely exclusively on integrins but rather a combined process through involving GFRs, integrins, PIP_2 and other factors. While full length FAK could be detected in the cytosol the plasma membrane and the nuclei of cells in the embryo, tyrosine phosphorylated FAK was only found on the plasma membrane suggesting that activation takes place there. No FA-like structures could be detected and the staining appears to be uniform on the surface of these cells. In addition, active FAK was present in regions were only adherens junctions are present and that are clearly devoid of ECM components. However, at gastrula stages and specifically in the deep cells of the ectoderm which are in contact with the FN matrix of the BCR, phospho-FAK is elevated and displays foci of higher signal intensity that resemble FA-like structures. On the other hand, in the superficial cells of the ectoderm we detected equal levels of phosphorylated FAK on the apical surface of the plasma membrane compared to the basolateral regions. Since the apical region of the plasma membrane is free from integrins and isolated from the basolateral with tight junctions this supports the notion that FAK activation in these areas of the cell during early development can be integrin independent. Another possibility is that activated FAK at the basolateral region of these cells diffuses through the cytosol and re-localizes on the apical side of the plasma membrane. This is unlikely though because this would presumably generate a gradient of higher levels of phospho-FAK at the periphery of the apical membrane vs the center. This does not appear to be the case since the intensity of phospho-FAK signal is uniform on the apical membrane of superficial cells.

We have shown that FRNK, which has been shown to act as a DN and block integrin-based FAK activation (Richardson, Malik et al. 1997), fails to reduce FAK activation in the embryo, as determined by the undiminished levels of FAK's tyrosine phosphorylation on key residues including tyrosine 397 and 576. It was previously shown that FRNK does in fact reduce endogenous FAK phosphorylation of mesodermal explants plated on FN (Stylianou and Skourides 2009) and the same is true in *Xenopus* cell lines. In all these cases however, FAK phosphorylation primarily derives from cell-ECM adhesion, whereas we present evidence suggesting that this is not the case in the early embryo. In fact the inability of FRNK to act as a DN could itself be considered indirect evidence that FAK is not activated exclusively through integrins in this context. In addition FRNK, despite containing the FAT domain which has been

shown to be both necessary and sufficient for targeting FAK to FAs (Hildebrand, Schaller et al. 1993), fails to target FAK at the plasma membrane in the embryo and is specifically absent from the integrin-free apical region of the plasma membrane in superficial blastomeres. This inability may explain why it fails to block FAK activation since it is presumably unable to compete endogenous FAK off of its complexes at the plasma membrane. FRNK has also been shown to act as a DN during somitogenesis in *Xenopus* tadpoles. Specifically, FAK and other FA molecules, like paxillin as well as FN and integrins, have been shown to localize at the intersomitic boundaries leading to the conclusion that FA contacts mediate the stabilization of somite boundaries (Henry, Crawford et al. 2001, Crawford, Henry et al. 2003, Kragtorp and Miller 2006). Since FAK is activated through integrins in this context, these data confirm that FRNK is able to block integrin-based activation of FAK *in vivo*. Although FRNK has been shown to block GFR based activation of FAK in cultured cells, for example PDGF-induced activation of FAK in Vascular Smooth Muscle Cells is blocked by FRNK expression, it is possible that in this context where PDGF also induces the migration of these cells, FAK's activation is still largely integrin dependent and indirect (Sundberg, Galante et al. 2003). In addition, the FAT domain in FRNK has been shown to be the major determinant for FRNK's DN function (Richardson and Parsons 1996) showing that targeting to integrin-based complexes is the mechanism through which FRNK acts and suggesting that in the absence of the ability to target non integrin-based FAK complexes FRNK would not be able to act in a DN fashion. All these data support the notion that in the context of the early embryo, FAK activation and function is not sufficiently regulated through interactions of its C-terminal domain and suggest that interactions involving other domains of the FAK molecule might also be required.

Exploring the domains of FAK that might be responsible for targeting FAK to integrin-free regions of the plasma membrane we found that the N-terminal region of FAK is both necessary and sufficient for membrane localization. Exogenously expressed FERM recapitulates the localization of tyrosine phosphorylated FAK while FRNK fails to do so. In addition, deletion of the FERM domain leads to the reduction of plasma membrane localization of full length FAK. Overall these data suggest that the major determinant for localization of FAK on the plasma membrane of superficial cells of the embryo is the N-terminus. However, in DMZ cells which display the highest levels of FAK phosphorylation during gastrulation neither the FERM domain nor the FAT domain are sufficient to strongly target FAK to the plasma membrane suggesting that in these cells both the FAT and the FERM domain may cooperate to target active FAK on the plasma membrane and apparently this is the case since the FF construct

(consisting of the N- and C-termini of FAK) exhibits tight membrane localization as activated FAK.

The fact that exogenously expressed FERM has such a dramatically different localization compared to full length FAK in the integrin-free regions of the embryo, is most likely due to the fact that the majority of FAK in the cell is in the closed conformation with the FERM domain unavailable to bind growth factor receptors and PIP_2 (Cai, Lietha et al. 2008). When expressed autonomously it is no longer impeded by its interaction with the kinase domain and it is free to bind targets on the plasma membrane. The strong membrane localization of the FERM domain coupled with the fact that it was shown to block FAK activation *in trans* raised the possibility that exogenously expressed FERM could block endogenous FAK activation *in vivo*. However, FERM expression in the integrin-free regions of the ectodermal cells led to activation of endogenous FAK in a tyrosine 397 dependent fashion. This was not the case however, when expressed in *Xenopus* cell lines where FERM transfected cells displayed reduced levels of FAK phosphorylation, confirming that FERM dependent activation of endogenous FAK in the context of the embryo is not a *Xenopus* specific phenotype, but rather that it results from different activation mechanisms according to the cell context. Exogenous FERM on the epidermal cells of *Xenopus* is heavily phosphorylated on tyrosine 397 at the plasma membrane, presumably *in trans* by active endogenous FAK which is also at the plasma membrane. The fact that tyrosine 397 is necessary for the FERM induced activation of endogenous FAK leads to the conclusion that the exogenous phosphorylated FERM recruits Src to the plasma membrane leading to additional FAK phosphorylation. It is possible that the FERM domain in the context of non-integrin based activation has a greater affinity for the plasma membrane (PIP_2 and GFRs) than for the kinase domain of endogenous FAK and thus fails to block endogenous FAK *in trans* but rather leads to further activation via Src recruitment. This interpretation is in agreement with recent data showing that Src is required for PDGF dependent activation of FAK whereas FAK is actually necessary for Src activation at integrin-based adhesions (Seong, Ouyang et al. 2011). In addition, FERM domain expression has been shown to partially rescue the EGF stimulated migration defect of FAK null cells. This coupled with the fact that the FERM domain can autonomously interact with EGFR suggests that the FERM domain can in fact promote GFR based FAK signaling while blocking integrin-based activation (Cooper, Shen et al. 2003, Cohen and Guan 2005).

This set of results suggest that in the early *Xenopus* embryos, there are integrin dependent and integrin independent mechanisms of FAK activation and that the FERM domain is the primary determinant for FAK's localization at the plasma membrane, at least in integrin-free regions of

the cell. In addition, the data suggest an important role of the FERM domain in the *in vivo* activation of FAK and provide new insights regarding the differences between integrin and GFR activation of FAK.

3.3.2. Elucidating the role of FAK in FA turnover through the use of the FF DN

Since neither the FERM domain nor the FAT domains can mimic the conformation of active FAK in mesodermal and other tissues we postulated that open conformation activated FAK may localize on the plasma membrane through the cooperation of these two domains. As mentioned above, a fusion of these two domains (FF) shows strong localization at the plasma membrane in the embryo, mimicking the localization of active FAK. This result shows that despite the fact that the FAT domain is both necessary and sufficient for FA localization the FERM domain is also required for correct localization *in vivo*. By utilizing this new tool we went on to characterize further the role of FAK in cell migration *in vitro*.

We show that FF has a higher affinity for FA complexes, displaying significantly longer residence times on these complexes compared to FRNK, demonstrating that the FERM domain has a significant role regulating the dynamics of FAK on FAs. This result also explains previous findings showing that phosphorylation of FAK on Tyr397 increases residence times of FAK at FAs (Hamadi, Bouali et al. 2005), since tyrosine phosphorylated active FAK acquires an open conformation similarly to FF and this conformation seems to increase the residence time of FAK at FAs. In addition, we show that FF becomes enriched on newly formed FCs prior to FRNK, suggesting a role of the FERM domain in the recruitment of FAK to these complexes. This may be due to the ability of the FERM domain to bind locally generated PIP_2, keeping FF in close proximity to nascent adhesions, however another possibility is that the FERM domain is binding integrins at the early stages of FA formation, since it was shown that the FERM domain can bind to peptides mimicking the integrin β1 cytoplasmic domain (Schaller, Otey et al. 1995, Cai, Lietha et al. 2008). This initial binding may be transient but important for FAK's recruitment to the newly formed FCs and is subsequently competed off by proteins like talin. FAK may then be stabilized at FAs through interactions of the FAT domain with other FA proteins (Hayashi, Vuori et al. 2002). This explanation is supported by the fact that FAK has been shown to bind integrins and be activated by them and in addition, by work showing that talin recruitment to FCs is compromised in FAK null cells (Lawson, Lim et al. 2012). A recent study that came out after these results were obtained, gives another possible explanation for the high affinity of FF for FAs. It was suggested that dimerization of FAK molecules occurs at the FAs through intermolecular FERM:FERM interactions and is stabilized through FERM:FAT

interactions (Brami-Cherrier, Gervasi et al. 2014). Moreover, the fact that the paxillin binding deficient FF mutant (FF L1034S) displays reduced affinity for FAs than WT FF, can be explained by the observation that paxillin binding on the FAT domain was found to reinforce the FERM:FAT interaction and induce dimerization (Brami-Cherrier, Gervasi et al. 2014).

FF displaces FAK from FAs resulting in the loss of FAK phosphorylation. This leads to a dramatic reduction of FA turnover and an increase in size and number of FAs, recapitulating the phenotype of FAK null MEFs (Ilic, Furuta et al. 1995). When compared to FRNK, FF elicits a much stronger phenotype. Disassembly defects are generalized and are seen both at the cell front as well as at the cell rear. The significant differences between FRNK and FF expressing cells with respect to their ability to turnover FAs may be attributed to the higher affinity that FF displays for FAs. The long residence times of FF suggest a slower off rate from these complexes compared to FRNK and as a result, at steady state, and given fixed levels of expression, FF should be more effective in displacing endogenous FAK from FAs. In addition, while FRNK can compete FAK from a subset of target proteins that bind the C terminus, FF can compete with endogenous FAK for a wider array of FAK partners. These defects in FA disassembly have a direct impact on cell migration, since FF expression leads to inhibition of cell migration both in single cells in culture and in collective tissue migration of mesodermal tissue explants from *Xenopus* embryos.

3.3.3. Elucidating the role of FAK in *Xenopus* embryogenesis through the use of the FF DN

The strong DN activity of FF *in vitro* translated to a strong DN activity *in vivo*, providing evidence that during *Xenopus* early embryogenesis, FAK plays a crucial role in processes regulated by FN-integrin signaling. Although as described above, prior to gastrulation and in a minor subset of the gastrula embryo (apical surface of the cells of the outermost epithelial cell layer) FAK activation must originate through an integrin independent mechanism, during gastrulation and later on in development both FAK's localization and activation pattern correlates well with the areas where FN-integrin interactions take place (such as at the BCR, MZ, intersomitic boundaries). However, despite the central role of FAK in the transduction of FN-integrin signaling and the importance of this signaling in early morphogenesis in *Xenopus*, so far the reported effects of FAK knockdown or inhibition via expression of FRNK are relatively mild. MO based knockdown of FAK in *Xenopus* resulted in abnormal proliferation of the myocytes that are necessary for chamber outgrowth and heart tube morphogenesis leading to defective cardiac development and reduced expression of posterior neural markers

(Doherty, Conlon et al. 2010, Fonar, Gutkovich et al. 2011). In addition, expression of FRNK blocks mesoderm migration and leads to aberrant somitogenesis (Kragtorp and Miller 2006, Stylianou and Skourides 2009). It was quite surprising that no severe developmental defects were reported in the above studies given the lethal phenotype of the FAK knockout mice, including the severe abnormalities in the mesodermal tissues (Furuta, Ilic et al. 1995). However, expression of FF in the mesoderm lead to smaller curved embryos with disorganized somite formation. The shortening of the A-P axis is probably not due to defects in mesodermal movements such as CE but due to survival issues as can be concluded by the strong reduction in MyoD expression suggesting loss of mesodermal tissues in agreement with the FAK knockout mice (Furuta, Ilic et al. 1995). This loss of mesoderm was due to increased apoptosis which appears to be secondary to defects in mitosis, since we detected multipolar spindles and anaphase bridges in FF expressing embryos. A Ser732 point mutant FF displays a much milder phenotype without any apparent loss of mesodermal tissues again supporting that apoptosis in FF expressors is secondary to defects in mitosis. Cdk5 has been shown to regulate phosphorylation of FAK at Ser732 and the phosphorylated form of FAK co-localizes with γ-tubulin at the centrosome (Xie, Sanada et al. 2003, Park, Shen et al. 2009). FAK null endothelial cells exhibit mitotic defects, similar to what we observed by FF expression (Park, Shen et al. 2009). These include alterations in the mitotic spindle and centrosome organization and are rescued by re-expression of WT FAK, but not by a mutant defective for phosphorylation at Ser732 (Park, Shen et al. 2009). We noted that phosphorylation of endogenous FAK on Ser732 is reduced in FF expressing embryos suggesting that FF may be competing with endogenous FAK for phosphorylation by Cdk5.

In order to overcome the survival defects induced in FF mesodermal expressing cells so as we could study further the roles of FAK in later embryogenesis we generated an inducible FF construct, based on the hormone binding properties of the GR. The use of this inducible construct enabled us to separate the effects of loss of FAK function in survival and morphogenesis of the vascular system. By inducing FF at stages at which the angioblasts had already migrated and generated the primary vessels, we identified that FAK is involved in the angiogenesis process and in the maintenance of the vessel integrity.

Interestingly, expression of FF in epithelial tissues presented a different phenotype of that in mesodermal tissues, with no apoptosis or survival issues. Inhibition of FAK function by FF expression in the AC leads to BCR thickening, spindle misorientation and loss of deep cell polarity leading to defective epiboly. In addition, FF expression in the AC led to severe gastrulation defects. Similar effects have been reported in experiments where the fibrillar FN

matrix of the AC is prevented from forming (Marsden and DeSimone 2001, Davidson, Marsden et al. 2006, Rozario, Dzamba et al. 2009). However, the FN fibrillar matrix of FF injected BCRs was present, despite exhibiting thicker and denser fibrils than the matrix in control BCRs, probably stemming from disrupted turnover of the FA complexes in these cells. These results taken together with the similar phenotypes described in FN, FAK and integrin α5 mouse knockouts suggest that FAK has a central role in the transduction of FN-integrin signaling and that FF can block this signaling (George, Georges-Labouesse et al. 1993, Yang, Rayburn et al. 1993, Furuta, Ilic et al. 1995). Interestingly, rescuing FA turnover rates in the cells of FF injected ACs by downregulating vinculin or disrupting FF-paxillin interaction, did not rescue AC thickening indicating that the source of defective epiboly in FF injected embryos is not a defective fibrillary matrix that is unable to provide proper polarizing signals, but rather that FAK is involved in the transduction of the FN-integrin derived polarizing signal that guides epiboly.

Specifically in the AC, radial intercalation requires integrin dependent contact of deep cells with FN. Signaling from the FN fibrillar matrix is also required for the polarized cell divisions taking place in the deep cells of the AC (Marsden and DeSimone 2001). We show through radial intercalation explants that FF expression in the cells in contact with the FN matrix is sufficient to block intercalative behavior, while expression in the cells overlying these cells does not, confirming that a FN-integrin signal can direct intercalative behaviors at a distance and FAK has a critical role in its transduction.

Block of epiboly through a variety of experimental approaches as described above leads to gastrulation defects in the mesoderm including partial block of involution and delay or failure of blastopore closure. However, it was shown that BCR-less embryos close their blastopores without any problems (Keller and Jansa 1992). In fact in these embryos, a speeding up of blastopore closure is observed suggesting that the mesoderm is actually excreting forces on the AC and is held back by this interaction (Keller and Jansa 1992). We now show that this is in fact the case. In FF expressors, generation of a small incision on the AC leads to the abrupt speeding up of blastopore closure suggesting that the failure of blastopore closure is due to the fact that the mesoderm is held back by the AC. The AC in FF expressors not only displays loss of polarity but in addition, displays increased stiffness as evidenced by the elevation of phosphorylation of MLC and the pattern of the actin cytoskeleton. This would suggest that the inability of FF expressing ACs to thin and allow vegetal translocation of the blastopore results in increased tension imposed on this tissue and the tissue responds by increasing its stiffness. In agreement with this interpretation, use of a ROCK inhibitor rescues blastopore closure and

BCR thinning. It appears that under conditions of low contractility, improved tissue rheology allows the AC to deform in response to the forces generated by mesoderm involution. This suggests that epiboly requires the forces generated by the mesoderm in order to take place.

Interestingly, a study by Campinho et al., exploring the mechanisms of epiboly during *Zebrafish* gastrulation, showed that tension dependent spindle orientation in the EVL (enveloping layer, superficial cell layer of the ectoderm) is an efficient mechanism by which the EVL releases anisotropic tension during epiboly (Campinho, Behrndt et al. 2013). Similarly in the case of *Xenopus* epiboly, it seems that loss of spindle orientation in the epithelial cells leads to a thickened AC with increased tension, blocking blastopore closure. We propose that forces derived from mesoderm involution and from the plane of the epithelium orients these cells to divide parallel to their apical surface promoting epithelial cell spreading and that epiboly progression releases tension allowing the blastopore to close. What is interesting however, is that the loss of FN-integrin interactions in the *Xenopus* BCR by injecting FN blocking antibodies in the blastocoel leads to spindle misorientation only in the deep epithelial cell layers and not in the outermost layer (Marsden and DeSimone 2001). In contrast, FF expression in the AC leads to spindle misorientation with respect to the epithelial plane also in the cells of the outermost epithelium, suggesting that the role of FAK in orienting the mitotic spindle in these cells is independent of FN-integrin interactions. These data raised the possibility that FAK has an ECM independent role in determining the division plane, a question that was extensively studied and described in the results section of Chapter II of this thesis.

Although loss of FAK in mesodermal tissues leads to mitosis progression defects (multipolar spindles, anaphase bridges) associated with FAK's centrosomal function (Ser732 phosphorylation dependent) and resulting in apoptosis, this phenotype was absent when FAK function was inhibited in the ectoderm (spindle misorientation, without defects in the integrity of the spindle structure). These discrepancies may be attributed to differential mechanisms of FAK regulation and function in different contexts. For example, the phenotype of FF injected embryos in the mesoderm is extremely similar to the phenotype of FAK null mice including diminished mesodermal tissues suggesting defects in the survival of these tissues (Furuta, Ilic et al. 1995). Thus, an FA-derived survival signal might drive mesodermal morphogenesis, since the FN and integrin a5 knockout mice display loss of mesodermally derived tissues (George, Georges-Labouesse et al. 1993, Yang, Rayburn et al. 1993). Moreover, since the mesodermally derived tissues display elevated levels of FAK phosphorylation, it is highly possible that this survival/mitosis signal is purely kinase dependent. Support comes from a study showing that the mitosis defects exhibited in FAK null endothelial cells depend on FAK's kinase activity

(Park, Shen et al. 2009). However, in epithelial tissues no spindle integrity issues are present probably attributed to the epithelial character of the cells, i.e. no ECM is surrounding these cells and FAK phosphorylation levels are much lower when compared to the mesodermal cells (except the inner epithelial cells facing the blastocoel).

Overall, these results suggest that in the *Xenopus* embryo, FAK exhibits differential mechanisms of regulation depending on the tissue context. Although FAK was initially established as a tyrosine kinase involved in cell migration, more recently kinase dependent and independent functions have been uncovered and there is evidence that it is also involved in processes not directly associated with cell migration (cell division, proliferation, survival). Here we provide *in vivo* data that in the context of the *Xenopus* embryo, FAK can drive several developmental processes simultaneously (mesoderm migration, epithelial cell polarization and radial intercalation, apoptosis and cell division), according to its spatiotemporal pattern of activation and the differential interactions of its domains with multiple binding partners, highlighting the importance of this multifunctional protein in embryogenesis.

4. Chapter II

4.1. Introduction Chapter II

4.1.1. Mitotic spindle orientation

4.1.1.1. Importance of spindle orientation in development and disease

Oriented cell division is the process determining the division axis of the cell so as the daughter cells acquire their correct positions either with respect to their substrate or with their neighboring cells. Aberrant spindle orientation is associated with defective embryogenesis and more importantly, the development of severe diseases including neurological disorders, polycystic kidney disease and tumorigenesis (Siller and Doe 2009, Castanon and Gonzalez-Gaitan 2011, Pease and Tirnauer 2011, Noatynska, Gotta et al. 2012). Cells can either divide asymmetrically so as the daughter cells acquire different determinants regulating in this way cell fate or symmetrically promoting tissue growth along an axis and maintaining epithelial integrity (Bergstralh, Haack et al. 2013).

Representative examples of the important role of oriented cell division during embryonic development exist in several model systems. One of the best characterized systems in which spindle orientation is fundamental for embryonic development is the *C. elegans* embryo, where a series of asymmetric cell divisions establish the principal axes of the body plan (A-P, D-V, L-R) and guide cell specification and differentiation. Specifically, five asymmetric divisions produce six founder cells. The first division produces a larger anterior blastomere and a smaller posterior blastomere, where the latter divides asymmetrically several times to produce the founder cells which each one is a progenitor of a different cell type (Gonczy and Rose 2005) (**Figure 57A**). Asymmetric division in *Drosophila* is also evident in the embryonic neuroblasts, which delaminate from the neuroectoderm and divide perpendicularly to the plane of the neuroectoderm to produce one cell that self-renews (neuroblast) and one smaller cell that initiates differentiation (ganglion mother cell) (Gonzalez 2007) (**Figure 57B**). Spindle orientation regulates the development of bristle mechanosensory organs in *Drosophila* which are composed of four different cells that originate from one progenitor through asymmetric divisions (Gho and Schweisguth 1998) (**Figure 57B**). Oriented cell division is also required for proper organogenesis in *Drosophila*, such as in the imaginal disks that give rise to most adult organs (**Figure 57C**) and for the preservation of the follicular epithelium monolayer (Baena-Lopez, Baonza et al. 2005, Fernandez-Minan, Martin-Bermudo et al. 2007). Moreover, oriented

symmetric divisions were shown to drive epithelial morphogenesis vertebrates, such as epiboly during *Xenopus* and *Zebrafish* gastrulation (Marsden and DeSimone 2001, Campinho, Behrndt et al. 2013) and neurulation (Geldmacher-Voss, Reugels et al. 2003, Kieserman and Wallingford 2009). Finally, oriented cell division controls epidermal development in the mouse mammalian skin (**Figure 57D**) and regulates organ morphogenesis, such as the branching of the lungs, elongation of the kidney tubules and intestinal crypt formation (Lechler and Fuchs 2005, Fischer, Legue et al. 2006, Barker, van Es et al. 2007, Chen and Krasnow 2012).

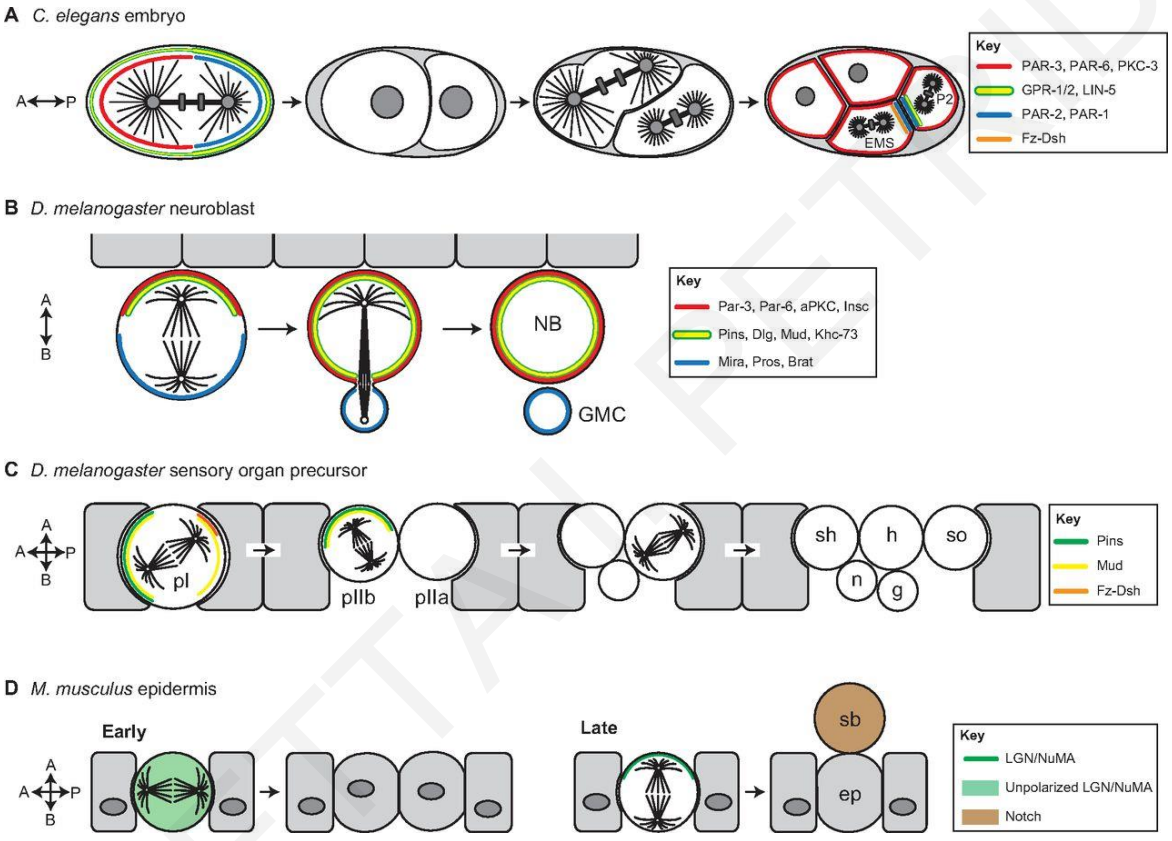

Figure 57: Spindle orientation and embryonic development.

Representative examples of how oriented cell divisions orchestrate embryonic development such as establishment of the body axes in *C.elegans* (A), neural development (B) and sensory organ formation in *Drosophila* (C) and embryonic epithelial morphogenesis and stratification of the epidermis in mice (D). Adapted from (Lu and Johnston 2013).

Oriented cell division is not only important for embryonic development, but also for the adult organism since aberrant spindle orientation is associated with the appearance of several diseases. Although the cause and effect relationship between spindle misorientation and disease development is not clear, due to the fact that many disease-linked genes required for spindle orientation also carry out additional cellular functions, several lines of evidence correlate the

two. Specifically, spindle misorientation has been linked with neurological disorders such as microcephaly, lissencephaly and Huntington's disease (Noatynska, Gotta et al. 2012). Loss of oriented cell division was also associated with the development of polycystic kidney disease, since the lengthening of the renal tubules is driven by mitosis along the tubule axis and a model has emerged in which loss of this orientation leads to tubule dilation and cyst formation (Fischer, Legue et al. 2006). Carcinogenesis is also linked with randomized divisions since spindle orientation defects alter the balance between asymmetric and symmetric divisions affecting tissue homeostasis and disrupting epithelial integrity and tissue architecture allowing malignant transformation (Pease and Tirnauer 2011). The molecular evidence linking spindle orientation and tumorigenesis stems from the fact that tumor suppressor genes and oncogenes such as adenomatous polyposis coli (APC), E-cadherin, von Hippel-Lindau, VEGF and PTEN are implicated in spindle orientation (Pease and Tirnauer 2011, Noatynska, Gotta et al. 2012).

4.1.1.2. Mitotic of spindle orientation – intrinsic and extrinsic signals

Mitotic spindle orientation refers to the process that establishes the division axis followed by the alignment of the spindle along this axis (Lu and Johnston 2013). The division axis is determined by both intrinsic and extrinsic factors. Intrinsic factors include molecules and cortical cues that localize in a polarized fashion at the cell cortex, whereas the extrinsic signals refer to external factors such as cell shape, cell adhesion geometry and external forces that often influence the localization and polarity of internal factors (Nestor-Bergmann, Goddard et al. 2014). During symmetric divisions, the spindle is oriented in two major manners; In the case of single adherent cells in culture the spindle is parallel to the cell-ECM interface (**Figure 58**), whereas in epithelial tissues the spindle is usually aligned to the plane of the epithelium, i.e. parallel to the apical surface of the cell, referred to as spindle orientation along the Z-axis of the cell (Toyoshima and Nishida 2007, Bergstralh, Haack et al. 2013). This type of spindle orientation in adherent cells is achieved through the retraction fibers (RFs), which are actin-rich filaments that maintain adhesion to the substrate when the cell rounds up during mitosis and most of its adhesion complexes are disassembled (Mitchison 1992) (**Figure 58**). Moreover, the spindle can be oriented within the XY plane of the cell, a mechanism that in adherent cells is mainly controlled by cell adhesion geometry, RF distribution and external forces (**Figure 58**), whereas in tissues is determined mainly by the cell shape and external forces (Thery, Racine et al. 2005, Thery, Jimenez-Dalmaroni et al. 2007, Minc, Burgess et al. 2011).

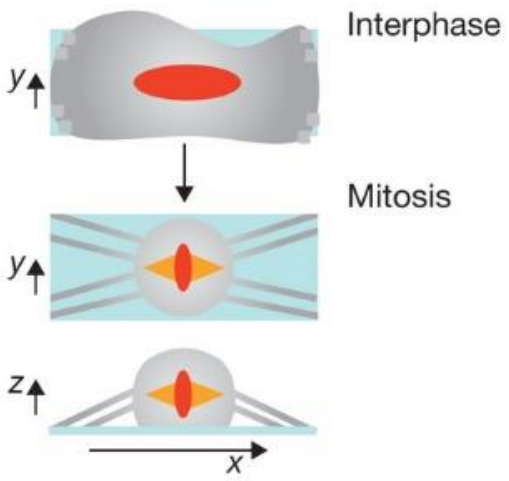

Figure 58: Spindle orientation in adherent cells.

During mitosis, the cell rounds up and retains adhesion to its substrate through the actin-rich containing tubes called RFs. Adherent single cells orient their spindle in the XY plane according to the distribution of the RFs and at the same time along the Z-axis, so as the spindle axis is parallel to the substrate. Adapted from (Lancaster and Baum 2011).

Intracellular machinery, intrinsic signals and guidance cues

Regarding the intrinsic pathway of spindle orientation, the mitotic spindle is positioned within a cell according to the "cortical pulling" model, where the astral microtubules are anchored on specific regions on the cortex, called the spindle captures sites. The minus end directed microtubule motor cytoplasmic dynein which is attached at the cell cortex at the spindle capture sites, exerts pulling forces on the plus ends of the astral microtubules and positions the mitotic spindle (McNally 2013). Evidence for the existence of force generating events on the cortex comes from a study by Redemann and coworkers, where cortical stiffness was reduced so as it was visible that microtubule plus ends pull the tubular invaginations of the plasma membrane inwards (Redemann, Pecreaux et al. 2010). The localization of dynein/dynactin complex at the spindle capture sites is guided by a conserved core protein complex, called cortical capture machinery which is composed by the proteins LGN (Leu-Gly-Asn repeat-enriched protein), NuMA (Nuclear Mitotic Apparatus) and the G-protein subunit Gαi (Bergstralh, Haack et al. 2013). LGN (Pins, Partner of Inscuteable in *Drosophila* / GPR-1/2 G-protein Regulators 1 and 2 in *C.elegans*) localizes asymmetrically at the cell cortex of dividing cells, enriched at the spindle capture sites (Du, Stukenberg et al. 2001, Kaushik, Yu et al. 2003). LGN acts as a scaffold in the cortical capture machinery since it interacts through its N-terminal tetratricopeptide repeats (TPRs) with NuMA and through its C-terminal GoLoco motifs with GDP-bound Gai at the plasma membrane (**Figure 59**) (Bergstralh, Haack et al. 2013). The N-

and C-termini of LGN interact to keep the protein in an inactive conformation which is released upon NuMA and Gai binding (Du and Macara 2004, Nipper, Siller et al. 2007). NuMA (Mud in *Drosophila* / LIN-5, abnormal cell lineage-5 in *C.elegans*) is a dynein binding protein (**Figure 59**) it localizes at the spindle and at the cell cortex (Du, Stukenberg et al. 2001). GDP-bound Gai localizes at the plasma membrane through myristoylation modification and it anchors LGN at the plasma membrane (Bergstralh, Haack et al. 2013) (**Figure 59**). The LGN/NuMA/Gαi complex is enriched at the spindle capture sites both in adherent cells and in epithelial tissues, creating a lateral belt, determining the localization of the dynein/dynactin complex and as a result spindle orientation (Kaushik, Yu et al. 2003, Peyre, Jaouen et al. 2011).

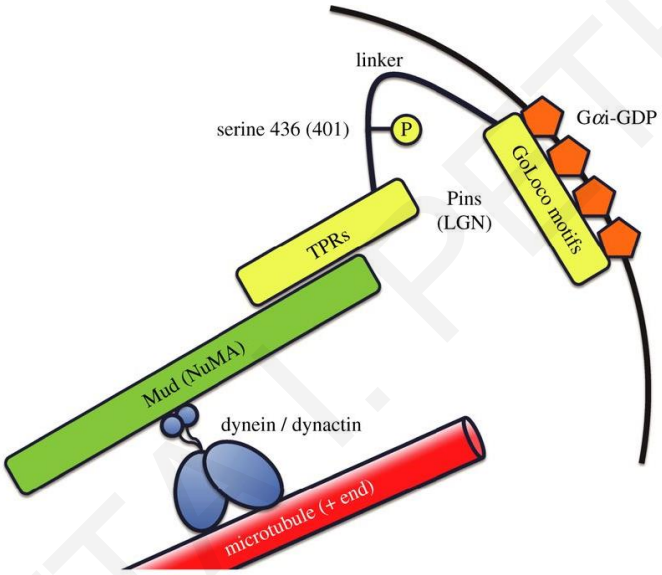

Figure 59: The cortical capture machinery.

Schematic illustration of the LGN/NuMA/Gai complex with respect to the plus end of the astral microtubules and the cortex. Adapted from (Bergstralh, Haack et al. 2013).

Extensive research has been carried out in order to identify how the distribution of these polarity cues is achieved. Initial experiments have shown that the actin cytoskeleton is important for the accumulation of LGN on the cortex, since treatment of cells with latrunculin B leads to loss of LGN cortical localization (Kaushik, Yu et al. 2003). The same was true for NuMA however in this case, only the cortical localization of NuMA was affected and not the one on the spindle. More importantly, when treating cells with nocodazole to depolymerize astral microtubules, the cortical localization of NuMA is unaffected suggesting that the accumulation of these proteins on the cortex depends on the actin cytoskeleton (Seldin, Poulson et al. 2013). It was shown that disruption of LGN lateral polarity by broadening its localization at the cortex leads to randomization of spindle orientation. Interestingly however, in the absence of LGN cells were

still oriented parallel to the substrate (Matsumura, Hamasaki et al. 2012) suggesting that an alternative mechanism orients the mitotic spindle in adherent cells in the absence of LGN. It was suggested that a PI3K-PIP_3 dependent pathway orients the mitotic spindle under these conditions (Toyoshima, Matsumura et al. 2007, Matsumura, Hamasaki et al. 2012). The interplay between the cortical machinery and phosphoinositides (PIP) was recently supported by another study showing that NuMA interacts with PIP and PIP_2 and that this interaction is important for cortical localization of NuMA during anaphase (Kotak, Busso et al. 2014). However, in another study in the absence of LGN and Gai, the localization of NuMA at the cell cortex was compromised (Matsumura, Hamasaki et al. 2012, Kotak, Busso et al. 2014), suggesting an LGN dependent mechanism of localization and indicating that the recruitment of the capture machinery on the cell cortex is regulated by multiple mechanisms which are likely context dependent. Other factors that influence the localization of the complex is phosphorylation of NuMA by ABL1 (Abelson murine leukemia viral oncogene homolog 1) (Matsumura, Hamasaki et al. 2012) and activation of the membrane-actin linkers ezrin, radixin, moesin (ERMs) (Machicoane, de Frutos et al. 2014). Interestingly, work from Kiyomitsou and colleagues has shown that signals from the metaphase plate and the centrosomes can also polarize the cortical capture machinery. Specifically, it was shown that the Polo-like kinase (Plk1) localizes on the spindle poles and when the pole is near the cortex, Plk1 causes dynein to dissociate from the LGN/NuMA complex leading to the movement of the spindle towards the other side of the cortex, thus centering the mitotic spindle. In addition, a chromosome-derived Ran-GTP gradient can cause dissociation of the LGN/NuMA complex from the cortex when the chromosomes are close to the cortex, in order to exclude LGN/NuMA accumulation at the areas away from the spindle poles, indicating that intrinsic signals can also influence positioning of the mitotic spindle (Kiyomitsu and Cheeseman 2012).

The situation is even more complex in epithelial tissues where polarity molecules come into play. Several studies using epithelial cysts as models to study symmetric cell divisions in epithelial cells suggest that most of the upstream regulators of the cortical machinery are molecules involved in the establishment of apicobasal polarity, including Par3, Par6, atypical PKC (αPKC) and Cdc42 (Rodriguez-Fraticelli, Galvez-Santisteban et al. 2011). However, in this context loss of LGN, or disruption of its association with NuMA or Gai leads to spindle misorientation and cystogenesis in MDCK cells (Zheng, Zhu et al. 2010). In these cells Gai is localized throughout the cell cortex and theoretically the LGN/NuMA complex can be distributed as Gai. However Par3 mediated apical localization of αPKC was shown to be necessary for the exclusion of LGN from the apical cortex, a process involving phosphorylation

of Ser401 of LGN by αPKC. This phosphorylation creates a binding site for the adaptor protein 14-3-3 which leads to LGN dissociation from Gai at the apical surface, thus restricting its localization and subsequently the spindle in a planar orientation (Hao, Du et al. 2010).

Extrinsic signals

In addition to the intrinsic molecular pathways that guide spindle orientation, many studies have shown that external stimuli can regulate and guide spindle orientation. The first observation that external factors can influence spindle orientation comes from over 120 years ago from experiments performed in confined frog embryos so as they acquire a clear cell shape anisotropy, documenting a correlation between the division plane and the cell shape. This observation has been termed the "Hertwig rule", or "long axis rule": The mitotic spindle bisects the cell perpendicularly to its longest axis (Hertwig 1983) (**Figure 60**). Although this is an empirical rule, it is still widely accepted and can be used to effectively predict the cell division plane. More recent studies exploring Hertwig's rule support that cell geometry determines the division plane along the longest axis of the cell albeit with exceptions in certain cell shapes (Minc and Piel 2012). Minc and coworkers developed a computational model of predicting the division plane based on experiments where sea urchin eggs were placed into microfabricated chambers in order to adopt a certain geometry leading to refinements of the Hertwig's rule. They propose that the cell geometry is translated as the length of the astral microtubules emerging from the spindle poles, a model that predicts division axis orientation probability for various shapes (Minc, Burgess et al. 2011).

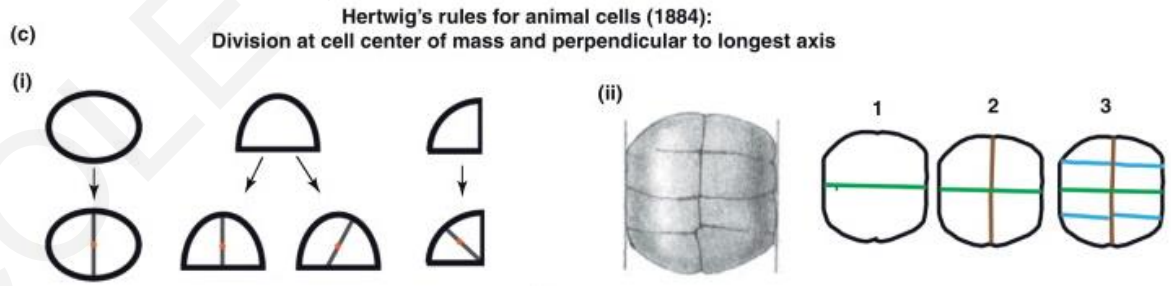

Figure 60: Hertwig's rule for predicting the cell division plane.
Schematic illustration of the division planes in cells of various shapes and in shape-manipulated *Xenopus* embryos following the "long axis rule". Adapted from (Minc and Piel 2012).

However, cell geometry is not expected to have a role in mitotic cells in culture since as mentioned above they round up during mitosis. Surprisingly, what is important in single cells is the cell adhesion geometry prior to mitosis which is defined through the distribution of the RFs. It was initially suggested that these cells follow the Hertwig's rule since the RFs resemble the cell shape in interphase and it was believed that the RFs act as a "memory" mechanism of the cell in order to divide according to its interphase long axis (Thery and Bornens 2006). This interpretation stems from the fact that the axis of cell division can be predicted when growing cultured cells on adhesive substrates of different shapes where the distribution of the RFs is predetermined, indicating that the adhesion geometry alone can regulate spindle orientation (Thery, Racine et al. 2005) (**Figure 61**). Seeding cells on these microprints leads to the polarized distribution of the members of the cortical machinery LGN and NuMA and of actin-associated proteins (such as ezrin, cortactin and Src) that promote tension on the astral microtubules, according to the local density of the RFs terminating on the cell cortex (Thery, Racine et al. 2005, Machicoane, de Frutos et al. 2014). Moreover, a theoretical analysis of these data was performed taking into consideration three parameters: the spherical shape of the cell, the fact that the RFs mimic the adhesive pattern and the density of the RFs. This quantitative description of spindle orientation in adherent cells was found to predict the distribution of force generators and subsequently spindle orientation (**Figure 61**) (Thery, Jimenez-Dalmaroni et al. 2007).

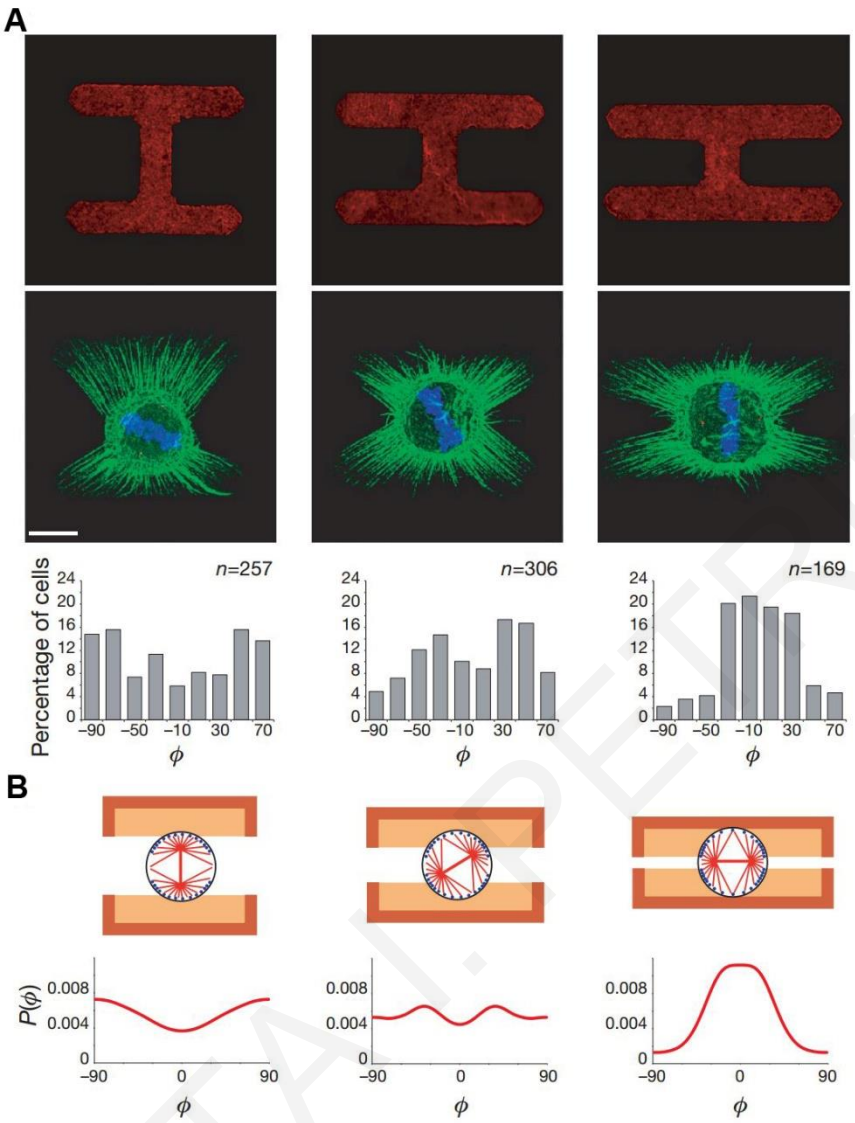

Figure 61: Prediction of spindle orientation and forces exerted on the cortex based on the cell adhesion geometry.

(A) Examples of adhesive patterns of different shapes, showing the RF distribution according to the interphase cell shape and angular distributions of spindle orientation in each case. (B) Theoretical distribution of force generators (blue dots on the schematic illustrations) and the potential energy landscapes plotted against the angular probability density of spindle orientation. Adapted from (Thery, Jimenez-Dalmaroni et al. 2007).

However, the fact that the RF distribution seems to be crucial for spindle orientation raised the question if the information of the external environment is transmitted in real time through the RFs to the spindle and that the RFs are not just anchoring cables that resemble the interphase cell shape. Fink and coworkers addressed this question and have elegantly shown that external forces transmitted through the RFs can guide mitotic spindle orientation in real time. Specifically, they grew HeLa cells on adhesive substrates of either bar-shaped or cross-shaped FN micropatterns. Under normal conditions the spindles aligned along the long axis of the

pattern. Once the spindles had aligned, laser ablations were performed to disrupt the RFs along the adhesion axis. Interestingly, the spindles on cross-shaped patterns rotated and became aligned with the new adhesive axis whereas the spindles on bar-shaped patterns did not change their orientation (**Figure 62**). These results together with further experiments showing that the RFs are under high tension suggested that the mitotic spindle can sense and respond in real time according to the external forces that are applied on the cortex through the RFs and its alignment is not a result of a memory mechanism provided at interphase (Fink, Carpi et al. 2011).

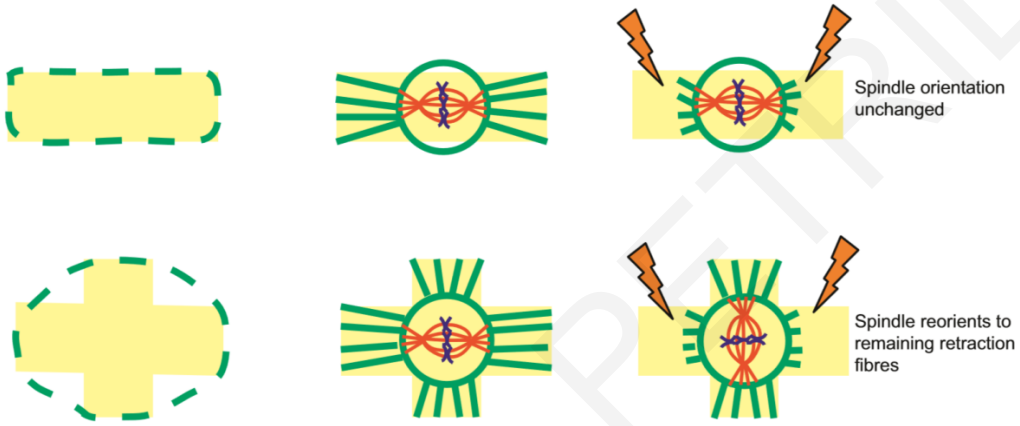

Figure 62: External forces transmitted through the RFs guide spindle orientation.
Schematic illustration of the RF distribution according to the interphase cell shape and adhesion geometry defined either on a bar- or cross-shaped micropattern. Laser ablations performed disrupt the RFs along the long axis of the pattern and the spindle in cross-shaped patterns responds by orientating itself along the remaining adhesion axis. Adapted from (Nestor-Bergmann, Goddard et al. 2014).

Even if in the above experiments the cell rounds up during mitosis, it is still possible that the initial cell shape anisotropy plays a role in orienting the spindle. In an effort to separate the contributions of cell shape and mechanical force on spindle orientation, Fink et al. grew cells on elliptical FN coated patterns on silicon thin films where the spindle was aligned according to the RF pattern and unidirectional stretch was applied on the cells to adopt a circular shape. Although, in un-stretched cells the mitotic spindle was aligned with the long axis of the ellipse, when cells were stretched the spindle aligned with the axis of stretch without the cells exhibiting a long adhesive axis (**Figure 63**), providing clear evidence for force dependent and shape independent mechanisms of spindle orientation (Fink, Carpi et al. 2011).

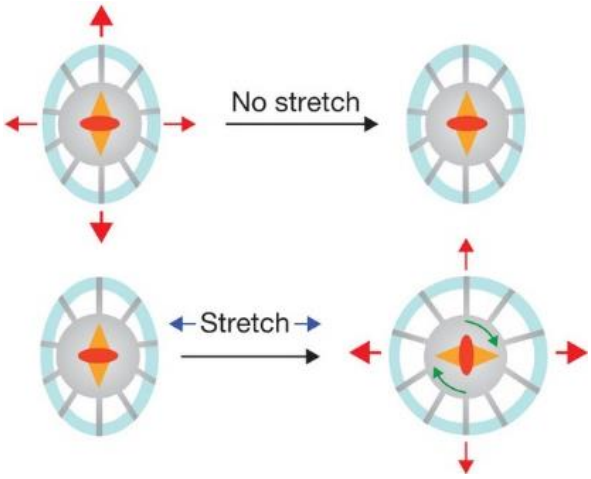

Figure 63: External forces transmitted through the RFs guide spindle orientation independently of cell geometry.

Schematic representation of spindle rotation along the stretch axis in cells exhibiting no cell shape anisotropy. Adapted from (Lancaster and Baum 2011).

The importance of aligning the mitotic spindle with external forces is also supported by work in in the fruit fly and *Zebrafish*, where it was shown to be important for proper embryogenesis (Campinho, Behrndt et al. 2013, Legoff, Rouault et al. 2013, Mao, Tournier et al. 2013). The *Drosophila* wing disc epithelium displays cell divisions aligned with the proximal-distal axis at the center, and cell divisions perpendicular to the proximal-distal axis at the periphery. It was suggested that differential proliferation rates in the disc generate anisotropic tension in the peripheral/proximal regions of the disc and that this pattern of force anisotropy determines spindle orientation (Legoff, Rouault et al. 2013, Mao, Tournier et al. 2013). It was shown that the cells in the periphery are mechanically stretched, whereas in the center are compressed suggesting that tension in the proximal-distal cell junctions (junctions oriented orthogonally to the proximal-distal axis) increases towards the periphery of the disc (Legoff, Rouault et al. 2013). Another study showed through laser ablations that at the periphery, tension is increased in the axis perpendicular to the proximal-distal axis causing elongation of these cells. This together with the higher proliferation rates at the center of the disc than at the periphery, were suggested to differentially orient the mitotic spindle throughout the disc (Mao, Tournier et al. 2013). During *Zebrafish* epiboly the EVL spreads and covers the yolk cell and at the same time displays fast proliferation rates with the spindles oriented both with the plane of the epithelium and with the axis of tissue spreading, the animal-vegetal axis. Interestingly, Campinho and coworkers have shown by measuring the recoil velocities of the EVL after laser cuts that the greatest tension is along the animal-vegetal axis of the embryo correlating with the orientation of the mitotic spindle. Moreover, by locally inducing a new tension axis on a diving cell through

laser ablations, it was shown that the spindle similarly to the *in vitro* situation (Fink, Carpi et al. 2011), responded in real time and rotated along the major force vector (Campinho, Behrndt et al. 2013). Laser ablations were performed in two neighboring cells of the dividing cell, in the axis perpendicularly to the axis of the spindle. Laser ablations lead to the extrusion of the ablated cells creating wounds and as the wounds close, stretching forces are exerted in this axis leading to elongation of the dividing cell and spindle rotation. However, the change in cell shape in response to the tensile forces makes the contribution of each parameter in spindle orientation difficult to separate, concluding that in the tissue context where cells retain their interphase shape during mitosis, separating the two is quite challenging (Nestor-Bergmann, Goddard et al. 2014).

4.1.1.3. Intracellular translation of the extrinsic signals that guide spindle orientation

Although the relationship between mechanical forces and spindle orientation is now well established, information on how these forces are translated into biochemical signals that orient the mitotic spindle is still lacking. Besides the cortical capture machinery, many regulators of mitotic spindle orientation were identified to date and these include microtubule and actin associated proteins (EB1, myosin X, cortactin, ezrin), kinases (ABL1, PI3K, Src, Aurora), members of the Planar Cell Polarity pathway and of the intraflagellar transport machinery in cilia and transmembrane receptors (EGFR, integrins) (Thery, Racine et al. 2005, Toyoshima, Matsumura et al. 2007, Toyoshima and Nishida 2007, Mitsushima, Toyoshima et al. 2009, Delaval, Bright et al. 2011, Matsumura, Hamasaki et al. 2012, Banon-Rodriguez, Galvez-Santisteban et al. 2014, Carvalho, Moreira et al. 2015). However, only a few examples exist in the literature that provide direct evidence that force transduction can influence the function of the above proteins.

It was initially proposed that a dynamic subcortical actin pool is formed in mitotic cells according to the adhesion geometry and associates with spindle movement during metaphase. Interestingly, laser ablations on cells seeded on cross-shaped patterns to induce spindle re-orientation as described above (**Figure 62**), revealed that these actin structures are dynamically polarized along the remaining adhesive axis guiding spindle response to external forces. These results suggest that the subcortical actin pool provides a link between the external forces and the spindle (Fink, Carpi et al. 2011). The movement of the spindle towards the actin structures was lost upon disruption of the astral microtubules through nocodazole treatment suggesting that actin and motor proteins of the astral microtubules communicate to align the spindle (Fink, Carpi et al. 2011). A recent study revealed that the unconventional myosin 10 has a similar

distribution to the actin clouds and that is required to pull the centrosomes towards these clouds acting as a link between the subcortical actin and the spindle (Kwon, Bagonis et al. 2015).

Moreover, there is evidence that the molecules of the cortical capture machinery can localize at the cell cortex in response to external forces. Both LGN and NuMA, but not Gai, displayed a strong polarized cortical localization in metaphase cells seeded on L-FN microprints (Machicoane, de Frutos et al. 2014) (**Figure 64**). What is interesting is that in prometaphase, LGN and NuMA cortical localization resembles the adhesive zone of the pattern, i.e. forming a rounded-shaped "L" (**Figure 64**), suggesting that it dynamically responds to the RF-derived adhesion forces and then is eventually restricted at the two spindle capture sites probably through chromosome derived signals discussed above (Kiyomitsu and Cheeseman 2012, Machicoane, de Frutos et al. 2014). Moreover, application of unidirectional stretching in keratinocytes was shown to induce enrichment of NuMA on the cortex and spindle rotation along the stretch axis, a response that was lost upon NuMA knockdown. Interestingly, NuMA dependent spindle re-orientation in response to force requires the binding domain of NuMA to the 4.1 family of proteins, which link the actin cytoskeleton to the cortex (Seldin, Poulson et al. 2013).

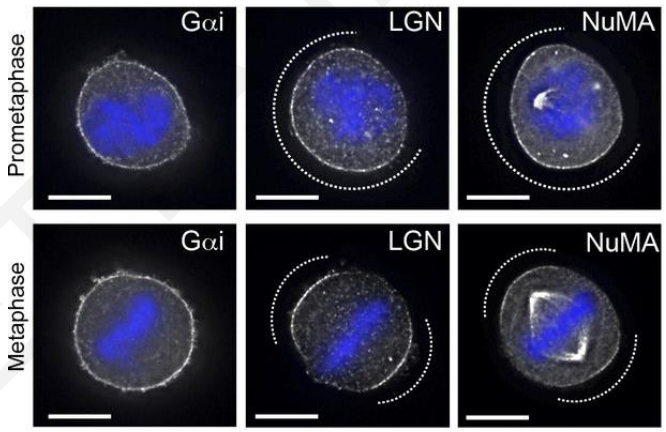

Figure 64: Distribution of the members of the cortical machinery on micropatterned surfaces.
Cortical localization of Gai, LGN and NuMA in prometaphase and metaphase cells seeded on L-FN microprints. Adapted from (Machicoane, de Frutos et al. 2014).

4.1.2. Integrins and spindle orientation

One of the major regulators of mitotic spindle orientation are integrins, which as mentioned in the general introduction section, facilitate cell-ECM adhesion (Campbell and Humphries 2011). Since spindle orientation both along the Z-axis and at the XY plane requires RF formation, integrins are expected to be involved in this process since they ensure proper cell-ECM adhesion (Toyoshima and Nishida 2007, Bergstralh, Haack et al. 2013). The first evidence that integrins are required for spindle orientation came from a study by Toyoshima and co-workers where studying symmetric cell divisions in adherent cells, they identified that integrin β1 is necessary for the determination of the division axis parallel to the substrate. Specifically, by using several approaches to disrupt integrin β1 function in HeLa cells (growing cells on PLL - a substrate which does not bind to integrins -, inhibition of integrin-FN interaction by RGD peptide treatment, integrin β1 downregulation, integrin loss of function using functional-blocking antibodies), led to spindle misorientation along the Z-axis (Toyoshima and Nishida 2007) (**Figure 65**).

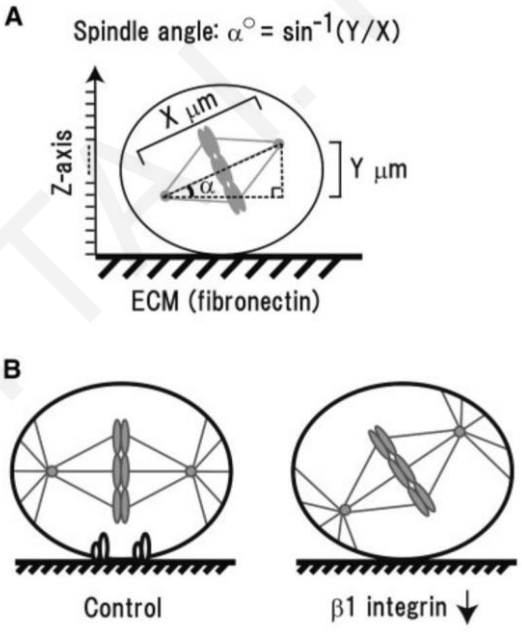

Figure 65: Spindle orientation parallel to the substrate in adherent cells.
Disruption of integrin β1 function leads to spindle misorientation along the Z-axis, creating an angle between the spindle axis the substrate. Adapted from (Toyoshima and Nishida 2007).

It was suggested that integrin-mediated adhesion signaling promotes the accumulation of PIP_3 at the cortex of mitotic cells which act as a cortical cue to orient the mitotic spindle (Toyoshima, Matsumura et al. 2007). Moreover, integrin binding partners were found to be involved in

spindle orientation of adherent cells. ILK was proposed to regulate spindle orientation by linking the subunits of the dynein/dynactin complex, dynactin-1 and 2, with integrins at the basal surface of mitotic cells, the cell-ECM interface (Morris, Assi et al. 2015).

In addition, a study in the mammalian skin has shown that integrin β1 knockout mice display spindle randomization during stratification. Normally, the basal keratinocytes in the embryonic mouse skin undergo asymmetric cell divisions to promote stratification, a phenotype that was lost upon integrin β1 knockout. The cortical polarity cues LGN/NuMA and the epithelial polarity protein αPKC were mislocalized in the integrin β1 knockout embryonic skin (Lechler and Fuchs 2005). Concerning integrins role in spindle orientation during embryonic development, integrin β1 was also found to be essential for the development of the mouse airway epithelium where spindle misorientation was associated with multilayered lung epithelium and defective lung branching (Chen and Krasnow 2012). However, a direct role of integrins in spindle orientation in epithelial tissues is difficult to be assessed due to the fact that integrins control basement membrane deposition, a process that is required for the establishment of epithelial polarity, which is necessary for correct spindle orientation. This suggests that spindle orientation defects in epithelia caused by disruption of integrin function may arise from secondary effects of aberrant epithelial polarity (Ojakian and Schwimmer 1994). Moreover, integrins were identified to be important for spindle orientation of the follicle cells of ovarian epithelium monolayer in *Drosophila*. Interestingly, it was shown that in this context integrin signaling rather integrin-based adhesion was required for spindle orientation, providing the first evidence that integrins may have a direct role in orienting the mitotic spindle independently of cell-ECM adhesion (Fernandez-Minan, Martin-Bermudo et al. 2007).

4.2. Results Chapter II: A mechanosensory complex composed of FA proteins forms on the mitotic cortex upon ligand independent integrin β1 activation and guides spindle orientation

4.2.1. FF expression in the outermost epithelium leads to spindle misorientation

We have shown in the previous chapter that FAK transduces a FN-derived polarity signal that guides radial intercalation of the inner epithelial cells of the BCR and spindle orientation along the plane of the epithelium in order to guide epithelial cell spreading during epiboly. As described above, before gastrulation the *Xenopus* epithelium consists of three epithelial cell layers, the outermost cell layer which has tight junctions and two innermost epithelial layers that associate with each other and the outermost layer through adherens junctions (Keller 1980, Fesenko, Kurth et al. 2000, Winklbauer 2012). The innermost cell layer is in contact with the FN matrix that polarizes the two deep cell layers to intercalate radially and merge into one during epiboly (Marsden and DeSimone 2001). Moreover, these cells know how to orient their mitotic spindle through FN-integrin mediated signaling, since inhibition of FN fibrillogenesis or FN loss of function leads to spindle misorientation in the inner cells (Marsden and DeSimone 2001, Rozario, Dzamba et al. 2009). Spindle orientation of the cells of the outermost epithelium however is not regulated by this FN-derived polarizing signal since no FN fibrillar matrix exists underneath these cells, and inhibition of FN function through blocking antibodies did not affect spindle orientation of the outer cells (Marsden and DeSimone 2001). However, we have noticed spindle misorientation in the cells of the outermost epithelium in FF expressing embryos (**Figure 51C** and **Figure 66C**), raising the possibility that FAK has a central role in spindle orientation. It is possible however, that spindle misorientation in these cells might be a secondary effect of the increased mechanical tension that is generated through epiboly failure in FF injected embryos. In order to overcome this, we injected FF at the AP at the one cell stage, let embryos to grow until stage 9 and ACs were dissected and cultured until stage 15. Spindle orientation in dissected ACs would presumably be unaffected by defects in morphogenesis (such as blastopore closure failure) and it would permit a clearer evaluation of the role of FAK in spindle orientation in the outer cells. As can be seen in **Figure 66A**, and from the quantification of the spindle to apical surface angles, FF expression led to spindle misorientation a phenotype that was rescued by expression of WT FAK (**Figure 66A, B**). These results suggest that FAK has an essential role in the determination of the division axis.

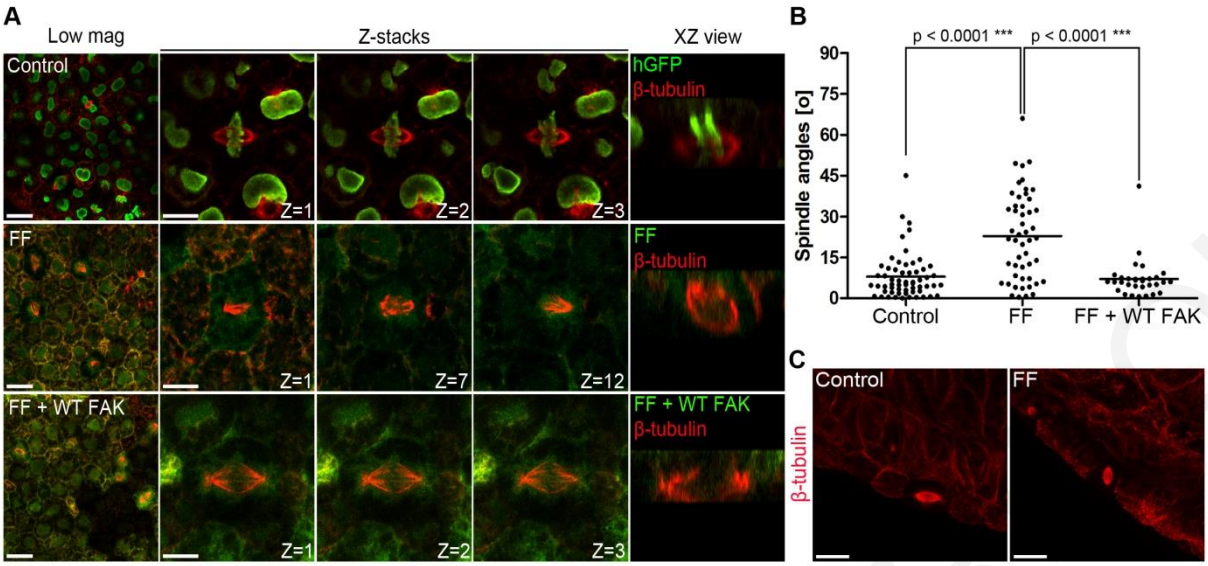

Figure 66: FAK loss of function through FF expression leads to spindle misorientation in the cells of the outermost epithelium of *Xenopus*.

(A) A low magnification image of the *Xenopus* epithelium, optical sections from a Z-stack of a high magnification image of a metaphase epithelial cell and the corresponding XZ projection of a control embryo injected with histone GFP, an embryo injected with FF (800 pg F-GFP-F, green signal), and of a rescued embryo (800 pg F-GFP-F co-injected with 300 pg WT FAK). *Xenopus* epithelia were stained with β-tubulin and anti-GFP antibodies. (B) Scatter plots of the spindle to plane of the epithelium angles of control, FF injected and rescued embryos. The average spindle angle is 7.913 ± 1.086º (n=59) for control cells, 22.86 ± 2.258º (n=50) for FF expressing cells and 7.083 ± 1.301º (n=31) for rescued cells. Analysis of spindle orientation with a Mann-Whitney test showed statistically significant differences of the means of the spindle angles between the above samples, p<0.0001***; n, number of metaphase cells, three independent experiments. (C) Sagittal sections of mid-neurula stage *Xenopus* embryos. In control embryos the long axis of the spindle is parallel to the apical surface whereas in FF injected embryos, it is not. Scale bars: (A) low mag: 20 μm, high mag: 10 μm.

4.2.2. FAK is required for spindle orientation in adherent cells

The fact that integrins have been shown to play a critical role in spindle orientation in several systems (Lechler and Fuchs 2005, Toyoshima and Nishida 2007) coupled with the central role of FAK in the transduction of integrin signaling (Guan 1997), prompted us to investigate the role of FAK in spindle orientation further. As an initial approach we examined spindle orientation in FAK null MEFs and compared the results to those from FAK nulls re-expressing WT FAK. The mitotic spindle in adherent cells has been shown to be oriented parallel to the substratum (Toyoshima and Nishida 2007), so for each metaphase cell, thin optical sections along the Z-axis were acquired and the angle between the two spindle poles with respect to the substrate was measured from Z reconstructions (**Figure 67A, B**). The average spindle angle in FAK null cells was 20.3 ± 1.368º (n=116), whereas this angle was 8.849 ± 0.7483º (n=95) in

FAK re-expressing cells (**Figure 67B, C**). In addition, 75% of the FAK null cells showed a spindle angle greater than 10^{o} compared with 32% in FAK re-expressing cells (**Figure 67D**), showing that FAK is required for spindle orientation parallel to the substrate in MEFs.

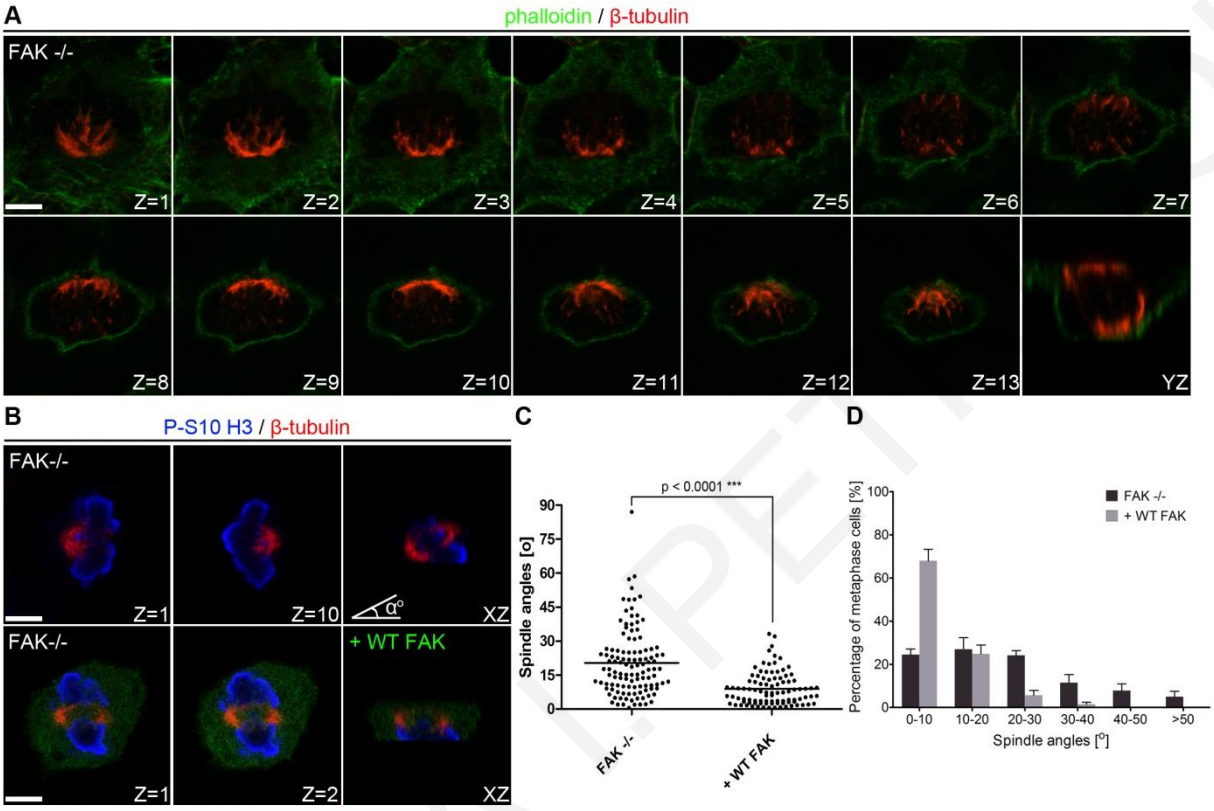

Figure 67: FAK null cells display spindle misorientation along the Z-axis.

(A) Thin optical sections (0.37 μm) of a FAK null metaphase cell and the corresponding YZ projection image. (B) First and last optical sections from a Z-stack, showing the two spindle poles and the XZ projection of a FAK null metaphase cell and a FAK reconstituted cell (transfected with GFP FAK). The diagram shows how the substrate to spindle angle was measured. (C) Scatter plots of the substrate to spindle angles (angle α shown in B) of FAK null and WT FAK reconstituted cells. The average spindle angle in FAK null cells is 20.30 ± 1.368^{o} (n=116) and in WT FAK reconstituted cells 8.849 ± 0.7483^{o} (n=95). Data are Means ± S.E.M (Standard Error of the Mean). Analysis of spindle orientation with a Mann-Whitney test showed statistically significant differences of the means of the spindle angles between the two samples, p<0.0001***; n, number of metaphase cells, six independent experiments. (D) Quantification of the percentage of metaphase cells with substrate to spindle angles greater than 10^{o}. 75% of FAK null cells displayed spindle angles greater than 10^{o} compared with 32% of FAK reconstituted cells. Scale bars: (A, B) 5 μm.

In addition, we examined the possibility that spindle misorientation of FAK null cells is a secondary effect of spindle centering or spindle integrity defects. Spindle positioning effects were examined by measuring the distances from the two spindle poles to their respective nearest cortex (**Figure 68A**) and then dividing the distance with the greatest value by the distance with

the smallest value. FAK null and FAK re-expressing cells had an average ratio near 1 indicating proper spindle centering, without any statistically significant differences (**Figure 68B**), and the percentage of off-center spindles was comparable between the two samples (**Figure 68C**). Moreover, in order to ensure that the changes in the spindle angle in FAK knockout cells do not arise from indirect effects of the spindle integrity, we examined the spindle size in FAK deficient and FAK re-expressing cells, by measuring the spindle length and width as shown in **Figure 68D**. Quantification of our results showed that the lengths and widths of the mitotic spindles hardly changed in FAK deficient cells (**Figure 68E**). These results indicate that the effects on spindle orientation do not originate from defects in spindle integrity or centering (Toyoshima and Nishida 2007).

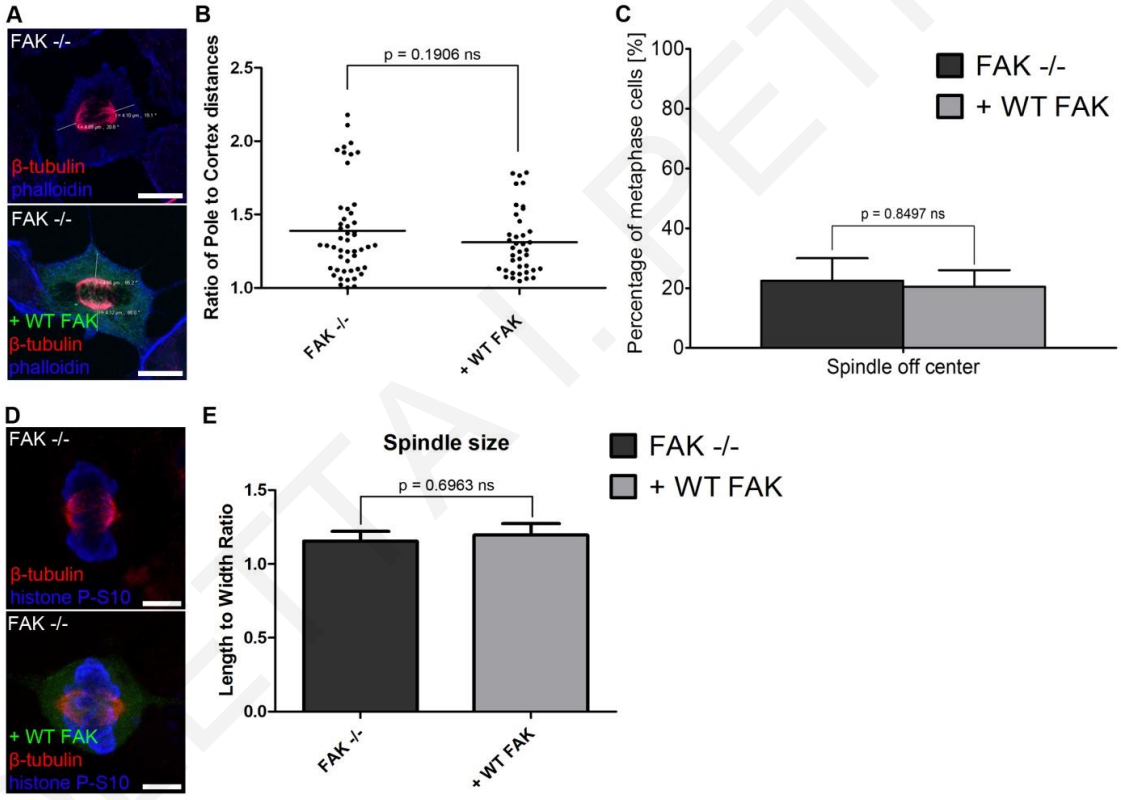

Figure 68: Spindle misorientation of FAK null cells is not a secondary effect of spindle integrity and centering issues.

(A) Representative images of FAK null and FAK reconstituted metaphase cells indicating how the measurements of spindle centering were carried out. (B) Scatter plots of the ratio of pole to cortex distances of FAK null and WT FAK reconstituted cells. The average ratio in FAK nulls is 1.390 ± 0.04560 (n=49) and 1.310 ± 0.03583 (n=39) in FAK reconstituted cells. Analysis of spindle centering with a two-tailed unpaired t-test showed no statistically significant differences of the means of the above ratio between the two samples, p=0.1906 ns; n, number of mitotic spindles, two independent experiments. (C) The percentage of metaphase cells with off-center spindles in FAK nulls is 22.5 ± 7.5 % (n=96) and 20.5 ± 5.5 % in WT FAK reconstituted cells (n=71); n, number of metaphase

cells. (D) Representative images of a FAK null and a FAK reconstituted metaphase cell showing similar spindle size. (E) Quantification of the spindle size. FAK nulls had an average spindle length to width ratio of 1.154 ± 0.06600 µm (n=96) and 1.196 ± 0.07685 µm in FAK reconstituted cells (n=71). Statistical analysis with an unpaired t-test showed no statistically significant differences of the means between the two samples, p=0.6963 ns; n, number of metaphase cells, four independent experiments. Scale bars (A, D) 5 µm.

We went on to examine if loss of FAK function in other cell types also leads to spindle misorientation. Both electroporation of a previously characterized FAK MO (Fonar, Gutkovich et al. 2011) in *Xenopus* XL177 cells (**Figure 69A, B**), as well as expression of the FF FAK DN composed of the N and C termini of FAK in NIH3T3 cells (**Figure 69C**), lead to spindle misorientation confirming a requirement for FAK in spindle orientation.

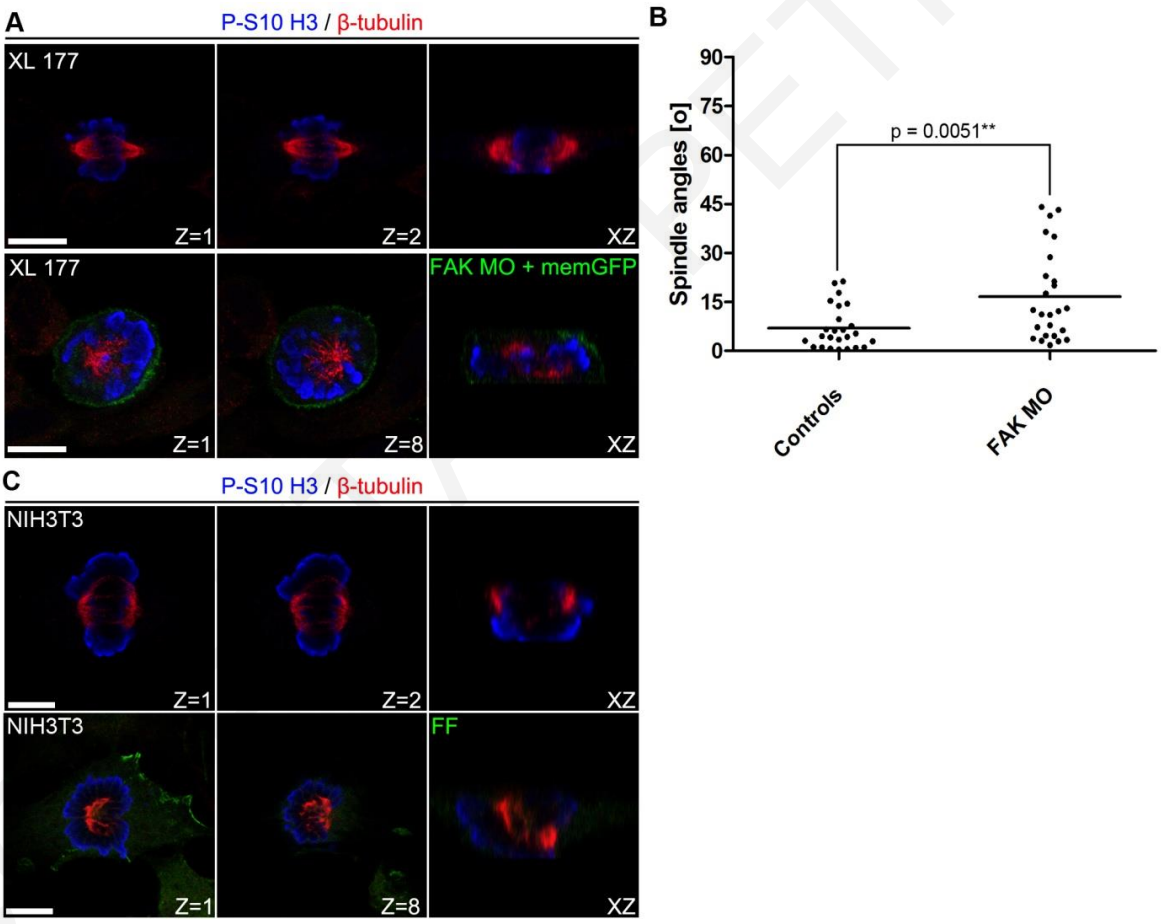

Figure 69: FAK is required for spindle orientation along the Z-axis in several adherent cell lines.
(A) Optical sections and a side view of a control XL177 cell and a cell electroporated with FAK MO (together with memGFP). (B) Quantification of the average spindle angles of the samples in (A); controls 6.932 ± 1.306º (n=25), FAK morphants 16.63 ± 2.777º (n=25). Statistical analysis using a Mann-Whitney test shows that the difference in the average spindle angles between the two samples is statistically significant (p=0.0051**); n, number of metaphase cells, two independent experiments. (C) Optical sections and a side view of a control NIH3T3 cell and a cell transfected with FF. Scale bars: (A, C) 5 µm.

The mitotic spindle of adherent cells is normally parallel to the substratum while it is oriented through mechanical forces exerted by RFs in the XY plane (Thery, Racine et al. 2005, Fink, Carpi et al. 2011). It is thus possible to force the spindle of adherent cells into a defined orientation by plating cells onto micropatterned surfaces (Thery, Jimenez-Dalmaroni et al. 2007). To determine whether loss of FAK affects XY spindle orientation we used L-shaped FN micropatterns. The mitotic spindle of cells grown on this pattern is normally parallel to the hypotenuse of the triangle formed by the L (Thery, Racine et al. 2005). Examination of spindle orientation on L-shaped microprints revealed loss of spindle orientation of FAK null cells along the XY axis (**Figure 70A**). Specifically, under these conditions FAK-null cells display randomized spindles with an average angle of deviation of 49.77 ± 5.119º (n=31), compared with 14.82 ± 1.426º (n=20) in FAK reconstituted cells (**Figure 70B**). These results show that FAK is required both for spindle alignment with the substrate as well as for force dependent orientation associated with RFs. Since both cell shape and forces have been shown to influence spindle orientation (Fink, Carpi et al. 2011, Minc, Burgess et al. 2011, Campinho, Behrndt et al. 2013) we also quantified spindle orientation on bar-shaped patterns which generate greater cell shape anisotropy. FAK nulls on such patterns display a moderate but statistically significant reduction of misorientation compared to cells on L-shapes suggesting that the primary defect on FAK nulls is in force dependent orientation (**Figure 70C**).

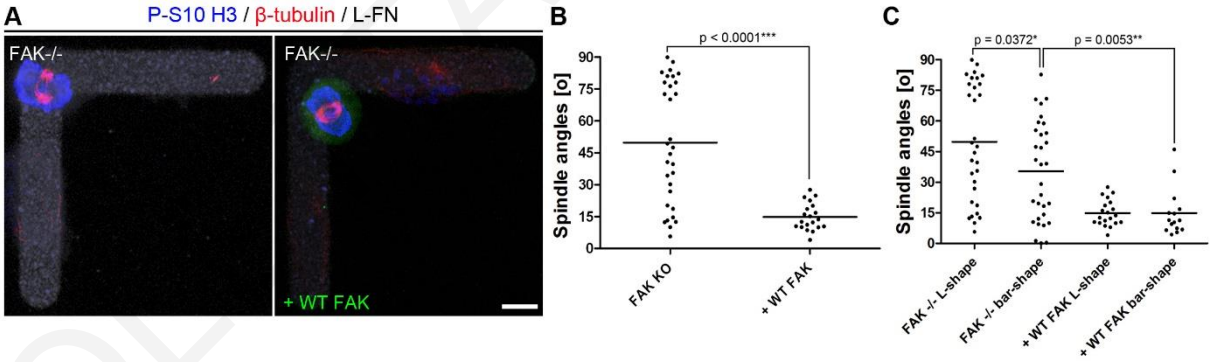

Figure 70: FAK is required for force dependent spindle orientation.

(A) Representative images of FAK null and FAK reconstituted metaphase cells on L- FN micropatterns. (B) Scatter plots of XY spindle angles of the cells described in (A). The average spindle angle in FAK null cells is 49.77 ± 5.119º (n=31) and in WT FAK reconstituted cells is 14.82 ± 1.426º (n=20). Quantification of spindle orientation with a Mann-Whitney test showed statistically significant differences of the means of the spindle angles between the two samples, p<0.0001***; n, number of metaphase cells, two independent experiments. (C) Scatter plot of the spindle angles of FAK null and FAK reconstituted cells dividing on L or on bar FN microprints. The average spindle angle of FAK nulls on bars is 35.30 ± 4.365º (n=31) and of the reconstituted cells on bars 14.83 ± 3.014º (n=15). Statistical analysis was performed using Mann-Whitney tests. Scale bars: (A) 10 μm.

4.2.3. Spindle orientation is controlled by the 3D distribution of the ECM

During mitosis adherent cultured cells round up becoming spherical however, they maintain RFs connecting them to the ECM in a pattern closely resembling their adhesion geometry prior to rounding up (Mitchison 1992). Use of 2D micropatterned adhesive substrates revealed that the spatial distribution of ECM components is responsible for the orientation of the spindle of adherent cells through resulting variations in the distribution of forces applied to the spherical cell cortex by the RFs (Thery, Racine et al. 2005, Thery, Jimenez-Dalmaroni et al. 2007). The spindle becomes aligned in the XY plane with the greatest force vector and has been shown to reorient when the direction of maximum force changes (Fink, Carpi et al. 2011). Before the effects of RFs and force on spindle orientation had been uncovered, it was shown that integrin-based cell adhesion to ECM components also orients the mitotic spindle of cultured cells parallel to the plane of the substrate (Toyoshima and Nishida 2007). Although the mechanism through which this Z-axis orientation is accomplished is sometimes assumed to be the same as in the case of orientation in the XY plane (Lancaster and Baum 2011) this has never been addressed directly. The fact that FAK null cells fail to orient their spindle both in response to micropatterns as well as with respect to the plane of the substrate would suggest that the two orientation processes do in fact share a common mechanism. It is likely that the absence of RFs at the apical area of a spherical mitotic cell automatically would lead to the exclusion of a vertical division with respect to the substrate since no force is applied in that direction. However, other possibilities cannot be excluded. For example, cortical cues responsible for spindle orientation could be excluded from the basal area of a cell through integrin signaling thus preventing spindle capture in that region. In order to determine if RF dependent forces applied to the lateral regions of mitotic cells are in fact responsible for the parallel orientation of the spindle to the substrate we exposed cells to two parallel substrate planes by sandwiching them between coverslips. After cells attached to the first coverslip, a second was positioned over them using silicone grease bridges to hold it in place (**Figure 71A**). As shown, HeLa cells primarily adhere and spread on the bottom coverslip while maintaining a small area in contact with the top coverslip (**Figure 71A, B**). Once they round up, the majority of RFs are formed on the bottom coverslip however, RFs also form at the top (**Figure 71A, B**). Cells under these conditions fail to orient their spindles parallel to the substrate and often divide completely perpendicular to the substratum (**Figure 71B-D**). This suggests that RFs under these conditions apply forces perpendicular to the substrate plane leading to the change in spindle orientation. In order to ensure that spindle reorientation is a result of integrin-dependent adhesion we repeated the experiment using FN bottom coverslips and PLL coverslips on top (**Figure 71A**).

In agreement with previous work, spindles under these conditions remain parallel to the substratum (**Figure 71C, D**) indicating that integrin based adhesions are required to elicit spindle orientation changes (Toyoshima and Nishida 2007). Overall, these results suggest that the mechanism for spindle orientation in the XY and Z-axis is common and depends on the spatial distribution of the ECM which defines the distribution of RFs and subsequently, the spatial distribution of forces applied on the cell cortex.

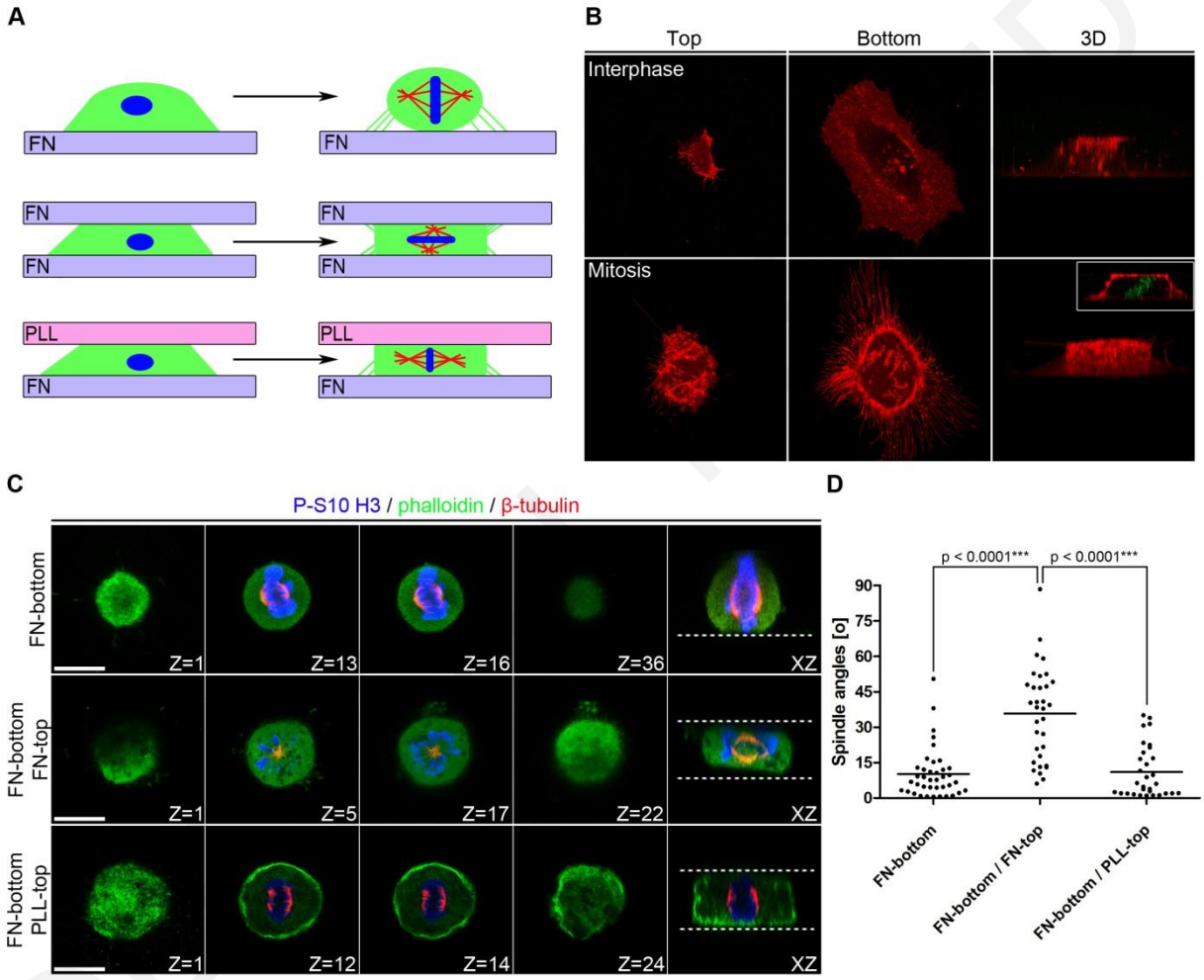

Figure 71: The mechanism of spindle orientation in the XY and Z-axis is common and depends on the spatial distribution of the RFs.

(A) Schematic representation of the experimental setup to determine the role of RFs in Z axis spindle orientation: cells seeded on a FN coated coverslip, sandwiched between two FN coated coverslips, or sandwiched between a FN coated coverslip and a PLL coated coverslip and imaged during cell division. (B) Confocal images of live memCherry transfected HeLa cells confined between two FN coated coverslips. Optical sections showing the top and the bottom of an interphase cell and a 3D reconstruction show how the cell adheres on both coverslips. In the lower panel optical sections of the top and the bottom of a mitotic cell and a 3D reconstruction show the distribution of the RFs. The small rectangle in the 3D reconstruction of the lower panel shows a side view of the mitotic cell where the metaphase plate (green) is not perpendicular to the substrate. (C) Z-stacks (0.37 μm interval) and the

corresponding XZ side view of representative mitotic cells grown under the experimental settings shown in (A). Cells were fixed and stained for actin, β-tubulin and P-S10 H3. The white dashed lines represent the coverslips. (D) Scatter plots of spindle angles relative to the substrate of the cells grown under the three conditions. The average spindle angle for cells grown in 2D is 10.17 ± 1.699º (n=39), in cells grown between two FN coated coverslips 35.72 ± 3.405º (n=33) and in cells grown between a FN coated and a PLL coated coverslip 11.01 ± 1.987º (n=31). Quantification of spindle orientation with a Mann-Whitney test shows statistically significant differences of the means of the spindle angles between the indicated samples, p<0.0001***; n, number of metaphase cells, three independent experiments. Scale bars: (B, C) 10 μm.

4.2.4. FAK's kinase activity is dispensable for spindle orientation

One of the main mechanisms through which FAK transduces integrin signals and controls FA turnover is through phosphorylation of downstream targets (Mitra, Hanson et al. 2005). We thus examined if FAK´s kinase activity is important in spindle orientation by transfecting FAK null cells with the kinase inactive mutant FAK K454R (Lim, Chen et al. 2010). The results from these experiments were nearly identical to those for WT FAK suggesting that FAK's kinase activity is dispensable for correct spindle orientation both along the Z-axis and the XY plane (**Figure 72A-D**). Due to the unexpected nature of this result we went on to confirm it using the FAK kinase inhibitor PF-228 in HeLa and NIH3T3 cells (Slack-Davis, Martin et al. 2007). Both cell lines were treated with the inhibitor for 24 hours and inhibitor effectiveness was evaluated by western blotting (**Figure 72G, J**). Quantification of spindle angles in inhibitor treated cells confirmed that inhibition of FAK's kinase activity does not affect spindle orientation, confirming that spindle orientation does not require FAK´s enzymatic activity (**Figure 72E, F** and **H, I**).

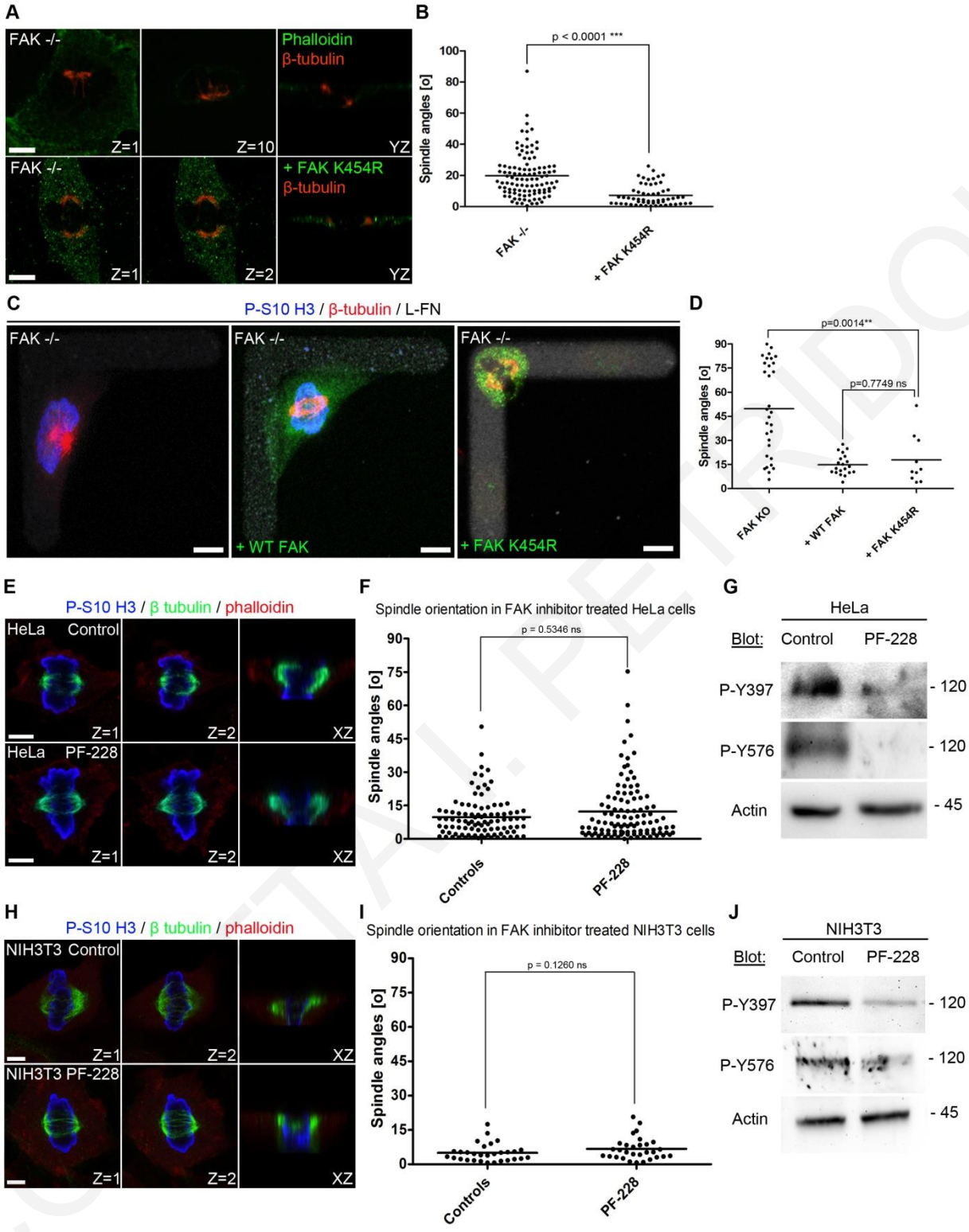

Figure 72: FAK's enzymatic activity is not required for spindle orientation in adherent cells.

(A) Representative images of FAK nulls and FAK nulls expressing a KD mutant of FAK (FAK K454R). (B) Scatter plots of substrate to spindle angles of FAK -/- and FAK -/- + FAK K454R expressing metaphase cells. The average spindle angle in FAK nulls transfected with FAK K454R is 7.200 ± 0.8812° (n=58). Analysis with Mann-Whitney tests showed statistically significant differences of the means of the spindle angles for the indicated samples, p<0.0001***; n, number of metaphase cells, three independent experiments. (C) Representative images of FAK null, and FAK nulls transfected with the WT FAK or FAK K454R constructs on L- FN micropatterns. (D)

Scatter plots of XY spindle angles of the samples in (C). The average spindle angle in FAK K454R is 17.82 ± 4.912º (n=10). Statistical analysis with Mann-Whitney tests showed statistically significant differences of the means of the spindle angles between FAK null and FAK K454R expressing cells (p=0.014**), but no statistically significant differences between WT FAK and FAK K454R expressing cells (p=0.7749 ns); n, number of metaphase cells, two independent experiments. (E) Optical sections and the XZ projection from HeLa metaphase cells with and without FAK inhibitor treatment (10 μM FAK inhibitor PF-228). (F) Scatter plots of the spindle to ECM angles of control and FAK inhibitor treated HeLa cells. The average spindle angle of controls is 9.765 ± 0.9342º (n=96) and of FAK inhibitor treated cells 12.24 ± 1.320º (n=107). Analysis with a Mann-Whitney test showed no statistically significant differences of the means of the spindle angles between the two samples, p=0.5346 ns; n, number of metaphase cells, three independent experiments. (G) Western blotting of total cell lysates from the above samples using specific antibodies against phosphorylated FAK on Tyr397 and Tyr576 and actin for loading control. (H) Optical sections showing the spindle pole positions and XZ projection from NIH3T3 metaphase cells without FAK inhibitor and after treatment with 5 μM of the FAK inhibitor PF-228. (I) Scatter plots of the spindle to ECM angles of control and FAK inhibitor treated NIH3T3 cells. The average spindle angle of control cells is 4.980 ± 0.7127º (n=30) and for FAK inhibitor treated cells 6.726 ± 0.8993º (n=30). Analysis with a Mann-Whitney test showed no statistically significant differences of the means of the spindle angles between the two samples, p=0.1260 ns; n, number of metaphase cells, two independent experiments. (J) Western blot analysis from total cell lysates from the above samples blotted against phosphorylated FAK on Tyr397 and Tyr576. Actin was used as a loading control. Scale bars: (A, E, H) 5 μm, (C) 10 μm.

4.2.5. FAK's Kinase and FAT domains are required for spindle orientation

The above results suggest that FAK's function in spindle orientation is a scaffolding one. Given the previously identified role of integrins in spindle orientation we postulated that FA localization would be required for FAK's role in this process. The FAT domain is both necessary and sufficient for FAK's FA localization (Hildebrand, Schaller et al. 1993) and as shown, a FAK ΔFAT mutant failed to rescue the spindle orientation defects suggesting that the FAT domain and FA localization are important (**Figure 73A-C**). We went on to examine a possible role of the FERM domain, which has been shown to interact with several proteins involved in spindle orientation, such as the Arp2/3 complex and integrins (Schaller, Otey et al. 1995, Serrels, Serrels et al. 2007). FAK nulls were transfected with a KD mutant of FAK that lacks the FERM domain (ΔFERM/K454R). As shown, expression of ΔFERM/K454R rescued the phenotype of spindle misorientation with the same efficiency as WT FAK and FAK K454R suggesting that the FERM domain is dispensable (**Figure 73A-C**). Given the fact that the kinase activity and the FERM domain are both dispensable, we went on to express the C-terminal non-catalytic part of the protein referred to as FRNK (Nolan, Lacoste et al. 1999). FRNK failed to rescue spindle orientation indicating that the FAT containing C-terminus is not sufficient (**Figure 73A-C**). This result suggests that despite the fact that the kinase activity is not necessary for correct spindle orientation, the kinase domain itself is, revealing a novel kinase

domain dependent but kinase activity independent function. Alternatively, the kinase domain may also be dispensable however, since FRNK lacks Tyr397 while FAK ΔFERM retains its binding of Src which has been previously shown to be involved in spindle orientation, may be required (Thery, Racine et al. 2005).

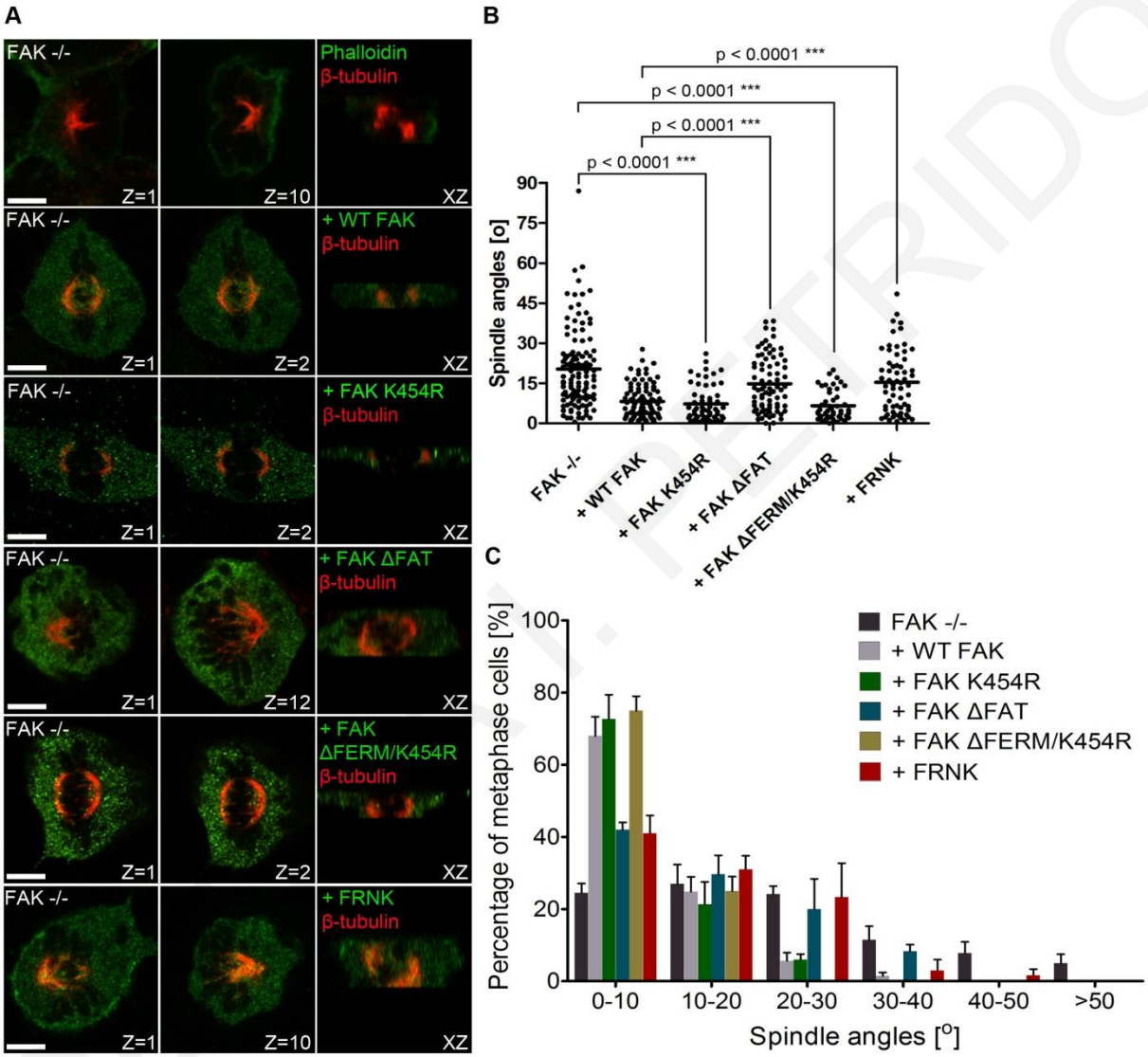

Figure 73: The FAK Kinase and FAT domains, but not the kinase activity, are required for correct spindle orientation.

(A) First and last optical sections from Z-stacks and the corresponding XZ projections of a FAK null metaphase cell and FAK nulls transfected with WT FAK, FAK K454R, FAK ΔFAT, ΔFERM/K454R and FRNK. (B) Scatter plots of substrate to spindle angles from nulls and cells transfected with the constructs in (A). The average spindle angle in FAK nulls transfected with FAK K454R is 7.200 ± 0.8812° (n=58), FAK ΔFAT 15.08 ± 1.333° (n=61), ΔFERM/K454R 6.586 ± 0.7927° (n=48) and FRNK 15.37 ± 1.478° (n=63). A Kruskal-Wallis test gave statistically significant results (p<0.0001***) indicating that at least one of the sample distributions is different from the other samples. Analysis with Mann-Whitney tests showed statistically significant differences of the means of the spindle angles for the indicated samples, p<0.0001***; n, number of metaphase cells, three independent experiments.

Comparison between WT FAK and FAK K454R, WT FAK and ΔFERM/K454R, FAK-/- and FAK ΔFAT, and FAK-/- and FRNK with Mann-Whitney tests revealed that the differences in the average spindle angles are statistically insignificant (p=0.1713 ns, p=0.1627 ns, p=0.6755 ns and p=0.6455 ns, respectively). (C) Plots (Means ± S.E.M) showing the percentage of cells that displayed spindle angles greater than 10^{o}, which were 27%, 58%, 25% and 59% for the FAK nulls transfected with FAK K454R, FAKΔFAT, ΔFERM/K454R and FRNK, respectively. Scale bars: (A) 5 μm.

4.2.6. FAK is required for spindle orientation in the developing embryo

Mechanisms controlling spindle orientation have been shown to be conserved between adherent cells and the *in vivo* setting (Toyoshima and Nishida 2007, Bergstralh, Haack et al. 2013). Spindle orientation has been studied extensively especially in epithelia as oriented cell divisions are critical to several aspects of embryonic morphogenesis. Since FF expression in the cells of the outermost epithelium in which its well documented that cell divisions are parallel to the plane of the epithelium, led to spindle misorientation (Marsden and DeSimone 2001, Woolner and Papalopulu 2012), we went on and characterize the requirement of FAK in spindle orientation in epithelial tissues. We microinjected 50 ng of a previously characterized FAK MO (Fonar, Gutkovich et al. 2011) at the one-cell stage and imaged cell divisions of the outermost epithelial layer in dissected ACs at early neurula stages. The effectiveness of the MO was confirmed by examining the levels of endogenous FAK (**Figure 74D**). As shown, injection of the FAK MO led to loss of spindle orientation while expression of WT FAK effectively rescued the phenotype (**Figure 74A-C**). We went on to examine if the functional requirements revealed from experiments in FAK null MEFs were conserved in the embryo. FAK MO was co-injected with mutants of FAK as shown in **Figure 74A-C**. Expression of the kinase dead mutant of FAK (K454R) and of the construct lacking the FERM domain (ΔFERM/K454R) rescued spindle misorientation cause by FAK downregulation as effectively as re-expression of WT FAK. Moreover, similarly to the *in vitro* situation, expression of the FAKΔFAT construct failed to rescue the phenotype. These results show that both the kinase activity and the FERM domain are dispensable, while the kinase and FAT domains are both essential for correct spindle orientation in the epithelium (**Figure 74A-C**).

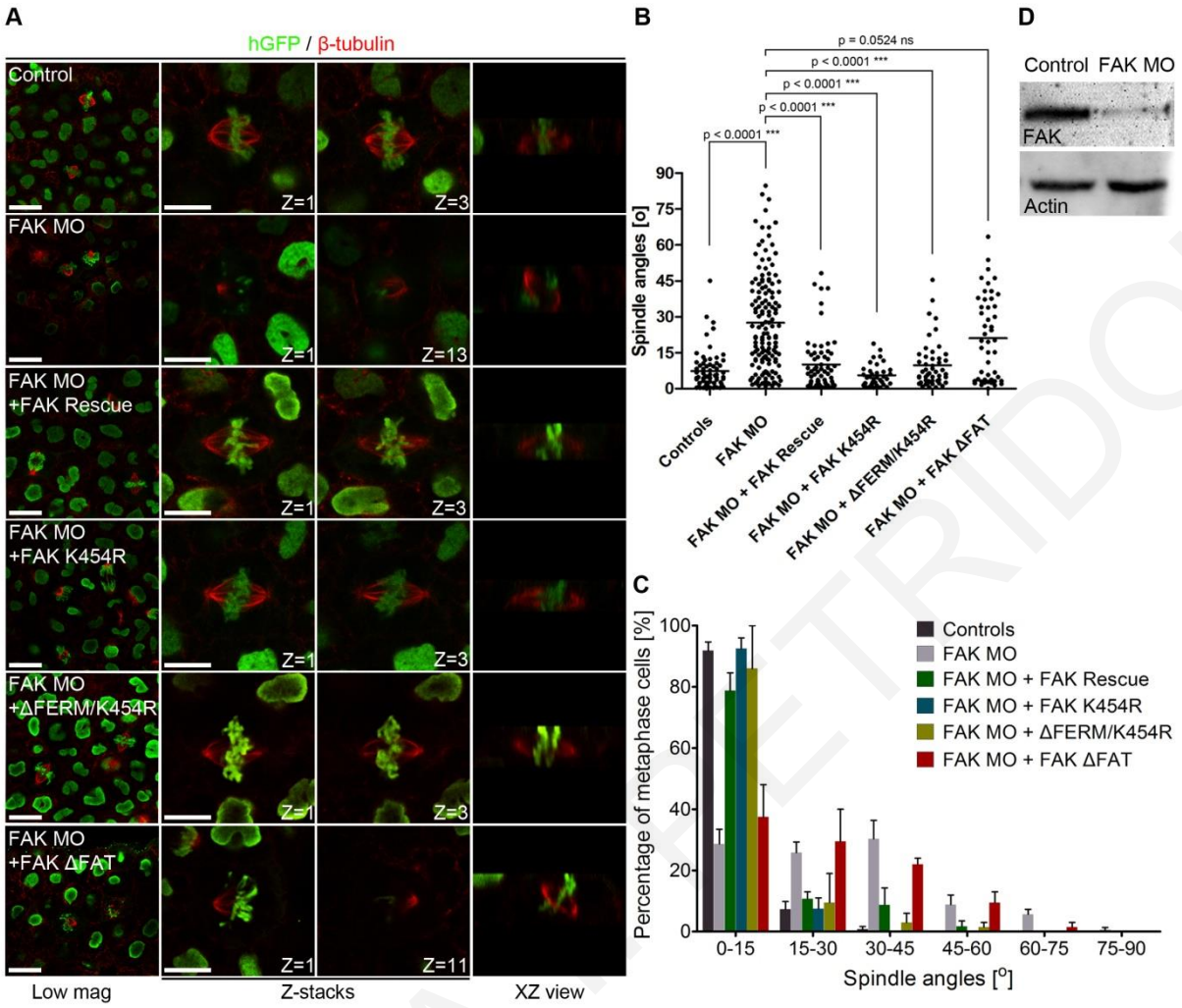

Figure 74: FAK is necessary for spindle orientation in the *Xenopus* epithelium and displays similar functional determinants as in adherent cells.

(A) Low magnification images of the *Xenopus* outer epithelium showing mitotic cells, optical sections showing each spindle pole and XZ projections from representative metaphase cells of control, morphant and embryos rescued with indicated FAK mutants (co-injected with histone GFP). *Xenopus* epithelia were stained with β-tubulin and anti-GFP antibodies. (B) Scatter plots of the spindle to plane of the epithelium angles from embryos shown in (A). The average angle in control cells is 7.343 ± 0.9881º (n=67), in FAK morphants 27.50 ± 1.682º (n=142), in cells rescued with the FAK Rescue construct 10.09 ± 1.429º (n=64), in cells rescued with the FAK K454R construct 5.617 ± 0.7739º (n=36), in cells rescued with the ΔFERM/K454R construct 9.700 ± 1.377º (n=50), and in FAK MO epithelial co-injected with the FAK ΔFAT construct 21.03 ± 2.530º (n=48). A Kruskal-Wallis test gave statistically significant results (p<0.0001***). Analysis with Mann-Whitney tests showed statistically significant differences of the means of the spindle angles between the indicated samples, p<0.0001***; n, number of metaphase cells, three independent experiments. Comparison between FAK Rescue and FAK K454R, FAK Rescue and ΔFERM/K454R, FAK MO and FAK ΔFAT with Mann-Whitney tests showed statistically insignificant differences of the means of the spindle angles (p=0.1343 ns, p=0.6498 ns and p=0.0524 ns, respectively). (C) Plots (Means ± S.E.M) showing the percentage of metaphase cells with spindle to plane of the epithelium angles greater than 15º. These were 8%, 71%, 21%, 8%, 14% and 62.5% for control, FAK MO, FAK MO + FAK Rescue, FAK MO + FAK K454R, FAK MO + ΔFERM/K454R and FAK MO + FAK ΔFAT,

respectively. (D) Western blot from total lysates of control and 50 ng FAK MO injected mid-neurula stage embryos blotted for FAK and actin confirming FAK downregulation. Scale bars: (a) low mag: 20 μm, high mag: 10 μm.

Since loss of apicobasal polarity in epithelia has been associated with spindle misorientation (Bergstralh, Haack et al. 2013), we examined the integrity of the FAK morphant epithelia. Staining with the tight junction marker ZO-1 revealed that apicobasal polarity is not affected in FAK morphants while other polarized molecules involved in spindle orientation, like the Par6/3-αPKC complex also remain properly localized even in cells with completely misoriented spindles (Hao, Du et al. 2010, Durgan, Kaji et al. 2011) (**Figure 75A-C**). These results suggest that loss of FAK in polarized epithelia does not lead to spindle misorientation through defects in the apicobasal polarity of the epithelia. In order to gain insight into how FAK orients the mitotic spindle, we examined if the distribution of the cortical capture machinery was affected in FAK morphants. As shown, LGN is localized at the cell cortex and is enriched at the areas across the spindle in both control and FAK morphant cells (**Figure 75D, E**). These data show that LGN is properly localized on the cell cortex in the areas that correspond to the spindle capture sites in the absence of FAK and suggest that LGN localization at the spindle capture sites is not affected by loss of FAK.

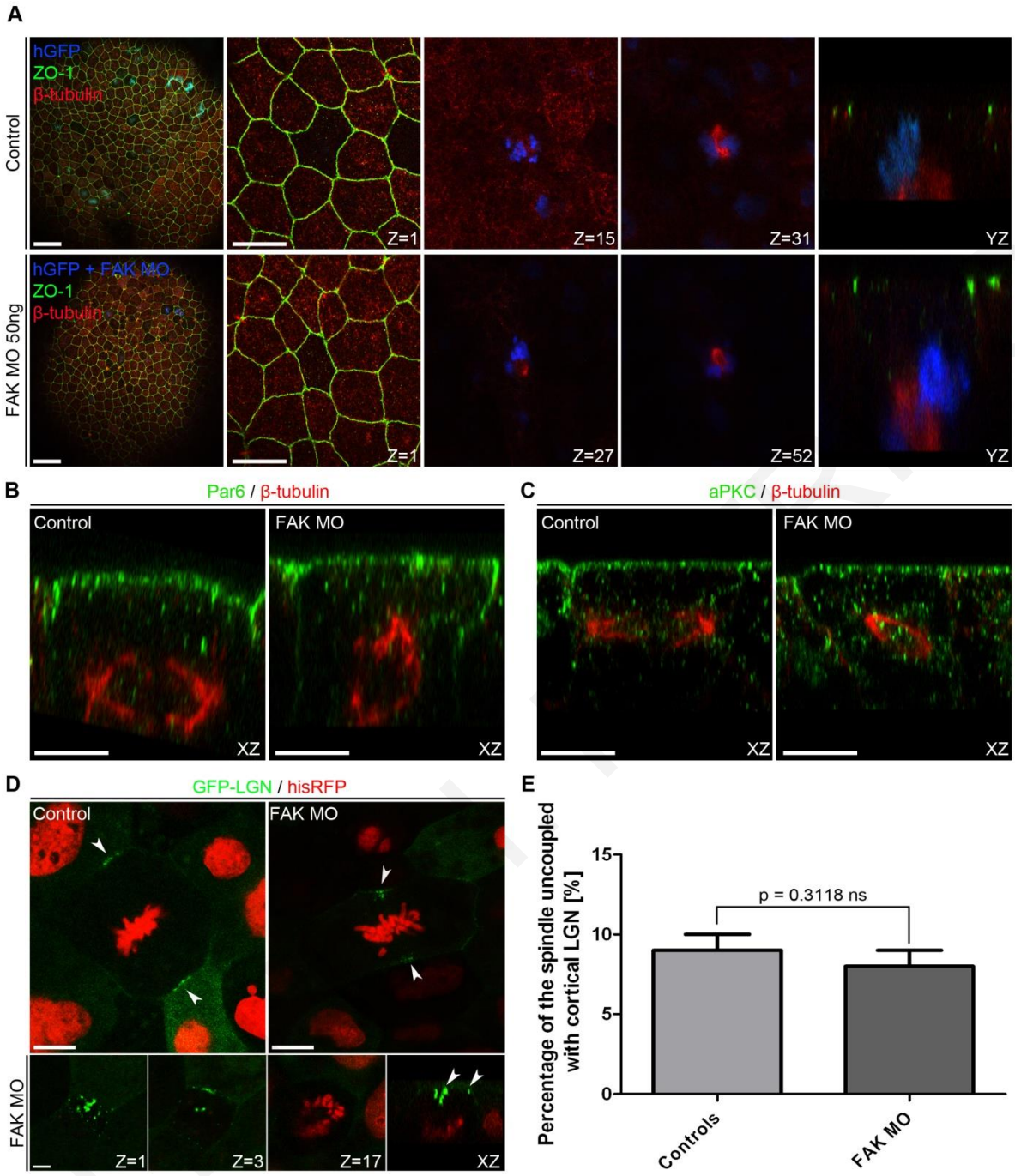

Figure 75: FAK downregulation leads to spindle misorientation without affecting apicobasal cell polarity or LGN cortical enrichment.

(A) Low magnification image of a *Xenopus* AC (first column) injected either with histone GFP (upper panel) or with histone GFP and 50 ng of FAK MO (lower panel) and stained with ZO-1 and β-tubulin. The representative Z-stacks of a metaphase cell of the AC (second to fourth column) and the XZ projection (fifth column) shows that ZO-1 is localized at the tight junctions and its localization is unaffected in morphant cells with misoriented spindles. (B) XZ projections of control and FAK morphant metaphase cells injected with 300pg of HA Par6 and stained with β-tubulin and HA showing enriched apical localization in both cases. (C) XZ projections of control and FAK morphant metaphase cells stained with aPKC and β-tubulin showing enriched apical localization in both cases. (D) Optical sections of GFP-LGN and histone RFP injected control cells and cells from an embryo injected with 50 ng of FAK MO showing cortical enrichment of LGN near the spindle poles (indicated by the white

arrowheads). In the lower panel a FAK morphant cell which displays spindle misorientation along the Z-axis is imaged, showing LGN localization at the apical surface of the epithelial cell (white arrowheads). (E) Quantification of the spindles that are not coupled with the LGN cortical crescent (angle between the line extending from the center of the metaphase plate perpendicularly to the cell cortex and the line extending from the center of the metaphase plate towards the LGN crescent between 30º and 90º). Scale bars: (A) low mag: 50 μm, high mag: 20 μm, (B, C, D lower panel) 10 μm, (D upper panel) 5μm.

4.2.7. FAK facilitates the transduction of external forces to the spindle

As discussed in the introduction, recent work revealed that external forces can induce mitotic spindle rotation in adherent mammalian cells (Fink, Carpi et al. 2011, Lancaster and Baum 2011). In addition, it has been shown that cells of the EVL in *Zebrafish* orient their mitotic spindle preferentially along the main axis of tension promoting tissue spreading during epiboly (Campinho, Behrndt et al. 2013). To determine if external forces can induce spindle rotation in *Xenopus* we placed mid-gastrula embryos in silicone chambered slides and imaged them live under conditions of absence of external force and conditions were the embryo was being slightly depressed exerting mechanical force on the epithelium. As shown, under mechanical stimulation (MS) the average spindle rotation increased by 50% and the same was true with respect to the frequency of rotation (**Figure 76A-C**). These results show that application of external force can induce spindle rotation *in vivo* in a similar fashion to what has been observed in cultured cells (Fink, Carpi et al. 2011). We went on to test if MS would lead to increased spindle rotation in FAK morphants. Despite the fact that under basal conditions FAK morphants display similar average spindle rotation and frequency of rotation with controls, under conditions of MS morphants fail to respond suggesting that FAK is required for the spindle rotation response (**Figure 76A-C**). Due to variations in the size of embryos that could lead to variations of the force exerted on each embryo this experiment was repeated in embryos unilaterally injected with the FAK MO leading to similar results (**Figure 76D, E**).

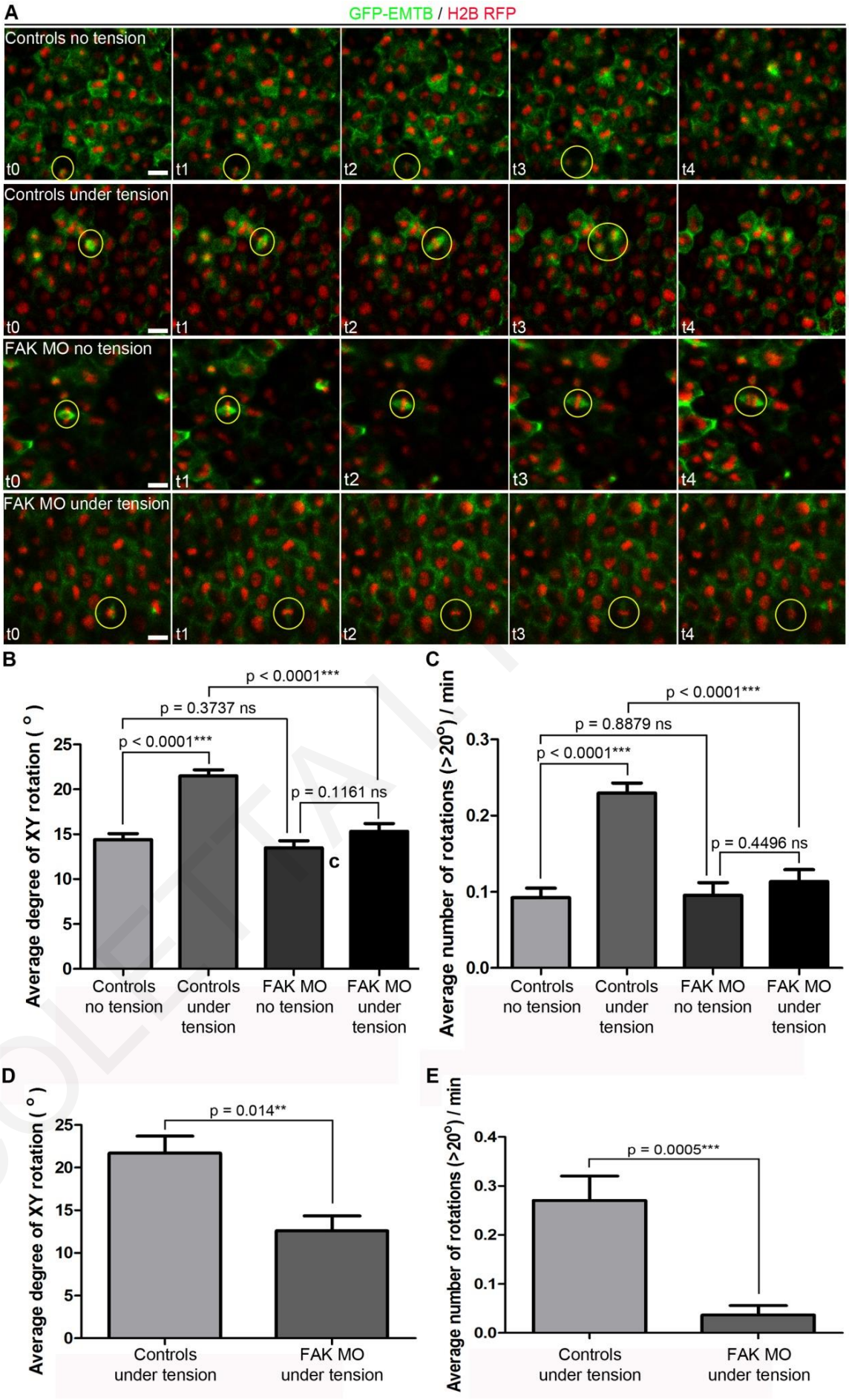

Figure 76: FAK is required in the response of the spindle to external forces.

(A) Stills (4 minutes interval) from time lapse recordings from stage 11 embryos expressing GFP-EMTB and histone RFP, showing rotations of the mitotic spindle in controls and FAK morphant embryos under normal conditions and conditions of MS. Yellow circles indicate representative mitotic cells from each condition. (B) The average spindle rotation for control embryos without MS is 14.41 ± 0.6600º (n=267), for control embryos under MS 21.51 ± 0.6631º (n=405), for FAK morphants without MS 13.48 ± 0.7861º (n=165) and for FAK morphant embryos under MS 15.33 ± 0.8635º (n=174). Analysis of spindle rotation with a two-tailed unpaired t-test showed statistically significant differences of the means between controls without MS and controls under MS ($p<0.0001$***) and between controls under MS and FAK morphants under MS ($p<0.0001$***) but no statistically significant differences between controls without MS and FAK morphants without MS ($p=0.3737$ ns) or between FAK morphants without and with MS ($p=0.1161$ ns); n, number of spindle rotations, three independent experiments. Error bands are S.E.M. (C) Quantification of the frequency of mitotic spindle rotation. The average frequency of rotation per minute is 0.09238 ± 0.01245 (n=82) for control embryos without MS, 0.2296 ± 0.01329 (n=120) for control embryos under MS, 0.09532 ± 0.01688 (n=47) for FAK morphants without MS and 0.1133 ± 0.01588 (n=68) for FAK morphant embryos under MS. The results were analyzed with a two-tailed unpaired t-test, showing statistically significant differences of the means of the rotation frequencies between controls without and with MS ($p<0.0001$***) and between controls under tension and FAK morphants under MS ($p<0.0001$***) but no statistically significant differences between controls and FAK morphants without MS ($p=0.8879$ ns) or between FAK morphants without and with MS ($p=0.4496$ ns); n, number of divisions. (D) Plots of the average degree of spindle rotation in the XY plane from unilaterally injected embryos with 25ng of FAK MO that were imaged under conditions of application of mechanical stimuli. The average degree of rotation for control cells within the same embryo was 21.69 ± 2.008º (n=43) and for FAK morphant cells 12.59 ± 1.741º (n=34); n, number of spindle rotations. Statistical analysis using a two-tailed unpaired t-test revealed that the average degree of spindle rotation between the two samples was statistically significant ($p=0.014$**), two independent experiments. (E) Quantification of the frequency of spindle rotation. The frequency of spindle rotation in control cells is 0.2705 ± 0.04977 (n=11) and in FAK morphants 0.0365 ± 0.01941 (n=10); n, number of divisions. Analysis with a two-tailed unpaired t-test showed that the differences between the frequency of rotation between the two samples was statistically significant ($p=0.0005$***), two independent experiments. Scale bars: (A) 20 μm.

Decoupling the spindle from the cortex could explain this defect, however high resolution imaging of mitotic spindles of morphant cells revealed that both spindle capture and spindle centering are unaffected in agreement with the *in vitro* data showing that both spindle integrity and centering are unaffected in FAK null cells (**Figure 77A**). Moreover, mitosis in FAK morphants progresses smoothly with no delays which may be responsible for spindle misorientation due to defects in the spindle assembly checkpoint (**Figure 77B**).

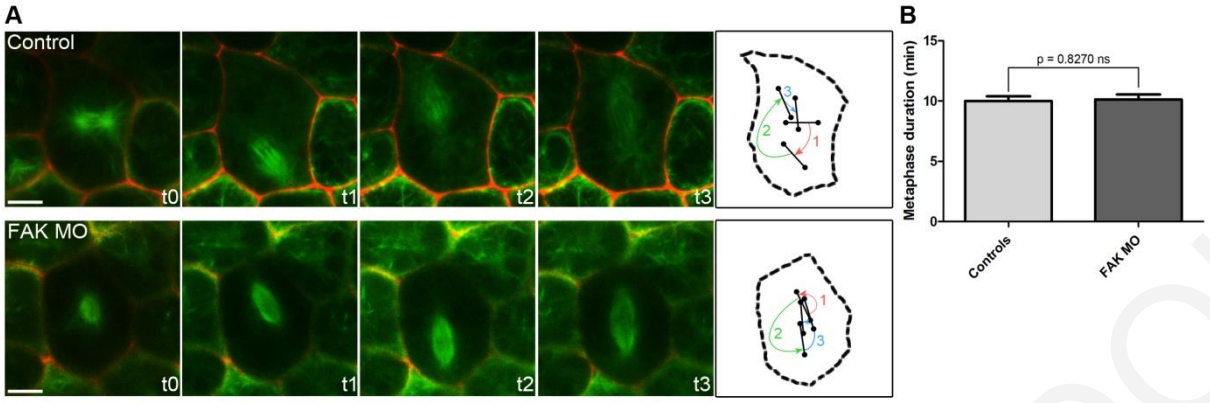

Figure 77: FAK morphant cells display normal astral microtubule capture by the cortex and normal progress of mitosis at metaphase.

(A) Stills from a time lapse recording (2 minutes interval) of control and FAK morphant late gastrula stage embryos injected with GFP-EMTB (green) and memCherry (red) showing the movements of the mitotic spindle during astral microtubule capture at the cell cortex. In the schematic diagrams the black line with two dots represents the long axis of the spindle, and the arrows define the path of the spindle from formation to the point it becomes centered. (B) Plot of the average time that control and FAK morphant *Xenopus* epithelial cells spend in metaphase. The average metaphase duration in controls is 10 minutes (n=15) and 10.133 minutes in FAK morphants (n=15). Analysis with a Mann-Whitney test showed no statistically significant differences between the two samples (p=0.8270 ns); n, number of metaphase cells. Scale bars (A) 20 μm.

We went on to use laser ablation to generate pulling forces perpendicular to the axis of the spindle of mitotic cells in a similar approach to what was described by Campinho et al. in *Zebrafish* (Campinho, Behrndt et al. 2013). Two cells positioned above and below the mitotic cell in a line perpendicular to the orientation of the spindle were laser ablated. Laser ablation leads to the extrusion of the ablated cell creating a wound. As the epithelium stretches to close the wound, it imposes tension to the tissue between the ablation sites causing the mitotic cell to change shape and stretch along the axis perpendicular to the spindle. As shown, the spindle of the control cell begins to rotate concomitant with cell stretching eventually becoming aligned with the imposed force (**Figure 78A, B** and **Movie 11**). In FAK morphants however, the spindle fails to respond and remains at a right angle to the force vector (**Figure 78A, B** and **Movie 12**). These results suggest that FAK is required for spindle reorientation in response to external forces.

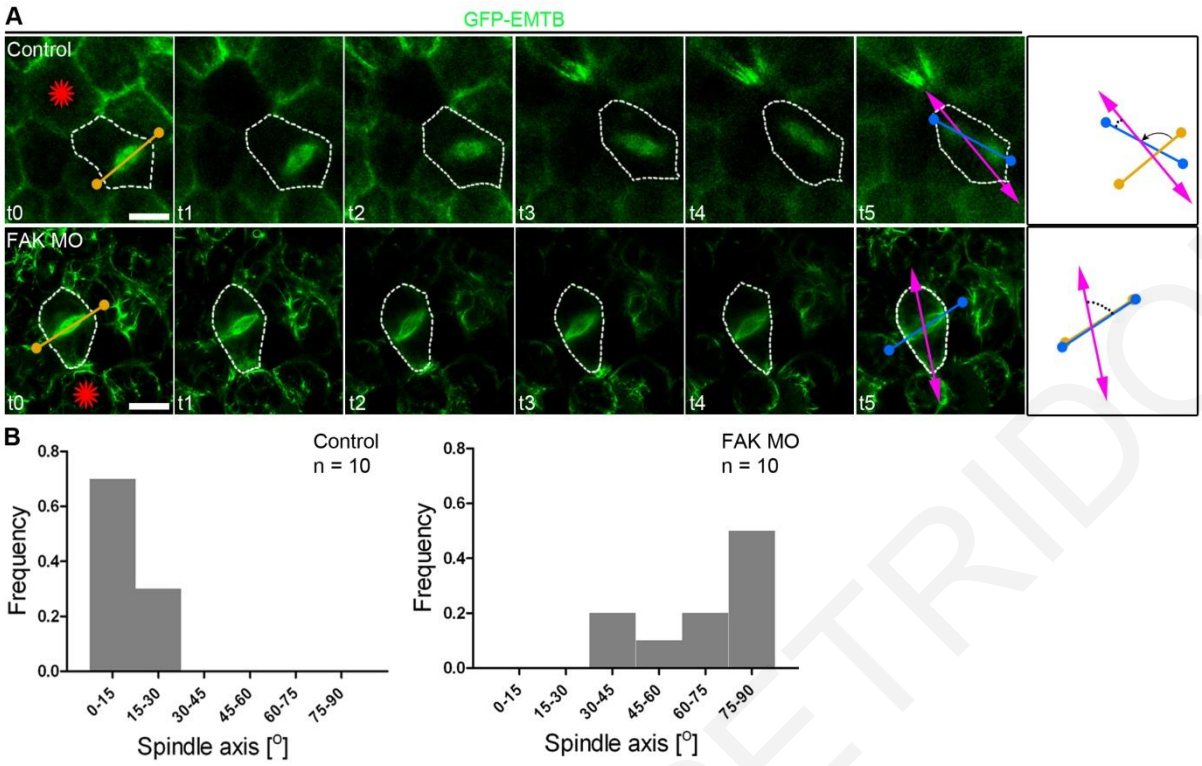

Figure 78: FAK is required for the transduction of the extracellular forces that guide spindle orientation. (A) Stills (2 minutes interval) from a time lapse recording where neighboring cells of a mitotic cell were laser ablated (red star) to generate tension perpendicular to the initial axis of the spindle (orange axis). The white dashed line delineates the cell boundary. (B) Quantification was performed by measuring the angle (black dashed line) between the final spindle axis (blue) and the induced tension axis (magenta axis). The histograms show the frequency distributions of the observed angles for control and morphant embryos. A two-tailed unpaired t-test showed statistically significant differences of the means of the spindle angles between the two samples, $p<0.0001$***; control spindle angle 10.99 ± 2.417°, FAK MO spindle angle 67.04 ± 5.671°, 10 embryos per sample, two independent experiments. Scale bars: (A) 20 μm.

As mentioned above, the forces generated by the wounds deform the mitotic cell elongating it along the axis of force. Cells have been shown to orient their spindle in response to force and cell shape (Fink, Carpi et al. 2011, Minc, Burgess et al. 2011), both of which share the same axis in the above experiment, making the contribution of each parameter in spindle orientation difficult to assert. In an effort to pinpoint the defect, we carried out laser ablation of single cells at regions perpendicular to their long axis in high salt conditions. Ablating a single cell ensured that wound derived forces would not lead to large cell shape changes and high salt that wounds would close rapidly giving rise to relatively brief application of force on the mitotic cell. Imaging of control cells in which a long axis was present prior to wound closure but the cell became symmetric after would closure, revealed that the spindle rotates to align with the imposed force despite the absence of a clearly defined long axis (**Figure 79A**). Time lapse

imaging of cells under conditions where the original long axis remained after wound closure revealed that during wound closure, spindles display a transient rotation to align with the applied force but eventually realign (albeit not always completely) with the long axis, once the wound closes and presumably the applied force dissipates. These cells eventually divide along their long axis suggesting that spindle orientation is determined by a combination of both sensing of forces and cell shape (**Figure 79B**). What the contribution of each parameter to the final spindle orientation is difficult to assess however, the transient rotation in cells with a clearly defined long axis away from that axis suggests that external forces may override cell shape. We went on to carry the same experiment in FAK morphant embryos and in this case, cells failed to display any transient rotations as expected given their inability to rotate even in response to double wounds and significant cell shape change (**Figure 79C**). These data suggest that FAK is required in order for mitotic cells to respond to external forces and reposition their spindle but do not rule out the possibility that it is also required for orientation with respect to cell shape.

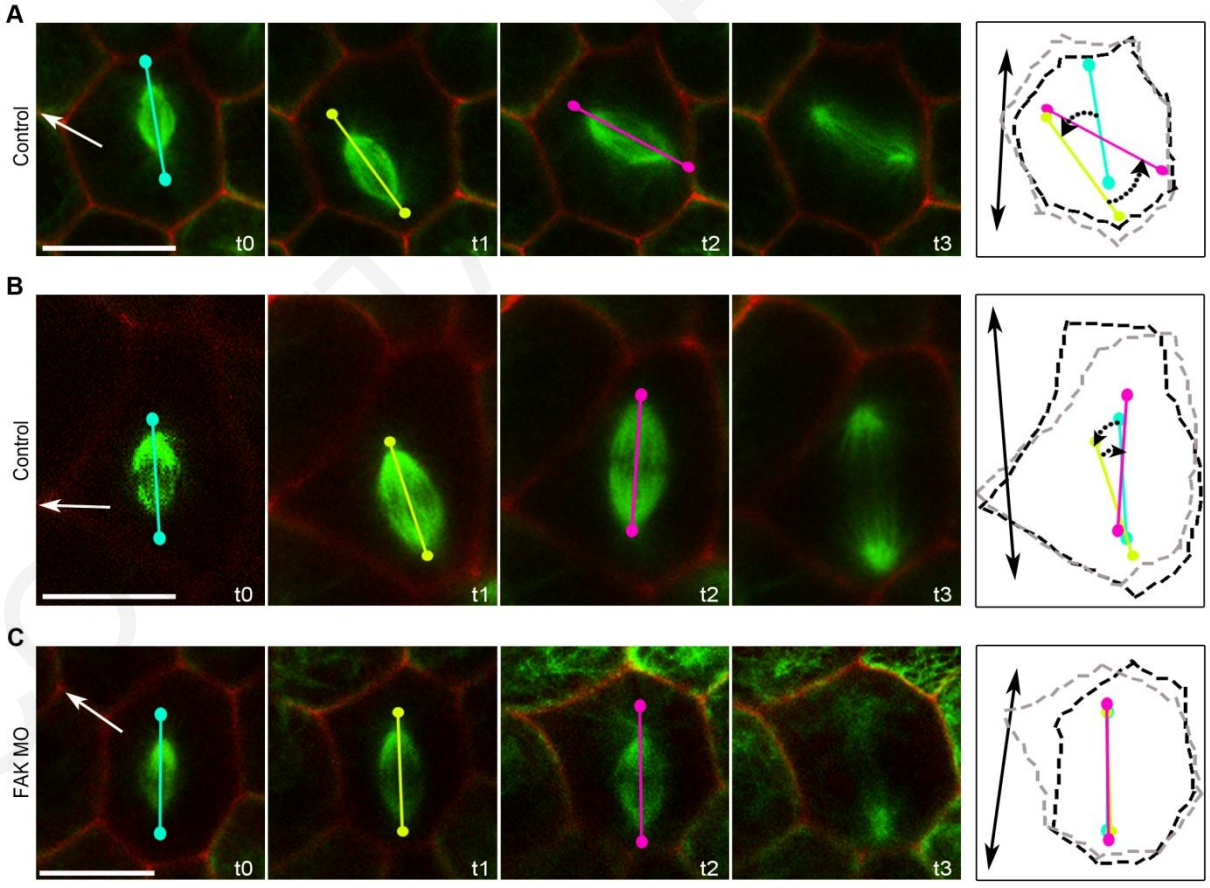

Figure 79: FAK morphants display defective spindle response in mechanical stimuli.

(A) Stills from a time lapse movie (2 minutes interval) of an epithelial cell from a late gastrula stage control embryo injected with memCherry and GFP-EMTB. A single cell at a right angle to the initial long axis of the cell was laser

ablated and the mitotic cells long axis (black axis), is lost after the wound has healed leading to a symmetric cell. The spindle rotates towards the direction of the imposed force despite the absence of a long axis (white arrow). (B) Stills from a time lapse recording (2 minutes interval) in which the initial long axis (black axis) remained after wound closure. Under these conditions the spindle transiently rotates towards the direction of applied force (white arrow), however, when the wound closes the spindle realigns with the initial long axis. (C) Stills from a time lapse recording (2 minutes interval) of a FAK morphant mitotic cell. Although force was applied on the mitotic spindle, no spindle rotation was observed towards the direction of imposed force (white arrow). The schematic diagrams represent the different positions of the mitotic spindle and the arrows define the path of the mitotic spindle. The black and grey dashed shapes represent the initial and final shape of the cell, respectively. Scale bars: (A-C) 20 μm.

If spindle orientation is determined via a multi parameter mechanism where both external forces and cell shape contribute to the final axis of division, since the majority of cells would be elongated along the axis of greatest force, the synthesis of information would make alignment along the long axis more robust. It's possible that due to an inability to properly transduce force alignment cues, FAK morphants fail to align unless the cell shape anisotropy is very high. In order to address this possibility, we generated linear wounds on control and morphant tailbuds using the gastromaster microsurgery instrument. Embryos were allowed to heal and fixed an hour later, to allow for the tension within the tissue to subside. Cells from these embryos display a great range of shape anisotropy with cells close to the wounds becoming very elongated. While imaging these cells it became evident that in FAK morphant cells that were highly anisotropic, the spindle was always oriented along the long axis like controls (**Figure 80A**). Use of low concentration nocodazole to depolymerize astral microtubules in control embryos on the other hand, gave rise to mitotic cells which failed to become oriented along the long axis irrespective of the extent of cell shape anisotropy (**Figure 80A**). Quantification of spindle angles in relation to shape anisotropy from control, FAK morphant and nocodazole treated embryos confirms these observations (**Figure 80B**). Although FAK morphants fail to orient along the long axis at low cell shape anisotropy they start behaving like controls above a threshold (Length to Width ratio = 3), while spindles of cells from nocodazole treated embryos remain randomized irrespective of cell shape (**Figure 80B**). Overall, the above data suggest that FAK is required for the transduction of mechanical signals from the cell exterior to the cortex which in turn bias cortical cues resulting in correct spindle alignment.

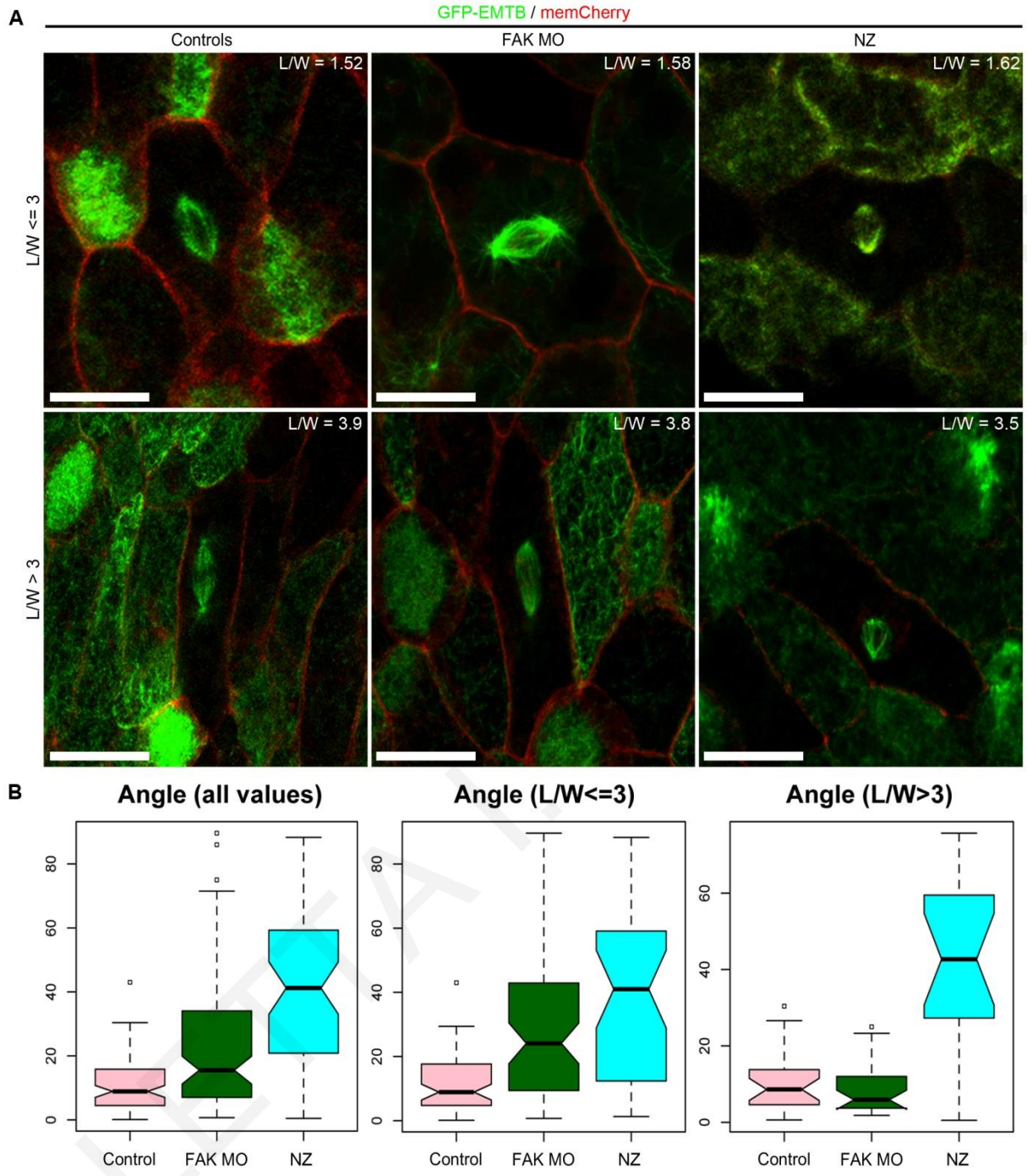

Figure 80: The mitotic spindle of FAK morphants can respond to extreme cell shape changes.

(A) Representative images of mitotic cells from wounded tailbuds that displayed small (L/W<=3) or large (L/W>3) shape anisotropy from control, FAK morphants and NZ treated control embryos. (B) L/W ratio was calculated for each cell and correlated to the spindle angle which was defined as the angle between the line connecting the two spindle poles and the long axis of the cell. Box-Whisker plots of the angle values are presented for the three experimental conditions. The first box-plot shows all the angles that were measured from all the cells from each sample, the second pox-plot shows angles measured from cells with L/W<=3 and the third box-plot angles measured from cells with L/W>3. Kruskal-Wallis test revealed that the three samples show statistical significant differences in each case ($p<0.01$). Mann-Whitney test between the three samples in the first box-plot showed that all three display statistically significant differences ($p<0.01$). In contrast, in the second plot (L/W<=3) only the

comparisons between Control - FAK MO and Control - NZ display statistically significant differences ($p<0.01$), while FAK MO and NZ ($p=0.22$) do not. In the third box-plot (L/W>3) only the comparisons between Control – NZ and FAK MO – NZ display statistically significant differences ($p<0.01$), while Control and FAK MO do not ($p=1$). Scale bars: (A) 20 μm. Abbreviations: NZ, Nocodazole; L/W: Length to Width ratio.

4.2.8. FAK's role in spindle orientation is required for epithelial morphogenesis

In order to assess the significance of the spindle orientation defects arising from FAK loss of function in the embryo we turned to two morphogenetic events known to require oriented cell divisions, epiboly and the development of the pronephros (Marsden and DeSimone 2001, Fischer, Legue et al. 2006). The *Xenopus* AC is initially three cell layers and rearranges into two layers via radial intercalation and is maintained as such through oriented cell divisions at the plane of the epithelium (Keller 1980, Marsden and DeSimone 2001). As shown above, loss of FAK function leads to block of epiboly through inhibition of radial intercalation and loss of spindle orientation. In order to decouple the two processes and examine the effects of loss of spindle orientation on epithelial morphogenesis independently from radial intercalation, we utilized the inducible FF DN. We thus induced FF-GR injected embryos at stage 10.5 to ensure that radial intercalation had been completed and assessed blastopore closure and AC thickness. As shown, FF expression delayed blastopore closure (**Figure 81A**) and led to thickening of the AC (**Figure 81B, C**), even after radial intercalation was completed, suggesting that loss of spindle orientation alone is sufficient to interfere with epiboly. In addition, the presence of heavily pigmented cells within the deep layers of the AC suggests that pigmented cells of the outermost epithelium divide asymmetrically, ingressing into the deep layer and contributing to the increase of AC thickness (**Figure 81D, E**). These results show that FAK's role in spindle orientation is indispensable for correct epithelial morphogenesis during epiboly, a process conserved in all vertebrates (Solnica-Krezel 2005).

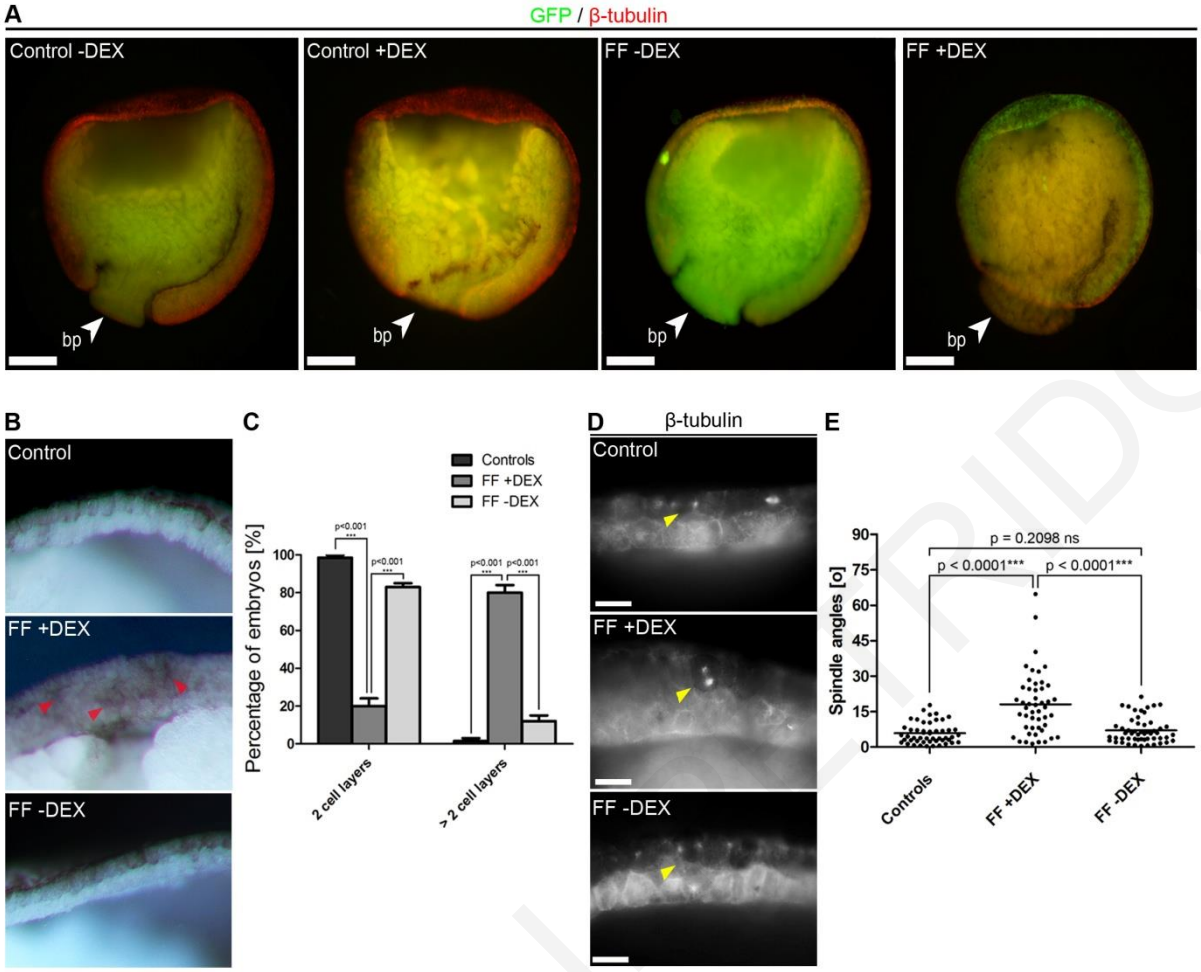

Figure 81: FAK's role in spindle orientation is necessary for epiboly during *Xenopus* gastrulation.

(A) Wide field images of sagittally sectioned late gastrula stage control embryos or embryos injected with 800 pg of FF-GR either treated or not with 10 μM DEX at early gastrula stage. The white arrowheads indicate the blastopore and show that FF expression leads to open blastopore, even if FF induction is carried out after radial intercalation is complete. (B) Sectioned control, FF-GR injected and FF-GR injected and DEX treated (at stage 10.5) embryos. In FF-GR +DEX embryos epiboly is blocked and pigmented cells of the outermost layer can be seen in the deep layers (red arrowheads). (C) Percentage of embryos with a 2-cell layered AC at stage 12. 98.5% in controls (n=50), 20% in FF-GR +DEX (n=71) and 83% in FF-GR –DEX injected embryos (n=26). Analysis with a 2way-ANOVA test revealed that these differences are statistically significant ($p<0.001$***); n, number of embryos, two independent experiments. (D) Fluorescence images of mitotic spindles (yellow arrowheads) in sectioned control, FF-GR -DEX and FF-GR +DEX injected embryos. (E) Scatter plots of the spindle angles. The average spindle angle in controls is 5.807 ± 0.6240º (n=50), in FF-GR +DEX 18.05 ± 1.924º (n=48) and in FF-GR –DEX 7.039 ± 0.7434º (n=53). Quantification of spindle orientation with an unpaired t-test showed statistically significant differences of the mean spindle angle between controls and FF-GR +DEX ($p<0.0001$***) and between FF-GR +DEX and FF-GR –DEX ($p<0.0001$***) but not between controls and FF-GR –DEX injected cells ($p=0.2098$ ns); n, number of metaphase cells, two independent experiments. Abbreviations: bp, blastopore. Scale bars: (A) 200 μm, (D) 20 μm.

Another tissue in which oriented cell divisions are known to be important is the kidney. A model has emerged in which oriented cell divisions are critical for the normally thin elongated tubes to develop with evidence suggesting that misoriented divisions lead to cystic kidney disease in animal models (Simons and Walz 2006). We thus targeted the inducible FF at the pronephros and induced the construct at stage 32/33. FF expression resulted in spindle misorientation (**Figure 82D**) and pronephros defects including dilated tubules while the pronephric duct was also dilated compared to controls (**Figure 82A-C**). Overall, these data suggest that FAK's role in spindle orientation is important for epithelial morphogenesis.

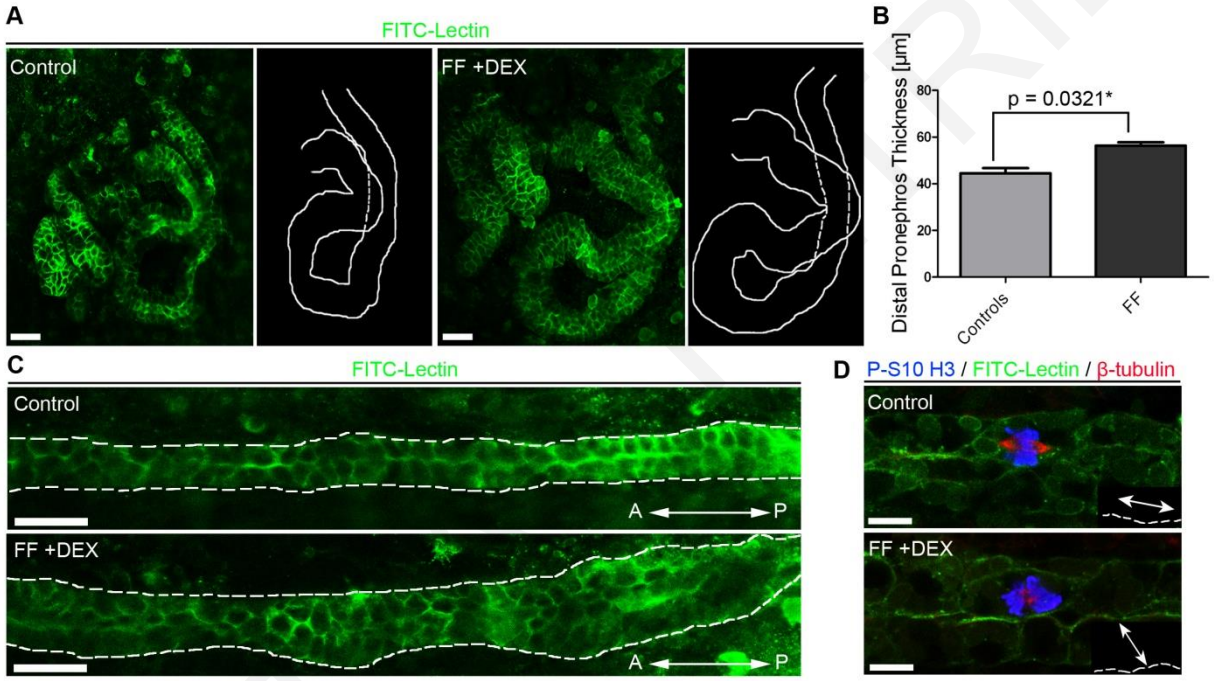

Figure 82: FAK is required for proper pronephros development in *Xenopus*.

(A) Maximum Intensity Projections from Z-stacks of the *Xenopus* pronephros including outlines of the distal pronephros from stage 40 control and FF-GR injected embryos. (B) Quantification of distal pronephros thickness. The average diameter in controls is 44.52 ± 0.8598 µm and in FF-GR injected 56.33 ± 1.396 µm. Analysis of the pronephros thickness with a 2way-ANOVA test showed statistically significant differences of the means between the samples, $p<0.0321^*$ (n = 6; n, number of embryos). (C) Optical sections of the pronephric duct in control and FF-GR injected tadpoles. The white dashed line defines the pronephric duct. (D) Confocal images of mitotic spindles in the duct of control and FF-GR injected tadpoles. In control cells the mitotic spindle is parallel to the long axis of the duct whereas in FF-GR injected cells, it's oriented orthogonally to the long axis of the duct. The black boxes show a schematic diagram of how the spindle is oriented (white axis) with respect to the duct lumen (dashed line). Scale bars: (A, C) 50 µm, (D) 10 µm.

4.2.9. The interaction of FAK with paxillin is necessary for spindle orientation both in adherent cells and in the developing embryo

In order to explore the mechanism by which FAK orients the mitotic spindle in response to force both in adherent cells and in the embryo, we focused on the role of FAK in mechanotransduction. FAK's role in mechanotransduction stems from its role in the integrin based complexes, FAs. The prime candidates for mechanotransduction in adherent cells are integrins and the protein members of the FA complexes that are formed in response to integrin activation (Goldmann 2012). Thus, we went on and examined if the interaction of FAK with other FA proteins is important for the orientation of the mitotic spindle.

Since the role of FAK in spindle orientation relies on its FAT domain which is necessary and sufficient for FAK's localization at the FAs (Hildebrand, Schaller et al. 1993), we initially probed the role of the FAT domain further. Thus, we expressed different variants of FAK with point mutations that abolish interactions with known FAK binding partners. The FAK C-terminus has been shown to be necessary for interactions with several proteins including talin, paxillin, RhoGEF and Grb2 (Schlaepfer, Hanks et al. 1994, Zhai, Lin et al. 2003, Scheswohl, Harrell et al. 2008, Lawson, Lim et al. 2012). Specifically, several lines of evidence suggest that the interactions with paxillin and talin are important for FAK's localization at FAs. We thus initially used two previously characterized point mutants FAK E1015A and FAK L1034S, which have been shown to abolish the interaction of FAK with talin and paxillin respectively, while retaining FA localization (Sieg, Hauck et al. 1999, Lawson, Lim et al. 2012). As shown, expression of the FAK E1015A mutant can effectively rescue misorientation defects indicating that the FAK-talin interaction is not necessary (**Figure 83A, B**). However, expression of the FAK L1034S point mutant failed to rescue spindle orientation defects (**Figure 83A, B**). Since the L1034S mutation has been shown to affect the structure of the four helix bundle that makes up the FAT domain and in addition, leads to loss of the FAK-RhoGEF interaction (Hayashi, Vuori et al. 2002, Zhai, Lin et al. 2003), we confirmed this result using the FAK I936E/I998E mutant that specifically abolishes paxillin binding without affecting FAT structure (Hayashi, Vuori et al. 2002). Expression of this mutant into FAK null cells did not rescue spindle misorientation (**Figure 83A, B**) further confirming that the interaction of paxillin with FAK is essential for proper spindle orientation.

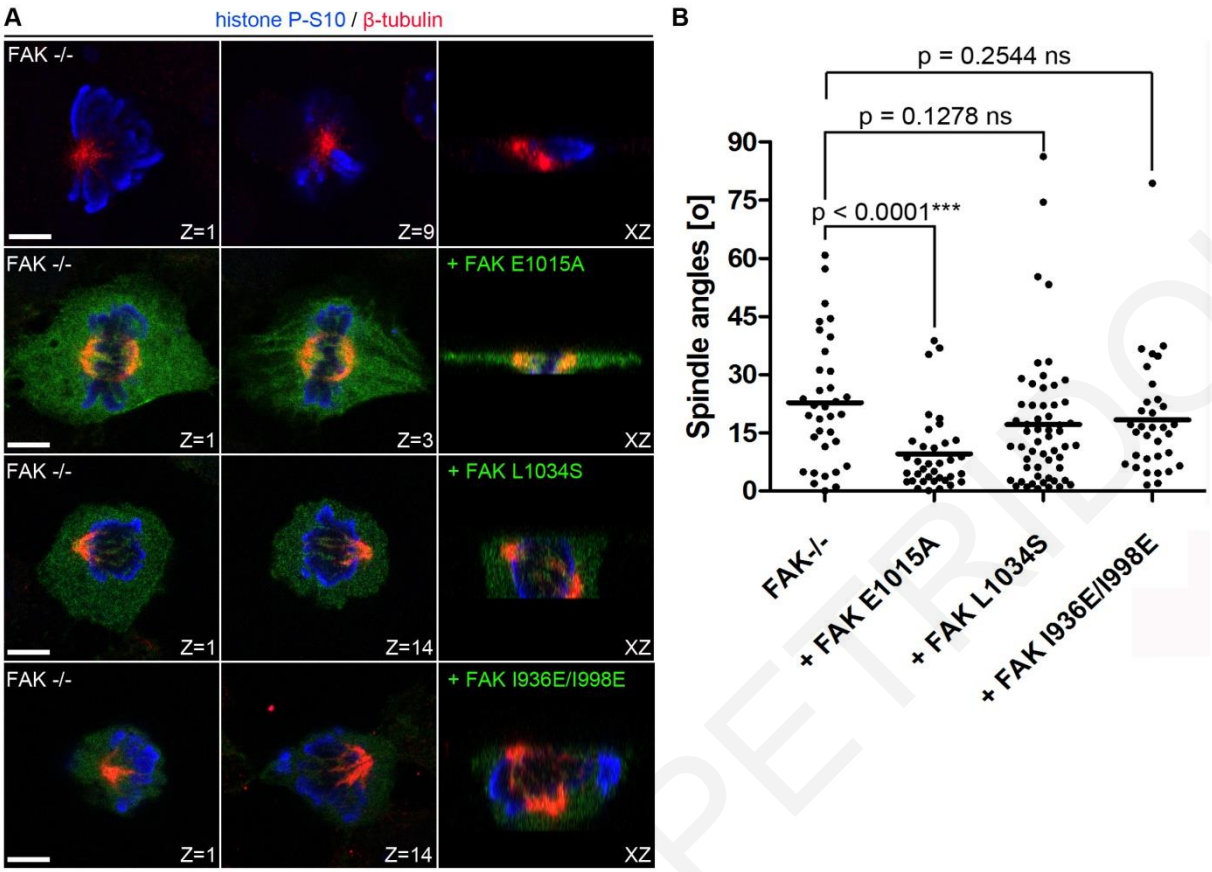

Figure 83: FAK-paxillin interaction is necessary for proper spindle orientation in adherent cells.

(A) Optical sections from Z-stacks, showing the position of each spindle pole and the XZ projections from a FAK null metaphase cell and FAK nulls transfected with the indicated mutants. (B) Scatter plots of measured substrate to spindle angles for FAK nulls and FAK nulls transfected with the indicated mutants. The average spindle angle in FAK nulls is 22.77 ± 2.780º (n=34), in FAK null cells transfected with FAK E1015A 9.527 ± 1.651º (n=36), in FAK null cells transfected with FAK L1034S 17.14 ± 2.303º (n=56) and in FAK null cells transfected with FAK I936E/I998E 18.37 ± 2.624º (n=33). Quantification of spindle orientation with a Mann-Whitney test showed statistically significant differences of the means of the spindle angles between FAK null and FAK E1015A ($p<0.0001$***) but not statistically significant differences between FAK null and FAK L1034S ($p=0.1278$ ns) and between FAK null and FAK I936E/I998E expressing cells ($p=0.2544$ ns); n, number of metaphase cells, two independent experiments. Scale bars: (A) 5 µm.

We went on to probe the role of the FAT domain of FAK in spindle orientation further, by performing rescue experiments with the FAK mutant Y925F, in which the major tyrosine of the FAT domain that gets phosphorylated by Src is mutated (Brunton, Avizienyte et al. 2005). Phosphorylated Tyr925 creates a binding site for Grb2 and it was shown that is required in microtubule dependent FA disassembly and that is required for paxillin phosphorylation at FAs (Schlaepfer, Hanks et al. 1994, Ezratty, Partridge et al. 2005, Deramaudt, Dujardin et al. 2011). Expression of this construct in FAK nulls rescued spindle misorientation of FAK null cells but not as effectively as WT FAK (**Figure 84A, B**). It has been shown that expression of this mutant

blocks FA turnover, a process that is necessary during mitosis so as the cell acquires a round morphology, through increased interaction with unphosphorylated paxillin leading to FA stabilization (Deramaudt, Dujardin et al. 2011). These results support the finding that FAK-paxillin interactions are required for spindle orientation in adherent cells. However, the fact that this mutant provides a partial rescue of the phenotype is indicative that the role of FAK in spindle orientation may not be exclusively based in its function at FAs and it is possible that the inability of this construct to fully rescue the phenotype might be due to impaired FA disassembly during mitosis.

Several reports supported a role for FAK at centrosomes and basal bodies. Deletion of FAK has been shown to lead to defective ciliogenesis, increases in centrosome numbers, defects in microtubule organization and nuclear movement as well as multipolar and disorganized spindles (Xie and Tsai 2004, Park, Shen et al. 2009, Antoniades, Stylianou et al. 2014). We wanted to examine if spindle misorientation in FAK nulls was related to the centrosomal functions of FAK and took advantage of the central role that phosphorylation of Ser732 by CDK5 has in this context (Xie and Tsai 2004). Expression of the S732A mutant effectively rescued spindle misorientation suggesting that phosphorylation of this residue by CDK5 is not important for FAK's function in spindle orientation (**Figure 84A, B**).

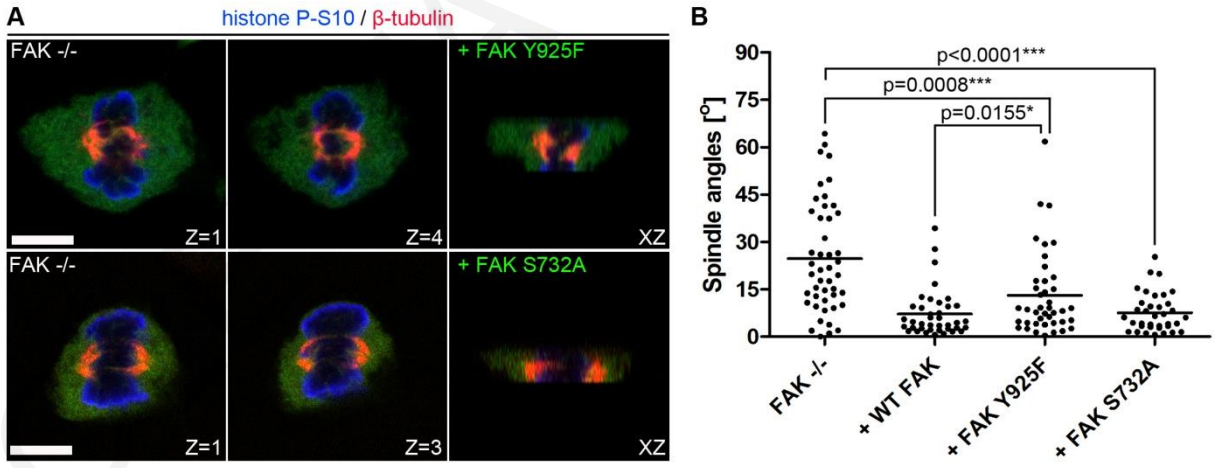

Figure 84: Phosphorylation of the FAT domain on Tyr925 is essential for spindle orientation, whereas on Ser732 is dispensable.

(A) Optical sections from Z-stacks, showing the position of each spindle pole and the XZ projections from FAK nulls transfected with the indicated mutants. (B) Scatter plots of measured substrate to spindle angles for the cells shown in (A). The average spindle angle in FAK nulls transfected with FAK Y925F is 13.10 ± 2.055° (n=41) and in FAK nulls transfected with FAK S732A is 7.542 ± 1.021° (n=36). P-values were calculated by unpaired t-tests, n, number of metaphase cells, two independent experiments. Scale bars: (A) 5 μm.

In order to gain insight into how FAK and paxillin regulate spindle orientation in adherent cells we examined their localization in mitotic cells. In agreement with the role of the FAT domain of FAK in spindle orientation, we observed that although most FA complexes disassemble in mitotic cells, small FAK and Paxillin positive adhesive complexes are retained along the RFs at areas where the fibers contact the ECM (**Figure 85A, B**). This suggests that FAK may be regulating spindle orientation by facilitating the transduction of external forces, generated at the ECM-RF interface, to the cell cortex, a notion supported by the fact that FAK null MEFs do form RFs (**Figure 85A**). On the other hand, the amount of FAK found at RF terminations is low with most of the protein retained in the cell body and since FAK's enzymatic activity is not required in this process, the question how would an ECM-RF signal be transmitted in real time along the RFs is hard to answer.

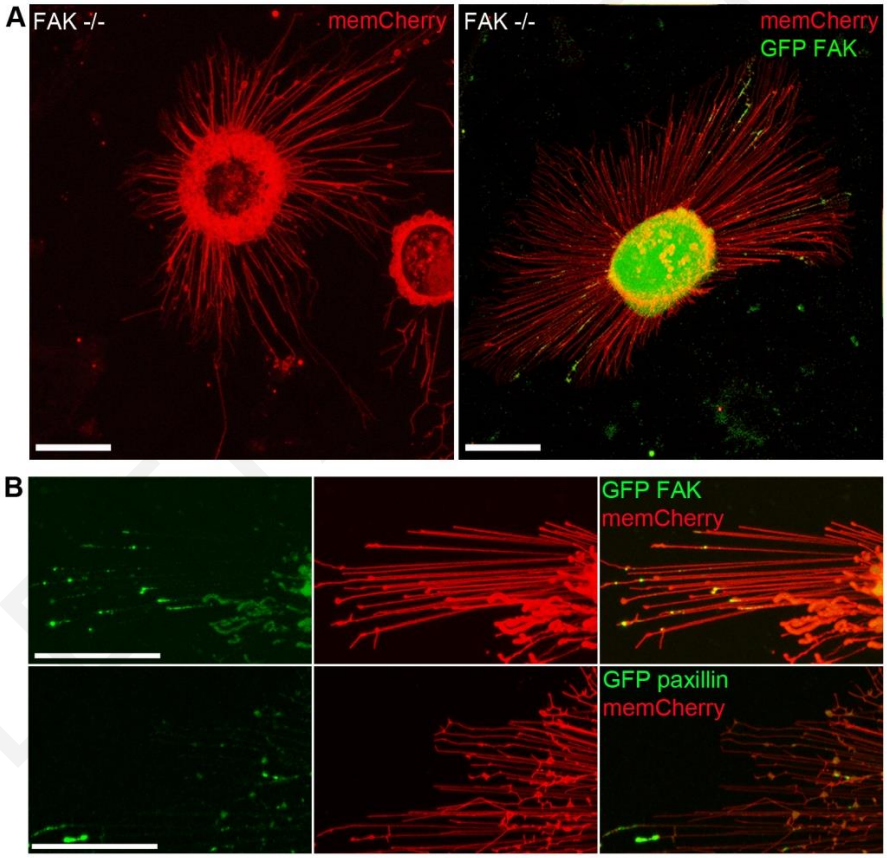

Figure 85: FAK and Paxillin localize at RFs tips in adherent cells.

(A) Confocal images of FAK null metaphase cells transfected with memCherry alone to visualize RFs, or memCherry and GFP FAK, showing FAK localization at the RFs. Although there was cell to cell variation no consistent differences were observed in the number density or length of RFs between FAK reconstituted and null cells. (B) High magnification optical sections of the RFs of mitotic cells transfected with memCherry and GFP FAK (upper panel) or GFP paxillin (lower panel), showing localization of FAK and paxillin respectively at the tips of RFs. Scale bars: (A, B) 20 μm.

We went on to examine if the requirement of the FAK-Paxillin interaction in spindle orientation is conserved in the *Xenopus* epithelium. We initially performed rescue experiments in FAK morphants using the FAK L1034S paxillin biding mutant which as shown failed to rescue spindle orientation defects (**Figure 86A, B**). We then confirmed the role of paxillin in spindle orientation by downregulating paxillin with the use of a paxillin MO in the *Xenopus* epithelia (Iioka, Iemura et al. 2007) (**Figure 86C**). Paxillin downregulation lead to spindle misorientation and these defects were rescued by the expression of a paxillin-Rescue construct (**Figure 86D, E**), suggesting that the paxillin-FAK interaction is also critical, for FAK's function in this process, *in vivo*.

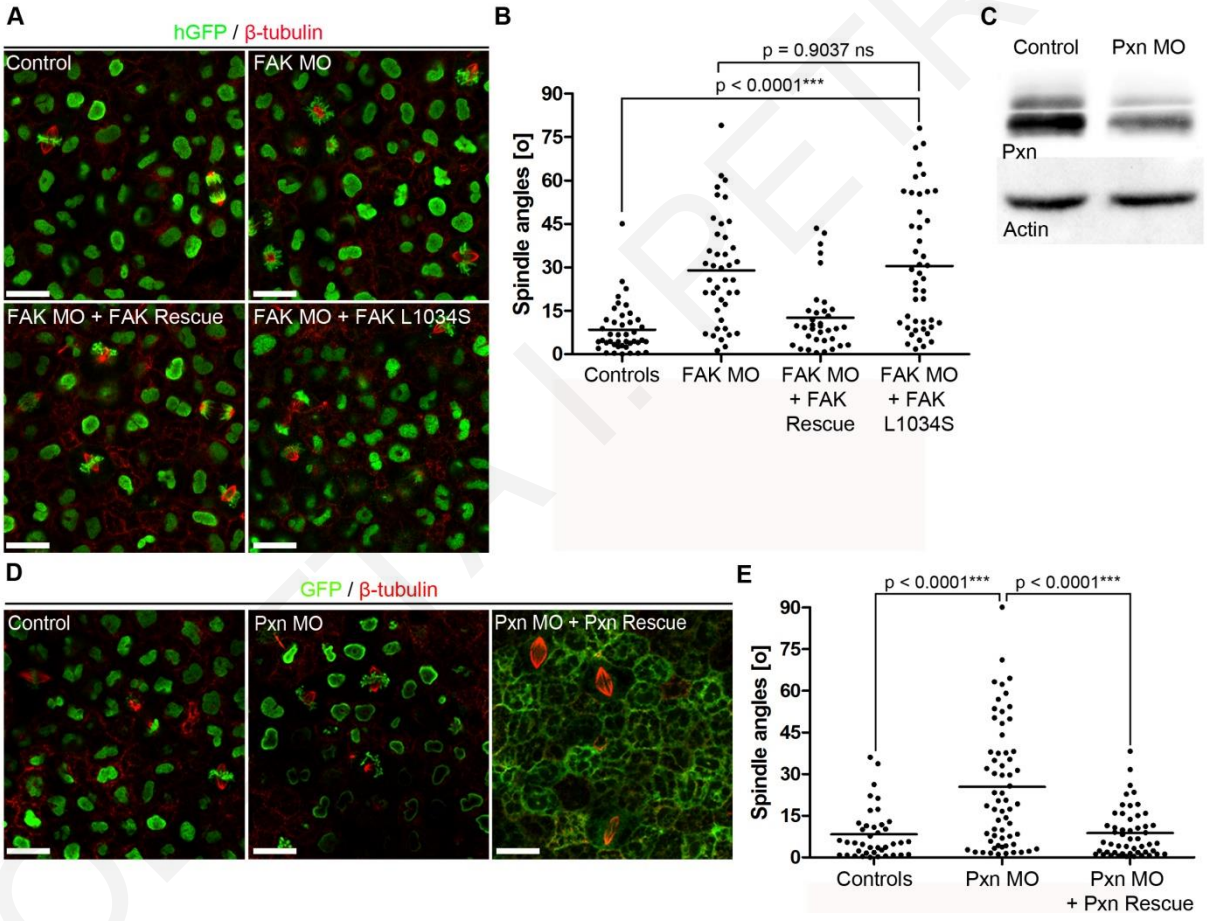

Figure 86: The FAK-Paxillin interaction is necessary for spindle orientation of *Xenopus* epithelial cells.
(A) Confocal images of epithelial cells from a control embryo, an embryo injected with FAK MO alone, FAK MO + FAK Rescue and FAK MO + FAK L1034S. Histone GFP was used as a linage tracer and embryos were stained for β-tubulin and GFP. (B) Scatter plots of spindle to plane of the epithelium angles. The average angle in control cells is 8.462 ± 1.324º (n=42), in FAK morphants 28.88 ± 2.909º (n=41), in rescued cells 12.57 ± 1.980º (n=35) and in FAK MO + FAK L1034S injected cells 30.42 ± 3.372º (n=45). Statistical analysis with a Mann-Whitney test showed statistically significant differences of the means of the spindle angles between control and FAK MO + FAK L1034S (p<0.0001***) but no statistically significant differences between FAK morphants and FAK MO

+ FAK L1034S injected embryos (p=0.9037 ns); n, number of metaphase cells, two independent experiments. (C) Western blot from total lysates of control and 100 ng Paxillin MO injected mid-neurula stage embryos blotted for paxillin and actin showing paxillin downregulation. (D) *Xenopus* epithelium of a control embryo injected with histone GFP, Pxn MO (100 ng Pxn MO + histone GFP) and Pxn MO + Pxn Rescue construct. *Xenopus* epithelia were stained for β-tubulin and GFP. (E) Scatter plots of spindle to plane of the epithelium angles. The average spindle angle in control cells is 8.282 ± 1.433º (n=40), in paxillin morphants 25.37 ± 2.774º (n=62) and in rescued cells 8.761 ± 1.226º (n=51). Statistical analysis with a Mann-Whitney test shows statistically significant differences of the means of the spindle angles between the indicated samples, p<0.0001***; n, number of metaphase cells, two independent experiments. Abbreviations: Pxn, paxillin. Scale bars: (A, D) 20 μm.

Additional support comes from experiments showing that both FAK and paxillin localize throughout the cell cortex of mitotic cells (**Figure 87A, B**). Overall, these results suggest that FAK's role in spindle orientation is conserved in the embryo.

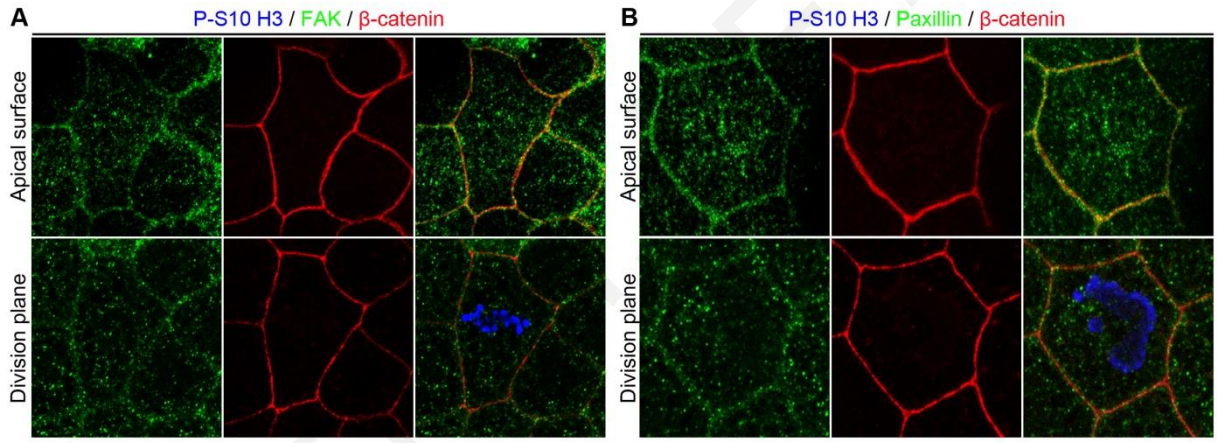

Figure 87: FAK and Paxillin localize at the cortex of cells of the *Xenopus* epidermis.
(A) High magnification optical sections of *Xenopus* outermost epithelial cells at their apical surface (upper panel) and at the plane of the spindle (lower panel) stained with FAK, β-catenin and P-S10 H3 antibodies showing that FAK localizes at the cell cortex. (B) High magnification optical sections of the apical surface (upper panel) or at the plane of the spindle (lower panel) of cells of the outermost epithelium of *Xenopus* stained with paxillin, β-catenin and P-S10 H3 antibodies showing cortical localization of paxillin. Scale bars: (A, B) 5 μm.

4.2.10. Integrin β1 is activated in a polarized fashion at the mid-lateral cortex of cultured mitotic cells

As described above when cells in culture enter mitosis, they round up and most of the FAs disassemble however, cells retain RFs connecting them to the ECM and small adhesive complexes are maintained at the terminations of RFs (Mitchison 1992), that contain the FA proteins FAK and paxillin. The fact that RFs have been shown to exert forces on the cell cortex

and the mitotic spindle becomes aligned with these forces (Fink, Carpi et al. 2011), suggests that these adhesive complexes may be purely mechanical links to the ECM. However, as shown above, FAK null cells form RFs normally, yet the spindle in these cells fails to respond to external forces. This suggested that the small adhesive complexes at RF terminations may in fact signal to the cell via the RFs, acting as mechanosensors. Since force application has been shown to lead to integrin activation (Friedland, Lee et al. 2009, Ferraris, Schulte et al. 2014), we decided to examine if RF terminations contain active integrin β1. To do so, we compared the distribution of active and total integrin β1, using two well characterized antibodies, HUTS-21 (Luque, Gomez et al. 1996, Byron, Humphries et al. 2009) and AIIB2 (Takada and Puzon 1993), respectively. As shown, in interphase cells total integrin β1 localizes uniformly throughout the cell cortex and in FA-like structures, while active β1 is found almost exclusively at FAs while it is excluded from the lateral cortex (**Figure 88A, C**). Quantification of basal / mid-lateral ratio of active and total β1 confirms this observation (**Figure 88C**). In mitotic cells although total integrin β1 is localized uniformly throughout the cell cortex and RFs, no active β1 enrichment could be detected on the RFs suggesting that the adhesive complexes at the ends of RFs are purely mechanical anchoring points and that they probably do not have signaling roles (**Figure 88B**, yellow arrowheads). Surprisingly however, we noted that active β1 is enriched at the lateral regions of the cell cortex at the plane of the spindle (**Figure 88B, D**, white arrowheads), while it is almost absent from the apical areas of the cortex (**Figure 88B, D**, magenta arrowheads). Quantification of mid-lateral / apical cortex intensity ratios of mitotic cells confirms these observations (**Figure 88D**) while quantification of basal / mid-lateral cortex intensity ratios of active β1 confirms the activation of β1 at the mid-lateral regions of the cortex during mitosis (**Figure 88E**).

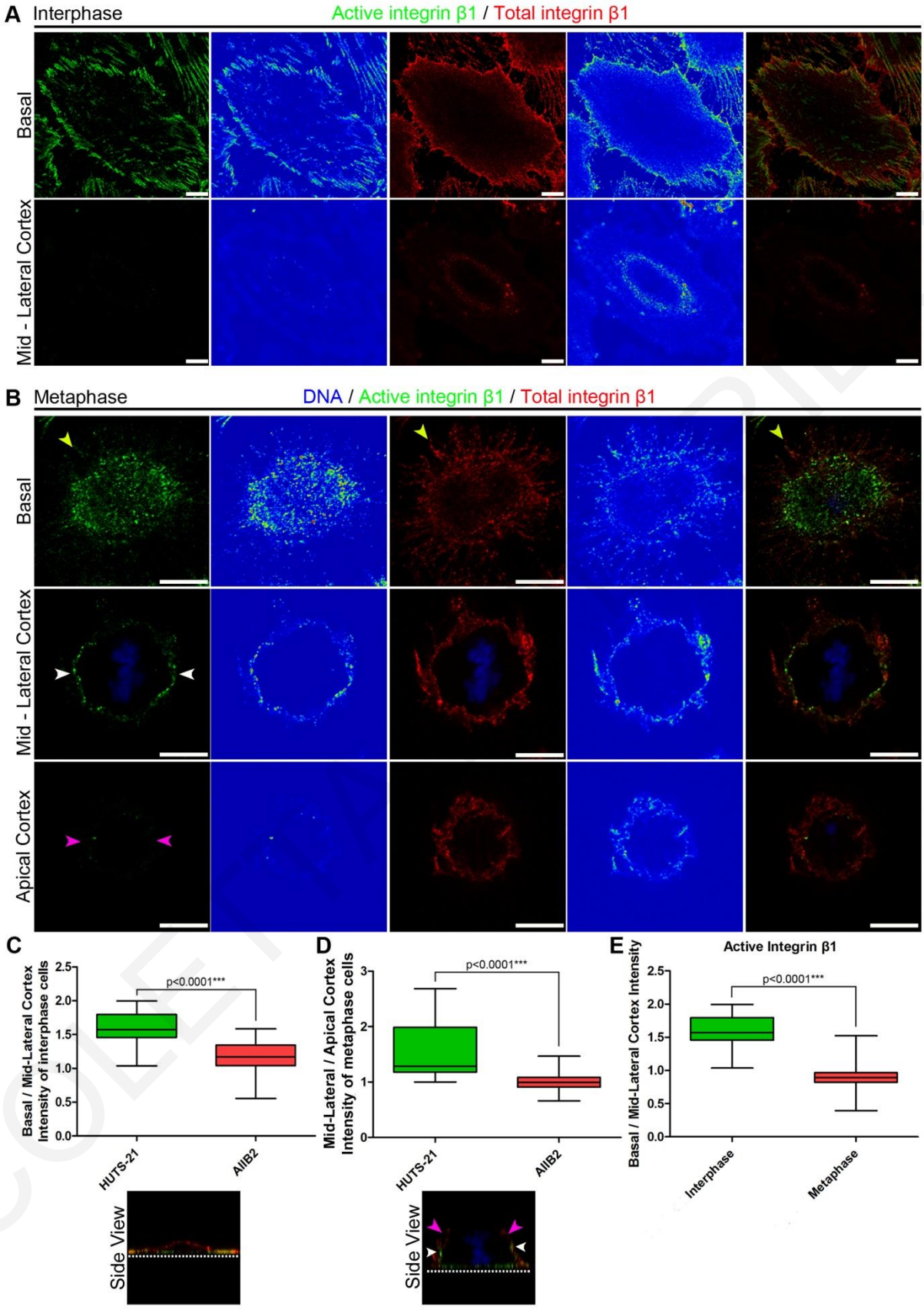

Figure 88: Integrin β1 becomes activated at the lateral cortex of mitotic cells.

(A) Representative optical sections, intensity coded and merged images at the cell-ECM interface and the lateral cortex of interphase HeLa cells stained for active (HUTS-21) and total (AIIB2) integrin β1. (B) Representative

optical sections, color intensity coded and merged images at the cell-ECM interface, mid-lateral and apical areas of the cortex of metaphase cells stained with same antibodies as (A) and TO-PRO. Yellow arrowheads indicate integrin β1 positive RFs without enrichment of active β1. White arrowheads indicate active β1 enrichment at the lateral cortex at the plane of the spindle. Magenta arrowheads show absence of active β1 from the apical cortex. (C) Box-plot of the basal to mid-lateral cortex intensity ratio of active and total integrin β1 in interphase cells and a side view of the cell shown in (A) (dashed line shows the ECM). Mean ± S.E.M: HUTS-21 1.572 ± 0.05921, n=20; AIIB2 1.158 ± 0.05203, n=20; p values were calculated by t-test; n, number of interphase cells, two independent experiments. (D) Box-plot of the mid-lateral to apical cortex intensity ratio of active and total integrin β1 in metaphase cells and a side view of the cell shown in (B) (dashed line represents the ECM, white arrowheads indicate integrin β1 activation at the lateral cortex, magenta arrowheads show absence of active β1 at the apical areas of the cortex). Mean ± S.E.M: HUTS-21 1.523 ± 0.1099, n=20; AIIB2 1.010 ± 0.03892, n=20; p values were calculated by t-test; n, number of metaphase cells, two independent experiments. (E) Box-plot of the basal to mid-lateral cortex intensity ratio of active integrin β1 in interphase and metaphase cells. Mean ± S.E.M: Interphase 1.572 ± 0.05921, n=20; Metaphase 0.8887 ± 0.04829, n=20; p values were calculated by t-test; n, number of cells, two independent experiments. Scale bars: (A, B) 10 μm.

Activation of β1 at the cortex of mitotic cells was verified using a different combination of antibodies (9EG7 for active integrin β1 and TS2/16 for total integrin β1) (**Figure 89A, B**) (Lenter, Uhlig et al. 1993, Bazzoni, Shih et al. 1995, Tsuchida, Ueki et al. 1997).

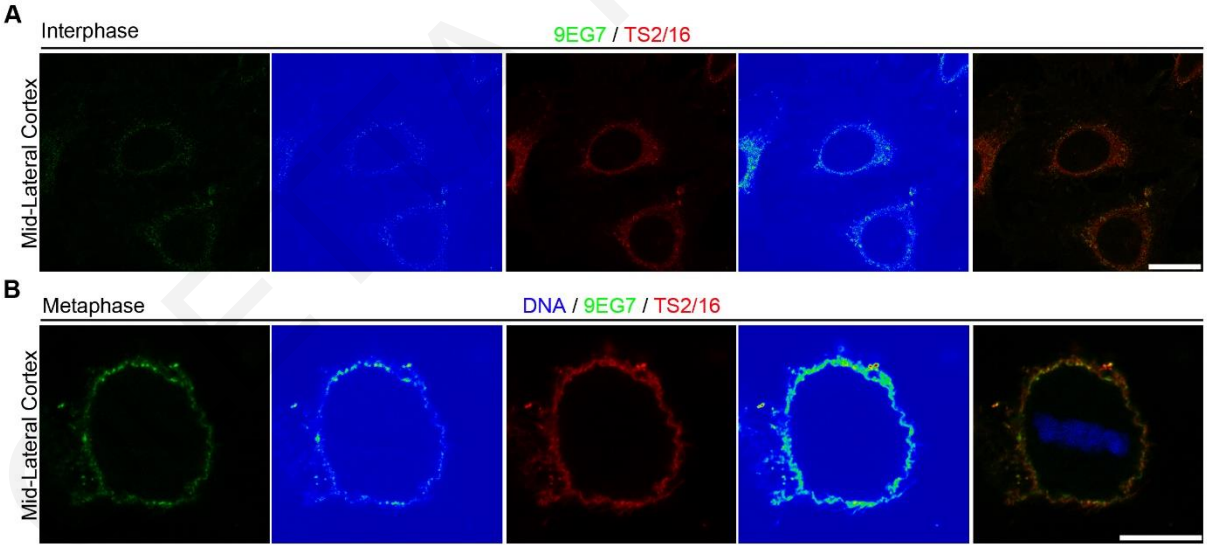

Figure 89: Active integrin β1 is localized at the lateral cortex of mitotic cells.
Optical sections, color intensity coded images and merged images at the plane of the lateral cortex of interphase (A) and metaphase (B) cells stained for total integrin β1 (TS2/16 antibody), active integrin β1 (9EG7 antibody) and TO-PRO for DNA labeling. Scale bars: (A) 20 μm, (B) 10 μm.

In addition, integrin β1 activation appeared to be polar in most cells (**Figure 88B**, white arrowheads at the mid-lateral cortex plane). Live immunostaining of active integrin β1 gave a clearer signal with lower background and the polarity became more pronounced. As shown, active β1 at the lateral regions of the cortex is distributed asymmetrically in metaphase cells with a polarity crescent preferentially accumulating at regions proximal to the spindle poles. Plotting the cortical distribution of active integrin β1 confirms this (**Figure 90A**). The distribution of active β1 is highly reminiscent of that of the cortical machinery that captures astral microtubules (LGN, NuMA, dynein) (McNally 2013). To examine if the active β1 distribution correlates with that of LGN we used live immunostaining and imaging of active β1 in cells expressing GFP-LGN. As shown, the distributions of LGN and active β1 on the cell cortex are quite similar both localizing asymmetrically and preferentially accumulating at regions proximal to the spindle poles (**Figure 90B,** white arrowheads). Similarly, active integrin β1 partially co-localizes with NuMA at regions proximal to the spindle poles, supporting the notion that integrin β1 activation takes place preferentially at the spindle capture sites (**Figure 90C**).

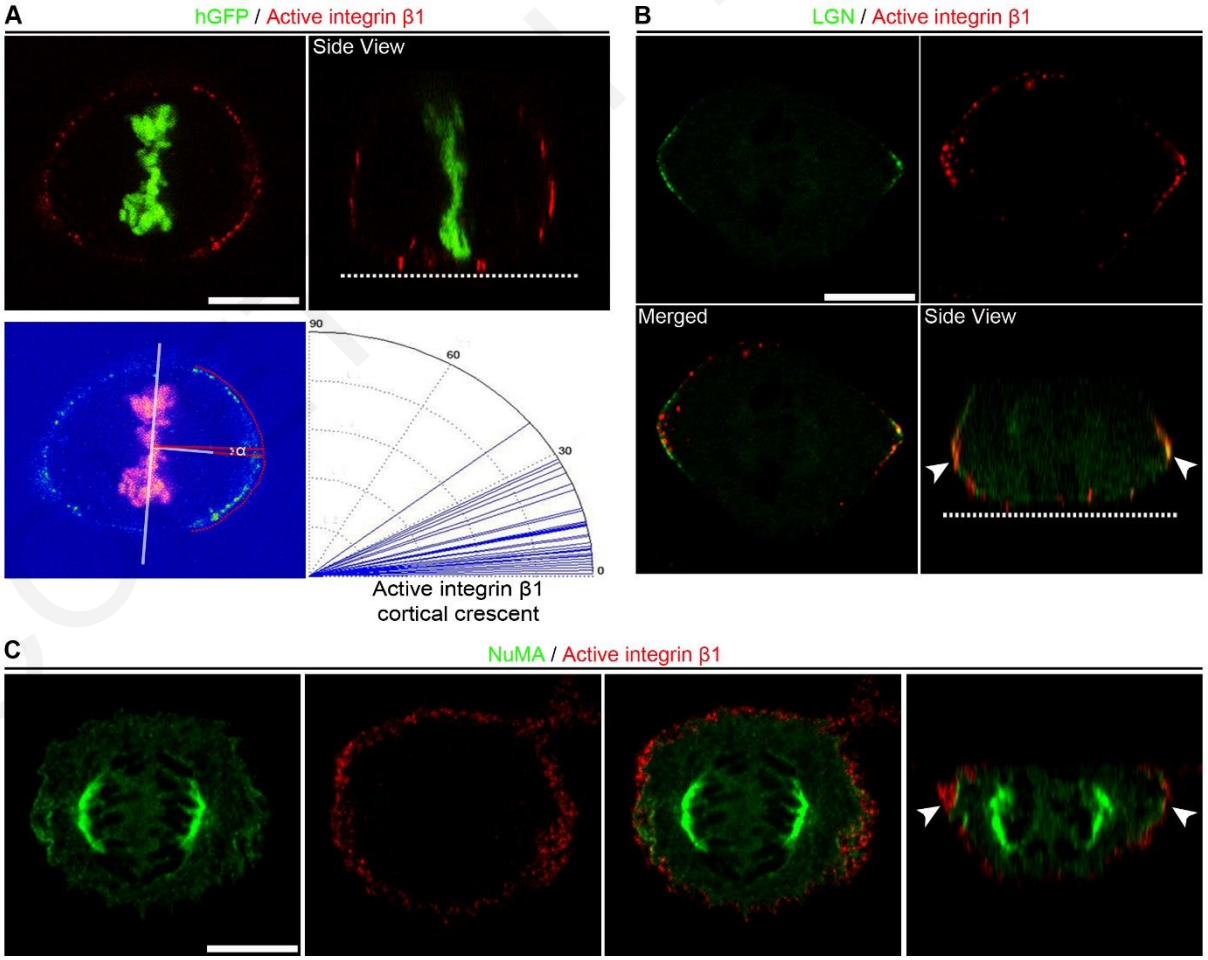

Figure 90: Integrin β1 is activated preferentially at the spindle capture sites at the mitotic cortex.
(A) A representative optical section and a side view (dashed line represents the ECM) of a live metaphase cell expressing histone GFP and stained for active integrin β1 (9EG7). Color intensity image showing how the polarity crescent of active β1 was correlated with the spindle capture sites and an angular distribution plot of the angle α; Mean ± S.E.M: 11.34 ± 1.55°, n=35; n, number of metaphase cells, two independent experiments. (B) Labeling of active β1 in live metaphase cells expressing GFP-LGN and a side view showing active β1 at the cell-ECM interface (dashed line) and co-localization with LGN at the lateral cortex of the cell (white arrowheads). (C) Immunostaining of HeLa cells showing co-localization of NuMA and active integrin β1 at the spindle capture sites (white arrowheads). Scale bars: (A, B, C) 10 μm.

Recent evidence suggests that integrin β1 can be activated by membrane tension in a ligand independent fashion raising the possibility that integrin β1 at the lateral regions of the cortex is elicited by forces deriving from RFs (Fink, Carpi et al. 2011, Ferraris, Schulte et al. 2014). In an effort to examine if there is a correlation between RFs and β1 activation we stained live HeLa cells expressing GFP-Utrophin with the 9EG7 antibody. High resolution optical sections of live metaphase cells revealed that active β1 displays the highest density at areas where the RFs terminate on the cortex (**Figure 91A**), a finding that was also confirmed by staining fixed mitotic cells with 9EG7 and phalloidin (**Figure 91B**), providing support to the notion that integrin β1 is activated at the cell cortex through force application from the RFs (Fink, Carpi et al. 2011). In order to test this hypothesis we stained active integrin β1 in cells seeded on L-FN microprints, where both the distribution of RFs and the areas of the cell in which maximal forces are exerted are predetermined (Thery, Racine et al. 2005, Thery, Jimenez-Dalmaroni et al. 2007). As shown, in interphase cells active integrin β1 is found exclusively on FAs all along the interface between the L-FN and the cell, while there is little or no cortical staining at the plane of the nucleus (**Figure 91C**). In early mitotic and metaphase cells when the cell rounds up and RFs are formed, active integrin β1 becomes enriched at the cell-FN interface at the areas where the RFs attach to the L and displays a polarized distribution becoming enriched at the areas where maximal forces are exerted, both at the basal and at the spindle plane (**Figure 91C,** white arrowheads). These are the areas with the highest density of RFs and as a result receive the strongest forces suggesting that force distribution around the cortex determines the distribution of active β1.

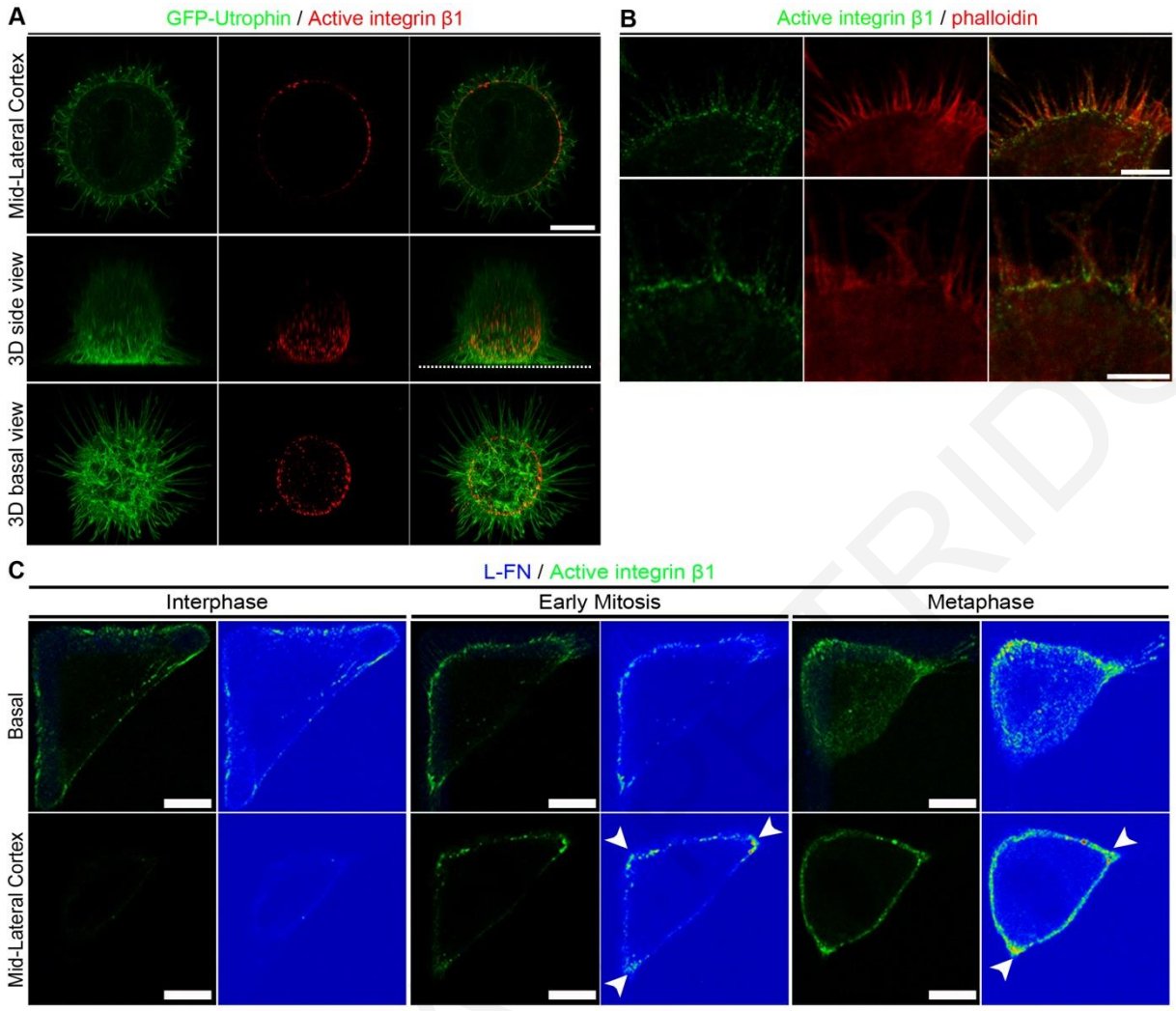

Figure 91: Integrin β1 is activated at the cell cortex through force application from the RFs.
(A) Optical section at the mid-lateral cortex, a side view (dashed line represents the ECM) and basal view of a 3D reconstruction of a representative live metaphase cell expressing GFP-Utrophin stained for active β1 (9EG7) showing integrin activation at the areas where the RFs merge with the cell cortex. (B) Thin optical sections and close-ups of metaphase HeLa cells stained for active integrin β1 (HUTS-21) and actin. (C) Representative optical sections and color intensity coded images at the cell-ECM interface and the lateral cortex of interphase, early mitotic and metaphase cells seeded on L-FN microprints and stained for active β1 (HUTS-21). Arrowheads indicate the areas with the highest active β1 signal. These correspond to the areas where maximal forces are exerted. Scale bars: (A, C) 10 μm, (B) 5 μm.

4.2.11. Cortical activation of integrin β1 depends on the presence of RFs in adherent cells

As discussed above integrin β1 can be activated by membrane tension independently of ligand binding (Ferraris, Schulte et al. 2014), so it is possible that in mitotic cells, lateral integrin β1 becomes activated as a consequence of forces exerted on the cortex. Such activating forces may derive from the RFs (Fink, Carpi et al. 2011) in agreement with our data suggesting a good

correlation between RFs and active β1. However, the possibility that these are intrinsic, such as the pulling forces that astral microtubules exert on the cell cortex cannot be excluded (McNally 2013), since the sites of maximal RF-derived forces coincide with the spindle capture sites (Thery, Jimenez-Dalmaroni et al. 2007). To distinguish between these two possibilities, we treated cells with low dose nocodazole to specifically disrupt astral microtubules (Jordan, Thrower et al. 1992). As shown, although nocodazole treatment led to spindle misorientation, there was no effect on β1 activation (**Figure 92A-C**) confirmed by the lack of a correlation between the degree of spindle misorientation and the ratio of basal to lateral active β1 intensity (**Figure 92D**). Moreover, nocodazole treatment of cells seeded on L-FN had no effect on the asymmetric distribution of active β1 (**Figure 92E**, yellow arrowheads). These results preclude the possibility that integrin β1 activation at the sites of spindle capture is a consequence of the pulling forces that astral microtubules exert on the cortex. We went on to examine the role of RFs. It has been previously shown that use of cytochalasin D to disrupt the actin cytoskeleton leads to loss of RFs (Mitchison 1992). Cytochalasin D treatment lead to spindle misorientation and nearly eliminated integrin β1 cortical activation (**Figure 92A-C, E**). Importantly, the degree of spindle misorientation was positively correlated with the change of the ratio of basal to lateral cortex intensity of active β1 (**Figure 92D**). However, cytochalasin D treatment had a visible effect on cortical actin. To ensure that the loss of active β1 is not an indirect effect of the disruption of cortical actin we seeded cells on PLL, a substrate on which cells fail to form FAs and RFs (Bershadsky, Chausovsky et al. 1996). Cells seeded on PLL displayed loss of cortical active integrin β1 and spindle misorientation despite normal cortical actin, confirming that activation of β1 on the lateral cortex during mitosis depends on RFs (**Figure 92F-H**). Overall, these data suggest that integrin β1 becomes activated at the lateral regions of the cortex in a RF dependent fashion.

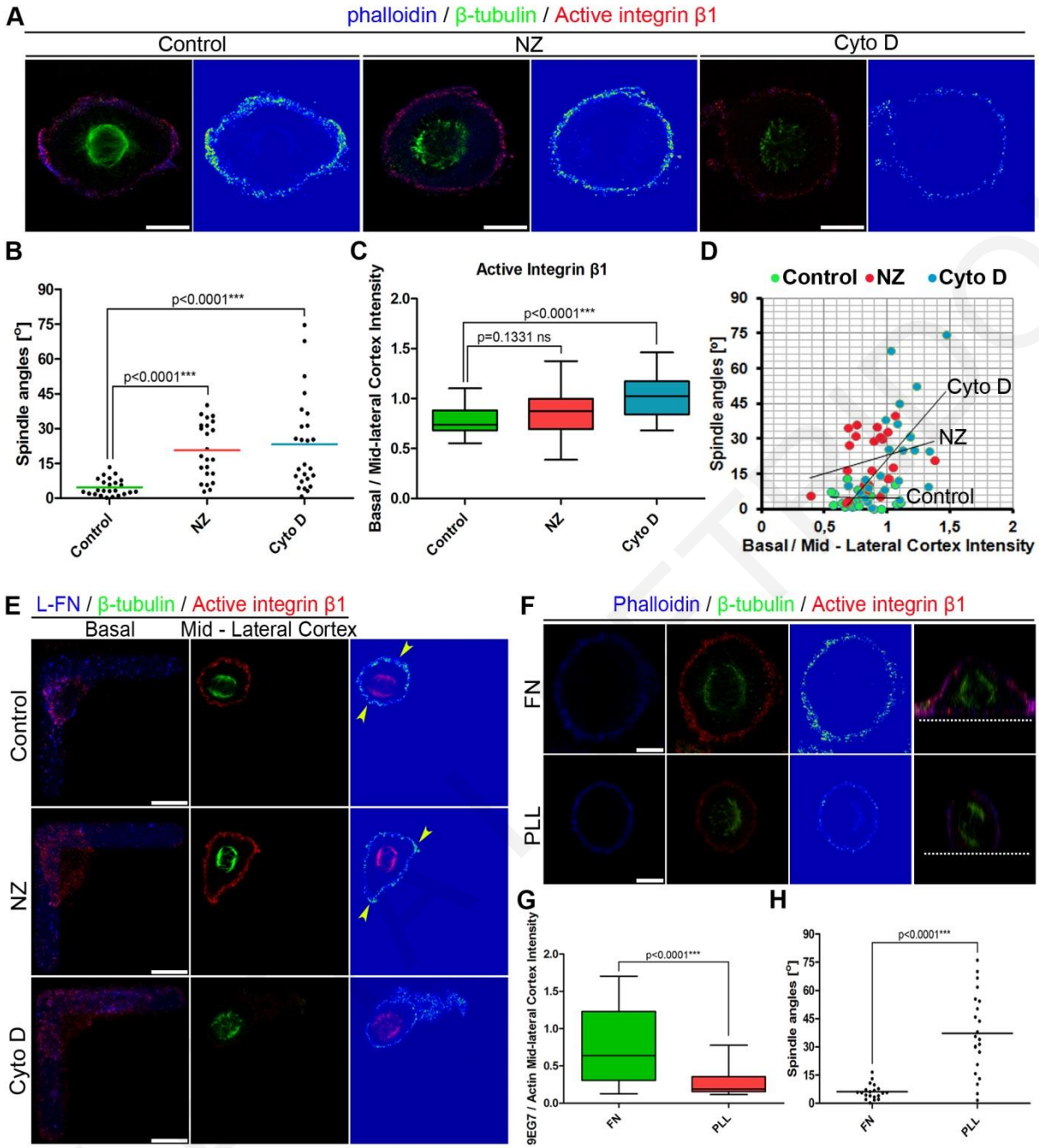

Figure 92: Integrin β1 cortical activation depends on the presence of RFs.

(A) Optical sections at the plane of the spindle and the corresponding color intensity coded image of a representative control, NZ or Cyto D treated cell. Cells were stained with β-tubulin and 9EG7 antibodies and phalloidin. All cells were imaged under the same conditions. (B) Scatter plot of substrate to spindle angles of metaphase cells under the above conditions. Mean ± S.E.M: Control 4.696 ± 0.7338°, n = 24; NZ 20.60 ± 2.527°, n=23; Cyto D 23.20 ± 4.037°, n=25; p values were calculated by t-test; n, number of metaphase cells, two independent experiments. (C) Box-plot of the basal to mid-lateral cortex intensity ratio of active integrin β1 of the cells analyzed in (B). Mean ± S.E.M: Control 0.7807 ± 0.03210, n=24; NZ 0.8597 ± 0.04068, n=23; Cyto D 1.030 ± 0.03908, n=25; p values were calculated by t-test; n, number of metaphase cells, two independent experiments. (D) Correlation of the degree of spindle misorientation with the ratio of basal to mid-lateral cortex intensity of active β1. Pearson's correlation coefficients: Control r = -0.0289, weak correlation, NZ r = 0.2547 weak

correlation, Cyto D $r = 0.5919$ moderate positive correlation. (E) Optical sections at the cell-ECM interface and at the plane of the spindle of Control, NZ treated and Cyto D treated cells seeded on L-FN microprints. Yellow arrowheads indicate the cortical polarity of active integrin β1. (F) Optical sections, color intensity coded images and side views of cells seeded on FN or PLL, stained for β-tubulin, active β1 (9EG7) and actin. (G) Box-plot of the ratio of the intensity of mid-lateral cortical active integrin β1 to the intensity of cortical actin of metaphase cells seeded on FN and PLL. Mean ± S.E.M: FN 0.7494 ± 0.1131, n=20; PLL 0.2628 ± 0.03568, n=22; $p<0.0001$*** analyzed by t-test; n, number of metaphase cells, two independent experiments. (H) Scatter plot of the substrate to spindle angles of the cells analyzed in (G). Mean ± S.E.M: FN 6.085 ± 0.8938°, n=20; PLL 37.07 ± 4.551°, n=22; $p<0.0001$*** analyzed by t-test; n, number of metaphase cells, two independent experiments. Abbreviations: NZ, Nocodazole; CytoD, Cytochalasin D. Scale bars: (A, E) 10 μm, (F) 5 μm.

4.2.12. Cortically polarized active integrin β1 guides spindle orientation of adherent cells

Given the RF dependent activation of integrin β1 on the lateral cortex of mitotic cells we wanted to then explore the possibility that this activation has a role in sensing the RF-derived forces that control spindle orientation. To do so, we needed to preferentially block ligand unoccupied integrin β1 on the lateral cortex without affecting ligand bound β1 on the cell-ECM interface. We took advantage of the blocking antibody P4C10, which has been shown to preferentially bind unoccupied integrin β1 (Mould, Akiyama et al. 1996, Mould, Askari et al. 1997). This antibody would presumably selectively inactivate the cortical pool of integrin β1 which is not ligand bound, whereas engaged integrins at the cell-ECM interface would remain unaffected. In agreement with the above, treatment of cells seeded on FN with P4C10 resulted in the reduction of cortically localized active integrin β1 in mitotic cells (**Figure 93A, C**), while cell adhesion was unaffected (**Figure 94A**). Loss of active β1 from the lateral aspect of the cortex led to spindle misorientation (**Figure 93B**) and importantly, the degree of spindle misorientation was positively correlated with the degree of loss of active β1 from the lateral cortex (**Figure 93D**), suggesting that force dependent activation of β1 is necessary for correct spindle orientation.

The above data strongly suggest that integrin β1 activation on the lateral cortex is necessary for spindle orientation however, effects of the antibody on adhesive complexes at the RF-FN interface cannot be ruled out. To address this, we took advantage of cell adhesion to VN. VN interacts with cells through its RGD integrin-binding sequence, however several integrin heterodimers recognize this substrate and the major one is αvβ3, so cell attachment does not depend exclusively on integrin β1 as in the case of adhesion on FN (Preissner 1991). Moreover, multiple cell types including HeLa cells were shown to also rely on uPAR for their adhesion to VN and inhibition of integrin-dependent adhesion on VN does not eliminate cell attachment

(Deng, Curriden et al. 2001). We initially confirmed that integrin β1 is not important for adhesion to VN. As shown, both total and active integrin β1 are nearly absent from FAs when cells are seeded on this substrate (**Figure 94B-D**). Importantly, despite the near undetectable levels of active integrin β1 in interphase cells, cortical activation of β1 in mitotic cells on VN was unaffected and spindles were properly oriented (**Figure 93A-C**). Treatment of cells seeded on VN with P4C10 resulted in loss of cortically active integrin β1 and elicited spindle misorientation despite a lack of any effect on cell adhesion (**Figure 93A-D, Figure 94A**). This result confirms that even when cell adhesion is β1 independent, β1 activation on the lateral cortex is necessary for correct spindle orientation.

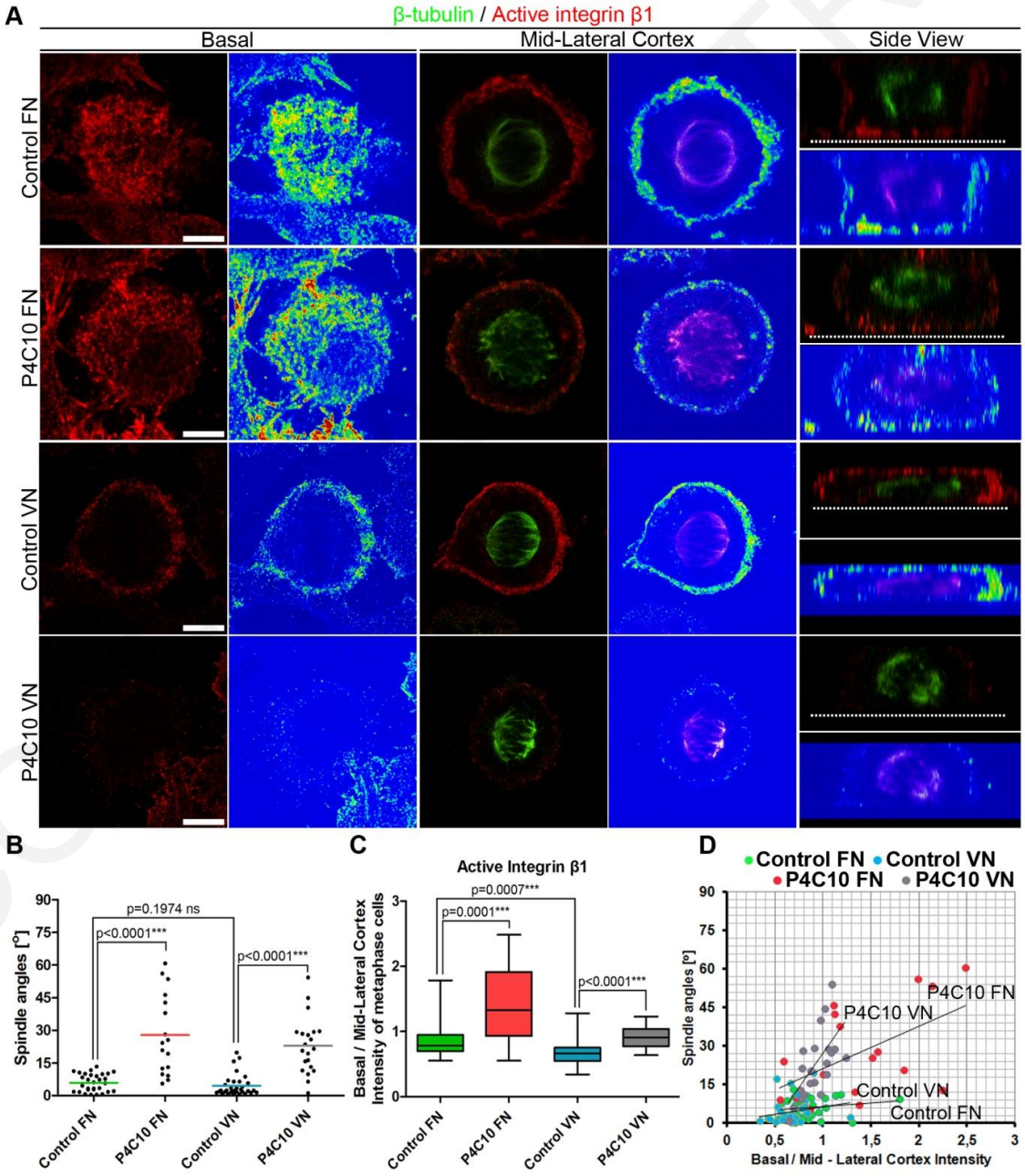

Figure 93: Inhibition of integrin β1 cortical activation leads to spindle misorientation.

(A) Optical sections at the cell-ECM interface and at the spindle plane, color intensity coded images and side views of representative metaphase control or P4C10 antibody treated HeLa cells seeded on FN or VN. All cells were imaged under the same conditions. Cells were stained with β-tubulin and 9EG7 antibodies. The dashed lines show the cell-ECM interface. (B) Scatter plot of substrate to spindle angles of metaphase cells from the above conditions. Mean ± S.E.M: Control FN 5.920 ± 0.7391°, n=30; P4C10 FN 27.76 ± 4.455°, n=17; Control VN 4.427 ± 0.8606°, n=33; P4C10 VN 22.84 ± 2.824°, n=21; p values were calculated by t-test; n, number of metaphase cells, two independent experiments. (C) Box-plot of the basal to mid-lateral cortex intensity ratio of active integrin β1 of the cells analyzed in (B). Mean ± S.E.M: Control FN 0.8482 ± 0.04543, n=30; P4C10 FN 1.388 ± 0.1422, n=17; Control VN 0.6639 ± 0.02926, n=33; P4C10 VN 0.9175 ± 0.03423, n=21; p values were calculated by t-test; n, number of metaphase cells, two independent experiments. (D) Correlation of the spindle angle and the ratio of basal to mid-lateral cortex intensity of active integrin β1. Pearson's correlation coefficient: Control FN r = 0.1755 weak correlation, Control VN r = 0.2006 weak correlation, P4C10 FN r = 0.5601 moderate positive correlation, P4C10 VN r = 0.645 moderate positive correlation. Scale bars: (A) 5 μm.

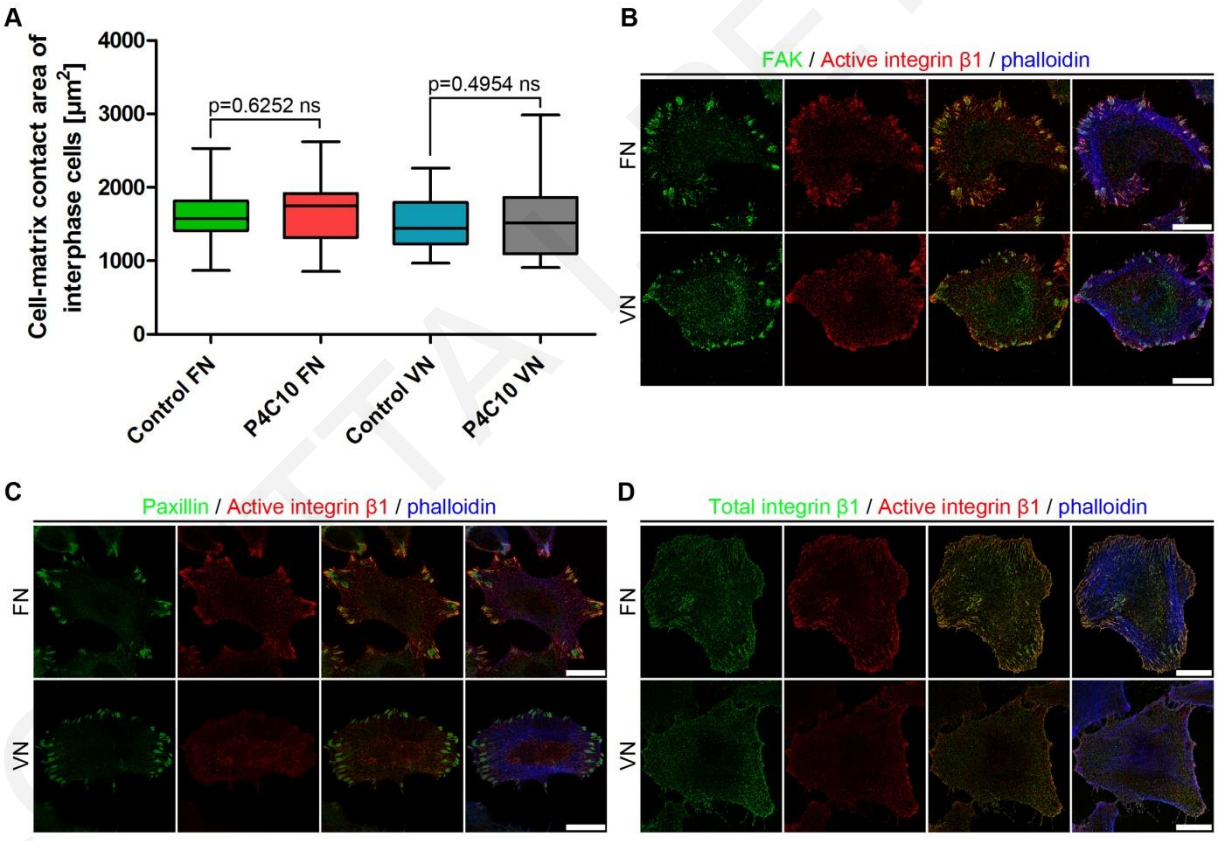

Figure 94: Adhesion of HeLa cells on VN does not rely on integrin β1.

(A) Box-plot of the cell-matrix contact area of interphase control cells or P4C10 treated cells seeded on FN or VN. Mean ± S.E.M: Control FN 1602 ± 85.95 μm², n=20; P4C10 FN 1667 ± 99.87 μm², n=20; Control VN 1499 ± 74.48 μm², n=20; P4C10 VN 1599 ± 124.9 μm², n=20; p values were calculated by t-test; n, number of metaphase cells, two independent experiments. (B, C, D) Optical sections of HeLa cells seeded on FN or VN and stained for active integrin β1 (9EG7), actin and the FA proteins FAK (B), paxillin (C) or total integrin β1 (K20 antibody). Scale bars: (B, C, D) 20 μm.

Given the importance of integrin β1 cortical activation in spindle orientation, we then asked if the asymmetric distribution of active β1 is also important. We postulated that if integrin β1 has a role in determining the capture sites of astral microtubules, integrin β1 overactivation would lead to spindle misorientation. Treatment of HeLa cells with RGD peptides at concentrations that disrupt integrin-dependent cell adhesion (400 μg/ml) via competition for binding to the substrate has been shown to lead to spindle misorientation (Toyoshima and Nishida 2007). We postulated that treatment of cells adhering on FN with low concentrations of RGD peptide would fail to compete with immobilized FN on the cells basal region and thus not disrupt adhesion, but bind to and activate unoccupied cortically localized integrins. We found that at 50 μg/ml of RGD peptide (8-fold lower concentration than previously used) did not detectably perturb cell adhesion and active integrin β1 levels in interphase (**Figure 95A-C**) or cell adhesion and RF formation during mitosis (**Figure 96A, C**), yet was sufficient to elicit integrin β1 activation on the entire cell cortex (**Figure 96B, E**, yellow arrowheads) and spindle misorientation (**Figure 96A, D**). This suggests that the polar distribution of active β1 in mitotic cells is required for correct spindle orientation. Similar results were obtained when using an alternative approach to activate integrin β1. Cells were treated with the activating 9EG7 antibody. However, 9EG7 treatment was not sufficient to either lead to ectopic integrin activation or spindle misorientation (**Figure 96B**) probably due to the fact that the 9EG7 epitope (at the EGF like repeats which are masked when the integrin molecule is bent) was shown to be exposed when integrin β1 was bound to RGD peptide (Bazzoni, Shih et al. 1995). These data suggest that inactive integrins at the apical cortex are in a bent conformation and cannot become activated by 9EG7 treatment alone. To overcome this, we pre-treated cells with very low concentrations of RGD peptide (10 μg/ml) for 30 minutes in order to expose the 9EG7 epitope in all integrin molecules around the cortex, and then incubated them with the 9EG7 antibody so as "primed" integrin molecules would become fully activated. Treatment of cells with 10 μg/ml RGD peptide alone had no effect on spindle orientation, RF formation, integrin cortical activation during mitosis or integrin basal activation during interphase. However, evaluation of spindle orientation and integrin β1 activation in RGD + 9EG7 treated cells, revealed that mitotic spindles were misoriented, integrin β1 was activated throughout the cortex (both in basal, lateral and apical cortex) but at the same time there was no effect on RF formation and cell adhesion surface area during mitosis and integrin β1 activation in interphase (**Figure 95, Figure 96**). Overall, the above data show that both inhibition and overactivation of integrin β1 on the lateral cortex of mitotic cells leads to spindle misorientation.

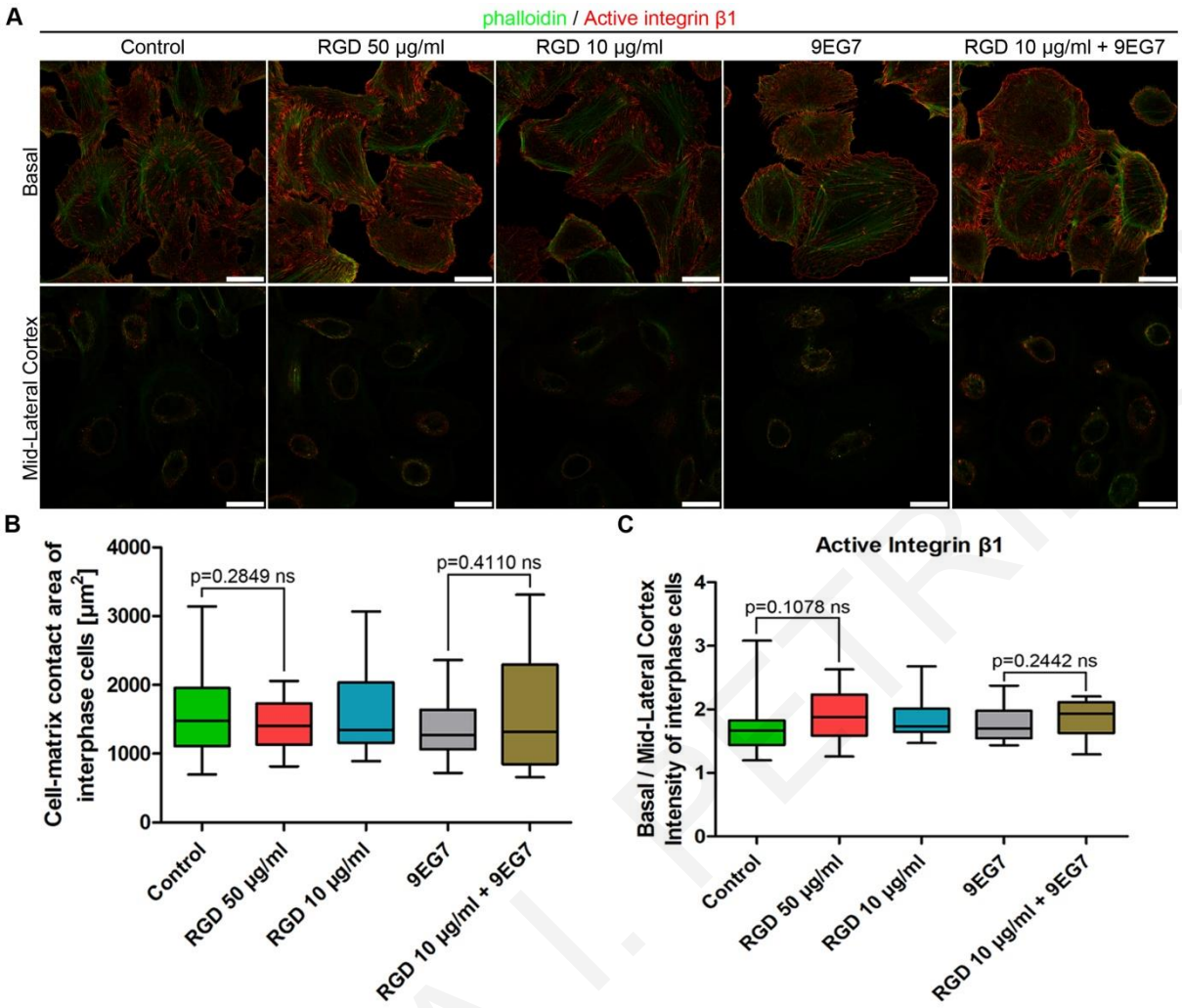

Figure 95: RGD-mediated cortical integrin β1 overactivation does not affect cell-ECM adhesion or the distribution of active integrin β1 during interphase.

(A) Optical sections at the cell-ECM interface and at the plane of the nucleus of interphase control cells, or cells treated as indicated and stained for actin and active integrin β1 (HUTS-21). (B) Box-plot of the cell-matrix contact area of interphase cells described in (A). Mean ± SEM: Control 1591 ± 148.6 µm², n=20; RGD 50 µg/ml 1407 ± 80.36 µm², n=20; RGD 10 µg/ml 1553 ± 129.2 µm², n=20; 9EG7 1371 ± 95.35 µm², n=20; RGD 10 µg/ml + 9EG7 1539 ± 177.8 µm², n=20; p values were calculated by t-test; n, number of metaphase cells, two independent experiments. (C) Box-plot of the ratio of basal to mid-lateral cortex intensity of active integrin β1 of the cells described in (A). Control 1.713 ± 0.09153, n=20; RGD 50 µg/ml 1.918 ± 0.08440, n=20; RGD 10 µg/ml 1.850 ± 0.07315, n=20; 9EG7 1.768 ± 0.05489, n=20; RGD 10 µg/ml + 9EG7 1.868 ± 0.06438, n=20; p values were calculated by t-test; n, number of metaphase cells, two independent experiments. Scale bars: (A) 20 µm.

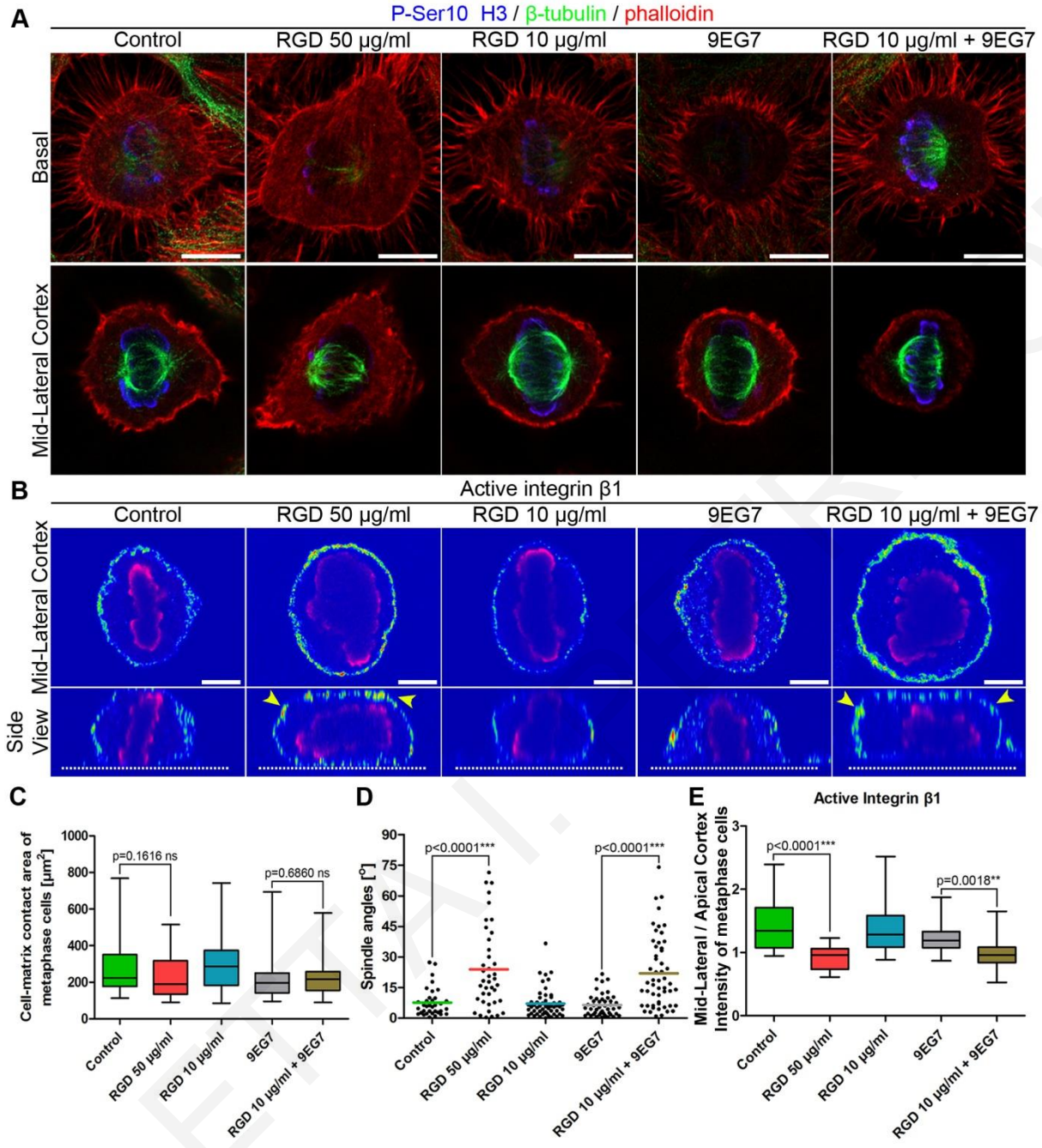

Figure 96: Disruption of the asymmetric distribution of cortical integrin β1 leads to spindle misorientation. (A) Optical sections at the RF plane and at the spindle plane of control and treated metaphase cells stained with P-Ser10 H3 and β-tubulin antibodies, and phalloidin. Treatments are RGD 50 µg/ml, RGD 10 µg/ml, 9EG7, RGD 10 µg/ml + 9EG7. (B) Color intensity coded optical sections at the spindle plane and the corresponding side view from metaphase cells under the same conditions as (A) stained with HUTS-21 and P-Ser10 H3 antibodies. All cells were imaged under the same conditions. The dashed lines show the cell-ECM interface. Yellow arrowheads indicate integrin β1 activation throughout the cell cortex. (C) Box-plot of the cell-matrix contact area of metaphase cells under indicated treatments. Mean ± S.E.M: Control 278.4 ± 24.09 µm^2, n=35; RGD 50 µg/ml 235.0 ± 19.48 µm^2, n=40; RGD 10 µg/ml 298.6 ± 20.95 µm^2, n=54; 9EG7 225.1 ± 18.42 µm^2, n=48; RGD 10 µg/ml + 9EG7 216.5 ± 11.43 µm^2, n=53; p values were calculated by t-test ; n, number of metaphase cells, three independent experiments. (D) Scatter plot of substrate to spindle angles of cells analyzed in (C). Mean ± S.E.M: Control 7.607

± 1.163°, n=35; RGD 50 μg/ml 23.91 ± 3.219°, n=40; RGD 10 μg/ml 7.100 ± 0.9431°, n=54; 9EG7 6.385 ± 0.7696°, n=48; RGD 10 μg/ml +9EG7 21.97 ± 2.408°, n=53; p values were calculated by t-test; n, number of metaphase cells, three independent experiments. (E) Box-plot of the mid-lateral to apical cortex intensity ratio of metaphase cells under indicated treatments. Mean ± S.E.M: Control 1.438 ± 0.09659, n=21; RGD 50 μg/ml 0.9443 ± 0.04263, n=19; RGD 10 μg/ml 1.393 ± 0.08771, n=20; 9EG7 1.222 ± 0.04880, n=20; RGD 10 μg/ml + 9EG7 0.9646 ± 0.05918, n=19; p values were calculated by t-test; n, number of metaphase cells, two independent experiments. Scale bars (A) 10 μm, (B) 5 μm.

4.2.13. A conserved integrin β1 based cortical mechanosensory complex is formed in a polarized fashion during mitosis

As shown above, integrin β1 becomes activated at the lateral cortex of mitotic cells in a RF dependent but ligand independent fashion and this activation is critical for correct spindle orientation. How is this activation guiding spindle orientation? Integrin activation at FAs leads to the formation of a multiprotein complex responsible for mechanosensing at the cell-ECM interface (Schwartz 2010). However, since the adhesive complexes at the tips of the RFs which are in contact the ECM probably serve an anchoring role, raised the possibility that integrin β1 activation at the lateral cortex may lead to the formation of an FA similar multiprotein complex that sense the external forces and transmits them to the spindle. Combining with the above findings concerning the role of FAK in mechanotransduction and response of the spindle to external forces we examined if integrin β1 activation on the lateral cortex leads to the recruitment of downstream effectors and the formation of a cortical signaling complex. We began by examining the localization of phosphorylated FAK and while active FAK is localized at FAs in interphase cells (Ballestrem, Erez et al. 2006), as shown during mitosis it is detected on the cell cortex (**Figure 97A**). Given previous data showing that ligand independent activation of integrin β1 elicits Cas phosphorylation (Ferraris, Schulte et al. 2014) and its direct interaction with FAK (Polte and Hanks 1995, Harte, Hildebrand et al. 1996), we also examined the localization of phosphorylated Cas. As shown, P-Cas also becomes localized at the cell cortex in mitotic cells (**Figure 97A,** white arrowheads) and the same is true for Src, the principle kinase known to phosphorylate Cas (**Figure 97A,** white arrowheads) (Nakamoto, Sakai et al. 1996, Pellicena and Miller 2001). In addition to localizing at the lateral aspect of the cortex, the active forms of all three proteins also display lateral cortical polarity in a similar fashion to active β1 (**Figure 97A,** white arrowheads). Importantly, treatment with the inhibitory antibody P4C10 led to a reduction of cortically localized P-Cas and P-Src suggesting that the localization and phosphorylation of these proteins on the cell cortex is dependent on β1 activation (**Figure**

97B). These results suggest that a cortical mechanosensory complex (CMC) forms at the lateral regions of the cell on force activated integrin β1 in non-polar adherent cells.

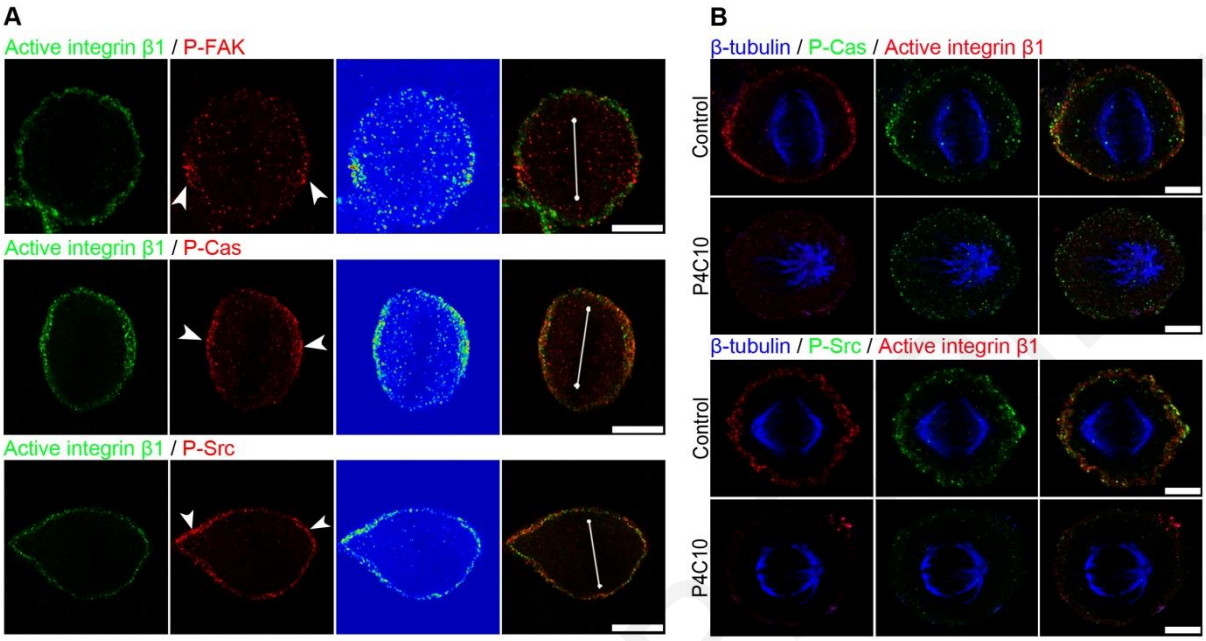

Figure 97: A cortical mechanosensory complex forms in a polarized fashion at the lateral cortex of mitotic cells in response to ligand independent integrin β1 activation.

(A) Optical sections and color intensity coded images of representative metaphase HeLa cells co-stained for active β1 and phosphorylated active forms of FAK, Cas or Src. The white arrowheads indicate the polarized cortical crescent of the phosphorylated forms of the above proteins. The white line in the merged images represents the metaphase plate. (B) Optical sections at the spindle plane of metaphase control HeLa cells or cells treated with the P4C10 antibody. All cells were imaged under the same conditions. Cells were co-stained for β-tubulin, active β1 (9EG7) and phosphorylated Cas or Src. Scale bars: (A) 10 μm, (B) 5 μm.

We then asked if this complex also forms in polarized epithelia. Staining of MDCK monolayers revealed that active integrin β1, P-FAK, P-Cas and P-Src are localized at the lateral aspect of the cortex specifically in mitotic cells in a similar fashion to HeLa cells (**Figure 98A, B,** white arrowheads).

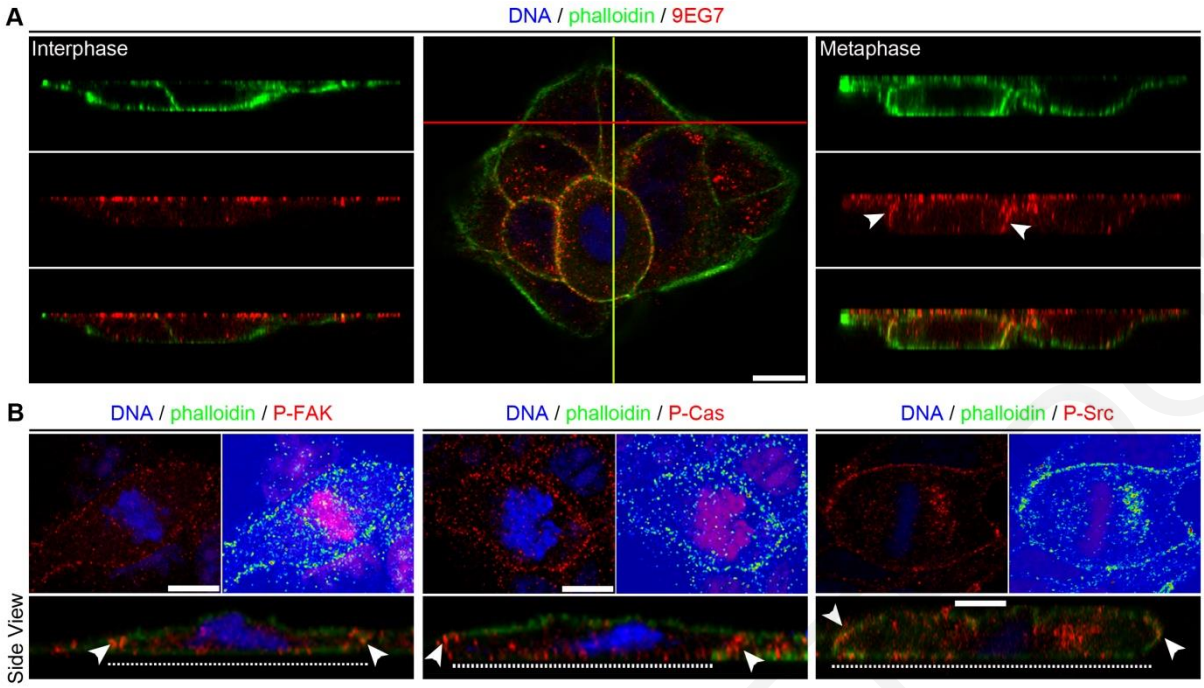

Figure 98: CMC is conserved in the mammalian epithelial monolayer.

(A) Optical section and side views of interphase (section at the red line) and mitotic (section at the yellow line) cells in the same colony of MDCK cells. Cells were stained with the 9EG7 antibody, phalloidin and TO-PRO. Cell-ECM interface is represented by the white dashed line. Arrowheads show integrin β1 activation at the lateral cortex of the mitotic cell. (B) Optical sections at the spindle plane, color intensity coded images and side views of representative MDCK cells stained with phalloidin, TO-PRO and antibodies against phosphorylated FAK, Cas or Src. White arrowheads show enrichment of the phosphorylated proteins at the lateral cortex of mitotic cells, white dashed line represents the ECM. Scale bars: (A, B) 10 μm.

As shown above, the determinants of FAK function in spindle orientation (requirement of FAT and kinase domain of FAK, of FAK-paxillin interaction and dispensable role of FAK's catalytic activity) were identical both in adherent cells and in the outermost epithelial cells of the vertebrate epidermis. This was a surprising finding since, the outermost epithelial cells of *Xenopus* embryos are not in contact with the ECM (**Figure 99A**), thus they do not form FAs or RFs and yet they orient their spindles parallel to the plane of the epithelium (Marsden and DeSimone 2001, Woolner and Papalopulu 2012). Since both FA proteins are involved in spindle orientation, FAK and paxillin localize at the cortex of mitotic cells we attributed their involvement in spindle orientation to possible interactions with members of the adherens junctions or tight junctions (Sun, Shikata et al. 2009, Dubrovskyi, Tian et al. 2012). However, based on the above findings suggesting that ligand independent integrin β1 activation creates a mechanosensory complex composed by FA proteins at the lateral cortex of mitotic cells, it is possible that also in the context of the embryo spindle orientation is regulated by the CMC

through the same mechanism we proposed for adherent cells in culture. Support for this notion stems from the fact that despite the absence of an ECM integrin β1 is expressed in these cells and is localized at the basolateral regions of the cell cortex (**Figure 99B**). In order to address the possibility that integrins are involved in controlling spindle orientation in the outermost cells of the *Xenopus* epithelium we interfered with β1 function through the expression of a previously characterized DN (Marsden and DeSimone 2001, Marsden and DeSimone 2003). This construct is a chimeric molecule composed of the *Xenopus* integrin β1 subunit cytoplasmic tail fused to the transmembrane and extracellular domains of HA, allowing it to localize at the plasma membrane. However, this construct is believed to act as a DN of integrin β1 since it is able to dimerize at the plasma membrane irrespective of extracellular signals, leading to cytoplasmic β1 tail clustering, recruiting in this way the cytoplasmic components that are needed for the activation of endogenous β1 to a defective complex that does not respond to external cues or tension dependent activation (LaFlamme, Thomas et al. 1994). Expression of this construct in the *Xenopus* epidermis lead to spindle misorientation (**Figure 99C**), strongly suggesting that integrin β1 has a role in spindle orientation in a ligand independent fashion in this tissue.

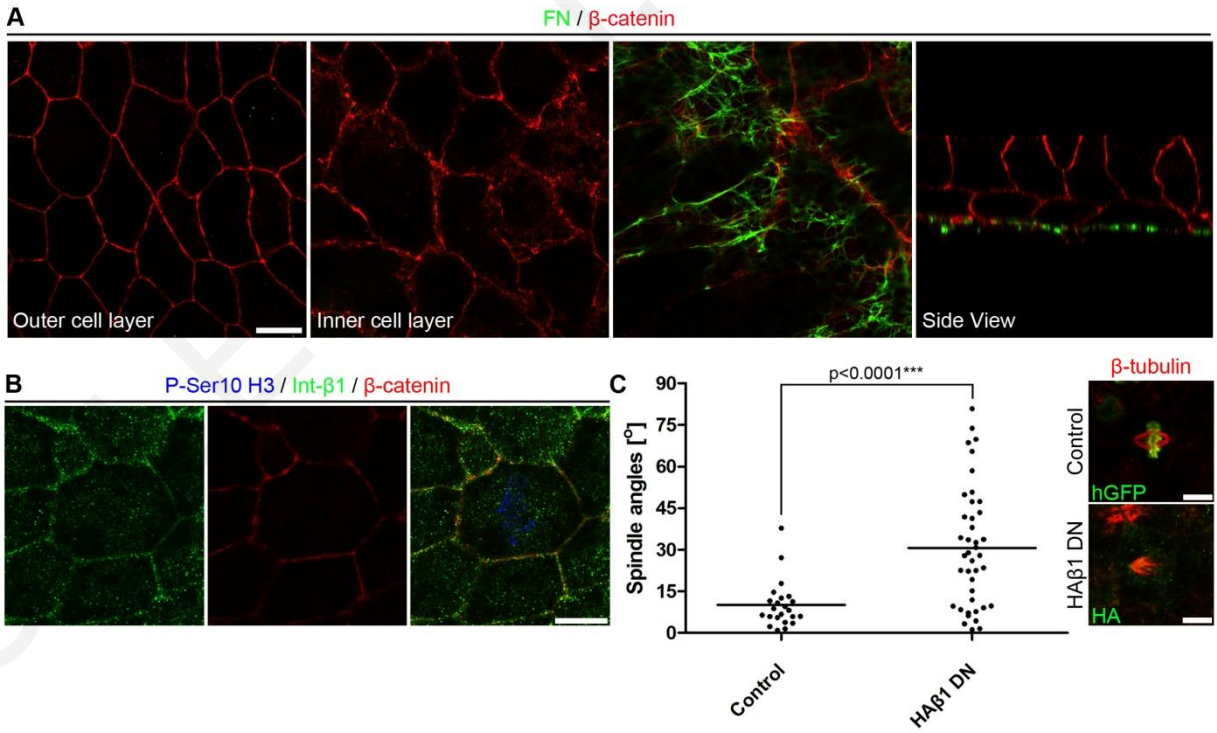

Figure 99: Spindle orientation of the outermost epithelial cells of the *Xenopus* epidermis depends on integrin β1 function.

(A) Optical sections of the *Xenopus* epidermis at the outermost epithelial layer, the innermost epithelial cell layer, the basal surface of the cells of the inner epithelial layer and a side view of these cells. Embryos were stained with

FN and β-catenin antibodies. (B) Optical section at the mid-lateral cortex of a mitotic cell of the *Xenopus* outermost epidermis stained with phospho-Ser10 H3, total integrin β1 and β-catenin antibodies. (C) Representative top views of mitotic control cells (injected with histone GFP) or cells injected with integrin β1 DN (HAβ1) of the *Xenopus* epidermis and a scatter plot of the apical surface to spindle angles of these cells. Mean ± S.E.M: Control 10.06 ± 1.758º, n=23; HAβ1 DN 30.66 ± 3.389º, n=41; p<0.0001*** analyzed by t-test; n, number of metaphase cells, two independent experiments. Cells were stained with β-tubulin and GFP or HA antibodies. Scale bars: (A-C) 10 μm.

Furthermore, examining the localization of the members of the CMC in these cells, P-FAK, P-Cas and P-Src, reveals that although all cells of the epithelium display staining on the lateral aspect of the cortex (especially in terminally differentiated ciliated cells), in mitotic cells there is clear elevation of the signal of the active forms of all three proteins at the lateral cortex (**Figure 100**, white arrowheads**).** Overall, the above data suggest that integrin β1, FAK, Cas and Src form a ligand independent CMC in response to external force.

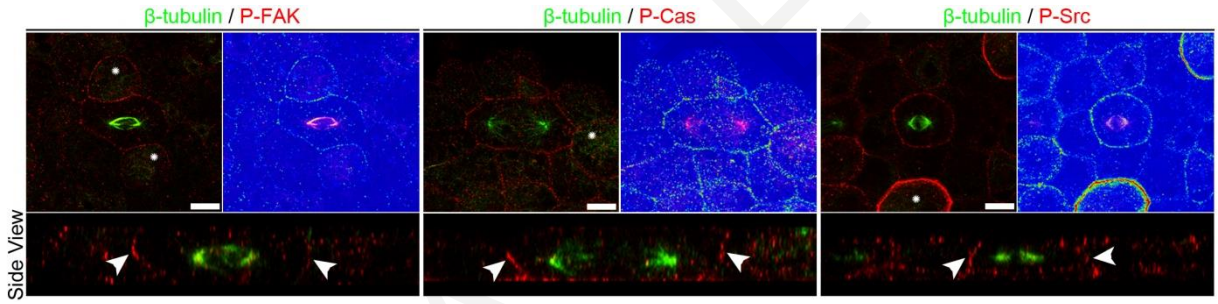

Figure 100: CMC is conserved in the cells of the vertebrate epidermis.
Optical sections at the plane of the spindle, color intensity coded images and side views of representative epithelial cells of the superficial cell layer of the *Xenopus* embryonic epidermis. Staining for β-tubulin and the phosphorylated forms of FAK, Cas and Src reveals elevated levels of the above proteins on the cortex of mitotic cells (white stars indicate the ciliated cells). The white arrowheads show enrichment of the phosphorylated proteins at the lateral cortex of mitotic cells. Scale bars: 10 μm.

4.2.14. The members of the CMC interact to orient the mitotic spindle both in adherent cells and in the vertebrate embryos

Our data so far suggest that a complex composed of known FA proteins (FAK, paxillin, Cas and Src) forms on active β1 at the lateral cortex of mitotic cells and regulates spindle responses to external forces. We went on to explore the interactions between its members that are important in this process. We first examined the interaction of FAK with Cas, since Cas has a well characterized role in mechanotransduction which is primarily based on the notion that mechanical stretching can induce conformational changes on the Cas molecule by extending

the SD and exposing the 15 tyrosine residues for phosphorylation by Src (Sawada, Tamada et al. 2006). FAK-Cas interaction is mediated by the binding of the N-terminal SH3 domain of Cas to the PR2 of FAK, with amino acid sequence APPKPSR (Polte and Hanks 1995, Harte, Hildebrand et al. 1996). In order to address the necessity of the interaction of Cas with FAK in spindle orientation we generated the FAK point mutant P712/715A in which this interaction is abolished (Polte and Hanks 1995) and introduced it in FAK null cells. Expression of the Cas binding defective mutant of FAK failed to rescue spindle orientation defects in FAK null cells (**Figure 101A, B**). Since Cas had not been previously implicated in this process we also examined Cas null cells (Honda, Oda et al. 1998). As shown in **Figure 102A, B,** Cas null cells exhibit spindle misorientation compared to Cas reconstituted cells showing Cas is directly involved in spindle orientation. Moreover, active integrin β1 is localized properly on the lateral cortex of Cas null cells, indicating that Cas acts downstream of integrin activation to guide spindle orientation (**Figure 102C**). Furthermore, we confirmed that the FAK-Cas interaction is crucial for spindle orientation by transfecting Cas null cells with the CasΔSH3 mutant, which fails to bind FAK (Polte and Hanks 1995). Expression of this construct failed to rescue spindle misorientation when compared with expression of WT Cas (**Figure 102A, B**).

Since the interaction of FAK with Cas is necessary for spindle orientation in adherent cells, we went on and to explore the functional determinants of Cas in the selection of the division axis. To do this, we transfected Cas nulls with previously characterized Cas mutants (Meenderink, Ryzhova et al. 2010). Given the previously established role of the SD of Cas in mechanotransduction from FAs (Sawada, Tamada et al. 2006), we then asked if phosphorylation of the Cas SD is important. As shown expression of the 15F Cas mutant in Cas nulls, in which all the tyrosines of the SD are mutated to phenylalanines, failed to rescue spindle misorientation indicating that phosphorylation and subsequently mechanotransduction through Cas, is required for the orientation of the mitotic spindle (**Figure 102A, B**). The SD domain of Cas is a well characterized substrate of Src kinases (Nakamoto, Sakai et al. 1996, Pellicena and Miller 2001) and it has been previously shown that the Src kinase activity is indispensable for force dependent spindle orientation *in vitro* (Thery, Racine et al. 2005). This raised the possibility that during mitosis Cas is phosphorylated by Src to regulate spindle orientation. SD domain phosphorylation is mediated via two distinct mechanisms; either through direct binding of the SH3 domain of Src to the C-terminal polyproline region of Cas or via indirect association of Src with Cas through a FAK scaffold (Fonseca, Shin et al. 2004). As shown, expression of the Cas mPR mutant in which the Src-Cas interaction is impaired rescues as effectively as WT Cas (Meenderink, Ryzhova et al. 2010) (**Figure 102A, B**), suggesting that direct binding of Src

on Cas is dispensable. Expression of a Src binding mutant of FAK (Y397F) (Cobb, Schaller et al. 1994, Schaller, Hildebrand et al. 1994) in FAK nulls was significantly less effective in rescuing spindle orientation defects compared to WT FAK, suggesting that Src binding on FAK is important (**Figure 101A, B**). However, expression of FAK Y397F led to a partial rescue of the phenotype (**Figure 101A, B**), probably due to weak recruitment of Src to the CMC. Compared to FAK nulls, FAK Y397F cells would be able to recruit Cas to the complex, while Src might also be recruited to the complex through binding to the PR1 of FAK through the Src SH3 domain (Thomas, Ellis et al. 1998). This interaction could enable this mutant to elicit limited phosphorylation of Cas since it was shown that despite a large drop, some phosphorylation of Cas still exists in Y397F expressing FAK null cells (Cary, Han et al. 1998, Ruest, Shin et al. 2001).

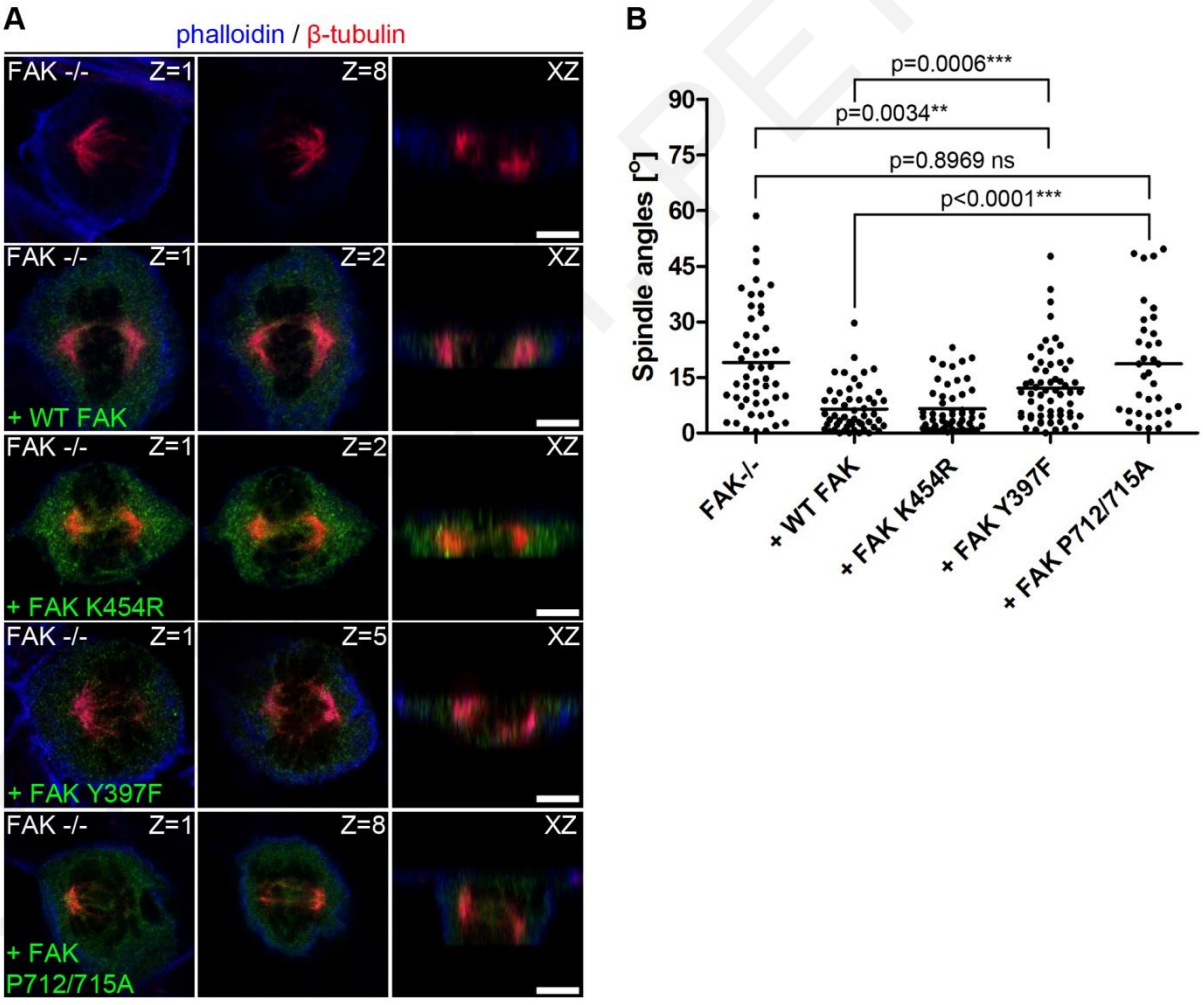

Figure 101: FAK-Src and FAK-Cas interactions are required for spindle orientation in adherent cells.

(A) Optical sections (0.37 μm interval) at the plane of each spindle pole and side views of FAK nulls, or FAK nulls transfected with the indicated constructs (signal shown in green) stained for β-tubulin and actin. (B) Scatter plot of the substrate to spindle angles of metaphases cells described in (A). Mean ± S.E.M: FAK-/- 19.04 ± 2.028°,

n=50; FAK-/- + WT FAK 6.507 ± 0.8685º, n=52; FAK-/- + FAK Y397F 12.14 ± 1.263º, n=61; FAK-/- + FAK P712/715A 18.63 ± 2.501º, n=35; p values were calculated by t-test; n, number of metaphase cells, two independent experiments. Scale bars: (A) 5 µm.

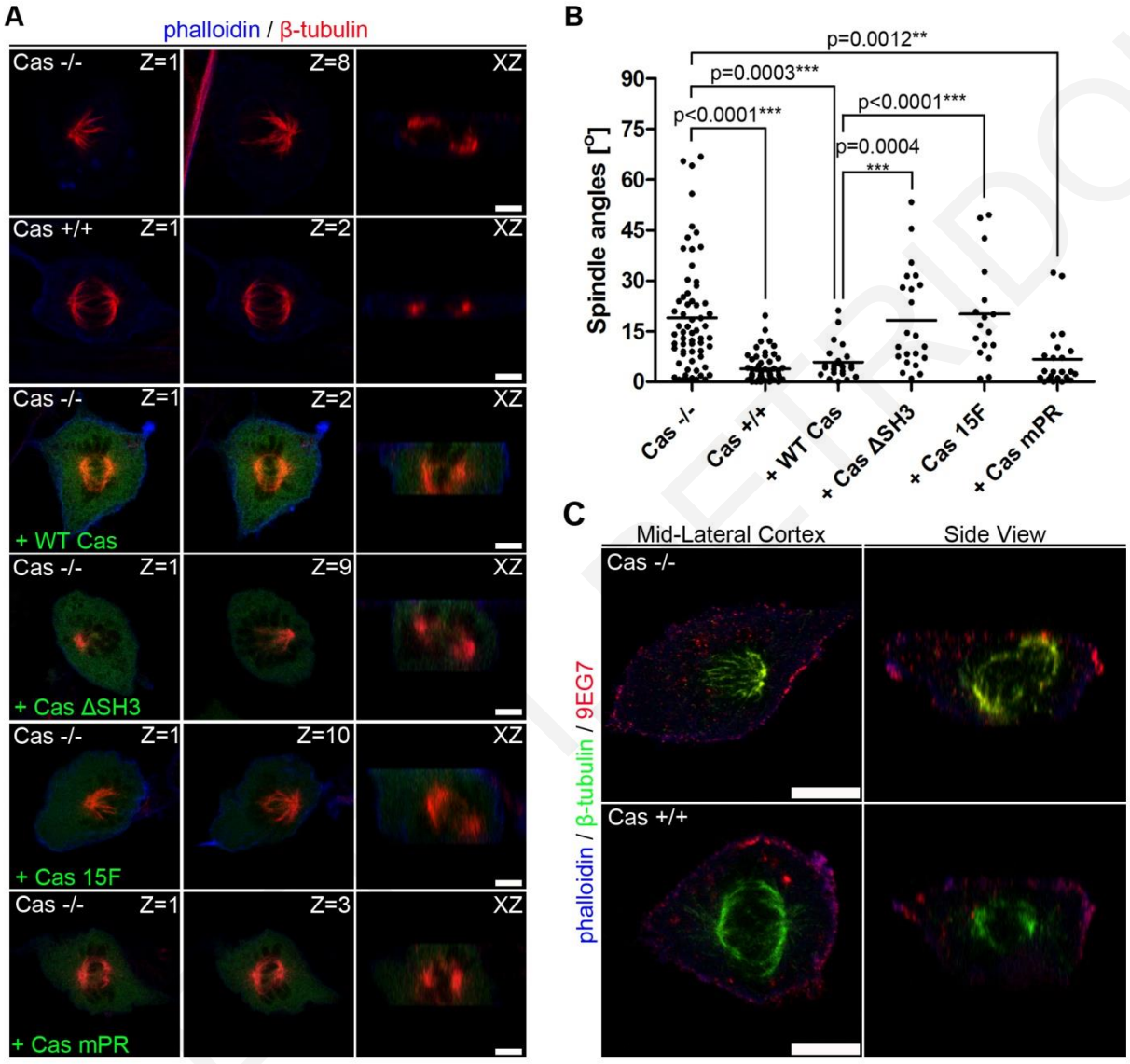

Figure 102: Cas phosphorylation by Src through a FAK scaffold is required for spindle orientation in adherent cells.

(A) Optical sections (0.37 µm interval) at the plane of each spindle pole and side views of Cas nulls, Cas re-constituted cells or Cas nulls transfected with the indicated constructs (shown in green) stained for β-tubulin and actin. (B) Scatter plot of the substrate to spindle angles of metaphases cells described in (A). Mean ± S.E.M: Cas-/- 18.97 ± 2.102º, n=63; Cas+/+ 3.825 ± 0.5526º, n=57; Cas-/- + WT Cas 5.805 ± 1.062º, n=24; Cas-/- + Cas ΔSH3 18.24 ± 3.173º, n=22; Cas-/- + Cas 15F 20.09 ± 3.660º, n=17; Cas-/- + Cas mPR 6.703 ± 1.882º, n=23; p values were calculated by t-test; n, number of metaphase cells, two independent experiments. (C) Representative optical sections and side views of Cas null and Cas reconstituted cells stained for active β1, β-tubulin and actin. Scale bars: (A) 5 µm, (C) 10 µm.

In order to address if the same interactions between the members of the CMC are required for spindle orientation *in vivo*, we downregulated FAK in the *Xenopus* epithelium and performed rescue experiments with either WT FAK as a positive control, or the mutants FAK P712/715A and FAK Y397F to examine the requirement of FAK/Cas or FAK/Src interactions on mitotic spindle orientation, respectively. Similarly to the *in vitro* results, expression of both constructs failed to rescue spindle misorientation induced by FAK downregulation (**Figure 103A**) confirming that both interactions are necessary for the determination of the division axis in the epidermal cells of the *Xenopus* embryo. Since disruption of the Src kinase activity through pharmacological approaches was shown to disrupt spindle orientation in adherent cells (Thery, Racine et al. 2005), and our data suggesting that Src dependent phosphorylation and mechanotransduction through Cas guide spindle orientation, we decided to address if the kinase activity of Src is also necessary in the *in vivo* situation. To do that, we treated blastula stage embryos with 8 μM of the selective Src kinase inhibitor PP2 and evaluated its effects on spindle orientation. As shown, inhibition of Src kinase activity in the context of the embryo leads to spindle misorientation (**Figure 103B**), providing additional support for the notion that the integrin β1 dependent CMC is conserved. Overall, these data show that direct interaction of FAK with Cas and Src is critical for correct spindle orientation and suggest that during mitosis a complex forms downstream of force dependent integrin β1 activation in which FAK acts as a scaffold to elicit Src dependent Cas phosphorylation.

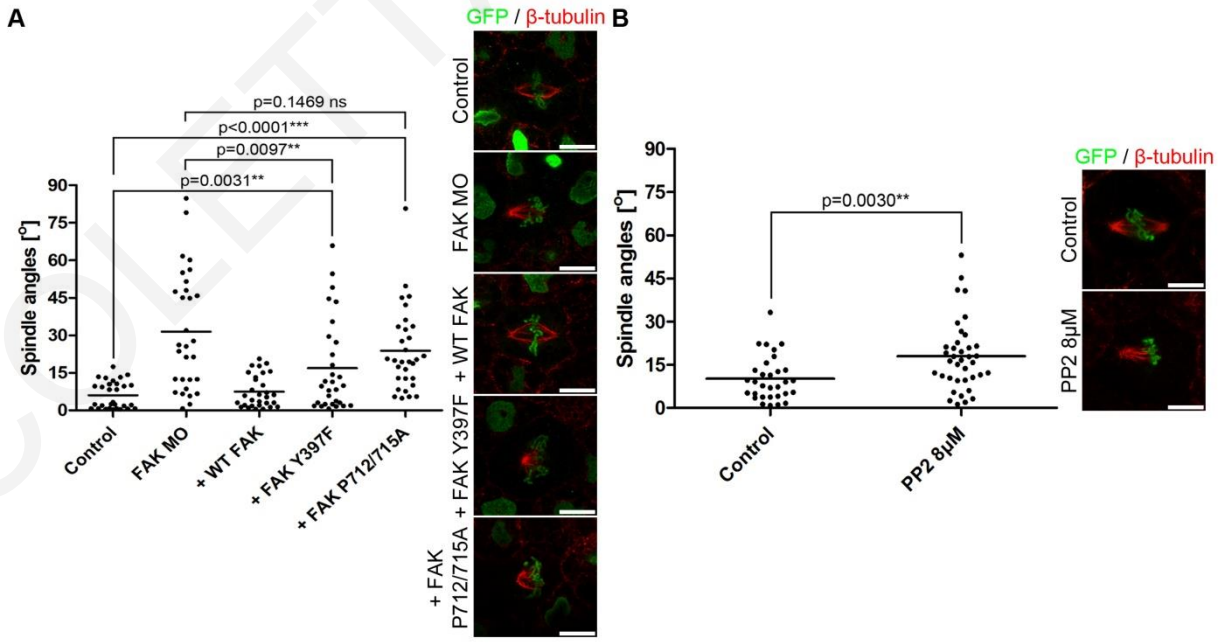

Figure 103: Interactions between the members of the CMC are required to orient the mitotic spindle in the cells of *Xenopus* outermost epithelium.

(A) Representative top views of mitotic control cells (injected with histone GFP) or cells injected with histone GFP, FAK MO and the indicated FAK constructs of the *Xenopus* epidermis and scatter plot of the apical surface to spindle angles of these cells. Mean ± S.E.M: Control 6.033 ± 0.9885º, n=30; FAK MO 31.46 ± 4.301º, n=30; FAK MO + WT FAK 7.442 ± 1.176º, n=30; FAK MO + FAK Y397F 16.85 ± 3.358º, n=30; FAK MO + FAK P712/715A 23.81 ± 2.979º, n=31; p values were calculated by t-test; n, number of metaphase cells, two independent experiments. Cells were stained with β-tubulin and GFP antibodies. (B) Representative top views of mitotic histone GFP injected control or PP2 treated cells of the *Xenopus* epidermis and a scatter plot of the apical surface to spindle angles of these cells. Mean ± S.E.M: Control 10.17 ± 1.389º, n=31; PP2 17.93 ± 1.972º, n=38; p=0.0030** analyzed by t-test; n, number of metaphase cells, two independent experiments. Cells were stained with β-tubulin and GFP antibodies. Scale bars: (A, B) 10 μm.

4.3. Discussion Chapter II

4.3.1. FAK's role in spindle orientation and its physiological significance during epithelial morphogenesis

Although significant progress has been made towards understanding how cells couple cortical polarity signals and spindle positioning, how cells sense external stimuli and how these are translated at the cortex is poorly understood (Lu and Johnston 2013). In this study we provide evidence of how external forces are translated into biochemical signals in order to guide spindle orientation. We initially showed that FAK is involved in spindle orientation both in cultured cells and in the epithelia of the developing vertebrate embryo. In an effort to address if loss of FAK function has a direct impact on mitotic spindle orientation we ensured that other factors that could influence the orientation of the mitotic spindle indirectly were unaffected in the absence of FAK, such as spindle integrity, centering, cortical microtubule capture and metaphase duration. Further experiments revealed that in the absence of FAK the mitotic spindles both in cells in culture and in epithelial tissues fail to respond to external guiding forces, suggesting that FAK's involvement in spindle orientation stems from a defect in the transduction of the external forces to the spindle.

In the case of adherent cells in culture, we evaluated spindle orientation along the Z-axis and within the XY plane. In control cells the spindle is parallel to the substrate and orients according to the adhesion geometry in the XY (Thery, Racine et al. 2005, Toyoshima and Nishida 2007). Both types of spindle orientation depend on the formation of RFs (Lancaster and Baum 2011). We noted that although FAK null cells display RFs during mitosis in a similar fashion as FAK reconstituted cells, they fail to orient their spindle parallel to the matrix, while they also fail to orient according to extracellular cues in the XY plane. By performing experiments to address if mitotic spindle orientation along the Z-axis and at the XY plane is driven by similar mechanisms, we concluded that the distribution of the RFs as determined by the ECM distribution is principally responsible for spindle orientation, rather than other factors such as the cell shape. Since the RF distribution determines the distribution of the external forces that are exerted on the mitotic cortex (Thery, Jimenez-Dalmaroni et al. 2007, Fink, Carpi et al. 2011) and since FAK null cells display normal RFs, it is possible that the presence of the RFs is not sufficient for force transmission to the spindle of adherent cells but rather that forces are transmitted via a cytoskeletal link from the adhesive complex to the spindle involving FAK mediated signaling.

In the context of the embryo we evaluated effects of loss of FAK in spindle orientation both at the plane of the epithelium (Z-axis, spindle axis should be parallel to the apical surface of the epithelium) and at the XY plane (determined by cell shape and external forces exerted on the cell) (Minc, Burgess et al. 2011, Woolner and Papalopulu 2012). FAK morphant cells show defective spindle orientation since the spindle axis forms an angle with respect to the epithelial plane instead of being parallel, showing that FAK is required for epithelial cells to maintain cell divisions in the plane of the epithelium. This is in agreement with data in Medaka showing that planar divisions in the neuroepithelium are randomized in FAK morphant cells (Tsuda, Kitagawa et al. 2010). During early embryonic development, mechanical forces are believed to play a critical role in morphogenesis in part through control of cell division orientation (Mammoto and Ingber 2010). Experiments in invertebrates and vertebrates have shown that tissue level forces influence spindle orientation during embryonic development (Campinho, Behrndt et al. 2013, Legoff, Rouault et al. 2013, Mao, Tournier et al. 2013). By manipulating the external forces applied on a dividing cell of the *Zebrafish* EVL it was specifically shown that the mitotic spindle becomes aligned with the major force vector applied on the mitotic cell, a process that during EVL spreading releases anisotropic tension to guide proper epithelial morphogenesis during *Zebrafish* gastrulation (Campinho, Behrndt et al. 2013). We now show by performing laser ablations in a similar fashion to what was described in the *Zebrafish* EVL, that external forces can orient mitotic cells in *Xenopus* epithelia and provide direct evidence that FAK is required for spindle responses to such forces. Although these experiments strongly suggest that FAK orients the mitotic spindle by enabling force sensing by the spindle, another possibility is that FAK also transmits guiding signals derived from cell shape changes that are generated while the external forces elongate the mitotic cell so as the cell acquires a long axis which is coincident with the tension axis (Nestor-Bergmann, Goddard et al. 2014). In an effort to decouple the effects of cell shape and external forces on spindle orientation, we performed laser ablations such as the external forces exerted on the mitotic cell would lead to isotropic cell shapes. Under these conditions the mitotic spindle became aligned to the major force vector which in this case was not the same with the long axis of the cell, suggesting that in the context of the embryo the major determinant of spindle orientation is the external forces. These data together with the fact that in the presence of high cell shape anisotropy FAK morphants orient correctly, strongly suggest that the primary defect of FAK downregulation is loss of the ability to orient depending on force.

In an effort to address if the role of FAK in spindle orientation is physiologically significant in epithelial morphogenesis, we examined if FAK inhibition affects the development of tissues

that require oriented cell division. The first tissue that we examined was the prospective ectoderm that undergoes epiboly during *Xenopus* gastrulation. As mentioned in the Results section of chapter I, FAK regulates epiboly by guiding radial intercalation and maintaining spindle orientation at the plane of the epithelium. To examine the effects of spindle orientation on epiboly independently from radial intercalation, we inhibited FAK function after radial intercalation was completed and the AC was already 2-cell layers thick, using the inducible DN of FAK, FF-GR. Under these conditions, FAK inhibition led to spindle misorientation and cells of the superficial cell layer were found in the deep epithelial cell layers leading to increased thickness of the AC and gastrulation failure suggesting that epithelial spreading is largely dependent on oriented cell division. Another tissue that requires oriented cell division for proper morphogenesis is the kidney (Simons and Walz 2006). Blocking FAK function is this tissue with the inducible DN led to defective pronephros development including dilated tubules and ducts, thus highlighting the importance of FAK dependent spindle orientation during epithelial organ development.

4.3.2. Ligand independent integrin β1 activation guides spindle orientation

One of the most surprising findings of this project was that FAK inhibition in the *Xenopus* epithelium resulted in spindle misorientation at the cells of the epidermis, the outermost superficial cell layer. This observation was of special interest since the outermost cells of the prospective neuroectoderm are not in contact with the ECM and do not form FAs. These cells are attached to one another via tight junctions at their apical surface and via adherens junctions in their lateral regions (Fesenko, Kurth et al. 2000, Winklbauer 2012). They are also anchored to the deep cell layer via adherens junctions and only the deep layer is in contact with the ECM (Lee, Hynes et al. 1984). This suggests that cell-ECM interactions are not required for spindle orientation in the outer epithelium. This is supported by the fact that these cells are not in contact with the FN matrix and that inhibition of FN matrix assembly fails to affect oriented cell divisions in the outer epithelial layer (Marsden and DeSimone 2001), showing that spindle orientation in the cells of the *Xenopus* epidermis is ECM independent. If cell-ECM interactions are dispensable for oriented divisions in the outer epithelium, then is FAK's role in this context integrin independent? Cadherins have been shown to be required for proper spindle orientation, raising the possibility that FAK acts through adherens junctions to position the spindle in the epithelium, especially given the fact that both FAK and paxillin were localized at the lateral cortex of these cells and they have been previously shown to interact with adherens junction proteins (Sun, Shikata et al. 2009, Dubrovskyi, Tian et al. 2012). Alternatively, FAK may guide

spindle orientation downstream of integrin signaling in a ligand independent manner. This suggests that the role of integrins in epithelial tissue spindle orientation is independent from their role in cell-ECM interactions and FAK's role in this context is again stemming from transducing integrin dependent signals.

As mentioned above, integrins have a well documented role in the determination of the division axis, however in every case this has been attributed to their role in ECM adhesion and signaling. Some examples include; defective asymmetric division of basal keratinocytes during stratification in integrin β1 knockout mice (Lechler and Fuchs 2005) and during symmetric divisions of non-polarized cultured cells where disruption of integrin β1 dependent cell adhesion leads to spindle misorientation with respect to the substrate (Toyoshima and Nishida 2007). In addition, studies have implicated integrins in the regulation of divisions in polarized epithelial cells (Chen and Krasnow 2012, Akhtar and Streuli 2013). However, a direct role in spindle orientation in this context is difficult to conclude given the fact that integrins regulate basement membrane deposition and apicobasal polarity, raising the possibility that the observed spindle orientation defects may be secondary to defects in epithelial polarity (Ojakian and Schwimmer 1994). Overall, integrins are broadly implicated in the regulation of spindle orientation through their interactions with ECM components and signaling from FAs. However, a hint of an ECM independent role of integrins in spindle orientation comes from studies in the fly showing that although integrin signaling is required for the correct orientation of the mitotic apparatus and maintenance of the ovarian monolayer epithelium, cell-ECM interactions are dispensable (Fernandez-Minan, Martin-Bermudo et al. 2007). Interestingly, integrins are expressed in the *Xenopus* outer epithelium and disrupting integrin β1 function in these cells resulted in spindle misorientation supporting our hypothesis that an integrin based mechanosensory complex might guide spindle orientation, in the absence though of ligand binding. In agreement with our hypothesis, a recent study provided the first evidence of ligand independent integrin β1 activation. Through a series of experiments taking advantage of uPAR´s ability to bind VN, the authors showed that integrin β1 can be activated through membrane tension in cells adhering in an integrin independent fashion. In addition, the authors showed that this activation leads to signaling from active β1 including phosphorylation of the downstream target Cas (Ferraris, Schulte et al. 2014).

In this study, by using integrin monoclonal antibodies that specifically recognize the active conformation of integrins (Byron, Humphries et al. 2009), we show that integrin β1 becomes activated at the lateral cortex of mitotic adherent cells in culture in areas that are not in contact with the ECM. The activation of integrin β1 displays asymmetry throughout the cortex, both

along the apicobasal axis and at the plane of the spindle. The asymmetric activation of integrin β1 depends on the asymmetry in the distribution of the RFs and consequently of the external forces applied on the cortex. Specifically, there is apicobasal polarity with active β1 enriched at the basolateral regions of the cortex where the RFs terminate and no active β1 at the apical regions where there is no ECM, or RF terminations. Moreover, the distribution of active β1 at the plane of the spindle displays an asymmetry where integrin β1 is preferentially activated at the areas where maximal forces are exerted on the cortex, corresponding to the spindle capture sites. This finding is supported by data showing that cortically active integrin β1 co-localizes with the members of the cortical capture machinery, LGN and NuMA. The asymmetric distribution of active β1 in areas not in contact with ECM suggests that force transmitted through the RFs activates β1. This is also supported by data showing that integrin β1 activation on the cortex is independent of astral microtubules but relies on the presence of intact RFs and RF distribution dictates the distribution of active integrin β1, similarly to the case of RF-dependent cortical accumulation of LGN and NuMA (Kaushik, Yu et al. 2003, Seldin, Poulson et al. 2013). Importantly, the activation of β1 on the cortex is independent of β1 activation at the cell-ECM interface, since cells seeded on VN, a substrate that cells can adhere in an integrin β1 independent manner, display integrin β1 lateral cortical activation and orient their spindles properly. As mentioned above, a ligand independent integrin β1 activation was suggested in a study by the Sidenius group in which a system was developed where cells adhered in an integrin independent fashion (Ferraris, Schulte et al. 2014). The physiological relevance of this mode of activation and if it actually occurs in parallel with ligand dependent activation was not clear, given the artificial nature of the system used. Nevertheless, the authors convincingly demonstrated that integrin β1 can be activated by membrane tension and here we provide evidence that ligand dependent and independent activation of integrin β1 co-exist in mitotic cells. The activation of integrin β1 on the cortex of mitotic cells in conjunction with previous work implicating it in spindle orientation, raised the possibility that β1 has both ligand dependent as well as ligand independent roles in this process. Interestingly, we noted that the ligand independent pool of active integrin β1 at the spindle capture sites co-localizes with the cortical capture machinery whereas the ligand engaged pool of active β1 at the basal cortex is not associated with the capture machinery. This raises the possibility that the two integrin β1 based complexes that are formed in the mitotic cortex have different signaling properties that might contribute to orient the mitotic spindle. Although it is possible that the ligand engaged pool of active β1 can provide an exclusion signal at the basal cortex so as the cortical capture machinery would not accumulate in this area, this is highly unlikely since in the cells in the 3D adhesion assay the spindle capture points correspond to ligand engaged active integrin β1 sites.

Thus, the exclusion of the LGN/NuMA from the basal cortex under physiological conditions probably stems from the metaphase plate derived Ran-GTP dependent signal that promotes dissociation of the complex in regions near the chromosomes (Kiyomitsu and Cheeseman 2012). Because the RFs that terminate at the lateral cortex are larger and are expected to exert greater forces in these areas than at the basal surface, we propose that the force activated pool of integrin β1 is principally responsible for guiding the spindle capture (at the areas where the RFs exert maximal forces). Ligand dependent roles of integrin β1 in spindle orientation clearly stem from the role of integrins as receptors for cell adhesion but additionally, through the requirement of signaling through β1 for proper polarization of epithelia (Ojakian and Schwimmer 1994). For this reason separating the ligand dependent from ligand independent roles is not trivial however, our data showing that both loss of active β1 from the cortex as well as loss of its asymmetric distribution lead to spindle misorientation, are highly suggestive that cortical activation of β1 is critical for correct spindle orientation. Importantly, inhibition of β1 activation on cells seeded on VN provides strong support for a ligand independent role of β1 in this process. These results together with the *in vivo* data in which disruption of integrin β1 function or of the downstream targets of integrin β1 signaling FAK and paxillin, led to spindle misorientation in the *Xenopus* epidermis, provide additional support for the notion that integrin β1 has a ligand independent role in spindle orientation.

4.3.3. Conserved interactions between the members of an integrin based cortical mechanosensory complex (CMC) guide spindle orientation independently of cell context

Integrin activation is linked with the formation of the FAs, which are composed of a multitude of FA proteins many of which are in their active/phosphorylated state. Our experiments revealed that four core members of the FA complex are required for spindle orientation both in adherent cells and in the *Xenopus* epithelium, including FAK, paxillin, Src and Cas. In an effort to understand how these proteins orient the mitotic spindle we initially examined their distribution in mitotic cells in culture and in the *Xenopus* epithelium. In adherent cells, despite the fact that the majority of FAs disassemble during mitosis, FAK and paxillin positive basal adhesion complexes were retained at the areas where the RFs contact the substrate. Although this suggests that these complexes might transmit the external guiding stimuli to the spindle, these complexes are not enriched in active integrin β1 suggesting that the adhesive complex has diminished signaling properties and probably fulfills a mechanical anchoring requirement rather than having a signaling role. In other words, it is possible that their presence at the cell-

ECM interface is required for proper cell adhesion and anchoring of the RFs to the substrate and that is indirectly required for spindle orientation. In contrast, the active forms of several FA proteins including FAK, Src and Cas localize preferentially at the lateral cortex where the bulk of active integrin β1 is localized, suggesting that a cortical mechanosensory complex (CMC) is formed at the spindle capture sites. Importantly, we have shown that the CMC forms in response to integrin β1 activation, suggesting that β1 activation leads to the formation of a cortical signaling complex important for spindle orientation. The fact that integrin β1 becomes activated on the cortex in response to force together with the data showing that the members of the CMC become phosphorylated in response to integrin β1 activation suggest that the CMC is responsible for facilitating signal transduction from force activated β1 to the spindle. This is supported by the results showing that loss of FAK leads to spindle misorientation due to defective force sensing by the spindle. Importantly, we have shown that the CMC is formed in several cell types including the mammalian epithelial monolayer (MDCK cells) and the *Xenopus* outermost epithelium. In the epithelial tissues, the active forms of integrin, FAK, Src and Cas are enriched on the lateral cortex specifically in mitotic cells. Here we propose the following models of how integrin β1 guides spindle orientation irrespective of cell context (**Figure 104**). Our results suggest that in cultured mitotic cells there are two pools of active β1; one at the cell-ECM interface which is ligand dependent and one at the mid-lateral regions of the cortex, which is ligand independent. The adhesive complex at the RF-ECM interface is composed of integrin β1, FAK and paxillin and likely has an anchoring role to link the RFs to the substrate and maintain proper cell adhesion during mitosis, since there is no enrichment of active β1. However, the cortical pool of integrin β1 is highly activated at the spindle capture sites and co-localizes with the members of the cortical machinery LGN and NuMA. We suggest that cortical integrin β1 becomes activated by forces exerted on the mitotic cortex transmitted by the RFs and/or cell-cell junctions. Integrin β1 activation leads to the formation of the CMC which guides astral microtubule capture. In the case of the embryo, although we do not have information of how active β1 is distributed in the cells of the *Xenopus* outermost epithelium, we have shown that integrin β1, FAK and paxillin localize on the basolateral cortex (**Figure 104**). However, in mitotic cells the CMC (P-FAK, P-Cas and P-Src) is localized specifically on the lateral cortex of mitotic cells similarly to the *in vitro* situation.

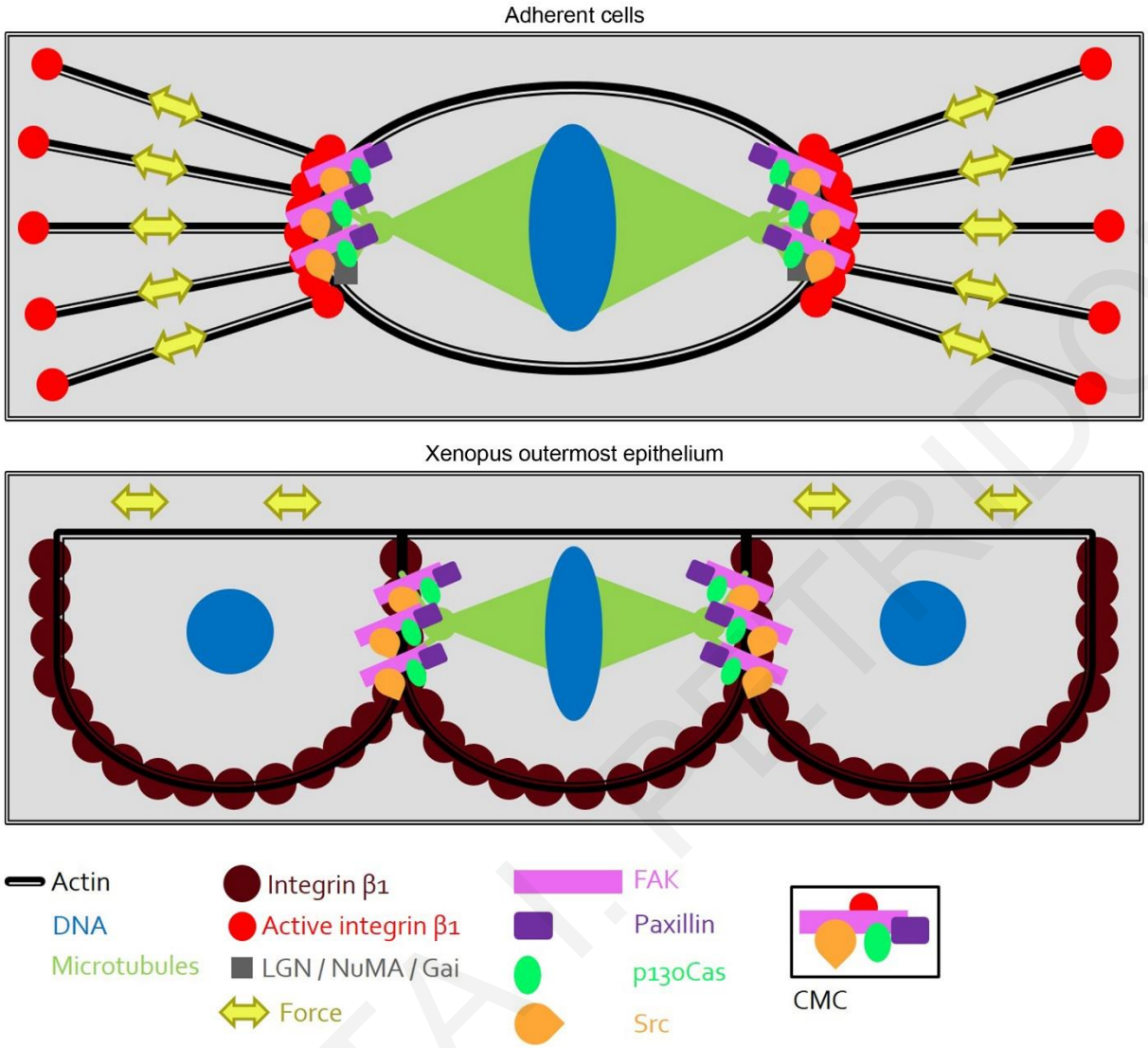

Figure 104: Model of integrin based CMC formation in mitotic adherent and epithelial cells.
In adherent mitotic cells in culture integrin β1 is activated at the cell-ECM interface and at the lateral cortex. Cortical integrin β1 becomes activated in a ligand independent fashion by force transduction through the RFs at the spindle capture sites co-localizing with the cortical capture machinery. Integrin β1 activation leads to the formation of the CMC at the spindle capture sites which subsequently orients the mitotic spindle. At the vertebrate epithelium integrin β1 is localized at the basolateral region of epithelial cells and the CMC is formed at the lateral cortex of mitotic cells. The formation of the CMC in this context is probably driven by forces exerted at the plane of the epithelium.

Functional analysis of the interactions between the members of the CMC that are required to promote spindle orientation revealed that these interactions are conserved both in mitotic cells in culture and *in vivo* supporting the hypothesis that the CMC has a conserved role in orienting the mitotic spindle irrespective of tissue context. We also examined important interactions of the CMC proteins by utilizing FAK and Cas null MEFs as well as FAK morphant epithelia that exhibit spindle misorientation by introducing several mutant forms of the proteins and

evaluating the ability to rescue. Initial experiments to identify the determinants of FAK function in spindle orientation revealed that although the kinase domain of FAK is required, the kinase activity of FAK is dispensable in this process. This is the first report of a kinase domain dependent but kinase activity independent role of FAK. Although this result suggested that the kinase activity is dispensable for spindle orientation, later experiments revealed that autophosphorylation of FAK on Tyr397 is necessary and subsequent Src binding on FAK, raising the question how can the KD mutant fully rescue spindle misorientation? Previous studies provided evidence that when this mutant is expressed in FAK null cells, although it fails to elicit phosphorylation of downstream targets of FAK (such as paxillin) it retains some phosphorylation on Tyr397 (Sieg, Hauck et al. 1999, Lim, Chen et al. 2010) which is evidently sufficient for Src binding (Schlaepfer and Hunter 1996). This suggests that either the retained basal kinase activity of the K454R mutant is sufficient for spindle orientation or more likely that Tyr397 phosphorylation during mitosis is carried out by another kinase. Further experiments revealed that bindings of Cas on the PR2 of FAK and of paxillin on the FAT domain of FAK are both necessary for FAK's role in spindle orientation. Thus, we suggest that FAK acts as a bridge to recruit Src, Cas and paxillin in a complex to promote force transduction to the spindle. Experiments performed in Cas null cells showed that phosphorylation of Cas at the SD is required but the direct binding of Cas with Src (the kinase phosphorylating Cas SD) is dispensable. However, Src kinase activity was previously reported to be required for spindle orientation in adherent cells (Thery, Racine et al. 2005), a finding that we have expanded to the *Xenopus* epithelium. These data suggest that FAK acts as a scaffold so as Src and Cas come in close proximity allowing Src to phosphorylate Cas and to facilitate mechanotransduction to the spindle. This is additionally supported by prior work showing that FAK's kinase activity is dispensable for Cas SD phosphorylation (Lim, Chen et al. 2010), since the FAK K454R mutant is able to promote Cas SD phosphorylation acting as a docking protein for Src recruitment and Cas (Ruest, Shin et al. 2001). The observation however, that the Y397F mutant can partially rescue the phenotype can be attributed to the fact that this mutant can presumably retain some Src binding capacity through its SH3 domain on the PR1 of FAK which is located near the Tyr397 site (Thomas, Ellis et al. 1998). However, it should be noted that the Y397F mutant also abolishes PI3K binding on FAK (Chen, Appeddu et al. 1996). Since PI3K has been previously involved in spindle orientation in adherent cells by accumulating PIP_3 at the mid-cortex of mitotic cells in an integrin dependent manner (Toyoshima, Matsumura et al. 2007), it is possible that the CMC and PI3K dependent pathways may act together to promote correct spindle orientation. However, since the PIP_3 dependent mechanism of spindle orientation is not

conserved in the polarized MDCK cells (Toyoshima, Matsumura et al. 2007) in contrast to the CMC, suggests that the two mechanisms may be independent.

How does Cas phosphorylation can directly control spindle capture is not clear. One possibility stems from the fact that the established role of the FA proteins is to link the external stimuli to the actin cytoskeleton (DeMali, Wennerberg et al. 2003). It has been suggested that a subcortical actin pool influences the capture sites of astral microtubules by generating pulling forces on the centrosomes (Fink, Carpi et al. 2011). Moreover, it has been recently shown that the binding of myosin10 at the astral microtubules is required for centrosome positioning according to the actin clouds (Kwon, Bagonis et al. 2015). These data raise the possibility that Cas phosphorylation may alter the dynamics of the subcortical actin that orients the mitotic spindle. In fact there is evidence that phosphorylation of Cas at the SD acts as a binding site for Nck (Li, Fan et al. 2001) and Nck adaptors play a crucial role in regulating actin dynamics (Rivera, Antoku et al. 2006). In addition, it has been shown that Cas phosphorylation leads to Rac activation (Sharma and Mayer 2008) suggesting that it is possible that the subcortical actin pool is regulated through localized activation of Rac downstream of Cas phosphorylation during mitosis. In agreement with such an explanation, Rac activity is polarized and regulates anchoring of the spindle in mammalian oocytes (Halet and Carroll 2007). Moreover, several lines of evidence show that the binding of Nck on the phosphorylated SD of Cas is crucial for the interaction of Rac with PAK in order to promote PAK activation and PAK dependent actin reorganization (Szczepanowska 2009). Since the members of the PAK family interact with paxillin (Turner, Brown et al. 1999, Hashimoto, Tsubouchi et al. 2001) and are necessary for mitotic spindle orientation (Mitsushima, Toyoshima et al. 2009, Bompard and Morin 2012, deLeon, Puglise et al. 2012, Bompard, Rabeharivelo et al. 2013) it is possible that the CMC orients the mitotic spindle through interactions with the Rac/Nck/PAK cytoskeletal rearrangement pathway.

The notion that the role of the CMC is to link the external mechanical stimuli to the actin cytoskeleton similarly to what the FA complex does in cell-ECM adhesion is quite attractive since it suggests that the members of the FA protein family exhibit conserved functions independently from the cell context and that these functions can regulate biological processes shared among a wide range of organisms. A detailed comparison of the composition of the CMC and the FA complexes would be quite useful in understanding how the FA proteins evolved in order to retain conserved functions in distinct developmental processes.

5. Conclusions

In conclusion, we have explored the role of FAK in *Xenopus* embryonic development by performing a descriptive analysis of its expression and spatiotemporal pattern of activation during development, a detailed characterization of the role of the major domains in different cell contexts utilizing several loss of function approaches both in epithelial and mesodermal tissues. Moreover, we have expanded this work to address conserved functions of FA proteins in general, not only during *Xenopus* embryonic development but also in human cultured cells.

The results obtained from this study have shown that FAK displays versatile roles during *Xenopus* embryonic development and that its mechanisms of function strongly depend on tissue context. We have concluded that in mesodermal tissues FAK exhibits the highest phosphorylation levels and that active phosphorylated FAK is tightly localized on the plasma membrane. By performing experiments to identify the determinants of the plasma membrane localization of active FAK we noted that this localization pattern requires both the N-terminus and C-terminus of FAK. We utilized a construct composed of these two regions of FAK (FF) as a DN and were able to effectively block FAK function in the mesoderm, resulting in a phenotype very similar to that of the FAK null mice (Furuta, Ilic et al. 1995). We have shown that FAK is required for the survival of mesodermal tissues, a role associated with the function of FAK on the centrosome during mitosis and involving the phosphorylation of FAK on Ser732 (Park, Shen et al. 2009) (**Figure 105**). Inhibition of FAK in the prospective ectoderm however, which is the other embryonic tissue that exhibits high levels of phosphorylated FAK (BCR cells) resulted in a much earlier phenotype. FAK inhibition in the epithelial layers led to blastopore closure failure, defective internalization of the mesendoderm and gastrulation arrest. This was a surprising result since inhibition of FAK in the mesodermal belt which is the tissue driving blastopore closure (Keller and Shook 2008), did not significantly affect blastopore closure whereas FAK inhibition in the ectoderm arrested gastrulation. Further experiments revealed that loss of FAK blocks the morphogenetic movement of epiboly of the inner epithelial cell layers by inhibiting radial intercalation and spindle orientation of these cells, processes that are regulated by the FN fibrillar matrix that lies the BCR (**Figure 105**). In an effort to understand how epiboly affects blastopore closure and to comprehend how the epithelial AC tissue is mechanically linked to the mesodermal belt we came into the conclusion that epiboly plays an essential but permissive role during *Xenopus* gastrulation and that under physiological conditions the ectoderm holds back the mesoderm and through epiboly tissue tension is released allowing blastopore closure. Moreover, we have shown that FAK has a central role in determining spindle orientation and that is required for proper epithelial morphogenesis during

embryonic development such as the morphogenesis of the prospective ectoderm during *Xenopus* epiboly and of epithelial organs such as the kidney during organogenesis (**Figure 105**). We have shown that FAK in involved in spindle orientation by regulating the sensing and responses of the spindle to the external forces that are applied on the mitotic cell (**Figure 105**) (Fink, Carpi et al. 2011, Campinho, Behrndt et al. 2013). Interestingly, FAK's involvement in spindle orientation relies almost exclusively on its scaffolding abilities rather than on its kinase signaling properties.

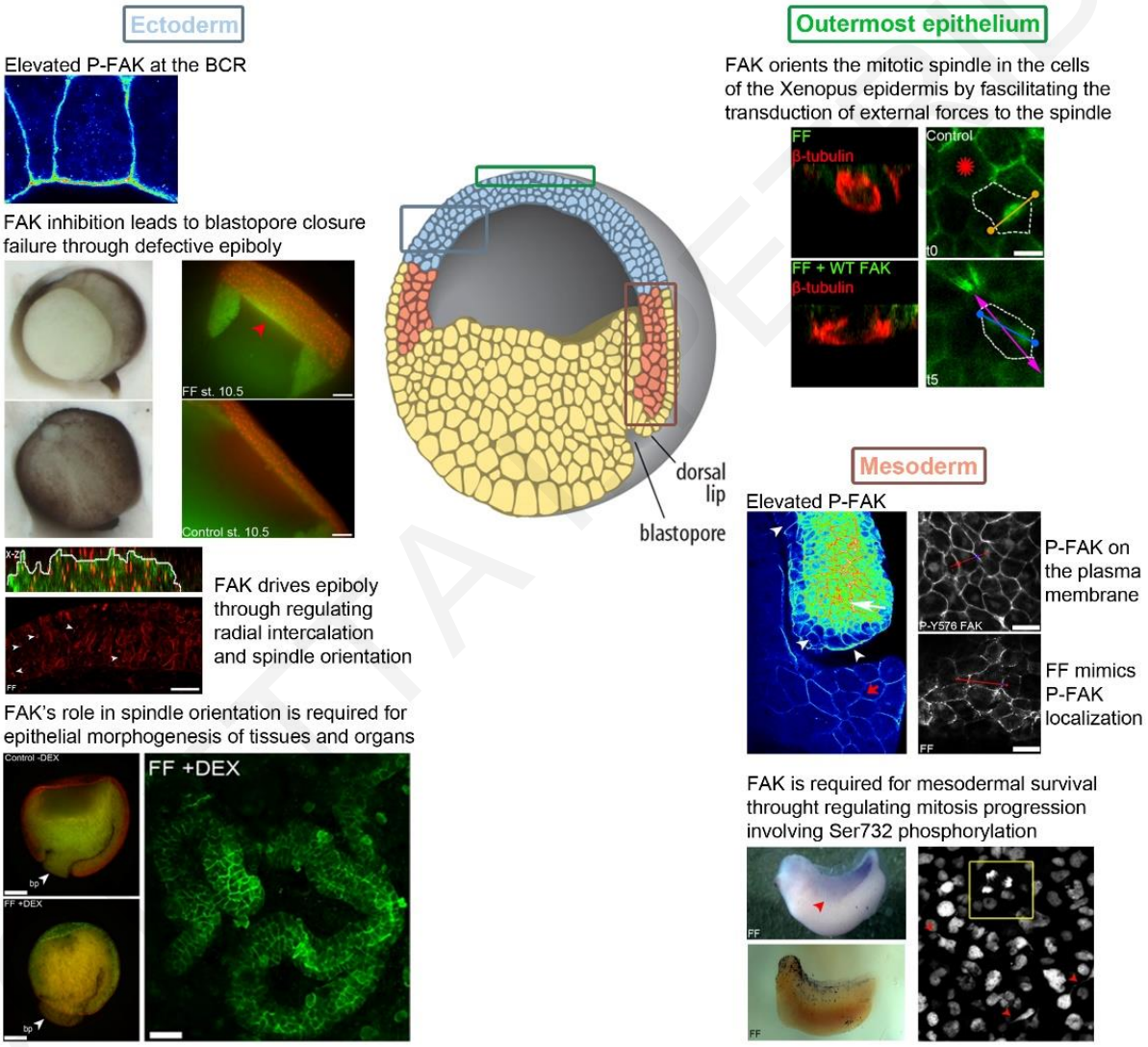

Figure 105: Versatile roles of FAK during *Xenopus* embryonic development.

Schematic summary of the differential functions of FAK in the mesoderm, ectoderm and epidermis.

The last part of this project focused on understanding how the well characterized FA protein FAK has a role in determining the cell division axis in a tissue context that is ECM independent. The results of this part of the work led to the surprising conclusion that FAK and several core

members of the FA complex, including Src and p130Cas, form a mechanosensory complex at the mitotic cortex downstream of ligand independent integrin β1 activation. The conservation of the CMC in the embryo suggests a possible broader role for this complex during vertebrate development. The fact that during embryogenesis cells are exposed to mechanical stimuli from multiple sources due to massive movements and tissue rearrangements raises the possibility that the CMC may have additional roles in tissue morphogenesis independent of cell division. These findings may also have a broader significance not only in developmental biology but also in understanding the evolution of the FA complex. Since the CMC is formed in an adhesion independent manner it may suggest that FA proteins also serve adhesion independent functions. Support for this comes from a recent study from our lab showing that the FA proteins FAK, paxillin and vinculin are also involved in motile ciliogenesis by forming ciliary adhesions, complexes formed at the basal bodies in an ECM independent fashion and link basal bodies to the actin cytoskeleton (Antoniades, Stylianou et al. 2014). Thus, the distinct roles of the FA proteins suggest that these proteins retain conserved features that allow them to form actin associated complexes which however, can be adapted for differential functions, depending for example on the presence of an adhesive environment. The conservation of this protein complex independently of cell context highlights the importance of this protein family for proper cell function. Such possibility deserves further investigation since it could provide evidence in understanding how these proteins were co-opted for differential functions over the course of metazoan evolution.

6. References

Abbi, S., H. Ueda, C. Zheng, L. A. Cooper, J. Zhao, R. Christopher and J. L. Guan (2002). "Regulation of focal adhesion kinase by a novel protein inhibitor FIP200." Mol Biol Cell **13**(9): 3178-3191.

Akhtar, N. and C. H. Streuli (2013). "An integrin-ILK-microtubule network orients cell polarity and lumen formation in glandular epithelium." Nat Cell Biol **15**(1): 17-27.

Alexandrova, A. Y., K. Arnold, S. Schaub, J. M. Vasiliev, J. J. Meister, A. D. Bershadsky and A. B. Verkhovsky (2008). "Comparative dynamics of retrograde actin flow and focal adhesions: formation of nascent adhesions triggers transition from fast to slow flow." PLoS One **3**(9): e3234.

Alfandari, D., H. Cousin, A. Gaultier, K. Smith, J. M. White, T. Darribere and D. W. DeSimone (2001). "Xenopus ADAM 13 is a metalloprotease required for cranial neural crest-cell migration." Curr Biol **11**(12): 918-930.

Antoniades, I., P. Stylianou and P. A. Skourides (2014). "Making the connection: ciliary adhesion complexes anchor basal bodies to the actin cytoskeleton." Dev Cell **28**(1): 70-80.

Arold, S. T. (2011). "How focal adhesion kinase achieves regulation by linking ligand binding, localization and action." Curr Opin Struct Biol **21**(6): 808-813.

Askari, J. A., C. J. Tynan, S. E. Webb, M. L. Martin-Fernandez, C. Ballestrem and M. J. Humphries (2010). "Focal adhesions are sites of integrin extension." J Cell Biol **188**(6): 891-903.

Baena-Lopez, L. A., A. Baonza and A. Garcia-Bellido (2005). "The orientation of cell divisions determines the shape of Drosophila organs." Curr Biol **15**(18): 1640-1644.

Balaban, N. Q., U. S. Schwarz, D. Riveline, P. Goichberg, G. Tzur, I. Sabanay, D. Mahalu, S. Safran, A. Bershadsky, L. Addadi and B. Geiger (2001). "Force and focal adhesion assembly: a close relationship studied using elastic micropatterned substrates." Nat Cell Biol **3**(5): 466-472.

Ballestrem, C., N. Erez, J. Kirchner, Z. Kam, A. Bershadsky and B. Geiger (2006). "Molecular mapping of tyrosine-phosphorylated proteins in focal adhesions using fluorescence resonance energy transfer." J Cell Sci **119**(Pt 5): 866-875.

Banon-Rodriguez, I., M. Galvez-Santisteban, S. Vergarajauregui, M. Bosch, A. Borreguero-Pascual and F. Martin-Belmonte (2014). "EGFR controls IQGAP basolateral membrane localization and mitotic spindle orientation during epithelial morphogenesis." EMBO J **33**(2): 129-145.

Barker, N., J. H. van Es, J. Kuipers, P. Kujala, M. van den Born, M. Cozijnsen, A. Haegebarth, J. Korving, H. Begthel, P. J. Peters and H. Clevers (2007). "Identification of stem cells in small intestine and colon by marker gene Lgr5." Nature **449**(7165): 1003-1007.

Bass, M. D., B. Patel, I. G. Barsukov, I. J. Fillingham, R. Mason, B. J. Smith, C. R. Bagshaw and D. R. Critchley (2002). "Further characterization of the interaction between the cytoskeletal proteins talin and vinculin." Biochem J **362**(Pt 3): 761-768.

Bate, N., A. R. Gingras, A. Bachir, R. Horwitz, F. Ye, B. Patel, B. T. Goult and D. R. Critchley (2012). "Talin contains a C-terminal calpain2 cleavage site important in focal adhesion dynamics." PLoS One **7**(4): e34461.

Bazzoni, G., D. T. Shih, C. A. Buck and M. E. Hemler (1995). "Monoclonal antibody 9EG7 defines a novel beta 1 integrin epitope induced by soluble ligand and manganese, but inhibited by calcium." J Biol Chem **270**(43): 25570-25577.

Beauvais, D. M. and A. C. Rapraeger (2004). "Syndecans in tumor cell adhesion and signaling." Reprod Biol Endocrinol **2**: 3.

Beckerle, M. C. (1997). "Zyxin: zinc fingers at sites of cell adhesion." Bioessays **19**(11): 949-957.

Beckerle, M. C., K. Burridge, G. N. DeMartino and D. E. Croall (1987). "Colocalization of calcium-dependent protease II and one of its substrates at sites of cell adhesion." Cell **51**(4): 569-577.

Bellis, S. L., J. T. Miller and C. E. Turner (1995). "Characterization of tyrosine phosphorylation of paxillin in vitro by focal adhesion kinase." J Biol Chem **270**(29): 17437-17441.

Bergstralh, D. T., T. Haack and D. St Johnston (2013). "Epithelial polarity and spindle orientation: intersecting pathways." Philos Trans R Soc Lond B Biol Sci **368**(1629): 20130291.

Bershadsky, A., A. Chausovsky, E. Becker, A. Lyubimova and B. Geiger (1996). "Involvement of microtubules in the control of adhesion-dependent signal transduction." Curr Biol **6**(10): 1279-1289.

Bertolucci, C. M., C. D. Guibao and J. Zheng (2005). "Structural features of the focal adhesion kinase-paxillin complex give insight into the dynamics of focal adhesion assembly." Protein Sci **14**(3): 644-652.

Bianchi, M., S. De Lucchini, O. Marin, D. L. Turner, S. K. Hanks and E. Villa-Moruzzi (2005). "Regulation of FAK Ser-722 phosphorylation and kinase activity by GSK3 and PP1 during cell spreading and migration." Biochem J **391**(Pt 2): 359-370.

Bjerke, M. A., B. J. Dzamba, C. Wang and D. W. DeSimone (2014). "FAK is required for tension-dependent organization of collective cell movements in Xenopus mesendoderm." Dev Biol **394**(2): 340-356.

Bompard, G. and N. Morin (2012). "p21-activated kinase 4 regulates mitotic spindle positioning and orientation." Bioarchitecture **2**(4): 130-133.

Bompard, G., G. Rabeharivelo, J. Cau, A. Abrieu, C. Delsert and N. Morin (2013). "P21-activated kinase 4 (PAK4) is required for metaphase spindle positioning and anchoring." Oncogene **32**(7): 910-919.

Brami-Cherrier, K., N. Gervasi, D. Arsenieva, K. Walkiewicz, M. C. Boutterin, A. Ortega, P. G. Leonard, B. Seantier, L. Gasmi, T. Bouceba, G. Kadare, J. A. Girault and S. T. Arold (2014). "FAK dimerization controls its kinase-dependent functions at focal adhesions." EMBO J **33**(4): 356-370.

Braren, R., H. Hu, Y. H. Kim, H. E. Beggs, L. F. Reichardt and R. Wang (2006). "Endothelial FAK is essential for vascular network stability, cell survival, and lamellipodial formation." J Cell Biol **172**(1): 151-162.

Brunton, V. G., E. Avizienyte, V. J. Fincham, B. Serrels, C. A. Metcalf, 3rd, T. K. Sawyer and M. C. Frame (2005). "Identification of Src-specific phosphorylation site on focal adhesion kinase: dissection of the role of Src SH2 and catalytic functions and their consequences for tumor cell behavior." Cancer Res **65**(4): 1335-1342.

Burgaya, F., A. Menegon, M. Menegoz, F. Valtorta and J. A. Girault (1995). "Focal adhesion kinase in rat central nervous system." Eur J Neurosci **7**(8): 1810-1821.

Bussolino, F., A. Mantovani and G. Persico (1997). "Molecular mechanisms of blood vessel formation." Trends Biochem Sci **22**(7): 251-256.

Byron, A., J. D. Humphries, J. A. Askari, S. E. Craig, A. P. Mould and M. J. Humphries (2009). "Anti-integrin monoclonal antibodies." J Cell Sci **122**(Pt 22): 4009-4011.

Cai, X., D. Lietha, D. F. Ceccarelli, A. V. Karginov, Z. Rajfur, K. Jacobson, K. M. Hahn, M. J. Eck and M. D. Schaller (2008). "Spatial and temporal regulation of focal adhesion kinase activity in living cells." Mol Cell Biol **28**(1): 201-214.

Calalb, M. B., T. R. Polte and S. K. Hanks (1995). "Tyrosine phosphorylation of focal adhesion kinase at sites in the catalytic domain regulates kinase activity: a role for Src family kinases." Mol Cell Biol **15**(2): 954-963.

Calalb, M. B., X. Zhang, T. R. Polte and S. K. Hanks (1996). "Focal adhesion kinase tyrosine-861 is a major site of phosphorylation by Src." Biochem Biophys Res Commun **228**(3): 662-668.

Campbell, I. D. and M. J. Humphries (2011). "Integrin structure, activation, and interactions." Cold Spring Harb Perspect Biol **3**(3).

Campinho, P., M. Behrndt, J. Ranft, T. Risler, N. Minc and C. P. Heisenberg (2013). "Tension-oriented cell divisions limit anisotropic tissue tension in epithelial spreading during zebrafish epiboly." Nat Cell Biol **15**(12): 1405-1414.

Carisey, A. and C. Ballestrem (2011). "Vinculin, an adapter protein in control of cell adhesion signalling." Eur J Cell Biol **90**(2-3): 157-163.

Carpenter, C. L. and L. C. Cantley (1996). "Phosphoinositide kinases." Curr Opin Cell Biol **8**(2): 153-158.

Carvalho, C. A., S. Moreira, G. Ventura, C. E. Sunkel and E. Morais-de-Sa (2015). "Aurora A triggers Lgl cortical release during symmetric division to control planar spindle orientation." Curr Biol **25**(1): 53-60.

Cary, L. A., J. F. Chang and J. L. Guan (1996). "Stimulation of cell migration by overexpression of focal adhesion kinase and its association with Src and Fyn." J Cell Sci **109 (Pt 7)**: 1787-1794.

Cary, L. A. and J. L. Guan (1999). "Focal adhesion kinase in integrin-mediated signaling." Front Biosci **4**: D102-113.

Cary, L. A., D. C. Han, T. R. Polte, S. K. Hanks and J. L. Guan (1998). "Identification of p130Cas as a mediator of focal adhesion kinase-promoted cell migration." J Cell Biol **140**(1): 211-221.

Castanon, I. and M. Gonzalez-Gaitan (2011). "Oriented cell division in vertebrate embryogenesis." Curr Opin Cell Biol **23**(6): 697-704.

Ceccarelli, D. F., H. K. Song, F. Poy, M. D. Schaller and M. J. Eck (2006). "Crystal structure of the FERM domain of focal adhesion kinase." J Biol Chem **281**(1): 252-259.

Chan, K. T., D. A. Bennin and A. Huttenlocher (2010). "Regulation of adhesion dynamics by calpain-mediated proteolysis of focal adhesion kinase (FAK)." J Biol Chem **285**(15): 11418-11426.

Chang, F., C. A. Lemmon, D. Park and L. H. Romer (2007). "FAK potentiates Rac1 activation and localization to matrix adhesion sites: a role for betaPIX." Mol Biol Cell **18**(1): 253-264.

Chen, C. S., J. L. Alonso, E. Ostuni, G. M. Whitesides and D. E. Ingber (2003). "Cell shape provides global control of focal adhesion assembly." Biochem Biophys Res Commun **307**(2): 355-361.

Chen, H. C., P. A. Appeddu, H. Isoda and J. L. Guan (1996). "Phosphorylation of tyrosine 397 in focal adhesion kinase is required for binding phosphatidylinositol 3-kinase." J Biol Chem **271**(42): 26329-26334.

Chen, H. C., P. A. Appeddu, J. T. Parsons, J. D. Hildebrand, M. D. Schaller and J. L. Guan (1995). "Interaction of focal adhesion kinase with cytoskeletal protein talin." J Biol Chem **270**(28): 16995-16999.

Chen, J. and M. A. Krasnow (2012). "Integrin Beta 1 suppresses multilayering of a simple epithelium." PLoS One **7**(12): e52886.

Chen, S. Y. and H. C. Chen (2006). "Direct interaction of focal adhesion kinase (FAK) with Met is required for FAK to promote hepatocyte growth factor-induced cell invasion." Mol Cell Biol **26**(13): 5155-5167.

Chen, T. H., P. C. Chan, C. L. Chen and H. C. Chen (2011). "Phosphorylation of focal adhesion kinase on tyrosine 194 by Met leads to its activation through relief of autoinhibition." Oncogene **30**(2): 153-166.

Chen, X. L., J. O. Nam, C. Jean, C. Lawson, C. T. Walsh, E. Goka, S. T. Lim, A. Tomar, I. Tancioni, S. Uryu, J. L. Guan, L. M. Acevedo, S. M. Weis, D. A. Cheresh and D. D. Schlaepfer (2012). "VEGF-induced vascular permeability is mediated by FAK." Dev Cell **22**(1): 146-157.

Choquet, D., D. P. Felsenfeld and M. P. Sheetz (1997). "Extracellular matrix rigidity causes strengthening of integrin-cytoskeleton linkages." Cell **88**(1): 39-48.

Chu, P. Y., L. Y. Huang, C. H. Hsu, C. C. Liang, J. L. Guan, T. H. Hung and T. L. Shen (2009). "Tyrosine phosphorylation of growth factor receptor-bound protein-7 by focal adhesion kinase in the regulation of cell migration, proliferation, and tumorigenesis." J Biol Chem **284**(30): 20215-20226.

Cobb, B. S., M. D. Schaller, T. H. Leu and J. T. Parsons (1994). "Stable association of pp60src and pp59fyn with the focal adhesion-associated protein tyrosine kinase, pp125FAK." Mol Cell Biol **14**(1): 147-155.

Cohen, L. A. and J. L. Guan (2005). "Residues within the first subdomain of the FERM-like domain in focal adhesion kinase are important in its regulation." J Biol Chem **280**(9): 8197-8207.

Coll, J. L., A. Ben-Ze'ev, R. M. Ezzell, J. L. Rodriguez Fernandez, H. Baribault, R. G. Oshima and E. D. Adamson (1995). "Targeted disruption of vinculin genes in F9 and embryonic stem cells changes cell morphology, adhesion, and locomotion." Proc Natl Acad Sci U S A **92**(20): 9161-9165.

Cooley, M. A., J. M. Broome, C. Ohngemach, L. H. Romer and M. D. Schaller (2000). "Paxillin binding is not the sole determinant of focal adhesion localization or dominant-negative activity of focal adhesion kinase/focal adhesion kinase-related nonkinase." Mol Biol Cell **11**(9): 3247-3263.

Cooper, L. A., T. L. Shen and J. L. Guan (2003). "Regulation of focal adhesion kinase by its amino-terminal domain through an autoinhibitory interaction." Mol Cell Biol **23**(22): 8030-8041.

Corsi, J. M., C. Houbron, P. Billuart, I. Brunet, K. Bouvree, A. Eichmann, J. A. Girault and H. Enslen (2009). "Autophosphorylation-independent and -dependent functions of focal adhesion kinase during development." J Biol Chem **284**(50): 34769-34776.

Cortesio, C. L., L. R. Boateng, T. M. Piazza, D. A. Bennin and A. Huttenlocher (2011). "Calpain-mediated proteolysis of paxillin negatively regulates focal adhesion dynamics and cell migration." J Biol Chem **286**(12): 9998-10006.

Cousin, H. and D. Alfandari (2004). "A PTP-PEST-like protein affects alpha5beta1-integrin-dependent matrix assembly, cell adhesion, and migration in Xenopus gastrula." Dev Biol **265**(2): 416-432.

Crawford, B. D., C. A. Henry, T. A. Clason, A. L. Becker and M. B. Hille (2003). "Activity and distribution of paxillin, focal adhesion kinase, and cadherin indicate cooperative roles during zebrafish morphogenesis." Mol Biol Cell **14**(8): 3065-3081.

Critchley, D. R. (2009). "Biochemical and structural properties of the integrin-associated cytoskeletal protein talin." Annu Rev Biophys **38**: 235-254.

Cukierman, E., R. Pankov, D. R. Stevens and K. M. Yamada (2001). "Taking cell-matrix adhesions to the third dimension." Science **294**(5547): 1708-1712.

Dale, L. and J. M. Slack (1987). "Fate map for the 32-cell stage of Xenopus laevis." Development **99**(4): 527-551.

Danker, K., H. Hacke, J. Ramos, D. DeSimone and D. Wedlich (1993). "V(+)-fibronectin expression and localization prior to gastrulation in Xenopus laevis embryos." Mech Dev **44**(2-3): 155-165.

Davidson, L. A. (2011). "Embryo mechanics: balancing force production with elastic resistance during morphogenesis." Curr Top Dev Biol **95**: 215-241.

Davidson, L. A., B. D. Dzamba, R. Keller and D. W. Desimone (2008). "Live imaging of cell protrusive activity, and extracellular matrix assembly and remodeling during morphogenesis in the frog, Xenopus laevis." Dev Dyn **237**(10): 2684-2692.

Davidson, L. A., R. Keller and D. W. DeSimone (2004). "Assembly and remodeling of the fibrillar fibronectin extracellular matrix during gastrulation and neurulation in Xenopus laevis." Dev Dyn **231**(4): 888-895.

Davidson, L. A., M. Marsden, R. Keller and D. W. Desimone (2006). "Integrin alpha5beta1 and fibronectin regulate polarized cell protrusions required for Xenopus convergence and extension." Curr Biol **16**(9): 833-844.

Deakin, N. O. and C. E. Turner (2008). "Paxillin comes of age." J Cell Sci **121**(Pt 15): 2435-2444.

Defilippi, P., P. Di Stefano and S. Cabodi (2006). "p130Cas: a versatile scaffold in signaling networks." Trends Cell Biol **16**(5): 257-263.

del Rio, A., R. Perez-Jimenez, R. Liu, P. Roca-Cusachs, J. M. Fernandez and M. P. Sheetz (2009). "Stretching single talin rod molecules activates vinculin binding." Science **323**(5914): 638-641.

Delaval, B., A. Bright, N. D. Lawson and S. Doxsey (2011). "The cilia protein IFT88 is required for spindle orientation in mitosis." Nat Cell Biol **13**(4): 461-468.

deLeon, O., J. M. Puglise, F. Liu, J. Smits, M. B. ter Beest and M. M. Zegers (2012). "Pak1 regulates the orientation of apical polarization and lumen formation by distinct pathways." PLoS One **7**(7): e41039.

DeMali, K. A., K. Wennerberg and K. Burridge (2003). "Integrin signaling to the actin cytoskeleton." Curr Opin Cell Biol **15**(5): 572-582.

Deng, G., S. A. Curriden, G. Hu, R. P. Czekay and D. J. Loskutoff (2001). "Plasminogen activator inhibitor-1 regulates cell adhesion by binding to the somatomedin B domain of vitronectin." J Cell Physiol **189**(1): 23-33.

Deramaudt, T. B., D. Dujardin, A. Hamadi, F. Noulet, K. Kolli, J. De Mey, K. Takeda and P. Ronde (2011). "FAK phosphorylation at Tyr-925 regulates cross-talk between focal adhesion turnover and cell protrusion." Mol Biol Cell **22**(7): 964-975.

Di Paolo, G., L. Pellegrini, K. Letinic, G. Cestra, R. Zoncu, S. Voronov, S. Chang, J. Guo, M. R. Wenk and P. De Camilli (2002). "Recruitment and regulation of phosphatidylinositol phosphate kinase type 1 gamma by the FERM domain of talin." Nature **420**(6911): 85-89.

Dixon, R. D., Y. Chen, F. Ding, S. D. Khare, K. C. Prutzman, M. D. Schaller, S. L. Campbell and N. V. Dokholyan (2004). "New insights into FAK signaling and localization based on detection of a FAT domain folding intermediate." Structure **12**(12): 2161-2171.

Doherty, J. T., F. L. Conlon, C. P. Mack and J. M. Taylor (2010). "Focal adhesion kinase is essential for cardiac looping and multichamber heart formation." Genesis **48**(8): 492-504.

Du, Q. and I. G. Macara (2004). "Mammalian Pins is a conformational switch that links NuMA to heterotrimeric G proteins." Cell **119**(4): 503-516.

Du, Q., P. T. Stukenberg and I. G. Macara (2001). "A mammalian Partner of inscuteable binds NuMA and regulates mitotic spindle organization." Nat Cell Biol **3**(12): 1069-1075.

Dubash, A. D., M. M. Menold, T. Samson, E. Boulter, R. Garcia-Mata, R. Doughman and K. Burridge (2009). "Chapter 1. Focal adhesions: new angles on an old structure." Int Rev Cell Mol Biol **277**: 1-65.

Dubrovskyi, O., X. Tian, V. Poroyko, B. Yakubov, A. A. Birukova and K. G. Birukov (2012). "Identification of paxillin domains interacting with beta-catenin." FEBS Lett **586**(16): 2294-2299.

Dumbauld, D. W., H. Shin, N. D. Gallant, K. E. Michael, H. Radhakrishna and A. J. Garcia (2010). "Contractility modulates cell adhesion strengthening through focal adhesion kinase and assembly of vinculin-containing focal adhesions." J Cell Physiol **223**(3): 746-756.

Durgan, J., N. Kaji, D. Jin and A. Hall (2011). "Par6B and atypical PKC regulate mitotic spindle orientation during epithelial morphogenesis." J Biol Chem **286**(14): 12461-12474.

Dzamba, B. J., K. R. Jakab, M. Marsden, M. A. Schwartz and D. W. DeSimone (2009). "Cadherin adhesion, tissue tension, and noncanonical Wnt signaling regulate fibronectin matrix organization." Dev Cell **16**(3): 421-432.

Eide, B. L., C. W. Turck and J. A. Escobedo (1995). "Identification of Tyr-397 as the primary site of tyrosine phosphorylation and pp60src association in the focal adhesion kinase, pp125FAK." Mol Cell Biol **15**(5): 2819-2827.

Elinson, R. P. (2011). Cleavage and gastrulation in *Xenopus laevis* embryos. L. C. eLS. John Wiley & Sons.

Ezratty, E. J., M. A. Partridge and G. G. Gundersen (2005). "Microtubule-induced focal adhesion disassembly is mediated by dynamin and focal adhesion kinase." Nat Cell Biol **7**(6): 581-590.

Fassler, R. and M. Meyer (1995). "Consequences of lack of beta 1 integrin gene expression in mice." Genes Dev **9**(15): 1896-1908.

Fernandez-Minan, A., M. D. Martin-Bermudo and A. Gonzalez-Reyes (2007). "Integrin signaling regulates spindle orientation in Drosophila to preserve the follicular-epithelium monolayer." Curr Biol **17**(8): 683-688.

Ferraris, G. M., C. Schulte, V. Buttiglione, V. De Lorenzi, A. Piontini, M. Galluzzi, A. Podesta, C. D. Madsen and N. Sidenius (2014). "The interaction between uPAR and vitronectin triggers ligand-independent adhesion signalling by integrins." EMBO J **33**(21): 2458-2472.

Fesenko, I., T. Kurth, B. Sheth, T. P. Fleming, S. Citi and P. Hausen (2000). "Tight junction biogenesis in the early Xenopus embryo." Mech Dev **96**(1): 51-65.

Fey, J. and P. Hausen (1990). "Appearance and distribution of laminin during development of Xenopus laevis." Differentiation **42**(3): 144-152.

Fink, J., N. Carpi, T. Betz, A. Betard, M. Chebah, A. Azioune, M. Bornens, C. Sykes, L. Fetler, D. Cuvelier and M. Piel (2011). "External forces control mitotic spindle positioning." Nat Cell Biol **13**(7): 771-778.

Fischer, E., E. Legue, A. Doyen, F. Nato, J. F. Nicolas, V. Torres, M. Yaniv and M. Pontoglio (2006). "Defective planar cell polarity in polycystic kidney disease." Nat Genet **38**(1): 21-23.

Fonar, Y., Y. E. Gutkovich, H. Root, A. Malyarova, E. Aamar, V. M. Golubovskaya, S. Elias, Y. M. Elkouby and D. Frank (2011). "Focal adhesion kinase protein regulates Wnt3a gene expression to control cell fate specification in the developing neural plate." Mol Biol Cell **22**(13): 2409-2421.

Fonseca, P. M., N. Y. Shin, J. Brabek, L. Ryzhova, J. Wu and S. K. Hanks (2004). "Regulation and localization of CAS substrate domain tyrosine phosphorylation." Cell Signal **16**(5): 621-629.

Fraley, S. I., Y. Feng, R. Krishnamurthy, D. H. Kim, A. Celedon, G. D. Longmore and D. Wirtz (2010). "A distinctive role for focal adhesion proteins in three-dimensional cell motility." Nat Cell Biol **12**(6): 598-604.

Frame, M. C., H. Patel, B. Serrels, D. Lietha and M. J. Eck (2010). "The FERM domain: organizing the structure and function of FAK." Nat Rev Mol Cell Biol **11**(11): 802-814.

Franco, S. J., M. A. Rodgers, B. J. Perrin, J. Han, D. A. Bennin, D. R. Critchley and A. Huttenlocher (2004). "Calpain-mediated proteolysis of talin regulates adhesion dynamics." Nat Cell Biol **6**(10): 977-983.

Franke, T. F., D. R. Kaplan, L. C. Cantley and A. Toker (1997). "Direct regulation of the Akt proto-oncogene product by phosphatidylinositol-3,4-bisphosphate." Science **275**(5300): 665-668.

Friedland, J. C., M. H. Lee and D. Boettiger (2009). "Mechanically activated integrin switch controls alpha5beta1 function." Science **323**(5914): 642-644.

Furuta, Y., D. Ilic, S. Kanazawa, N. Takeda, T. Yamamoto and S. Aizawa (1995). "Mesodermal defect in late phase of gastrulation by a targeted mutation of focal adhesion kinase, FAK." Oncogene **11**(10): 1989-1995.

Gabarra-Niecko, V., P. J. Keely and M. D. Schaller (2002). "Characterization of an activated mutant of focal adhesion kinase: 'SuperFAK'." Biochem J **365**(Pt 3): 591-603.

Galbraith, C. G., K. M. Yamada and M. P. Sheetz (2002). "The relationship between force and focal complex development." J Cell Biol **159**(4): 695-705.

Gallegos, L., M. R. Ng and J. S. Brugge (2011). "The myosin-II-responsive focal adhesion proteome: a tour de force?" Nat Cell Biol **13**(4): 344-346.

Gao, G., K. C. Prutzman, M. L. King, D. M. Scheswohl, E. F. DeRose, R. E. London, M. D. Schaller and S. L. Campbell (2004). "NMR solution structure of the focal adhesion targeting domain of focal adhesion kinase in complex with a paxillin LD peptide: evidence for a two-site binding model." J Biol Chem **279**(9): 8441-8451.

Garces, C. A., E. V. Kurenova, V. M. Golubovskaya and W. G. Cance (2006). "Vascular endothelial growth factor receptor-3 and focal adhesion kinase bind and suppress apoptosis in breast cancer cells." Cancer Res **66**(3): 1446-1454.

Garcia-Alvarez, B., J. M. de Pereda, D. A. Calderwood, T. S. Ulmer, D. Critchley, I. D. Campbell, M. H. Ginsberg and R. C. Liddington (2003). "Structural determinants of integrin recognition by talin." Mol Cell **11**(1): 49-58.

Garton, A. J. and N. K. Tonks (1999). "Regulation of fibroblast motility by the protein tyrosine phosphatase PTP-PEST." J Biol Chem **274**(6): 3811-3818.

Gee, E. P., D. E. Ingber and C. M. Stultz (2008). "Fibronectin unfolding revisited: modeling cell traction-mediated unfolding of the tenth type-III repeat." PLoS One **3**(6): e2373.

Geiger, B. (1979). "A 130K protein from chicken gizzard: its localization at the termini of microfilament bundles in cultured chicken cells." Cell **18**(1): 193-205.

Geiger, B. and K. M. Yamada (2011). "Molecular architecture and function of matrix adhesions." Cold Spring Harb Perspect Biol **3**(5).

Geldmacher-Voss, B., A. M. Reugels, S. Pauls and J. A. Campos-Ortega (2003). "A 90-degree rotation of the mitotic spindle changes the orientation of mitoses of zebrafish neuroepithelial cells." Development **130**(16): 3767-3780.

George, E. L., E. N. Georges-Labouesse, R. S. Patel-King, H. Rayburn and R. O. Hynes (1993). "Defects in mesoderm, neural tube and vascular development in mouse embryos lacking fibronectin." Development **119**(4): 1079-1091.

Gho, M. and F. Schweisguth (1998). "Frizzled signalling controls orientation of asymmetric sense organ precursor cell divisions in Drosophila." Nature **393**(6681): 178-181.

Gingras, A. R., K. P. Vogel, H. J. Steinhoff, W. H. Ziegler, B. Patel, J. Emsley, D. R. Critchley, G. C. Roberts and I. L. Barsukov (2006). "Structural and dynamic characterization of a vinculin binding site in the talin rod." Biochemistry **45**(6): 1805-1817.

Goksoy, E., Y. Q. Ma, X. Wang, X. Kong, D. Perera, E. F. Plow and J. Qin (2008). "Structural basis for the autoinhibition of talin in regulating integrin activation." Mol Cell **31**(1): 124-133.

Goldmann, W. H. (2012). "Mechanotransduction and focal adhesions." Cell Biol Int **36**(7): 649-652.

Golubovskaya, V. M., R. Finch and W. G. Cance (2005). "Direct interaction of the N-terminal domain of focal adhesion kinase with the N-terminal transactivation domain of p53." J Biol Chem **280**(26): 25008-25021.

Gonczy, P. and L. S. Rose (2005). "Asymmetric cell division and axis formation in the embryo." WormBook: 1-20.

Gonzales, M., B. Weksler, D. Tsuruta, R. D. Goldman, K. J. Yoon, S. B. Hopkinson, F. W. Flitney and J. C. Jones (2001). "Structure and function of a vimentin-associated matrix adhesion in endothelial cells." Mol Biol Cell **12**(1): 85-100.

Gonzalez, C. (2007). "Spindle orientation, asymmetric division and tumour suppression in Drosophila stem cells." Nat Rev Genet **8**(6): 462-472.

Goult, B. T., M. Bouaouina, D. S. Harburger, N. Bate, B. Patel, N. J. Anthis, I. D. Campbell, D. A. Calderwood, I. L. Barsukov, G. C. Roberts and D. R. Critchley (2009). "The structure of the N-terminus of kindlin-1: a domain important for alphaiibbeta3 integrin activation." J Mol Biol **394**(5): 944-956.

Guan, J. L. (1997). "Focal adhesion kinase in integrin signaling." Matrix Biol **16**(4): 195-200.

Guan, J. L. (1997). "Role of focal adhesion kinase in integrin signaling." Int J Biochem Cell Biol **29**(8-9): 1085-1096.

Hagel, M., E. L. George, A. Kim, R. Tamimi, S. L. Opitz, C. E. Turner, A. Imamoto and S. M. Thomas (2002). "The adaptor protein paxillin is essential for normal development in the mouse and is a critical transducer of fibronectin signaling." Mol Cell Biol **22**(3): 901-915.

Halet, G. and J. Carroll (2007). "Rac activity is polarized and regulates meiotic spindle stability and anchoring in mammalian oocytes." Dev Cell **12**(2): 309-317.

Hall, J. E., W. Fu and M. D. Schaller (2011). "Focal adhesion kinase: exploring Fak structure to gain insight into function." Int Rev Cell Mol Biol **288**: 185-225.

Hamadi, A., M. Bouali, M. Dontenwill, H. Stoeckel, K. Takeda and P. Ronde (2005). "Regulation of focal adhesion dynamics and disassembly by phosphorylation of FAK at tyrosine 397." J Cell Sci **118**(Pt 19): 4415-4425.

Hamasaki, K., T. Mimura, H. Furuya, N. Morino, T. Yamazaki, I. Komuro, Y. Yazaki and Y. Nojima (1995). "Stretching mesangial cells stimulates tyrosine phosphorylation of focal adhesion kinase pp125FAK." Biochem Biophys Res Commun **212**(2): 544-549.

Han, D. C. and J. L. Guan (1999). "Association of focal adhesion kinase with Grb7 and its role in cell migration." J Biol Chem **274**(34): 24425-24430.

Hanahan, D. (1997). "Signaling vascular morphogenesis and maintenance." Science **277**(5322): 48-50.

Hanks, S. K., M. B. Calalb, M. C. Harper and S. K. Patel (1992). "Focal adhesion protein-tyrosine kinase phosphorylated in response to cell attachment to fibronectin." Proc Natl Acad Sci U S A **89**(18): 8487-8491.

Hannigan, G. E., C. Leung-Hagesteijn, L. Fitz-Gibbon, M. G. Coppolino, G. Radeva, J. Filmus, J. C. Bell and S. Dedhar (1996). "Regulation of cell adhesion and anchorage-dependent growth by a new beta 1-integrin-linked protein kinase." Nature **379**(6560): 91-96.

Hao, Y., Q. Du, X. Chen, Z. Zheng, J. L. Balsbaugh, S. Maitra, J. Shabanowitz, D. F. Hunt and I. G. Macara (2010). "Par3 controls epithelial spindle orientation by aPKC-mediated phosphorylation of apical Pins." Curr Biol **20**(20): 1809-1818.

Harburger, D. S. and D. A. Calderwood (2009). "Integrin signalling at a glance." J Cell Sci **122**(Pt 2): 159-163.

Harte, M. T., J. D. Hildebrand, M. R. Burnham, A. H. Bouton and J. T. Parsons (1996). "p130Cas, a substrate associated with v-Src and v-Crk, localizes to focal adhesions and binds to focal adhesion kinase." J Biol Chem **271**(23): 13649-13655.

Harunaga, J. S. and K. M. Yamada (2011). "Cell-matrix adhesions in 3D." Matrix Biol **30**(7-8): 363-368.

Hashimoto, S., A. Tsubouchi, Y. Mazaki and H. Sabe (2001). "Interaction of paxillin with p21-activated Kinase (PAK). Association of paxillin alpha with the kinase-inactive and the Cdc42-activated forms of PAK3." J Biol Chem **276**(8): 6037-6045.

Hayashi, I., K. Vuori and R. C. Liddington (2002). "The focal adhesion targeting (FAT) region of focal adhesion kinase is a four-helix bundle that binds paxillin." Nat Struct Biol **9**(2): 101-106.

Hazel L. Sive, R. M. G., Richard M. Harland (2000). Early development of *Xenopus laevis*. Cold Spring Harbor, New York, Cold Spring Harbor Laboratory Press.

Hazel L. Sive, R. M. G., Richard M. Harland (2000). Early Development of *Xenopus laevis*, A Laboratory Manual. Cold Spring Harbor, New York, Cold Spring Harbor Laboratory Press.

Heisenberg, C. P. and R. Fassler (2012). "Cell-cell adhesion and extracellular matrix: diversity counts." Curr Opin Cell Biol **24**(5): 559-561.

Hemmings, L., D. J. Rees, V. Ohanian, S. J. Bolton, A. P. Gilmore, B. Patel, H. Priddle, J. E. Trevithick, R. O. Hynes and D. R. Critchley (1996). "Talin contains three actin-binding sites each of which is adjacent to a vinculin-binding site." J Cell Sci **109 (Pt 11)**: 2715-2726.

Henderson, B., S. Nair, J. Pallas and M. A. Williams (2011). "Fibronectin: a multidomain host adhesin targeted by bacterial fibronectin-binding proteins." FEMS Microbiol Rev **35**(1): 147-200.

Henry, C. A., B. D. Crawford, Y. L. Yan, J. Postlethwait, M. S. Cooper and M. B. Hille (2001). "Roles for zebrafish focal adhesion kinase in notochord and somite morphogenesis." Dev Biol **240**(2): 474-487.

Hens, M. D. and D. W. DeSimone (1995). "Molecular analysis and developmental expression of the focal adhesion kinase pp125FAK in Xenopus laevis." Dev Biol **170**(2): 274-288.

Hertwig, O. (1983). "Über den Werth der ersten Furchungszellen für die Organbildung des Embryos. Experimentelle Studien am Frosch und Tritonei." Archiv für mikroscopische Anatomie **42**: 662–807.

Hildebrand, J. D., M. D. Schaller and J. T. Parsons (1993). "Identification of sequences required for the efficient localization of the focal adhesion kinase, pp125FAK, to cellular focal adhesions." J Cell Biol **123**(4): 993-1005.

Hildebrand, J. D., M. D. Schaller and J. T. Parsons (1995). "Paxillin, a tyrosine phosphorylated focal adhesion-associated protein binds to the carboxyl terminal domain of focal adhesion kinase." Mol Biol Cell **6**(6): 637-647.

Hildebrand, J. D., J. M. Taylor and J. T. Parsons (1996). "An SH3 domain-containing GTPase-activating protein for Rho and Cdc42 associates with focal adhesion kinase." Mol Cell Biol **16**(6): 3169-3178.

Hirata, H., H. Tatsumi and M. Sokabe (2008). "Mechanical forces facilitate actin polymerization at focal adhesions in a zyxin-dependent manner." J Cell Sci **121**(Pt 17): 2795-2804.

Hoellerer, M. K., M. E. Noble, G. Labesse, I. D. Campbell, J. M. Werner and S. T. Arold (2003). "Molecular recognition of paxillin LD motifs by the focal adhesion targeting domain." Structure **11**(10): 1207-1217.

Honda, H., T. Nakamoto, R. Sakai and H. Hirai (1999). "p130(Cas), an assembling molecule of actin filaments, promotes cell movement, cell migration, and cell spreading in fibroblasts." Biochem Biophys Res Commun **262**(1): 25-30.

Honda, H., H. Oda, T. Nakamoto, Z. Honda, R. Sakai, T. Suzuki, T. Saito, K. Nakamura, K. Nakao, T. Ishikawa, M. Katsuki, Y. Yazaki and H. Hirai (1998). "Cardiovascular anomaly, impaired actin bundling and resistance to Src-induced transformation in mice lacking p130Cas." Nat Genet **19**(4): 361-365.

Horwitz, A., K. Duggan, C. Buck, M. C. Beckerle and K. Burridge (1986). "Interaction of plasma membrane fibronectin receptor with talin--a transmembrane linkage." Nature **320**(6062): 531-533.

Hsia, D. A., S. K. Mitra, C. R. Hauck, D. N. Streblow, J. A. Nelson, D. Ilic, S. Huang, E. Li, G. R. Nemerow, J. Leng, K. S. Spencer, D. A. Cheresh and D. D. Schlaepfer (2003). "Differential regulation of cell motility and invasion by FAK." J Cell Biol **160**(5): 753-767.

Humphries, J. D., A. Byron and M. J. Humphries (2006). "Integrin ligands at a glance." J Cell Sci **119**(Pt 19): 3901-3903.

Humphries, J. D., P. Wang, C. Streuli, B. Geiger, M. J. Humphries and C. Ballestrem (2007). "Vinculin controls focal adhesion formation by direct interactions with talin and actin." J Cell Biol **179**(5): 1043-1057.

Humphries, M. J. (1996). "Integrin activation: the link between ligand binding and signal transduction." Curr Opin Cell Biol **8**(5): 632-640.

Huttenlocher, A. and A. R. Horwitz (2011). "Integrins in cell migration." Cold Spring Harb Perspect Biol **3**(9): a005074.

Hynes, R. O. (2002). "Integrins: bidirectional, allosteric signaling machines." Cell **110**(6): 673-687.

Hytonen, V. P. and V. Vogel (2008). "How force might activate talin's vinculin binding sites: SMD reveals a structural mechanism." PLoS Comput Biol **4**(2): e24.

Iioka, H., S. Iemura, T. Natsume and N. Kinoshita (2007). "Wnt signalling regulates paxillin ubiquitination essential for mesodermal cell motility." Nat Cell Biol **9**(7): 813-821.

Ilic, D., Y. Furuta, S. Kanazawa, N. Takeda, K. Sobue, N. Nakatsuji, S. Nomura, J. Fujimoto, M. Okada and T. Yamamoto (1995). "Reduced cell motility and enhanced focal adhesion contact formation in cells from FAK-deficient mice." Nature **377**(6549): 539-544.

Iwanicki, M. P., T. Vomastek, R. W. Tilghman, K. H. Martin, J. Banerjee, P. B. Wedegaertner and J. T. Parsons (2008). "FAK, PDZ-RhoGEF and ROCKII cooperate to regulate adhesion movement and trailing-edge retraction in fibroblasts." J Cell Sci **121**(Pt 6): 895-905.

Jaalouk, D. E. and J. Lammerding (2009). "Mechanotransduction gone awry." Nat Rev Mol Cell Biol **10**(1): 63-73.

Jacamo, R. O. and E. Rozengurt (2005). "A truncated FAK lacking the FERM domain displays high catalytic activity but retains responsiveness to adhesion-mediated signals." Biochem Biophys Res Commun **334**(4): 1299-1304.

Johnson, M. S., N. Lu, K. Denessiouk, J. Heino and D. Gullberg (2009). "Integrins during evolution: evolutionary trees and model organisms." Biochim Biophys Acta **1788**(4): 779-789.

Joos, T. O., C. A. Whittaker, F. Meng, D. W. DeSimone, V. Gnau and P. Hausen (1995). "Integrin alpha 5 during early development of Xenopus laevis." Mech Dev **50**(2-3): 187-199.

Jordan, M. A., D. Thrower and L. Wilson (1992). "Effects of vinblastine, podophyllotoxin and nocodazole on mitotic spindles. Implications for the role of microtubule dynamics in mitosis." J Cell Sci **102 (Pt 3)**: 401-416.

Kadare, G., M. Toutant, E. Formstecher, J. C. Corvol, M. Carnaud, M. C. Boutterin and J. A. Girault (2003). "PIAS1-mediated sumoylation of focal adhesion kinase activates its autophosphorylation." J Biol Chem **278**(48): 47434-47440.

Kaplan, K. B., J. R. Swedlow, D. O. Morgan and H. E. Varmus (1995). "c-Src enhances the spreading of src-/- fibroblasts on fibronectin by a kinase-independent mechanism." Genes Dev **9**(12): 1505-1517.

Katsumi, A., T. Naoe, T. Matsushita, K. Kaibuchi and M. A. Schwartz (2005). "Integrin activation and matrix binding mediate cellular responses to mechanical stretch." J Biol Chem **280**(17): 16546-16549.

Kaushik, R., F. Yu, W. Chia, X. Yang and S. Bahri (2003). "Subcellular localization of LGN during mitosis: evidence for its cortical localization in mitotic cell culture systems and its requirement for normal cell cycle progression." Mol Biol Cell **14**(8): 3144-3155.

Keller, R. (2000). "The origin and morphogenesis of amphibian somites." Curr Top Dev Biol **47**: 183-246.

Keller, R. and S. Jansa (1992). "Xenopus Gastrulation without a blastocoel roof." Dev Dyn **195**(3): 162-176.

Keller, R., J. Shih and A. Sater (1992). "The cellular basis of the convergence and extension of the Xenopus neural plate." Dev Dyn **193**(3): 199-217.

Keller, R. and D. Shook (2008). "Dynamic determinations: patterning the cell behaviours that close the amphibian blastopore." Philos Trans R Soc Lond B Biol Sci **363**(1495): 1317-1332.

Keller, R., D. Shook and P. Skoglund (2008). "The forces that shape embryos: physical aspects of convergent extension by cell intercalation." Phys Biol **5**(1): 015007.

Keller, R. E. (1980). "The cellular basis of epiboly: an SEM study of deep-cell rearrangement during gastrulation in Xenopus laevis." J Embryol Exp Morphol **60**: 201-234.

Kieserman, E. K. and J. B. Wallingford (2009). "In vivo imaging reveals a role for Cdc42 in spindle positioning and planar orientation of cell divisions during vertebrate neural tube closure." J Cell Sci **122**(Pt 14): 2481-2490.

Kiyomitsu, T. and I. M. Cheeseman (2012). "Chromosome- and spindle-pole-derived signals generate an intrinsic code for spindle position and orientation." Nat Cell Biol **14**(3): 311-317.

Klemke, R. L., J. Leng, R. Molander, P. C. Brooks, K. Vuori and D. A. Cheresh (1998). "CAS/Crk coupling serves as a "molecular switch" for induction of cell migration." J Cell Biol **140**(4): 961-972.

Kloeker, S., M. B. Major, D. A. Calderwood, M. H. Ginsberg, D. A. Jones and M. C. Beckerle (2004). "The Kindler syndrome protein is regulated by transforming growth factor-beta and involved in integrin-mediated adhesion." J Biol Chem **279**(8): 6824-6833.

Kolm, P. J. and H. L. Sive (1995). "Efficient hormone-inducible protein function in Xenopus laevis." Dev Biol **171**(1): 267-272.

Kong, F., A. J. Garcia, A. P. Mould, M. J. Humphries and C. Zhu (2009). "Demonstration of catch bonds between an integrin and its ligand." J Cell Biol **185**(7): 1275-1284.

Kong, F., Z. Li, W. M. Parks, D. W. Dumbauld, A. J. Garcia, A. P. Mould, M. J. Humphries and C. Zhu (2013). "Cyclic mechanical reinforcement of integrin-ligand interactions." Mol Cell **49**(6): 1060-1068.

Kotak, S., C. Busso and P. Gonczy (2014). "NuMA interacts with phosphoinositides and links the mitotic spindle with the plasma membrane." EMBO J **33**(16): 1815-1830.

Kragtorp, K. A. and J. R. Miller (2006). "Regulation of somitogenesis by Ena/VASP proteins and FAK during Xenopus development." Development **133**(4): 685-695.

Kragtorp, K. A. and J. R. Miller (2007). "Integrin alpha5 is required for somite rotation and boundary formation in Xenopus." Dev Dyn **236**(9): 2713-2720.

Krammer, A., H. Lu, B. Isralewitz, K. Schulten and V. Vogel (1999). "Forced unfolding of the fibronectin type III module reveals a tensile molecular recognition switch." Proc Natl Acad Sci U S A **96**(4): 1351-1356.

Krylyshkina, O., I. Kaverina, W. Kranewitter, W. Steffen, M. C. Alonso, R. A. Cross and J. V. Small (2002). "Modulation of substrate adhesion dynamics via microtubule targeting requires kinesin-1." J Cell Biol **156**(2): 349-359.

Kwon, M., M. Bagonis, G. Danuser and D. Pellman (2015). "Direct Microtubule-Binding by Myosin-10 Orients Centrosomes toward Retraction Fibers and Subcortical Actin Clouds." Dev Cell.

Ladoux, B. and A. Nicolas (2012). "Physically based principles of cell adhesion mechanosensitivity in tissues." Rep Prog Phys **75**(11): 116601.

LaFlamme, S. E., L. A. Thomas, S. S. Yamada and K. M. Yamada (1994). "Single subunit chimeric integrins as mimics and inhibitors of endogenous integrin functions in receptor localization, cell spreading and migration, and matrix assembly." J Cell Biol **126**(5): 1287-1298.

Lancaster, O. M. and B. Baum (2011). "Might makes right: Using force to align the mitotic spindle." Nat Cell Biol **13**(7): 736-738.

Lawson, C., S. T. Lim, S. Uryu, X. L. Chen, D. A. Calderwood and D. D. Schlaepfer (2012). "FAK promotes recruitment of talin to nascent adhesions to control cell motility." J Cell Biol **196**(2): 223-232.

Lawson, C. and D. D. Schlaepfer (2012). "Integrin adhesions: who's on first? What's on second? Connections between FAK and talin." Cell Adh Migr **6**(4): 302-306.

Lechler, T. and E. Fuchs (2005). "Asymmetric cell divisions promote stratification and differentiation of mammalian skin." Nature **437**(7056): 275-280.

Lee, G., R. Hynes and M. Kirschner (1984). "Temporal and spatial regulation of fibronectin in early Xenopus development." Cell **36**(3): 729-740.

Lee, S. E., R. D. Kamm and M. R. Mofrad (2007). "Force-induced activation of talin and its possible role in focal adhesion mechanotransduction." J Biomech **40**(9): 2096-2106.

Legoff, L., H. Rouault and T. Lecuit (2013). "A global pattern of mechanical stress polarizes cell divisions and cell shape in the growing Drosophila wing disc." Development **140**(19): 4051-4059.

Lenter, M., H. Uhlig, A. Hamann, P. Jeno, B. Imhof and D. Vestweber (1993). "A monoclonal antibody against an activation epitope on mouse integrin chain beta 1 blocks adhesion of lymphocytes to the endothelial integrin alpha 6 beta 1." Proc Natl Acad Sci U S A **90**(19): 9051-9055.

Leu, T. H. and M. C. Maa (2002). "Tyr-863 phosphorylation enhances focal adhesion kinase autophosphorylation at Tyr-397." Oncogene **21**(46): 6992-7000.

Li, W., J. Fan and D. T. Woodley (2001). "Nck/Dock: an adapter between cell surface receptors and the actin cytoskeleton." Oncogene **20**(44): 6403-6417.

Li, W., D. G. Metcalf, R. Gorelik, R. Li, N. Mitra, V. Nanda, P. B. Law, J. D. Lear, W. F. Degrado and J. S. Bennett (2005). "A push-pull mechanism for regulating integrin function." Proc Natl Acad Sci U S A **102**(5): 1424-1429.

Liddington, R. C. (2014). "Structural aspects of integrins." Adv Exp Med Biol **819**: 111-126.

Lietha, D., X. Cai, D. F. Ceccarelli, Y. Li, M. D. Schaller and M. J. Eck (2007). "Structural basis for the autoinhibition of focal adhesion kinase." Cell **129**(6): 1177-1187.

Lim, S. T., X. L. Chen, Y. Lim, D. A. Hanson, T. T. Vo, K. Howerton, N. Larocque, S. J. Fisher, D. D. Schlaepfer and D. Ilic (2008). "Nuclear FAK promotes cell proliferation and survival through FERM-enhanced p53 degradation." Mol Cell **29**(1): 9-22.

Lim, S. T., X. L. Chen, A. Tomar, N. L. Miller, J. Yoo and D. D. Schlaepfer (2010). "Knock-in mutation reveals an essential role for focal adhesion kinase activity in blood vessel morphogenesis and cell motility-polarity but not cell proliferation." J Biol Chem **285**(28): 21526-21536.

Lim, Y., I. Han, J. Jeon, H. Park, Y. Y. Bahk and E. S. Oh (2004). "Phosphorylation of focal adhesion kinase at tyrosine 861 is crucial for Ras transformation of fibroblasts." J Biol Chem **279**(28): 29060-29065.

Lim, Y., S. T. Lim, A. Tomar, M. Gardel, J. A. Bernard-Trifilo, X. L. Chen, S. A. Uryu, R. Canete-Soler, J. Zhai, H. Lin, W. W. Schlaepfer, P. Nalbant, G. Bokoch, D. Ilic, C. Waterman-Storer and D. D. Schlaepfer (2008). "PyK2 and FAK connections to p190Rho guanine nucleotide exchange factor regulate RhoA activity, focal adhesion formation, and cell motility." J Cell Biol **180**(1): 187-203.

Lim, Y., H. Park, J. Jeon, I. Han, J. Kim, E. H. Jho and E. S. Oh (2007). "Focal adhesion kinase is negatively regulated by phosphorylation at tyrosine 407." J Biol Chem **282**(14): 10398-10404.

Liu, E., J. F. Cote and K. Vuori (2003). "Negative regulation of FAK signaling by SOCS proteins." EMBO J **22**(19): 5036-5046.

Liu, G., C. D. Guibao and J. Zheng (2002). "Structural insight into the mechanisms of targeting and signaling of focal adhesion kinase." Mol Cell Biol **22**(8): 2751-2760.

Liu, S., S. M. Thomas, D. G. Woodside, D. M. Rose, W. B. Kiosses, M. Pfaff and M. H. Ginsberg (1999). "Binding of paxillin to alpha4 integrins modifies integrin-dependent biological responses." Nature **402**(6762): 676-681.

Liu, Y., J. C. Loijens, K. H. Martin, A. V. Karginov and J. T. Parsons (2002). "The association of ASAP1, an ADP ribosylation factor-GTPase activating protein, with focal adhesion kinase contributes to the process of focal adhesion assembly." Mol Biol Cell **13**(6): 2147-2156.

Lo, S. H., Q. An, S. Bao, W. K. Wong, Y. Liu, P. A. Janmey, J. H. Hartwig and L. B. Chen (1994). "Molecular cloning of chick cardiac muscle tensin. Full-length cDNA sequence, expression, and characterization." J Biol Chem **269**(35): 22310-22319.

Lock, J. G., B. Wehrle-Haller and S. Stromblad (2008). "Cell-matrix adhesion complexes: master control machinery of cell migration." Semin Cancer Biol **18**(1): 65-76.

Lu, M. S. and C. A. Johnston (2013). "Molecular pathways regulating mitotic spindle orientation in animal cells." Development **140**(9): 1843-1856.

Luo, B. H. and T. A. Springer (2006). "Integrin structures and conformational signaling." Curr Opin Cell Biol **18**(5): 579-586.

Luo, S. W., C. Zhang, B. Zhang, C. H. Kim, Y. Z. Qiu, Q. S. Du, L. Mei and W. C. Xiong (2009). "Regulation of heterochromatin remodelling and myogenin expression during muscle differentiation by FAK interaction with MBD2." EMBO J **28**(17): 2568-2582.

Luque, A., M. Gomez, W. Puzon, Y. Takada, F. Sanchez-Madrid and C. Cabanas (1996). "Activated conformations of very late activation integrins detected by a group of antibodies (HUTS) specific for a novel regulatory region (355-425) of the common beta 1 chain." J Biol Chem **271**(19): 11067-11075.

Ma, A., A. Richardson, E. M. Schaefer and J. T. Parsons (2001). "Serine phosphorylation of focal adhesion kinase in interphase and mitosis: a possible role in modulating binding to p130(Cas)." Mol Biol Cell **12**(1): 1-12.

Machicoane, M., C. A. de Frutos, J. Fink, M. Rocancourt, Y. Lombardi, S. Garel, M. Piel and A. Echard (2014). "SLK-dependent activation of ERMs controls LGN-NuMA localization and spindle orientation." J Cell Biol **205**(6): 791-799.

Malikova, M. A., M. Van Stry and K. Symes (2007). "Apoptosis regulates notochord development in Xenopus." Dev Biol **311**(2): 434-448.

Mammoto, T. and D. E. Ingber (2010). "Mechanical control of tissue and organ development." Development **137**(9): 1407-1420.

Mao, Y., A. L. Tournier, A. Hoppe, L. Kester, B. J. Thompson and N. Tapon (2013). "Differential proliferation rates generate patterns of mechanical tension that orient tissue growth." EMBO J **32**(21): 2790-2803.

Margadant, C., H. N. Monsuur, J. C. Norman and A. Sonnenberg (2011). "Mechanisms of integrin activation and trafficking." Curr Opin Cell Biol **23**(5): 607-614.

Marsden, M. and D. W. DeSimone (2001). "Regulation of cell polarity, radial intercalation and epiboly in Xenopus: novel roles for integrin and fibronectin." Development **128**(18): 3635-3647.

Marsden, M. and D. W. DeSimone (2003). "Integrin-ECM interactions regulate cadherin-dependent cell adhesion and are required for convergent extension in Xenopus." Curr Biol **13**(14): 1182-1191.

Martel, V., C. Racaud-Sultan, S. Dupe, C. Marie, F. Paulhe, A. Galmiche, M. R. Block and C. Albiges-Rizo (2001). "Conformation, localization, and integrin binding of talin depend on its interaction with phosphoinositides." J Biol Chem **276**(24): 21217-21227.

Matsuda, M., B. J. Mayer, Y. Fukui and H. Hanafusa (1990). "Binding of transforming protein, P47gag-crk, to a broad range of phosphotyrosine-containing proteins." Science **248**(4962): 1537-1539.

Matsumura, S., M. Hamasaki, T. Yamamoto, M. Ebisuya, M. Sato, E. Nishida and F. Toyoshima (2012). "ABL1 regulates spindle orientation in adherent cells and mammalian skin." Nat Commun **3**: 626.

McLean, G. W., N. O. Carragher, E. Avizienyte, J. Evans, V. G. Brunton and M. C. Frame (2005). "The role of focal-adhesion kinase in cancer - a new therapeutic opportunity." Nat Rev Cancer **5**(7): 505-515.

McNally, F. J. (2013). "Mechanisms of spindle positioning." J Cell Biol **200**(2): 131-140.

Meenderink, L. M., L. M. Ryzhova, D. M. Donato, D. F. Gochberg, I. Kaverina and S. K. Hanks (2010). "P130Cas Src-binding and substrate domains have distinct roles in sustaining focal adhesion disassembly and promoting cell migration." PLoS One **5**(10): e13412.

Minc, N., D. Burgess and F. Chang (2011). "Influence of cell geometry on division-plane positioning." Cell **144**(3): 414-426.

Minc, N. and M. Piel (2012). "Predicting division plane position and orientation." Trends Cell Biol **22**(4): 193-200.

Mitchison, T. J. (1992). "Actin based motility on retraction fibers in mitotic PtK2 cells." Cell Motil Cytoskeleton **22**(2): 135-151.

Mitra, S. K., D. A. Hanson and D. D. Schlaepfer (2005). "Focal adhesion kinase: in command and control of cell motility." Nat Rev Mol Cell Biol **6**(1): 56-68.

Mitsushima, M., F. Toyoshima and E. Nishida (2009). "Dual role of Cdc42 in spindle orientation control of adherent cells." Mol Cell Biol **29**(10): 2816-2827.

Monkley, S. J., X. H. Zhou, S. J. Kinston, S. M. Giblett, L. Hemmings, H. Priddle, J. E. Brown, C. A. Pritchard, D. R. Critchley and R. Fassler (2000). "Disruption of the talin gene arrests mouse development at the gastrulation stage." Dev Dyn **219**(4): 560-574.

Montanez, E., S. Ussar, M. Schifferer, M. Bosl, R. Zent, M. Moser and R. Fassler (2008). "Kindlin-2 controls bidirectional signaling of integrins." Genes Dev **22**(10): 1325-1330.

Morgan, M. R., M. J. Humphries and M. D. Bass (2007). "Synergistic control of cell adhesion by integrins and syndecans." Nat Rev Mol Cell Biol **8**(12): 957-969.

Morris, E. J., K. Assi, B. Salh and S. Dedhar (2015). "Integrin-linked kinase links dynactin-1/dynactin-2 with cortical integrin receptors to orient the mitotic spindle relative to the substratum." Sci Rep **5**: 8389.

Mould, A. P., S. K. Akiyama and M. J. Humphries (1996). "The inhibitory anti-beta1 integrin monoclonal antibody 13 recognizes an epitope that is attenuated by ligand occupancy. Evidence for allosteric inhibition of integrin function." J Biol Chem **271**(34): 20365-20374.

Mould, A. P., J. A. Askari, S. Aota, K. M. Yamada, A. Irie, Y. Takada, H. J. Mardon and M. J. Humphries (1997). "Defining the topology of integrin alpha5beta1-fibronectin interactions using inhibitory anti-alpha5 and anti-beta1 monoclonal antibodies. Evidence that the synergy sequence of fibronectin is recognized by the amino-terminal repeats of the alpha5 subunit." J Biol Chem **272**(28): 17283-17292.

Na, S., O. Collin, F. Chowdhury, B. Tay, M. Ouyang, Y. Wang and N. Wang (2008). "Rapid signal transduction in living cells is a unique feature of mechanotransduction." Proc Natl Acad Sci U S A **105**(18): 6626-6631.

Nakamoto, T., R. Sakai, K. Ozawa, Y. Yazaki and H. Hirai (1996). "Direct binding of C-terminal region of p130Cas to SH2 and SH3 domains of Src kinase." J Biol Chem **271**(15): 8959-8965.

Nestor-Bergmann, A., G. Goddard and S. Woolner (2014). "Force and the spindle: mechanical cues in mitotic spindle orientation." Semin Cell Dev Biol **34**: 133-139.

Nethe, M. and P. L. Hordijk (2011). "A model for phospho-caveolin-1-driven turnover of focal adhesions." Cell Adh Migr **5**(1): 59-64.

Ng, T., A. Squire, G. Hansra, F. Bornancin, C. Prevostel, A. Hanby, W. Harris, D. Barnes, S. Schmidt, H. Mellor, P. I. Bastiaens and P. J. Parker (1999). "Imaging protein kinase Calpha activation in cells." Science **283**(5410): 2085-2089.

Nieuwkoop, P. D. a. F., J. (1994). Normal table of Xenopus laevis (Daudin). New York, Garland.

Nipper, R. W., K. H. Siller, N. R. Smith, C. Q. Doe and K. E. Prehoda (2007). "Galphai generates multiple Pins activation states to link cortical polarity and spindle orientation in Drosophila neuroblasts." Proc Natl Acad Sci U S A **104**(36): 14306-14311.

Noatynska, A., M. Gotta and P. Meraldi (2012). "Mitotic spindle (DIS)orientation and DISease: cause or consequence?" J Cell Biol **199**(7): 1025-1035.

Nolan, K., J. Lacoste and J. T. Parsons (1999). "Regulated expression of focal adhesion kinase-related nonkinase, the autonomously expressed C-terminal domain of focal adhesion kinase." Mol Cell Biol **19**(9): 6120-6129.

Nowakowski, J., C. N. Cronin, D. E. McRee, M. W. Knuth, C. G. Nelson, N. P. Pavletich, J. Rogers, B. C. Sang, D. N. Scheibe, R. V. Swanson and D. A. Thompson (2002). "Structures of the cancer-related Aurora-A, FAK, and EphA2 protein kinases from nanovolume crystallography." Structure **10**(12): 1659-1667.

Oberhauser, A. F., C. Badilla-Fernandez, M. Carrion-Vazquez and J. M. Fernandez (2002). "The mechanical hierarchies of fibronectin observed with single-molecule AFM." J Mol Biol **319**(2): 433-447.

Ojakian, G. K. and R. Schwimmer (1994). "Regulation of epithelial cell surface polarity reversal by beta 1 integrins." J Cell Sci **107 (Pt 3)**: 561-576.

Olson, J. H. and D. E. Chandler (1999). "Xenopus laevis egg jelly contains small proteins that are essential to fertilization." Dev Biol **210**(2): 401-410.

Ossovskaya, V., S. T. Lim, N. Ota, D. D. Schlaepfer and D. Ilic (2008). "FAK nuclear export signal sequences." FEBS Lett **582**(16): 2402-2406.

Otey, C. A., F. M. Pavalko and K. Burridge (1990). "An interaction between alpha-actinin and the beta 1 integrin subunit in vitro." J Cell Biol **111**(2): 721-729.

Owen, K. A., F. J. Pixley, K. S. Thomas, M. Vicente-Manzanares, B. J. Ray, A. F. Horwitz, J. T. Parsons, H. E. Beggs, E. R. Stanley and A. H. Bouton (2007). "Regulation of lamellipodial persistence, adhesion turnover, and motility in macrophages by focal adhesion kinase." J Cell Biol **179**(6): 1275-1287.

Pankov, R., E. Cukierman, B. Z. Katz, K. Matsumoto, D. C. Lin, S. Lin, C. Hahn and K. M. Yamada (2000). "Integrin dynamics and matrix assembly: tensin-dependent translocation of alpha(5)beta(1) integrins promotes early fibronectin fibrillogenesis." J Cell Biol **148**(5): 1075-1090.

Pankov, R. and K. M. Yamada (2002). "Fibronectin at a glance." J Cell Sci **115**(Pt 20): 3861-3863.

Papagrigoriou, E., A. R. Gingras, I. L. Barsukov, N. Bate, I. J. Fillingham, B. Patel, R. Frank, W. H. Ziegler, G. C. Roberts, D. R. Critchley and J. Emsley (2004). "Activation of a vinculin-binding site in the talin rod involves rearrangement of a five-helix bundle." EMBO J **23**(15): 2942-2951.

Park, A. Y., T. L. Shen, S. Chien and J. L. Guan (2009). "Role of focal adhesion kinase Ser-732 phosphorylation in centrosome function during mitosis." J Biol Chem **284**(14): 9418-9425.

Parsons, J. T. (2003). "Focal adhesion kinase: the first ten years." J Cell Sci **116**(Pt 8): 1409-1416.

Parsons, J. T., A. R. Horwitz and M. A. Schwartz (2010). "Cell adhesion: integrating cytoskeletal dynamics and cellular tension." Nat Rev Mol Cell Biol **11**(9): 633-643.

Parsons, J. T. and S. J. Parsons (1997). "Src family protein tyrosine kinases: cooperating with growth factor and adhesion signaling pathways." Curr Opin Cell Biol **9**(2): 187-192.

Parsons, J. T., J. Slack-Davis, R. Tilghman and W. G. Roberts (2008). "Focal adhesion kinase: targeting adhesion signaling pathways for therapeutic intervention." Clin Cancer Res **14**(3): 627-632.

Parsons, S. J. and J. T. Parsons (2004). "Src family kinases, key regulators of signal transduction." Oncogene **23**(48): 7906-7909.

Pearson, M. A., D. Reczek, A. Bretscher and P. A. Karplus (2000). "Structure of the ERM protein moesin reveals the FERM domain fold masked by an extended actin binding tail domain." Cell **101**(3): 259-270.

Pease, J. C. and J. S. Tirnauer (2011). "Mitotic spindle misorientation in cancer--out of alignment and into the fire." J Cell Sci **124**(Pt 7): 1007-1016.

Pelham, R. J., Jr. and Y. Wang (1997). "Cell locomotion and focal adhesions are regulated by substrate flexibility." Proc Natl Acad Sci U S A **94**(25): 13661-13665.

Pellicena, P. and W. T. Miller (2001). "Processive phosphorylation of p130Cas by Src depends on SH3-polyproline interactions." J Biol Chem **276**(30): 28190-28196.

Peng, X., E. S. Nelson, J. L. Maiers and K. A. DeMali (2011). "New insights into vinculin function and regulation." Int Rev Cell Mol Biol **287**: 191-231.

Petit, V. and J. P. Thiery (2000). "Focal adhesions: structure and dynamics." Biol Cell **92**(7): 477-494.

Peyre, E., F. Jaouen, M. Saadaoui, L. Haren, A. Merdes, P. Durbec and X. Morin (2011). "A lateral belt of cortical LGN and NuMA guides mitotic spindle movements and planar division in neuroepithelial cells." J Cell Biol **193**(1): 141-154.

Pietri, T., O. Eder, M. A. Breau, P. Topilko, M. Blanche, C. Brakebusch, R. Fassler, J. P. Thiery and S. Dufour (2004). "Conditional beta1-integrin gene deletion in neural crest cells causes severe developmental alterations of the peripheral nervous system." Development **131**(16): 3871-3883.

Plow, E. F., T. A. Haas, L. Zhang, J. Loftus and J. W. Smith (2000). "Ligand binding to integrins." J Biol Chem **275**(29): 21785-21788.

Pollard, T. D. (2007). "Regulation of actin filament assembly by Arp2/3 complex and formins." Annu Rev Biophys Biomol Struct **36**: 451-477.

Polte, T. R. and S. K. Hanks (1995). "Interaction between focal adhesion kinase and Crk-associated tyrosine kinase substrate p130Cas." Proc Natl Acad Sci U S A **92**(23): 10678-10682.

Poullet, P., A. Gautreau, G. Kadare, J. A. Girault, D. Louvard and M. Arpin (2001). "Ezrin interacts with focal adhesion kinase and induces its activation independently of cell-matrix adhesion." J Biol Chem **276**(40): 37686-37691.

Pourquie, O. (2001). "Vertebrate somitogenesis." Annu Rev Cell Dev Biol **17**: 311-350.

Prager-Khoutorsky, M., A. Lichtenstein, R. Krishnan, K. Rajendran, A. Mayo, Z. Kam, B. Geiger and A. D. Bershadsky (2011). "Fibroblast polarization is a matrix-rigidity-dependent process controlled by focal adhesion mechanosensing." Nat Cell Biol **13**(12): 1457-1465.

Preissner, K. T. (1991). "Structure and biological role of vitronectin." Annu Rev Cell Biol **7**: 275-310.

Prutzman, K. C., G. Gao, M. L. King, V. V. Iyer, G. A. Mueller, M. D. Schaller and S. L. Campbell (2004). "The focal adhesion targeting domain of focal adhesion kinase contains a hinge region that modulates tyrosine 926 phosphorylation." Structure **12**(5): 881-891.

Puklin-Faucher, E., M. Gao, K. Schulten and V. Vogel (2006). "How the headpiece hinge angle is opened: New insights into the dynamics of integrin activation." J Cell Biol **175**(2): 349-360.

Ramos, J. W. and D. W. DeSimone (1996). "Xenopus embryonic cell adhesion to fibronectin: position-specific activation of RGD/synergy site-dependent migratory behavior at gastrulation." J Cell Biol **134**(1): 227-240.

Redemann, S., J. Pecreaux, N. W. Goehring, K. Khairy, E. H. Stelzer, A. A. Hyman and J. Howard (2010). "Membrane invaginations reveal cortical sites that pull on mitotic spindles in one-cell C. elegans embryos." PLoS One **5**(8): e12301.

Reiske, H. R., S. C. Kao, L. A. Cary, J. L. Guan, J. F. Lai and H. C. Chen (1999). "Requirement of phosphatidylinositol 3-kinase in focal adhesion kinase-promoted cell migration." J Biol Chem **274**(18): 12361-12366.

Ren, X. D., W. B. Kiosses, D. J. Sieg, C. A. Otey, D. D. Schlaepfer and M. A. Schwartz (2000). "Focal adhesion kinase suppresses Rho activity to promote focal adhesion turnover." J Cell Sci **113 (Pt 20)**: 3673-3678.

Reynolds, A. B., S. B. Kanner, H. C. Wang and J. T. Parsons (1989). "Stable association of activated pp60src with two tyrosine-phosphorylated cellular proteins." Mol Cell Biol **9**(9): 3951-3958.

Richardson, A., R. K. Malik, J. D. Hildebrand and J. T. Parsons (1997). "Inhibition of cell spreading by expression of the C-terminal domain of focal adhesion kinase (FAK) is rescued by coexpression of Src or catalytically inactive FAK: a role for paxillin tyrosine phosphorylation." Mol Cell Biol **17**(12): 6906-6914.

Richardson, A. and T. Parsons (1996). "A mechanism for regulation of the adhesion-associated proteintyrosine kinase pp125FAK." Nature **380**(6574): 538-540.

Rico, B., H. E. Beggs, D. Schahin-Reed, N. Kimes, A. Schmidt and L. F. Reichardt (2004). "Control of axonal branching and synapse formation by focal adhesion kinase." Nat Neurosci **7**(10): 1059-1069.

Risau, W. (1997). "Mechanisms of angiogenesis." Nature **386**(6626): 671-674.

Riveline, D., E. Zamir, N. Q. Balaban, U. S. Schwarz, T. Ishizaki, S. Narumiya, Z. Kam, B. Geiger and A. D. Bershadsky (2001). "Focal contacts as mechanosensors: externally applied local mechanical force induces growth of focal contacts by an mDia1-dependent and ROCK-independent mechanism." J Cell Biol **153**(6): 1175-1186.

Rivera, G. M., S. Antoku, S. Gelkop, N. Y. Shin, S. K. Hanks, T. Pawson and B. J. Mayer (2006). "Requirement of Nck adaptors for actin dynamics and cell migration stimulated by platelet-derived growth factor B." Proc Natl Acad Sci U S A **103**(25): 9536-9541.

Rodriguez-Fraticelli, A. E., M. Galvez-Santisteban and F. Martin-Belmonte (2011). "Divide and polarize: recent advances in the molecular mechanism regulating epithelial tubulogenesis." Curr Opin Cell Biol **23**(5): 638-646.

Rottner, K., B. Behrendt, J. V. Small and J. Wehland (1999). "VASP dynamics during lamellipodia protrusion." Nat Cell Biol **1**(5): 321-322.

Rozario, T., B. Dzamba, G. F. Weber, L. A. Davidson and D. W. DeSimone (2009). "The physical state of fibronectin matrix differentially regulates morphogenetic movements in vivo." Dev Biol **327**(2): 386-398.

Ruest, P. J., N. Y. Shin, T. R. Polte, X. Zhang and S. K. Hanks (2001). "Mechanisms of CAS substrate domain tyrosine phosphorylation by FAK and Src." Mol Cell Biol **21**(22): 7641-7652.

Sai, X., K. Naruse and M. Sokabe (1999). "Activation of pp60(src) is critical for stretch-induced orienting response in fibroblasts." J Cell Sci **112 (Pt 9)**: 1365-1373.

Sakai, R., A. Iwamatsu, N. Hirano, S. Ogawa, T. Tanaka, H. Mano, Y. Yazaki and H. Hirai (1994). "A novel signaling molecule, p130, forms stable complexes in vivo with v-Crk and v-Src in a tyrosine phosphorylation-dependent manner." EMBO J **13**(16): 3748-3756.

Saunders, R. M., M. R. Holt, L. Jennings, D. H. Sutton, I. L. Barsukov, A. Bobkov, R. C. Liddington, E. A. Adamson, G. A. Dunn and D. R. Critchley (2006). "Role of vinculin in regulating focal adhesion turnover." Eur J Cell Biol **85**(6): 487-500.

Sawada, Y. and M. P. Sheetz (2002). "Force transduction by Triton cytoskeletons." J Cell Biol **156**(4): 609-615.

Sawada, Y., M. Tamada, B. J. Dubin-Thaler, O. Cherniavskaya, R. Sakai, S. Tanaka and M. P. Sheetz (2006). "Force sensing by mechanical extension of the Src family kinase substrate p130Cas." Cell **127**(5): 1015-1026.

Schaller, M. D. (2010). "Cellular functions of FAK kinases: insight into molecular mechanisms and novel functions." J Cell Sci **123**(Pt 7): 1007-1013.

Schaller, M. D., C. A. Borgman, B. S. Cobb, R. R. Vines, A. B. Reynolds and J. T. Parsons (1992). "pp125FAK a structurally distinctive protein-tyrosine kinase associated with focal adhesions." Proc Natl Acad Sci U S A **89**(11): 5192-5196.

Schaller, M. D., J. D. Hildebrand, J. D. Shannon, J. W. Fox, R. R. Vines and J. T. Parsons (1994). "Autophosphorylation of the focal adhesion kinase, pp125FAK, directs SH2-dependent binding of pp60src." Mol Cell Biol **14**(3): 1680-1688.

Schaller, M. D., C. A. Otey, J. D. Hildebrand and J. T. Parsons (1995). "Focal adhesion kinase and paxillin bind to peptides mimicking beta integrin cytoplasmic domains." J Cell Biol **130**(5): 1181-1187.

Scheswohl, D. M., J. R. Harrell, Z. Rajfur, G. Gao, S. L. Campbell and M. D. Schaller (2008). "Multiple paxillin binding sites regulate FAK function." J Mol Signal **3**: 1.

Schlaepfer, D. D., S. K. Hanks, T. Hunter and P. van der Geer (1994). "Integrin-mediated signal transduction linked to Ras pathway by GRB2 binding to focal adhesion kinase." Nature **372**(6508): 786-791.

Schlaepfer, D. D. and T. Hunter (1996). "Evidence for in vivo phosphorylation of the Grb2 SH2-domain binding site on focal adhesion kinase by Src-family protein-tyrosine kinases." Mol Cell Biol **16**(10): 5623-5633.

Schwartz, M. A. (2010). "Integrins and extracellular matrix in mechanotransduction." Cold Spring Harb Perspect Biol **2**(12): a005066.

Schwartz, M. A. and D. W. DeSimone (2008). "Cell adhesion receptors in mechanotransduction." Curr Opin Cell Biol **20**(5): 551-556.

Seldin, L., N. D. Poulson, H. P. Foote and T. Lechler (2013). "NuMA localization, stability, and function in spindle orientation involve 4.1 and Cdk1 interactions." Mol Biol Cell **24**(23): 3651-3662.

Seong, J., M. Ouyang, T. Kim, J. Sun, P. C. Wen, S. Lu, Y. Zhuo, N. M. Llewellyn, D. D. Schlaepfer, J. L. Guan, S. Chien and Y. Wang (2011). "Detection of focal adhesion kinase activation at membrane microdomains by fluorescence resonance energy transfer." Nat Commun **2**: 406.

Serrels, B., A. Serrels, V. G. Brunton, M. Holt, G. W. McLean, C. H. Gray, G. E. Jones and M. C. Frame (2007). "Focal adhesion kinase controls actin assembly via a FERM-mediated interaction with the Arp2/3 complex." Nat Cell Biol **9**(9): 1046-1056.

Seufferlein, T. and E. Rozengurt (1994). "Lysophosphatidic acid stimulates tyrosine phosphorylation of focal adhesion kinase, paxillin, and p130. Signaling pathways and cross-talk with platelet-derived growth factor." J Biol Chem **269**(12): 9345-9351.

Sharma, A. and B. J. Mayer (2008). "Phosphorylation of p130Cas initiates Rac activation and membrane ruffling." BMC Cell Biol **9**: 50.

Sharma, C. P., R. M. Ezzell and M. A. Arnaout (1995). "Direct interaction of filamin (ABP-280) with the beta 2-integrin subunit CD18." J Immunol **154**(7): 3461-3470.

Shen, T. L., A. Y. Park, A. Alcaraz, X. Peng, I. Jang, P. Koni, R. A. Flavell, H. Gu and J. L. Guan (2005). "Conditional knockout of focal adhesion kinase in endothelial cells reveals its role in angiogenesis and vascular development in late embryogenesis." J Cell Biol **169**(6): 941-952.

Shook, D. and R. Keller (2003). "Mechanisms, mechanics and function of epithelial-mesenchymal transitions in early development." Mech Dev **120**(11): 1351-1383.

Sieg, D. J., C. R. Hauck, D. Ilic, C. K. Klingbeil, E. Schaefer, C. H. Damsky and D. D. Schlaepfer (2000). "FAK integrates growth-factor and integrin signals to promote cell migration." Nat Cell Biol **2**(5): 249-256.

Sieg, D. J., C. R. Hauck and D. D. Schlaepfer (1999). "Required role of focal adhesion kinase (FAK) for integrin-stimulated cell migration." J Cell Sci **112 (Pt 16)**: 2677-2691.

Siller, K. H. and C. Q. Doe (2009). "Spindle orientation during asymmetric cell division." Nat Cell Biol **11**(4): 365-374.

Simons, M. and G. Walz (2006). "Polycystic kidney disease: cell division without a c(l)ue?" Kidney Int **70**(5): 854-864.

Singh, P., C. Carraher and J. E. Schwarzbauer (2010). "Assembly of fibronectin extracellular matrix." Annu Rev Cell Dev Biol **26**: 397-419.

Slack-Davis, J. K., K. H. Martin, R. W. Tilghman, M. Iwanicki, E. J. Ung, C. Autry, M. J. Luzzio, B. Cooper, J. C. Kath, W. G. Roberts and J. T. Parsons (2007). "Cellular characterization of a novel focal adhesion kinase inhibitor." J Biol Chem **282**(20): 14845-14852.

Slack, J. K., R. B. Adams, J. D. Rovin, E. A. Bissonette, C. E. Stoker and J. T. Parsons (2001). "Alterations in the focal adhesion kinase/Src signal transduction pathway correlate with increased migratory capacity of prostate carcinoma cells." Oncogene **20**(10): 1152-1163.

Smith, H. W. and C. J. Marshall (2010). "Regulation of cell signalling by uPAR." Nat Rev Mol Cell Biol **11**(1): 23-36.

Smith, W. C. and R. M. Harland (1991). "Injected Xwnt-8 RNA acts early in Xenopus embryos to promote formation of a vegetal dorsalizing center." Cell **67**(4): 753-765.

Solnica-Krezel, L. (2005). "Conserved patterns of cell movements during vertebrate gastrulation." Curr Biol **15**(6): R213-228.

Soriano, P., C. Montgomery, R. Geske and A. Bradley (1991). "Targeted disruption of the c-src proto-oncogene leads to osteopetrosis in mice." Cell **64**(4): 693-702.

Stephens, L. E., A. E. Sutherland, I. V. Klimanskaya, A. Andrieux, J. Meneses, R. A. Pedersen and C. H. Damsky (1995). "Deletion of beta 1 integrins in mice results in inner cell mass failure and peri-implantation lethality." Genes Dev **9**(15): 1883-1895.

Strauss, B., R. J. Adams and N. Papalopulu (2006). "A default mechanism of spindle orientation based on cell shape is sufficient to generate cell fate diversity in polarised Xenopus blastomeres." Development **133**(19): 3883-3893.

Stylianou, P. and P. A. Skourides (2009). "Imaging morphogenesis, in Xenopus with Quantum Dot nanocrystals." Mech Dev **126**(10): 828-841.

Sulzmaier, F. J., C. Jean and D. D. Schlaepfer (2014). "FAK in cancer: mechanistic findings and clinical applications." Nat Rev Cancer **14**(9): 598-610.

Sun, X., Y. Shikata, L. Wang, K. Ohmori, N. Watanabe, J. Wada, K. Shikata, K. G. Birukov, H. Makino, J. R. Jacobson, S. M. Dudek and J. G. Garcia (2009). "Enhanced interaction between focal adhesion and adherens junction proteins: involvement in sphingosine 1-phosphate-induced endothelial barrier enhancement." Microvasc Res **77**(3): 304-313.

Sundberg, L. J., L. M. Galante, H. M. Bill, C. P. Mack and J. M. Taylor (2003). "An endogenous inhibitor of focal adhesion kinase blocks Rac1/JNK but not Ras/ERK-dependent signaling in vascular smooth muscle cells." J Biol Chem **278**(32): 29783-29791.

Szczepanowska, J. (2009). "Involvement of Rac/Cdc42/PAK pathway in cytoskeletal rearrangements." Acta Biochim Pol **56**(2): 225-234.

Tachibana, K., T. Urano, H. Fujita, Y. Ohashi, K. Kamiguchi, S. Iwata, H. Hirai and C. Morimoto (1997). "Tyrosine phosphorylation of Crk-associated substrates by focal adhesion kinase. A putative mechanism for the integrin-mediated tyrosine phosphorylation of Crk-associated substrates." J Biol Chem **272**(46): 29083-29090.

Tada, M., M. A. O'Reilly and J. C. Smith (1997). "Analysis of competence and of Brachyury autoinduction by use of hormone-inducible Xbra." Development **124**(11): 2225-2234.

Tadokoro, S., S. J. Shattil, K. Eto, V. Tai, R. C. Liddington, J. M. de Pereda, M. H. Ginsberg and D. A. Calderwood (2003). "Talin binding to integrin beta tails: a final common step in integrin activation." Science **302**(5642): 103-106.

Takada, Y. and W. Puzon (1993). "Identification of a regulatory region of integrin beta 1 subunit using activating and inhibiting antibodies." J Biol Chem **268**(23): 17597-17601.

Takagi, J. (2004). "Structural basis for ligand recognition by RGD (Arg-Gly-Asp)-dependent integrins." Biochem Soc Trans **32**(Pt3): 403-406.

Taylor, J. M., C. P. Mack, K. Nolan, C. P. Regan, G. K. Owens and J. T. Parsons (2001). "Selective expression of an endogenous inhibitor of FAK regulates proliferation and migration of vascular smooth muscle cells." Mol Cell Biol **21**(5): 1565-1572.

Taylor, J. M., M. M. Macklem and J. T. Parsons (1999). "Cytoskeletal changes induced by GRAF, the GTPase regulator associated with focal adhesion kinase, are mediated by Rho." J Cell Sci **112 (Pt 2)**: 231-242.

Thery, M. and M. Bornens (2006). "Cell shape and cell division." Curr Opin Cell Biol **18**(6): 648-657.

Thery, M., A. Jimenez-Dalmaroni, V. Racine, M. Bornens and F. Julicher (2007). "Experimental and theoretical study of mitotic spindle orientation." Nature **447**(7143): 493-496.

Thery, M., V. Racine, A. Pepin, M. Piel, Y. Chen, J. B. Sibarita and M. Bornens (2005). "The extracellular matrix guides the orientation of the cell division axis." Nat Cell Biol **7**(10): 947-953.

Thomas, J. W., B. Ellis, R. J. Boerner, W. B. Knight, G. C. White, 2nd and M. D. Schaller (1998). "SH2- and SH3-mediated interactions between focal adhesion kinase and Src." J Biol Chem **273**(1): 577-583.

Tilghman, R. W. and J. T. Parsons (2008). "Focal adhesion kinase as a regulator of cell tension in the progression of cancer." Semin Cancer Biol **18**(1): 45-52.

Tilghman, R. W., J. K. Slack-Davis, N. Sergina, K. H. Martin, M. Iwanicki, E. D. Hershey, H. E. Beggs, L. F. Reichardt and J. T. Parsons (2005). "Focal adhesion kinase is required for the spatial organization of the leading edge in migrating cells." J Cell Sci **118**(Pt 12): 2613-2623.

Tomar, A., S. T. Lim, Y. Lim and D. D. Schlaepfer (2009). "A FAK-p120RasGAP-p190RhoGAP complex regulates polarity in migrating cells." J Cell Sci **122**(Pt 11): 1852-1862.

Toutant, M., A. Costa, J. M. Studler, G. Kadare, M. Carnaud and J. A. Girault (2002). "Alternative splicing controls the mechanisms of FAK autophosphorylation." Mol Cell Biol **22**(22): 7731-7743.

Toyoshima, F., S. Matsumura, H. Morimoto, M. Mitsushima and E. Nishida (2007). "PtdIns(3,4,5)P3 regulates spindle orientation in adherent cells." Dev Cell **13**(6): 796-811.

Toyoshima, F. and E. Nishida (2007). "Integrin-mediated adhesion orients the spindle parallel to the substratum in an EB1- and myosin X-dependent manner." EMBO J **26**(6): 1487-1498.

Toyoshima, F. and E. Nishida (2007). "Spindle orientation in animal cell mitosis: roles of integrin in the control of spindle axis." J Cell Physiol **213**(2): 407-411.

Tsuchida, J., S. Ueki, Y. Saito and J. Takagi (1997). "Classification of 'activation' antibodies against integrin beta1 chain." FEBS Lett **416**(2): 212-216.

Tsuda, S., T. Kitagawa, S. Takashima, S. Asakawa, N. Shimizu, H. Mitani, A. Shima, M. Tsutsumi, H. Hori, K. Naruse, Y. Ishikawa and H. Takeda (2010). "FAK-mediated extracellular signals are essential for interkinetic nuclear migration and planar divisions in the neuroepithelium." J Cell Sci **123**(Pt 3): 484-496.

Turner, C. E., M. C. Brown, J. A. Perrotta, M. C. Riedy, S. N. Nikolopoulos, A. R. McDonald, S. Bagrodia, S. Thomas and P. S. Leventhal (1999). "Paxillin LD4 motif binds PAK and PIX through a novel 95-kD ankyrin repeat, ARF-GAP protein: A role in cytoskeletal remodeling." J Cell Biol **145**(4): 851-863.

Valdembri, D. and G. Serini (2012). "Regulation of adhesion site dynamics by integrin traffic." Curr Opin Cell Biol **24**(5): 582-591.

Vicente-Manzanares, M., C. K. Choi and A. R. Horwitz (2009). "Integrins in cell migration--the actin connection." J Cell Sci **122**(Pt 2): 199-206.

Vicente-Manzanares, M., K. Newell-Litwa, A. I. Bachir, L. A. Whitmore and A. R. Horwitz (2011). "Myosin IIA/IIB restrict adhesive and protrusive signaling to generate front-back polarity in migrating cells." J Cell Biol **193**(2): 381-396.

Vogel, V. (2006). "Mechanotransduction involving multimodular proteins: converting force into biochemical signals." Annu Rev Biophys Biomol Struct **35**: 459-488.

Vogel, W. F., R. Abdulhussein and C. E. Ford (2006). "Sensing extracellular matrix: an update on discoidin domain receptor function." Cell Signal **18**(8): 1108-1116.

Volberg, T., L. Romer, E. Zamir and B. Geiger (2001). "pp60(c-src) and related tyrosine kinases: a role in the assembly and reorganization of matrix adhesions." J Cell Sci **114**(Pt 12): 2279-2289.

Wacker, S., A. Brodbeck, P. Lemaire, C. Niehrs and R. Winklbauer (1998). "Patterns and control of cell motility in the Xenopus gastrula." Development **125**(10): 1931-1942.

Wade, R., J. Bohl and S. Vande Pol (2002). "Paxillin null embryonic stem cells are impaired in cell spreading and tyrosine phosphorylation of focal adhesion kinase." Oncogene **21**(1): 96-107.

Wang, F., Z. Shi, Y. Cui, X. Guo, Y. B. Shi and Y. Chen (2015). "Targeted gene disruption in Xenopus laevis using CRISPR/Cas9." Cell Biosci **5**: 15.

Wang, H. B., M. Dembo, S. K. Hanks and Y. Wang (2001). "Focal adhesion kinase is involved in mechanosensing during fibroblast migration." Proc Natl Acad Sci U S A **98**(20): 11295-11300.

Wang, P., C. Ballestrem and C. H. Streuli (2011). "The C terminus of talin links integrins to cell cycle progression." J Cell Biol **195**(3): 499-513.

Webb, D. J., K. Donais, L. A. Whitmore, S. M. Thomas, C. E. Turner, J. T. Parsons and A. F. Horwitz (2004). "FAK-Src signalling through paxillin, ERK and MLCK regulates adhesion disassembly." Nat Cell Biol **6**(2): 154-161.

Wegener, K. L., A. W. Partridge, J. Han, A. R. Pickford, R. C. Liddington, M. H. Ginsberg and I. D. Campbell (2007). "Structural basis of integrin activation by talin." Cell **128**(1): 171-182.

Whitaker, M. (2006). "Calcium at fertilization and in early development." Physiol Rev **86**(1): 25-88.

Wiesner, S., K. R. Legate and R. Fassler (2005). "Integrin-actin interactions." Cell Mol Life Sci **62**(10): 1081-1099.

Wilson, P. A., G. Oster and R. Keller (1989). "Cell rearrangement and segmentation in Xenopus: direct observation of cultured explants." Development **105**(1): 155-166.

Winklbauer, R. (1998). "Conditions for fibronectin fibril formation in the early Xenopus embryo." Dev Dyn **212**(3): 335-345.

Winklbauer, R. (2009). "Cell adhesion in amphibian gastrulation." Int Rev Cell Mol Biol **278**: 215-275.

Winklbauer, R. (2012). "Cadherin function during Xenopus gastrulation." Subcell Biochem **60**: 301-320.

Winklbauer, R. and R. E. Keller (1996). "Fibronectin, mesoderm migration, and gastrulation in Xenopus." Dev Biol **177**(2): 413-426.

Winklbauer, R., M. Nagel, A. Selchow and S. Wacker (1996). "Mesoderm migration in the Xenopus gastrula." Int J Dev Biol **40**(1): 305-311.

Winklbauer, R. and M. Schurfeld (1999). "Vegetal rotation, a new gastrulation movement involved in the internalization of the mesoderm and endoderm in Xenopus." Development **126**(16): 3703-3713.

Winklbauer, R. and C. Stoltz (1995). "Fibronectin fibril growth in the extracellular matrix of the Xenopus embryo." J Cell Sci **108 (Pt 4)**: 1575-1586.

Winograd-Katz, S. E., R. Fassler, B. Geiger and K. R. Legate (2014). "The integrin adhesome: from genes and proteins to human disease." Nat Rev Mol Cell Biol **15**(4): 273-288.

Wiseman, P. W., C. M. Brown, D. J. Webb, B. Hebert, N. L. Johnson, J. A. Squier, M. H. Ellisman and A. F. Horwitz (2004). "Spatial mapping of integrin interactions and dynamics during cell migration by image correlation microscopy." J Cell Sci **117**(Pt 23): 5521-5534.

Woolner, S. and N. Papalopulu (2012). "Spindle position in symmetric cell divisions during epiboly is controlled by opposing and dynamic apicobasal forces." Dev Cell **22**(4): 775-787.

Xiao, T., J. Takagi, B. S. Coller, J. H. Wang and T. A. Springer (2004). "Structural basis for allostery in integrins and binding to fibrinogen-mimetic therapeutics." Nature **432**(7013): 59-67.

Xie, B., J. Zhao, M. Kitagawa, J. Durbin, J. A. Madri, J. L. Guan and X. Y. Fu (2001). "Focal adhesion kinase activates Stat1 in integrin-mediated cell migration and adhesion." J Biol Chem **276**(22): 19512-19523.

Xie, Z., K. Sanada, B. A. Samuels, H. Shih and L. H. Tsai (2003). "Serine 732 phosphorylation of FAK by Cdk5 is important for microtubule organization, nuclear movement, and neuronal migration." Cell **114**(4): 469-482.

Xie, Z. and L. H. Tsai (2004). "Cdk5 phosphorylation of FAK regulates centrosome-associated miocrotubules and neuronal migration." Cell Cycle **3**(2): 108-110.

Xiong, J. P., T. Stehle, B. Diefenbach, R. Zhang, R. Dunker, D. L. Scott, A. Joachimiak, S. L. Goodman and M. A. Arnaout (2001). "Crystal structure of the extracellular segment of integrin alpha Vbeta3." Science **294**(5541): 339-345.

Xu, W., H. Baribault and E. D. Adamson (1998). "Vinculin knockout results in heart and brain defects during embryonic development." Development **125**(2): 327-337.

Yamaguchi, R., Y. Mazaki, K. Hirota, S. Hashimoto and H. Sabe (1997). "Mitosis specific serine phosphorylation and downregulation of one of the focal adhesion protein, paxillin." Oncogene **15**(15): 1753-1761.

Yang, J. T., H. Rayburn and R. O. Hynes (1993). "Embryonic mesodermal defects in alpha 5 integrin-deficient mice." Development **119**(4): 1093-1105.

Yu, D. H., C. K. Qu, O. Henegariu, X. Lu and G. S. Feng (1998). "Protein-tyrosine phosphatase Shp-2 regulates cell spreading, migration, and focal adhesion." J Biol Chem **273**(33): 21125-21131.

Yu, J. A., N. O. Deakin and C. E. Turner (2009). "Paxillin-kinase-linker tyrosine phosphorylation regulates directional cell migration." Mol Biol Cell **20**(22): 4706-4719.

Zachary, I. (1997). "Focal adhesion kinase." Int J Biochem Cell Biol **29**(7): 929-934.

Zaidel-Bar, R., C. Ballestrem, Z. Kam and B. Geiger (2003). "Early molecular events in the assembly of matrix adhesions at the leading edge of migrating cells." J Cell Sci **116**(Pt 22): 4605-4613.

Zhai, J., H. Lin, Z. Nie, J. Wu, R. Canete-Soler, W. W. Schlaepfer and D. D. Schlaepfer (2003). "Direct interaction of focal adhesion kinase with p190RhoGEF." J Biol Chem **278**(27): 24865-24873.

Zhang, X., A. Chattopadhyay, Q. S. Ji, J. D. Owen, P. J. Ruest, G. Carpenter and S. K. Hanks (1999). "Focal adhesion kinase promotes phospholipase C-gamma1 activity." Proc Natl Acad Sci U S A **96**(16): 9021-9026.

Zhang, X., G. Jiang, Y. Cai, S. J. Monkley, D. R. Critchley and M. P. Sheetz (2008). "Talin depletion reveals independence of initial cell spreading from integrin activation and traction." Nat Cell Biol **10**(9): 1062-1068.

Zhang, X., C. V. Wright and S. K. Hanks (1995). "Cloning of a Xenopus laevis cDNA encoding focal adhesion kinase (FAK) and expression during early development." Gene **160**(2): 219-222.

Zhao, J. and J. L. Guan (2009). "Signal transduction by focal adhesion kinase in cancer." Cancer Metastasis Rev **28**(1-2): 35-49.

Zhao, X., X. Peng, S. Sun, A. Y. Park and J. L. Guan (2010). "Role of kinase-independent and -dependent functions of FAK in endothelial cell survival and barrier function during embryonic development." J Cell Biol **189**(6): 955-965.

Zheng, D., E. Kurenova, D. Ucar, V. Golubovskaya, A. Magis, D. Ostrov, W. G. Cance and S. N. Hochwald (2009). "Targeting of the protein interaction site between FAK and IGF-1R." Biochem Biophys Res Commun **388**(2): 301-305.

Zheng, Y., Y. Xia, D. Hawke, M. Halle, M. L. Tremblay, X. Gao, X. Z. Zhou, K. Aldape, M. H. Cobb, K. Xie, J. He and Z. Lu (2009). "FAK phosphorylation by ERK primes ras-induced

tyrosine dephosphorylation of FAK mediated by PIN1 and PTP-PEST." Mol Cell **35**(1): 11-25.

Zheng, Z., H. Zhu, Q. Wan, J. Liu, Z. Xiao, D. P. Siderovski and Q. Du (2010). "LGN regulates mitotic spindle orientation during epithelial morphogenesis." J Cell Biol **189**(2): 275-288.

Zhong, C., M. Chrzanowska-Wodnicka, J. Brown, A. Shaub, A. M. Belkin and K. Burridge (1998). "Rho-mediated contractility exposes a cryptic site in fibronectin and induces fibronectin matrix assembly." J Cell Biol **141**(2): 539-551.

Zhou, Z., H. Feng and Y. Bai (2006). "Detection of a hidden folding intermediate in the focal adhesion target domain: Implications for its function and folding." Proteins **65**(2): 259-265.

Zhu, J., K. Motejlek, D. Wang, K. Zang, A. Schmidt and L. F. Reichardt (2002). "beta8 integrins are required for vascular morphogenesis in mouse embryos." Development **129**(12): 2891-2903.

Ziegler, W. H., R. C. Liddington and D. R. Critchley (2006). "The structure and regulation of vinculin." Trends Cell Biol **16**(9): 453-460.

7. Annexes

7.1. Abbreviations

A-P: anterior-posterior

ABL1: Abelson murine leukemia viral oncogene homolog 1

AC: Animal Cap

ADAM: A Disintegrin And Metalloproteinase

AP: Animal Pole

APC: Adenomatous Polyposis Coli

aPKC: atypical PKC

ASAP1: ARF [ADP Ribosylation Factor] GTPase-activating protein GAP

BCR: Blastocoel Roof

BSA: Bovine Serum Albumin

Cas: Crk-associate substrate

CDK5: Cyclin-dependent-like Kinase 5

CE: Convergent Extension

Chrd: Chordin

CMC: Cortical Mechanosensory Complex

CRISPR: Clustered Regularly Interspaced Short Palindromic Repeats

D-V: dorsal-ventral

DA: Dorsal Aorta

DFA: Danilchik's for Amy

DEX: Dexamethasone

DLAV: Dorsal Lateral Anastomosing Vessel

DMZ: Dorsal Marginal Zone

DN: Dominant Negative

ECM: Extracellular Matrix

EGFR: Epidermal Growth Factor Receptor

EMT: Epithelial to Mesenchymal Transition

ERK: Extracellular signal Related Kinase

ERM: Ezrin Radixin Moesin

EVL: Enveloping Layer

FA: Focal Adhesion

FAK: Focal adhesion Kinase

FAT: Focal Adhesion Targeting

FB: Fibrillar Adhesion

FBS: Fetal Bovine Serum

FC: Focal Complex

FERM: Four-point-one, Ezrin, Radaxin, Moesin

FF: FERM-FRNK

FIP200: FAK family Interacting Protein 200

FLIP: Fluorescence Loss In Photobleaching

FN: Fibronectin

FRAP: Fluorescence Recovery After Photobleaching

FRNK: FAK-Related Non Kinase

GFP: Green Fluorescent Protein

GFR: Growth Factor Receptor

GR: Glucocorticoid Receptor

GRAF: GTPase regulator associated with FAK

Grb2: Growth factor receptor Bound protein 2

Grb7: Growth factor receptor Bound protein 7

Gsc: Goosecoid

HA: Hemagglutinin

hCG: human Chorionic Gonadotropin

HDAC1: Histone Deacetylase 1

HGFR: Hepatocyte Growth Factor Receptor

HSP90: Heat-Shock Protein 90

HRP: Horseradish Peroxide

ICAM-4: InterCellular Adhesion Molecule

IGF-IR: Insulin-like Growth Factor Receptor

ILK: Integrin Linked Kinase

IMZ: Involuting Marginal Zone

ISH: *In Situ* Hybridization

ISV: Intersomitic Vessels

KD: Kinase Dead

L-R: Left-Right

LD: Leucine and Aspartate rich

LGN: Leu-Gly-Asn repeat-enriched protein

LIM: Lin11, Isl-1, Mec-3

LPA: Lysophosphatidic Acid

MAB: Maleic Acid Buffer

MAdCAM-1: Mucosal Addressin Cell Adhesion Molecule-1

MAPK: Mitogen Activated Protein Kinase

MBD2: Methyl CpG Binding protein 2

MDM2: Mouse Double Minute 2 homolog

MEFs: Mouse Embryonic Fibroblasts

MLC: Myosin Light Chain

MMR: Marc's modified Ringer's

MO: Morpholino

MS: Mechanical Stimulation

MTOC: Microtubule Organizing Center

MZ: Marginal Zone

NES: Nuclear Export Signal

NIMZ: Non Involuting Marginal Zone

NLS: Nuclear Localization Signal

NuMA: Nuclear Mitotic Apparatus

PAK: p-21 Activated Kinase

PCV: Posterior Cardinal Vein

PDGFR: Platelet-Derived Growth Factor Receptor

PFA: Paraformaldehyde

PI3K: Phosphoinositide 3 Kinase

PIP: Phosphoinositides

PIP_2: Phosphatidylinositol-4,5-biphosphate

PIP_3: Phosphatidylinositol-3,4,5-triphosphate

PIPKIγ: Phosphatidylinositol-4-phosphate 5-kinase type 1γ

PKC: Protein Kinase C

PKL: Paxillin Kinase Linker

PLCγ: Phospholipase Cγ

Plk1: Polo-like kinase 1

PLL: Poly-L-Lysine

PR: Proline-rich Region

PTEN: Phosphatase and Tensin homolog

Pyk2: Protein Tyrosine Kinase

QDs: Quantum Dots

RFs: Retraction Fibers

RFP: Red Fluorescent Protein

RGD: Arg-Gly-Asp

ROCK: Rho-associated protein Kinase

RT: Room Temperature

SBD: Src Binding Domain

SD: Substrate Domain

SEM: Standard Error of the Mean

SH: Src Homology

STAT1: Signal Transducer and Activator of Transcription

SYFs: Src Family Kinases

TALEN: Transcription Activator-Like Effector Nuclease

TEO: Triethanolamine

uPAR: Urokinase-type Plasminogen Activator Receptor

VASP: Vasodilator-stimulated Phosphoprotein

VBS: Vinculin Binding Sites

VCAM-1: Vascular Cell Adhesion Molecule 1

VEGFR: Vascular Endothelial Growth Factor Receptor

VN: Vitronectin

VP: Vegetal Pole

WASP: Wiskott-Aldrich syndrome protein

WAVE: WASP-family verprolin-homologous protein

WT: Wild Type

Xbra: *Xenopus* Brachyury

7.2. Buffers, solutions and media

10xMMR

0.1 M NaCl

1.8 mM KCl

1 mM $MgSO_4$

2 mM $CaCl_2$

5 mM HEPES

pH 7.8

0.05 mg/ml Gentamycin

1xMAB (1 L)

11.61 g Maleic Acid (100 mM)

30 ml 5 M NaCl

800 ml distilled water

pH 7.5

add distilled water to 1 L

Autoclave

1xMEMFA (100 ml)

0.1 M MOPS (pH 7.4)

2 mM EGTA

1 mM $MgSO_4$

3.7% Formaldehyde

Prepare 10x solution of MEM and autoclave (turns yellow)

Before use add formaldehyde and dilute 1:10 (1xMEMFA)

Alkaline Phosphatase Buffer (1 L)

100 ml 1 M Tris (pH 9.5)

20 ml 5 M NaCl

50 ml 1 M $MgCl_2$

pH 9.5

Bleaching Solution (50 ml)

1.25 ml 20xSSC

2.5 ml Formamide

2 ml 30% Peroxide

BMB blocking solution

10 g BMB block in 1xMAB (100 ml final)

Autoclave

2 ml 10xBMB in 1xMAB (10 ml final)

Cystein

1.8 g L-Cystein diluted in 0.33xMMR

pH 7.8

DFA

53 mM $NaCl_2$

5 mM Na_2CO_3

4.5 mM Potassium gluconate

32 mM Sodium gluconate

1mM $CaCl_2$

1mM $MgSO_4$

Ficoll

4 g Ficoll diluted in 0.33xMMR

Hybridization Buffer (1 L)

10 g Boehringer Block

500 ml Formamide

250 ml 20xSSC

Heat to 65^{o}C for 1 hour

120 ml distilled water

100 ml Torula RNA (10 mg/ml in distilled water, dissolved at 65^{o}C, filtered)

2 ml Heparin (50 mg/ml in 1xSSC, pH 7)

5 ml 20% Tween-20

10 ml 10% CHAPS

10 ml 0.5 M EDTA

Filter (5 μm)

MK's modified lysis buffer

50 mM Tris pH 8

150 mM NaCl

0.5% NP40

0.5% Triton-X100

1 mM EGTA

5 mM NaF

PBST

1xPBS

0.5% Triton-X

1% dimethyl sulfoxide

RIPA lysis buffer

50 mM TrisHCl pH 7.4

150 mM NaCl

2 mM EDTA

1% NP-40

0.1% SDS

1% deoxycholate 24 mM

7.3. Publications

A ligand independent integrin β1 mechanosensory complex guides spindle responses to external forces (under revision)

Petridou NI and Skourides PA

FAK transduces extracellular forces that orient the mitotic spindle and control tissue morphogenesis

Petridou NI and Skourides PA

Nat Commun. 2014 Oct 24;5:5240

A dominant-negative provides new insights into FAK regulation and function in early embryonic morphogenesis

Petridou NI, Stylianou P and Skourides PA

Development. 2013 Oct; 140(20):4266-76

Activation of endogenous FAK via its amino terminal domain in Xenopus embryos

Petridou NI*, Stylianou P*, Christodoulou N, Rhoads D, Guan JL and Skourides PA

PLoS One. 2012;7(8):e42577

* Equal contribution

OPEN ACCESS Freely available online

PLoS one

Activation of Endogenous FAK via Expression of Its Amino Terminal Domain in *Xenopus* Embryos

Nicoletta I. Petridou[1☯], Panayiota Stylianou[1☯], Neophytos Christodoulou[1], Daniel Rhoads[1], Jun-Lin Guan[2], Paris A. Skourides[1]*

1 Department of Biological Sciences, University of Cyprus, Nicosia, Cyprus, **2** Department of Internal Medicine-MMG, University of Michigan Medical School, Ann Arbor, Michigan, United States of America

Abstract

Background: The Focal Adhesion Kinase is a well studied tyrosine kinase involved in a wide number of cellular processes including cell adhesion and migration. It has also been shown to play important roles during embryonic development and targeted disruption of the FAK gene in mice results in embryonic lethality by day 8.5.

Principal Findings: Here we examined the pattern of phosphorylation of FAK during Xenopus development and found that FAK is phosphorylated on all major tyrosine residues examined from early blastula stages well before any morphogenetic movements take place. We go on to show that FRNK fails to act as a dominant negative in the context of the early embryo and that the FERM domain has a major role in determining FAK's localization at the plasma membrane. Finally, we show that autonomous expression of the FERM domain leads to the activation of endogenous FAK in a tyrosine 397 dependent fashion.

Conclusions: Overall, our data suggest an important role for the FERM domain in the activation of FAK and indicate that integrin signalling plays a limited role in the in vivo activation of FAK at least during the early stages of development.

Citation: Petridou NI, Stylianou P, Christodoulou N, Rhoads D, Guan J-L, et al. (2012) Activation of Endogenous FAK via Expression of Its Amino Terminal Domain in *Xenopus* Embryos. PLoS ONE 7(8): e42577. doi:10.1371/journal.pone.0042577

Editor: Effie C. Tsilibary, National Center for Scientific Research Demokritos, Greece

Received March 29, 2012; **Accepted** July 9, 2012; **Published** August 6, 2012

Funding: Funding was provided by the Cyprus Research Promotion Foundation (ΥΓΕΙΑ/ΒΙΟΣ/0609(BE)/14). The funder had no role in study design, data collection and analysis, decision to publish, or preparation of the manuscript.

Competing Interests: The authors have declared that no competing interests exist.

* E-mail: skourip@ucy.ac.cy

☯ These authors contributed equally to this work.

Introduction

Cell adhesion and migration are essential processes for embryonic development, wound healing and inflammation. Cell movements and specifically cell migration require coordinated adhesion and detachment of cells from the extracellular matrix (ECM) [1,2]. The Focal Adhesion Kinase (FAK) is a 125-kDa non-receptor tyrosine kinase that is recruited to focal adhesions and shown to be activated by integrin signalling [3]. As a key mediator of cell-ECM signalling, FAK has an important role in cell adhesion and migration, yet our understanding of the regulation of its activity in these processes remains incomplete [4,5,6].

The study of FAK has for a long time primarily focused on its role in cell adhesion and cell migration and as a result a lot of research has been carried out regarding the ways FAK becomes activated downstream of integrin signalling. Upon integrin-mediated adhesion, FAK becomes tyrosine phosphorylated and subsequently activated [7]. Signalling molecules, like Src and phosphatidylinositol 3-kinase (PI3K), are recruited into complexes with FAK, leading to the transduction of biochemical signals that control a wide number of biological processes including cell migration, proliferation, and survival [5,8,9]. The involvement of FAK in one or more of these processes is necessary for normal embryonic development, since FAK knockout mice exhibit embryonic lethality [10]. In addition, cells lacking FAK display impaired integrin-dependent cell migration, whereas expression of the dominant negative protein FRNK (FAK Related Non-Kinase) blocks endogenous FAK phosphorylation in vivo and in vitro and suppresses the ability of cells to spread on fibronectin and to elicit integrin-induced signals [10,11,12].

FRNK is the C-terminal domain of FAK which contains the focal adhesion targeting (FAT) sequence and the region between the catalytic domain and FAT (a region which contains docking sites for SH3 domain-containing proteins including p130Cas) [11,13,14]. The FAT domain has been shown to be both necessary and sufficient for focal adhesion targeting of FAK although the mechanism of focal adhesion targeting has not been fully elucidated [15]. However, focal adhesion targeting has been shown to be necessary for FRNK's dominant negative activity [16]. FAK contains two additional domains, an N-terminal domain which exhibits homology with FERM domains and a central tyrosine kinase domain [17]. One of the main ways that FAK is regulated is via tyrosine phosphorylation. Several sites of tyrosine phosphorylation have been identified including two tyrosine residues in the activation loop (tyrosines 576 and 577) which regulate its catalytic activity and the major site of autophosphorylation, tyrosine 397 [18,19]. Tyrosine 397 is located between the catalytic and the FERM domains and in its

phosphorylated state serves as a binding site for SH2 domain containing proteins, including Src family kinases as well as PI3K [20,21]. While the roles of the catalytic and C-terminal domains of FAK have been explored extensively, more recently studies have begun exploring the function of the N-terminal domain in detail.

As mentioned above, the N-terminal domain of FAK exhibits homology with FERM domains, which are structurally conserved domains found in many proteins. The FAK FERM domain has been shown to mediate protein-protein interactions and several binding partners have been identified, including the cytoplasmic tails of the β1 integrin subunit, growth factor receptors and phosphatidylinositol-4,5-bisphosphate (PtdIns(4,5)P_2–PIP2) [22,23,24,25]. In general, FAK's FERM domain is primarily viewed as having an inhibitory role on FAK's activity. Several reports have demonstrated that deletion of the N-terminal domain of FAK leads to elevation of FAK's catalytic activity, maintaining however responsiveness to integrin signalling [26,27]. In addition, the FAK FERM domain can bind the FAK kinase domain and can inhibit FAK activity in trans. Specifically, exogenous FERM impairs the catalytic activity of full-length FAK in vitro and FAK signalling in adherent cells in culture [27]. Mutations which partially relieve the FERM binding onto the kinase domain also lead to elevated kinase activity [28]. From the above, a direct auto-inhibitory mechanism for FAK regulation was proposed and the crystal structure of the FERM and kinase domains of FAK support this model. Specifically, the FERM inhibition of FAK's kinase activity is thought to result from steric inhibition of target protein access to the catalytic cleft and to tyrosine 397 [29]. Release of the FERM binding would presumably allow FAK autophosphorylation on tyrosine 397 and the subsequent recruitment of Src leading to full activation through phosphorylation of the kinase activation loop.

Despite FAK's importance in development little is known about FAK's specific role and activation mechanisms in the embryo [30]. In this study, the data presented suggest an important role for the FERM domain in the in vivo activation of FAK during early embryogenesis. Furthermore, we conclude that despite the importance attributed to integrin signalling in the activation of FAK, it appears that integrin signalling plays a limited role in the in vivo setting at least during the early stages of development. This conclusion is supported by two major findings. First, FRNK fails to localize at the plasma membrane where the bulk of phosphorylated FAK is localized and second, expression of FRNK even at very high levels fails to block endogenous FAK phosphorylation in the early embryo. In addition, we show that the FERM domain is both necessary and sufficient for targeting FAK to the plasma membrane. Expression of the FERM domain leads to elevated phosphorylation of endogenous FAK as well as elevated phosphorylation of FAK-Src complex downstream target proteins like p130Cas and paxillin, suggesting that FERM expression can lead to FAK activation. This elevation is dependent on an intact tyrosine 397 site on the N-terminal domain suggesting that FERM activates endogenous FAK through Src.

Results

Expression and Phosphorylation of FAK during *Xenopus* Development

Xenopus FAK was originally cloned by Zhang et al. and its expression was analyzed in detail by the DeSimone group. It was determined that FAK is expressed maternally and that elevated levels are found in the highly mophogenetically active mesodermal tissues and in addition at the somitic boundaries. Additionally, increased levels of expression and phosphorylation of FAK were observed during gastrulation indicating that FAK may be involved in regulating embryonic cell adhesive behaviour and morphogenesis [31,32]. In an effort to better characterize the spatiotemporal expression and phosphorylation of FAK in the embryo we examined the endogenous levels of phosphorylation on tyrosines 397, 576 and 861 in western blotting (Figure 1A) and whole mount immunofluorescence experiments (Figure 1B) using previously characterized antibodies against the phosphorylated forms of the above sites. As shown in Figure 1 all three sites are phosphorylated in all developmental stages we examined including pre-gastrula stages. Phosphorylation of tyrosine 397 follows a similar pattern to what was reported by Hens and DeSimone for total phospho-FAK, ie phosphorylation increases during development with an increase observed during gastrulation [32]. A similar increase is observed for phosphorylation of tyrosines 576 and 861 however for these two sites a drop is observed during neurulation (Figure 1A). Whole mount indirect immunofluorescence shows that phosphorylated FAK is localized at the plasma membrane of the cells (Figure 1B) suggesting that FAK activation takes place at the plasma membrane as expected. Elevated levels of phosphorylated FAK are seen in the highly morphogenetic mesodermal tissues suggesting a possible involvement of FAK in these movements (Figure 1B). Examination of the localization pattern of tyrosine phosphorylated paxillin (Y-31) at these stages reveals a very similar pattern to that of phosphorylated FAK (Figure 1B, 4th row). High magnification optical sections at the blastopore lip reveal that the mesoderm contains much higher levels of phosphorylated FAK (Figure 2A, white arrow) compared to the adjacent endoderm of the blastopore (Figure 2A, red arrow) as well as the single layer of endodermal cells that will line the archenteron and surround the mesoderm (Figure 2A, white arrowheads). In addition, the superficial cells of the ectoderm on the animal cap display lower levels of FAK phosphorylation compared to the deep cells (Figure 2B). The detection of phosphorylated FAK prior to gastrulation including early blastula stages and the presence of phosphorylated FAK on the apical surface of superficial cells is surprising (Figure 1B, 1st column and Figure 2C). Prior to gastrulation there is no fibronectin secretion [33], and no laminin expression [34]. In addition, cells from *Xenopus* embryos are unable to spread or migrate on fibronectin prior to gastrulation [35]. These taken together suggest that there is little, if any cell-ECM signalling at these early stages of development and thus FAK phosphorylation is most likely integrin-independent. This notion is also supported by the presence of phosphorylated FAK at the apical surface of superficial blastomeres which are clearly not exposed to the ECM (Figure 2C). The apical surface of each superficial cell is isolated from the basolateral region with tight junctions which prevent diffusion of membrane bound molecules between the two areas [36]. Thus it is likely that activated FAK at the apical surface of these cells is exclusively activated through mechanisms independent of integrin signalling.

FAK is Phosphorylated in Integrin-free Regions of the Cell and FRNK Expression Fails to Block FAK Phosphorylation in the Early Embryo

To further explore the possibility that FAK activation in the early embryo is integrin-independent we compared the localization of phosphorylated FAK in relation to that of integrins. Double whole mount in situ immunofluorescence using P-Y397 and integrin-β1 antibodies where carried out and embryos were imaged on a confocal microscope (Figure 2E–J). α5β1-integrin is ubiquitously expressed and is the primary integrin heterodimer responsible for both mesoderm migration on fibronectin as well as

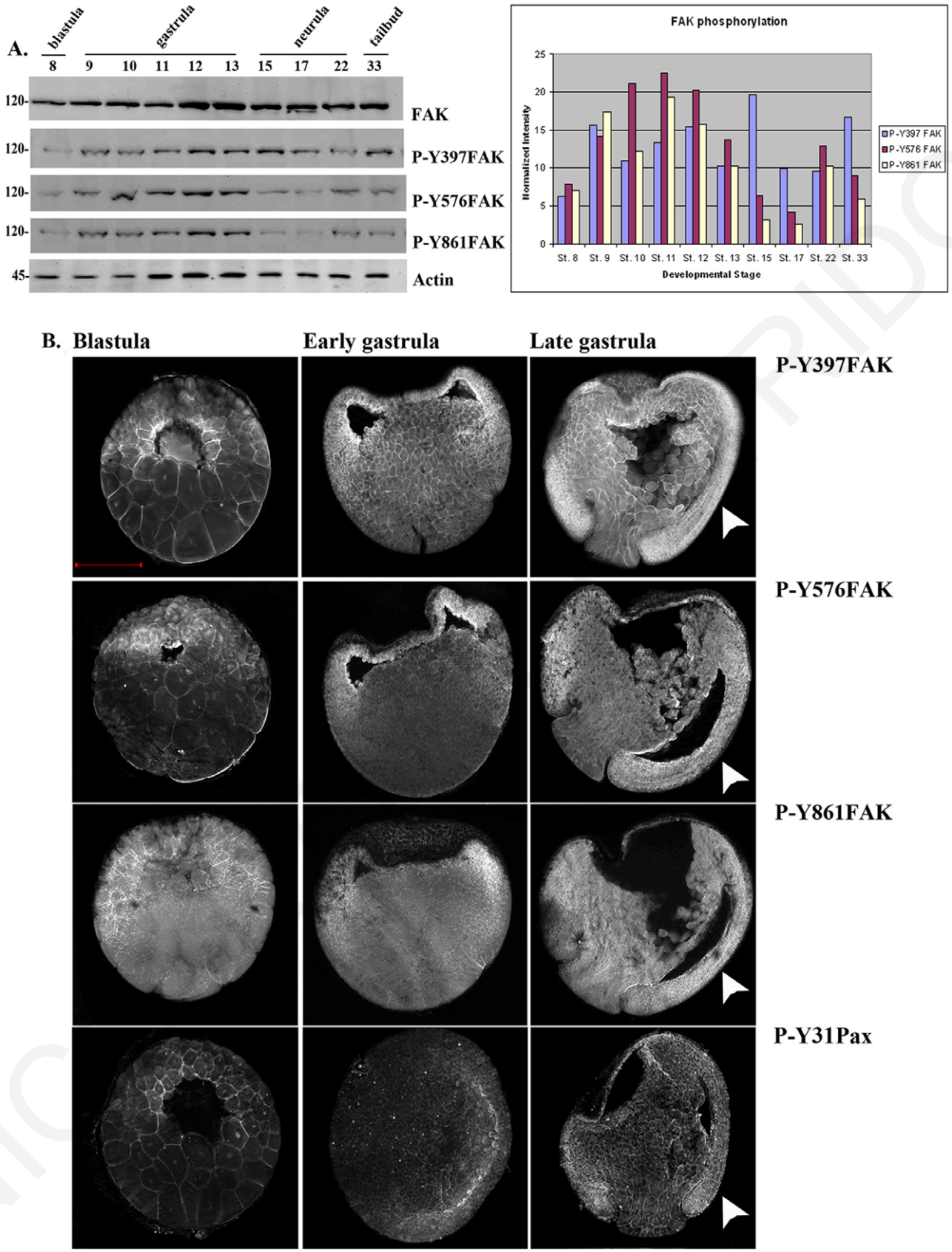

Figure 1. FAK expression and phosphorylation during development. (A) Western Blots from extracts of equal numbers of embryos probed with a monoclonal antibody against the C-terminus of FAK or polyclonal antibodies against the phosphorylated tyrosine residues indicated. FAK is phosphorylated on all three residues both before and after gastrulation. The intensity values from the densitometry analysis of the western blots

were normalized against total FAK amount. (B) Blastula (1st column), early gastrula (2nd column) and late gastrula embryos (3rd column) stained with P-Y397, P-Y576, P-Y861 and P-Y31paxillin antibodies as indicated. Phosphorylated FAK and paxillin can be detected on the plasma membrane from early blastula stages including the apical region of superficial blastomeres. During gastrulation elevated levels of phosphorylation are detected in the highly morphogenetic mesodermal tissues (white arrowheads). Scale bar: 400 μm.
doi:10.1371/journal.pone.0042577.g001

control of fibronectin deposition by animal cap cells on the blastocoel roof (BCR) [37]. As seen in Figure 2G phosphorylated FAK is localized tightly on the membrane in a similar fashion to integrin-β1 at sites of cell–cell contact (white arrowhead). However, despite strong phospho-FAK signal on the apical surface of superficial cells, no integrin-β1 staining can be detected in this region of the cell (Figure 2E, red arrow). This is in agreement with previous reports indicating that integrin-α5 is also not detectable on the apical surface of these cells [37]. On the other hand, in cells facing the blastocoel where fibronectin fibrils are assembled [38,39], both activated FAK and integrins are found on the apical side of the membrane where they colocalize (Figure 2I). Importantly high magnification optical sections from superficial ectodermal cells of the animal cap reveal that the level of FAK phosphorylation is identical between the apical and basolateral regions in these cells suggesting that either FAK activation is completely integrin independent in both cases or that FAK is activated through different mechanisms in the basolateral vs the apical region of these cells (Figure 2C). On the other hand, high magnification optical sections of the deep cells of the ectoderm facing the blastocoel reveals an elevation of FAK phosphorylation at the apical compared to the basolateral region in these cells (Figure 2D). This could be interpreted as integrin based elevation since fibronectin is lining the blastocoel and both α5 and β1 integrins are present in this region [37,40]. It should also be noted that in these high magnification images of deep ectodermal cells the phospho-FAK signal in the basolateral region appears relatively uniform and no focal adhesion like structures can be detected. However on the apical surface of these cells which is facing the fibronectin network of the BCR, the phospho-FAK staining is of higher intensity with clearly visible high intensity foci which may represent focal adhesion like structures (Figure 2D).

To further examine the integrin component of FAK activation in the early embryo we overexpressed FRNK and examined its effect on the endogenous phosphorylation of FAK on tyrosines 397 and 576. Overexpression of FRNK has been shown to block cell spreading and tyrosine phosphorylation of endogenous FAK, paxillin, and tensin [41]. Although focal adhesion localization and thus integrin colocalization of FRNK is not the sole determinant for its dominant negative activity, it is required for this dominant negative activity suggesting that FRNK exerts its effect by blocking FAK specifically at integrin based activation sites [16]. However, as shown in Figure 3 expression of FRNK in DMZ cells has no effect on the levels of phosphorylation of FAK on tyrosines 397 and 576 during gastrulation in vivo as determined by immunofluorescence and western blotting (Figure 3 A–H, Q). This is in contrast to the clear downregulation of phosphorylation on both tyrosine 397 and 576 seen when we expressed FRNK via transfection in the *Xenopus* A6 cell line (Figure 3I–L, M–P respectively). In agreement with the lack of dominant negative activity FRNK fails to localize at the plasma membrane in animal cap cells unlike phosphorylated endogenous FAK which is found exclusively on the plasma membrane in these cells (Figure 3R, S). These results demonstrate a strong context dependence with regards to the dominant negative activity of FRNK and are in agreement with the possibility that the bulk of phosphorylated FAK in the early embryo results through integrin independent mechanisms.

The FERM Domain is both Necessary and Sufficient for Plasma Membrane Localization of FAK in Integrin-free Regions of the Cell

The above data raised the possibility that FAK is primarily activated through integrin-independent mechanisms in the early *Xenopus* embryo. Since the C-terminus of FAK which is both necessary and sufficient for focal adhesion localization fails to localize at the plasma membrane of animal cap cells (Figure 3S) we postulated that the N-terminus which has been shown to bind PIP2 and growth factor receptors may in fact be the major determinant for the localization of active FAK in vivo [4,5,6]. To explore the role of the FERM domain in the localization of endogenous FAK on the plasma membrane, a series of constructs were generated (based on chicken FAK which shares a 91% identity and 95% similarity at the amino acid level with *Xenopus* FAK and conservation of all tyrosine phosphorylation sites) and examined with respect to their localization in cells of the animal pole and their ability to specifically localize to the integrin-free apical surface of these cells. Each construct was expressed as an HA tagged protein through mRNA injection at the two AP-dorsal blastomeres of four-cell stage embryos, and embryos were subsequently processed for whole mount immunofluorescence using a monoclonal anti-HA antibody. As shown in Figure 4 the FERM domain, unlike FRNK, displays strong plasma membrane localization and is also found on plasma membrane associated vesicles (Figure 4A). This pattern closely matches that of phosphorylated FAK (Figure 4B) suggesting that the FERM domain rather than the FAT domain is responsible for membrane localization of active FAK in the embryo. To further investigate the role of the FERM domain in the localization of activated FAK we examined the localization of the full length FAK K38A point mutant, in which the FERM kinase domain interaction is compromised, and compared it to that of the Δ375 mutant, which lacks the FERM domain. Both constructs are constitutively active due to the loss in the case of the K38A mutant of the FERM kinase inhibitory interaction and absence of the FERM domain in the case of the Δ375. The two constructs exhibit significant differences in terms of their ability to localize to the plasma membrane with the K38A exhibiting strong membrane localization while the Δ375 is very diffuse and appears completely absent from the plasma membrane in the cells of the animal cap (Figure 4C and D respectively).

These results suggest that the FERM domain is both necessary and sufficient for the localization of FAK on the plasma membrane.

Expression of the N-terminal Domain of FAK Leads to Elevated Phosphorylation of Endogenous FAK and Downstream Targets in a Src Dependent Manner

To further explore the role of the FERM domain in the activation of FAK in *Xenopus* we examined the effects of FERM domain overexpression in the developing embryo. Embryos were injected with the FERM domain either at the animal pole or at the two dorsal blastomeres of four cell stage embryos and were allowed to develop to tadpole stages. FERM expressing embryos developed normally and were identical to controls suggesting that FAK function was not being affected (data not shown). To examine the

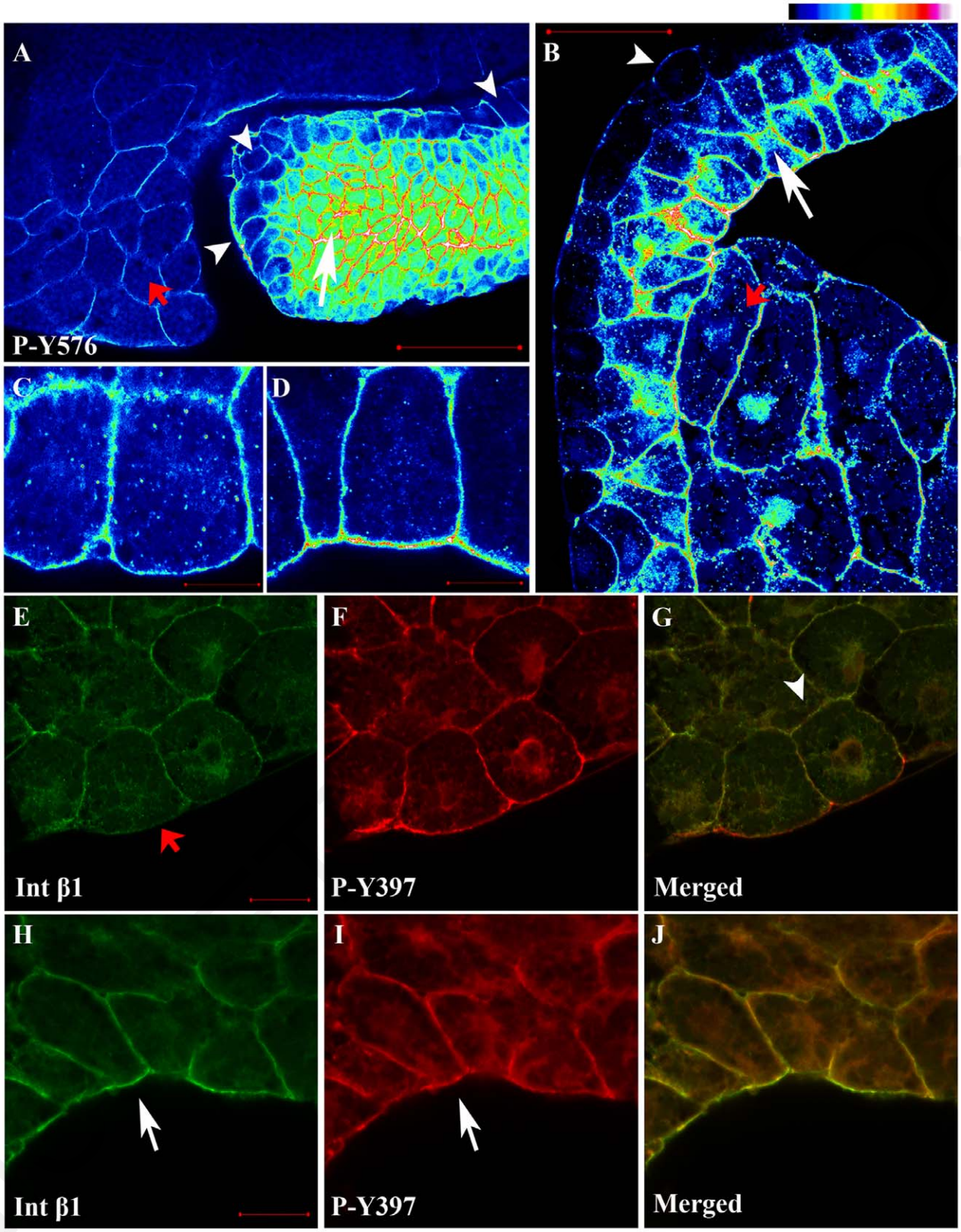

Figure 2. FAK is heavily phosphorylated in mesodermal tissues and integrin-free regions of cells. (A) Intensity color coded confocal section of the dorsal lip region from a whole mount immunostained gastrula stage embryo using a P-Y576 FAK antibody. Mesodermal cells (white arrow) display much higher levels of phospho-FAK than endodermal cells lining the forming archenteron (white arrowheads) and the endodermal cells of the blastopore (red arrow). (B) Same as A but showing the anterior mesendoderm and the animal cap from a whole mount immunostained gastrula stage embryo. The superficial cells of the animal cap (white arrowhead) show lower levels of phospho-FAK signal compared to deep cells

(white arrow) and mesendodermal cells (red arrow). (C) High magnification color coded narrow optical section of superficial cells of the animal cap reveals that the apical surface of these cells display similar levels of phospho-FAK compared to the basolateral region while (D) the apical region of the deep cells of the animal cap facing the fibronectin ECM display significantly elevated levels of phospho-FAK compared to the basolateral region. In addition, in the deep cells of the ectoderm labeling of phospho-FAK in the basolateral region is relatively uniform but the apical region displays distinct foci of higher signal intensity (E–G) Confocal optical sections from whole mount immunostained embryos using integrin-β1 (green) and P-Y397 FAK antibodies (red). Integrin-β1 and P-Y397 FAK colocalize on the plasma membrane at cell–cell boundaries (white arrowhead). However phosphorylated FAK is also present on the apical region of the outermost cells of the embryo where integrin-β1 is absent (red arrow). (H–J) Same embryo as above but the cells facing the blastocoel cavity are imaged. Integrin-β1 and P-Y397 FAK colocalize on the apical surface of the cells facing the blastocoel (white arrows). Scale bars: (A) 100 μm, (B) 50 μm, (C, D) 10 μm, (E) 30 μm, (H) 20 μm.
doi:10.1371/journal.pone.0042577.g002

effects of FERM expression on endogenous FAK the experiment was repeated and embryos were either fixed or lysed at gastrula stage. As shown in Figure 5, cells expressing FERM, show elevated levels of endogenous phosphorylated FAK on tyrosines 576 and 861 compared to un-injected neighbouring cells suggesting that FERM expression leads to activation of endogenous FAK (Figure 5A–D, 5I–L respectively, red stars: injected cells, white stars: control cells). This is a surprising finding and several experiments were carried out to ensure that the phospho-FAK antibodies used were in fact specific in this context. These control experiments are described in detail in the methods section and presented in Figure S1. To confirm the activation of FAK in FERM overexpressing embryos western blotting experiments and densitometry analysis were carried out. Lysates from FERM injected embryos contain comparable levels of total FAK as controls but elevated phosphorylation on tyrosines 397, 576 and 861 (Figure 5Q). It should be noted that only a subset of the cells in the embryo are expressing the construct (~50%) so the upregulation is effectively underestimated in western blotting experiments. In addition blotting of the HA-FERM with an anti P-Y397 antibody shows that the exogenously expressed protein is phosphorylated on tyrosine 397 in agreement with previously published work (Figure 5Q, 2nd row) [25,42]. Expression of the N-terminus of FAK has been previously shown to block integrin-dependent FAK activation [27,28]. To preclude the possibility that the observed effect is *Xenopus* specific we expressed the FERM domain in *Xenopus* A6 cells and examined the effects on endogenous levels of phospho-576 via indirect immunofluorescence. As shown in Figure 5 (R–U) FERM expression in *Xenopus* adherent cells results in a moderate reduction (compared to the more drastic effects of FRNK expression, Figure 3M–P) of phospho-576 levels indicating that FERM does in fact block FAK activation in cultured *Xenopus* cells. The opposite results obtained in vivo and in vitro with regard to the effects of FERM expression may be explained by a differential effect of FERM expression in integrin vs non integrin-based activation of FAK. Expression of the N-terminus of FAK in FAK null cells has been shown to actually partially rescue the EGF induced cell migration defect suggesting that the FERM domain can partially transduce growth factor based signals autonomously supporting this possibility [25].

Since tyrosine 397 is a known Src binding site [21] and tyrosines 576 and 861 are targets of Src [18,43] we went on to examine the possibility that an intact tyrosine 397 was required for the FERM induced activation of FAK. We generated a FERM Y397F construct and the construct was overexpressed in *Xenopus* embryos. As shown in Figure 5, cells expressing FERM Y397F do not display elevated levels of phosphorylation on tyrosines 576 and 861 (Figure 5E–H and M–P) suggesting that the observed activation of endogenous FAK is dependent on Src. This is also supported by the fact that in embryos treated with the Src inhibitor PP2, tyrosine phosphorylation on both 576 and 861 is severely reduced indicating that, in the developing embryo, FAK phosphorylation of the above residues is dependent on Src (Figure S1). Finally, to confirm the FERM induced activation of endogenous FAK we examined the phosphorylation status of p130Cas and paxillin, two FAK-Src downstream targets [44,45]. Expression of FERM, but not FERM Y397F, leads to elevated phosphorylation of both paxillin and p130Cas but not of Akt which is a substrate of PI3K (Figure 6A–D, E–H, I–L) [46]. These results show that FERM expression leads to activation of endogenous FAK and subsequent phosphorylation of FAK-Src targets in a tyrosine 397 dependent manner.

Discussion

The Focal Adhesion Kinase is a cytoplasmic kinase shown to be involved in a number of diverse processes including cell adhesion, migration, proliferation and survival. It has also been shown to be necessary for embryonic development since FAK knockout mice die early during development due to defects of the axial mesoderm [10]. FAK as a focal adhesion protein has been primarily studied with respect to integrin-based activation on 2D matrices. On such matrices it has been shown to be activated downstream of integrin clustering and to have an important role in the assembly and disassembly of focal adhesions [47,48,49,50,51,52]. However, focal adhesions are much smaller on soft matrices and different in structure, localization, and function in cells embedded in 3D matrices which resemble the in vivo setting better [53,54,55]. In addition cell polarization is also dependent on matrix rigidity and controlled by mechanosensing at the focal adhesions [55]. FAK's phosphorylation is much lower in cells grown on soft matrices and surprisingly no tyrosine 397 phosphorylation can be detected on 3D-matrix adhesions [56,57,58]. In fact downregulation of some proteins has the opposite effect in terms of their role in cell migration when tested on 2D vs 3D matrices. Overall it appears that regulation of 2D cell motility by focal adhesion proteins is not necessarily predictive of regulation of cell motility in a 3D matrix [53]. Things get even more complicated when examining focal adhesion proteins in the context of a living organism in which case not only the cell is faced with a 3D matrix but it also faces a 3D cell–cell adhesion network. These differences raise the need for the study of adhesion molecules like FAK in an in vivo setting in order to allow the integration of the valuable knowledge generated on FAK signaling in vitro back to a more physiologically relevant context.

Here we explore the activation of the Focal Adhesion Kinase in the context of the *Xenopus* embryo. We initially examined FAK phosphorylation on three major tyrosine residues 397, 576 and 861 during development. In agreement with previously published work, we observed elevated FAK phosphorylation on all three residues during gastrulation suggesting a possible role of FAK in embryonic morphogenesis. Specifically, phospho-FAK levels were elevated in the mesoderm compared to the endoderm in gastrula stage embryos and deep cells of the animal cap displayed elevated levels of phospho-FAK compared to the cells of the outermost epithelium. Surprisingly, phosphorylation was detected on all three residues from early blastula stages before the mid-blastula transition and well before the initiation of gastrulation and cell

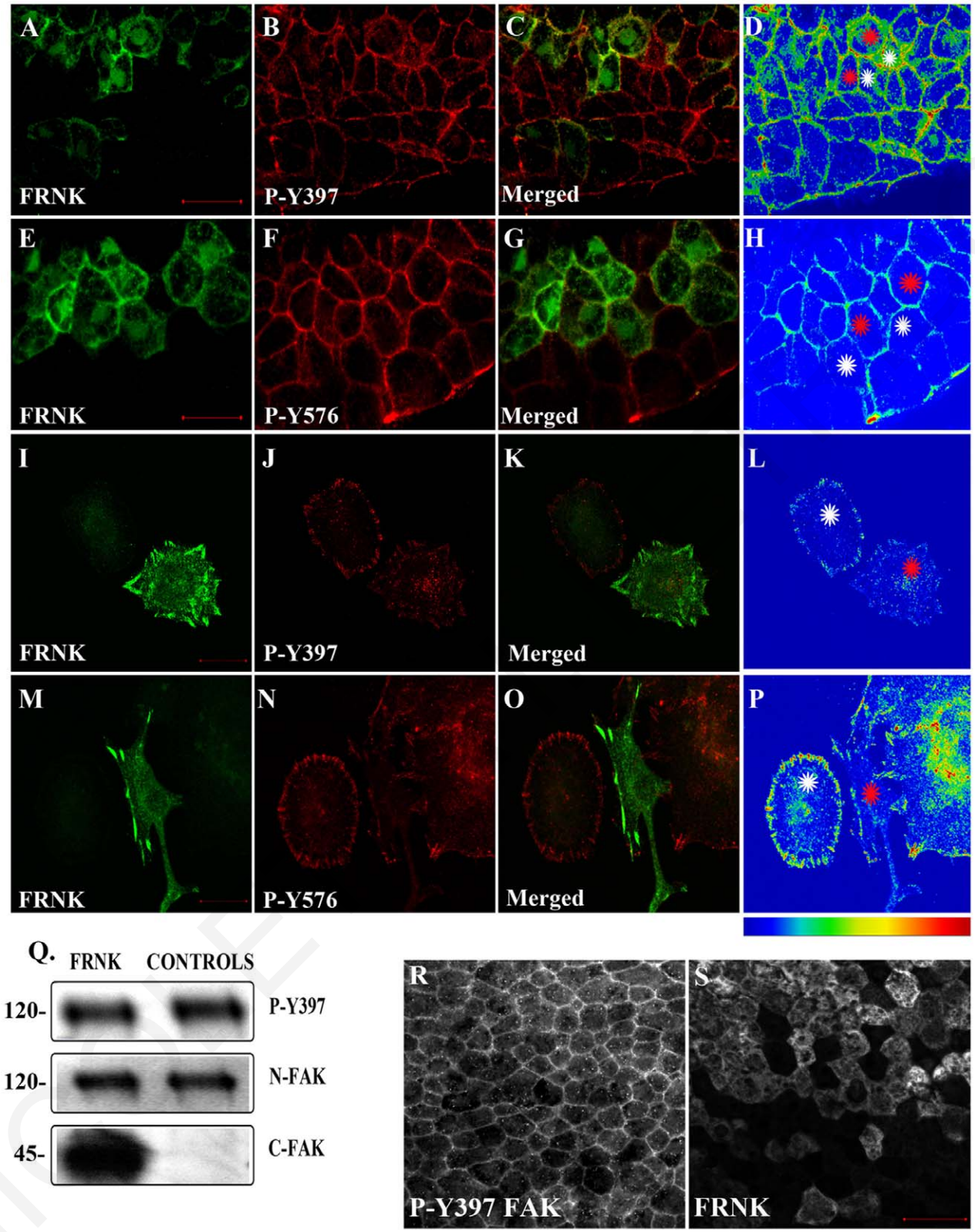

Figure 3. FRNK does not act as a dominant negative in early *Xenopus* embryos. (A–D) Optical sections of whole mount immunostained embryos injected with 1 ng GFP-FRNK at the two dorsal blastomeres at the four-cell stage. Embryos were stained with anti-GFP (A) and anti-P-Y397 (B). C is the merged image and D an intensity color coded image of the anti-P-Y397 signal. FRNK injected cells are indicated with red stars and control cells with white stars. FRNK expression fails to reduce the phosphorylation levels of endogenous FAK on tyrosine 397. (E–H) Same as A–D, but the embryos were stained with anti-GFP (E) and anti-P-Y576 (F). FRNK expressing cells display similar levels of phosphorylation on tyrosine 576 as neighboring control cells. (I–L) Confocal images of A6 *Xenopus* cells transfected with GFP-FRNK. Cells were stained with anti-GFP (I) and anti-P-Y397

(J). K is the merged image and L an intensity color coded image of the anti-P-Y397 signal. FRNK expression leads to reduction of the phosphorylation levels of FAK on tyrosine 397 at the focal adhesions. (M–P) Same as I–L but the cells were stained with anti-GFP (M) and anti-P-Y576 (N) antibodies. FRNK expression leads to downregulation of the endogenous phosphorylation levels of FAK on tyrosine 576 at the focal adhesions. (Q) Western blot analysis of control and injected gastrula stage embryos with 1 ng FRNK at the animal pole of both blastomeres of two cell stage embryos. FRNK expression fails to reduce endogenous FAK phosphorylation on tyrosine 397. FRNK expression was verified using a FAK antibody raised against the C-terminus of the protein. (R–S) Localization of P-Y397 FAK (R) and FRNK (S) in animal pole cells of stage 10 *Xenopus* embryos. P-Y397 FAK shows strong membrane localization while FRNK is primarily cytoplasmic in these cells. Scale bars: (A) 40 μm, (E) 30 μm, (I) 20 μm, (M) 20 μm, (R–S) 40 μm.
doi:10.1371/journal.pone.0042577.g003

movements. What the role of FAK during these early developmental stages might be is not known but the mechanism of activation is not likely to be through integrins but rather through growth factor receptors. While FAK could be detected in the cytosol the plasma membrane and the nuclei of cells in the embryo, tyrosine phosphorylated FAK was only found on the plasma membrane suggesting that activation takes place there. No focal adhesion like structures could be detected and the staining

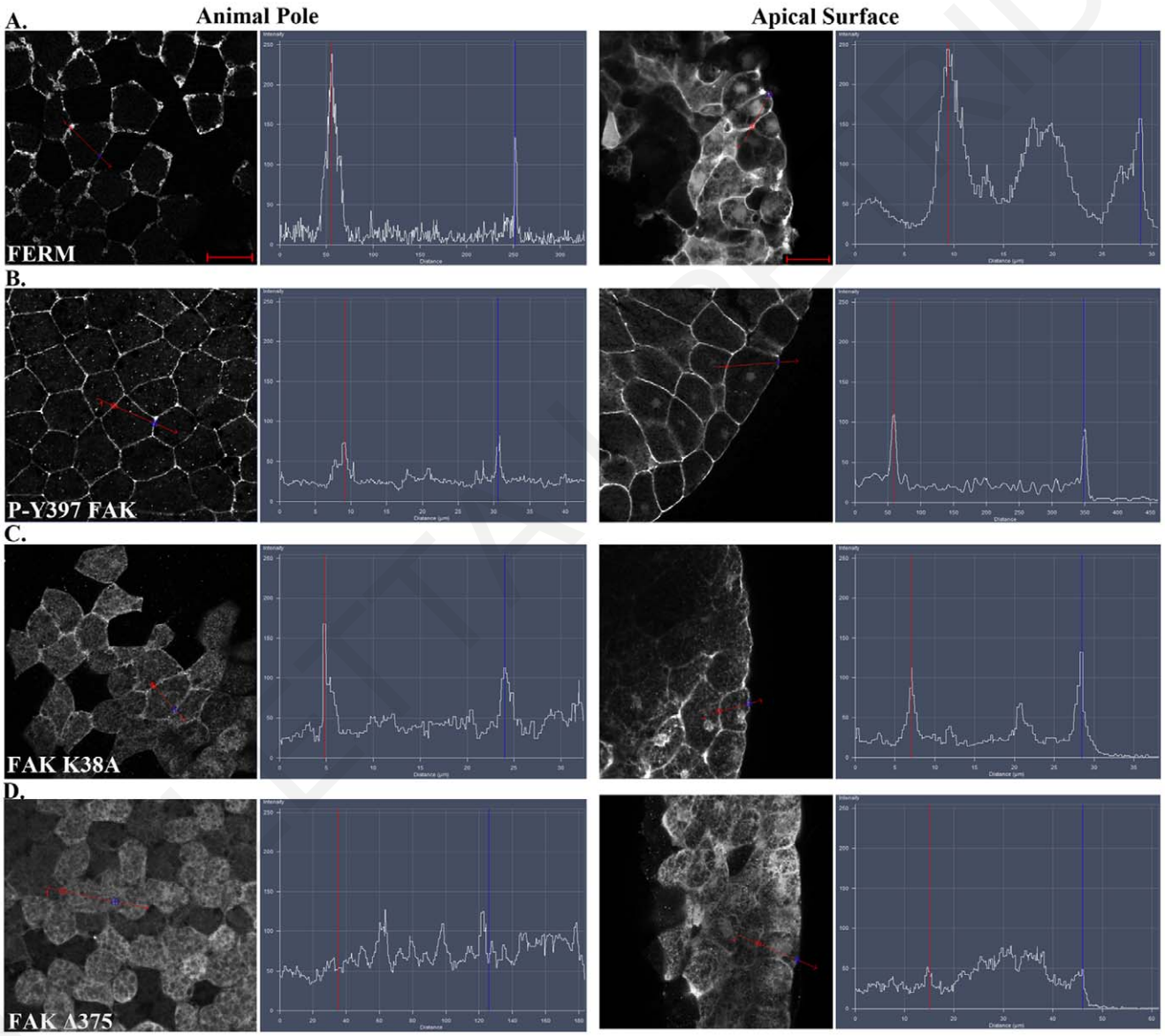

Figure 4. The FERM domain is necessary and sufficient for membrane localization of FAK at integrin-free regions. Confocal images and intensity profiles of the indicated constructs after whole mount immunostaining. The first column are top views of superficial cells of the animal cap in intact embryos and the second column are views from sagittally sectioned embryos that reveal the localization of each construct on the apical surface of superficial cells. Apical region of superficial blastomeres is to the right. (A) The FERM domain shows strong plasma membrane localization in the top view and is strongly localized to the apical surface. (B) Endogenous phosphorylated FAK shows very strong plasma membrane localization in the top view and is localized on the basolateral and apical surface of the cell. (C) Full length FAK with the point mutation K38A exhibits strong membrane localization. (D) Deletion of the FERM domain (HA-Δ375 FAK construct) abolishes the plasma membrane localization of FAK. Scale bars: 25 μm.
doi:10.1371/journal.pone.0042577.g004

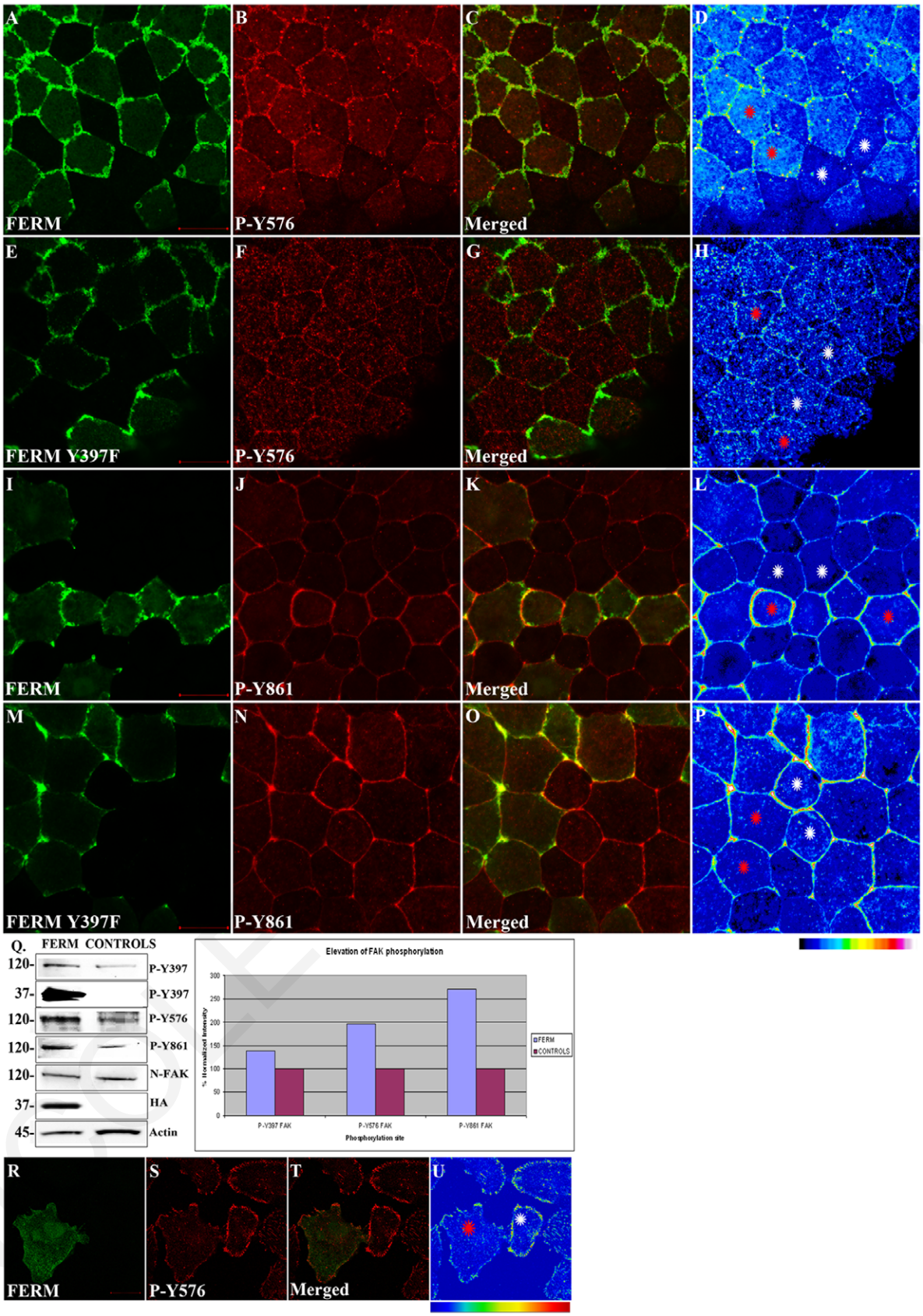

Figure 5. The FERM domain leads to activation of endogenous FAK in a tyrosine 397 dependent manner. HA-FERM and HA-FERM Y397F injected embryos in one blastomere at the animal pole of two cell stage embryos were processed for whole mount immunostaining using an HA antibody (green) to reveal expressing cells and the respective phospho-specific antibodies (red) as indicated. In each case individual signals for

each secondary are shown in addition to a merged image and finally an intensity color coded image of the respective phospho-specific antibody signal. HA-FERM and HA-FERM Y397F injected cells are indicated with red stars and un-injected cells with white stars. (A–D) Levels of phosphorylated tyrosine 576 are elevated in HA-FERM overexpressing cells compared to controls. (E–H) Overexpression of HA-FERM Y397F has no effect on the endogenous levels of phosphorylated tyrosine 576. HA-FERM Y397F expressing cells have the same levels of phosphorylated endogenous FAK on tyrosine 576 with neighboring control cells. (I–L) Levels of phosphorylated tyrosine 861 are elevated in HA-FERM expressing cells compared to controls. (M–P) Overexpression of HA-FERM Y397F has no effect on the endogenous levels of phosphorylated tyrosine 861. HA-FERM Y397F expressing cells have the same levels of phosphorylated endogenous FAK on tyrosine 861 with neighboring control cells. (Q) Total lysates from HA-FERM injected gastrula stage embryos contain comparable levels of endogenous FAK as un-injected controls but elevated levels of phosphorylated FAK on tyrosines 397, 576 and 861. Blotting using the anti-P-Y397 antibody shows that the exogenously expressed FERM is heavily in trans phosphorylated on tyrosine 397 (2nd row). The intensity values from the densitometry analysis were normalized against total FAK and present the average increase in phosphorylation from three independent experiments (R–U) Confocal images of A6 *Xenopus* cells transfected with HA-FERM. Cells were stained with anti-HA (R) and anti-P-Y576 (S). T is the merged image and U an intensity color coded image of the anti-P-Y576 signal. Transfected cells are shown with red stars and controls with white stars. HA-FERM transfected cells show reduced levels of tyrosine 576 phosphorylation suggesting that FERM expression blocks FAK activation in these cells. Scale bars: (A) 40 μm, (E) 30 μm, (I) 20 μm, (M) 50 μm, (R) 20 μm.
doi:10.1371/journal.pone.0042577.g005

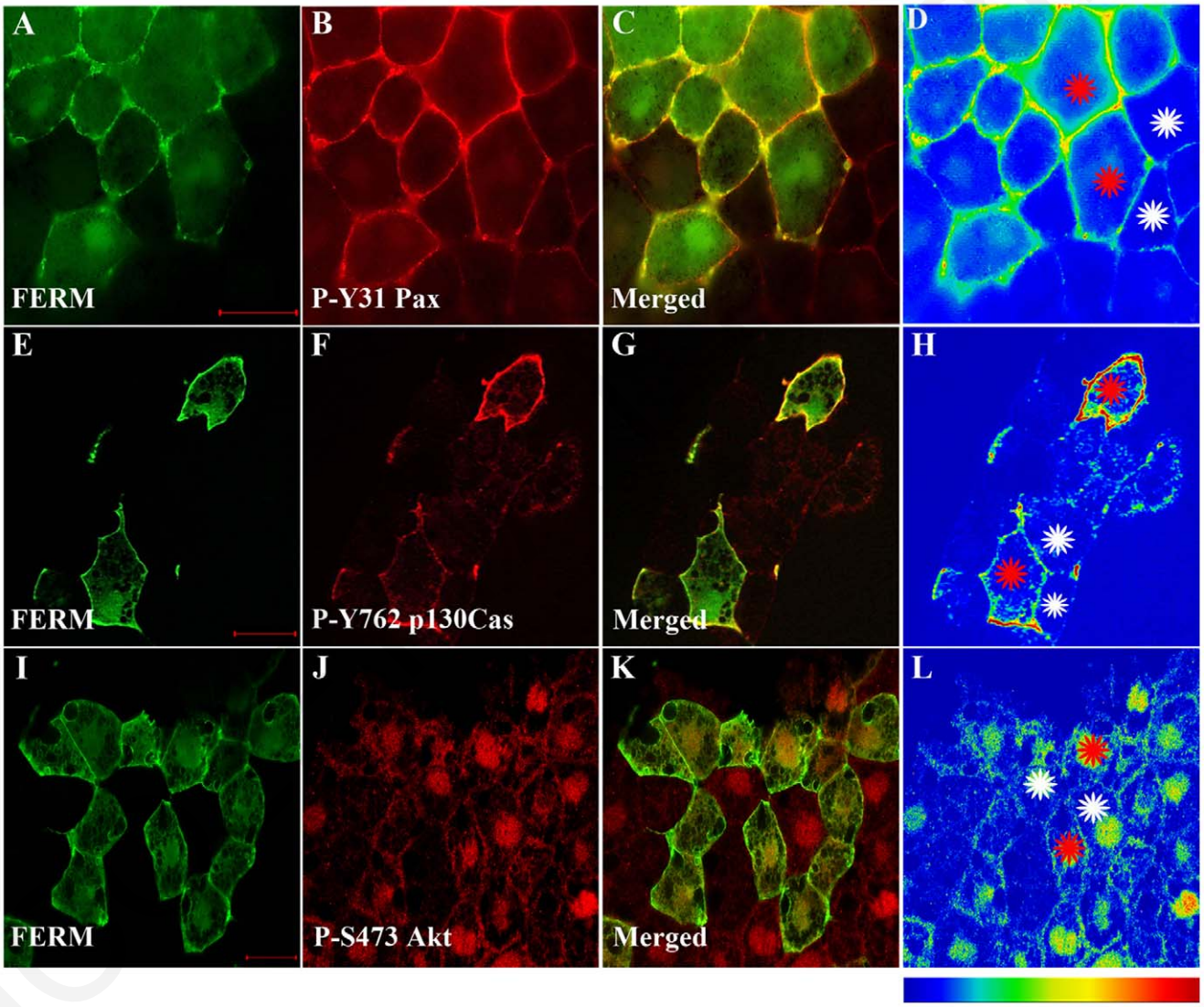

Figure 6. The FERM domain activates endogenous FAK leading to increased phosphorylation of FAK/Src targets. (A–D) Embryos injected with HA-FERM mRNA in two blastomeres, at the animal pole, at the four cell stage were processed for immunofluorescence using anti-HA (green) and anti-P-Y31 paxillin (red) antibodies. C is the merged image and D is an intensity color coded image. FERM expressing cells display elevated levels of phosphorylated paxillin (red stars) when compared with un-injected neighbouring cells (white stars). (E–H) Same as (A–D) but comparing phosphorylation levels of p130Cas on tyrosine 762 between FERM expressing and control cells. FERM expressing cells show elevated levels of phosphorylated p130Cas (red stars), when compared with un-injected cells (white stars). (I–L) Same as (A–D) but comparing levels of phosphorylated Akt on serine 473 between FERM expressing and control cells. Levels of phosphorylated Akt are comparable in FERM expressing cells to those of control neighboring cells. Scale bars: 20 μm.
doi:10.1371/journal.pone.0042577.g006

appears to be uniform on the surface of these cells. However at gastrula stages and specifically in the deep cells of the ectoderm which are in contact with the fibronectin matrix of the BCR, phospho-FAK is elevated and displays foci of higher signal intensity that resemble focal adhesion like structures. On the other hand, in superficial cells of the ectoderm we detected equal levels of phosphorylated FAK on the apical surface of the plasma membrane compared to the basolateral regions. Since the apical region of the plasma membrane is free from integrins and isolated from the basolateral with tight junctions this supports the notion that FAK activation during early development can be integrin-independent. Another possibility is that FAK activated at the basolateral region of these cells diffuses through the cytosol and relocalizes on the apical side of the plasma membrane. This is unlikely though because this would presumably generate a gradient of higher levels of phospho-FAK at the periphery of the apical membrane vs the center. This does not appear to be the case since the intensity of phospho-FAK signal is uniform on the apical plasma membrane of superficial cells.

We go on to show that FRNK, which has been shown to act as a dominant negative and block integrin-based FAK activation, fails to reduce FAK activation in the embryo, as determined by undiminished levels of FAK's tyrosine phosphorylation on key residues including tyrosine 397 and 576 [44]. We have in the past shown that FRNK does in fact reduce endogenous FAK phosphorylation of mesodermal explants plated on fibronectin and show now that it can do the same in *Xenopus* cell lines [59]. In all these cases however, FAK phosphorylation primarily derives from cell-ECM adhesion, whereas we present evidence suggesting that this is not the case in the early embryo. In fact the inability of FRNK to act as a dominant negative could itself be considered indirect evidence that FAK is activated independently of integrins in this context. In addition FRNK, despite containing the FAT domain which has been shown to be both necessary and sufficient for targeting FAK to focal adhesions, fails to target FAK at the plasma membrane in the embryo and is specifically absent from the integrin-free apical region of the plasma membrane in superficial blastomeres. This inability may explain why it fails to block FAK activation since it is presumably unable to compete endogenous FAK off of its complexes at the plasma membrane. FRNK has also been shown to act as a dominant negative during somitogenesis in *Xenopus* tadpoles. Specifically, FAK and other focal adhesion molecules, like paxillin as well as fibronectin and integrins, have been shown to localize at the intersomitic boundaries leading to the conclusion that focal adhesion contacts mediate the stabilization of somite boundaries [60,61,62]. Since FAK is activated through integrins in this context these data confirm that FRNK is able to block integrin-based activation of FAK in vivo. Although FRNK has been shown to block GFR based activation of FAK in cultured cells, for example PDGF induced activation of FAK in Vascular Smooth Muscle Cells is blocked by FRNK expression, it is possible that in this context where PDGF also induces the migration of these cells, FAK's activation is still largely integrin-dependent and indirect [63]. In addition, the FAT domain in FRNK has been shown to be the major determinant for FRNK's dominant negative function [41] suggesting that targeting to integrin-based complexes is the mechanism through which FRNK acts, suggesting that in the absence of the ability to target non integrin-based FAK complexes FRNK would not be able to act in a dominant negative fashion.

Exploring the domains of FAK that might be responsible for targeting of FAK to integrin-free regions of the plasma membrane we found that the N-terminal region of FAK is both necessary and sufficient for membrane localization. Exogenously expressed FERM recapitulates the localization of tyrosine phosphorylated FAK while FRNK fails to do so. In addition, deletion of the FERM domain leads to the reduction of plasma membrane localization of full length FAK. Overall these data suggest that the major determinant for localization of FAK on the plasma membrane of superficial cells of the embryo is the N-terminus. However, it should be noted that in DMZ cells which display the highest levels of FAK phosphorylation during gastrulation neither the FERM domain nor the FAT domain are sufficient to strongly target FAK to the plasma membrane (Figure S2) suggesting that in these cells both the FAT and the FERM domain may cooperate to target active FAK on the plasma membrane.

The fact that exogenously expressed FERM has such a dramatically different localization compared to full length FAK is most likely due to the fact that the majority of FAK in the cell is in the closed conformation with the FERM domain unavailable to bind growth factor receptors and PIP2 [64]. Expressed autonomously it no longer is impeded by its interaction with the kinase domain and free to bind targets on the plasma membrane. The strong membrane localization of the FERM domain coupled with the fact that it was shown to block FAK activation in trans raised the possibility that exogenously expressed FERM could block endogenous FAK activation in vivo. However, FERM expression lead to activation of endogenous FAK in a tyrosine 397 dependent fashion. Exogenous FERM is heavily phosphorylated on tyrosine 397 at the plasma membrane, presumably in trans by active endogenous FAK which is also at the plasma membrane. The fact that tyrosine 397 is necessary for the FERM induced activation of endogenous FAK leads to the conclusion that the exogenous phosphorylated FERM recruits Src to the plasma membrane leading to additional FAK phosphorylation. It is possible that the FERM domain in the context of non integrin-based activation has a greater affinity for the plasma membrane (PIP2 and GFRs) than for the kinase domain of endogenous FAK and thus fails to block endogenous FAK in trans but rather leads to further activation via Src. This interpretation is in agreement with recent data showing that Src is required for PDGF dependent activation of FAK whereas FAK is actually necessary for Src activation at integrin-based adhesions [65]. In addition, FERM domain expression has been shown to partially rescue the EGF stimulated migration defect of FAK null cells. This coupled with the fact that the FERM domain can autonomously interact with EGFR suggests that the FERM domain can in fact promote GFR based FAK signaling while blocking integrin-based activation [27,28]. The fact that FERM expression leads to FAK activation rather than downregulation in the early embryo supports the notion that FAK activation in this context is largely integrin-independent.

The results presented in this paper suggest that FAK is activated primarily through integrin-independent mechanisms in the early embryo and that the FERM domain and not the FAT domain is the primary determinant for FAK's localization at the plasma membrane, at least in integrin-free regions of the cell. In addition, the data suggest an important role of the FERM domain in the in vivo activation of FAK and provide new insights regarding the differences between integrin and GFR activation of FAK. Finally, these experiments suggest kinase dependent roles for FAK, which are independent of cell movement and cell-ECM interactions, very early during development. The generation of a dominant negative mutant that enables inhibition of FAK activity in early embryos would be an important step in order to begin exploring the possible roles of FAK at these early embryonic stages.

Methods

Embryos, Explants and Microinjections

Xenopus laevis embryos from induced spawning were staged according to Nieuwkoop and Faber (1967). Operation techniques and buffers have been described [66]. *Xenopus* embryos were fertilized in vitro and dejellied using 1.8% L-cysteine, pH 7.8, then maintained in 0.1X Marc's Modified Ringer's (0.1X MMR). Microinjections were performed in 4% Ficoll in 0.33X MMR. The embryos were injected with mRNA at the 2 and 4-cell stage according to established protocols [67]. The injections amounts per embryo were the following: GFP-FRNK 500 pg –1 ng, HA-FAK 100–200 pg, HA-FERM 500 pg, HA-FERM Y397F 500 pg, HA-FAKΔ375 500 pg, HA FAK K38A 300 pg. After the injections the embryos were cultured in 4% Ficoll in 0.33X MMR until stage 8 and then cultured in 0.1X MMR at room temperature.

Cell Culture and Transfections

The *Xenopus* cell line A6 [68] was grown in L-15 medium Leibovitz plus 10% FCS at room temperature. Transfection of A6 cells with the constructs HA-FRNK pCS108 and HA-FERM pCS108 was performed using Lipofectamine (Lipofectamine 2000, Invitrogen, UK) according to the manufacturer's protocol. The NIH3T3 (ATCC) and $FAK^{-/-}$ (ATCC) cell lines were grown in DMEM medium plus 10% FBS at 37°C. These cell lines were used in immunofluorescence experiments for the specificity of the phospho antibodies.

Antibodies and Surface Labelling

Indirect immunofluorescence assays were carried out as described [69,70] with modifications. Transfected and control A6 *Xenopus* cells were plated on glass coverslips (charged with HCl) washed three times with phosphate buffered saline (PBS) containing 0.5 mM $MgCl_2$ and 0.5 mM $CaCl_2$ (PBS++) and then fixed for 10 min in 4% paraformaldehyde solution in PBS. Fixation was followed by addition of 50 mM glycine solution in PBS and then the cells were permeabilized using 0.2% Triton-X solution in PBS for 10 min. Permeabilized cells were blocked using 10% normal donkey serum (Jackson Immunoresearch, USA) for 30 min. Cells were incubated with primary antibodies diluted in 10% normal donkey serum solution in PBS for one hour. The primary antibodies used were P-Y397 FAK rabbit polyclonal (1:500, 44624G-Invitrogen, UK) or P-Y576 FAK rabbit polyclonal (1:500, 44652G-eBiosource Invitrogen, UK) in combination with HA mouse monoclonal (1:500, sc-7392-Santa Cruz, USA). Cells were then washed five times in PBS. Secondary antibodies used were Cy3 anti-rabbit (1:500, 711-165-152, Jackson Immunoresearch, USA) and Alexa 488 anti-mouse (1:500, A11029, Molecular probes Invitrogen, UK).

For whole mount immunostaining, embryos were fixed in 10% 10XMEMFA-0.1 mM MOPS pH 7.4, 2 mM EGTA, 1 mM $MgSO_4$, 3.7% formaldehyde-10% formaldehyde and 80% water for 2 hours at room temperature and the vitelline envelope was removed manually. Embryos were then bisected and permeabilized for at least 5 hours in 1XPBS, 0.5% Triton, 1% DMSO (Perm solution) and blocked for 2 hours in 10% Normal Goat or Normal Donkey serum in Perm solution. Embryos were then incubated with primary antibodies. These included P-Y397FAK rabbit polyclonal (1:2000, ab4803-Abcam, USA), P-Y397 FAK mouse monoclonal (1:500, MAB1144-Chemicon Millipore, USA), P-Y397 FAK rabbit polyclonal (1:500, 44624G-Invitrogen, UK), P-Y576 FAK rabbit polyclonal (1:500, 44652G-eBiosource Invitrogen, UK), P-Y576 FAK rabbit recombinant monoclonal (1:500, 700013-Invitrogen, UK), P-Y576 rabbit polyclonal (1:1500, sc-16563-R, Santa Cruz), P-Y861 FAK rabbit polyclonal (1:500, 44-626G-eBiosource Invitrogen, UK), P-Y31 Paxillin rabbit polyclonal (1:150, sc-14035-Santa Cruz, USA), P-S473 Akt rabbit polyclonal (1:300, sc-7985-Santa Cruz, USA), HA mouse monoclonal (1:100, sc-7392-Santa Cruz, USA), HA rabbit polyclonal (1:500, NB600-363-Novus, UK). The incubation was performed overnight at 4°C. Embryos were then washed four times in Perm solution for 20 min, incubated for 2 hours RT with secondary antibodies Alexa 488 anti-mouse (1:500, A11029, Molecular probes Invitrogen, UK), Alexa 488 anti-rabbit (A11034, Molecular probes Invitrogen, UK), Cy3 anti-mouse (1:500, 715-165-150, Jackson Immunoresearch, USA), Cy3 anti-rabbit (1:500, 711-165-152, Jackson Immunoresearch, USA) at RT and then washed four times in Perm solution for 20 min. Clearing of embryos was performed by immersing the embryos in two parts Benzyl Benzoate and one part Benzyl Alcohol after dehydration (Murray's Clearing Medium).

The phosphospecific FAK antibodies although previously characterized used in the figures were tested further for specificity in the context they were used. Two-cell stage embryos were treated with 20 μM of the Src inhibitor PP2 (P0042, Sigma) until gastrula stages in order to block phosphorylation of endogenous FAK. Use of the Src inhibitor led to dramatic reduction of the signal of both the P-Y576 and P-Y861 in gastrula stage embryos (Figure S1A). In addition, both the P-Y397 and P-Y576 antibodies which were used extensively were tested in FAK knockout cells where they fail to detect focal adhesions in immunofluorescence experiments (Figure S1B and data not shown). To ensure that neither the P-Y576 nor the P-Y861 antibodies bind exogenous phosphorylated FERM western blotting experiments were carried out where FERM was initially probed with either a P-Y576 or a P-Y861 antibody, then striped and reprobed using a P-Y397 antibody. Neither P-Y576 nor P-Y861 bind exogenous FERM (Figure S1C). Moreover, colocalization analysis was performed in HA-FERM expressing embryos double stained for HA and P-Y576 or P-Y397. Although HA colocalizes strongly with P-Y397 as expected it does not with anti P-Y576 suggesting that no cross reactivity or bleed through is present (Figure S1D). Additionally, 30 ng of FAK morpholino (TTGGGTCCAGGTAAGCCG-CAGCCAT) was injected on both blastomeres of two cell-stage embryos to knock down endogenous FAK expression [71]. An approximately 50% drop of FAK protein level was observed at gastrula stages but more severe reduction was seen at tadpole stages via western blotting. In morphant tadpoles staining of the intersomitic boundaries with the anti P-Y576 antibody (Figure S1E) is significantly reduced suggesting that the antibody is specific. Finally, embryo lysates were phosphatase treated and we confirmed that no protein was detected under these conditions (not shown).

Western Blot Analysis

Protein lysates were prepared by homogenizing explants or embryos in ice cold RIPA lysis buffer (50 mM TrisHCl pH7.4, 150 mM NaCl, 2 mM EDTA, 1% NP-40, 0.1% SDS, 1% deoxycholate 24 mM) supplemented with phosphatase inhibitors (5 mM Sodium Orthovanatate, Na_3VO_4) and protease inhibitors (1 mM PMSF, Protease cocktail, Sigma). Homogenates were cleared by centrifugation at 15000 g for 30 min at 4°C [60]. Protein levels were determined by bicinchoninic acid assay (BCA) using the Magellan™ Data Analysis software (Tecan). The lysates were loaded on 7.5% SDS-polyacrylamide gels with the WesternC ladder (161-0376 Bio-Rad, USA). The proteins were transferred onto nitrocellulose membrane, blocked in 5% BSA (in TBST: 1X

TBS & 0.1% Tween). The blotting was performed by incubation of the primary antibodies in 3% BSA, overnight at 4°C. Blots were incubated with anti-FAK mouse monoclonal (1:200, 2A7-Upstate Biotechnology, USA), anti-FAK (1:500, 05–537, monoclonal from Millipore, USA) or phospho-FAK antibodies, P-Y397 FAK mouse monoclonal (1:200, MAB1144-Chemicon Millipore, USA), P-Y397 FAK rabbit polyclonal (1:3000, ab4803-Abcam, USA), P-Y576 FAK rabbit polyclonal (1:200, 44652G-eBiosource Invitrogen, UK), P-Y576 FAK rabbit recombinant monoclonal (1:500, 700013-Invitrogen), P-Y861 FAK rabbit polyclonal (1:200, 44-626G-eBiosource Invitrogen, USA), HA rabbit polyclonal (1:500, NB600-363-Novus, UK). The incubation was performed overnight at 4°C. Visualization was performed using HRP-conjugated antibodies (1 hour incubation RT) (Santa Cruz Biotechnology anti-rabbit and anti-mouse, USA) and detected with LumiSensor (GeneScript) on UVP iBox. For loading control an actin rabbit polyclonal antibody (1:1000, sc-1616-Santa cruz, USA) was used in every blot. Densitometry analysis was carried out using the Vision Works LS Software. The analysis of the results at Figures 1 and 5 included normalization of the intensity values of phospho-FAK signal against total FAK and averaging from three independent experiments.

Plasmids and Cloning

All plasmids were constructed using standard molecular biology techniques and they were sequenced to verify correct coding.

pCS108 HA-FERM. A PCR fragment amplified with F/HA-FERM (5′-ATGCGGCCGCATGTACCCATACGATGTTC-CAGATTACGCT-3′) and R/FERM (5′-TTTCTCGAGT-TAATCTATTATCTCTGCATAGTCATCTGT-3′) encoding HA FERM (up to amino acids 402 including tyrosine 397), using pKH3 HA-FAK plasmid (kindly provided by Dr. Guan laboratory) as template, was inserted into the multiple cloning site of the pCS108 vector by restriction enzyme digest with NotI/XhoI.

pCS108 HA-FERM Y397F. A PCR fragment amplified with F/HA-FERM primer and R/FERM Y397F primer (5′-TTTCTCGAGTTAATCTATTATCTCTGCAAAGT-CATCTGT-3′) encoding HA-FERM Y397F, using pKH3 HA-FAK Y397F plasmid as template was inserted into the multiple cloning site of the pCS108 vector by restriction enzyme digest with NotI/XhoI.

pCS2++ GFP-FRNK. GFP-FRNK construct in the adenoviral shuttle vector pShuttle was transferred to the CS2++ vector using the restriction enzymes BglII/NotI.

HA-FAKΔ375 construct (N-term 375 amino acids truncated) in pKH3 vector (kindly provided by Dr. Guan laboratory) was amplified by PCR techniques using the primers F/HA tag: 5′-ATGCGGCCGCATGTACCCATACGATGTTCCAGAT-TACGCT-3′and R/FRNK: 5′-TTTCTCGAGT-TAGTGGGGCCTGGACTGGCTGATCATTTT-3′ and cloned into the pCS108 vector.

All mutants were generated from FAK chicken variant.

The DNA amplification reactions were performed using AccuPrime^{TM} Pfx SuperMix (1234-040, Invitrogen, UK) which contains 22 U/ml Thermococcus species KOD thermostable polymerase complexed with anti-KOD antibodies, 66 mM Tris-SO_4 (pH 8.4), 30.8 mM $(NH_4)_2SO_4$, 11 mM KCl, 1.1 mM $MgSO_4$, 330 μM dNTPs, AccuPrime proteins and stabilizers.

All plasmids were transcribed into RNA using mMessage mMachine Sp6 kit (Ambion, UK) and the mRNAs were purified using the Mega Clear kit (Ambion, UK).

Imaging Analysis

Embryos were observed either under a Zeiss Axio Imager Z1 microscope, using a Zeiss Axiocam MR3 and the Axiovision software 4.8.2 or under a confocal LSM710 microscope (Zeiss, Germany). For the generation of the intensity profiles and the color coded pixel intensity profiles of the localization of the mutants the ZEN 2009 software was used.

Supporting Information

Figure S1 Characterization of the phosphospecific FAK antibodies. (A) Confocal images of mid-gastrula control and Src inhibitor treated embryos stained with the phosphospecific antibodies P-Y576 and P-Y861 showing a reduction in staining intensity in the presence of the inhibitors. (B) High magnification confocal images of the focal adhesions of NIH 3T3 and FAK −/− cells stained with the P-Y576 phosphospecific antibody showing lack of FAK staining in FAK knockout cells (C) Western blot of control and FERM expressing embryo lysates blotted with the P-Y576 and P-Y861 antibodies. Membranes were stripped and reprobed with a P-Y397 antibody to visualize the phophorylated FERM. Exogenous phosphorylated FERM is not recognized by the two phosphospecific antibodies. The blot with the P-Y576 antibody has two background bands slightly above and below the size of the FERM domain (black arrowhead) but these are also present at the control lane. (D) High magnification confocal images of immunostained FERM injected embryos either with HA and P-Y397 FAK (1st row) or HA and P-Y576 FAK (2nd row). Colocalization analysis of these images using the Zen 2010 Software shows strong colocalization between FERM and P-Y397 indicating recognition of the Tyr397 site of the exogenously expressed FERM domain by the P-Y397 antibody but very little between FERM and P-Y576 suggesting lack of bleedthrough artifacts and crossreactivity of the antibodies. (E) Maximum Intensity Projections of confocal Z-stacks from an immunostained control and a 30 ng of FAK morpholino injected tadpole using the P-Y576 antibody. Injected tadpoles show much lower P-Y576 levels suggesting that the antibody is specific when used in whole mount immunofluorecence experiments in *Xenopus*. Western blot analysis of lysates from FAK morpholino injected and control embryos with the C-903 FAK antibody showing an aproximately 50% reduction of endogenous FAK at the gastrula stage.
(TIF)

Figure S2 Localization of the HA-FERM (A) and HA-FRNK (B) constructs in DMZ injected cells. (C) Localization pattern of P-Y397 FAK in DMZ cells.
(TIF)

Acknowledgments

We thank Dr. Chenbei Chang for comments on the paper and to Drs. Niovi Santama and Kevin Pumiglia for generously providing reagents.

Author Contributions

Conceived and designed the experiments: PS JLG NIP PAS. Performed the experiments: NIP PAS NC. Analyzed the data: PS JLG NIP PAS NC DR. Contributed reagents/materials/analysis tools: DR JLG. Wrote the paper: PS.

References

1. Ridley AJ, Schwartz MA, Burridge K, Firtel RA, Ginsberg MH, et al. (2003) Cell migration: integrating signals from front to back. Science 302: 1704–1709.
2. Lauffenburger DA, Horwitz AF (1996) Cell migration: a physically integrated molecular process. Cell 84: 359–369.
3. Mitra SK, Hanson DA, Schlaepfer DD (2005) Focal adhesion kinase: in command and control of cell motility. Nat Rev Mol Cell Biol 6: 56–68.
4. Hall JE, Fu W, Schaller MD (2011) Focal adhesion kinase: exploring Fak structure to gain insight into function. Int Rev Cell Mol Biol 288: 185–225.
5. Peng X, Guan JL (2011) Focal adhesion kinase: from in vitro studies to functional analyses in vivo. Curr Protein Pept Sci 12: 52–67.
6. Schaller MD (2010) Cellular functions of FAK kinases: insight into molecular mechanisms and novel functions. J Cell Sci 123: 1007–1013.
7. Zachary I (1997) Focal adhesion kinase. Int J Biochem Cell Biol 29: 929–934.
8. Reiske HR, Kao SC, Cary LA, Guan JL, Lai JF, et al. (1999) Requirement of phosphatidylinositol 3-kinase in focal adhesion kinase-promoted cell migration. J Biol Chem 274: 12361–12366.
9. Parsons JT, Parsons SJ (1997) Src family protein tyrosine kinases: cooperating with growth factor and adhesion signaling pathways. Curr Opin Cell Biol 9: 187–192.
10. Ilic D, Furuta Y, Kanazawa S, Takeda N, Sobue K, et al. (1995) Reduced cell motility and enhanced focal adhesion contact formation in cells from FAK-deficient mice. Nature 377: 539–544.
11. Schaller MD, Borgman CA, Parsons JT (1993) Autonomous expression of a noncatalytic domain of the focal adhesion-associated protein tyrosine kinase pp125FAK. Mol Cell Biol 13: 785–791.
12. Taylor JM, Mack CP, Nolan K, Regan CP, Owens GK, et al. (2001) Selective expression of an endogenous inhibitor of FAK regulates proliferation and migration of vascular smooth muscle cells. Mol Cellular Biol 21: 1565–1572.
13. Harte MT, Hildebrand JD, Burnham MR, Bouton AH, Parsons JT (1996) p130Cas, a substrate associated with v-Src and v-Crk, localizes to focal adhesions and binds to focal adhesion kinase. J Biol Chem 271: 13649–13655.
14. Hayashi I, Vuori K, Liddington RC (2002) The focal adhesion targeting (FAT) region of focal adhesion kinase is a four-helix bundle that binds paxillin. Nat Struct Biol 9: 101–106.
15. Hildebrand JD, Schaller MD, Parsons JT (1993) Identification of sequences required for the efficient localization of the focal adhesion kinase, pp125FAK, to cellular focal adhesions. J Cell Biol 123: 993–1005.
16. Cooley MA, Broome JM, Ohngemach C, Romer LH, Schaller MD (2000) Paxillin binding is not the sole determinant of focal adhesion localization or dominant-negative activity of focal adhesion kinase/focal adhesion kinase-related nonkinase. Mol Biol Cell 11: 3247–3263.
17. Frame MC, Patel H, Serrels B, Lietha D, Eck MJ (2010) The FERM domain: organizing the structure and function of FAK. Nat Rev Mol Cell Biol 11: 802–814.
18. Calalb MB, Polte TR, Hanks SK (1995) Tyrosine phosphorylation of focal adhesion kinase at sites in the catalytic domain regulates kinase activity: a role for Src family kinases. Mol Cell Biol 15: 954–963.
19. Eide BL, Turck CW, Escobedo JA (1995) Identification of Tyr-397 as the primary site of tyrosine phosphorylation and pp60src association in the focal adhesion kinase, pp125FAK. Mol Cell Biol 15: 2819–2827.
20. Chen HC, Appeddu PA, Isoda H, Guan JL (1996) Phosphorylation of tyrosine 397 in focal adhesion kinase is required for binding phosphatidylinositol 3-kinase. J Biol Chem 271: 26329–26334.
21. Schaller MD, Hildebrand JD, Shannon JD, Fox JW, Vines RR, et al. (1994) Autophosphorylation of the focal adhesion kinase, pp125FAK, directs SH2-dependent binding of pp60src. Mol Cell Biol 14: 1680–1688.
22. Schaller MD, Otey CA, Hildebrand JD, Parsons JT (1995) Focal adhesion kinase and paxillin bind to peptides mimicking beta integrin cytoplasmic domains. J Cell Biol 130: 1181–1187.
23. Chen TH, Chan PC, Chen CL, Chen HC (2011) Phosphorylation of focal adhesion kinase on tyrosine 194 by Met leads to its activation through relief of autoinhibition. Oncogene 30: 153–166.
24. Chen SY, Chen HC (2006) Direct interaction of focal adhesion kinase (FAK) with Met is required for FAK to promote hepatocyte growth factor-induced cell invasion. Mol Cell Biol 26: 5155–5167.
25. Sieg DJ, Hauck CR, Ilic D, Klingbeil CK, Schaefer E, et al. (2000) FAK integrates growth-factor and integrin signals to promote cell migration. Nat Cell Biol 2: 249–256.
26. Jacamo RO, Rozengurt E (2005) A truncated FAK lacking the FERM domain displays high catalytic activity but retains responsiveness to adhesion-mediated signals. Biochem Biophys Res Commun 334: 1299–1304.
27. Cooper LA, Shen TL, Guan JL (2003) Regulation of focal adhesion kinase by its amino-terminal domain through an autoinhibitory interaction. Mol Cell Biol 23: 8030–8041.
28. Cohen LA, Guan JL (2005) Residues within the first subdomain of the FERM-like domain in focal adhesion kinase are important in its regulation. J Biol Chem 280: 8197–8207.
29. Ceccarelli DF, Song HK, Poy F, Schaller MD, Eck MJ (2006) Crystal structure of the FERM domain of focal adhesion kinase. J Biol Chem 281: 252–259.
30. Chatzizacharias NA, Kouraklis GP, Theocharis SE (2010) The role of focal adhesion kinase in early development. Histol Histopathol 25: 1039–1055.
31. Zhang X, Wright CV, Hanks SK (1995) Cloning of a Xenopus laevis cDNA encoding focal adhesion kinase (FAK) and expression during early development. Gene 160: 219–222.
32. Hens MD, DeSimone DW (1995) Molecular analysis and developmental expression of the focal adhesion kinase pp125FAK in Xenopus laevis. Dev Biol 170: 274–288.
33. Danker K, Hacke H, Ramos J, DeSimone D, Wedlich D (1993) V(+)-fibronectin expression and localization prior to gastrulation in Xenopus laevis embryos. Mech Dev 44: 155–165.
34. Fey J, Hausen P (1990) Appearance and distribution of laminin during development of Xenopus laevis. Differentiation 42: 144–152.
35. Ramos JW, Whittaker CA, DeSimone DW (1996) Integrin-dependent adhesive activity is spatially controlled by inductive signals at gastrulation. Development 122: 2873–2883.
36. Fesenko I, Kurth T, Sheth B, Fleming TP, Citi S, et al. (2000) Tight junction biogenesis in the early Xenopus embryo. Mech Dev 96: 51–65.
37. Joos TO, Whittaker CA, Meng F, DeSimone DW, Gnau V, et al. (1995) Integrin alpha 5 during early development of Xenopus laevis. Mech Dev 50: 187–199.
38. Winklbauer R, Stoltz C (1995) Fibronectin fibril growth in the extracellular matrix of the Xenopus embryo. J Cell Sci 108 (Pt 4): 1575–1586.
39. Sarrazin S, Lamanna WC, Esko JD (2011) Heparan sulfate proteoglycans. Cold Spring Harb Perspect Biol 3.
40. Marsden M, DeSimone DW (2001) Regulation of cell polarity, radial intercalation and epiboly in Xenopus: novel roles for integrin and fibronectin. Development 128: 3635–3647.
41. Richardson A, Parsons T (1996) A mechanism for regulation of the adhesion-associated proteintyrosine kinase pp125FAK. Nature 380: 538–540.
42. Toutant M, Costa A, Studler JM, Kadare G, Carnaud M, et al. (2002) Alternative splicing controls the mechanisms of FAK autophosphorylation. Mol Cell Biol 22: 7731–7743.
43. Calalb MB, Zhang X, Polte TR, Hanks SK (1996) Focal adhesion kinase tyrosine-861 is a major site of phosphorylation by Src. Biochem Biophys Res Commun 228: 662–668.
44. Richardson A, Malik RK, Hildebrand JD, Parsons JT (1997) Inhibition of cell spreading by expression of the C-terminal domain of focal adhesion kinase (FAK) is rescued by coexpression of Src or catalytically inactive FAK: a role for paxillin tyrosine phosphorylation. Mol Cell Biol 17: 6906–6914.
45. Tachibana K, Urano T, Fujita H, Ohashi Y, Kamiguchi K, et al. (1997) Tyrosine phosphorylation of Crk-associated substrates by focal adhesion kinase. A putative mechanism for the integrin-mediated tyrosine phosphorylation of Crk-associated substrates. J Biol Chem 272: 29083–29090.
46. Franke TF, Kaplan DR, Cantley LC, Toker A (1997) Direct regulation of the Akt proto-oncogene product by phosphatidylinositol-3,4-bisphosphate. Science 275: 665–668.
47. Webb DJ, Donais K, Whitmore LA, Thomas SM, Turner CE, et al. (2004) FAK-Src signalling through paxillin, ERK and MLCK regulates adhesion disassembly. Nat Cell Biol 6: 154–161.
48. Ren XD, Kiosses WB, Sieg DJ, Otey CA, Schlaepfer DD, et al. (2000) Focal adhesion kinase suppresses Rho activity to promote focal adhesion turnover. J Cell Sci 113 (Pt 20): 3673–3678.
49. Hamadi A, Bouali M, Dontenwill M, Stoeckel H, Takeda K, et al. (2005) Regulation of focal adhesion dynamics and disassembly by phosphorylation of FAK at tyrosine 397. J Cell Sci 118: 4415–4425.
50. Guan JL (1997) Focal adhesion kinase in integrin signaling. Matrix Biol 16: 195–200.
51. Guan JL (1997) Role of focal adhesion kinase in integrin signaling. Int J Biochem Cell Biol 29: 1085–1096.
52. Cary LA, Guan JL (1999) Focal adhesion kinase in integrin-mediated signaling. Front Biosci 4: D102–113.
53. Fraley SI, Feng Y, Krishnamurthy R, Kim DH, Celedon A, et al. (2010) A distinctive role for focal adhesion proteins in three-dimensional cell motility. Nat Cell Biol 12: 598–604.
54. Harunaga JS, Yamada KM (2011) Cell-matrix adhesions in 3D. Matrix Biol 30: 363–368.
55. Prager-Khoutorsky M, Lichtenstein A, Krishnan R, Rajendran K, Mayo A, et al. (2011) Fibroblast polarization is a matrix-rigidity-dependent process controlled by focal adhesion mechanosensing. Nat Cell Biol 13: 1457–1465.
56. Pelham RJ Jr, Wang Y (1997) Cell locomotion and focal adhesions are regulated by substrate flexibility. Proc Natl Acad Sci U S A 94: 13661–13665.
57. Cukierman E, Pankov R, Stevens DR, Yamada KM (2001) Taking cell-matrix adhesions to the third dimension. Science 294: 1708–1712.
58. Gonzales M, Weksler B, Tsuruta D, Goldman RD, Yoon KJ, et al. (2001) Structure and function of a vimentin-associated matrix adhesion in endothelial cells. Mol Biol Cell 12: 85–100.
59. Stylianou P, Skourides PA (2009) Imaging morphogenesis, in Xenopus with Quantum Dot nanocrystals. Mech Dev 126: 828–841.
60. Kragtorp KA, Miller JR (2006) Regulation of somitogenesis by Ena/VASP proteins and FAK during Xenopus development. Development 133: 685–695.
61. Henry CA, Crawford BD, Yan YL, Postlethwait J, Cooper MS, et al. (2001) Roles for zebrafish focal adhesion kinase in notochord and somite morphogenesis. Dev Biol 240: 474–487.

62. Crawford BD, Henry CA, Clason TA, Becker AL, Hille MB (2003) Activity and distribution of paxillin, focal adhesion kinase, and cadherin indicate cooperative roles during zebrafish morphogenesis. Mol Biol Cell 14: 3065–3081.
63. Sundberg LJ, Galante LM, Bill HM, Mack CP, Taylor JM (2003) An endogenous inhibitor of focal adhesion kinase blocks Rac1/JNK but not Ras/ERK-dependent signaling in vascular smooth muscle cells. J Biol Chem 278: 29783–29791.
64. Cai X, Lietha D, Ceccarelli DF, Karginov AV, Rajfur Z, et al. (2008) Spatial and temporal regulation of focal adhesion kinase activity in living cells. Mol Cell Biol 28: 201–214.
65. Seong J, Ouyang M, Kim T, Sun J, Wen PC, et al. (2011) Detection of focal adhesion kinase activation at membrane microdomains by fluorescence resonance energy transfer. Nat Commun 2: 406.
66. Ubbels GA, Hara K, Koster CH, Kirschner MW (1983) Evidence for a functional role of the cytoskeleton in determination of the dorsoventral axis in Xenopus laevis eggs. J Embryol Exp Morphol 77: 15–37.
67. Smith WC, Harland RM (1991) Injected Xwnt-8 RNA acts early in Xenopus embryos to promote formation of a vegetal dorsalizing center. Cell 67: 753–765.
68. Rafferty KA Jr, Sherwin RW (1969) The length of secondary chromosomal constrictions in normal individuals and in a nucleolar mutant of Xenopus laevis. Cytogenetics 8: 427–438.
69. Skourides PA, Perera SA, Ren R (1999) Polarized distribution of Bcr-Abl in migrating myeloid cells and co-localization of Bcr-Abl and its target proteins. Oncogene 18: 1165–1176.
70. Demetriou MC, Stylianou P, Andreou M, Yiannikouri O, Tsaprailis G, et al. (2007) Spatially and temporally regulated alpha6 integrin cleavage during Xenopus laevis development. Biochem Biophys Res Commun 3: 779–785.
71. Fonar Y, Gutkovich YE, Root H, Malyarova A, Aamar E, et al. (2011) Focal adhesion kinase protein regulates Wnt3a gene expression to control cell fate specification in the developing neural plate. Mol Biol Cell 22: 2409–2421.

Development 140, 4266-4276 (2013) doi:10.1242/dev.096073

A dominant-negative provides new insights into FAK regulation and function in early embryonic morphogenesis

Nicoletta I. Petridou, Panayiota Stylianou and Paris A. Skourides*

SUMMARY

FAK is a non-receptor tyrosine kinase involved in a wide variety of biological processes and crucial for embryonic development. In this manuscript, we report the generation of a new FAK dominant negative (FF), composed of the C terminus (FRNK) and the FERM domain of the protein. FF, unlike FRNK and FERM, mimics the localization of active FAK in the embryo, demonstrating that both domains are necessary to target FAK to its complexes *in vivo*. We show that the FERM domain has a role in the recruitment of FAK on focal adhesions and controls the dynamics of the protein on these complexes. Expression of FF blocks focal adhesion turnover and, unlike FRNK, acts as a dominant negative *in vivo*. FF expression in *Xenopus* results in an overall phenotype remarkably similar to the FAK knockout in mice, including loss of mesodermal tissues. Expression of FF in the animal cap revealed a previously unidentified role of FAK in early morphogenesis and specifically epiboly. We show that a fibronectin-derived signal transduced by FAK governs polarity and cell intercalation. Finally, failure of epiboly results in severe gastrulation problems that can be rescued by either mechanical or pharmacological relief of tension within the animal cap, demonstrating that epiboly is permissive for gastrulation. Overall, this work introduces a powerful new tool for the study of FAK, uncovers new roles for FAK in morphogenesis and reveals new mechanisms through which the FERM domain regulates the localization and dynamics of FAK.

KEY WORDS: FAK, FERM, *Xenopus*, Dominant negative, Epiboly

INTRODUCTION

The focal adhesion kinase (FAK) is a 125 kDa non-receptor tyrosine kinase shown to be activated by integrin signaling and act as a phosphorylation-regulated signaling scaffold to control adhesion turnover, cell migration, proliferation and survival (Mitra et al., 2005). FAK is composed of three major domains, the N-terminal FERM (4.1-band, ezrin, radixin, moesin) domain, followed by the central catalytic kinase domain and the C-terminal focal adhesion targeting (FAT) domain. The FERM domain of FAK is an important regulator of FAK activity as deletion or overexpression of the FERM domain leads to enhanced or suppressed tyrosine phosphorylation status, respectively (Cooper et al., 2003; Jácamo and Rozengurt, 2005). Specifically, the FERM domain promotes FAK interactions that cause conformational changes on the FAK molecule: from a closed inactive form where the FERM domain interacts with the kinase domain, to an open active form where this intramolecular interaction is relieved and Y397 becomes phosphorylated (Ceccarelli et al., 2006). This phosphorylation leads to exposure of the FAK activation loop and full catalytic activation, through binding of Src and subsequent phosphorylation on Y576 and Y577 (Calalb et al., 1995). The FERM domain was also found to bind to peptides of the β1-integrin cytoplasmic tail, the Arp2/3 complex, PIP_2 [PtdIns(4,5)P_2] and growth factor receptors (GFRs) (Cai et al., 2008; Chen and Chen, 2006; Schaller et al., 1995; Serrels et al., 2007; Sieg et al., 2000). However, exogenously expressed FERM domain does not localize to focal adhesions (FAs) and no direct *in vivo* binding has been demonstrated between FAK and integrins (Lawson and Schlaepfer, 2012). By contrast, the C terminus of FAK contains the FAT domain, a four-helix bundle that has been shown to be both necessary and sufficient for FA targeting (Chen et al., 1995; Hayashi et al., 2002; Hildebrand et al., 1993; Hildebrand et al., 1995). FRNK (FAK-related non kinase), which encompasses the FAK C-terminus, has been shown to act as a dominant-negative, possibly through competition with endogenous FAK at FAs (Richardson et al., 1997; Sieg et al., 1999).

Cells isolated from E8.0 FAK-null embryos display reduced mobility *in vitro* and an increased number of FAs, indicating that FAK is involved in the turnover of FAs (Ilić et al., 1995). Several lines of evidence have since confirmed a crucial role for FAK in FA turnover through a variety of mechanisms, including a spatially and temporally resolved role in Rho activation and inhibition, and interactions between the FERM domain of FAK and dynamin 2, which promote microtubule-dependent FA disassembly (Ezratty et al., 2005; Lim et al., 2008b; Ren et al., 2000; Tomar et al., 2009).

FAK has also been shown to play a role in cell survival and apoptosis through p53 and PI3K-dependent signaling (Golubovskaya et al., 2005; Lim et al., 2008a; Xia et al., 2004). FAK-null endothelial cells exhibit cell proliferation problems and high levels of apoptosis (Ilic et al., 2003). In addition, FAK was found to be phosphorylated on several serine residues during mitosis (Yamakita et al., 1999), and Ser732 specifically was shown to be phosphorylated by Cdk5 and to regulate centrosome function during mitosis and neuronal migration (Park et al., 2009; Xie et al., 2003).

Disruption of FAK in mice leads to early embryonic lethality by E8.5 due to generalized mesodermal defects (Furuta et al., 1995). The phenotype of the FAK null is similar to the fibronectin (FN) and integrin α5 knockouts, which also exhibit early embryonic lethality due to defects in mesodermally derived tissues, shortening of the anterior-posterior (A-P) axis and abnormal vascular development (George et al., 1993; Yang et al., 1993). The similarity of the FAK, FN and integrin knockouts provides strong evidence that FAK mediates the FN-integrin signaling required for early embryonic development. Studies in *Xenopus* have shown that FN-integrin interactions are essential for proper embryonic development, regulating major morphogenetic movements during

Department of Biological Sciences, University of Cyprus, Nicosia 2109, Cyprus.

*Author for correspondence (skourip@ucy.ac.cy)

Accepted 8 August 2013

gastrulation and neurulation. Disruption of these interactions leads to radial intercalation failure and loss of polarity in the deep ectodermal cells of the animal cap (AC) (Davidson et al., 2006; Marsden and DeSimone, 2001; Rozario et al., 2009). Both processes are required for epiboly, the morphogenetic movement that drives the thinning and expansion that allow the ectoderm to encompass the entire embryo by the end of gastrulation (Keller, 1980). However, studies of FAK in *Xenopus* with the use of morpholino (MO)-based knockdown have failed to identify any early morphogenetic roles for FAK. One study showed that FAK regulates Wnt3a expression and cell fate specification during neurulation (Fonar et al., 2011), and another revealed that FAK also plays an important role in *Xenopus* cardiogenesis (Doherty et al., 2010). However, we have shown that FAK-MO reduces FAK protein levels by about 50% at gastrula stages (Petridou et al., 2012); given the fact that the mouse $FAK^{+/-}$, which also display a 50% reduction of FAK protein levels, develops normally, it is likely that this reduction in not sufficient to reveal early roles of FAK in morphogenesis (Kostourou et al., 2013).

In this study, we have generated a new FAK construct that contains the N and C termini of FAK, termed FF. In the embryo, FF mimics the localization of active endogenous FAK, primarily localizing at sites of cell-cell contact. We show that the FERM domain is important for both the recruitment of FAK to nascent adhesions, as well as for the affinity and dynamics of FAK on FAs. Finally, we show that FF acts as a strong dominant-negative both *in vivo* and *in vitro*, and present data suggesting that FAK has a role in the transduction of a FN-integrin signal required for epiboly.

MATERIALS AND METHODS

Cell culture and transfections

XL177 cells were grown in 70% L-15, 15%FBS and 100 mM L-Glutamine at room temperature. Electroporation was carried out according to the manufacturer's protocol (Invitrogen).

Embryos, microinjections and explants

Xenopus laevis embryos were staged according to Nieuwkoop and Faber (Nieuwkoop and Faber, 1967). Embryos were fertilized *in vitro* and dejellied using 1.8% L-cysteine (pH 7.8), then maintained in 0.1× Marc's Modified Ringer's (MMR). Microinjections were performed in 4% Ficoll in 0.3×MMR. Capped mRNAs were *in vitro* transcribed using mMessage machine (Ambion). Rho kinase (ROCK) inhibitor (Sigma) (7 mM) was injected in the blastocoel at stage 10 as described previously (Woolner and Papalopulu, 2012).

Radial intercalation explants and induced AC explants were performed as described (Alfandari et al., 2001; Marsden and DeSimone, 2001) but with the use of glass bridges to hold the AC in place. AC elongation assays have been described previously (Stylianou and Skourides, 2009).

DNA constructs and morpholinos

All plasmids generated were verified by sequencing. Primers used are listed in supplementary material Table S1. HA-FF construct in pCS108 vector was generated by amplifying the FERM domain up to 402 amino acids from the HA-FAK pKH3 plasmid (Zhao et al., 1998) using the primers F/HA and R/FERM. FRNK was amplified from the same plasmid using F/FRNK and R/FAK with the inserted linker segment GGTAGCGGCAGCGGTAGC in the forward primer and ligated to the FERM domain. GFP sequence from pEGFP-N1 or mCherry sequence from pShuttle mCherry-tubulin (Addgene) was inserted at the *Xba*I site to generate the FF-GFP or FF-mCherry, respectively. GFP-FRNK and HA-FERM have been described previously (Petridou et al., 2012). HA-FRNK and HA-FAK K38A were subcloned from pKH3 (Zhao et al., 1998) using F/HA and R/FAK into pCS108 or pCS2++, respectively. HA-FF S732A was generated by site-directed mutagenesis of the HA-FF pCS108 plasmid with the primer FF732. All FAK mutants were generated from chicken FAK (GenBank AAA48765.1).

The sequence of FAK-MO is TTGGGTCCAGGTAAGCCGCAGCCAT (Fonar et al., 2011) and of Vinculin-MO is TATGGAAGACCGGCAT-CTTGGCAAT.

Whole-mount *in situ* hybridization

Whole-mount *in situ* hybridization of *Xenopus* embryos has been described previously (Smith and Harland, 1991).

RT-PCR

cDNA was prepared via reverse transcription (SuperScriptIII First strand synthesis, Invitrogen) from RNA extracted from FF-injected and control embryos. PCR was carried out using specific primer pairs for each marker.

TUNEL assay

TUNEL assay of *Xenopus* embryos was performed according to the Harland protocol (Conlon laboratory, North Carolina). Apoptotic nuclei were quantified by using the ImageJ ICTN plug-in.

Immunofluorescence

Immunofluorescence on XL177 cells and whole embryos has been described (Petridou et al., 2012). Primary antibodies used were: anti-vinculin (Hybridoma Bank), GFP (Invitrogen), P-Y576FAK (Santa Cruz), P-S732FAK (Invitrogen), HA (Santa Cruz), β-tubulin (Hybridoma Bank), FN (4H2, kindly provided by Dr Douglas DeSimone, Virginia, USA), β-catenin (Santa Cruz), P-MLC (Abcam) and H3 histone (Novus).

Western blot and analysis

Protein lysate preparation and western blotting have been described previously (Petridou et al., 2012). Antibodies used were: N-FAK (Millipore), P-S732FAK, HA, FN (4H2), actin (Santa Cruz) and P-Y20 (Santa Cruz). Densitometry analysis was carried out using the Vision Works LS Software. The analysis of the results in Fig. 6 included normalization of the intensity values of phospho-FAK signal against total FAK and averaging values from three independent experiments.

Immunoprecipitation

Immunoprecipitation was performed as described previously (Klymkowsky Lab Methods, see http://klymkowskylab.colorado.edu/Methods/Precipitation.htm) using anti-GFP antibody (Invitrogen).

Imaging analysis

Embryos were imaged either under a Zeiss AxioImager Z1 microscope, using a Zeiss Axiocam MR3 and Axiovision 4.8 or a Zeiss Lumar V12 stereomicroscope, or an LSM710 (Zeiss). The generation of the intensity profiles and the data analysis of FRAP and FLIP experiments were performed using the ZEN2010 software. FRAP experiments were conducted using a Plan-Apochromat 63×/1.40 oil. Relative recovery rates were compared using half time for recovery of fluorescence towards the asymptote. The fluorescence recovery curve was fitted by single exponential function, given by $F(t)=A(1-e^{-R})+B$; where F(t) is the intensity at time t, A and B are the amplitudes of the time-dependent and time-independent terms, respectively; τ is the lifetime of the exponential term; and the recovery rate is given by $R=1/\tau$. Immobile fractions were calculated by comparing the intensity ratio in the bleached area just before bleaching and after recovery.

RESULTS

The FERM and FAT domains cooperate to target FAK at the plasma membrane in the embryo, and at FAs in cultured cells

In the embryo, FAK can be detected in the cytosol, the nucleus and the plasma membrane; however, phosphorylated FAK is found almost exclusively on the plasma membrane (Petridou et al., 2012). The FAT domain has been shown to be both necessary and sufficient for FA targeting of FAK (Hildebrand et al., 1993). However, we have recently shown that neither the FAT nor the FERM domain alone can place FAK on the plasma membrane in the embryo (Petridou et al., 2012). We wanted to explore the possibility that the FERM and FAT

domains cooperate to target active FAK at the plasma membrane. We thus generated FERM-FRNK (FF), a construct which contains the N and C terminus sequences of FAK (supplementary material Fig. S1A). By removing the kinase domain, we wanted to mimic the active conformation of FAK in which the FERM domain is free to bind PIP_2 and GFRs (Cai et al., 2008; Chen and Chen, 2006; Sieg et al., 2000). Combining the two regions resulted in a dramatic change in localization, as shown in Fig. 1A. FF is almost exclusively localized at the plasma membrane, unlike FRNK and FERM, mimicking the localization of endogenous phosphorylated FAK. To explore the role of the FERM domain in the localization of FAK further, we compared the localization of FF and FRNK in cultured cells after generating GFP fusions of the two constructs. As shown in Fig. 1B, FRNK localizes in the cytosol and FAs, whereas FF is predominantly localized on FAs with little signal in the cytosol. In addition, FF expressors have FAs throughout the cell, whereas, in FRNK expressors, FAs are primarily found in the cell periphery (Fig. 1B; supplementary material Fig. S1B). To preclude the possibility that FF appeared to have stronger localization on FAs, due to the fact that FF expression induces stronger and more abundant FAs, we co-transfected GFP-FRNK with FF-mCherry. As shown in supplementary material Fig. S1C, FF displays lower cytoplasmic signal than FRNK, suggesting a role for the FERM domain in the localization of FAK at FA complexes. In addition, FF expression displaces full-length FAK from FAs and nearly eliminates FAK phosphorylation on these complexes, demonstrating a strong dominant-negative activity (Fig. 1C,D).

To better understand the mechanism underlying the higher affinity of FF for FAs, we carried out FRAP and FLIP experiments on cells expressing GFP-FRNK and FF-GFP (Fig. 2A,B). As shown in Fig. 2A, FF displays a slower recovery and has a larger immobile fraction compared with FRNK, suggesting slower turnover on FAs (FF t1/2, 11.01±1.74 seconds; FRNK t1/2, 2.6±0.4 seconds; Fig. 2A′; immobile fraction FF, 30.3±4.5%; FRNK, 9.78±1.4%; Fig. 2A″). To preclude the possibility that these differences arise due to differences induced by FF on the FA complexes, we carried out FRAP experiments in cells co-transfected with FF-mCherry and GFP-FRNK that gave similar results (supplementary material Fig. S1D). FLIP experiments on these cells showed that loss of FF from FAs is slower than loss of FRNK, confirming that FF has longer residence times on FAs (supplementary material Fig. S1E). These data show that the FERM domain is required for the localization of FAK in the embryo and has an important role for the affinity and dynamics of FAK on FA complexes in cultured cells.

FF expression blocks cell migration by blocking FA turnover

Fibroblasts from FAK-null mice show a significant increase in FA number and intensity and decreased migration rates (Ilić et al., 1995), which can be restored by re-expression of FAK, suggesting a role in FA turnover (Sieg et al., 1999). Overexpression of FRNK has been shown to reduce the rates of cell migration and induce the formation of enlarged FA complexes (Richardson et al., 1997; Sieg et al., 1999; Taylor et al., 2001).

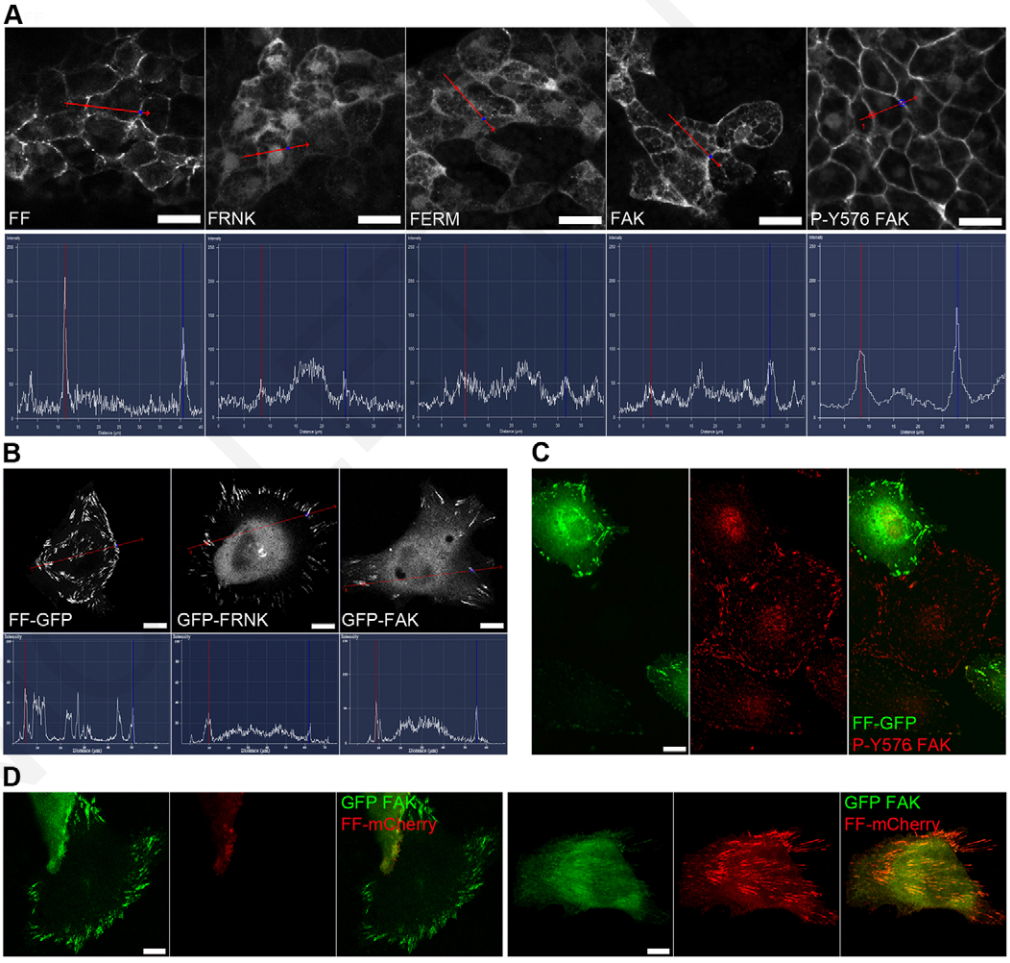

Fig. 1. The FERM and FAT domains cooperate to target FAK at the plasma membrane in the embryo and at FAs in cultured cells. (**A-A″**) Confocal images and intensity profiles of gastrula-stage embryos injected with 300 pg of wild-type FAK; of the DMZs of HA-tagged FAK mutants (FF, FRNK and FERM) stained with anti-HA antibody; or of control embryos stained with anti P-Y576 FAK. (**B**) Confocal images and intensity profiles of live XL177 cells transfected with FF-GFP, GFP-FRNK or GFP-FAK. (**C**) Wide-field images of XL177 cells transfected with FF-GFP and stained with P-Y576 FAK. (**D**) Confocal images of XL177 cells co-transfected with FF-mCherry and GFP-FAK, showing FAK displacement from FF-positive FAs. Scale bars: 20 μm in A,C; 10 μm in B,D.

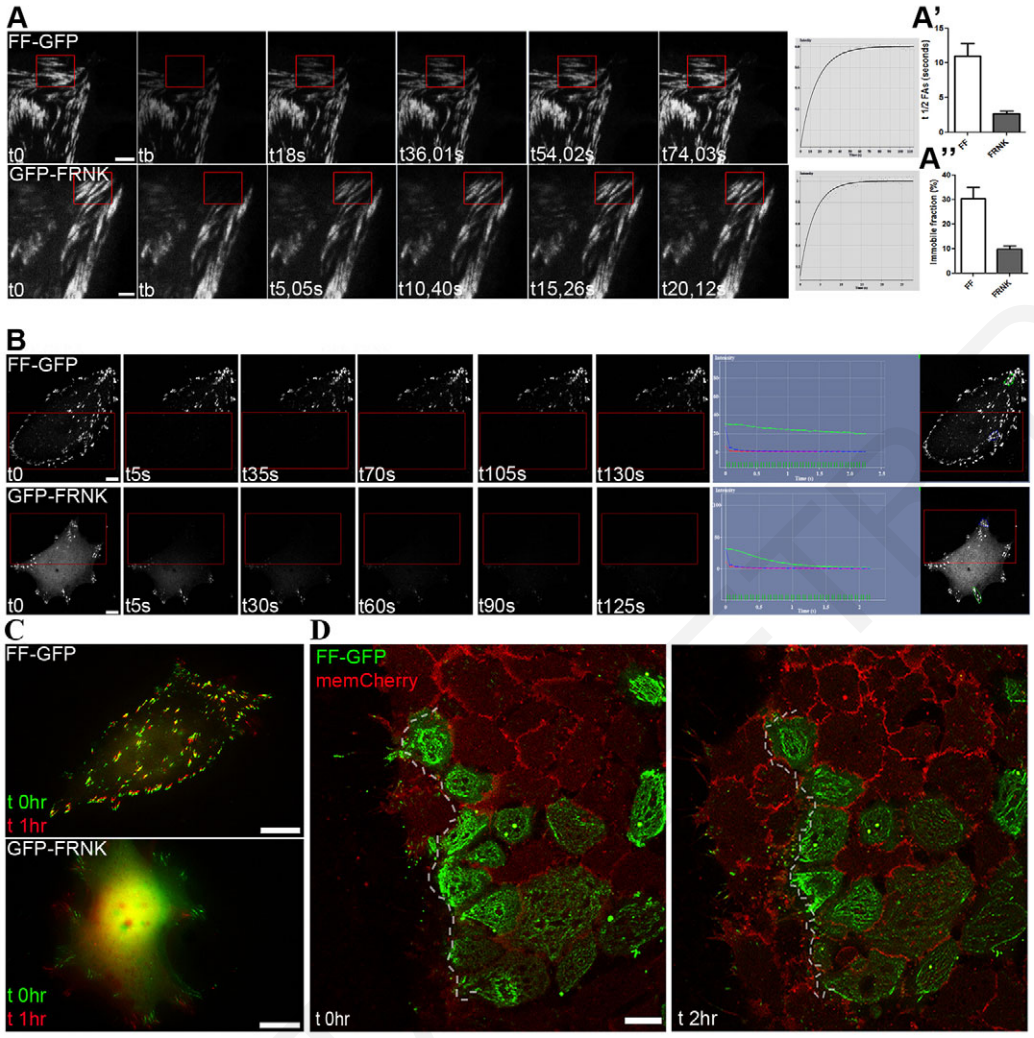

Fig. 2. FF exhibits longer residence times on FAs compared with FRNK, and blocks FA turnover and cell migration. (**A**) FRAP experiments comparing FF-GFP and GFP-FRNK. FF displays slower recovery and larger immobile fraction than FRNK. Data are mean+s.e.m. (**A′**) FF t1/2: 11.01±1.74 seconds; FRNK t1/2: 2.6±0.4 seconds, *n*=50. (**A″**) FF immobile fraction: 30.3±4.5%. FRNK immobile fraction: 9.78±1.4%, *n*=50. (**B**) FLIP experiments comparing loss of FF-GFP and GFP-FRNK. Rate of loss of FF is slower than FRNK. (**C**) High-magnification wide-field live imaging of FA turnover in FF-GFP or GFP-FRNK transfected XL177 cells. Cells were imaged for 1 hour. The merged image is composed from the first (green) and last time point (red). (**D**) The first (t 0hr) and last (t 2hr) time point of a 2-hour time-lapse movie of a mesodermal explant placed on FN-coated coverslips injected with memCherry (red) and FF-GFP (green), showing block of cell migration in FF-expressing cells. Scale bars: 2 μm in A; 10 μm in B; 20 μm in C,D.

As shown above, FF-expressing cells display a marked increase in the numbers and intensity of FAs compared with FRNK and control cells, suggesting that FF leads to a more dramatic reduction of FA turnover compared with FRNK. To explore this possibility further, FF- and FRNK-expressing cells were imaged using time-lapse fluorescence microscopy. As shown in Fig. 2C, a typical FF-expressing cell completely fails to disassemble its FAs while a FRNK-expressing cell has completely disassembled all its FAs and generated new ones within the same time frame.

FF displayed different dynamics on FAs and higher affinity compared with FRNK, and it has been suggested in previous studies that the FERM domain may have a role in the recruitment of FAK at the sites of FA formation, possibly via binding of locally generated PIP_2 (Cai et al., 2008). If this hypothesis is correct, one would expect FF to be recruited to nascent FAs prior to FRNK. To test this hypothesis, we co-transfected and imaged FF-mCherry and GFP-FRNK. As shown in the images from supplementary material Fig. S2A, FF (red) enrichment appears first on two nascent adhesions and FRNK enrichment follows (green). These results suggest that the FERM domain plays a role in the recruitment of FAK to nascent adhesions.

To further explore the effects of FF expression on cell migration, we expressed FF in mesodermal explants. As shown in Fig. 2D, FF-GFP-expressing cells (green) spread and form very strong FAs, normally absent from these cells (Stylianou and Skourides, 2009; Wacker et al., 1998). FF expression blocks FA turnover, preventing these cells from migrating (Fig. 2D; supplementary material Movie 1). In addition, expression of FF in activin-induced ACs, which normally spread and migrate as a cohesive sheet in all directions when plated on FN (supplementary material Movie 2), blocks spreading, and migration is reduced in the GFP-positive areas (as shown in supplementary material Movie 3).

FAK signals cell polarity during *Xenopus* epiboly

FAK is a major transducer of integrin signaling, and the earliest integrin-dependent process described in *Xenopus* is the FN

fibrillogenesis taking place on the blastocoel roof (BCR). In addition, FAK is expressed in the AC of *Xenopus* embryos and is specifically expressed in the deep cells of the AC that colocalize with FN, suggesting a possible role in this process (Hens and DeSimone, 1995).

In an effort to address the role of FAK in *Xenopus* early morphogenesis, we decided to test whether FF expression could block endogenous FAK function in the embryo. As shown in Fig. 3A, expression of 500 pg of FF in the AC leads to severe gastrulation defects, including failure of blastopore closure. These defects are partially rescued by expression of a constitutively active FAK K38A point mutant, which speeds up blastopore closure but not FAK Δ375, stressing the requirement of the FERM domain for the function of FAK in this context (Fig. 3A; supplementary material Fig. S3A). In addition, in FF-expressing embryos, the blastocoel is displaced vegetally, the archenteron fails to form and the mesoderm (despite proper patterning) only involutes partially (Fig. 3B-D). In agreement with the failure of the Δ375 construct to rescue the FF phenotype, expression of FRNK, which lacks the FERM domain, does not induce any appreciable gastrulation defects, confirming the requirement of the FERM domain for the dominant-negative function in this context (Fig. 3B).

FF expression also leads to the visible thickening of the BCR, suggesting that epiboly and radial intercalation are blocked (Fig. 3E,

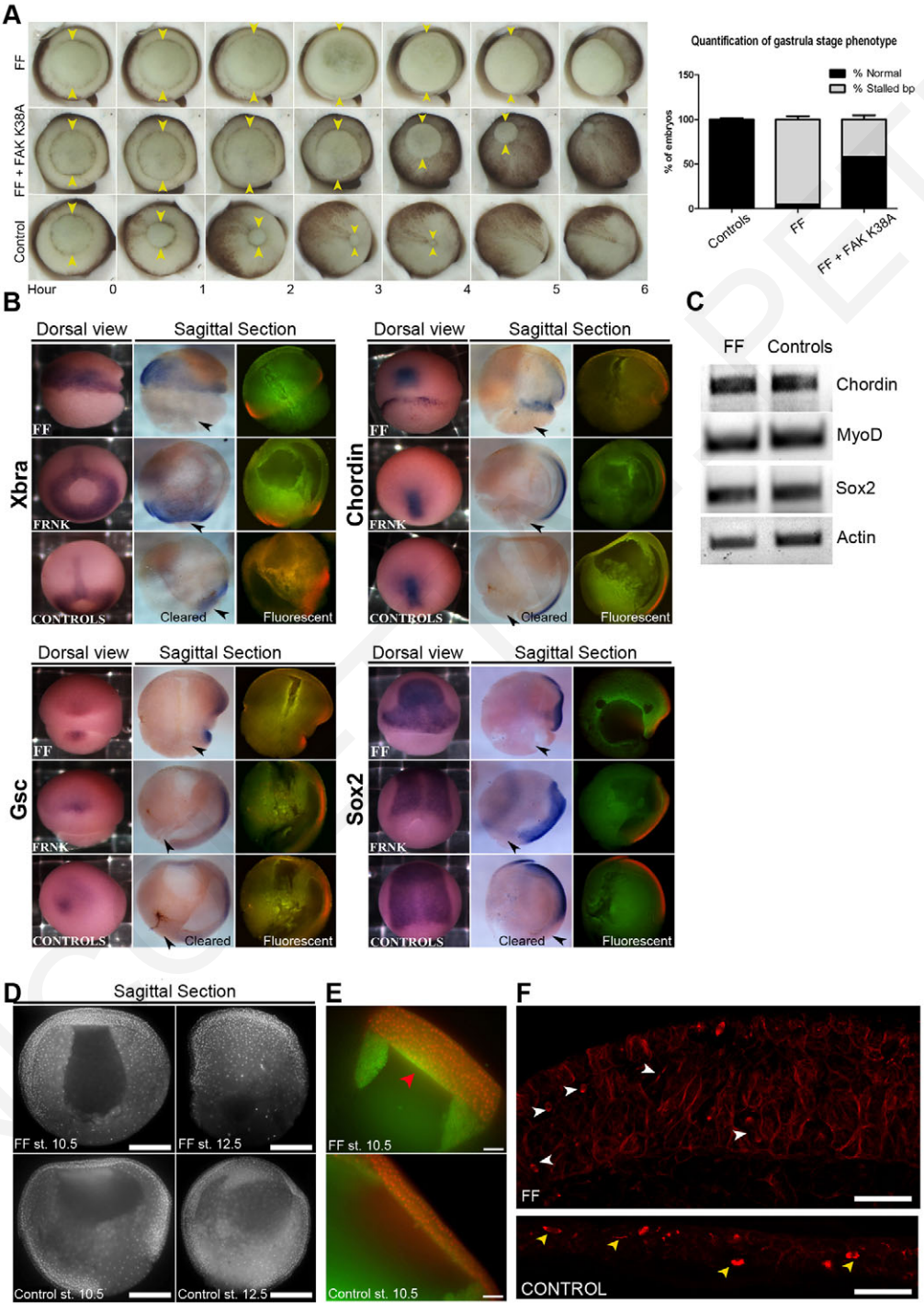

Fig. 3. FF expression in the AC leads to epiboly failure and gastrulation arrest. (**A**) Stills from a movie showing blastopore closure in controls and in embryos injected with 500 pg HA-FF (95.05±3.7% stalled blastopore, *n*=211) or with 500 pg HA-FF + 150 pg FAK K38A (41.97±4.7% stalled blastopore, *n*=128) from three independent experiments. Yellow arrowheads indicate the size of the blastopore. Data are mean±s.e.m. (**B**) Whole-mount *in situ* hybridization of control and embryos injected with HA-FF and HA-FRNK for the mesodermal markers Xbra, chordin and MyoD, and the neural marker Sox2. Black arrowheads show the blastopore. (**C**) RT-PCR for the markers chordin, MyoD and Sox2 and for actin as a loading control from control and FF-injected mid-gastrula stage embryos. (**D**) Wide-field images of sagittal sections of early and late gastrula stage control and HA-FF-injected embryos stained with Hoechst, showing thick AC in FF-expressing embryos. (**E**) Wide-field images of the AC of the same embryos showing epiboly failure after HA-FF injection (red arrowhead). (**F**) HA-FF-injected and control stage 11 embryos stained with β-tubulin antibody to image spindle orientation (78.7% misoriented spindles, *n*=61, three independent experiments). Yellow and white arrowheads indicate oriented and unoriented spindles, respectively. Scale bars: 500 μm in D; 100 μm in E; 50 μm in F.

red arrowhead). In addition, although normally cell divisions in the BCR occur in the horizontal plane of the epithelium, spindle orientation in FF expressors is randomized, showing loss of polarity (Fig. 3F, white arrowheads). Dose response of a previously characterized FAK-MO showed no early gastrulation defects (Fonar et al., 2011). However, sectioning of morphant embryos at gastrula stages revealed epiboly defects, albeit milder than those induced by FF expression (supplementary material Fig. S3B). Epiboly occurs in two distinct phases, beginning in the AC and spreading to the marginal zones as gastrulation proceeds (Keller, 1980); and morphants display more prominent thickening in the marginal zone, suggesting that the MO is more effective in preventing later intercalative activities as the maternal pool of FAK is slowly depleted. This is in agreement with previous work showing that the FAK-MO only reduces FAK protein levels by 50% at gastrula stages (Petridou et al., 2012).

The gastrulation defects observed in FF expressors are quite similar to what was observed when FN fibrillogenesis is blocked (Davidson et al., 2006; Marsden and DeSimone, 2001), suggesting that FF may be eliciting these by preventing FN fibrillogenesis. FN staining of stage 11 FF-expressing embryos shows that a dense fibrillar matrix is present (Fig. 4A) and FN protein levels are unaffected (Fig. 4A′). Sagittal sections reveal a dense network of FN on the BCR and ectopic fibrils between the cells of the AC (Fig. 4A, red arrowhead), suggesting that FF does not elicit its effect through the loss of the FN matrix. Another possible mechanism through which FF may be blocking epiboly is through the inhibition of adhesive complex turnover. To explore this possibility, we used MOs against *Xenopus* vinculin. Vinculin-null cells adhere poorly and have been shown to display increased migration rates and faster FA turnover (Coll et al., 1995). FRAP experiments comparing FF-GFP recovery in FF alone and FF + vinculin-MO AC explants show

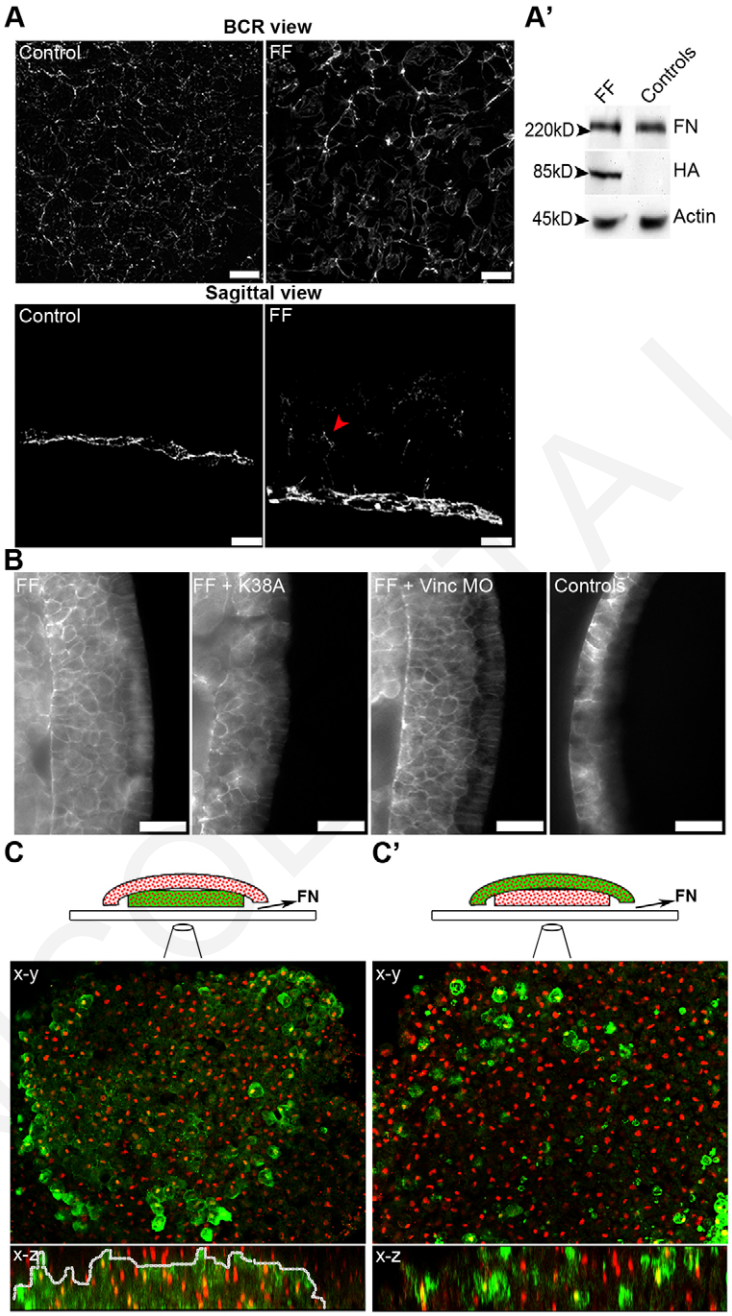

Fig. 4. FF expression blocks a FN-dependent polarizing signal during *Xenopus* epiboly. (**A**) Confocal images of the FN matrix on the BCR of control and FF-GFP-injected embryos at stage 11 and sagittal sections from embryos of the same experiment showing ectopic FN fibril formation between the inner cells of the AC in FF-injected embryos (red arrowhead). (**A′**) Western blot analysis shows similar expression levels of FN between FF and control embryos. (**B**) Wide-field images of gastrula stage control and embryos injected with FF, FF + FAK K38A, FF + vinculin-MO stained with β-catenin antibody to visualize the cell boundaries. (**C**) Radial intercalation explants from control and FF-GFP-injected embryos. The deep cell layer explant dissected from an FF-GFP-injected embryo (green) was placed on a FN-coated coverslip and another explant from an unlabeled control embryo was placed on top. Explants were cultured for 3 hours, fixed and stained with anti-histone H3 (nuclei) and anti-GFP antibodies. They were subsequently cleared and *z*-stacks were acquired on a confocal microscope. A single optical section at the level of the FN (*x-y*) and a vertical reconstruction of the *z*-stack (*x-z*) are shown. The FF-GFP-expressing explant (green with red dots) remains coherent and no GFP-negative cells have intercalated into it. A clear boundary is visible between the two explants (dashed line). (**C′**) In the reverse explant with control tissue placed on FN (red dots) and FF-GFP-injected explant on top (green with red dots), radial intercalation takes place normally and there is extensive cell mixing without any visible boundaries between the two explants. Scale bars: 20 μm in A; 50 μm in B.

that vinculin knockdown leads to increased turnover of FF in addition to fewer and smaller adhesions in a similar fashion to FAK K38A (supplementary material Fig. S4A). However, unlike FAK K38A, which rescues epiboly, vinculin knockdown fails to do so (Fig. 4B) suggesting that the effects of FF on FA turnover are not responsible for the phenotype. To confirm this, we generated an FF with a point mutation which abolishes binding of FAK to paxillin (FF-L1034S) (Tachibana et al., 1995). We postulated that as paxillin binding is one of the major determinants for FAK FA localization, this mutation would weaken the FF FA interaction and diminish its effects on FA turnover. FF-L1034S displays significantly faster turnover on FAs and fails to block FA disassembly; however, it blocks epiboly effectively uncoupling FA turnover from the epiboly defects (supplementary material Fig. S4B-D).

Previous studies in *Xenopus* have demonstrated that FN can provide signals that instruct cells to intercalate in the plane perpendicular to the matrix, and that these signals can act at a distance (Marsden and DeSimone, 2001). Our results suggest that FF expression leads to loss of polarity in the cells of the BCR by blocking these signals. If this is true one would expect that restricted FF expression in the cells in contact with the FN matrix would be sufficient to block directional intercalative behavior. To test this hypothesis, we took advantage of the deep layer explant developed by Marsden and DeSimone (Marsden and DeSimone, 2001). In this explant, dorsal marginal zone (DMZ) tissue is cut from one embryo and layers of deep cells lining the blastocoel are shaved and placed on a FN-coated coverslip. Another DMZ fragment is cut, the majority of deep cells removed and then positioned over the deep explant. As shown in Fig. 4C, when the deep explant in contact with the FN is expressing FF-GFP, little or no intercalation takes place from the overlying tissue and the GFP-positive FF explant remains coherent (dashed line). However, when a control deep explant is overlaid with an FF-GFP expressing superficial explant, FF cells intercalate into the control and GFP-positive cells can be seen interspersed between the controls (Fig. 4C′). This shows that FF expression specifically blocks the FN-dependent signal originating from the cells in direct contact with the substrate, and that FF-expressing cells can in fact polarize and intercalate if the signal is provided by control cells.

Epiboly plays an essential but permissive role during *Xenopus* gastrulation

The block of epiboly in FF expressors leads to failure of blastopore closure, as well as to partial block of involution. We postulated that this is due to the fact that in the absence of radial intercalation and BCR thinning, the mesodermal belt and the blastopore are held back, unable to move vegetally. This, coupled with the fact that mediolateral intercalation proceeds normally, leads to constriction of the embryo at the equatorial region and produces the characteristic mushroom-shaped embryos also seen in the 70 kDa FN experiments (Rozario et al., 2009). If this explanation is correct, one would expect increased tension in FF ACs. Phalloidin staining, in combination with β-catenin staining, shows that cells in FF-expressing ACs display stronger actin staining and have many protrusions compared with controls, suggesting they are under increased mechanical tension (Fig. 5A). The levels of β-catenin and C-cadherin are similar between FF and controls, suggesting that FF does not elicit its effect via strengthening of cell-cell adhesions (Fig. 5A; supplementary material Fig. S4E). Staining of FF and control ACs with a phospho-specific myosin light chain (MLC) antibody shows that in FF-expressing ACs, the apical surface of the deep cells displays elevated levels of phosphorylated MLC (Fig. 5B, white arrow), suggesting that FF BCRs are under increased mechanical tension and respond with increased contractility. In addition, levels of phosphorylated MLC are elevated both in expressing and in control cells, suggesting that FF expression does not cell autonomously lead to Rho activation, but rather the increased tension in the AC leads to elevated phosphorylation of MLC (Fig. 5B′, yellow box, white arrowhead). This result is consistent with the above postulated explanation with regards to the failure of blastopore closure being a result of the lack of epiboly and mechanical linkage of the mesodermal belt to the AC. To confirm this, we decided to relieve the tension within the FF ACs. To do so, we generated an incision on the BCR of FF-expressing embryos and monitored the progress of blastopore closure (Fig. 5C). Generating an incision on the BCR of an FF embryo (Fig. 5Ca) leads to the abrupt speeding up of blastopore closure compared with the FF control, which remains stalled (Fig. 5Cb). In agreement with previous reports, such small incisions only affect blastopore closure rates in control embryos marginally (data not shown) (Keller and Jansa, 1992). The incision on the BCR presumably relieves tension within the AC and allows the mesodermal belt to move vegetally, suggesting that epiboly plays an essential but permissive role during *Xenopus* gastrulation. Interestingly, injection of an inhibitor of ROCK in the blastocoel at stage 10 to chemically relive tension within the AC of FF-expressing embryos has the same effect, rescuing blastopore closure and dissection of ROCK inhibitor-treated FF-expressing embryos revealed a thinned AC (Fig. 5D,E). This result, in combination with the non-cell autonomy of MLC phosphorylation elevation, suggests that loss of polarity by FF expression leads to defective epiboly, which in turn leads to increased tension and stiffness in the AC. Inhibition of ROCK leads to a reduction of tissue stiffness and improved tissue rheology, allowing the AC tissue to deform in response to the pulling forces of the mesodermal belt, leading to thinning of the AC and rescuing blastopore closure.

FF expression in *Xenopus* leads to loss of mesodermal tissues

The major defect reported in FAK knockout mice is loss of mesodermally derived tissues. We, thus, decided to target FF to the dorsal mesoderm via DMZ injection at the four-cell stage. FF expression lead to smaller, curved and severely shortened embryos, the majority of which died by tadpole stages (Fig. 6A). The phenotype could be rescued via co-injection of 150 pg FAK K38A, indicating that the phenotype is specific (Fig. 6A). Interestingly, injection of 500 pg of FRNK has a very mild impact on development (Fig. 6A) and examination of the phosphorylation status of FAK shows that FF is more effective in blocking FAK phosphorylation *in vivo* (supplementary material Fig. S5A). To further address the specificity of the FF phenotype, we combined FAK-MO injections with FF expression and, as shown in supplementary material Fig. S5B, FF and FAK-MO act synergistically, suggesting that FF elicits the phenotype via inhibition of FAK activity. *In situ* hybridization and RT-PCRs showed that FF-expressing embryos, despite normal mesoderm induction and marker expression at gastrula and neurula stages (Xbra and MyoD), display extensive loss of somitic mesoderm (MyoD) at tadpole stages whereas no effect is seen in the expression of Sox2 (Fig. 6B-D). Despite normal patterning at gastrula stages, Xbra staining of the notochord appeared wider (Fig. 6B), whereas the MyoD expression domain at neurula stages was wider and positioned at the posterior (Fig. 6D). This, coupled with the dorsally bent tadpole-stage embryos, suggested that convergent extension

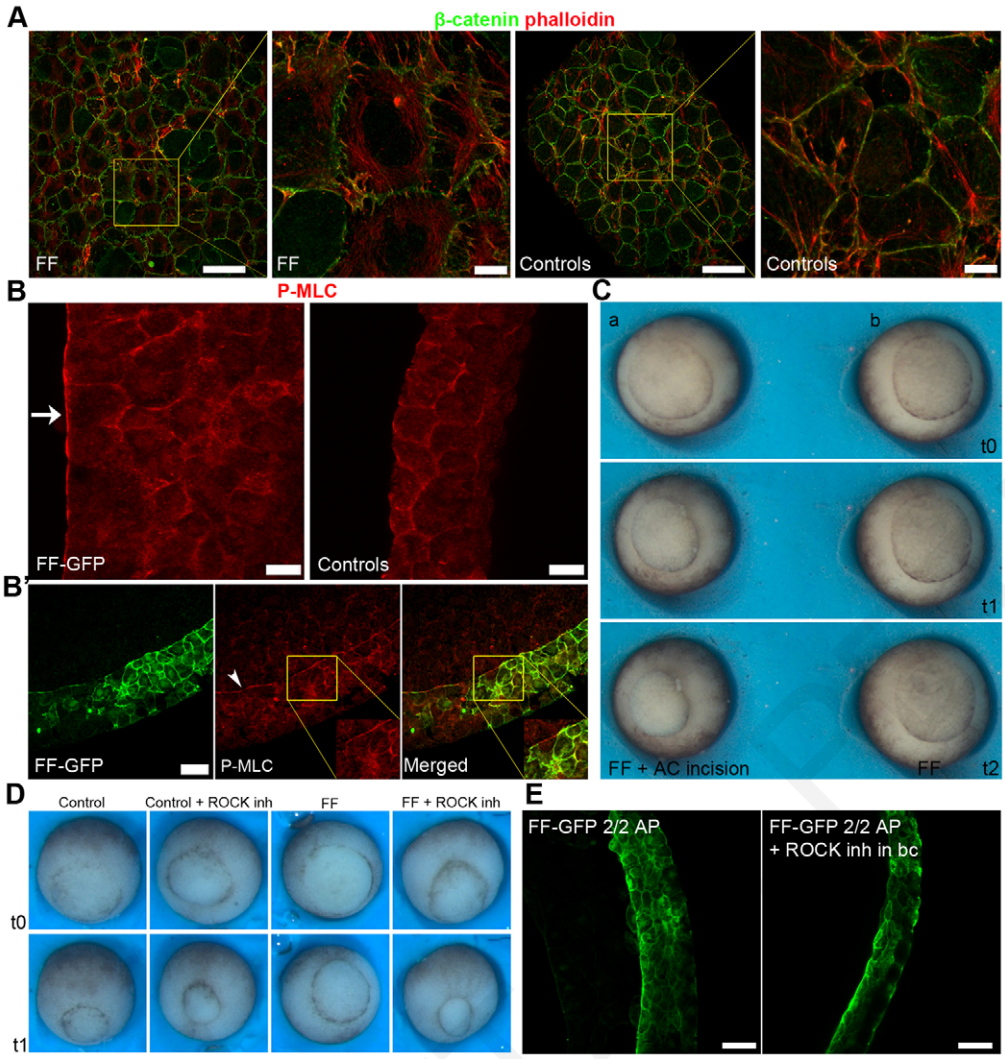

Fig. 5. FF ACs are under increased tension and epiboly has a permissive role during *Xenopus* gastrulation. (**A**) Low- and high-magnification confocal images and maximum intensity projections of the inner cell layer of the AC in FF-injected and control gastrula embryos stained with β-catenin (green) and phalloidin-488 (red). (**B**) Confocal images of FF-GFP-injected and control embryos stained for P-MLC (red) showing elevated P-MLC at the inner apical surface facing the blastocoel in FF-injected embryos (white arrow). (B′) Elevation of P-MLC is not cell-autonomous as elevation is seen in both FF-expressing (green) and non-expressing cells of the BCR (yellow box, white arrowhead). (**C**) FF blastopore closure failure is rescued by a small incision on the BCR (a). t0, FF-injected embryos before AC incision; t1, first time point immediately after incision; t2, second time point after incision. (b) FF injected embryo without any manipulation. (**D**) FF blastopore closure failure is also rescued by pharmacological release of tension by injecting the ROCK inhibitor in the blastocoel at stage 10. (**E**) Sagittal sections of FF-GFP-injected embryos, non-treated or treated with the ROCK inhibitor, showing thinning of the AC and epiboly rescue. Scale bars: 10 µm in A; 50 µm in A,B′,E; 20 µm in B.

movements may be affected; however, AC elongation assays showed that FF-expressing ACs elongate to the same extent as controls, suggesting that the mild early mesodermal morphogenesis problems may be due to defective mesoderm migration and possibly radial intercalation of the mesoderm (supplementary material Fig. S5C). Immunofluorescence experiments of FF-expressing embryos co-injected with histone-GFP revealed a large number of anaphase bridges from late gastrula stages onwards (Fig. 6F), and TUNEL staining of FF-expressing embryos showed increased apoptosis beginning at neurula stages (Fig. 6E), suggesting that FF expression induces mitotic defects and apoptosis. As Ser732 phosphorylation of FAK has been shown to play a role in centrosome function during mitosis (Park et al., 2009), we examined the effects of FF expression on the levels of endogenous P-Ser732. FF expression leads to a reduction of P-Ser732 levels and FF itself is heavily phosphorylated on Ser732 (Fig. 6G). As phosphorylation of Ser732 has been shown to be essential for the association of endogenous FAK with dynein, we postulated that FFs dominant-negative activity with respect to centrosomal function would require this residue. We thus generated a Ser732 point mutant that substituted serine to alanine (FF-S732A), and compared the effects of its expression to that of FF. As shown in Fig. 6F, FF-S732A expression fails to induce mitotic defects, resulting in a much milder phenotype compared with FF (Fig. 6H), suggesting that at least part of the FF phenotype is due to effects of FF on centrosome function through Ser732. Interestingly, FF-S732A expression induced identical phenotypes, as FF both in terms of FA turnover *in vitro* as well as block of epiboly *in vivo* (data not shown, supplementary material Fig. S5D). These results suggest that FFs effects on FA turnover and epiboly are related to the function of FAK at FAs and strengthen the conclusion that the defects elicited in the mesoderm are primarily dependent on the role of FAK in cell division and survival.

DISCUSSION

The FERM domain has been shown to bind several molecules that are important for FAK activation, as well as downstream effectors, including PIP_2, integrins, p53, Arp2/3 and GFRs (Cai et al., 2008; Chen and Chen, 2006; Schaller et al., 1994; Serrels et al., 2007; Sieg et al., 2000). Here, we show that despite the fact that the FAT domain is both necessary and sufficient for FA localization, the FERM domain is also required for correct localization *in vivo*. We go on to show that FF has a higher affinity for FA complexes, displaying significantly longer residence times compared with FRNK and demonstrating that the FERM domain regulates the dynamics of FAK on FAs. In addition, we show that FF becomes enriched on nascent adhesions prior to FRNK, suggesting a role of the FERM domain in the recruitment of FAK to these complexes. This may be due to the ability of the FERM domain to bind locally

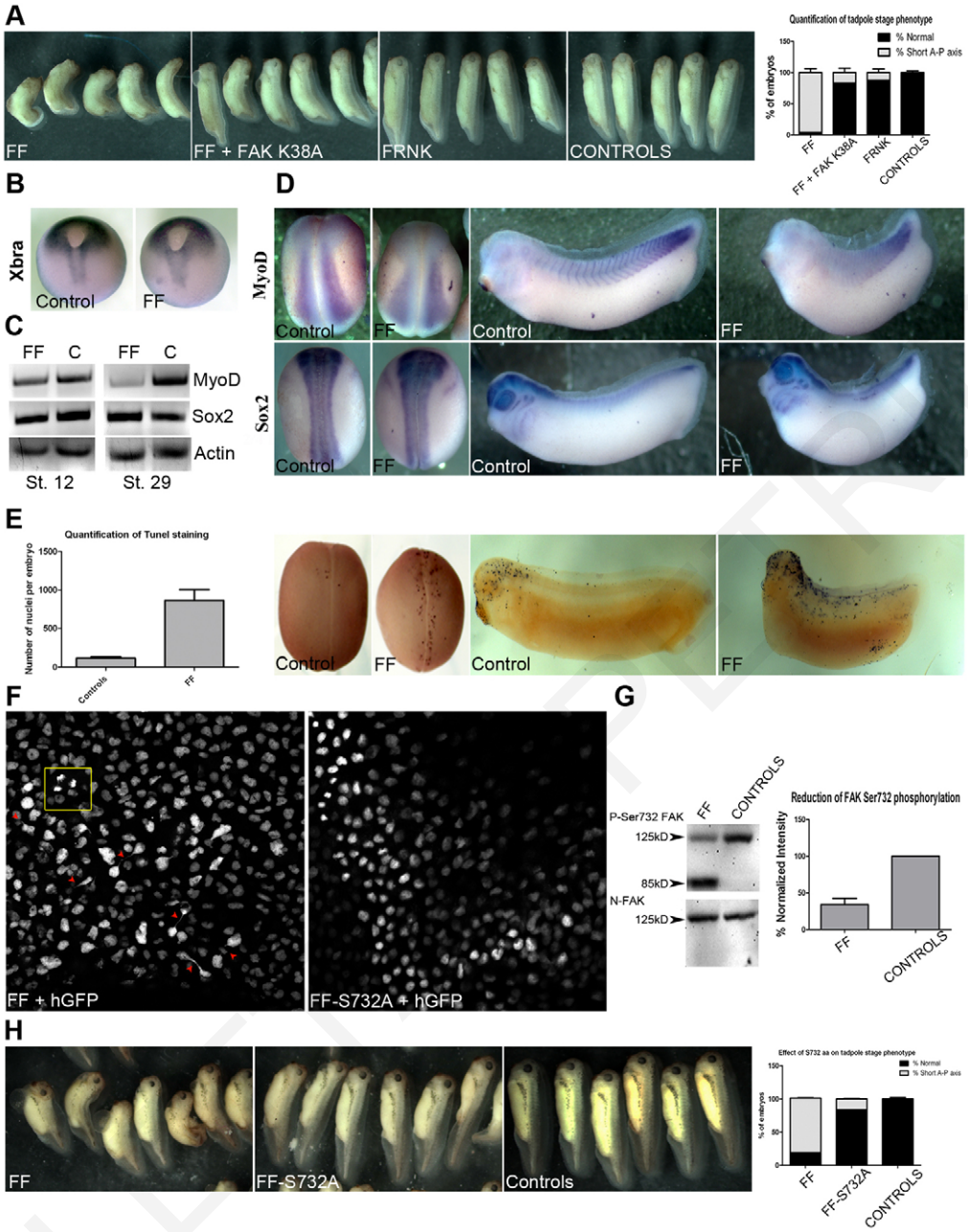

Fig. 6. FF expression leads to loss of mesoderm in a Ser732-dependent manner. (**A**) Injection of 500 pg FF into the DMZ of four-cell stage embryos leads to severe shortening of the A-P axis when compared with control (95.83±6.45%, *n*=149) and with FRNK-injected (12.45±5.87%, *n*=136) embryos. This phenotype is rescued by co-injection of 150 pg of FAK K38A (16.41±7.1%, *n*=136). (**B**) Whole-mount *in situ* hybridization for Xbra of gastrula stage control embryos or embryos injected with 500 pg FF into two dorsal blastomeres at the four-cell stage. (**C**) RT-PCR of gastrula (St. 12) and tadpole (St. 29) stages of control embryos or embryos injected with 500 pg FF into two out of four blastomeres at the DMZ. MyoD, Sox2 and actin levels were analyzed, showing loss of MyoD in FF-injected embryos. (**D**) Whole-mount *in situ* hybridization for MyoD and Sox2 of neurula- and tadpole-stage control embryos and embryos injected with FF as described above. (**E**) TUNEL assay of control and DMZ FF-injected embryos at the four-cell stage. Quantification of the apoptotic nuclei at the tadpole stages shows a sevenfold increase in apoptosis in FF expressors (861.67±140.96 apoptotic nuclei compared with 114.67±17.79 apoptotic nuclei in controls, *n*=6, two independent experiments). (**F**) Confocal images of embryos co-injected with histone-GFP and HA-FF or HA-FF S732A to visualize mitotic cells showing the formation of anaphase bridges (red arrowheads) and multipolar spindles (yellow box) in FF expressors. (**G**) Western blot and densitometry analysis of the effect of HA-FF expression on the reduction of the phosphorylation levels of P-Ser732 endogenous FAK and Ser732 phosphorylation of FF (lower band in FF lane). (**H**) Control embryos and embryos in which FF or FF-S732A has been injected into the DMZ at the four-cell stage. Graph shows statistical analysis of the shortened A-P axis phenotype. Data are mean+s.e.m.

generated PIP_2, keeping FF in close proximity to nascent adhesions; however, another possibility is that the FERM domain is transiently binding integrins at the early stages of FA formation (Cai et al., 2008; Schaller et al., 1995).

FF displaces FAK from FAs, resulting in the loss of FAK phosphorylation. This leads to a dramatic reduction of FA turnover and an increase in size and number of FAs. When compared with FRNK, FF elicits a much stronger phenotype with expressors

resembling FAK-null fibroblasts. The significant differences between FRNK and FF expressors with respect to their ability to turnover FAs, may be attributed to the higher affinity that FF displays for FAs. The long residence times of FF suggest a slower off rate from these complexes and, as a result, at steady state and at given fixed levels of expression, FF would be more effective in displacing endogenous FAK than would FRNK. In addition, although FRNK can compete FAK from a subset of target proteins that bind the C terminus, FF can presumably compete with endogenous FAK for a wider array of FAK partners.

Expression of FF in the AC leads to BCR thickening and severe gastrulation defects, whereas expression of FF in the mesoderm via DMZ injections leads to smaller curved embryos, in part due to loss of mesodermal tissues, similar to FAK knockout mice (Furuta et al., 1995). The mild defects induced by FF in mesodermal morphogenesis are in contrast to the severe defects induced in the AC and in agreement with the requirement of fibrillar FN for epiboly but not for convergent extension (Davidson et al., 2006; Marsden and DeSimone, 2001; Rozario et al., 2009). Here, we show that, despite the presence of a fibrillar matrix, both radial intercalation and cell polarity are lost in FF expressors, suggesting that an integrin-dependent polarizing signal is required for both processes. We also show that FF expression in the cells in direct contact with the FN blocks intercalative behavior, whereas expression in the overlying cells does not, confirming that a FN-integrin signal can direct intercalative behaviors at a distance and that FAK has a crucial role in its transduction.

Block of epiboly through a variety of experimental approaches leads to gastrulation defects in the mesoderm, including partial block of involution and delay or failure of blastopore closure. However, it has been shown that BCR-less embryos close their blastopores without any problems. In fact, in these embryos, a speeding up of blastopore closure is observed, suggesting that the mesoderm is actually exerting forces on the AC and is held back by this interaction (Keller and Jansa, 1992). In FF expressors, generation of a small incision on the AC leads to the abrupt speeding up of blastopore closure, suggesting that the failure of blastopore closure is due to the fact that the mesoderm is held back by the AC. The AC in FFs not only displays loss of polarity but in addition, displays increased stiffness, as evidenced by the elevation of phosphorylation of MLC and increased F-actin. This would suggest that the inability of FF-expressing ACs to thin and allow vegetal translocation of the blastopore results in increased tension imposed on this tissue, which responds by increasing its stiffness. In agreement with this interpretation, use of a ROCK inhibitor rescues blastopore closure and BCR thinning. It appears that under conditions of low contractility, improved tissue rheology allows the AC to deform in response to the forces generated by the mesoderm. This suggests that epiboly requires the forces generated by the mesoderm in order to take place.

Overall, our work identifies new roles for the FERM domain in the regulation of the dynamics of FAK on its signaling complexes *in vivo* and *in vitro*, and identifies epiboly as the earliest developmental process in which FAK plays a crucial role during *Xenopus* development. The new dominant negative that we have generated and characterized will be a valuable tool, through targeted injections and inducible expression, for future studies of the involvement of FAK in a variety of developmental processes.

Acknowledgments
We thank Dr Douglas DeSimone for kindly providing the fibronectin 4H2 antibody, Dr Jun-Lin Guan for providing the pKH3 FAK and pKH3 FRNK plasmids, and Drs Chenbei Chang and Chao Yun Irene Yan for comments on the paper.

Funding
Funding was provided by the Cyprus Research Promotion Foundation [ΥΓΕΙΑ/ΒΙΟΣ/0609(ΒΕ)/14]

Competing interests statement
The authors declare no competing financial interests.

Author contributions
N.I.P., P.S. and P.A.S. conceived and designed the experiments. N.I.P. and P.S. performed the experiments. N.I.P., P.S. and P.A.S. analyzed the data. N.I.P. and P.A.S. wrote the paper.

Supplementary material
Supplementary material available online at
http://dev.biologists.org/lookup/suppl/doi:10.1242/dev.096073/-/DC1

References

Alfandari, D., Cousin, H., Gaultier, A., Smith, K., White, J. M., Darribère, T. and DeSimone, D. W. (2001). Xenopus ADAM 13 is a metalloprotease required for cranial neural crest-cell migration. *Curr. Biol.* **11**, 918-930.
Cai, X., Lietha, D., Ceccarelli, D. F., Karginov, A. V., Rajfur, Z., Jacobson, K., Hahn, K. M., Eck, M. J. and Schaller, M. D. (2008). Spatial and temporal regulation of focal adhesion kinase activity in living cells. *Mol. Cell. Biol.* **28**, 201-214.
Calalb, M. B., Polte, T. R. and Hanks, S. K. (1995). Tyrosine phosphorylation of focal adhesion kinase at sites in the catalytic domain regulates kinase activity: a role for Src family kinases. *Mol. Cell. Biol.* **15**, 954-963.
Ceccarelli, D. F., Song, H. K., Poy, F., Schaller, M. D. and Eck, M. J. (2006). Crystal structure of the FERM domain of focal adhesion kinase. *J. Biol. Chem.* **281**, 252-259.
Chen, S. Y. and Chen, H. C. (2006). Direct interaction of focal adhesion kinase (FAK) with Met is required for FAK to promote hepatocyte growth factor-induced cell invasion. *Mol. Cell. Biol.* **26**, 5155-5167.
Chen, H. C., Appeddu, P. A., Parsons, J. T., Hildebrand, J. D., Schaller, M. D. and Guan, J. L. (1995). Interaction of focal adhesion kinase with cytoskeletal protein talin. *J. Biol. Chem.* **270**, 16995-16999.
Coll, J. L., Ben-Ze'ev, A., Ezzell, R. M., Rodríguez Fernández, J. L., Baribault, H., Oshima, R. G. and Adamson, E. D. (1995). Targeted disruption of vinculin genes in F9 and embryonic stem cells changes cell morphology, adhesion, and locomotion. *Proc. Natl. Acad. Sci. USA* **92**, 9161-9165.
Cooper, L. A., Shen, T. L. and Guan, J. L. (2003). Regulation of focal adhesion kinase by its amino-terminal domain through an autoinhibitory interaction. *Mol. Cell. Biol.* **23**, 8030-8041.
Davidson, L. A., Marsden, M., Keller, R. and Desimone, D. W. (2006). Integrin alpha5beta1 and fibronectin regulate polarized cell protrusions required for Xenopus convergence and extension. *Curr. Biol.* **16**, 833-844.
Doherty, J. T., Conlon, F. L., Mack, C. P. and Taylor, J. M. (2010). Focal adhesion kinase is essential for cardiac looping and multichamber heart formation. *Genesis* **48**, 492-504.
Ezratty, E. J., Partridge, M. A. and Gundersen, G. G. (2005). Microtubule-induced focal adhesion disassembly is mediated by dynamin and focal adhesion kinase. *Nat. Cell Biol.* **7**, 581-590.
Fonar, Y., Gutkovich, Y. E., Root, H., Malyarova, A., Aamar, E., Golubovskaya, V. M., Elias, S., Elkouby, Y. M. and Frank, D. (2011). Focal adhesion kinase protein regulates Wnt3a gene expression to control cell fate specification in the developing neural plate. *Mol. Biol. Cell* **22**, 2409-2421.
Furuta, Y., Ilić, D., Kanazawa, S., Takeda, N., Yamamoto, T. and Aizawa, S. (1995). Mesodermal defect in late phase of gastrulation by a targeted mutation of focal adhesion kinase, FAK. *Oncogene* **11**, 1989-1995.
George, E. L., Georges-Labouesse, E. N., Patel-King, R. S., Rayburn, H. and Hynes, R. O. (1993). Defects in mesoderm, neural tube and vascular development in mouse embryos lacking fibronectin. *Development* **119**, 1079-1091.
Golubovskaya, V. M., Finch, R. and Cance, W. G. (2005). Direct interaction of the N-terminal domain of focal adhesion kinase with the N-terminal transactivation domain of p53. *J. Biol. Chem.* **280**, 25008-25021.
Hayashi, I., Vuori, K. and Liddington, R. C. (2002). The focal adhesion targeting (FAT) region of focal adhesion kinase is a four-helix bundle that binds paxillin. *Nat. Struct. Biol.* **9**, 101-106.
Hens, M. D. and DeSimone, D. W. (1995). Molecular analysis and developmental expression of the focal adhesion kinase pp125FAK in Xenopus laevis. *Dev. Biol.* **170**, 274-288.
Hildebrand, J. D., Schaller, M. D. and Parsons, J. T. (1993). Identification of sequences required for the efficient localization of the focal adhesion kinase, pp125FAK, to cellular focal adhesions. *J. Cell Biol.* **123**, 993-1005.
Hildebrand, J. D., Schaller, M. D. and Parsons, J. T. (1995). Paxillin, a tyrosine phosphorylated focal adhesion-associated protein binds to the carboxyl terminal domain of focal adhesion kinase. *Mol. Biol. Cell* **6**, 637-647.

Ilić, D., Furuta, Y., Kanazawa, S., Takeda, N., Sobue, K., Nakatsuji, N., Nomura, S., Fujimoto, J., Okada, M. and Yamamoto, T. (1995). Reduced cell motility and enhanced focal adhesion contact formation in cells from FAK-deficient mice. *Nature* **377**, 539-544.
Ilic, D., Kovacic, B., McDonagh, S., Jin, F., Baumbusch, C., Gardner, D. G. and Damsky, C. H. (2003). Focal adhesion kinase is required for blood vessel morphogenesis. *Circ. Res.* **92**, 300-307.
Jácamo, R. O. and Rozengurt, E. (2005). A truncated FAK lacking the FERM domain displays high catalytic activity but retains responsiveness to adhesion-mediated signals. *Biochem. Biophys. Res. Commun.* **334**, 1299-1304.
Keller, R. E. (1980). The cellular basis of epiboly: an SEM study of deep-cell rearrangement during gastrulation in Xenopus laevis. *J. Embryol. Exp. Morphol.* **60**, 201-234.
Keller, R. and Jansa, S. (1992). Xenopus Gastrulation without a blastocoel roof. *Dev. Dyn.* **195**, 162-176.
Kostourou, V., Lechertier, T., Reynolds, L. E., Lees, D. M., Baker, M., Jones, D. T., Tavora, B., Ramjaun, A. R., Birdsey, G. M., Robinson, S. D. et al. (2013). FAK-heterozygous mice display enhanced tumour angiogenesis. *Nat Commun* **4**, 2020.
Lawson, C. and Schlaepfer, D. D. (2012). Integrin adhesions: who's on first? What's on second? Connections between FAK and talin. *Cell Adh. Migr.* **6**, 302-306.
Lim, S. T., Chen, X. L., Lim, Y., Hanson, D. A., Vo, T. T., Howerton, K., Larocque, N., Fisher, S. J., Schlaepfer, D. D. and Ilic, D. (2008a). Nuclear FAK promotes cell proliferation and survival through FERM-enhanced p53 degradation. *Mol. Cell* **29**, 9-22.
Lim, Y., Lim, S. T., Tomar, A., Gardel, M., Bernard-Trifilo, J. A., Chen, X. L., Uryu, S. A., Canete-Soler, R., Zhai, J., Lin, H. et al. (2008b). PyK2 and FAK connections to p190Rho guanine nucleotide exchange factor regulate RhoA activity, focal adhesion formation, and cell motility. *J. Cell Biol.* **180**, 187-203.
Marsden, M. and DeSimone, D. W. (2001). Regulation of cell polarity, radial intercalation and epiboly in Xenopus: novel roles for integrin and fibronectin. *Development* **128**, 3635-3647.
Mitra, S. K., Hanson, D. A. and Schlaepfer, D. D. (2005). Focal adhesion kinase: in command and control of cell motility. *Nat. Rev. Mol. Cell Biol.* **6**, 56-68.
Park, A. Y., Shen, T. L., Chien, S. and Guan, J. L. (2009). Role of focal adhesion kinase Ser-732 phosphorylation in centrosome function during mitosis. *J. Biol. Chem.* **284**, 9418-9425.
Petridou, N. I., Stylianou, P., Christodoulou, N., Rhoads, D., Guan, J. L. and Skourides, P. A. (2012). Activation of endogenous FAK via expression of its amino terminal domain in Xenopus embryos. *PLoS ONE* **7**, e42577.
Ren, X. D., Kiosses, W. B., Sieg, D. J., Otey, C. A., Schlaepfer, D. D. and Schwartz, M. A. (2000). Focal adhesion kinase suppresses Rho activity to promote focal adhesion turnover. *J. Cell Sci.* **113**, 3673-3678.
Richardson, A., Malik, R. K., Hildebrand, J. D. and Parsons, J. T. (1997). Inhibition of cell spreading by expression of the C-terminal domain of focal adhesion kinase (FAK) is rescued by coexpression of Src or catalytically inactive FAK: a role for paxillin tyrosine phosphorylation. *Mol. Cell. Biol.* **17**, 6906-6914.
Rozario, T., Dzamba, B., Weber, G. F., Davidson, L. A. and DeSimone, D. W. (2009). The physical state of fibronectin matrix differentially regulates morphogenetic movements in vivo. *Dev. Biol.* **327**, 386-398.
Schaller, M. D., Hildebrand, J. D., Shannon, J. D., Fox, J. W., Vines, R. R. and Parsons, J. T. (1994). Autophosphorylation of the focal adhesion kinase, pp125FAK, directs SH2-dependent binding of pp60src. *Mol. Cell. Biol.* **14**, 1680-1688.
Schaller, M. D., Otey, C. A., Hildebrand, J. D. and Parsons, J. T. (1995). Focal adhesion kinase and paxillin bind to peptides mimicking beta integrin cytoplasmic domains. *J. Cell Biol.* **130**, 1181-1187.
Serrels, B., Serrels, A., Brunton, V. G., Holt, M., McLean, G. W., Gray, C. H., Jones, G. E. and Frame, M. C. (2007). Focal adhesion kinase controls actin assembly via a FERM-mediated interaction with the Arp2/3 complex. *Nat. Cell Biol.* **9**, 1046-1056.
Sieg, D. J., Hauck, C. R. and Schlaepfer, D. D. (1999). Required role of focal adhesion kinase (FAK) for integrin-stimulated cell migration. *J. Cell Sci.* **112**, 2677-2691.
Sieg, D. J., Hauck, C. R., Ilic, D., Klingbeil, C. K., Schaefer, E., Damsky, C. H. and Schlaepfer, D. D. (2000). FAK integrates growth-factor and integrin signals to promote cell migration. *Nat. Cell Biol.* **2**, 249-256.
Smith, W. C. and Harland, R. M. (1991). Injected Xwnt-8 RNA acts early in Xenopus embryos to promote formation of a vegetal dorsalizing center. *Cell* **67**, 753-765.
Stylianou, P. and Skourides, P. A. (2009). Imaging morphogenesis, in Xenopus with Quantum Dot nanocrystals. *Mech. Dev.* **126**, 828-841.
Tachibana, K., Sato, T., D'Avirro, N. and Morimoto, C. (1995). Direct association of pp125FAK with paxillin, the focal adhesion-targeting mechanism of pp125FAK. *J. Exp. Med.* **182**, 1089-1099.
Taylor, J. M., Mack, C. P., Nolan, K., Regan, C. P., Owens, G. K. and Parsons, J. T. (2001). Selective expression of an endogenous inhibitor of FAK regulates proliferation and migration of vascular smooth muscle cells. *Mol. Cell. Biol.* **21**, 1565-1572.
Tomar, A., Lim, S. T., Lim, Y. and Schlaepfer, D. D. (2009). A FAK-p120RasGAP-p190RhoGAP complex regulates polarity in migrating cells. *J. Cell Sci.* **122**, 1852-1862.
Wacker, S., Brodbeck, A., Lemaire, P., Niehrs, C. and Winklbauer, R. (1998). Patterns and control of cell motility in the Xenopus gastrula. *Development* **125**, 1931-1942.
Woolner, S. and Papalopulu, N. (2012). Spindle position in symmetric cell divisions during epiboly is controlled by opposing and dynamic apicobasal forces. *Dev. Cell* **22**, 775-787.
Xia, H., Nho, R. S., Kahm, J., Kleidon, J. and Henke, C. A. (2004). Focal adhesion kinase is upstream of phosphatidylinositol 3-kinase/Akt in regulating fibroblast survival in response to contraction of type I collagen matrices via a beta 1 integrin viability signaling pathway. *J. Biol. Chem.* **279**, 33024-33034.
Xie, Z., Sanada, K., Samuels, B. A., Shih, H. and Tsai, L. H. (2003). Serine 732 phosphorylation of FAK by Cdk5 is important for microtubule organization, nuclear movement, and neuronal migration. *Cell* **114**, 469-482.
Yamakita, Y., Totsukawa, G., Yamashiro, S., Fry, D., Zhang, X., Hanks, S. K. and Matsumura, F. (1999). Dissociation of FAK/p130(CAS)/c-Src complex during mitosis: role of mitosis-specific serine phosphorylation of FAK. *J. Cell Biol.* **144**, 315-324.
Yang, J. T., Rayburn, H. and Hynes, R. O. (1993). Embryonic mesodermal defects in alpha 5 integrin-deficient mice. *Development* **119**, 1093-1105.
Zhao, J. H., Reiske, H. and Guan, J. L. (1998). Regulation of the cell cycle by focal adhesion kinase. *J. Cell Biol.* **143**, 1997-2008.

nature COMMUNICATIONS

ARTICLE

Received 11 Mar 2014 | Accepted 11 Sep 2014 | Published 24 Oct 2014

DOI: 10.1038/ncomms6240

FAK transduces extracellular forces that orient the mitotic spindle and control tissue morphogenesis

Nicoletta I. Petridou[1] & Paris A. Skourides[1]

Spindle orientation is critical for proper morphogenesis of organs and tissues as well as for the maintenance of tissue morphology. Although significant progress has been made in understanding the mechanisms linking the cell cortex to the spindle and the well-documented role that extracellular forces play in spindle orientation, how such forces are transduced to the cortex remains poorly understood. Here we report that focal adhesion kinase (FAK) is necessary for correct spindle orientation and as a result, indispensable for proper epithelial morphogenesis in the vertebrate embryo. We show that FAK's role in spindle orientation is dependent on its ability to localize at focal adhesions and its interaction with paxillin, but is kinase activity independent. Finally, we present evidence that FAK is required for external force-induced spindle reorientation, suggesting that FAK's involvement in this process stems from a role in the transduction of external forces to the cell cortex.

[1] Laboratory of Developmental Biology and BioImaging, Department of Biological Sciences, University of Cyprus, University Ave 1, Nicosia 2109, Cyprus. Correspondence and requests for materials should be addressed to P.A.S. (email: skourip@ucy.ac.cy).

Defective spindle orientation is associated with developmental abnormalities often associated with severe diseases, including neurological disorders, polycystic kidneys and tumorigenesis[1–3]. Cortical pulling forces generated by dynein on astral microtubules define the position and orientation of the spindle. A conserved core protein complex composed of several proteins including LGN, NuMA and the G-protein subunit Gαi recruit dynein to the cortex. LGN localizes at the cell cortex of dividing cells and interacts with the plasma membrane-bound Gαi-GDP through its C-terminus and with NuMA (which binds to dynein directly) through its N-terminus[4]. Through different mechanisms the LGN/NuMA/Gαi complex localizes asymmetrically at the cortex, leading to determined localization of dynein[5].

Several factors have been shown to influence mitotic spindle orientation including cell polarity, cell shape and, more recently, external forces[6,7]. Fink *et al.*[7], elegantly showed that external forces transmitted through the retraction fibres (RFs) can guide mitotic spindle orientation in adherent cells, whereas external forces have also been shown to control spindle orientation *in vivo* in the zebrafish EVL[8]. Despite an abundance of molecules identified as regulators of mitotic spindle positioning and orientation, including microtubule- and actin-associated proteins, kinases, cell polarity proteins, adherens junction proteins, transmembrane receptors and phosphoinositides[3,5,7–15], how are external forces transmitted to the cell cortex and bias cortical cues is still poorly understood.

The members of the focal adhesion (FA) complex are important mechanosensing molecules, and the FA complex itself can mature and change composition in response to external forces[16]. In this study, we explored the possibility that FAK, a major mechanosensing molecule regulated by mechanical forces, is involved in the regulation of spindle orientation[17,18]. We show that FAK is required for spindle orientation and that this function is related to FAK's role in the transduction of mechanical signals from the extracellular environment to the cell.

Results

FAK is required for spindle orientation in adherent cells. The fact that integrins have been shown to play a critical role in spindle orientation in several systems[15,19] coupled with the central role of FAK in the transduction of integrin signalling[20], prompted us to investigate a possible role of FAK in spindle orientation. We begun by examining spindle orientation in FAK-null mouse embryonic fibroblasts (MEFs) and compared the results to those from FAK-nulls re-expressing WT-FAK. The mitotic spindle of adherent cells is normally parallel to the substratum[15], so for each metaphase cell, thin optical sections were acquired along the *Z* axis and the angle between the two spindle poles with respect to the substrate was measured from Z reconstructions (Fig. 1a,b). The average spindle angle in FAK-null cells was $20.3 \pm 1.368°$ ($n = 116$), whereas this angle was $8.849 \pm 0.7483°$ ($n = 95$) in FAK re-expressing cells (Fig. 1b,c). In addition, 75% of the FAK-null cells showed a spindle angle greater than 10° compared with 32% in FAK re-expressing cells (Fig. 1d). Examination of spindle integrity and spindle centring revealed that loss of FAK does not affect spindle integrity or centring (Supplementary Fig. 1a–e)[15]. In addition, both electroporation of a previously characterized FAK morpholino (MO)[21] in *Xenopus* XL177 cells, as well as expression of a FAK dominant negative composed of the N and C termini of FAK (FF)[22] in NIH3T3 cells, lead to spindle misorientation confirming a requirement for FAK in spindle orientation (Supplementary Fig. 1f–h).

The mitotic spindle of adherent cells is normally parallel to the substratum, whereas it is oriented through mechanical forces exerted by RFs in the *XY*[23]. It is thus possible to force the spindle of adherent cells into a defined orientation by plating cells onto micropatterned surfaces. To determine whether loss of FAK affects *XY* spindle orientation, we used L-shaped fibronectin micropatterns. The mitotic spindle of cells grown on this pattern is normally parallel to the hypotenuse of the triangle formed by the L[23]. Examination of spindle orientation on L-shaped microprints revealed loss of spindle orientation of FAK-null cells in the *XY* plane. Specifically, under these conditions, FAK-null cells display randomized spindles with an average angle of deviation of $49.77 \pm 5.119°$ ($n = 31$), compared with $14.82 \pm 1.426°$ ($n = 20$) in FAK reconstituted cells (Fig. 1e,f). These results show that FAK is required both for spindle alignment with the substrate as well as for force-dependent orientation associated with RFs. As both cell shape and forces have been shown to influence spindle orientation[6–8], we also quantified spindle orientation on bar-shaped patterns, which generate greater cell shape anisotropy. FAK-nulls on such patterns display a moderate but statistically significant reduction of misorientation compared with cells on L-shapes, suggesting that the primary defect on FAK-nulls is in force-dependent orientation (Supplementary Fig. 1i).

Spindle orientation is determined by the ECM distribution. Integrin-based cell adhesion to extracellular matrix (ECM) components orients the mitotic spindle of cultured cells parallel to the plane of the substrate[15]. Although the mechanism through which this *Z* axis orientation is accomplished is sometimes assumed to be the same as in the case of orientation in the *XY* plane, this has never been addressed directly[24,25]. The fact that FAK-null cells fail to orient their spindle both in response to micropatterns as well as with respect to the plane of the substrate suggests that the two orientation processes share a common mechanism. It is likely that the absence of RFs at the basal and apical areas of a spherical mitotic cell would automatically lead to the exclusion of a vertical division with respect to the substrate, as no force is applied in that direction. In order to address this possibility, we exposed cells to two parallel substrate planes by sandwiching them between coverslips. After cells attached to the first coverslip, a second was positioned over them using silicone grease bridges to hold it in place (Fig. 2a). As shown, HeLa cells primarily adhere and spread on the bottom coverslip while maintaining a small area in contact with the top coverslip (Fig. 2a,b). Once they round up, the majority of RFs are formed on the bottom coverslip, however, RFs also form at the top (Fig. 2a,b). Cells under these conditions fail to orient their spindles parallel to the substrate and often divide completely perpendicular to the substratum (Fig. 2b–d). This suggests that RFs under these conditions apply forces perpendicular to the substrate plane leading to the change in spindle orientation. In order to ensure that spindle reorientation is a result of integrin-dependent adhesion, we repeated the experiment using fibronectin bottom coverslips and poly-L-lysine (PLL) coverslips on top (Fig. 2a). In agreement with previous work, spindles under these conditions remain parallel to the substratum (Fig. 2c,d), indicating that integrin-based adhesions are required to elicit spindle orientation changes[15]. Overall, these results suggest that the mechanism for spindle orientation in the *XY* and *Z* axis is common and depends on the spatial distribution of the ECM, which defines the distribution of RFs and subsequently, the spatial distribution of forces applied on the cell cortex.

FAK's kinase activity is dispensable for spindle orientation. One of the central mechanisms through which FAK transduces integrin signals and controls FA turnover is through

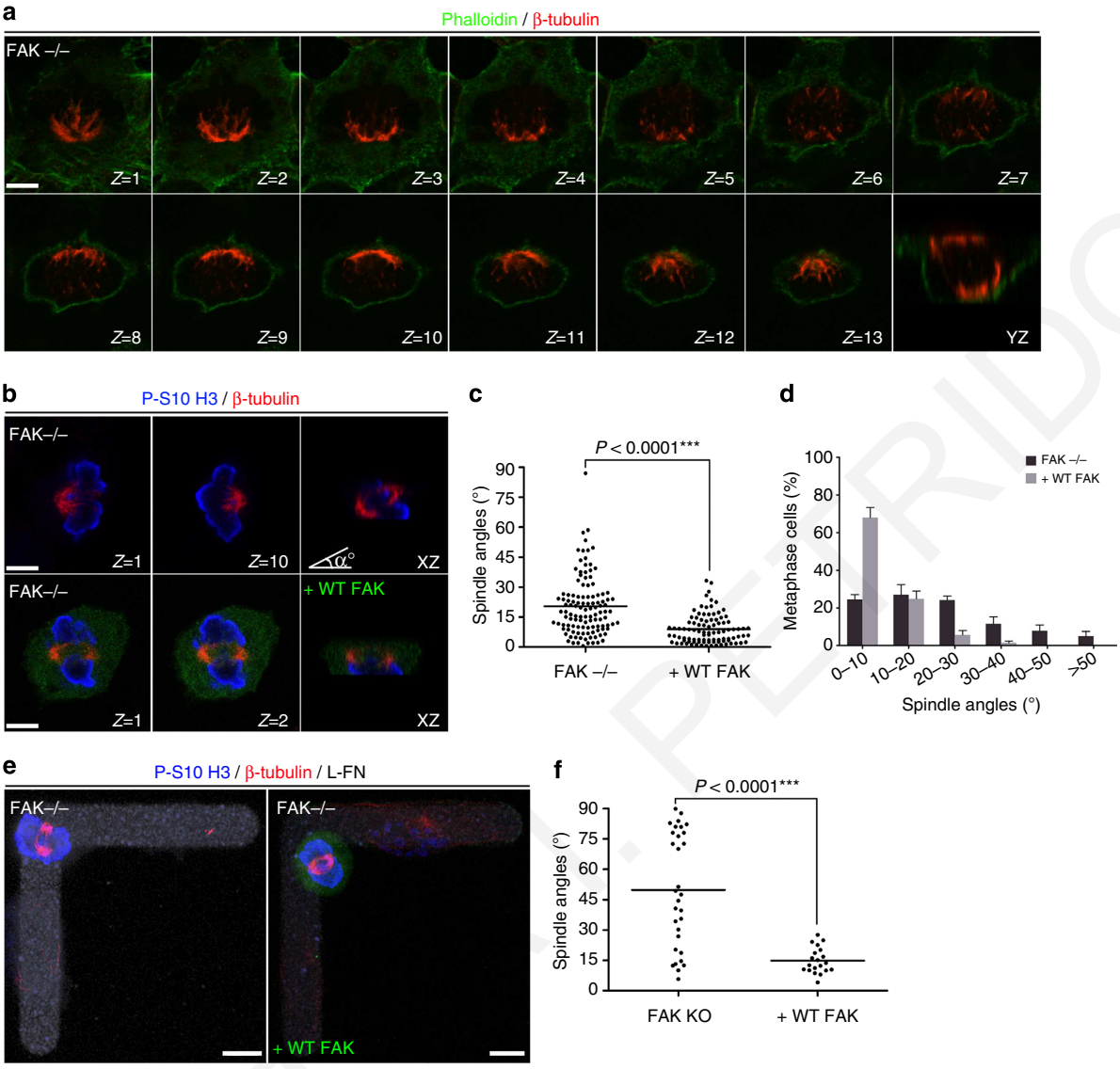

Figure 1 | FAK-null MEFs display spindle orientation defects. (**a**) Thin optical sections (0.37 μm) of a FAK-null metaphase cell and the corresponding *YZ*-projection image. (**b**) First and last optical sections from a Z-stack, showing the two spindle poles and the *XZ*-projection of a FAK-null metaphase cell and a FAK reconstituted cell (transfected with GFP FAK). (**c**) Scatter plots of the substrate to spindle angles (angle α shown in **b**) of FAK-null and WT-FAK reconstituted cells. The average spindle angle in FAK-null cells is 20.30 ± 1.368° ($n = 116$) and in WT-FAK reconstituted cells 8.849 ± 0.7483° ($n = 95$). Analysis of spindle orientation with a Mann–Whitney test showed statistically significant differences of the means of the spindle angles between the two samples, ***$P < 0.0001$; *n*, number of metaphase cells, six independent experiments. (**d**) Quantification of the percentage of metaphase cells with substrate to spindle angles greater than 10°. 75% of FAK-null cells displayed spindle angles greater than 10° compared with 32% of FAK reconstituted cells. Error bands are s.e.m. (**e**) Representative images of FAK-null and FAK reconstituted metaphase cells on L-shaped fibronectin micropatterns. (**f**) Scatter plots of *XY* spindle angles of FAK-null and WT-FAK reconstituted cells on L-shaped fibronectin micropatterns. The average spindle angle in FAK-null cells is 49.77 ± 5.119° ($n = 31$) and in WT-FAK reconstituted cells is 14.82 ± 1.426° ($n = 20$). Quantification of spindle orientation with a Mann–Whitney test showed statistically significant differences of the means of the spindle angles between the two samples, ***$P < 0.0001$; *n*, number of metaphase cells, two independent experiments. Scale bars (**a**,**b**), 5 μm, (**e**) 10 μm.

phosphorylation of downstream targets[26]. We thus examined if FAK's kinase activity is important in spindle orientation both in the Z axis and in the XY plane by transfecting FAK-null cells with the kinase-inactive mutant FAK-K454R[27]. The results from these experiments are nearly identical to those for WT-FAK suggesting that FAK's kinase activity is dispensable for correct spindle orientation (Fig. 3a,d). Due to the unexpected nature of this result we went on to confirm it using the FAK kinase inhibitor PF-228 in HeLa and NIH3T3 cells[28]. Both cell lines were treated with the inhibitor for 24 h and inhibitor effectiveness was evaluated by western blotting (Supplementary Fig. 2c,f). Quantification of spindle angles in inhibitor treated cells confirmed that inhibition of FAK's kinase activity does not affect spindle orientation, confirming that spindle orientation does not require FAK's enzymatic activity (Supplementary Fig. 2a,b and d,e).

The kinase and FAT domains are vital for spindle orientation. The above results suggest that FAK's function in spindle orientation is a scaffolding one. Given the previously identified role of integrins in spindle orientation, we postulated that FA localization of FAK would be necessary for its function in this

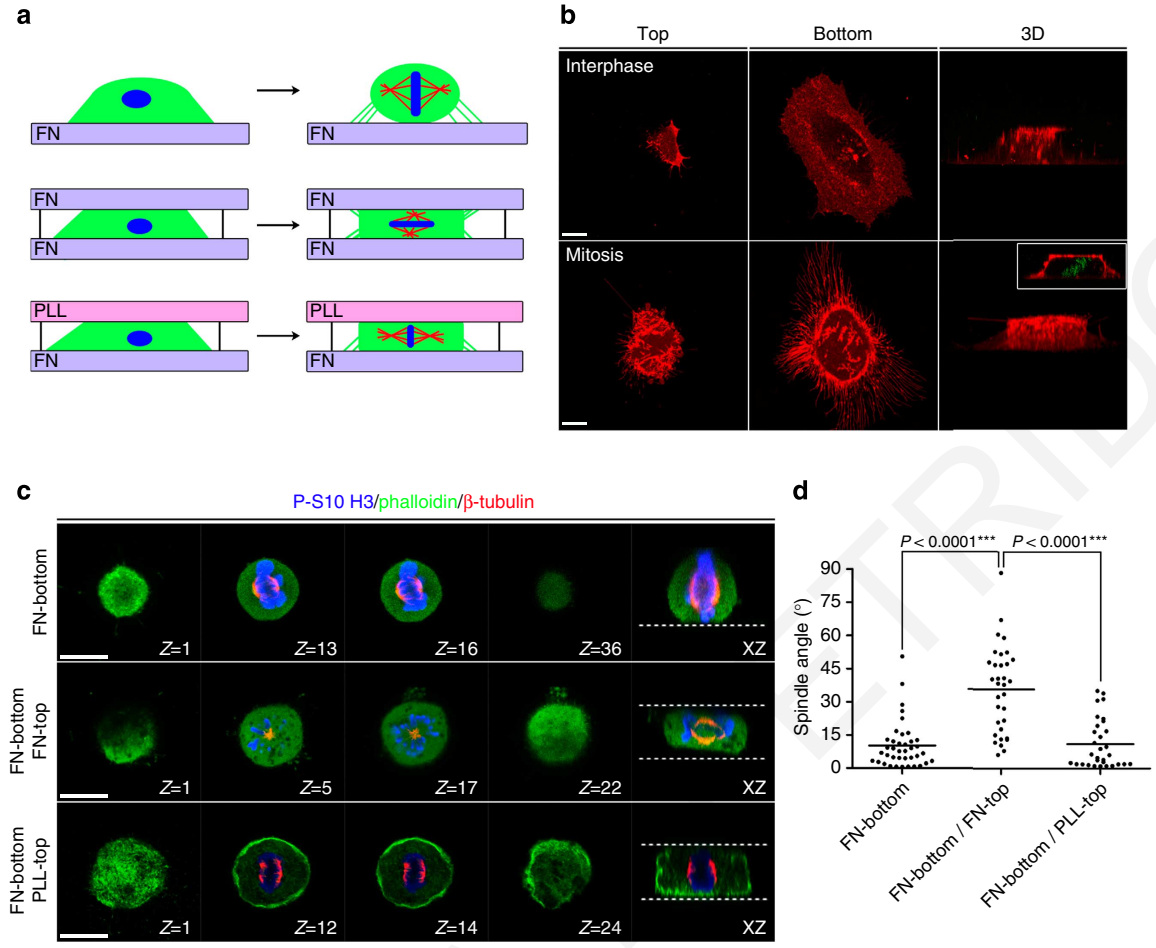

Figure 2 | The mechanism of spindle orientation in the *XY* and *Z* axis is common and depends on the spatial distribution of the retraction fibres. (**a**) Schematic representation of the experimental setup to determine the role of RFs in *Z* axis spindle orientation: cells seeded on a fibronectin (FN)-coated coverslip, sandwiched between two FN-coated coverslips or sandwiched between a FN-coated coverslip and a PLL-coated coverslip and imaged during cell division. (**b**) Confocal images of live memCherry-transfected HeLa cells confined between two FN-coated coverslips. Optical sections showing the top and the bottom of an interphase cell and a three-dimensional (3D) reconstruction show how the cell adheres on both coverslips. In the lower panel, optical sections of the top and the bottom of a mitotic cell and a 3D reconstruction show the distribution of the RFs. The small rectangle in the 3D reconstruction of the lower panel shows a side view of the mitotic cell where the metaphase plate (green) is not perpendicular to the substrate. (**c**) *Z*-stacks (0.37 μm interval) and the corresponding *XZ* side view of representative mitotic cells grown under the experimental settings shown in **a**. Cells were fixed and stained for actin, β-tubulin and P-S10 H3. The white dashed lines represent the coverslips. (**d**) Scatter plots of spindle angles relative to the substrate of the cells grown under the three conditions. The average spindle angle for cells grown in two-dimensional is 10.17 ± 1.699° ($n = 39$), in cells grown between two FN-coated coverslips 35.72 ± 3.405° ($n = 33$) and in cells grown between a FN-coated and a PLL-coated coverslip 11.01 ± 1.987° ($n = 31$). Quantification of spindle orientation with a Mann–Whitney test shows statistically significant differences of the means of the spindle angles between the indicated samples, ***$P < 0.0001$; *n*, number of metaphase cells, three independent experiments. Scale bars (**b**,**c**), 10 μm.

context. The FAT domain is both necessary and sufficient for FAK's FA localization[29]. Expression of a FAKΔFAT mutant in FAK nulls failed to rescue spindle orientation defects, suggesting that the FAT domain and FA localization are important (Fig. 3a–c). In agreement with this, we observed that although most FA complexes disassemble in mitotic cells, small FAK-positive adhesive complexes are retained along the RFs at areas where the fibres contact the ECM (Supplementary Fig. 3a,b). This suggests that FAK may be regulating spindle orientation by facilitating the transduction of external forces, generated at the ECM–RF interface, to the cell cortex, a notion supported by the fact that FAK-null MEFs do form RFs (Supplementary Fig. 3a).

We went on to examine a possible role of the FERM (4.1 protein, ezrin, radixin, moesin) domain, which has been shown to interact with several proteins involved in spindle orientation, such as the Arp2/3 complex and integrins[30,31]. FAK-nulls were transfected with a kinase-dead mutant of FAK that lacks the FERM domain (ΔFERM/K454R). As shown, expression of ΔFERM/K454R rescued the phenotype of spindle misorientation with the same efficiency as WT-FAK and FAK-K454R, suggesting that the FERM domain is dispensable (Fig. 3a–c). Given the fact that the kinase activity and the FERM domain are both dispensable, we went on to express the C-terminal non-catalytic part of the protein referred to as FAK-related non-kinase (FRNK)[32]. FRNK failed to rescue spindle orientation indicating that the FAT-containing C-terminus is not sufficient (Fig. 3a–c). This result suggests that despite the fact that the kinase activity is not necessary for correct spindle orientation, the kinase domain itself is revealing a novel kinase domain dependent but kinase activity-independent function.

A FAK paxillin interaction is critical for spindle orientation. In order to probe the role of the FAT domain further, we expressed variants of FAK with point mutations that abolish interactions

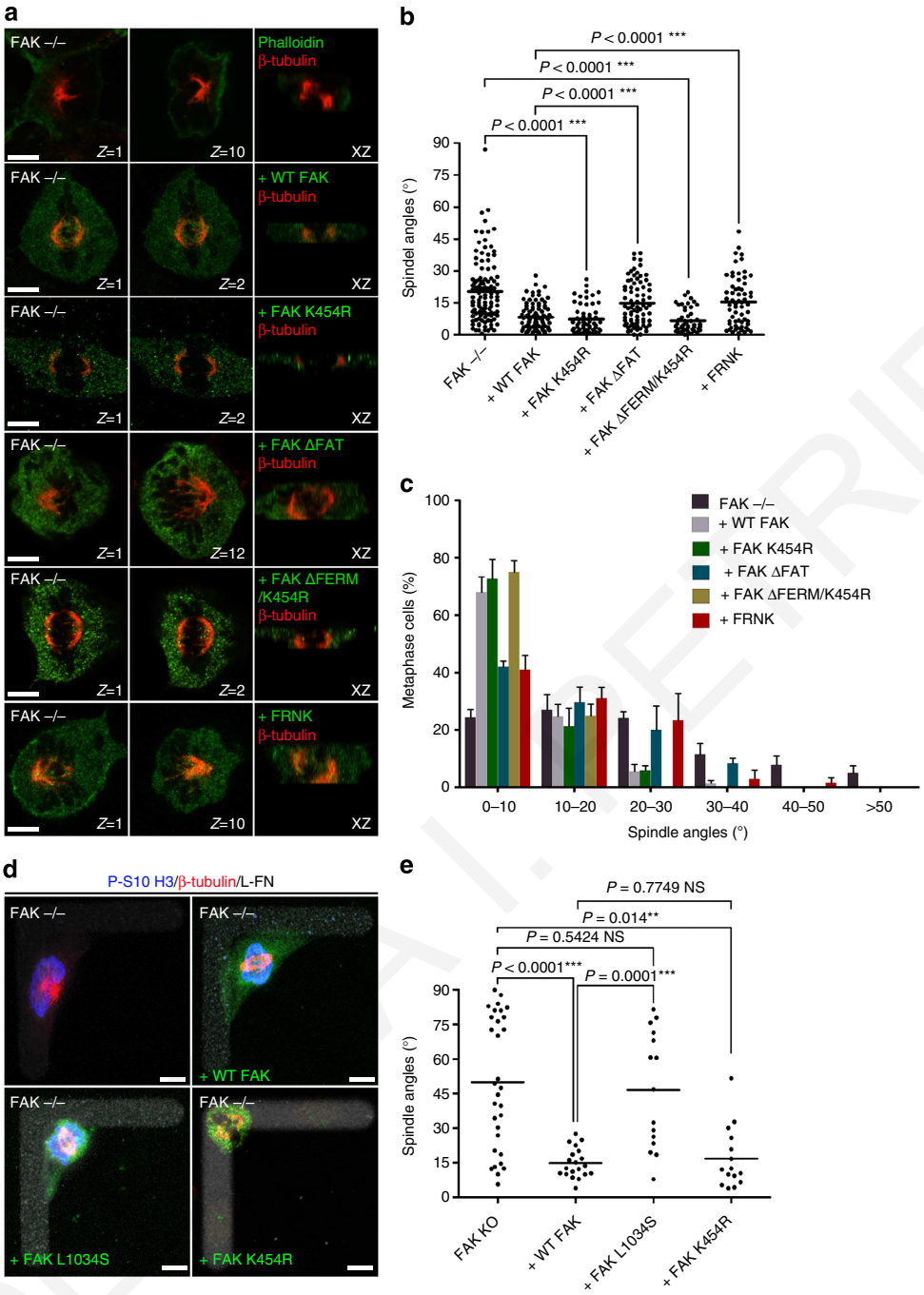

Figure 3 | The FAK kinase and FAT domains, but not the kinase activity, are required for correct spindle orientation. (**a**) First and last optical sections from *Z*-stacks and the corresponding *XZ*-projections of a FAK-null metaphase cell and FAK-nulls transfected with WT-FAK, FAK-K454R, FAKΔFAT, ΔFERM/K454R and FRNK. (**b**) Scatter plots of substrate to spindle angles from nulls and cells transfected with the constructs in **a**. The average spindle angle in FAK-nulls transfected with FAK-K454R is 7.200 ± 0.8812° ($n = 58$), FAKΔFAT 15.08 ± 1.333° ($n = 61$), ΔFERM/K454R 6.586 ± 0.7927° ($n = 48$) and FRNK 15.37 ± 1.478° ($n = 63$). A Kruskal–Wallis test gave statistically significant results (***$P < 0.0001$) indicating that at least one of the sample distributions is different from the other samples. Analysis with Mann–Whitney tests showed statistically significant differences of the means of the spindle angles for the indicated samples, ***$P < 0.0001$; *n*, number of metaphase cells, three independent experiments. Comparison between WT-FAK and FAK-K454R, WT-FAK and ΔFERM/K454R, FAK −/− and FAKΔFAT, and FAK −/− and FRNK with Mann–Whitney tests revealed that the differences in the average spindle angles are statistically insignificant (not significant (NS): $P = 0.1713$, NS: $P = 0.1627$, NS: $P = 0.6755$ and NS: $P = 0.6455$, respectively). (**c**) Plots (means ± s.e.m.) showing the percentage of cells that displayed spindle angles greater than 10°, which were 27%, 58%, 25% and 59% for the FAK-nulls transfected with FAK-K454R, FAKΔFAT, ΔFERM/K454R and FRNK, respectively. (**d**) Representative images of FAK-null, and FAK-nulls transfected with the WT-FAK, FAK-L1034S or FAK-K454R constructs on L-shaped fibronectin micropatterns. (**e**) Scatter plots of *XY* spindle angles of the samples in **d**. The average spindle angle in FAK-L1034S-transfected cells is 46.61 ± 6.538° ($n = 15$) and in FAK-K454R 17.82 ± 4.912° ($n = 10$). Statistical analysis with Mann–Whitney tests showed statistically significant differences of the means of the spindle angles between FAK-null- and FAK-K454R-expressing cells (**$P = 0.014$) and between FAK re-expressing cells and FAK-L1034S-expressing cells (***$P < 0.0001$), but no statistically significant differences between FAK-null- and FAK-L1034S-expressing cells (NS: $P = 0.5424$) or between WT-FAK- and FAK-K454R-expressing cells (NS: $P = 0.7749$); *n*, number of metaphase cells, two independent experiments. Scale bars (**a**), 5 μm, (**d**) 10 μm.

with known FAK-binding partners. The FAK C-terminus has been shown to be necessary for interactions with several proteins including talin, paxillin, RhoGEF and Grb2 (refs 33–36). Specifically, several lines of evidence suggest that the interactions with paxillin and talin are important for FAK's localization at FAs. We thus initially used two previously characterized point mutants FAK-E1015A and FAK-L1034S, which have been shown to abolish the interaction of FAK with talin and paxillin, respectively, whereas retaining FA localization[35,37]. As shown, expression of the FAK-E1015A mutant can effectively rescue orientation defects indicating that the FAK–talin interaction is not necessary (Fig. 4a,b). However, expression of the FAK-L1034S point mutant failed to rescue spindle orientation defects both in the *Z* axis and in the *XY* plane (Figs 3d,e and 4a,b). As the L1034S mutation has recently been shown to affect the structure of the four helix bundle that makes up the FAT domain and in addition, leads to loss of the FAK–RhoGEF interaction[33,38], we confirmed this result using the FAK-I936E/I998E mutant that specifically abolishes paxillin binding without affecting structure[38] (Fig. 4a,b). These results suggest that FA localization is not sufficient for FAK's function in spindle orientation and requires the interaction with paxillin, which similar to FAK, also localizes at RFs (Supplementary Fig. 3b).

Several reports revealed a role for FAK at centrosomes and basal bodies[39–41]. Deletion of FAK has been shown to lead to defective ciliogenesis, increases in centrosome numbers, defects in microtubule organization and nuclear movement as well as multipolar and disorganized spindles[39,41]. We wanted to examine if spindle misorientation in FAK nulls was related to the centrosomal functions of FAK and took advantage of the central role that phosphorylation of S732 by Cdk5 has in this context[41]. Expression of the S732A mutant effectively rescued spindle misorientation, suggesting that phosphorylation of this residue by Cdk5 is not important for FAK's function in spindle orientation (Fig. 4a,b).

FAK's role in spindle orientation is conserved in the embryo. Mechanisms controlling spindle orientation have been shown to be conserved between adherent cells and the *in vivo* setting[4,24]. Spindle orientation has been studied extensively especially in epithelia as oriented cell divisions are critical to several aspects of embryonic morphogenesis. We went on to examine a possible involvement of FAK in spindle orientation of epithelial tissues. The outer epithelium of *Xenopus* provides a good model as its well documented that cell divisions in this tissue are parallel to the plane of the epithelium[42,43]. Indirect immunofluorecence using FAK- and paxillin-specific antibodies revealed that both FAK and paxillin localize at the cell cortex and are enriched at the apical region of these cells (Supplementary Fig. 4a,b). We microinjected 50 ng of a previously characterized FAK MO[21,40,44] at the one-cell stage and imaged cell divisions of the

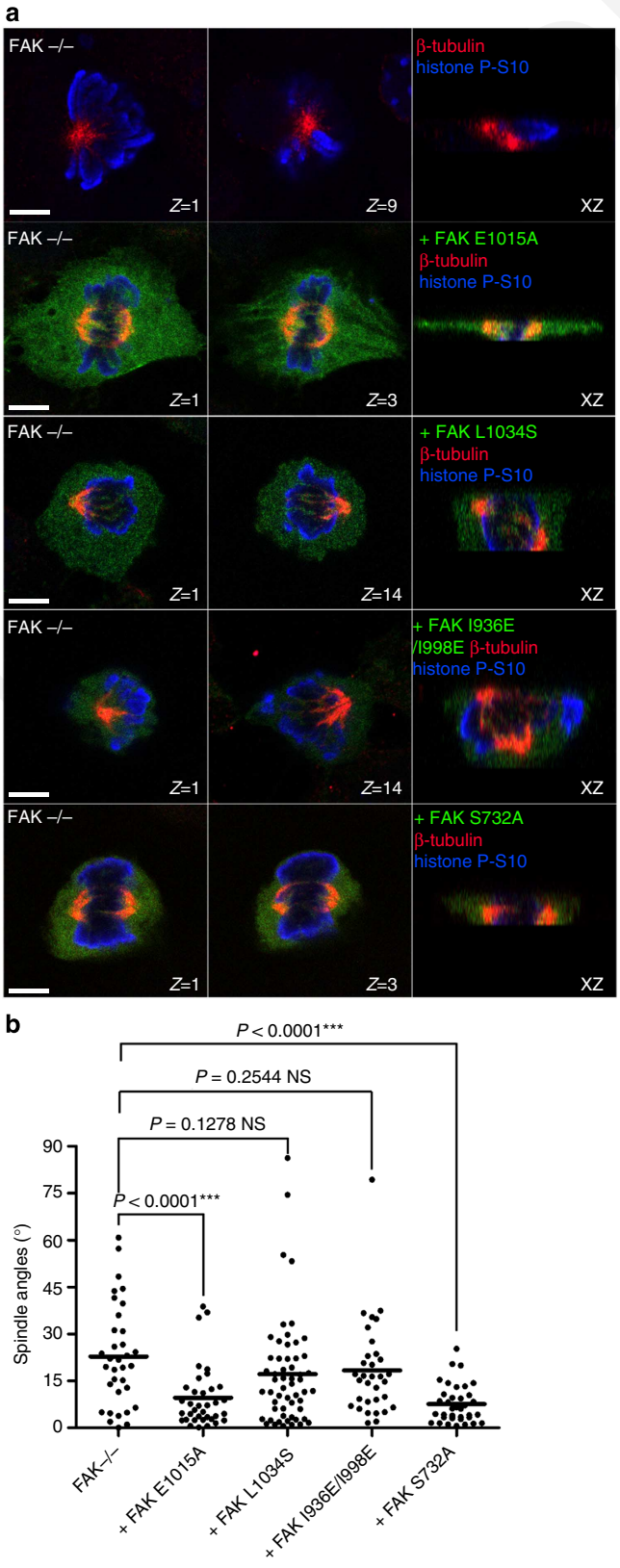

Figure 4 | FAK–paxillin interaction is necessary for proper spindle orientation in adherent cells. (**a**) Optical sections from *Z*-stacks, showing the position of each spindle pole and the *XZ*-projections from a FAK-null metaphase cell and FAK-nulls transfected with the indicated mutants. (**b**) Scatter plots of measured substrate to spindle angles for FAK-nulls and FAK-nulls transfected with the indicated mutants. The average spindle angle in FAK-nulls is 22.77 ± 2.780° ($n = 34$), in FAK-null cells transfected with FAK-E1015A is 9.527 ± 1.651° ($n = 36$), in FAK-null cells transfected with FAK-L1034S is 17.14 ± 2.303° ($n = 56$), in FAK-null cells transfected with FAK-I936E/I998E is 18.37 ± 2.624° ($n = 33$) and in FAK-nulls transfected with FAK-S732A is 7.542 ± 1.021° ($n = 36$). Quantification of spindle orientation with a Mann--Whitney test showed statistically significant differences of the means of the spindle angles between FAK-null and FAK-E1015A (***$P < 0.0001$) and FAK-null and FAK-S732A (***$P < 0.0001$) but not statistically significant differences between FAK-null and FAK-L1034S (not significant (NS): $P = 0.1278$) and between FAK-null- and FAK-I936E/I998E-expressing cells (NS: $P = 0.2544$); *n*, number of metaphase cells, two independent experiments. Scale bars (**a**), 5 μm.

outermost epithelial layer at early neurula. As shown, FAK knockdown (confirmed by western blot, Supplementary Fig. 5b) leads to spindle orientation defects in intact embryos, whereas expression of the FAK dominant-negative FF[22] also induces spindle misorientation (Supplementary Fig. 5a). In order to facilitate imaging and quantification, further analysis was carried out in dissected animal caps (ACs) from morphant control and rescued embryos. As shown, both the FAK MO as well as expression of FF lead to loss of spindle orientation, whereas expression of WT-FAK effectively rescued the phenotype (Fig. 5a–c and Supplementary Fig. 5d,e). Staining with the tight junction marker ZO-1 revealed that apicobasal polarity is not affected in FAK morphants, whereas other polarized molecules involved in spindle orientation like the Par6/3-aPKC complex also remain properly localized even in cells with completely misoriented spindles[45,46] (Supplementary Fig. 6a–c). We went on to examine if LGN cortical enrichment was affected, however, as shown, LGN is localized at the cell cortex and is enriched at the areas across the spindle in both control and FAK morphant cells (Supplementary Fig. 6d,e). Despite the fact that the spindle is misoriented in FAK morphants, LGN is clearly enriched at the spindle capture regions, suggesting that FAK is not required for spindle capture but for the correct localization of the NuMA, LGN and Gαi-GDP complex responsible for astral microtubule capture and spindle orientation.

We went on to examine if the functional requirements revealed from experiments in FAK-null MEFs were conserved in the embryo. FAK MO was co-injected with mutants of FAK as shown in Fig. 5a. These results show that both the kinase activity and the FERM domain are dispensable, whereas the kinase and FAT

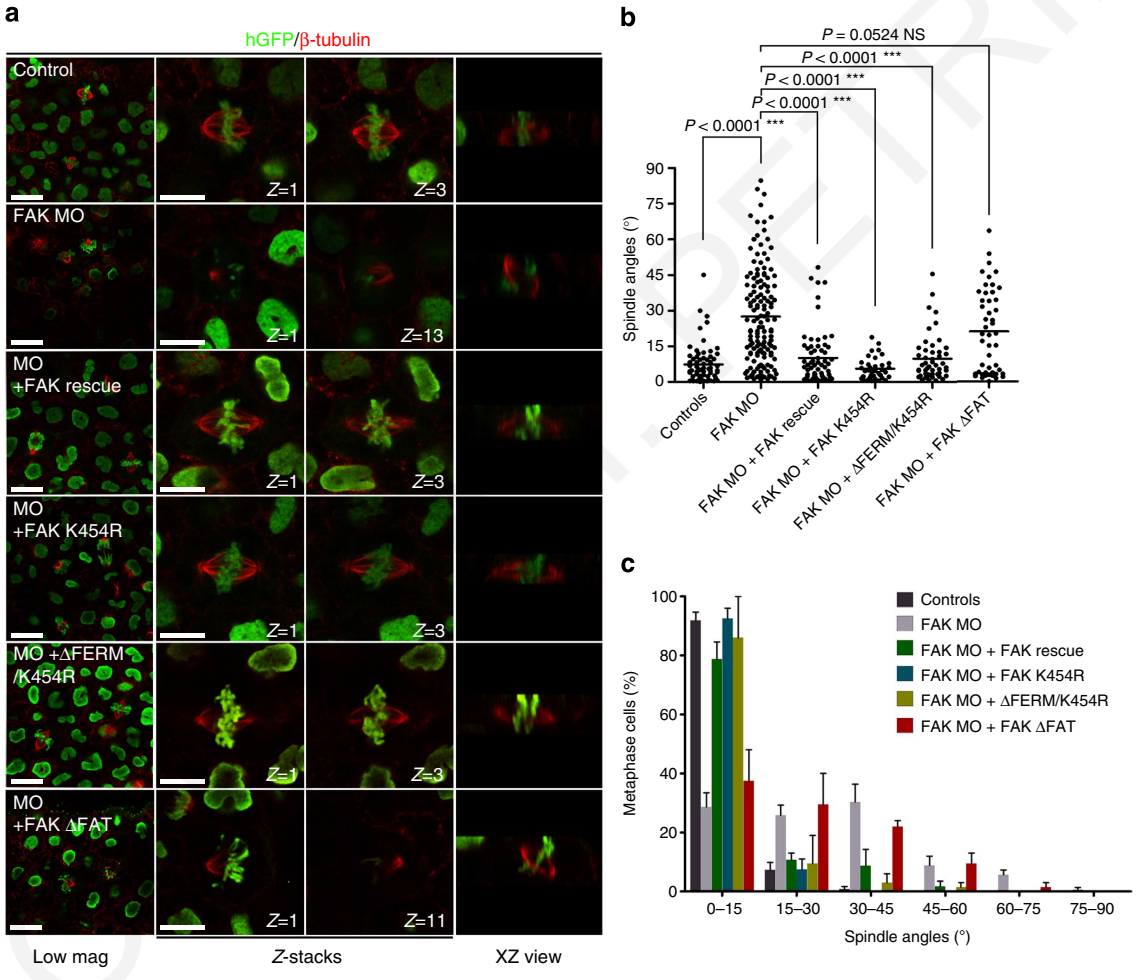

Figure 5 | FAK is necessary for spindle orientation in the *Xenopus* epithelium and displays similar functional determinants as in adherent cells. (**a**) Low-magnification images of the *Xenopus* outer epithelium showing mitotic cells (first column), optical sections showing each spindle pole (second, third column) and *XZ*-projections from representative metaphase cells of control, morphant and embryos rescued with indicated FAK mutants. *Xenopus* epithelia were stained with β-tubulin and anti-GFP antibodies. (**b**) Scatter plots of the spindle to plane of the epithelium angles from embryos shown in **a**. The average angle in control cells is 7.343 ± 0.9881° ($n = 67$), in FAK morphants is 27.50 ± 1.682° ($n = 142$), in cells rescued with the FAK-Rescue construct is 10.09 ± 1.429° ($n = 64$), in cells rescued with the FAK-K454R construct is 5.617 ± 0.7739° ($n = 36$), in cells rescued with the ΔFERM/K454R construct is 9.700 ± 1.377° ($n = 50$) and in FAK MO epithelial co-injected with the FAKΔFAT construct is 21.03 ± 2.530° ($n = 48$). A Kruskal–Wallis test gave statistically significant results (***$P < 0.0001$). Analysis with Mann–Whitney tests showed statistically significant differences of the means of the spindle angles between the indicated samples, ***$P < 0.0001$; *n*, number of metaphase cells, three independent experiments. Comparison between FAK-Rescue and FAK-K454R, FAK-Rescue and ΔFERM/K454R, FAK MO and FAKΔFAT with Mann–Whitney tests showed statistically insignificant differences of the means of the spindle angles (not significant (NS): $P = 0.1343$, NS: $P = 0.6498$ and NS: $P = 0.0524$, respectively). (**c**) Plots (means ± s.e.m) showing the percentage of metaphase cells with spindle to plane of the epithelium angles greater than 15°. These were 8%, 71%, 21%, 8%, 14% and 62.5% for control, FAK MO, FAK MO + FAK-Rescue, FAK MO + FAK-K454R, FAK MO + ΔFERM/K454R and FAK MO + FAKΔFAT, respectively. Scale bars: (**a**) low magnification: 20 μm, high magnification: 10 μm.

domains are essential for correct spindle orientation in the epithelium (Fig. 5a–c). In addition, a paxillin-binding mutant failed to rescue spindle orientation defects (Fig. 6a,b), whereas use of a paxillin MO[47] (paxillin downregulation was confirmed by western blot, Supplementary Fig. 5c) elicited spindle orientation defects. These defects were rescued by the expression of a Paxillin-Rescue construct (Fig. 6c,d), suggesting that the paxillin–FAK interaction is also critical, for FAK's function in this process, *in vivo*[47]. Overall, these results suggest that FAK's role in spindle orientation is conserved in the embryo.

FAK transduces external forces to the spindle. Recent work has revealed that external forces can induce mitotic spindle rotation in adherent mammalian cells[7,25], whereas cells of the EVL in zebrafish orient their mitotic spindle preferentially along the main axis of tension-promoting tissue spreading during epiboly[8]. To determine if external forces can induce spindle rotation in *Xenopus*, we placed mid-gastrula embryos in silicone-chambered slides and imaged them live under conditions where the embryo was being slightly depressed exerting mechanical force on the epithelium and in the absence of external force. As shown, under mechanical stimulation, the average spindle rotation increased by 50% and the same was true with respect to the frequency of rotation (Fig. 7a–c). These results show that application of external force can induce spindle rotation *in vivo* in a similar manner to what has been observed in cultured cells[7]. Presumably, the applied force on the embryo becomes distributed throughout the tissue changing the orientation of the maximum force vector on mitotic cells and the cells respond to reorient along the new axis. We went on to test if mechanical stimulation would lead to increased spindle rotation in FAK morphants. Despite the fact that under basal conditions FAK morphants display similar average spindle rotation and frequency of rotation with controls, under conditions of mechanical stimulation morphants fail to respond suggesting that FAK is required for the spindle rotation response (Fig. 7a–c). Owing to variations in the size of embryos that could lead to variations of the force exerted on each embryo, this experiment was repeated in embryos unilaterally injected with the FAK MO leading to similar results (Supplementary Fig. 7a,b). Decoupling the spindle from the cortex could explain this defect, however, high-resolution imaging of mitotic spindles

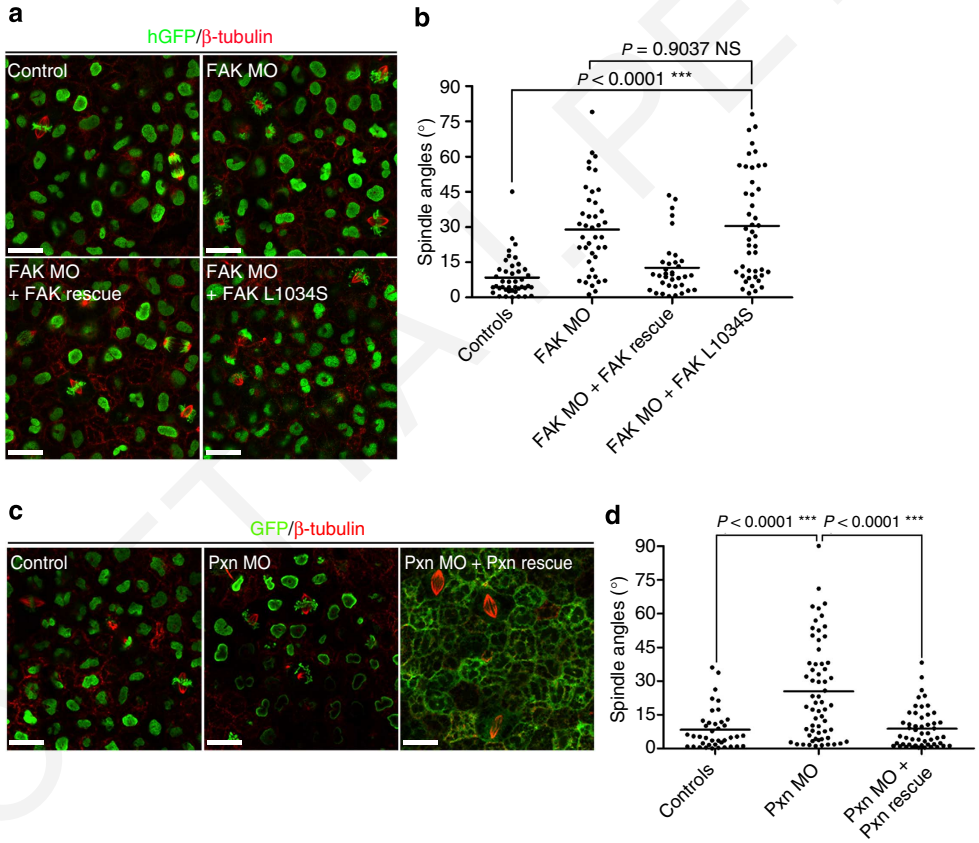

Figure 6 | The FAK–Paxillin interaction is necessary for spindle orientation of *Xenopus* epithelial cells. (**a**) Confocal images of epithelial cells from a control embryo, an embryo injected with FAK MO alone, FAK MO + FAK-Rescue and FAK MO + FAK-L1034S. HistoneGFP was used as a linage tracer and embryos were stained for β-tubulin and GFP. (**b**) Scatter plots of spindle to plane of the epithelium angles. The average angle in control cells is 8.462 ± 1.324° ($n = 42$), in FAK morphants is 28.88 ± 2.909° ($n = 41$), in rescued cells is 12.57 ± 1.980° ($n = 35$) and in FAK MO + FAK-L1034S-injected cells is 30.42 ± 3.372° ($n = 45$). Statistical analysis with a Mann–Whitney test showed statistically significant differences of the means of the spindle angles between control and FAK MO + FAK-L1034S (***$P < 0.0001$) but no statistically significant differences between FAK morphants and FAK MO + FAK-L1034S-injected embryos (not significant (NS): $P = 0.9037$); *n*, number of metaphase cells, two independent experiments. (**c**) *Xenopus* epithelium of a control embryo injected with histoneGFP, Pxn MO (100 ng Pxn MO + histoneGFP) and Pxn MO + Pxn-Rescue construct. *Xenopus* epithelia were stained for β-tubulin and GFP. (**d**) Scatter plots of spindle to plane of the epithelium angles. The average spindle angle in control cells is 8.282 ± 1.433° ($n = 40$), in Paxillin morphants is 25.37 ± 2.774° ($n = 62$) and in rescued cells is 8.761 ± 1.226° ($n = 51$). Statistical analysis with a Mann–Whitney test shows statistically significant differences of the means of the spindle angles between the indicated samples, ***$P < 0.0001$; *n*, number of metaphase cells, two independent experiments. Scale bars (**a**,**c**), 20 μm.

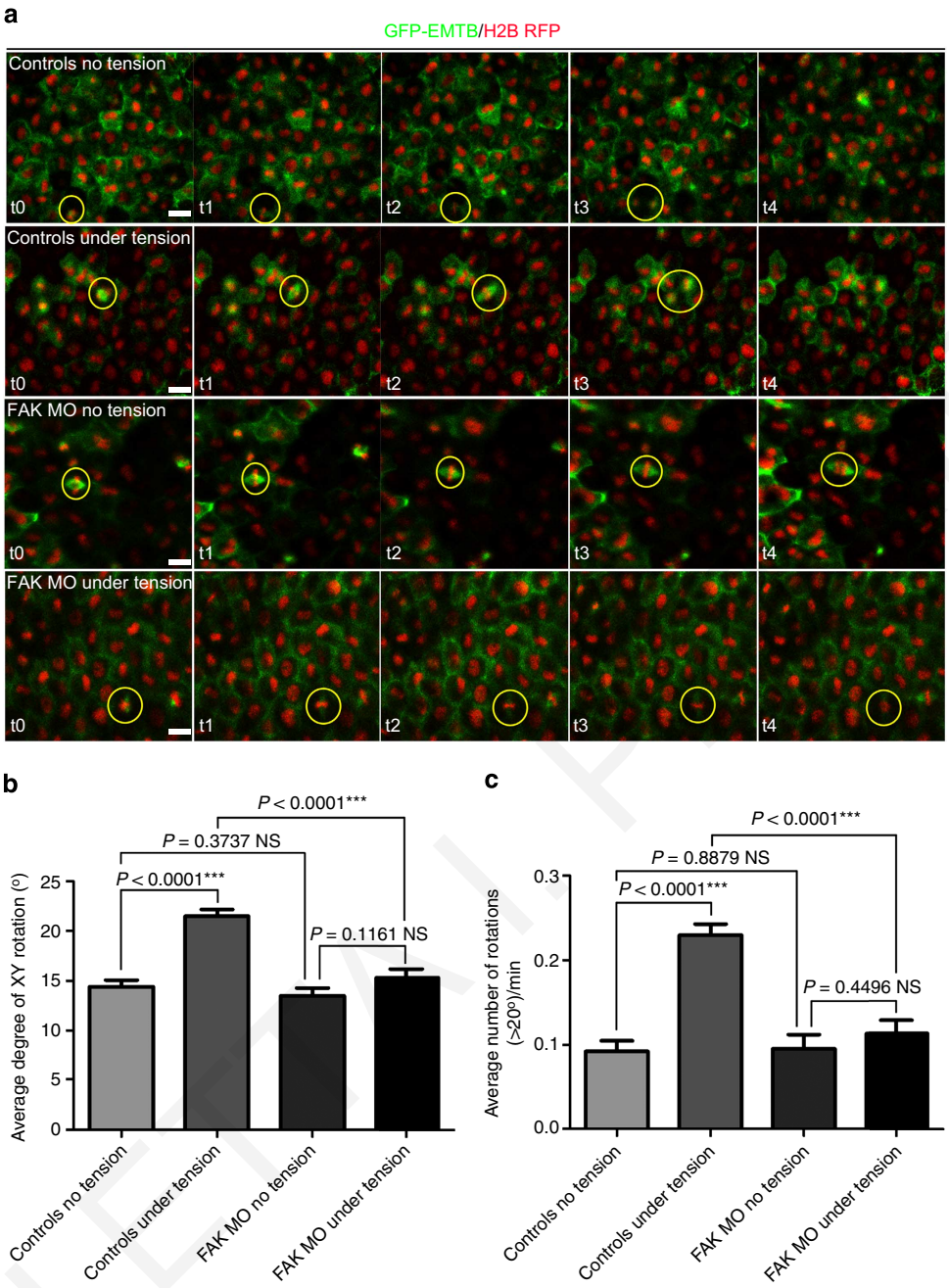

Figure 7 | FAK is required in the response of the spindle to external forces. (**a**) Stills (4 min interval) from time lapse recordings from stage 11 embryos expressing GFP-EMTB and histoneRFP, showing rotations of the mitotic spindle in controls and FAK morphant embryos under normal conditions and conditions of mechanical stimulation (MS). Yellow circles indicate representative mitotic cells from each condition. (**b**) The average spindle rotation for control embryos without MS is 14.41 ± 0.6600° ($n = 267$), for control embryos under MS is 21.51 ± 0.6631° ($n = 405$), for FAK morphants without MS is 13.48 ± 0.7861° ($n = 165$) and for FAK morphant embryos under MS is 15.33 ± 0.8635° ($n = 174$). Analysis of spindle rotation with a two-tailed unpaired *t*-test showed statistically significant differences of the means between controls without MS and controls under MS (***$P < 0.0001$) and between controls under MS and FAK morphants under MS (***$P < 0.0001$) but no statistically significant differences between controls without MS and FAK morphants without MS (not significant (NS): $P = 0.3737$) or between FAK morphants without and with MS (NS: $P = 0.1161$); *n*, number of spindle rotations, three independent experiments. Error bands are s.e.m. (**c**) Quantification of the frequency of mitotic spindle rotation. The average frequency of rotation per minute is 0.09238 ± 0.01245 ($n = 82$) for control embryos without MS, 0.2296 ± 0.01329 ($n = 120$) for control embryos under MS, 0.09532 ± 0.01688 ($n = 47$) for FAK morphants without MS and 0.1133 ± 0.01588 ($n = 68$) for FAK morphant embryos under MS. The results were analysed with a two-tailed unpaired *t*-test, showing statistically significant differences of the means of the rotation frequencies between controls without and with MS (***$P < 0.0001$) and between controls under tension and FAK morphants under MS (***$P < 0.0001$) but no statistically significant differences between controls and FAK morphants without MS (NS: $P = 0.8879$) or between FAK morphants without and with MS (NS: $P = 0.4496$); *n*, number of divisions. Scale bars (**a**), 20 μm.

of morphant cells revealed that both spindle capture and spindle centring are unaffected in agreement with the *in vitro* data showing that both spindle integrity and centring are unaffected in FAK-null cells (Supplementary Fig. 7d). Moreover, mitosis in FAK morphants progresses smoothly with no delays (Supplementary Fig. 7c). We went on to use laser ablation to generate pulling

forces perpendicular to the axis of the spindle of mitotic cells in a similar approach to what was described by Campinho *et al.*[8] in Zebrafish. Two cells positioned above and below the mitotic cell in a line perpendicular to the orientation of the spindle were laser ablated. Laser ablation leads to the extrusion of the ablated cell creating a wound. As the epithelium stretches to close the wound, it imposes tension on the tissue between the ablation sites causing the mitotic cell to change shape and stretch along the axis perpendicular to the spindle. As shown, the spindle of the control cell begins to rotate concomitant with cell stretching eventually becoming aligned with the imposed force (Fig. 8a,b). In FAK morphants, however, the spindle fails to respond and remains at a right angle to the force vector (Fig. 8a,b). These results suggest that FAK is required for spindle reorientation in response to external forces. As mentioned above, the forces generated by the wounds deform the mitotic cell elongating it along the axis of force. Cells have been shown to orient their spindle in response to force and cell shape[6,7], both of which share the same axis in the above experiment making the contribution of each parameter difficult to resolve. In an effort to pinpoint the defect, we carried out laser ablations of single cells at regions perpendicular to their long axis in high-salt conditions. Ablating a single cell ensured that wound-derived forces would not lead to large-cell shape changes and high salt that wounds would close rapidly giving rise to relatively brief application of force on the mitotic cell. Imaging of control cells in which a long axis was present before wound closure but the cell became symmetric after would closure revealed that the spindle rotates to align with the imposed force despite the absence of a clearly defined long axis (Supplementary Fig. 8a). Time-lapse imaging of cells under conditions where the original long axis remained after wound closure revealed that during wound closure, spindles display a transient rotation to align with the applied force but eventually realign (albeit not always completely) with the long axis, once the wound closes and presumably the applied force dissipates. These cells eventually divide along their long axis suggesting that spindle orientation is determined by a combination of both sensing of forces and cell shape (Supplementary Fig. 8b). The contribution of each parameter to the final spindle orientation is difficult to assess, however, the transient rotation in cells with a clearly defined long axis away from that axis suggests that external forces may override cell shape. We went on to carry out the same experiment in FAK morphant embryos, and in this case, cells failed to display any transient rotations as expected given their inability to rotate even in response to double wounds and significant cell shape change (Supplementary Fig. 8c). These data suggest that FAK is required in order for mitotic cells to respond to external forces and reposition their spindle but do not rule out the possibility that it is also required for orientation with respect to cell shape. If spindle orientation is determined via a multi-parameter mechanism where both external forces and cell shape contribute to the final axis of division, as the majority of cells would be elongated along the axis of greatest force, the synthesis of information would make alignment along the long axis more robust. It is possible that due to an inability to properly transduce force alignment cues, FAK morphants fail to align unless the cell shape anisotropy is very high. In order to address this possibility, we generated linear wounds on control and morphant tailbuds using the gastromaster microsurgery instrument. Embryos were allowed to heal and fixed an hour later, to allow for the tension within the tissue to subside. Cells from these embryos display a great range of shape anisotropy with cells close to the wounds becoming very elongated. Although imaging these cells it became evident that in FAK morphant cells that were highly anisotropic, the spindle was always oriented along the long axis just like in controls (Fig. 8c,d). Use of low-concentration nocodazole (Noc) to depolymerize astral microtubules in control embryos on the other hand, gave rise to mitotic cells which failed to become oriented along the long axis irrespective of the extent of cell shape anisotropy (Fig. 8c,d). Quantification of spindle angles in relation to shape anisotropy from control, FAK morphant- and Noc-treated embryos confirm these observations (Fig. 8d). Although FAK morphants fail to orient along the long axis at low cell shape anisotropy they start behaving like controls above a threshold (length to width ratio = 3), whereas spindles of cells from Noc-treated embryos remain randomized irrespective of cell shape (Fig. 8d). Overall, the above data suggest that FAK is required for the transduction of mechanical signals from the cell exterior to the cortex, which in turn bias cortical cues resulting in correct spindle alignment.

FAK is required for epithelial morphogenesis. In order to assess the significance of the spindle orientation defects arising from FAK loss of function in the embryo, we turned to two morphogenetic events known to require oriented cell divisions, epiboly and the development of the pronephros[43,48]. The *Xenopus* AC is initially three cell layers and rearranges into two layers via radial intercalation. This two-layer arrangement is maintained through oriented cell divisions at the plane of the epithelium[43,49]. We have previously shown that loss of FAK leads to block of epiboly through inhibition of radial intercalation and loss of spindle orientation[22]. In order to decouple the two processes and examine the effects of loss of spindle orientation on epithelial morphogenesis independently from radial intercalation, we generated an inducible FF dominant negative based on the hormone-binding domain of the glucocorticoid receptor[50]. The FF inducible construct was initially tested in adherent cells and as shown, in the absence of induction FF localizes primarily in the cytosol and becomes localized at FAs only upon induction (Supplementary Fig. 9a). We thus induced FF-injected embryos at stage 10.5 to ensure that radial intercalation had been completed and assessed blastopore closure and AC thickness. As shown, FF expression delayed blastopore closure (Supplementary Fig. 9b) and led to thickening of the AC (Fig. 9a,b), even after radial intercalation was completed, suggesting that loss of spindle orientation alone is sufficient to interfere with epiboly. In addition, the presence of heavily pigmented cells within the deep layers of the AC suggests that pigmented cells of the outermost epithelium divide asymmetrically, ingressing into the deep layer and contributing to the increase of AC thickness (Fig. 9c,d). These results show that FAK's role in spindle orientation is indispensable for correct epithelial morphogenesis during epiboly[51].

Another tissue in which oriented cell divisions are known to be important is the kidney. A model has emerged in which oriented cell divisions are critical for the normally thin elongated tubes to develop, with evidence suggesting that misoriented divisions lead to cystic kidney disease in animal models[52]. We thus targeted the inducible FF at the pronephros and induced the construct at stage 32/33. FF expression resulted in spindle misorientation and pronephros defects including dilated tubules, whereas the pronephric duct was also dilated compared with that of controls (Fig. 9e–h). Overall, these data suggest that FAK's role in spindle orientation is important for epithelial morphogenesis.

Discussion

In this manuscript, we provide evidence for the involvement of FAK in spindle orientation both in cultured cells as well as in the epithelia of the developing vertebrate embryo. We provide evidence that spindle integrity, centring and cortical microtubule capture are unaffected in the absence of FAK, yet these cells fail to respond to external forces suggesting that FAK's involvement in

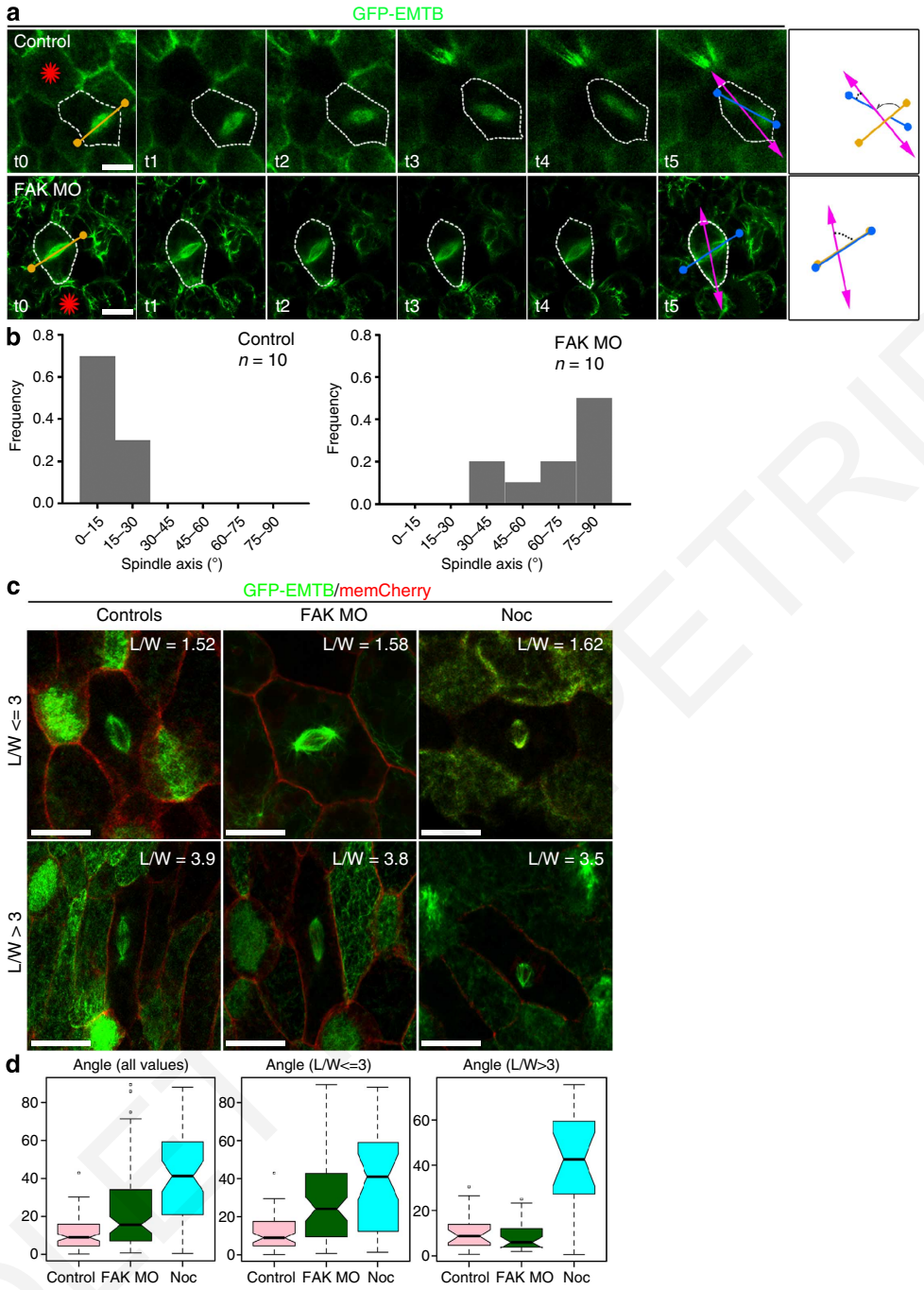

Figure 8 | FAK is required for the transduction of the extracellular forces to the cortex that guide spindle orientation. (**a**) Stills (2 min interval) from a time lapse recording where neighbouring cells of a mitotic cell were laser ablated (red star) to generate tension perpendicular to the initial axis of the spindle (orange axis). The white dashed line delineates the cell boundary. (**b**) Quantification was performed by measuring the angle (black dashed line) between the final spindle axis (blue) and the induced tension axis (magenta axis). The histograms show the frequency distributions of the observed angles for control and morphant embryos. A two-tailed unpaired *t*-test showed statistically significant differences of the means of the spindle angles between the two samples, ***$P<0.0001$; control spindle angle $10.99 \pm 2.417°$, FAK MO spindle angle $67.04 \pm 5.671°$, ten embryos per sample, two independent experiments. (**c**) Representative images of mitotic cells from wounded tailbuds that displayed small ($L/W \leq 3$) or large ($L/W > 3$) shape anisotropy from control, FAK morphants and Noc-treated control embryos. (**d**) L/W ratio was calculated for each cell and correlated to the spindle angle, which was defined as the angle between the line connecting the two spindle poles and the long axis of the cell. Box-Whisker plots of the angle values are presented for the three experimental conditions. The first box-plot shows all the angles that were measured from all the cells from each sample, the second pox-plot shows angles measured from cells with $L/W \leq 3$ and the third box-plot angles measured from cells with $L/W > 3$. Kruskal–Wallis test revealed that the three samples show statistical significant differences in each case ($P<0.01$). Mann–Whitney test between the three samples in the first box-plot showed that all three display statistically significant differences ($P<0.01$). In contrast, in the second plot ($L/W \leq 3$) only the comparisons between Control-FAK MO and Control-Noc display statistically significant differences ($P<0.01$), whereas FAK MO and Noc ($P=0.22$) do not. In the third box-plot ($L/W > 3$) only the comparisons between Control-Noc and FAK MO-Noc display statistically significant differences ($P<0.01$), whereas control and FAK MO ($P=1$) do not. Scale bars (**a**,**c**,**d**), 20 μm.

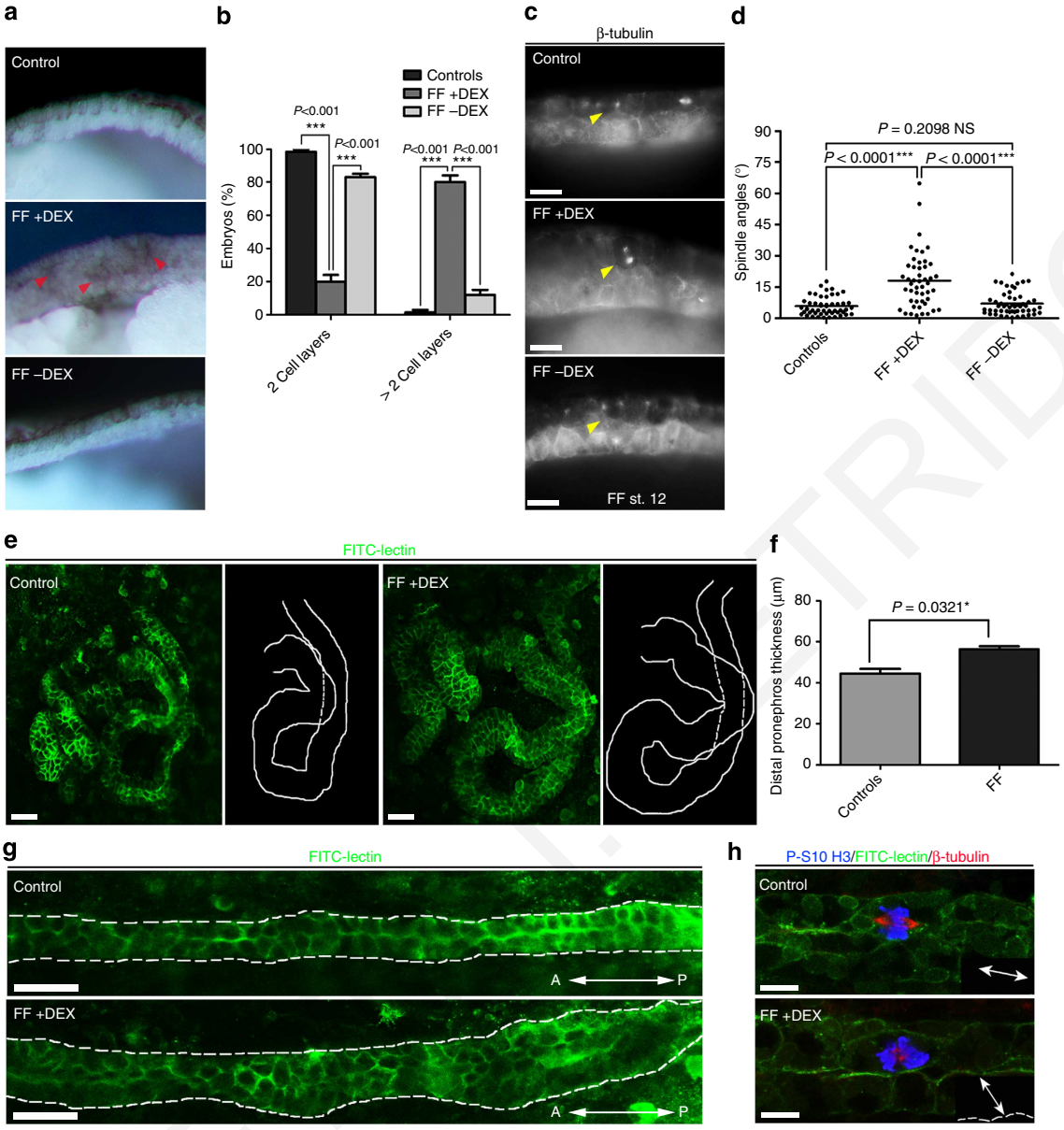

Figure 9 | FAK's role in spindle orientation is important for epithelial morphogenesis. (**a**) Sectioned control, FF-injected and FF-injected and dexamethasone-treated (at stage 10.5) embryos. In FF + DEX embryos epiboly is blocked and pigmented cells of the outermost layer can be seen in the deep layers (red arrowheads). (**b**) Percentage of embryos with a two-cell layered AC at stage 12. 98.5% in controls ($n = 50$), 20% in FF + DEX ($n = 71$) and 83% in FF-DEX-injected embryos ($n = 26$). Analysis with a two-way analysis of variance (ANOVA) test revealed that these differences are statistically significant (***$P < 0.001$); *n*, number of embryos, two independent experiments. (**c**) Fluorescence images of mitotic spindles (yellow arrowheads) in sectioned control, FF-DEX and FF + DEX-injected embryos. (**d**) Scatter plots of the spindle angles. The average spindle angle in controls is 5.807 ± 0.6240° ($n = 50$), in FF + DEX is 18.05 ± 1.924° ($n = 48$) and in FF-DEX is 7.039 ± 0.7434° ($n = 53$). Quantification of spindle orientation with an unpaired *t*-test showed statistically significant differences of the mean spindle angle between controls and FF + DEX (***$P < 0.0001$) and between FF + DEX and FF-DEX (***$P < 0.0001$) but not between controls and FF-DEX-injected cells (not significant (NS): $P = 0.2098$); *n*, number of metaphase cells, two independent experiments. (**e**) Maximum Intensity Projections from *Z*-stacks of the *Xenopus* pronephros including outlines of the distal pronephros from st.40 control and FF-injected embryos. (**f**) Quantification of distal pronephros thickness. The average diameter in controls is 44.52 ± 0.8598 µm and in FF-injected is 56.33 ± 1.396 µm. Analysis of the pronephros thickness with a two-way ANOVA test showed statistically significant differences of the means between the samples, *$P < 0.0321$ ($n = 6$; *n*, number of embryos). (**g**) Optical sections of the pronephric duct in control and FF-injected tadpoles. The white dashed line defines the pronephric duct. (**h**) Confocal images of mitotic spindles in the duct of control and FF-injected tadpoles. In control cells, the mitotic spindle is parallel to the long axis of the duct, whereas in FF-injected cells, it is oriented orthogonally to the long axis of the duct. The black boxes show a schematic diagram of how the spindle is oriented (white axis) with respect to the duct lumen (dashed line). Scale bars (**c**), 20 µm, (**e**,**g**) 50 µm, (**h**) 10 µm.

spindle orientation stems from a defect in the transmission of external forces to the cell cortex. Furthermore, our results suggest that an interaction between FAK and paxillin is critical for FAK's role in spindle positioning, whereas FAK's kinase activity is dispensable in this context, revealing the first kinase domain dependent but kinase activity independent function of FAK. Although the requirement for the presence of the kinase domain suggests a scaffolding function for this domain, it is also possible

that its presence is required in order to regulate or stabilize the conformation of the adjacent proline-rich regions or even that basal kinase activity is retained in the K454R mutant and is sufficient for this particular function.

FAK-null cells display RFs during mitosis in a similar manner as FAK reconstituted cells, yet fail to orient their spindle parallel to the matrix, whereas they also fail to orient according to extracellular cues in the *XY* plane. These results suggest that the presence of RFs is not sufficient for force transmission to the cortex of adherent cells but rather that forces are transmitted via a cytoskeletal link to the adhesive complex itself. Our results suggest that despite the fact that the majority of FAs disassemble during mitosis, a FAK-positive basal FA complex is retained at the RF–ECM interface. The composition of this complex warrants further study to determine which FA proteins other than FAK and paxillin remain localized at RFs during mitosis. We propose that these retraction adhesions anchor actin filaments to the ECM and through these, forces are transmitted to the cell cortex.

In the early embryo, the situation is different. The cells of the prospective neurectoderm encompass the entire embryo during gastrulation via epiboly, and at the end of gastrulation, the epithelium is composed of two cell layers[49]. The outer cells are attached to one another via tight junctions at their apical surface and via adherens junctions in their lateral regions[53,54]. They are also anchored to the deep cell layer via adherens junctions and only the deep layer is in contact with the ECM[55]. This suggests that cell–ECM interactions are not important for spindle orientation in the outer epithelium. This is also supported by the fact that fibronectin MOs as well as fibronectin antibodies that disrupt the fibronectin matrix assembly, thus disrupting cell–ECM interactions, fail to affect oriented cell divisions in the outer epithelial layer[43,56]. If cell–ECM interactions are dispensable for oriented divisions in the outer epithelium, is then FAK's role in this context integrin independent? As cadherins have been shown to be required for proper spindle orientation, it is possible that FAK acts through adherens junctions to position the spindle in the epithelium, especially given the fact that both FAK and paxillin have been shown to influence adherens junctions or interact with adherens junction proteins[57,58]. In addition, as we show, both FAK and paxillin co-localize with the adherens junctions of epithelial cells and are enriched at the apical region of the cell cortex in the outer epithelium of *Xenopus*. Another interesting possibility is that the role of integrins in epithelial tissue spindle orientation is independent from their role in cell–ECM interactions and FAK's role in this context is again stemming from the transduction of integrin-dependent signals. Support for this notion comes from studies in the fly showing that although integrin signalling is required for the correct orientation of the mitotic apparatus and maintenance of the ovarian monolayer epithelium, cell–ECM interactions are dispensable[59].

Although significant progress has been made towards understanding how cells couple cortical polarity signals and spindle positioning, how cells receive external stimuli and how these are translated at the cortex are poorly understood[3]. During early embryonic development, mechanical forces are believed to play a critical role in morphogenesis in part through control of cell division orientation[60]. Experiments in zebrafish showed that tissue level forces orient the mitotic spindle during epiboly thus releasing anisotropic tension in the EVL[8]. We show that in a similar manner, external forces can orient mitotic cells in *Xenopus* epithelia and provide direct evidence that FAK is required for spindle responses to such forces. Although both force and cell shape have been shown to control spindle orientation, our results suggest that the primary defect of FAK down-regulation is loss of the ability to orient depending on force, given the fact that in the presence of high cell shape anisotropy, FAK morphants orient correctly. FAK, however, is not only required for epithelial cells to orient their spindle along force vectors but it is also required to maintain cell divisions in the plane of the epithelium. This is in agreement with data in Medaka showing that planar divisions in the neuroepithelium are randomized in FAK morphant cells[61]. We show that blocking FAK function after radial intercalation has been completed, leads to failure of epiboly suggesting that correct spindle orientation is necessary for epithelial spreading, an important morphogenetic process shared by all vertebrates[51]. Blocking FAK function also leads to defective pronephros development highlighting the importance of proper spindle orientation in organogenesis.

Overall, our work identifies a novel role for FAK in spindle orientation and consequently for epithelial morphogenesis and reveals that this role stems from FAK's role in the transduction of external orienting forces to the cell cortex. We have recently shown that FAK is also involved in motile ciliogenesis by regulating ciliary adhesions, complexes formed at the basal bodies linking them to the actin cytoskeleton[40]. Thus, FAK is joining a number of proteins involved in both spindle orientation and cilia formation like IFT88, Msd1/SSX2IP Wtip and Vangl2 (refs 62–64). At least in one case, that of IFT88, it has been shown that the role in spindle orientation is not secondary to the protein's role in ciliogenesis, but independent[65]. Similarly, in the case of FAK, we propose that the two roles are distinct and stem from FAK's regulation of related but different complexes.

Methods

Cell culture. The FAK $-/-$ cell line (American Type Culture Collection (ATCC)) was cultured in DMEM with 10% fetal bovine serum (FBS) and 1 mM sodium pyruvate at 37 °C. HeLa (ATCC) and NIH3T3 (ATCC) cells were cultured in DMEM with 10% FBS at 37 °C. All cell lines were transfected with the indicated plasmids using Lipofectamin 2000 (11668019, Invitrogen) according to the manufacturer's protocol. FAK inhibitor PF-228 (Sigma) was added in HeLa and NIH3T3 cells at 10 and 5 μM for 24 h, respectively. Dexamethasone was added in HeLa cells at a concentration of 100 nM for 3 h. XL177 cells[66] were cultured in 70% L-15, 15% FBS and 100 mM L-glutamine at room temperature (RT), XL177 cells were transfected by electroporation (Invitrogen). Plating of the $FAK^{-/-}$ cells on fibronectin micropatterned coverslips (CYTOO) was performed according to the manufacturer's protocol.

Three-dimensional adhesion assay. The adhesion of HeLa cells between two coverslips was performed as follows: Bottom coverslips were charged, spotted with silicone grease at the edges and then coated with 50 μg ml^{-1} fibronectin (33010-018, Invitrogen) for 1 h at 37 °C. Top coverslips were also charged and coated either with poly-L-lysine (P8920, Sigma) or fibronectin. Cells were seeded on the bottom fibronectin-coated coverslips and allowed to adhere for 15 min. After initial attachment and while cells were still round, the second coverslip was secured in place on top using the silicone grease spots and carefully lowered under an inverted microscope until it contacted the cells. Cells were grown for 6 h at 37 °C and then were either imaged live or fixed and processed for immunofluorescence.

DNA constructs and MO oligonucleotides. All plasmids generated were verified by sequencing. The green fluorescent protein (GFP) and haemagglutinin (HA)-tagged versions of FAK, FRNK and FF plasmids have been described[22,44]. The HA FAK-K454R pCS2^{++} construct was generated by subcloning from the pKH3 HA FAK-K454R plasmid (kindly provided by the Guan lab) using the primers F/HA: 5′-ATGCGGCCGCATGTACCCATACGATGTTCCAGATTCCGCT-3′ and R/FAK: 5′-TTTCTCGAGTTAGTGGGGCCTGGACTGGCTGATCATTTT-3′. The GFP FAKΔFAT pCS108 construct was generated by PCR using the primers F/GFP: 5′-AAAGCGGCCGCATGGTGAGCAAGGGCGAGGAGCTG-3′ and R/ΔFAT: 5′-AACTCGAGTCTTCACGCCTTCGTTGTAGCTGTCCACGGGG-3′ and the template of GFP FAK pCS2^{++}. The HA ΔFERM/K454R pCS2^{++} construct was generated by subcloning a fragment of FAK containing the K454R mutation form the HA FAK-K454R pCS2^{++} plasmid followed by ligation to the plasmid of HA ΔFERM pCS2^{++} (ref. 44). The plasmids HA FAK-L1034S, GFP FAK-L1034S and GFP FAK-E1015A were generated by site-directed mutagenesis using the set of primers F/FAK-L1034S: 5′-GCTGTGGATGCCAAGAACTCGC TGGATGTCATCGATCAAGC-3′, R/FAK-L1034S: 5′-GCTTGATCGATCACATC CAGCGAGTTCTTGGCATCCACAGC-3′ for the L1034S mutation and the set of primers F/FAK-E1015A: 5′-CCAGCCTGCAGCAGGCGTACAAGAAGCAAAT GCT-3′ and R/FAK-E1015A: 5′-AGCATTTGCTTCTTGTACGCCTGCTGCAG GCTGG-3′ for the E1015A mutation. The GFP paxillin Rescue pCS2^{++} construct

was generated by a two-step directed mutagenesis, mutating the sequence recognized by Paxillin MO using the primers F/Pxn Rescue 1: 5′-ATGGAAGAA TTCGACGCCCTGCTGGCGGACTTGGAGTCTACC-3′ and R/Pxn Rescue 1: 5′-GGTAGACTCCAAGTCCGCCAGCAGGGCGTCGAATTCTTCCAT-3′ for the first step and the primers F/Pxn Rescue 2: 5′-ATGGAAGAATTCGATGCGCTC TTGGCGGACTTGGAGTCTACC-3′ and R/Pxn Rescue 2: 5′-GGTAGACTCCAA GTCCGCCAAGAGCGCATCGAATTCTTCCAT-3′ for the second step. The inducible FF dominant negative was generated in a three-step cloning as described below. Initially, a GFP-fused form of the FERM domain was amplified from the GFP FAK pCS2^{++} plasmid and cloned into the pCS108 vector using the primers F/GFP2: 5′-AAAGGATCCATGGTGAGCAAGGGCGAGGAGCTG-3′ and R/FERM: 5′-TTTGCGGCCGCATCTATTATCTCTGCATAGTCATCTGT-3′. Then the hormone-binding domain of the glucocorticoid receptor was PCR out from the Xbra-GR pSP64T plasmid (provided from Masazumi Tada lab) using the primers F/GR: 5′-AAAGCGGCCGCATCTGAAAATCCTGGTAACAAAACA-3′ and R/GR: 5′-TTTGATATCCTTTTGATGAAACAGAAGTTT-3′ and ligated to the GFP-FERM part in pCS108. Finally, the C-terminus FRNK domain was amplified from the GFP FAK pCS2^{++} plasmid and cloned into the GFP-FERM-GR part by using the primers F/FRNK_linker: 5′-AAGATATCGGTAGCGGCAGC GGTAGCAGGTTTACTGAACTTAAAGCAC-3′ and R/FAK, generating in this way an inducible from of the FF dominant negative with a GFP-tag on the N-terminus and the hormone-binding domain of the GR receptor in the middle of the construct.

The plasmids membraneCherry pCS2^{+} and histoneGFP pCS2^{+} were kindly provided by Chenbei Chang lab. The HA-Par6 pCS2+ plasmid was provided from Ira O. Daar lab. The H2B-mRFP1 pCS2 plasmid was provided by Reinhard Koster lab. The EMTB-3xGFP pCS2 was provided by Brian J. Mitchell lab. The pEGFP C1-LGN construct was kindly provided by Fumiko Toyoshima Lab.

All FAK mutants were generated from the FAK chicken variant (GenBank AAA48765.1).

The sequence of FAK MO is 5′-TTGGGTCCAGGTAAGCCGCAGCCAT-3′ (ref. 21) and of Paxillin MO is 5′-CAGCAATGCATCCAGGTCATCCATG-3′. This MO is based on a previously published Paxillin MO with slight differences[47].

Embryos and manipulations. *Xenopus laevis* embryos were staged according to the study by Nieuwkoop and Faber (1967). Embryos were fertilized *in vitro* and dejellied using 1.8% L-cysteine, pH 7.8, then maintained in 0.1 × Marc's Modified Ringer's (0.1xMMR). Microinjections were performed in 4% Ficoll in 0.3xMMR. Microinjections for the targeting of the AC performed at the one-cell stage, whereas microinjections for the targeting of the pronephros were performed at the two ventral vegetal blastomeres of eight-cell stage embryos.

ACs were dissected from stage 9 embryos and cultured in DFA (53 mM $NaCl_2$, 5 mM Na_2CO_3, 4.5 mM potassium gluconate, 32 mM sodium gluconate, 1 mM $CaCl_2$, 1 mM $MgSO_4$) until stage 15, when they were fixed and processed for immunofluorescence.

In order to generate high shape anisotropies in outer epithelial cells, linear parallel wounds were generated along the anterior–posterior axis of the embryo using the gastromaster microsurgery instrument. Embryos were allowed to heal in 1/3XMMR and were then fixed and imaged. Noc was used at 50 nM and was added to the embryos 20 min after the wounds were made and left for 40 min until fixation.

Activation of the inducible FF dominant negative for the radial intercalation experiments was performed by incubation of stage 10.5 embryos in 10 μM dexamethasome (sc-29059, Santa Cruz) at 14 °C. Activation of the inducible FF for the evaluation of the effects on pronephros morphogenesis was performed by incubating the embryos with 10 μM dexamethasome in 0.1xMMR from stage 33/34 until either stage 35/36 for imaging cell divisions or stage 40 for evaluation of the pronephros morphology.

Imaging. Embryos were imaged either under a Zeiss Axio Imager Z1 microscope, using a Zeiss Axiocam MR3 and the Axiovision software 4.8, or a Zeiss LumarV12 stereomicroscope or under a laser scanning confocal LSM710 microscope (Zeiss).

Live imaging of cell divisions described in Fig. 7 was performed as mentioned below. Imaging of gastrula embryos under conditions of reduced tension was performed by placing the embryos on a drop of Vaseline in a slide with a 2-mm silicone gasket and held in place by a glass coverslip, which was not in contact with the embryo. Optical sections were acquired every 2 min for a 40-min period. Imaging of embryos under conditions of increased tension was performed by placing the embryos in a slide with a 1-mm silicone gasket, applying in this way external mechanical force directly on the embryo and imaged as described above.

Laser ablation experiments were conducted using the LSM 710 confocal microscope and a Plan-Apochromat × 63/1.40 Oil DIC M27 objective lens (Zeiss). An early mitotic cell was selected and an image was acquired to determine the orientation of the division axis. For the data presented in Fig. 7a, wounds were performed in the two neighbouring cells in the axis perpendicular to the long axis of the spindle by using the 488- and 543-nm laser lines simultaneously, 50 iterations at 100% power and the mitotic cell was imaged every 15 s until the beginning of cytokinesis. For the data presented in Supplementary Fig. 7c,d,e, laser ablations were contacted as described above with the differences that the embryos were placed in high-salt solution (1x3 MMR) and only one cell near the mitotic cell was ablated in order to create a smaller wound that will not cause severe cell deformation.

Image of the spindle capture to the cell cortex was performed by using the LSM 710 confocal microscope and a Plan-Apochromat × 63/1.40 Oil DIC M27 objective lens (Zeiss) in embryos expressing GFP-EMTB and memCherry.

Immunofluorescence. Immunofluorescence on FAK −/−, HeLa, XL177 and NIH3T3 cells was carried out as follows: cells were plated on glass coverslips washed three times with PBS and then fixed for 10 min in 4% paraformaldehyde solution. Fixation was followed by addition of 50 mM glycine solution and then the cells were permeabilized using 0.2% Triton-X solution for 10 min. Permeabilized cells were blocked using 10% normal donkey or goat serum (017-000-121, Jackson Immunoresearch or 16210072, Invitrogen) for 30 min. Cells were incubated with primary antibodies for 1 h. Primary antibodies used were: β-tubulin (1:200, E7-c, Hybridoma Bank), Histone H3 phosphorylated Ser10 (1:1,000, 06-570, Millipore), HA (1:500, sc-805, Santa Cruz) and Paxillin (1:750, 610569, BD Biosciences). Cells were then washed several times in PBS. Secondary antibodies used were Cy3 (1:500, 711-165-152 or 715-165-150, Jackson Immunoresearch), Alexa fluor 488 (1:500, A11029 or A11034, Invitrogen), Alexa fluor 633 (1:500, A21052 or A21070, Invitrogen). Phalloidin was incubated together with the secondary antibodies, phalloidin 488 (1:500, A12379, Invitrogen), phalloidin 633 (1:500, A22284, Invitrogen). Immunfluorescence of *Xenopus* ACs was performed as whole mount immunostaining. ACs were fixed in 10% 10XMEMFA (0.1 mM 3-(*N*-morpholino)propanesulfonic acid, pH 7.4, 2 mM EGTA, 1 mM $MgSO_4$), 3.7% formaldehyde–10% formaldehyde and 80% water for 2 h at RT, dehydrated in ethanol and permeabilized for 2 h in 1 × PBS, 0.5% Triton, 1% dimethyl sulfoxide and blocked for 1 h in 10% Normal Goat or Normal Donkey serum. Primary antibodies used were: GFP (1:500, A11122, Invitrogen), HA (1:250, sc-805, Santa Cruz), β-tubulin (1:200, E7-c, Hybridoma Bank), ZO-1 (1:500, 61-7300, Invitrogen), Histone H3 phosphorylated Ser10 (1:1,000, 06-570, Millipore), aPKC (1:250, sc-216, Santa Cruz), FAK (1:100, 05-537, Millipore), Paxillin (1:500, 610569, BD Biosciences), β-catenin (1:500, sc-7199, Santa Cruz). The incubation was performed overnight at 4 °C. ACs were then washed four times for 20 min, incubated for 2 h RT with secondary antibodies: Alexa fluor 488 (1:500, A11029 or A11034, Invitrogen), Cy3 (1:500, 715-165-150 or 711-165-152, Jackson Immunoresearch) Alexa fluor 633 (1:500, A21052 or A21070, Invitrogen), at RT and then washed several times and post-fixed in 1XMEMFA. Clearing of the ACs was performed by immersing the embryos in Murray's Clearing Medium.

Immonofluorescence for the *Xenopus* pronephros was performed as whole-mount immunostaining with the difference that the tadpoles were treated with 0.01% Triton in 0.1xMMR prior fixation to avoid staining of the epidermis in order to facilitate imaging of the deep tissue. FITC-labelled *Lycopersicon Esculentum* (Tomato) Lectin (1:500, FL-1171, Vector Labs) was used for pronephros staining together with the secondary antibodies.

Western blot. Protein lysates were prepared by homogenizing cells or embryos in ice-cold radioimmunoprecipitation assay lysis buffer (50 mM Tris–HCl, pH 7.4, 150 mM NaCl, 2 mM EDTA, 1% NP-40, 0.1% SDS, 1% deoxycholate 24 mM) supplemented with phosphatase inhibitors (5 mM Sodium orthovanadate, Na_3VO_4) and protease inhibitors (1 mM phenylmethanesulfonyl fluoride, Protease cocktail, Sigma). Homogenates were cleared by centrifugation at 10,000 *g* for 5 min at 4 °C for cells or at 15,000*g* for 30 min at 4 °C for embryos. Protein levels were determined by bicinchoninic acid assay using the Magellan Data Analysis software (Tecan). The lysates were loaded on 7.5% SDS–polyacrylamide gels with the WesternC ladder (161-0376, Bio-Rad). The proteins were transferred onto nitrocellulose membrane, blocked in 5% milk (in TBST: 1 × TBS and 0.1% Tween). The blotting was performed by incubation of the primary antibodies overnight at 4 °C. Blots were incubated with N-FAK mouse monoconal (1:500, 05-537, Millipore), P-Y397 rabbit polyclonal (1:1,000, ab4803, Abcam), P-Y576 recombinant monoclonal (1:500, 700013, Invitrogen), Paxillin (1:5,000, 610569, BD Biosciences) and actin (1:1,000, sc-1616, Santa Cruz). Visualization was performed using HRP-conjugated antibodies (1:15,000, sc-2301 or sc-2302, Santa Cruz) and detected with LumiSensor (GeneScript) on UVP iBox.

Statistical analysis. Quantification of the orientation of the division axis of metaphase cultured and epithelial cells were carried out with the ImageJ software by using the Z-projections of the images, where the angle between the line from the one spindle pole parallel to the substrate and the line connecting the two spindle poles was measured. Statistical analysis including analysis of variance and two-tailed unpaired *t*-test for parametric distributions and Kruskal–Wallis and Mann–Whitney tests for non-parametric distributions and graph construction was performed by the GraphPad software.

The spindle size was determined by measuring the length and width of the mitotic spindle of metaphase cells. Maximum intensity projections were used for the measurements. The width was measured at the widest point of the mitotic spindle, usually at the centre of the spindle. As in the three dimensions, the spindle angle must also be considered and the actual length corresponds to the hypotenuse of the right triangle that connects the two poles, we calculated the length of the mitotic spindle as $\cos\alpha/A$, where α is the average spindle angle and A the length of

the spindle in the maximum intensity projections. This process was performed both in control and experimental samples.

Spindle centring was calculated by measuring the distance from each spindle pole of a metaphase cell to the nearest point at the cell cortex and then the distance with the greatest value was divided by the distance with the smallest value. Off centre spindles were defined when the above ratio was greater than 1.5.

The correlation of the spindle poles to the LGN cortical crescent was performed by measuring the angle formed between the line connecting the centre of the metaphase plate perpendicularly to the cell cortex and the line extending from the centre of the LGN cortical crescent towards the centre of the metaphase plate. The spindles that displayed an angle between 30° and 90° were considered as uncoupled with the LGN cortical localization.

The average degree of spindle rotation in *Xenopus* embryos was calculated by ImageJ and Graphpad software, where the angle between the long axis of the spindle at the first time and the next time point was measured. In order to calculate the average number of spindle rotations per frame, for each metaphase cell, the number of rotations above 20° was counted and divided by the number of total rotations. The frequency was calculated by dividing this result with the time interval between the frames.

The quantification of the spindle rotation after laser ablation was performed by measuring the angle between the final division axis before cytokinesis and the axis of the induced tension which corresponds to the long axis of the cell after it changes its shape. Histograms were generated with the GraphPad software where the frequency of the above spindle angle was calculated as the number of divisions that had a spindle angle in the indicated categories divided by the total number of divisions.

The correlation between cell shape and spindle angles was determined by measuring the length and width for each cell as well as the angle of deviation of each spindle from the cells long axis. For the statistical analysis both Kruskal–Wallis and Mann–Whitney tests were performed between controls, FAK MO- and Noc-treated cells comparing all values or after setting a length to width ratio (L/W) threshold of three.

The average thickness of the *Xenopus* distal pronephros was quantified by measuring the thickness of the pronephros in 20 different areas of the distal part in each embryo by using the Zen2009 Light Edition Software. The average thickness in each embryo was used for the two-way analysis of variance test to compare the thickness in control and experimental samples by using the GraphPad software.

References

1. Noatynska, A., Gotta, M. & Meraldi, P. Mitotic spindle (DIS)orientation and DISease: cause or consequence? *J. Cell Biol.* **199,** 1025–1035 (2012).
2. Rodriguez-Fraticelli, A. E., Galvez-Santisteban, M. & Martin-Belmonte, F. Divide and polarize: recent advances in the molecular mechanism regulating epithelial tubulogenesis. *Curr. Opin. Cell Biol.* **23,** 638–646 (2011).
3. Lu, M. S. & Johnston, C. A. Molecular pathways regulating mitotic spindle orientation in animal cells. *Development* **140,** 1843–1856 (2013).
4. Bergstralh, D. T., Haack, T. & St Johnston, D. Epithelial polarity and spindle orientation: intersecting pathways. *Philos. Trans. R. Soc. Lond. B Biol. Sci.* **368,** 20130291 (2013).
5. Siller, K. H. & Doe, C. Q. Spindle orientation during asymmetric cell division. *Nat. Cell Biol.* **11,** 365–374 (2009).
6. Minc, N., Burgess, D. & Chang, F. Influence of cell geometry on division-plane positioning. *Cell* **144,** 414–426 (2011).
7. Fink, J. *et al.* External forces control mitotic spindle positioning. *Nat. Cell Biol.* **13,** 771–778 (2011).
8. Campinho, P. *et al.* Tension-oriented cell divisions limit anisotropic tissue tension in epithelial spreading during zebrafish epiboly. *Nat. Cell Biol.* **15,** 1405–1414 (2013).
9. Kunda, P. & Baum, B. The actin cytoskeleton in spindle assembly and positioning. *Trends Cell Biol.* **19,** 174–179 (2009).
10. Lu, B., Roegiers, F., Jan, L. Y. & Jan, Y. N. Adherens junctions inhibit asymmetric division in the *Drosophila* epithelium. *Nature* **409,** 522–525 (2001).
11. den Elzen, N., Buttery, C. V., Maddugoda, M. P., Ren, G. & Yap, A. S. Cadherin adhesion receptors orient the mitotic spindle during symmetric cell division in mammalian epithelia. *Mol. Biol. Cell* **20,** 3740–3750 (2009).
12. Banon-Rodriguez, I. *et al.* EGFR controls IQGAP basolateral membrane localization and mitotic spindle orientation during epithelial morphogenesis. *EMBO J.* **33,** 129–145 (2014).
13. Matsumura, S. *et al.* ABL1 regulates spindle orientation in adherent cells and mammalian skin. *Nat. Commun.* **3,** 626 (2012).
14. Toyoshima, F., Matsumura, S., Morimoto, H., Mitsushima, M. & Nishida, E. PtdIns(3,4,5)P3 regulates spindle orientation in adherent cells. *Dev. Cell* **13,** 796–811 (2007).
15. Toyoshima, F. & Nishida, E. Integrin-mediated adhesion orients the spindle parallel to the substratum in an EB1- and myosin X-dependent manner. *EMBO J.* **26,** 1487–1498 (2007).
16. Goldmann, W. H. Mechanotransduction and focal adhesions. *Cell Biol. Int.* **36,** 649–652 (2012).
17. Wang, H. B., Dembo, M., Hanks, S. K. & Wang, Y. Focal adhesion kinase is involved in mechanosensing during fibroblast migration. *Proc. Natl Acad. Sci. USA* **98,** 11295–11300 (2001).
18. Zebda, N., Dubrovskyi, O. & Birukov, K. G. Focal adhesion kinase regulation of mechanotransduction and its impact on endothelial cell functions. *Microvasc. Res.* **83,** 71–81 (2012).
19. Lechler, T. & Fuchs, E. Asymmetric cell divisions promote stratification and differentiation of mammalian skin. *Nature* **437,** 275–280 (2005).
20. Guan, J. L. Focal adhesion kinase in integrin signaling. *Matrix Biol.* **16,** 195–200 (1997).
21. Fonar, Y. *et al.* Focal adhesion kinase protein regulates Wnt3a gene expression to control cell fate specification in the developing neural plate. *Mol. Biol. Cell* **22,** 2409–2421 (2011).
22. Petridou, N. I., Stylianou, P. & Skourides, P. A. A dominant-negative provides new insights into FAK regulation and function in early embryonic morphogenesis. *Development* **140,** 4266–4276 (2013).
23. Thery, M. *et al.* The extracellular matrix guides the orientation of the cell division axis. *Nat. Cell Biol.* **7,** 947–953 (2005).
24. Toyoshima, F. & Nishida, E. Spindle orientation in animal cell mitosis: roles of integrin in the control of spindle axis. *J. Cell Physiol.* **213,** 407–411 (2007).
25. Lancaster, O. M. & Baum, B. Might makes right: Using force to align the mitotic spindle. *Nat. Cell Biol.* **13,** 736–738 (2011).
26. Mitra, S. K., Hanson, D. A. & Schlaepfer, D. D. Focal adhesion kinase: in command and control of cell motility. *Nat. Rev. Mol. Cell Biol.* **6,** 56–68 (2005).
27. Lim, S. T. *et al.* Knock-in mutation reveals an essential role for focal adhesion kinase activity in blood vessel morphogenesis and cell motility-polarity but not cell proliferation. *J. Biol. Chem.* **285,** 21526–21536 (2010).
28. Slack-Davis, J. K. *et al.* Cellular characterization of a novel focal adhesion kinase inhibitor. *J. Biol. Chem.* **282,** 14845–14852 (2007).
29. Hildebrand, J. D., Schaller, M. D. & Parsons, J. T. Identification of sequences required for the efficient localization of the focal adhesion kinase, pp125FAK, to cellular focal adhesions. *J. Cell Biol.* **123,** 993–1005 (1993).
30. Serrels, B. *et al.* Focal adhesion kinase controls actin assembly via a FERM-mediated interaction with the Arp2/3 complex. *Nat. Cell Biol.* **9,** 1046–1056 (2007).
31. Schaller, M. D., Otey, C. A., Hildebrand, J. D. & Parsons, J. T. Focal adhesion kinase and paxillin bind to peptides mimicking beta integrin cytoplasmic domains. *J. Cell Biol.* **130,** 1181–1187 (1995).
32. Nolan, K., Lacoste, J. & Parsons, J. T. Regulated expression of focal adhesion kinase-related nonkinase, the autonomously expressed C-terminal domain of focal adhesion kinase. *Mol. Cell. Biol.* **19,** 6120–6129 (1999).
33. Zhai, J. *et al.* Direct interaction of focal adhesion kinase with p190RhoGEF. *J. Biol. Chem.* **278,** 24865–24873 (2003).
34. Schlaepfer, D. D., Hanks, S. K., Hunter, T. & van der Geer, P. Integrin-mediated signal transduction linked to Ras pathway by GRB2 binding to focal adhesion kinase. *Nature* **372,** 786–791 (1994).
35. Lawson, C. *et al.* FAK promotes recruitment of talin to nascent adhesions to control cell motility. *J. Cell Biol.* **196,** 223–232 (2012).
36. Scheswohl, D. M. *et al.* Multiple paxillin binding sites regulate FAK function. *J. Mol. Signal.* **3,** 1 (2008).
37. Sieg, D. J., Hauck, C. R. & Schlaepfer, D. D. Required role of focal adhesion kinase (FAK) for integrin-stimulated cell migration. *J. Cell Sci.* **112**(Pt 16): 2677–2691 (1999).
38. Hayashi, I., Vuori, K. & Liddington, R. C. The focal adhesion targeting (FAT) region of focal adhesion kinase is a four-helix bundle that binds paxillin. *Nat. Struct. Biol.* **9,** 101–106 (2002).
39. Park, A. Y., Shen, T. L., Chien, S. & Guan, J. L. Role of focal adhesion kinase Ser-732 phosphorylation in centrosome function during mitosis. *J. Biol. Chem.* **284,** 9418–9425 (2009).
40. Antoniades, I., Stylianou, P. & Skourides, P. A. Making the connection: ciliary adhesion complexes anchor Basal bodies to the actin cytoskeleton. *Dev. Cell* **28,** 70–80 (2014).
41. Xie, Z. & Tsai, L. H. Cdk5 phosphorylation of FAK regulates centrosome-associated miocrotubules and neuronal migration. *Cell Cycle* **3,** 108–110 (2004).
42. Woolner, S. & Papalopulu, N. Spindle position in symmetric cell divisions during epiboly is controlled by opposing and dynamic apicobasal forces. *Dev. Cell* **22,** 775–787 (2012).
43. Marsden, M. & DeSimone, D. W. Regulation of cell polarity, radial intercalation and epiboly in Xenopus: novel roles for integrin and fibronectin. *Development* **128,** 3635–3647 (2001).
44. Petridou, N. I. *et al.* Activation of endogenous FAK via expression of its amino terminal domain in Xenopus embryos. *PLoS One* **7,** e42577 (2012).
45. Hao, Y. *et al.* Par3 controls epithelial spindle orientation by aPKC-mediated phosphorylation of apical Pins. *Curr. Biol.* **20,** 1809–1818 (2010).
46. Durgan, J., Kaji, N., Jin, D. & Hall, A. Par6B and atypical PKC regulate mitotic spindle orientation during epithelial morphogenesis. *J. Biol. Chem.* **286,** 12461–12474 (2011).

47. Iioka, H., Iemura, S., Natsume, T. & Kinoshita, N. Wnt signalling regulates paxillin ubiquitination essential for mesodermal cell motility. *Nat. Cell Biol.* **9,** 813–821 (2007).
48. Fischer, E. *et al.* Defective planar cell polarity in polycystic kidney disease. *Nature Genet.* **38,** 21–23 (2006).
49. Keller, R. E. The cellular basis of epiboly: an SEM study of deep-cell rearrangement during gastrulation in *Xenopus laevis*. *J. Embryol. Exp. Morphol.* **60,** 201–234 (1980).
50. Tada, M., O'Reilly, M. A. & Smith, J. C. Analysis of competence and of Brachyury autoinduction by use of hormone-inducible Xbra. *Development* **124,** 2225–2234 (1997).
51. Solnica-Krezel, L. Conserved patterns of cell movements during vertebrate gastrulation. *Curr. Biol.* **15,** R213–R228 (2005).
52. Simons, M. & Walz, G. Polycystic kidney disease: cell division without a c(l)ue? *Kidney Int.* **70,** 854–864 (2006).
53. Winklbauer, R. Cadherin function during Xenopus gastrulation. *Subcell. Biochem.* **60,** 301–320 (2012).
54. Fesenko, I. *et al.* Tight junction biogenesis in the early Xenopus embryo. *Mech. Dev.* **96,** 51–65 (2000).
55. Lee, G., Hynes, R. & Kirschner, M. Temporal and spatial regulation of fibronectin in early Xenopus development. *Cell* **36,** 729–740 (1984).
56. Davidson, L. A., Marsden, M., Keller, R. & Desimone, D. W. Integrin alpha5beta1 and fibronectin regulate polarized cell protrusions required for Xenopus convergence and extension. *Curr. Biol.* **16,** 833–844 (2006).
57. Sun, X. *et al.* Enhanced interaction between focal adhesion and adherens junction proteins: involvement in sphingosine 1-phosphate-induced endothelial barrier enhancement. *Microvasc. Res.* **77,** 304–313 (2009).
58. Dubrovskyi, O. *et al.* Identification of paxillin domains interacting with beta-catenin. *FEBS Lett.* **586,** 2294–2299 (2012).
59. Fernandez-Minan, A., Martin-Bermudo, M. D. & Gonzalez-Reyes, A. Integrin signaling regulates spindle orientation in Drosophila to preserve the follicular-epithelium monolayer. *Curr. Biol.* **17,** 683–688 (2007).
60. Mammoto, T. & Ingber, D. E. Mechanical control of tissue and organ development. *Development* **137,** 1407–1420 (2010).
61. Tsuda, S. *et al.* FAK-mediated extracellular signals are essential for interkinetic nuclear migration and planar divisions in the neuroepithelium. *J. Cell Sci.* **123,** 484–496 (2010).
62. Delaval, B., Bright, A., Lawson, N. D. & Doxsey, S. The cilia protein IFT88 is required for spindle orientation in mitosis. *Nat. Cell Biol.* **13,** 461–468 (2011).
63. Hori, A., Ikebe, C., Tada, M. & Toda, T. Msd1/SSX2IP-dependent microtubule anchorage ensures spindle orientation and primary cilia formation. *EMBO Rep.* **15,** 175–184 (2014).
64. Bubenshchikova, E. *et al.* Wtip and Vangl2 are required for mitotic spindle orientation and cloaca morphogenesis. *Biol. Open* **1,** 588–596 (2012).
65. Borovina, A. & Ciruna, B. IFT88 plays a cilia- and PCP-independent role in controlling oriented cell divisions during vertebrate embryonic development. *Cell Rep.* **5,** 37–43 (2013).
66. Kanamori, A. & Brown, D. D. Cultured cells as a model for amphibian metamorphosis. *Proc. Natl Acad. Sci. USA* **90,** 6013–6017 (1993).
67. Nieuwkoop, P. D. & Faber, J. *Normal Table of Xenopus Laevis* (North Holland Publishing Co, 1967).

Acknowledgements

We thank Drs Chenbei Chang, Ira O. Daar, Reinhard Koster, Fumiko Toyoshima and Brian J. Mitchell for providing plasmids. We also thank Dr Vasilis Promponas for his help and guidance on the statistical analysis.

Author contributions

N.I.P. performed the experiments, N.I.P. and P.A.S. designed the experiments, analysed the data and wrote the manuscript.

Additional information

Supplementary Information accompanies this paper at http://www.nature.com/naturecommunications

Competing financial interests: The authors declare no competing financial interests.

Reprints and permission information is available online at http://npg.nature.com/reprintsandpermissions/

How to cite this article: Petridou, N. I. & Skourides, P. A. FAK transduces extracellular forces that orient the mitotic spindle and control tissue morphogenesis. *Nat. Commun.* 5:5240 doi: 10.1038/ncomms6240 (2014).